



University of  
**Nottingham**

UK | CHINA | MALAYSIA

***Alkaloids from *Alstonia scholaris*  
and *Ficus schwarzii****

**PREMANAND KRISHNAN**

School of Pharmacy

University of Nottingham Malaysia

Thesis submitted to the University of Nottingham  
for the degree of Doctor of Philosophy

November 2021

# Preface

This thesis is submitted for the degree of *Doctor of Philosophy* at the University of Nottingham. The study herein was conducted under the supervision of Professor Lim Kuan Hon of the Faculty of Science and Engineering, University of Nottingham Malaysia and Dr. Low Yun Yee of the Faculty of Science, University Malaya. This work is to the best of my knowledge original, except where acknowledgement and references are made to previous studies. This thesis has not been submitted for any degree and is not concurrently submitted for candidature of any other degree.

Parts of this work have been presented in the following publications:

## *Alstonia scholaris*

1. Krishnan, P.; Lee, F. K.; Chong, K. W.; Mai, C. W.; Muhamad, A.; Lim, S. H.; Low, Y. Y.; Ting, K. N.; Lim, K. H. *Org. Lett.* **2018**, *20* (24), 8014–8018.
2. Krishnan, P.; Mai, C. W.; Yong, K. T.; Low, Y. Y.; Lim, K. H. *Tetrahedron Lett.* **2019**, *60* (11), 789–791.

## *Ficus schwarzii*

3. Krishnan, P.; Lee, F. K.; Yap, V. A.; Low, Y. Y.; Kam, T. S.; Yong, K. T.; Ting, K. N.; Lim, K. H. *J. Nat. Prod.* **2020**, *83* (1), 152–158.

# Acknowledgements

First and foremost, I would like to express my sincerest gratitude to my main supervisor, Professor Lim Kuan Hon, for his patience, motivation, and immense knowledge, all of which contributed greatly to my PhD and related research. His advice was extremely helpful and supportive to me. I could not have asked for a better advisor and mentor in my PhD journey. I would also like to thank my co-supervisor, Dr. Low Yun Yee for his thoughtful ideas on how to overcome experimental barriers in my project.

My thanks also go to my fellow labmates, Dr. Lee Fong Kai, Dr. Chan Zi Yang, Dr. Amjad Ayad Qatran Al-Khdhairawi and Ms. Margret Chinonso, for the stimulating discussions and support they provided throughout my PhD journey.

I would like to thank Mr. Wong Soon Kit from the University of Malaya for his support in calculating the ECD data of several compounds described in this thesis, as well as Dr. Dawn Sim and Mr. Lim Jun Lee for their help with some spectroscopic measurements.

Professor Ting Kang Nee (UNM) and Professor Leong Chee Onn (IMU) deserve special recognition for evaluating the bioactivity of the selected alkaloids obtained from my project.

My heartfelt gratitude goes to my other half, Thaarani Vijayakumar and my children Hanushrey and Shrey Nhirav for their care, encouragement, and support throughout my research journey. Finally, I would like to express my special thanks to all my family and friends.

## Abstract

Alkaloids, which are the most studied secondary metabolites, are structurally diverse and well known for their biological activity. The aim of the present study is to perform phytochemical investigations on the alkaloidal composition of two selected plant species, namely, *Ficus schwarzii* (Moraceae) and *Alstonia scholaris* (Apocynaceae). (specimen from the West Coast of Peninsular Malaysia). The previously unexplored phytochemistry of *F. schwarzii* and the phytochemical variation of *A. scholaris* due to locality have motivated research into the two species collected from Peninsular Malaysia.

Phytochemical investigation of the leaves of *F. schwarzii* yielded nine novel alkaloids, namely, schwarzinicines A–G (**1–7**), and schwarzificusines A and B (**8** and **9**). The schwarzinicine alkaloids represent the first examples of 1,4 diarylbutanoid–phenethylamine conjugates, while schwarzificusines A and B (**8** and **9**) represent a pair of new diastereomeric 1-phenyl-3-aminotetralins that are structurally related to the schwarzinicines alkaloids. The structures of alkaloids **1–9** were elucidated by detailed analysis of their HRMS and NMR data. Plausible biogenetic pathways that furnish the skeletons of the schwarzinicine and schwarzificusine alkaloids were proposed.

Phytochemical investigation of the leaves, bark and flowers of *A. scholaris* cultivated on the West Coast of Peninsular Malaysia provided a total of 17 alkaloids, of which five are new, namely, alstoscholactine (**10**), alstolaxepine (**11**), *N*-formylyunnanensine (**12**), scholaphylline (**13**), and alstobrogaline (**19**). Alstoscholactine (**10**), alstolaxepine (**11**), and alstobrogaline (**19**) were established to contain novel ring systems. Alstoscholactine (**10**) represents a rearranged stemmadenine alkaloid with an unprecedented C-6-C-19 connectivity, while alstolaxepine (**11**) represents a 6,7-*seco*-angustilobine B-type alkaloid incorporating a rare  $\gamma$ -lactone-bridged oxepane ring system. On the other hand, alstobrogaline (**19**) is an

unusual monoterpenoid indole alkaloid incorporating a third *N* atom, and possessing an aldimine as well as a nitron function. *N*-Formilyunnanensine (**12**) is the *N*-formyl derivative of the known alkaloid yunnanensine, and it was isolated as a pair of unseparable *E/Z*-formamide rotamers. Scholaphylline (**13**) represents the first member of the *secostemmadenine-secovallesamine*-type bisindole alkaloid. The 12 known alkaloids obtained from *Alstonia scholaris* are 19,20-*E*-vallesamine (**14**), 19,20-*Z*-vallesamine (**15**), 19,20-*E*-vallesamine *N*-oxide (**16**), 6,7-*seco*angustilobine B (**17**), and 6,7-*seco*-19,20 $\alpha$ -epoxyangustilobine B (**18**), tetrahydroalstonine (**20**), picrinine (**21**), 16*R*-19,20-*Z*-isositsirikine (**22**), 16*R*-19,20-*E*-isositsirikine (**23**), scholaricine (**24**), *N*-demethylalstogustine *N*-oxide (**25**), and *E/Z*-vallesiachotamine (**26**).

# Table of Contents

Preface.....	II
Acknowledgements.....	III
Abstract.....	IV
Table of Contents.....	VI
List of Abbreviations.....	X
List of Figures.....	XII
List of Tables.....	XVII
List of Appendices.....	XIX
CHAPTER ONE: INTRODUCTION.....	1
1.0 Plant Metabolites.....	1
1.1 Alkaloids.....	2
1.3 Medicinal Use of Alkaloids.....	4
1.4 Classification of Alkaloids.....	6
1.5 The Genus <i>Ficus</i> .....	8
1.5.1 General.....	8
1.5.2 Alkaloids from the Genus <i>Ficus</i> .....	9
1.5.3 <i>Ficus schwarzii</i> Koord.....	19
1.6 The Genus <i>Alstonia</i> .....	21
1.6.1 General.....	21
1.6.2 Alkaloids of the Apocynaceae Family.....	23
1.6.2.1 Indole Alkaloids.....	23
1.6.2.2 Classification and Biogenesis of Monoterpenoid Indole Alkaloids.....	24
1.7 <i>Alstonia scholaris</i> (L.) R. Br.....	27
1.7.1 General.....	27
1.7.2 Alkaloids from <i>Alstonia scholaris</i> .....	29
1.8 Research Aim.....	43
CHAPTER TWO: ISOLATION AND STRUCTURE ELUCIDATION OF ALKALODS FROM <i>FICUS SCHWARZII</i> .....	44
2.1 Schwarzinicine A ( <b>1</b> ).....	45
2.2 Schwarzinicine B ( <b>2</b> ).....	51
2.3 Schwarzinicine C ( <b>3</b> ).....	57

2.4	Schwarzinicine D ( <b>4</b> ) .....	62
2.5	Schwarzinicine E ( <b>5</b> ).....	68
2.6	Schwarzinicine F ( <b>6</b> ) .....	74
2.7	Schwarzinicine G ( <b>7</b> ) .....	80
2.8	Schwarzificusine A and Schwarzificusine B ( <b>8 and 9</b> ).....	85
2.9	Proposed Biogenesis of Schwarzinicine and Schwarzificusine Alkaloids.....	94
CHAPTER THREE: ISOLATION AND STRUCTURE ELUCIDATION OF ALKALOIDS FROM <i>ALSTONIA SCHOLARIS</i> .....		96
3.1	Aspidospermatan-type Alkaloids.....	99
3.1.1	Alstoscholactine ( <b>10</b> ) .....	99
3.1.2	Alstolaxepine ( <b>11</b> ).....	106
3.1.3	<i>N</i> -Formylyunnanensine ( <b>12</b> ) .....	113
3.1.4	Scholaphylline ( <b>13</b> ).....	120
3.1.5	19,20- <i>E</i> -Vallesamine ( <b>14</b> ), 19,20- <i>Z</i> -vallesamine ( <b>15</b> ), 19,20- <i>E</i> -vallesamine <i>N</i> -oxide ( <b>16</b> ), 6,7- <i>seco</i> angustilobine B ( <b>17</b> ), and 6,7- <i>seco</i> -19,20 $\alpha$ -epoxyangustilobine B ( <b>18</b> ).....	126
3.2	Corynanthean-type Alkaloids .....	139
3.2.1	Alstobrogaline ( <b>19</b> ) .....	139
3.2.2	Tetrahydroalstonine ( <b>20</b> ), Picrinine ( <b>21</b> ), 16 <i>R</i> -19,20- <i>Z</i> -isositsirikine ( <b>22</b> ) and 16 <i>R</i> -19,20- <i>E</i> -isositsirikine ( <b>23</b> ) .....	146
3.3	Strychnan-type Alkaloids .....	156
3.3.1	Scholaricine ( <b>24</b> ) and <i>N</i> -demethylalstogustine <i>N</i> -oxide ( <b>25</b> ).....	156
3.4	Vallesiachotaman-type Alkaloids.....	161
3.4.1	<i>E/Z</i> -Vallesiachotamine ( <b>26</b> ) .....	161
3.5	Proposed Biogenesis of Alstoscholactine ( <b>10</b> ), Alstolaxepine ( <b>11</b> ), <i>N</i> -Formylyunnanensine - ( <b>12</b> ), Scholaphylline ( <b>13</b> ), and Alstobrogaline ( <b>19</b> ).....	164
CHAPTER FOUR: EXPERIMENTAL .....		168
4.1	Spectroscopic Techniques.....	168
4.1.1	NMR Spectroscopy .....	168
4.1.2	IR Spectroscopy .....	168
4.1.3	UV-Vis Spectroscopy .....	169
4.1.4	High-resolution MS .....	169
4.1.5	Optical Rotations .....	170
4.1.6	ECD Spectroscopy .....	170
4.2	Plant Materials, Extraction, and Isolation of Alkaloids .....	171
4.2.1	Source and Authentication of Plant Materials .....	171
4.2.2	Plant Processing and Extraction.....	171

4.2.3	Chromatographic Methods.....	173
4.2.3.1	Column Chromatography.....	173
4.2.3.2	Preparative Centrifugal Thin Layer Chromatography (CTLC).....	174
4.2.3.3	Thin Layer Chromatography (TLC) .....	175
4.2.3.4	High Performance Liquid Chromatography (HPLC).....	175
4.3	Spray Reagent (Dragendorff's reagent) .....	176
4.4	Isolation of Compounds <b>1 – 9</b> from the Leaves of <i>F. schwarzii</i> .....	176
4.5	Conversion of Schwarzinicine A ( <b>1</b> ) to Schwarzinicine B ( <b>2</b> ) via N-methylation.....	177
4.6	Isolation of Compounds <b>10 – 27</b> from <i>Alstonia scholaris</i> .....	178
4.6.1	Isolation of Compounds <b>10, 11, 14, 17, 19, 21 – 23</b> , and <b>25</b> from the Leaves of <i>A. scholaris</i> .....	178
4.6.2	Isolation of Compounds <b>12 – 16, 18, 24, 26</b> , and <b>27</b> from the Bark of <i>A. scholaris</i> .....	178
4.6.3	Isolation of Compounds <b>14, 20</b> , and <b>21</b> from the Flowers of <i>A. scholaris</i> .....	179
4.7	Transformation of 19,20- <i>E</i> -Vallesamine ( <b>14</b> ) to Alstoscholactine ( <b>10</b> ) .....	179
4.8	Summary of Physical Data.....	180
4.8.1	Alkaloids of <i>Ficus schwarzii</i> .....	180
4.8.1.1	Physical Data for Compound <b>1</b> .....	180
4.8.1.2	Physical Data for Compound <b>2</b> .....	180
4.8.1.3	Physical Data for Compound <b>3</b> .....	181
4.8.1.4	Physical Data for Compound <b>4</b> .....	181
4.8.1.5	Physical Data for Compound <b>5</b> .....	182
4.8.1.6	Physical Data for Compound <b>6</b> .....	182
4.8.1.7	Physical Data for Compound <b>7</b> .....	183
4.8.1.8	Physical Data for Compound <b>8</b> .....	183
4.8.1.9	Physical Data for Compound <b>9</b> .....	184
4.8.2	Alkaloids of <i>Alstonia scholaris</i> .....	184
4.8.2.1	Physical Data for Compound <b>10</b> .....	184
4.8.2.2	Physical Data for Compound <b>11</b> .....	185
4.8.2.3	Physical Data for Compound <b>12</b> .....	185
4.8.2.4	Physical Data for Compound <b>13</b> .....	186
4.8.2.5	Physical Data for Compound <b>14</b> .....	186
4.8.2.6	Physical Data for Compound <b>15</b> .....	187
4.8.2.7	Physical Data for Compound <b>16</b> .....	187
4.8.2.8	Physical Data for Compound <b>17</b> .....	188
4.8.2.9	Physical Data for Compound <b>18</b> .....	188

4.8.2.10	Physical Data for Compound <b>19</b> .....	189
4.8.2.11	Physical Data for Compound <b>20</b> .....	189
4.8.2.12	Physical Data for Compound <b>21</b> .....	190
4.8.2.13	Physical Data for Compound <b>22</b> .....	190
4.8.2.14	Physical Data for Compound <b>23</b> .....	191
4.8.2.15	Physical Data for Compound <b>24</b> .....	191
4.8.2.16	Physical Data for Compound <b>25</b> .....	192
4.8.2.17	Physical Data for Compound <b>26</b> .....	192
CHAPTER FIVE: CONCLUDING REMARKS .....		193
REFERENCES .....		196
APPENDICES .....		204

# List of Abbreviations

Ar	aryl group
ACN	acetonitrile
br	broadened (NMR signal)
CD <sub>3</sub> OD	deuterated methanol
CDCl <sub>3</sub>	deuterated chloroform
CHCl <sub>3</sub>	chloroform
COSY	Correlation Spectroscopy
CTLC	Centrifugal Thin Layer Chromatography
<i>c</i>	concentration
ca.	<i>Circa</i> , approximately
cm	centimeter
d	doublet
dd	doublet of doublets (NMR multiplicity)
dt	doublet of triplets (NMR multiplicity)
DCM	dichloromethane
DEA	diethylamine
DMSO	dimethylsulfoxide
ECD	electronic circular dichroism
E <sub>max</sub>	maximal efficacy
EC <sub>50</sub>	half maximal effective concentration
EtOH	ethanol
Et <sub>2</sub> O	diethyl ether
EtOAc	ethyl acetate
e.g.	<i>exempli gratia</i> , for example
etc	<i>et cetera</i> , and so forth
HPLC	High Performance Liquid Chromatography
HMBC	Heteronuclear Multiple Bond Correlation Spectroscopy
HRESIMS	High Resolution Electron Spray Ionisation Mass Spectrometry
HRDARTMS	High Resolution Direct Analysis in Real Time Mass Spectrometry
HSQC	Heteronuclear Single Quantum Coherence Spectroscopy
Hz	Hertz
IC <sub>50</sub>	half maximal inhibitory concentration
IR	Infrared
IUPAC	International Union of Pure and Applied Chemistry
<i>J</i>	coupling constant
kg	kilogram
m	multiplet (NMR multiplicity)
mp	melting point
<i>m/z</i>	mass-to-charge ratio
Me	methyl
MeOH	methanol
MHz	megahertz
mL	millilitre
mM	milimolar
min	minute
NMR	Nuclear Magnetic Resonance

NOESY	Nuclear Overhauser Effect Spectroscopy
nm	nanometer
OH	hydroxyl group
ppm	parts per million
PDA	photodiode array
q	quartet (NMR multiplicity)
R <sub>f</sub>	retention factor
R <sub>t</sub>	retention time
rtp	room temperature and pressure
s	singlet (NMR multiplicity)
sp.	unspecified species
spp.	several species
sx	sextet (NMR multiplicity)
SEM	standard error of the mean
SD	standard deviation
t	triplet (NMR multiplicity)
THF	tetrahydrofuran
TLC	Thin Layer Chromatography
TMS	tetramethylsilane
UV	ultraviolet
viz.	<i>videlicet</i> , which is

# List of Figures

<b>Figure 1.0</b> Selected examples of classes of alkaloids based on chemical structure (amino acid precursor stated in parentheses)	7
<b>Figure 1.1</b> Alkaloids from <i>Ficus</i> species	14 – 19
<b>Figure 1.2</b> Adult specimens of <i>Ficus schwarzii</i> Koord.: A - foliage; B - figs on tree trunk.	20
<b>Figure 1.3</b> Indole and related chromophores	23
<b>Figure 1.4</b> Adult specimens of <i>Alstonia scholaris</i> : A - tree; B – leaves and flowers; C - bark.	28
<b>Figure 1.5:</b> Alkaloids from <i>Alstonia scholaris</i>	35 – 40
<b>Figure 2.0:</b> Alkaloids from <i>Ficus schwarzii</i>	44
<b>Figure 2.1:</b> Schwarzinicine A (1)	45
<b>Figure 2.2:</b> COSY (blue, bold) and selected HMBC (red arrows) correlations of schwarzinicine A (1)	47
<b>Figure 2.3:</b> Chiral HPLC chromatogram of schwarzinicine A (1)	47
<b>Figure 2.4:</b> <sup>1</sup> H NMR spectrum of schwarzinicine A (1) (CDCl <sub>3</sub> , 600 MHz)	49
<b>Figure 2.5:</b> <sup>13</sup> C NMR spectrum of schwarzinicine A (1) (CDCl <sub>3</sub> , 150 MHz)	50
<b>Figure 2.6:</b> Schwarzinicine B (2)	51
<b>Figure 2.7:</b> COSY (blue, bold) and selected HMBC (red arrows) correlations of schwarzinicine B (2)	52
<b>Figure 2.8:</b> Chiral HPLC chromatogram of schwarzinicine B (2)	53
<b>Figure 2.9:</b> <sup>1</sup> H NMR spectrum of schwarzinicine B (2) (CDCl <sub>3</sub> , 600 MHz)	55
<b>Figure 2.10:</b> <sup>13</sup> C NMR spectrum of schwarzinicine B (2) (CDCl <sub>3</sub> , 150 MHz)	56
<b>Figure 2.11:</b> Schwarzinicine C (3)	57
<b>Figure 2.12:</b> COSY (blue, bold) and selected HMBC (red arrows) correlations of schwarzinicine C (3).	58
<b>Figure 2.13:</b> Chiral HPLC chromatogram of schwarzinicine C (3)	58
<b>Figure 2.14:</b> <sup>1</sup> H NMR spectrum of schwarzinicine c (3) (CDCl <sub>3</sub> , 600 MHz)	60
<b>Figure 2.15:</b> <sup>13</sup> C NMR spectrum of schwarzinicine C (3) (CDCl <sub>3</sub> , 150 MHz)	61
<b>Figure 2.16:</b> Schwarzinicine D (4)	62

<b>Figure 2.17:</b> COSY (blue, bold), selected HMBC (red arrows) and NOESY (blue arrow) correlations of schwarzinicine D ( <b>4</b> )	63
<b>Figure 2.18:</b> Chiral HPLC chromatogram of schwarzinicine D ( <b>4</b> )	64
<b>Figure 2.19:</b> $^1\text{H}$ NMR spectrum of schwarzinicine D ( <b>4</b> ) ( $\text{CDCl}_3$ , 600 MHz)	66
<b>Figure 2.20:</b> $^{13}\text{C}$ NMR spectrum of schwarzinicine D ( <b>4</b> ) ( $\text{CDCl}_3$ , 150 MHz)	67
<b>Figure 2.21:</b> Schwarzinicine E ( <b>5</b> )	68
<b>Figure 2.22:</b> COSY (blue, bold), selected HMBC (red arrows) and NOESY (blue arrow) correlations of schwarzinicine E ( <b>5</b> )	69
<b>Figure 2.23:</b> Chiral HPLC chromatogram of schwarzinicine E ( <b>5</b> )	70
<b>Figure 2.24:</b> $^1\text{H}$ NMR spectrum of schwarzinicine E ( <b>5</b> ) ( $\text{CDCl}_3$ , 600 MHz)	72
<b>Figure 2.25:</b> $^{13}\text{C}$ NMR spectrum of schwarzinicine E ( <b>5</b> ) ( $\text{CDCl}_3$ , 150 MHz)	73
<b>Figure 2.26:</b> Schwarzinicine F ( <b>6</b> )	74
<b>Figure 2.27:</b> COSY (blue, bold) and selected HMBC (red arrows) correlations of schwarzinicine F ( <b>6</b> )	75
<b>Figure 2.28:</b> Chiral HPLC chromatogram of schwarzinicine F ( <b>6</b> )	76
<b>Figure 2.29:</b> $^1\text{H}$ NMR spectrum of schwarzinicine F ( <b>6</b> ) ( $\text{CDCl}_3$ , 600 MHz)	78
<b>Figure 2.30:</b> $^{13}\text{C}$ NMR spectrum of schwarzinicine F ( <b>6</b> ) ( $\text{CDCl}_3$ , 150 MHz)	79
<b>Figure 2.31:</b> Schwarzinicine G ( <b>7</b> )	80
<b>Figure 2.32:</b> COSY (blue, bold) and selected HMBC (red arrows) correlations of schwarzinicine G ( <b>7</b> )	80
<b>Figure 2.33:</b> Chiral HPLC chromatogram of schwarzinicine G ( <b>7</b> )	81
<b>Figure 2.34:</b> $^1\text{H}$ NMR spectrum of schwarzinicine G ( <b>7</b> ) ( $\text{CDCl}_3$ , 600 MHz)	83
<b>Figure 2.35:</b> $^{13}\text{C}$ NMR spectrum of schwarzinicine G ( <b>7</b> ) ( $\text{CDCl}_3$ , 150 MHz)	84
<b>Figure 2.36:</b> Schwarzificusine A ( <b>8</b> ) and schwarzificusine B ( <b>9</b> )	85
<b>Figure 2.37:</b> COSY (blue bold bonds), selected HMBC (red arrows) and selected NOE (blue arrows) correlations of schwarzificusines A and B ( <b>8</b> and <b>9</b> )	87
<b>Figure 2.38:</b> Diastereomeric structures proposed for <b>8</b> and <b>9</b> ; stereochemistry shown is relative	88
<b>Figure 2.39:</b> $^1\text{H}$ NMR spectrum of schwarzificusine A ( <b>8</b> ) ( $\text{CDCl}_3$ , 600 MHz)	90
<b>Figure 2.40:</b> $^{13}\text{C}$ NMR spectrum of schwarzificusine A ( <b>8</b> ) ( $\text{CDCl}_3$ , 150 MHz)	91
<b>Figure 2.41:</b> $^1\text{H}$ NMR spectrum of schwarzificusine B ( <b>9</b> ) ( $\text{CDCl}_3$ , 600 MHz)	92
<b>Figure 2.42:</b> $^{13}\text{C}$ NMR spectrum of schwarzificusine B ( <b>9</b> ) ( $\text{CDCl}_3$ , 150 MHz)	93

<b>Figure 2.43:</b> Plausible biogenetic pathways to schwarzinicine and schwarzificusine alkaloids	95
<b>Figure 3.1:</b> Alkaloids isolated from <i>Alstonia scholaris</i>	97
<b>Figure 3.2:</b> Alstoscholactine ( <b>10</b> )	99
<b>Figure 3.3:</b> COSY (blue, bold) and selected HMBC (red arrows) correlations of alstoscholactine ( <b>10</b> )	101
<b>Figure 3.4:</b> Selected NOESY correlations of alstoscholactine ( <b>10</b> )	101
<b>Figure 3.5:</b> Experimental and calculated ECD spectra of alstoscholactine ( <b>10</b> )	102
<b>Figure 3.6:</b> <sup>1</sup> H NMR spectrum of alstoscholactine ( <b>10</b> ) (CDCl <sub>3</sub> , 600 MHz)	104
<b>Figure 3.7:</b> <sup>13</sup> C NMR spectrum of alstoscholactine ( <b>10</b> ) (CDCl <sub>3</sub> , 150 MHz)	105
<b>Figure 3.8:</b> Alstolaxepine ( <b>11</b> )	106
<b>Figure 3.9:</b> COSY (blue, bold) and selected HMBC (red arrows) correlations of alstolaxepine ( <b>11</b> )	108
<b>Figure 3.10:</b> Selected NOESY correlations of alstolaxepine ( <b>11</b> )	108
<b>Figure 3.11:</b> X-ray crystal structure of alstolaxepine ( <b>11</b> )	109
<b>Figure 3.12:</b> <sup>1</sup> H NMR spectrum of alstolaxepine ( <b>11</b> ) (CDCl <sub>3</sub> , 600 MHz)	111
<b>Figure 3.13:</b> <sup>13</sup> C NMR spectrum of alstolaxepine ( <b>11</b> ) (CDCl <sub>3</sub> , 150 MHz)	112
<b>Figure 3.14:</b> <i>N</i> -Formylyunnanensine ( <b>12</b> )	113
<b>Figure 3.15:</b> COSY (blue, bold) and selected HMBC (red arrows) correlations of <i>N</i> -formylyunnanensine ( <b>12</b> )	115
<b>Figure 3.16:</b> Selected NOESY correlations of <i>N</i> -formylyunnanensine ( <b>12</b> ) rotamers	116
<b>Figure 3.17:</b> <sup>1</sup> H NMR spectrum of <i>N</i> -formylyunnanensine ( <b>12</b> ) (CDCl <sub>3</sub> , 600 MHz)	118
<b>Figure 3.18:</b> <sup>13</sup> C NMR spectrum of <i>N</i> -formylyunnanensine ( <b>12</b> ) (CDCl <sub>3</sub> , 150 MHz)	119
<b>Figure 3.19:</b> Scholaphylline ( <b>13</b> )	120
<b>Figure 3.20:</b> COSY (blue, bold) and selected HMBC (red arrows) of scholaphylline ( <b>13</b> )	122
<b>Figure 3.21:</b> Selected NOESY correlations of scholaphylline ( <b>13</b> )	122
<b>Figure 3.22:</b> <sup>1</sup> H NMR spectrum of scholaphylline ( <b>13</b> ) (CDCl <sub>3</sub> , 700 MHz)	124
<b>Figure 3.23:</b> <sup>13</sup> C NMR spectrum of scholaphylline ( <b>13</b> ) (CDCl <sub>3</sub> , 175 MHz)	125
<b>Figure 3.24:</b> <sup>1</sup> H NMR spectrum of 19,20- <i>E</i> -vallesamine ( <b>14</b> ) (CDCl <sub>3</sub> , 600 MHz)	129
<b>Figure 3.25:</b> <sup>1</sup> H NMR spectrum of 19,20- <i>Z</i> -vallesamine ( <b>15</b> ) (CDCl <sub>3</sub> , 600 MHz)	130
<b>Figure 3.26:</b> <sup>1</sup> H NMR spectrum of 19,20- <i>E</i> -vallesamine <i>N</i> -oxide ( <b>16</b> ) (CDCl <sub>3</sub> , 600 MHz)	131

<b>Figure 3.27:</b> <sup>1</sup> H NMR spectrum of 6,7- <i>seco</i> angustilobine B ( <b>17</b> ) (CDCl <sub>3</sub> , 600 MHz)	132
<b>Figure 3.28:</b> <sup>1</sup> H NMR spectrum of 6,7- <i>seco</i> -19,20 $\alpha$ -epoxyangustilobine B ( <b>18</b> ) (CDCl <sub>3</sub> , 600 MHz)	133
<b>Figure 3.29:</b> <sup>13</sup> C NMR spectrum of 19,20- <i>E</i> -vallesamine ( <b>14</b> ) (CDCl <sub>3</sub> , 150 MHz)	134
<b>Figure 3.30:</b> <sup>13</sup> C NMR spectrum of 19,20- <i>Z</i> -vallesamine ( <b>15</b> ) (CDCl <sub>3</sub> , 150 MHz)	135
<b>Figure 3.31:</b> <sup>13</sup> C NMR spectrum of 19,20- <i>E</i> -vallesamine <i>N</i> -oxide ( <b>16</b> ) (CDCl <sub>3</sub> , 150 MHz)	136
<b>Figure 3.32:</b> <sup>13</sup> C NMR spectrum of 6,7- <i>seco</i> angustilobine B ( <b>17</b> ) (CDCl <sub>3</sub> , 150 MHz)	137
<b>Figure 3.33:</b> <sup>13</sup> C NMR spectrum of 6,7- <i>seco</i> -19,20 $\alpha$ -epoxyangustilobine B ( <b>18</b> ) (CDCl <sub>3</sub> , 150 MHz)	138
<b>Figure 3.34:</b> Structure of alstobrogaline ( <b>19</b> )	139
<b>Figure 3.35:</b> COSY (blue, bold) and selected HMBC (red arrows) correlations of alstobrogaline ( <b>19</b> )	140
<b>Figure 3.36:</b> Selected NOESY correlations of alstobrogaline ( <b>19</b> )	141
<b>Figure 3.37:</b> X-ray crystal structure of alstobrogaline ( <b>19</b> ) [Flack parameter, $x = -0.02(2)$ ]	142
<b>Figure 3.38:</b> <sup>1</sup> H NMR spectrum of alstobrogaline ( <b>19</b> ) (CDCl <sub>3</sub> , 600 MHz)	144
<b>Figure 3.39:</b> <sup>13</sup> C NMR spectrum of alstobrogaline ( <b>19</b> ) (CDCl <sub>3</sub> , 150 MHz)	145
<b>Figure 3.40:</b> <sup>1</sup> H NMR spectrum of tetrahydroalstonine ( <b>20</b> ) (CDCl <sub>3</sub> , 600 MHz)	148
<b>Figure 3.41:</b> <sup>1</sup> H NMR spectrum of picrinine ( <b>21</b> ) (CDCl <sub>3</sub> , 600 MHz)	149
<b>Figure 3.42:</b> <sup>1</sup> H NMR spectrum of 16 <i>R</i> -19,20- <i>Z</i> -isositsirikine ( <b>22</b> ) (CDCl <sub>3</sub> , 600 MHz)	150
<b>Figure 3.43:</b> <sup>1</sup> H NMR spectrum of 16 <i>R</i> -19,20- <i>E</i> -isositsirikine ( <b>23</b> ) (CDCl <sub>3</sub> , 600 MHz)	151
<b>Figure 3.44:</b> <sup>13</sup> C NMR spectrum of tetrahydroalstonine ( <b>20</b> ) (CDCl <sub>3</sub> , 150 MHz)	152
<b>Figure 3.45:</b> <sup>13</sup> C NMR spectrum of picrinine ( <b>21</b> ) (CDCl <sub>3</sub> , 150 MHz)	153
<b>Figure 3.46:</b> <sup>13</sup> C NMR spectrum of 16 <i>R</i> -19,20- <i>Z</i> -isositsirikine ( <b>22</b> ) (CDCl <sub>3</sub> , 150 MHz)	154
<b>Figure 3.47:</b> <sup>13</sup> C NMR spectrum of 16 <i>R</i> -19,20- <i>E</i> -isositsirikine ( <b>23</b> ) (CDCl <sub>3</sub> , 150 MHz)	155
<b>Figure 3.48:</b> <sup>1</sup> H NMR spectrum of scholaricine ( <b>24</b> ) (CDCl <sub>3</sub> , 600 MHz)	157

<b>Figure 3.49:</b> $^1\text{H}$ NMR spectrum of <i>N</i> -demethylalstogustine <i>N</i> -oxide ( <b>25</b> ) ( $\text{CDCl}_3$ , 600 MHz)	158
<b>Figure 3.50:</b> $^{13}\text{C}$ NMR spectrum of scholaricine ( <b>24</b> ) ( $\text{CDCl}_3$ , 150 MHz)	159
<b>Figure 3.51:</b> $^{13}\text{C}$ NMR spectrum of <i>N</i> -demethylalstogustine <i>N</i> -oxide ( <b>25</b> ) ( $\text{CDCl}_3$ , 150 MHz)	160
<b>Figure 3.52:</b> $^1\text{H}$ NMR spectrum of <i>E/Z</i> -vallesiachotamine ( <b>26</b> ) ( $\text{CDCl}_3$ , 600 MHz)	162
<b>Figure 3.53:</b> $^{13}\text{C}$ NMR spectrum of <i>E/Z</i> -vallesiachotamine ( <b>26</b> ) ( $\text{CDCl}_3$ , 150 MHz)	163
<b>Figure 3.54:</b> Plausible biogenetic pathways to alstoscholactine ( <b>10</b> ), alstolaxepine ( <b>11</b> ), <i>N</i> -formylyunnanensine ( <b>12</b> ), and scholaphylline ( <b>13</b> )	166
<b>Figure 3.55:</b> Plausible biogenetic pathway to alstobrogaline ( <b>19</b> )	167

# List of Tables

<b>Table 1.0:</b> Naturally occurring alkaloids marketed as medicines or drugs	5 – 6
<b>Table 1.1:</b> Biologically active <i>Ficus</i> Alkaloids	10
<b>Table 1.2:</b> Occurrence of alkaloids in <i>Ficus</i>	11 – 13
<b>Table 1.3:</b> Occurrence of alkaloids in <i>Alstonia scholaris</i>	29 – 34
<b>Table 1.4:</b> Biologically active <i>A. scholaris</i> alkaloids	41
<b>Table 2.1:</b> <sup>1</sup> H (600 MHz) and <sup>13</sup> C (150 MHz) NMR spectroscopic data (in CDCl <sub>3</sub> with TMS as internal reference) of schwarzinicine A ( <b>1</b> )	48
<b>Table 2.2:</b> <sup>1</sup> H (600 MHz) and <sup>13</sup> C (150 MHz) NMR spectroscopic data (in CDCl <sub>3</sub> with TMS as internal reference) of schwarzinicine B ( <b>2</b> )	54
<b>Table 2.3:</b> <sup>1</sup> H (600 MHz) and <sup>13</sup> C (150 MHz) NMR spectroscopic data (in CDCl <sub>3</sub> with TMS as internal reference) of schwarzinicine C ( <b>3</b> )	59
<b>Table 2.4:</b> <sup>1</sup> H (600 MHz) and <sup>13</sup> C (150 MHz) NMR spectroscopic data (in CDCl <sub>3</sub> with TMS as internal reference) of schwarzinicine D ( <b>4</b> )	65
<b>Table 2.5:</b> <sup>1</sup> H (600 MHz) and <sup>13</sup> C (150 MHz) NMR spectroscopic data (in CDCl <sub>3</sub> with TMS as internal reference) of schwarzinicine E ( <b>5</b> )	71
<b>Table 2.6:</b> <sup>1</sup> H (600 MHz) and <sup>13</sup> C (150 MHz) NMR spectroscopic data (in CDCl <sub>3</sub> with TMS as internal reference) of schwarzinicine F ( <b>6</b> )	77
<b>Table 2.7:</b> <sup>1</sup> H (600 MHz) and <sup>13</sup> C (150 MHz) NMR spectroscopic data (in CDCl <sub>3</sub> with TMS as internal reference) of schwarzinicine G ( <b>7</b> )	82
<b>Table 2.8:</b> <sup>1</sup> H (600 MHz) and <sup>13</sup> C (150 MHz) NMR spectroscopic data (in CDCl <sub>3</sub> with TMS as internal reference) of schwarzificusine A ( <b>8</b> ) and schwarzificusine B ( <b>9</b> )	89
<b>Table 3.1:</b> Source and yield of alkaloids obtained from <i>A. scholaris</i> .	98
<b>Table 3.2:</b> <sup>1</sup> H (600 MHz) and <sup>13</sup> C (150 MHz) NMR spectroscopic data (in CDCl <sub>3</sub> with TMS as internal reference) of alstoscholactine ( <b>10</b> )	103
<b>Table 3.3:</b> <sup>1</sup> H (600 MHz) and <sup>13</sup> C (150 MHz) NMR spectroscopic data (in CDCl <sub>3</sub> with TMS as internal reference) of alstolaxepine ( <b>11</b> )	110
<b>Table 3.4:</b> <sup>1</sup> H (600 MHz) and <sup>13</sup> C (150 MHz) NMR spectroscopic data (in CDCl <sub>3</sub> with TMS as internal reference) of <i>N</i> -formylyunnanensine ( <b>12</b> )	117

<b>Table 3.5:</b> $^1\text{H}$ (700 MHz) and $^{13}\text{C}$ (175 MHz) NMR spectroscopic data (in $\text{CDCl}_3$ with TMS as internal reference) of scholaphylline ( <b>13</b> )	123
<b>Table 3.6:</b> $^1\text{H}$ (600 MHz) and $^{13}\text{C}$ (150 MHz) NMR spectroscopic data (in $\text{CDCl}_3$ with TMS as internal reference) of 19,20- <i>E</i> -vallesamine ( <b>14</b> )	126
<b>Table 3.7:</b> $^1\text{H}$ (700 MHz) and $^{13}\text{C}$ (150 MHz) NMR spectroscopic data (in $\text{CDCl}_3$ with TMS as internal reference) of 19,20- <i>Z</i> -vallesamine ( <b>15</b> ) and 19,20- <i>E</i> -vallesamine <i>N</i> -oxide ( <b>16</b> )	127
<b>Table 3.8:</b> $^1\text{H}$ (700 MHz) and $^{13}\text{C}$ (175 MHz) NMR spectroscopic data (in $\text{CDCl}_3$ with TMS as internal reference) of 6,7- <i>seco</i> angustilobine B ( <b>17</b> ) and 6,7- <i>seco</i> -19,20 $\alpha$ -epoxyangustilobine B ( <b>18</b> )	128
<b>Table 3.9:</b> $^1\text{H}$ (600 MHz) and $^{13}\text{C}$ (150 MHz) NMR spectroscopic data (in $\text{CDCl}_3$ with TMS as internal reference) of alstobrogaline ( <b>19</b> )	143
<b>Table 3.10:</b> $^1\text{H}$ (600 MHz) and $^{13}\text{C}$ (150 MHz) NMR spectroscopic data (in $\text{CDCl}_3$ with TMS as internal reference) of tetrahydroalstonine ( <b>20</b> ) and picrinine ( <b>21</b> )	146
<b>Table 3.11:</b> $^1\text{H}$ (600 MHz) and $^{13}\text{C}$ (150 MHz) NMR spectroscopic data (in $\text{CDCl}_3$ with TMS as internal reference) of 16 <i>R</i> -19,20- <i>Z</i> -isositsirikine ( <b>22</b> ) and 16 <i>R</i> -19,20- <i>E</i> -isositsirikine ( <b>23</b> )	147
<b>Table 3.12:</b> $^1\text{H}$ (600 MHz) and $^{13}\text{C}$ (150 MHz) NMR spectroscopic data (in $\text{CDCl}_3$ with TMS as internal reference) of scholaricine ( <b>24</b> ) and <i>N</i> -demethylalstogustine <i>N</i> -oxide ( <b>25</b> )	156
<b>Table 3.13:</b> $^1\text{H}$ (600 MHz) and $^{13}\text{C}$ (150 MHz) NMR spectroscopic data (in $\text{CDCl}_3$ with TMS as internal reference) of <i>E/Z</i> -vallesiachotamine ( <b>26</b> )	161
<b>Table 4.1:</b> Source and authentication of plant materials	171
<b>Table 4.2:</b> Mass of dried plant materials and crude alkaloid	172
<b>Table 5.1:</b> Vasorelaxant activity of schwarzinicines A–D ( <b>1–4</b> ) against phenylephrine-Induced Contraction.	194
<b>Table 5.2:</b> Antiproliferative activity of scholaphylline ( <b>13</b> ) and alstobrogaline ( <b>19</b> )	195

# List of Appendices

<b>Appendix 1:</b> HR-DART-MS of schwarzinicine A (1)	206
<b>Appendix 2:</b> COSY Spectrum of schwarzinicine A (1)	207
<b>Appendix 3:</b> HSQC Spectrum of schwarzinicine A (1)	208
<b>Appendix 4:</b> HMBC Spectrum of schwarzinicine A (1)	209
<b>Appendix 5:</b> HR-DART-MS of schwarzinicine B (2)	210
<b>Appendix 6:</b> COSY Spectrum of schwarzinicine B (2)	211
<b>Appendix 7:</b> HSQC Spectrum of schwarzinicine B (2)	212
<b>Appendix 8:</b> HMBC Spectrum of schwarzinicine B (2)	213
<b>Appendix 9:</b> HR-DART-MS of schwarzinicine C (3)	214
<b>Appendix 10:</b> COSY Spectrum of schwarzinicine C (3)	215
<b>Appendix 11:</b> HSQC Spectrum of schwarzinicine C (3)	216
<b>Appendix 12:</b> HMBC Spectrum of schwarzinicine C (3)	217
<b>Appendix 13:</b> HR-DART-MS of schwarzinicine D (4)	218
<b>Appendix 14:</b> COSY Spectrum of schwarzinicine D (4)	219
<b>Appendix 15:</b> HSQC Spectrum of schwarzinicine D (4)	220
<b>Appendix 16:</b> HMBC Spectrum of schwarzinicine D (4)	221
<b>Appendix 17:</b> HR-DART-MS of schwarzinicine E (5)	222
<b>Appendix 18:</b> COSY Spectrum of schwarzinicine E (5)	223
<b>Appendix 19:</b> HSQC Spectrum of schwarzinicine E (5)	224
<b>Appendix 20:</b> HMBC Spectrum of schwarzinicine E (5)	225
<b>Appendix 21:</b> HR-DART-MS of schwarzinicine F (6)	226
<b>Appendix 22:</b> COSY Spectrum of schwarzinicine F (6)	227
<b>Appendix 23:</b> HSQC Spectrum of schwarzinicine F (6)	228
<b>Appendix 24:</b> HMBC Spectrum of schwarzinicine F (6)	229
<b>Appendix 25:</b> HR-DART-MS of schwarzinicine G (7)	230
<b>Appendix 26:</b> COSY Spectrum of schwarzinicine G (7)	231
<b>Appendix 27:</b> HSQC Spectrum of schwarzinicine G (7)	232
<b>Appendix 28:</b> HMBC Spectrum of schwarzinicine G (7)	233
<b>Appendix 29:</b> HR-DART-MS of schwarzificusine A (8)	234
<b>Appendix 30:</b> COSY of schwarzificusine A (8)	235
<b>Appendix 31:</b> HSQC of schwarzificusine A (8)	236

<b>Appendix 32:</b> HMBC of schwarzificusine A (8)	237
<b>Appendix 33:</b> NOESY of schwarzificusine A (8)	238
<b>Appendix 34:</b> HR-DART-MS of schwarzificusine B (9)	239
<b>Appendix 35:</b> COSY of schwarzificusine B (9)	240
<b>Appendix 36:</b> HSQC of schwarzificusine B (9)	241
<b>Appendix 37:</b> HMBC of schwarzificusine B (9)	242
<b>Appendix 38:</b> NOESY of schwarzificusine B (9)	243
<b>Appendix 39:</b> HR-DART-MS of alstoscholactine (10)	244
<b>Appendix 40:</b> COSY of alstoscholactine (10)	245
<b>Appendix 41:</b> HSQC of alstoscholactine (10)	246
<b>Appendix 42:</b> HMBC of alstoscholactine (10)	247
<b>Appendix 43:</b> NOESY of alstoscholactine (10)	248
<b>Appendix 44:</b> HR-DART-MS of alstolaxepine (11)	249
<b>Appendix 45:</b> COSY of alstolaxepine (11)	250
<b>Appendix 46:</b> HSQC of alstolaxepine (11)	251
<b>Appendix 47:</b> HMBC of alstolaxepine (11)	252
<b>Appendix 48:</b> NOESY of alstolaxepine (11)	253
<b>Appendix 49:</b> HR-DART-MS of <i>N</i> -formylyunnanensine (12)	254
<b>Appendix 50:</b> COSY of <i>N</i> -formylyunnanensine (12)	255
<b>Appendix 51:</b> HSQC of <i>N</i> -formylyunnanensine (12)	256
<b>Appendix 52:</b> HMBC of <i>N</i> -formylyunnanensine (12)	257
<b>Appendix 53:</b> NOESY of <i>N</i> -formylyunnanensine (12)	258
<b>Appendix 54:</b> HR-ESI-MS of scholaphylline (13)	259
<b>Appendix 55:</b> COSY of scholaphylline (13)	260
<b>Appendix 56:</b> HSQC of scholaphylline (13)	261
<b>Appendix 57:</b> HMBC of scholaphylline (13)	262
<b>Appendix 58:</b> NOESY of scholaphylline (13)	263
<b>Appendix 59:</b> HR-DART-MS of alstobrogaline (19)	264
<b>Appendix 60:</b> COSY of alstobrogaline (19)	265
<b>Appendix 61:</b> HSQC of alstobrogaline (19)	266
<b>Appendix 62:</b> HMBC of alstobrogaline (19)	267
<b>Appendix 63:</b> NOESY of alstobrogaline (19)	268
<b>Appendix 64:</b> Published articles	267 – 281

# CHAPTER ONE: INTRODUCTION

## 1.0 Plant Metabolites

Plants have long been a valuable source of a wide range of natural compounds known as plant metabolites. Plant metabolites can be classified into primary and secondary metabolites based on their role in plant growth and development. Since primary metabolites are crucial for the growth and development of plants, they are widely distributed in nature, occurring in one form or another in almost all species. Chlorophyll, amino acids, nucleotides, and carbohydrates, are examples of primary metabolites, which regulate metabolic processes such as photosynthesis, respiration, and nutrient assimilation.<sup>1</sup>

Secondary metabolites, on the other hand, are usually derived from primary metabolites.<sup>2</sup> They appear to play less apparent roles in plant growth and development, but may be needed for specific functions such as providing protection from environmental stress, defence against pathogens and herbivores,<sup>2</sup> discouraging competing plant species, and attracting pollinators or symbionts.<sup>3</sup> Interestingly, humans have used a variety of plant secondary metabolites as flavourings, fragrances, dyes, pesticides, and pharmaceuticals.<sup>4</sup>

Another distinguishing feature of secondary metabolites is that they are distributed differently among plant taxonomic groups.<sup>5</sup> In terms of chemical structure, plant secondary metabolites are usually small molecules with molecular weight of less than 1500 amu.<sup>6</sup> The production of secondary metabolites is dependent on the developmental process and physiological condition of a plant, and yields are typically very low, being less than 1% dry weight.<sup>7,8</sup> Plant secondary metabolites can be divided into five major structural classes, namely, polyketides, isoprenoids (terpenoids and steroids), alkaloids, phenylpropanoids, and flavonoids.<sup>9</sup>

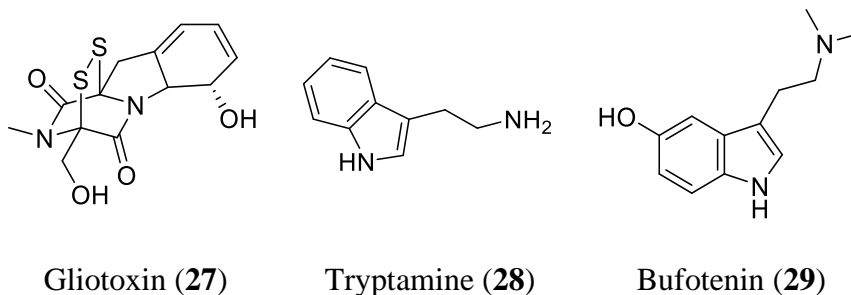
## 1.1 Alkaloids

Alkaloids are the most widely studied of the five major classes of secondary metabolites, with more than 27,000 alkaloid structures characterised to date.<sup>10</sup> The biosynthesis of a specific class of alkaloids is often restricted to specific plant families or genera.<sup>11,12</sup> The German chemist, Carl Friedrich Wilhelm Meissner, was the first to coin the term alkaloid, which means alkaline-like, in 1819.<sup>13</sup> According to his definition, alkaloids are basic nitrogen-containing compounds of plant origin. In 1983, Pelletier suggested a more comprehensive description, i.e., “*alkaloid is a cyclic compound containing nitrogen in a negative oxidation state which is of limited distribution in living organisms*”.<sup>13</sup> In 2002, Hesse suggested a simplified definition of alkaloid, i.e., “*Alkaloids are nitrogen-containing organic substances of natural origin with a greater or lesser degree of basic character*”.<sup>14</sup>

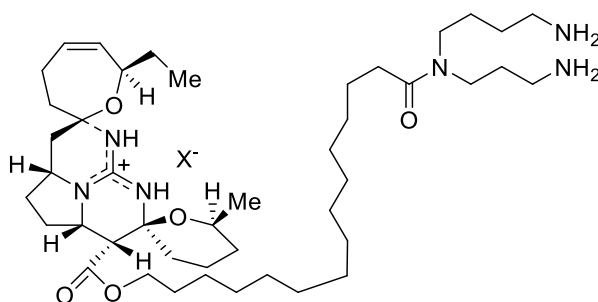
Alkaloids have limited distribution in higher plants and it is estimated that about 25% of plants contain alkaloids.<sup>15</sup> This is because the biosynthesis of alkaloids is often restricted to specific plant taxa. Alkaloids are primarily found in the flowering plants, also known as the angiosperms. Furthermore, certain families within the angiosperms, especially those belonging to the dicotyledons, have been found to produce more alkaloids than others. The major alkaloid-producing plant families include Apocynaceae, Berberidaceae, Papaveraceae, Ranunculaceae, Rubiaceae, Solanaceae, and Loganiaceae.<sup>16</sup> *Alstonia angustiloba* Miq. (Apocynaceae), for example, was reported to have at least 20 alkaloids in all of its organs.<sup>17</sup>

To a lesser extent, alkaloids have also been discovered in the lower plants,<sup>18</sup> bacteria, fungi and small animals.<sup>19</sup> For example, agrocybenine was isolated from the mushroom *Agrocybe cylindracea* by researchers from Korea in 1996.<sup>20</sup> Besides, a lichen was found to produce gliotoxin (**27**), a sulphur-containing alkaloid with antiviral, antifungal, and antibacterial properties.<sup>21</sup> A limited number of alkaloids has also been found in mammals,

amphibians, reptiles, and even arthropods that are capable of biosynthesizing alkaloids without the biogenetic capabilities of plants.<sup>22</sup> For instance, amphibians such as frogs and toads secrete toxic alkaloids on their skins as defence mechanism. Some species of toads elaborate indole alkaloids such as tryptamine (**28**) and bufotenin (**29**), which cause predators to undergo vivid hallucination. .<sup>23</sup>



Lastly, more and more alkaloids have been isolated from marine organisms, particularly those of the phylum Porifera, commonly known as sea sponges. For example, ptilomycalin A (**30**) is a polycyclic guanidine alkaloid previously isolated from the Caribbean sea sponge (*Ptilocaulis spiculifer*), which has demonstrated potent cytotoxic and antiviral activity.<sup>24,25</sup>



Ptilomycalin A (**30**)

### 1.3 Medicinal Use of Alkaloids

Alkaloids have a long history of use in human medicine. Although the knowledge of alkaloids is relatively recent, the use of alkaloid-containing plants like opium poppy dates back to at least 4000 years ago, as evidenced by the Assyrian clay tablets.<sup>19</sup> Besides, various medicinal plants from the Apocynaceae family have been exploited by the ancient “Dai” ethnopharmacy to treat infectious diseases in China.<sup>26</sup> In Europe, the infamous deadly nightshade (*Atropa belladonna*) has been used for centuries to treat symptoms ranging from headache to peptic ulcers to motion sickness. Phytochemical research into *A. belladonna* eventually yielded atropine, which is a tropane alkaloid drug valued for its anticholinergic activity. Today, *A. belladonna* is cultivated on a commercial scale for the pharmaceutical production of atropine and related tropane alkaloids. Its pharmacological effects include tachycardia, mydriasis, anti-secretion of salivary, sweat and mucus glands, and hallucinations. In fact, *A. belladonna* was used as a poison, with King Macbeth of Scotland rumoured to have poisoned the Danish army with the deadly nightshade before ascending to the throne.<sup>14</sup>

In the modern era, about 50 alkaloids or alkaloid-based drugs are clinically used to treat a wide range of human diseases. **Table 1.0** shows a list of naturally occurring alkaloids that are investigated or marketed as human medicines.<sup>27</sup> In addition to unaltered natural alkaloids, many drugs on the market are synthetic derivatives of alkaloids or synthetic compounds possessing alkaloid-inspired skeleton. Therefore, alkaloids continue to provide an important source of drug leads for the discovery of lifesaving therapeutic agents.

**Table 1.0:** Naturally occurring alkaloids marketed as medicines or drugs

<b>Alkaloid</b>	<b>Condition / Disease</b>
Aconitine	Rheumatism, neuralgia, sciatica
Adenine	Antiviral agent, pharmaceutical aid used to extend storage life of whole blood
Ajmaline	Antiarrhythmic agent
Atropine	Antispasmodic, anti-Parkinson, cycloplegic drug
Berberine	Eye irritations, AIDS, hepatitis
Boldine	Cholelithiasis, vomiting, constipation
Caffeine	Neonatal apnea, atopic dermatitis
Canescine	Antihypertensive agent
Cathine	Anorectic drug
Cinchonidine	Increases reflexes, epileptiform convulsions
Cocaine	Local anaesthetic
Codeine	Antitussive, analgesic
Colchicine	Amyloidosis treatment, acute gout
Diethanolamine	Base used in pharmaceuticals
Emetine	Intestinal amoebiasis, expectorant drug
Ephedrine	Nasal decongestant, bronchodilator
Ergometrine	Postpartum/postabortal haemorrhage
Ergotamine	Migraine treatment
Eserine	Ophthalmology, antidote/poisoning
Galanthamine	Muscle relaxant, Alzheimer's
Hydrastine	Gastrointestinal disorders
Hyoscine	Motion sickness
Hyoscyamine	Antispasmodic, anti-Parkinson, cycloplegic drug
Lobeline	Anti-smoking, asthma, cough
Morphine	Pain relief, diarrhoea
<i>N,N</i> -Diallylbisnortoxinerine	Short acting muscular relaxant
Narceine	Cough suppressant
Nicotine	Anti-smoking
Noscaphine	Cough suppressant
Papaverine	Vasodilator, gastrointestinal disorders
Pelletierine	Tenia infestations
Pilocarpine	Miotic in treatment of glaucoma, leprosy
Quinidine	Ventricular and supraventricular arrhythmias, malaria, cramping
Quinine	Malaria, babesiosis, myotonic disorders
Raubasine	Vascular disorders
Rescinnamine	Hypertension
Reserpine	Hypertension, psychoses
Rotundine	Analgesic, sedative, hypnotic agent
Sanguinarine	Antiplatelet agent

Sparteine	Uterine contractions, cardiac arrhythmias
Strychnine	Eye disorders
Synephrine	Vasoconstrictor, conjunctival decongestant, weight loss
Taxol	Mammary and ovary carcinoma
Theobromine	Asthma, diuretic agent
Theophylline	Asthma, bronchospasms
Turbocuranine	Muscle relaxant
Vinblastine	Hodgkin's disease, testicular cancer, blood disorders
Vincamine	Vasodilator
Vincristine	Burkitt's lymphoma
Vindesine	Chemotherapy
Yohimbine	Aphrodisiac, urinary incontinence

---

## 1.4 Classification of Alkaloids

Alkaloids have been classified by several methods in the past, and the most common ones include structural, taxonomical, and biosynthetic classifications.<sup>28</sup> The most widely accepted way to classify alkaloids is by their chemical structure, whereby alkaloids are categorised based on their common heterocyclic skeleton, e.g., indole, pyridine and tropane (**Figure 1.0**). On the other hand, the taxonomical classification is based on the restricted biogenetic occurrence of alkaloids across different taxa. For instance, distinctive classes of alkaloids can only be found in specific families of plants, such as the occurrence of atropine-type tropane alkaloids in the nightshade family (Solanaceae), and morphine-type isoquinoline alkaloids in the poppy family (Papaveraceae). To complement the above classification methods, alkaloids can be further classified according to their amino acid precursor such as ornithine, tyrosine and tryptophan (**Figure 1.0**), whereby a specific carbon-nitrogen skeleton of the amino acid is passed on to the alkaloid structure during alkaloid biosynthesis.<sup>29</sup>

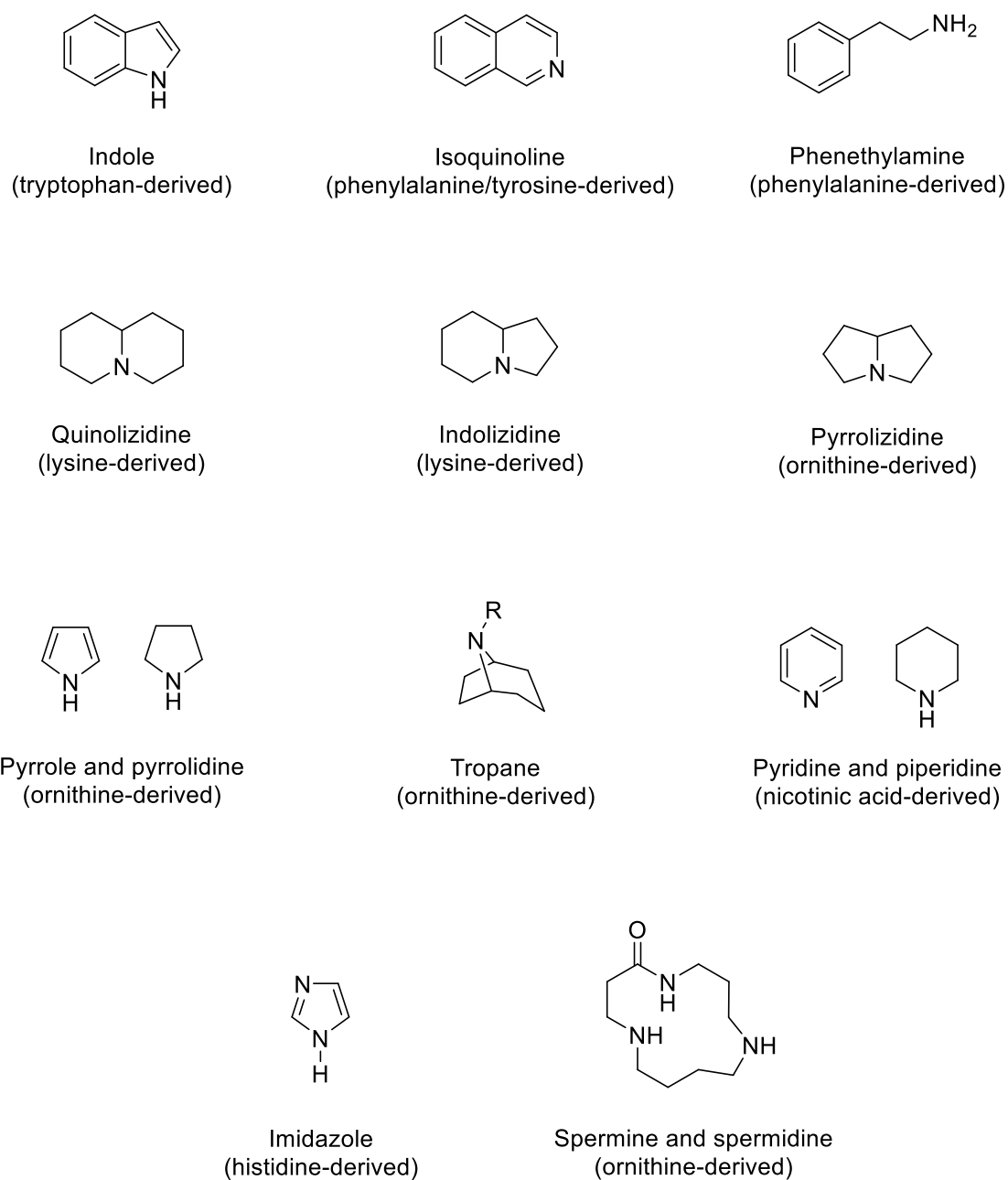


**Figure 1.0** Selected examples of alkaloid heterocyclic structures (amino acid precursor stated in parentheses).

## 1.5 The Genus *Ficus*

### 1.5.1 General

Moraceae, which is commonly known as the mulberry or fig family, is a diverse plant family that includes over 1000 species. Characteristic features of the Moraceae family include milky latex, parenchymatous tissues, unisexual flowers, anatropous ovules, and aggregated achenes.<sup>30</sup> Moraceae is further divided into five main tribes: Artocarpeae, Castillieae, Dorstenieae, Ficeae, and Morae.

The genus *Ficus*, classified under the Ficeae tribe of Moraceae, is one of the most ubiquitously diverse genera. Over 750 *Ficus* species exist as trees, shrubs, climbers, and hemiepiphytic stranglers in a wide variety of ecological niches throughout the tropics.<sup>31,32</sup> Approximately 100 species of *Ficus* are endemic to the rainforests of Malaysia. Various phytochemicals have previously been reported from several *Ficus* species. *Ficus racemosa* for example, was found to contain triterpenes, glycosides, flavonoids, phenolic compounds, and tannins.<sup>33</sup> *Ficus religiosa* was recorded to elaborate phenolic compounds, flavonoids, saponins, steroids, wax, terpenoids, cardiac glycosides, and tannins.<sup>34</sup> The leaf and stem-bark extracts of *F. capensis* contained alkaloids, flavonoids, anthraquinones, tannins, terpenes, resins, sterols, and saponins.<sup>35</sup>

Various *Ficus* species are valued by Ayurvedic medicine. It was reported that *F. benghalensis* is used to treat diarrhoea, dysentery, pain, bruises, and diabetes in India,<sup>36,37</sup> while the fruits, roots, and leaves of *F. carica* are traditionally used to treat gastrointestinal, respiratory, and cardiovascular disorders, as well as exhibiting anti-inflammatory and antispasmodic activities.<sup>38</sup> *Ficus racemosa* is used to treat aphthae, menorrhagia, diarrhoea,

hemorrhoids, diabetes, and dysentery.<sup>37</sup> *F. carica* is used traditionally to treat gastric disorders, inflammation, liver and spleen disorders, and also cancer.<sup>39</sup>

Recent phytochemical investigation further demonstrated that *Ficus religiosa* has a wide spectrum of *in vivo* and *in vitro* bioactivities, and it appeared to be a promising herbal remedy for asthma, diabetes, epilepsy, and sexual disorders.<sup>40</sup> *Ficus racemosa* is used to treat apthae, menorrhagia, diarrhoea, hemorrhoids, diabetes, and dysentery.<sup>37</sup>

### 1.5.2 Alkaloids from the genus *Ficus*

Out of over 750 species of *Ficus*, only eight species have been studied for their alkaloidal content, namely, *F. hispida*,<sup>41–44</sup> *F. fistulosa*,<sup>45–47</sup> *F. fistulosa* var. *tengerensis*,<sup>48</sup> *F. septica*,<sup>49–53</sup> *F. nota*,<sup>54</sup> *F. hirta*,<sup>55</sup> *F. pachyrhachis*,<sup>56</sup> and *F. pantoniana*.<sup>57</sup> These species predominantly produce phenanthroindolizidine-type alkaloids, e.g., *O*-methyltylophorinidine (**35**), dehydroantofine (**60**), dehydrotylophorine (**61**), and tylophoridicine D (**63**). The *seco*-phenanthroindolizidines are the second most common class of *Ficus* alkaloids, e.g., hispidine (**33**), ficushispidine (**40**), fistulopsine B (**46**), and *seco*dehydroantofine (**62**). The phenanthroindolizidine alkaloids exhibit prominent cytotoxic activity against a wide panel of cancer cells in addition to other bioactivities.<sup>58,59</sup> **Table 1.1** summarises the bioactivity of some of the alkaloids isolated from previously studied *Ficus* species.

**Table 1.1** Biologically active *Ficus* Alkaloids

<b>Compound</b>	<b>Reported bioactivity</b>	<b>Reference</b>
Hispidacine ( <b>32</b> )	vasorelaxant activity in rat isolated aorta	41
Hispiloscine ( <b>34</b> )	antiproliferative effect against MDA- MB-231 and MCF-7, lung carcinoma A549, colon carcinoma HCT-116 and human lung fibroblast MRC-5 cell lines	41
<i>O</i> -Methyltylophorinidine ( <b>35</b> )	antiproliferative effect against human colon (Col2), Lung (Lu1) nasopharyngeal (KB) and prostate (LNCaP) cell line	43
(-)-13 $\alpha$ -Antofine ( <b>43</b> )	antifungal activity against <i>Aspergillus fumigatus</i> and <i>Candida albicans</i>	45
Fistulopsines A ( <b>46</b> ) and B ( <b>49</b> )	antiproliferative effect against HCT 116 and MCF7 cell lines	46
Tengechlorenine ( <b>58</b> )	antiproliferative effect against MDA-MB-468, MDA-MB-231, and MCF7	48
(+)-Tengerensine ( <b>59</b> )	antiproliferative effect against MDA-MB-468 cells	
Dehydrotylophorine ( <b>61</b> ), secodehydroantofine ( <b>62</b> ) and tylophoridicine D ( <b>63</b> )	antimalarial activity against the 3D7 strain of <i>P. falciparum</i>	49
10 <i>S</i> ,13 <i>aR</i> -Tylocrebrine <i>N</i> -oxide ( <b>87</b> ) and 10 <i>S</i> ,13 <i>aR</i> -isotylocrebrine <i>N</i> -oxide ( <b>84</b> )	antiproliferative effect against HONE-1 and NUGC cell lines	51
Ficusnotins A ( <b>102</b> ) and B ( <b>103</b> )	antibacterial activity against <i>Bacillus subtilis</i>	54

Even though the *Ficus* genus contains a large number of species, alkaloidal research on *Ficus* is still very limited. Given that alkaloids represent one of the most important classes of secondary metabolites for drug discovery,<sup>60</sup> there is a need to discover novel and bioactive alkaloids from other unexplored *Ficus* species.

The occurrence of alkaloids in *Ficus* is summarized in **Table 1.2** (excluding the alkaloids isolated and published from the present work). The structures of these alkaloids are shown in **Figure 1.1**.

**Table 1.2** Occurrence of alkaloids in *Ficus*

<b>Plant</b>	<b>Plant part</b>	<b>Alkaloids</b>	<b>References</b>
<i>F. hispida</i> Linn.	Stem-bark	(+)-Deoxypergularinine ( <b>31</b> ) Hispidacine ( <b>32</b> )	41
	Leaves	Hispidine ( <b>33</b> ) Hispiloscine ( <b>34</b> ) 3,6,7-Trimethoxy-14-hydroxyphenanthroindolizidine ( <i>O</i> -Methyltylophorinidine) ( <b>35</b> ) 3,6,7-Trimethoxyphenanthroindolizidine ((-)-Deoxypergularinine) ( <b>36</b> )	41,42
	Leaves-twig	<i>O</i> -Methyltylophorinidine ( <b>35</b> )	38
	Twigs	Ficushispimine A ( <b>37</b> ) Ficushispimine B ( <b>38</b> ) Ficushispimine C ( <b>39</b> ) Ficushispidine ( <b>40</b> ) 1-(4-Hydroxyphenyl)-2-(2-pyrrolidinyl)ethanone ( <b>41</b> )	39
<i>F. fistulosa</i> Reinw. ex Blume	Stem-bark	Fistulosine ( <b>42</b> ) (-)-13 $\alpha$ -Antofine (13 $\alpha$ <i>R</i> -antofine) ( <b>43</b> ) (-)-14 $\beta$ -Hydroxyantofine ( <b>44</b> ) (-)-13 $\alpha$ - <i>Secoantofine</i> ((-)- <i>Secoantofine</i> ) ( <b>45</b> )	45
	Bark	Fistulopsine A ( <b>46</b> ) (+)-Septicine ( <b>47</b> ) (+)-Tylocrebrine ( <b>48</b> )	46
	Leaves	Fistulopsine B ( <b>49</b> ) (+)-Tylophorine ( <b>50</b> ) (-)-3,6-Didemethylisotylocrebrine ( <b>51</b> ) Aurantiamide acetate ( <b>52</b> )	42
	Leaves and stem-bark	Indole-3-carboxaldehyde ( <b>53</b> ) Palmanine ( <b>54</b> ) 3,4-Dihydro-6,7-dimethoxyisocarbostyryl ( <b>55</b> )	45

<i>F. fistulosa</i> var. <i>tengerensis</i> (Miq.) Kuntze	Leaves	(+)-Antofine ( <b>56</b> ) (±)-Fistulosine ( <b>57</b> ) (-)- <i>Secoantofine</i> ( <b>45</b> ) (+)-Tengechlorenine ( <b>58</b> ) (+)-Tengerensine ( <b>59</b> )	48
<i>F. septica</i> Burm f.	Twigs	Dehydroantofine ( <b>60</b> ) Dehydrotylophorine ( <b>61</b> ) <i>Secodehydroantofine</i> ( <b>62</b> ) Tylophoridicine D ( <b>63</b> )	49
	Leaves	Antofine ( <b>64</b> ) (+)-Antofine ( <b>56</b> ) Dehydrotylophorine ( <b>61</b> ) Ficuseptamine A ( <b>65</b> ) Ficuseptamine B ( <b>66</b> ) Ficuseptamine C ( <b>67</b> ) Ficuseptine A ( <b>68</b> ) (+)-Isotylocrebrine ( <b>69</b> ) Norruspoline ( <b>70</b> ) Phyllosterone ( <b>71</b> ) Septicine ( <b>72</b> ) (-)- <i>Secoantofine</i> ( <b>45</b> ) Tylocrebrine ( <b>73</b> ) (-)-Tylophorine (13a <i>R</i> -Tylophorine) ( <b>74</b> ) (+)-Tylocrebrine ( <b>48</b> ) (+)-Tylophorine ( <b>50</b> ) (+)-Tylophorine <i>N</i> -oxide ( <b>75</b> ) 14α-Hydroxyisocrebrine <i>N</i> -oxide ( <b>76</b> ) 14α-Hydroxyisotylocrebrine <i>N</i> -oxide ( <b>77</b> ) 14-Hydroxy-2,3,4,6,7- pentamethoxyphenanthroindolizidine ( <b>78</b> ) 14-Hydroxy-3,4,6,7- tetramethoxyphenanthroindolizidine ( <b>79</b> )	45,46
	Stem	Dehydrotylophorine ( <b>61</b> ) Ficuseptine B ( <b>80</b> ) Ficuseptine C ( <b>81</b> ) Ficuseptine D ( <b>82</b> ) (+)-Isotylocrebrine ( <b>69</b> ) Tylocrebrine ( <b>73</b> ) (-)-Tylophorine ( <b>74</b> ) 10 <i>S</i> ,13a <i>R</i> -Antofine <i>N</i> -oxide ( <b>83</b> ) 10 <i>S</i> ,13a <i>R</i> -Isotylocrebrine <i>N</i> -oxide ( <b>84</b> ) 10 <i>S</i> ,13a <i>S</i> -Isotylocrebrine <i>N</i> -oxide ( <b>85</b> ) 10 <i>R</i> ,13a <i>R</i> -Tylocrebrine <i>N</i> -oxide ( <b>86</b> ) 10 <i>S</i> ,13a <i>R</i> -Tylocrebrine <i>N</i> -oxide ( <b>87</b> )	63

		10 <i>R</i> ,13 <i>aR</i> -Tylophorine <i>N</i> -oxide ( <b>88</b> ) 10 <i>S</i> ,13 <i>aR</i> -Tylophorine <i>N</i> -oxide ( <b>89</b> )	
	Roots	Dehydrotylophorine ( <b>61</b> ) Ficuseptine A ( <b>68</b> ) Ficuseptine B ( <b>80</b> ) Ficuseptine E ( <b>90</b> ) Ficuseptine F ( <b>91</b> ) Ficuseptine G ( <b>92</b> ) Ficuseptine H ( <b>93</b> ) Ficuseptine I ( <b>94</b> ) Ficuseptine J ( <b>95</b> ) Ficuseptine K ( <b>96</b> ) Ficuseptine L ( <b>97</b> ) Ficuseptine M ( <b>98</b> ) Ficuseptine N ( <b>99</b> ) 13 <i>aR</i> -Antofine ( <b>43</b> ) 13 <i>aR</i> -Isotylocrebrine ( <b>100</b> ) 13 <i>aR</i> -Tylophorine ( <b>74</b> ) 13 <i>aR</i> -Tylocrebrine ( <b>101</b> ) 10 <i>S</i> ,13 <i>aR</i> -Isotylocrebrine <i>N</i> -oxide ( <b>84</b> ) 10 <i>S</i> ,13 <i>aR</i> -Tylocrebrine <i>N</i> -oxide ( <b>87</b> ) 10 <i>R</i> ,13 <i>aR</i> -Tylophorine <i>N</i> -oxide ( <b>88</b> )	48
<i>F. nota</i> (Blanco) Merr.	Leaves	Ficusnotin A ( <b>102</b> ) Ficusnotin B ( <b>103</b> ) Ficusnotin F ( <b>104</b> )	54
<i>F. hirta</i> Vahl.	Fruits	Methyl 1-methyl-1,2,3,4-tetrahydro- $\beta$ - carboline-3-carboxylate ( <b>105</b> ) 1-Methyl-1,2,3,4-tetrahydro- $\beta$ -carboline-3- carboxylic acid ( <b>106</b> )	55
<i>F. pachyrhachis</i> K.Schum. & Lauterb.	Leaves	(+)-Nor-reticuline ( <b>107</b> ) (-)-Reticuline ( <b>108</b> )	56
<i>F. pantoniana</i> King	(Not specified)	Ficine ( <b>109</b> ) Isoficine ( <b>110</b> )	57

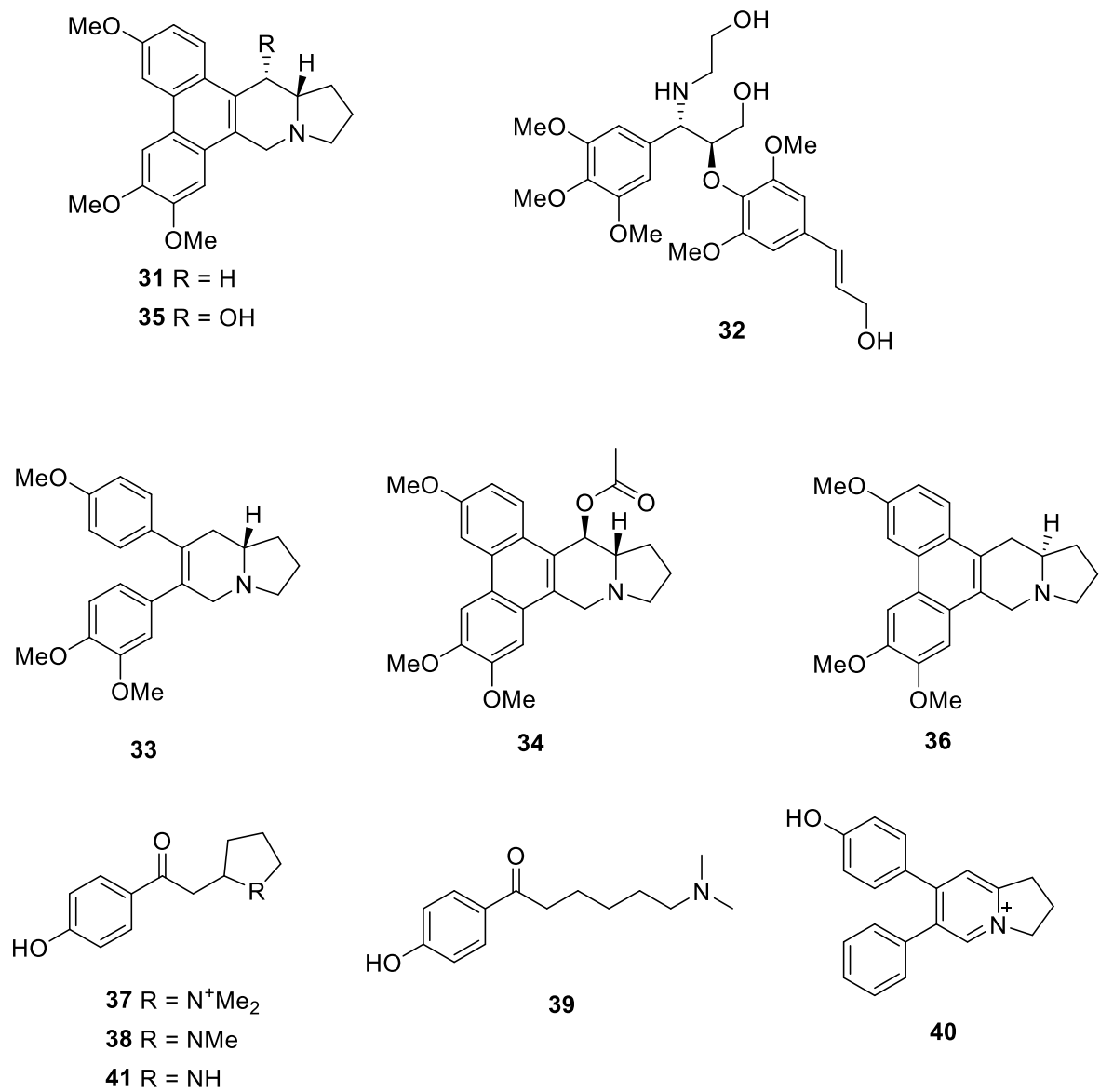


**Figure 1.1** Alkaloids from *Ficus* species

continued next page...

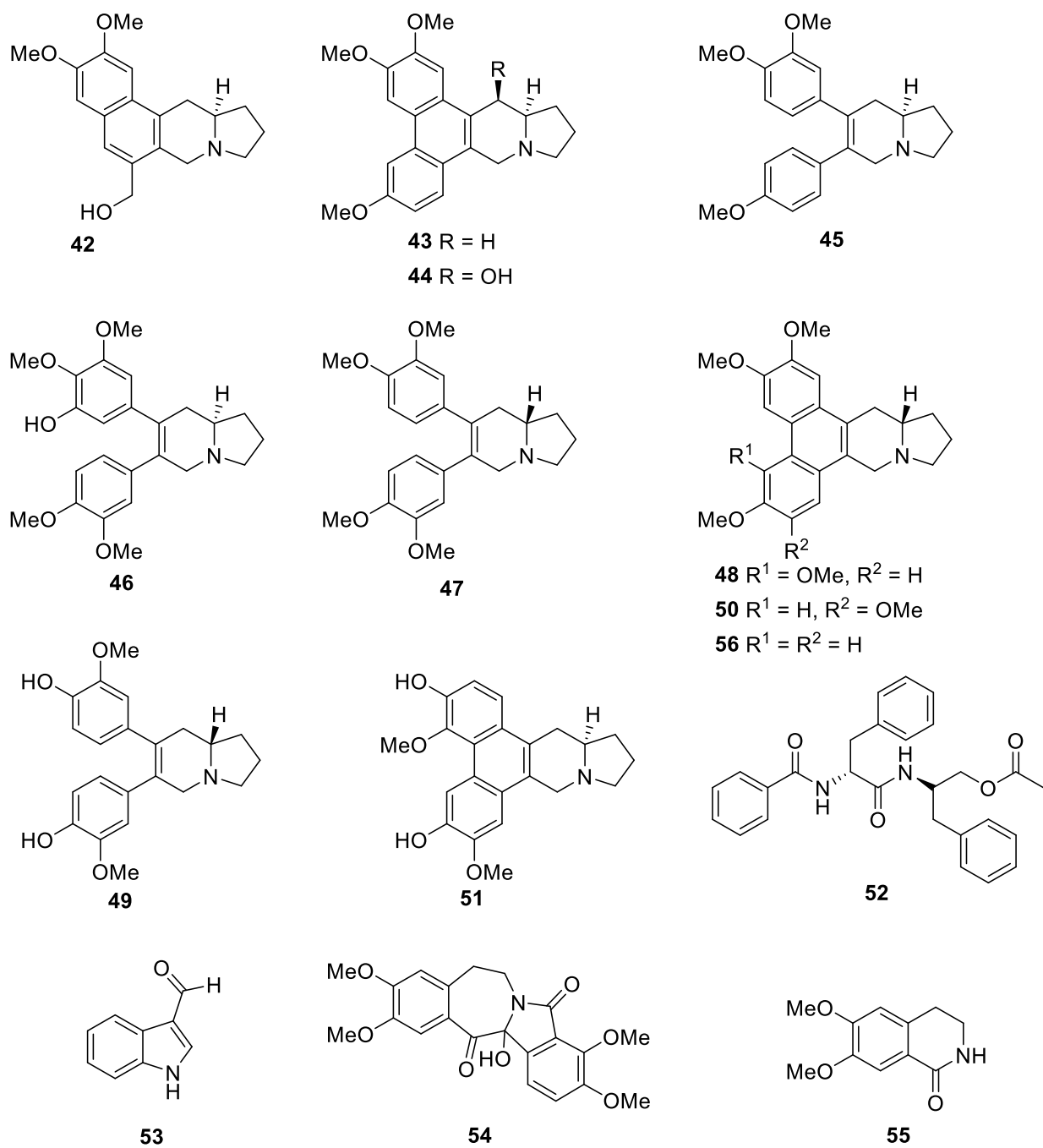


**Figure 1.1** Alkaloids from *Ficus* species

continued next page...

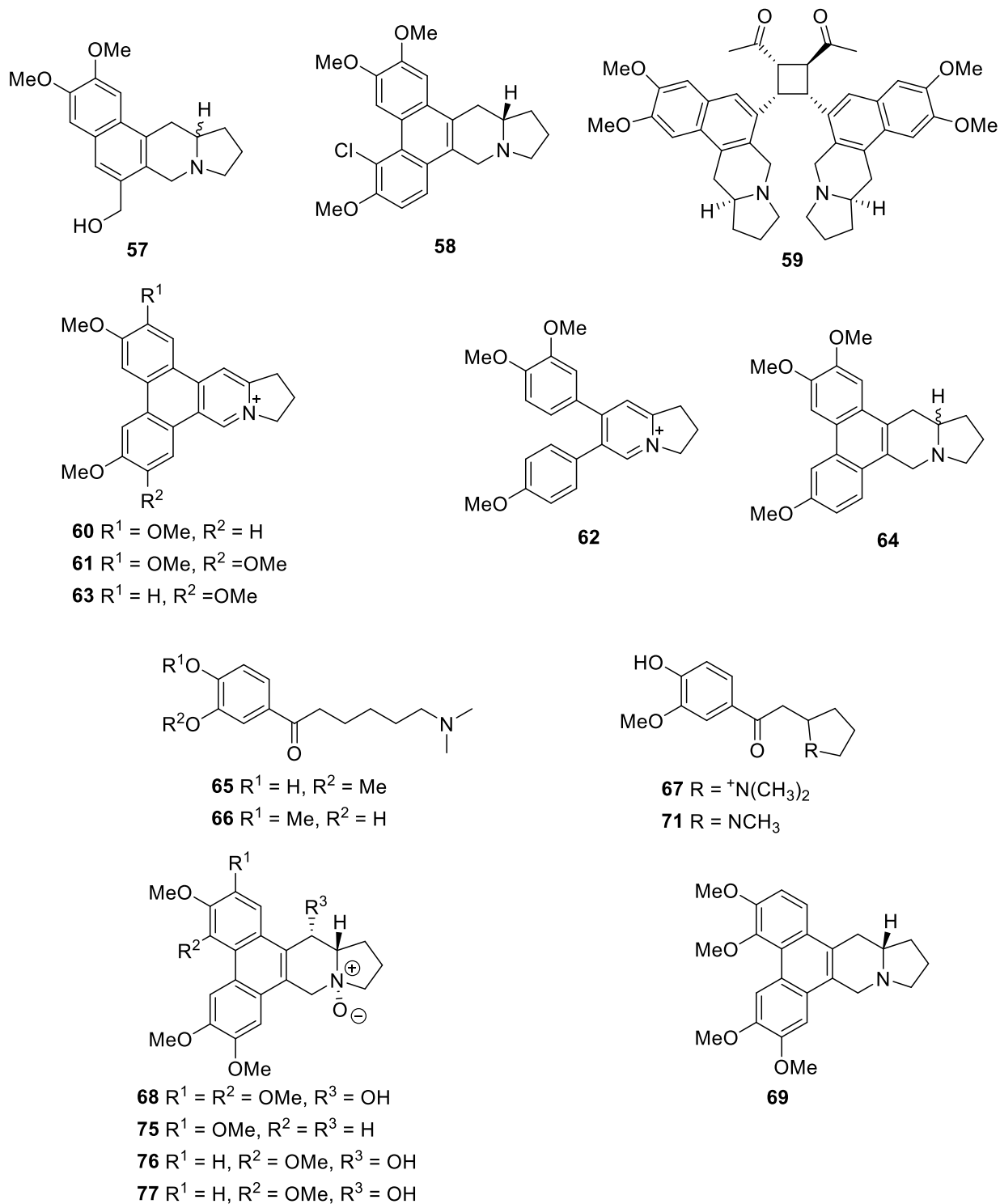


**Figure 1.1** Alkaloids from *Ficus* species

continued next page...

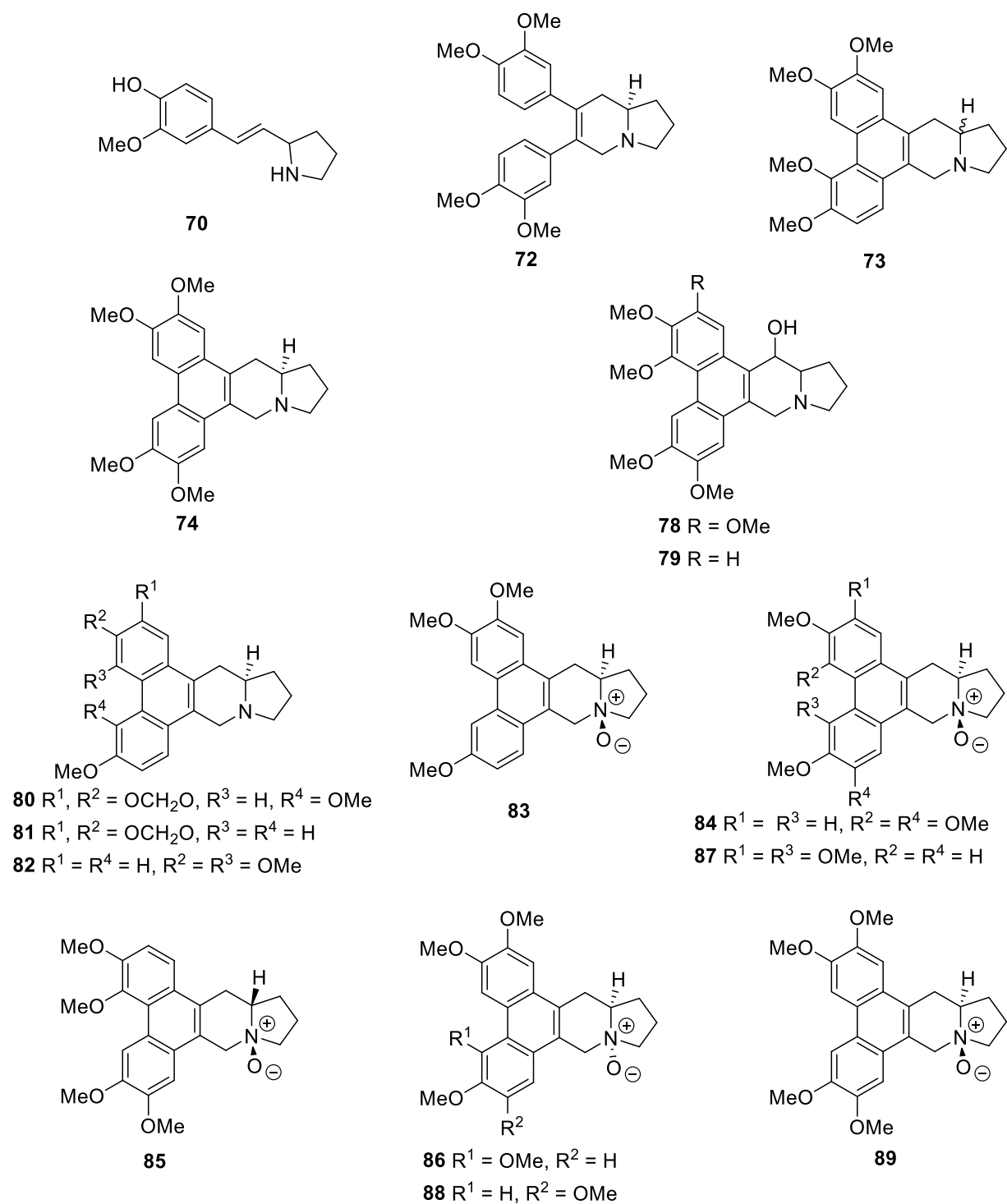


**Figure 1.1** Alkaloids from *Ficus* species

continued next page...

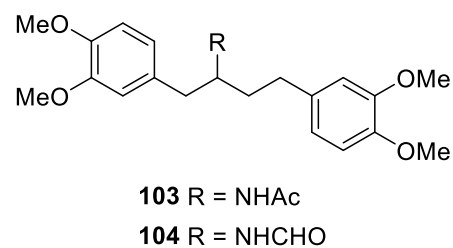
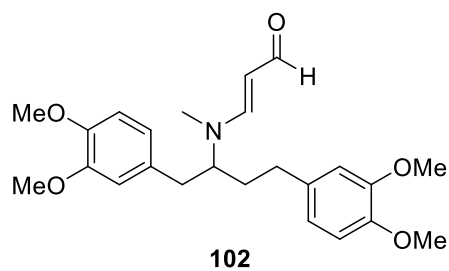
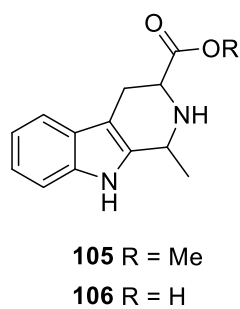
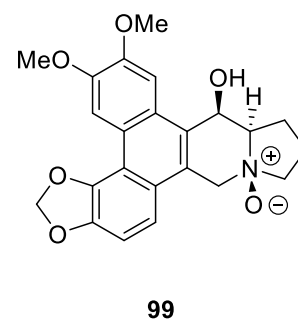
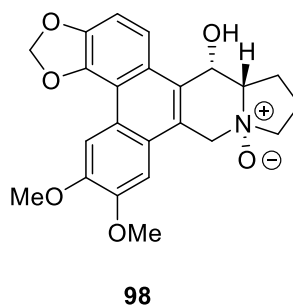
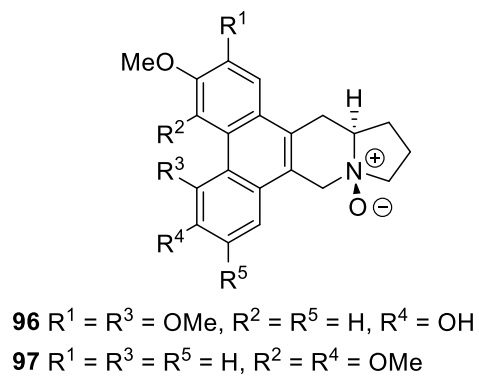
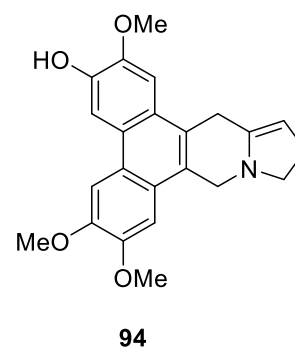
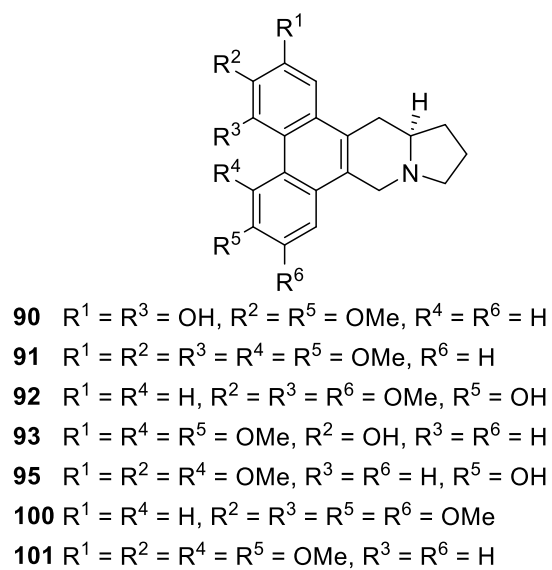


**Figure 1.1** Alkaloids from *Ficus* species

continued next page...

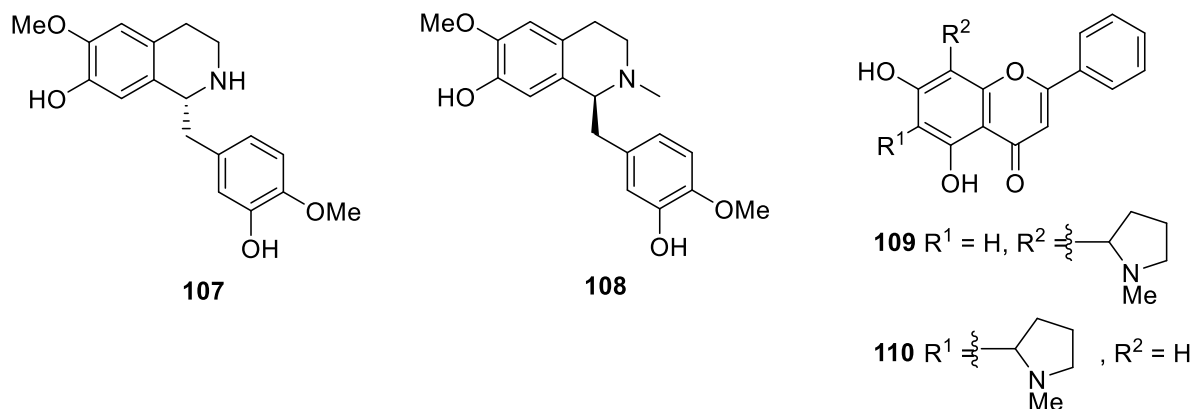


**Figure 1.1** Alkaloids from *Ficus* species

### 1.5.3 *Ficus schwarzii* Koord.

### 1.5.3 *Ficus schwarzii* Koord.

*Ficus schwarzii* Koord. is one of the 101 different *Ficus* species that can be found in Malaysia. It is locally known as ara, engkururoh, kahat ucang, kara, peranak (Dusun), engkunoh (Iban), or pipin (Bidayuh) in Borneo.<sup>64</sup> *F. schwarzii* is a tree that can reach a height of up to 20 m, and it is distributed around southern Myanmar, Thailand, and Malesia (Sumatra, Malay Peninsula and Borneo) (**Figure 1.2**). This species prefers habitats along forest streams and at altitudes of up to 1200 m.<sup>65,66</sup>

Our preliminary small-scale phytochemical investigation of *F. schwarzii* revealed the presence of alkaloids in the leaves, while only negligible amount of alkaloids were detected in the bark and stems. Since *F. schwarzii* has never been investigated phytochemically and pharmacologically, this represents a welcoming opportunity for the discovery of novel alkaloids with potentially beneficial biological activity. Furthermore, the crude alkaloid of *F. schwarzii* reported to inhibit the proliferation of HT-29 cells.<sup>67</sup> Therefore, the alkaloidal

composition of the leaves of *F. schwarzii* was investigated in the present study, along with exploration of the biological activity of the pure alkaloids obtained.



**Figure 1.2** Adult specimen of *Ficus schwarzii* Koord.: A - foliage; B - figs on tree trunk

## 1.6 The Genus *Alstonia*

### 1.6.1 General

*Alstonia* is a genus from the tribe Rauvolfiae, subfamily Plumerioideae of the dogbane family Apocynaceae. *Alstonia* species are widely distributed across tropical Africa, Central America, subtropical and tropical East and Southeast Asia, and Oceania. Plants of the genus *Alstonia* are mostly trees with only a few species being shrubs. The trees can reach up to 60 m and sometimes have pagoda-like branching. Typical of the Apocynaceae family, *Alstonia* species have opposite leaves without stipules, and barks that exude milky latex. The leaves are usually arranged in whorls, and the flowers are small and narrow, with mature buds no longer than 40 mm long. The fruits of *Alstonia* are usually a pair of follicles containing hairy seeds that are dispersed by wind. *Alstonia* species can be found in a wide range of habitats, including secondary and primary forests, as well as swamps and arid regions, at altitudes ranging from the sea level to 2870 m.<sup>68,69</sup>

There are approximately 43 *Alstonia* species worldwide,<sup>68,69</sup> many of which have been used traditionally to treat a variety of ailments. For example, *A. macrophylla* is employed in ethnopharmacy as a general tonic and antipyretic in Thailand.<sup>70</sup> *A. scholaris* has been used in both codified and non-codified drug systems in India for the treatment of malaria, jaundice, gastrointestinal problems, cancer, and a variety of other ailments.<sup>70</sup> *A. boonei*, a species endemic to sub-Saharan Africa, has been found to have powerful analgesic and antipyretic properties in human.<sup>71</sup> Of the 43 *Alstonia* species, 12 are native to Malaysia, namely:<sup>68</sup>

- *Alstonia actinophylla* (A.Cunn.) K.Schum.
- *Alstonia angustifolia* Wall. ex A.DC.

- *Alstonia angustiloba* Miq.
- *Alstonia iwahigensis* Elmer
- *Alstonia macrophylla* Wall. ex G.Don
- *Alstonia neriifolia* D.Don
- *Alstonia parvifolia* Merr.
- *Alstonia penangiana* Sidiyasa
- *Alstonia pneumatophora* Baker ex Den Berger
- *Alstonia rostrata* C.E.C. Fisch.
- *Alstonia scholaris* (L.) R. Br.
- *Alstonia sebusi* (Van Heurck & Müll.Arg.) Monach.

Among the Malaysian *Alstonia*, only eight species were previously investigated, namely, *A. actinophylla*, *A. angustifolia*, *A. angustiloba*, *A. macrophylla*, *A. pneumatophora*, *A. rostrata*, *Alstonia penangiana*, and *A. scholaris*.

## 1.6.2 Alkaloids of the Apocynaceae Family

### 1.6.2.1 Indole alkaloids

The plant family Apocynaceae, which incorporates the genus *Alstonia* predominantly elaborates indole alkaloids. Indole alkaloids are easily distinguished by an indole nucleus or its derivative. Indole alkaloids represent one of the largest groups of alkaloids. Oxidation, reduction, and substitution can lead to multiple variation of the indole chromophore. **Figure 1.3** outlines the actual structure of an indole chromophore, and those containing its derivatives, namely, indoline (dihydroindole), indolenine, hydroxyindolenine,  $\alpha$ -methylideneindoline, pseudoindoxyl, and oxindole. Natural tricyclic compounds such as carbazole,  $\beta$ -carboline, and  $\gamma$ -carboline (including their derivatives) are also regarded as indole alkaloids.<sup>72</sup>

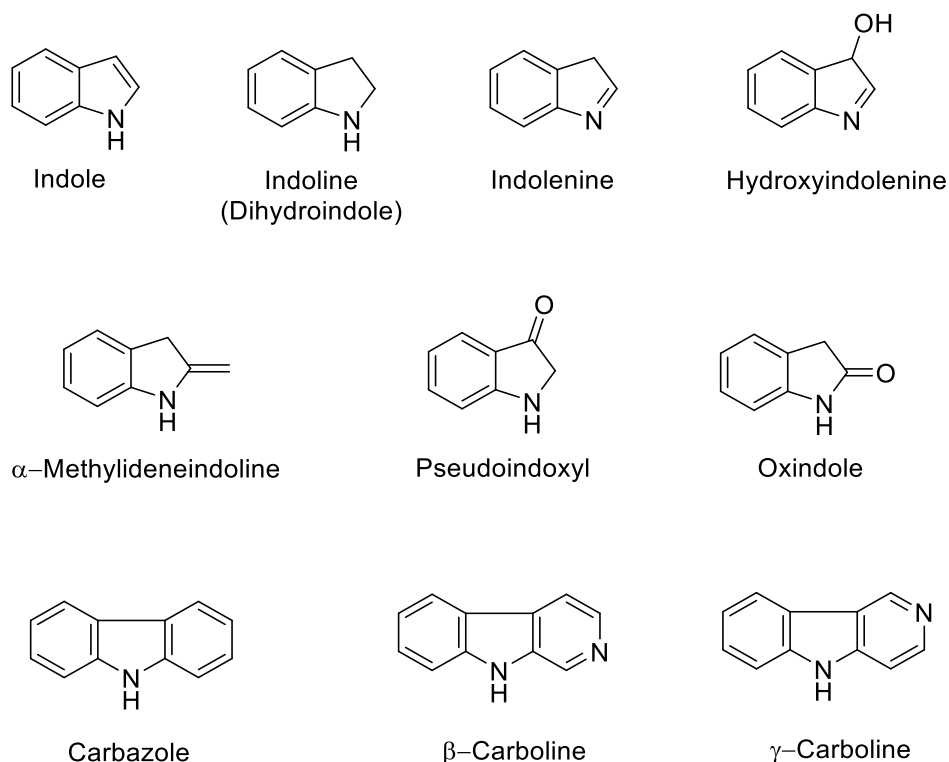
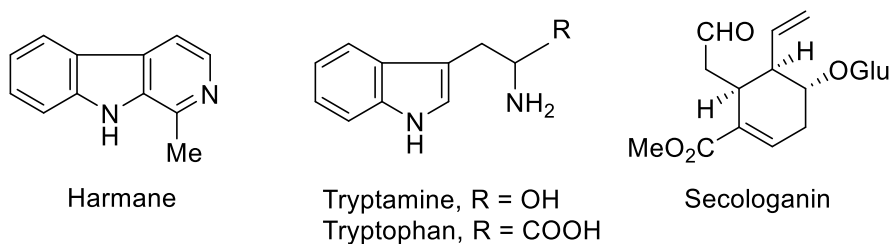


**Figure 1.3** Indole and related chromophores

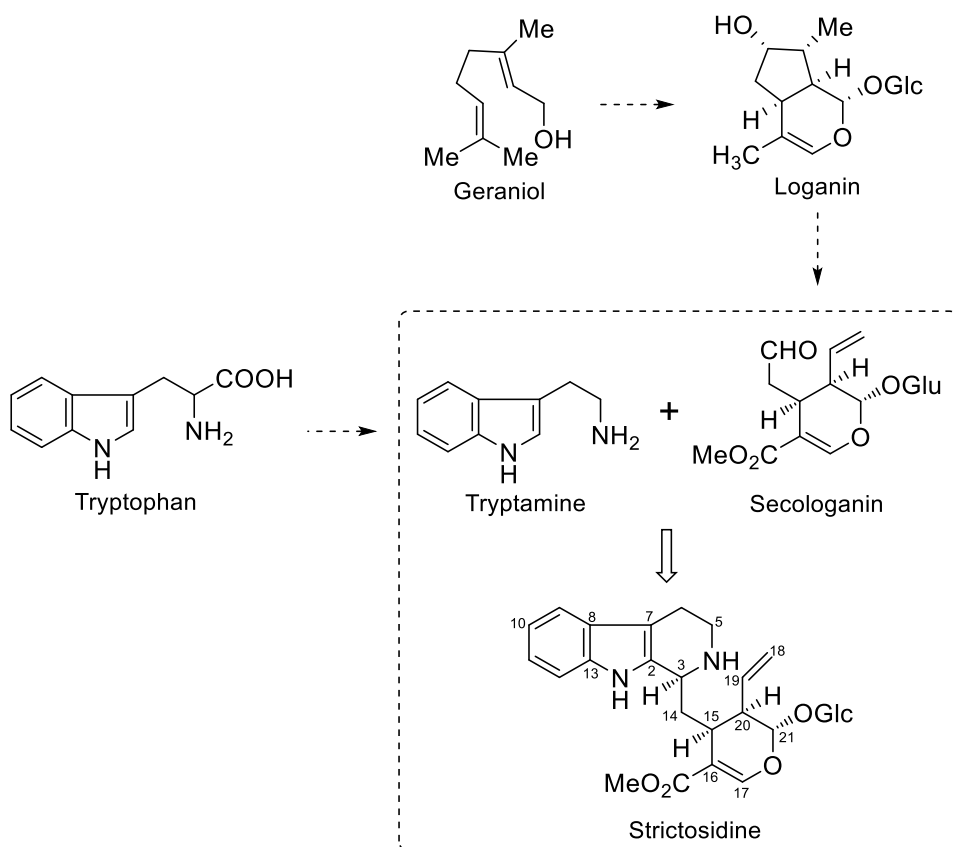
### 1.6.2.2 Classification and biogenesis of monoterpene indole alkaloids

Indole alkaloids are further divided into two main categories, i.e., simple indole alkaloids and monoterpene indole alkaloids. Generally, the simple indole alkaloids lack structural uniformity, with the indole nucleus or a direct derivative of it serving as the only common feature (e.g., harmaline).

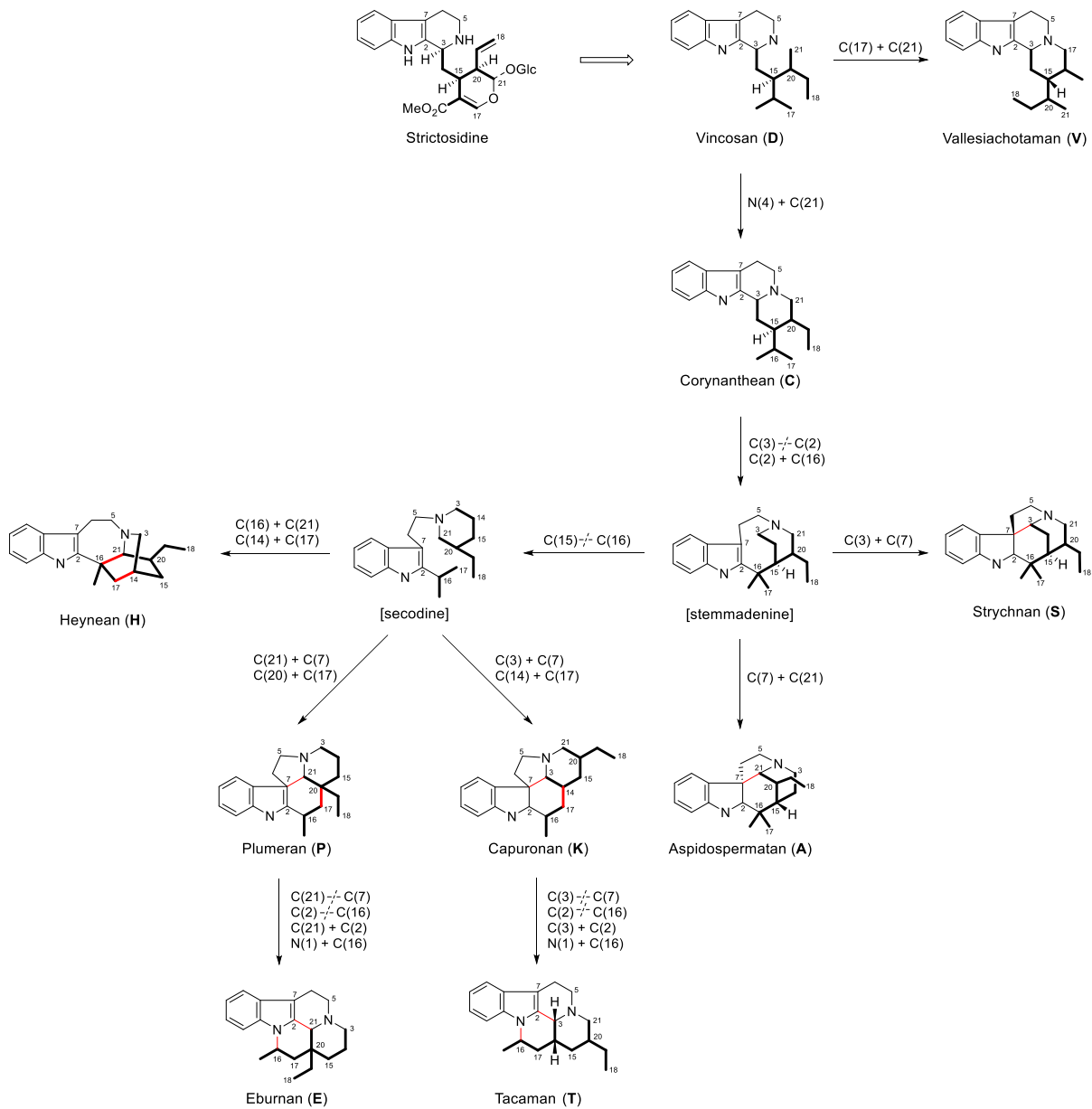


The monoterpene indole alkaloids on the other hand represent the largest class of indole alkaloids and their biogenesis was extensively studied. Through numerous experimentation, the biogenesis of the monoterpene indole alkaloids was traced back to strictosidine, which was also established to be derived from the condensation of a tryptamine/tryptophan moiety and a monoterpene moiety (originated from *secologanin*) via the Pictet-Spengler reaction. In other words, strictosidine is the common biogenetic precursor for all other monoterpene indole alkaloids (**Scheme 1.0**).<sup>14,73</sup> As a result, the biogenetic numbering system based on the structure of strictosidine was mostly consistently applied to all the monoterpene indole alkaloids reported in the literature. Inspection of the vast number of monoterpene indole alkaloids revealed that modifications to the indole (tryptamine) moiety are generally slight, with the major changes occurring in the monoterpene fragment instead. Extensive rearrangement of the terpenoid moiety eventually gave rise to many monoterpene indole alkaloids with distinctive structures, which can be broadly categorised into ten main skeletal types, i.e., vincosane (**D**), corynantheane (**C**), vallesiachotamine (**V**), strychnane (**S**), aspidospermatane (**A**), plumerane (**P**), capuronane (**K**), heyneane (**H**), eburnane (**E**), and tacamane

(T) (Scheme 1.1).<sup>74</sup> Scheme 1.1 presents a general molecular evolution from strictosidine to the 10 skeletal types, with the differences among them being in the rearranged terpenoid fragments, as indicated by a bolded fragment in each skeletal structure. Vincosan (D), corynanthean (C), vallesiachotaman (V), strychnan (S), and aspidospermatan (A) possess a non-rearranged secologanin skeletal system, while plumeran (P), capuronan (K), heynean (H), eburnan (E), and tacaman (T) possess a re-arranged terpenoid skeletons as a result of C–C bond cleavage and C–C bond formation via the intermediacy of secodine (Scheme 1.1).



**Scheme 1.0:** Formation of strictosidine



**Scheme 1.1:** Biogenetic inter-relationship between the ten main skeletal types of the monoterpene indole alkaloids

## 1.7 *Alstonia scholaris* (L.) R. Br.

### 1.7.1 General

*Alstonia scholaris* (syn. *Echites scholaris*)<sup>75</sup> is commonly known as ‘pulai’ or the devil tree in Malaysia.<sup>68</sup> The genus name *Alstonia* was coined to commemorate Professor Charles Alston, a Scottish botanist,<sup>76</sup> while the species name *scholaris* was inspired from the usage of the plant’s wood to construct school blackboards in Myanmar. *A. scholaris* occurs in a variety of habitats, from coastal lowlands to elevations of 1230 m. It is found in India, Sri Lanka, and from Southern China and Indochina through Malesia to northern Australia and the Pacific Islands.<sup>69</sup> The species is a medium-sized to large tree that can grow to be 50 – 60 m tall. The leaves form whorls of 4 to 8 and have an elliptic to obovate shape (**Figure 1.4**). The bark can be smooth, scaly, or slightly fissured, and produces a large amount of white latex when peeled off. The flowers are fragrant and come in white, yellow, or cream colour.<sup>68</sup>

Different parts of the plant are used in traditional medicine to treat a variety of acute and chronic diseases. The leaves are used to treat beriberi and malaria in Malaysia,<sup>71</sup> while in India, the bark is used as a tonic, which is indicated for fever, skin diseases, chronic diarrhoea and advanced stages of dysentery. It is also valued as a ‘heat-lowering’ drug, useful to treat gout and rheumatism, while promoting recovery from exhausting fever.<sup>77</sup> In China, the leaf extract of *A. scholaris* was available over the counter in pharmacies and hospitals as an expectorant and antipyretic agent.<sup>78</sup> On the island of Luzon, the bark is valued by natives as the most potent tonic and heat-reducing medicine, which has long been used as a decoction to treat severe, intermittent, and remittance fevers.<sup>77</sup>

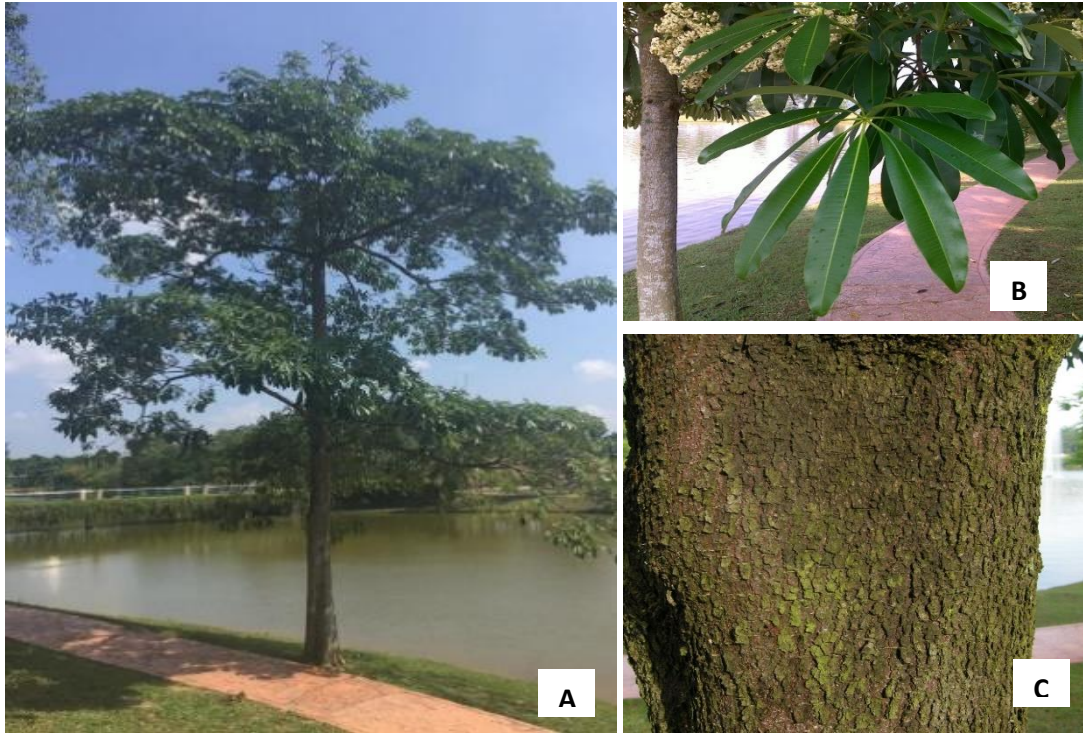


**Figure 1.4** Adult specimen of *Alstonia scholaris*: A - tree; B – leaves and flowers; C - bark.

### 1.7.2 Alkaloids from *Alstonia scholaris*

*A. scholaris* is well-known to be a rich source of alkaloids, particularly monoterpenoid indole alkaloids belonging to the corynanthean and strychnan type of alkaloids. Interestingly, the alkaloidal composition of *A. scholaris* differs tremendously with locality.<sup>86</sup> For example, Hua Zhou et al., (2015) isolated three akuammiline-type indole alkaloids from *A. scholaris* leaves collected from Xishuangbanna, Yunnan Province, China, whereas in 2010, Xiang et al. isolated two quinoline-type alkaloids from *A. scholaris* leaves collected from Simao, Yunnan Province, China. The observed variation of alkaloid production in *A. scholaris* supports the findings that secondary metabolites are significantly influenced by the ecological environment.<sup>87</sup> **Table 1.3** summarises the various alkaloids that have been isolated from *Alstonia scholaris* according to plant part and locality (excluding the alkaloids isolated and published from the present work). The structures of these alkaloids are shown in **Figure 1.5**.

**Table 1.3:** Occurrence of alkaloids in *Alstonia scholaris*

Locality	Plant part	Alkaloid	Reference
Thailand	Leaves	Alschomine ( <b>111</b> )	88
		Isoalschomine ( <b>112</b> )	88
		Nareline ( <b>113</b> )	88
		Picrinine ( <b>114</b> )	88
		Scholaricine ( <b>115</b> )	88
		Tubotaiwine ( <b>116</b> )	88
		Vallesamine ( <b>117</b> )	88
	Stem-bark	Echitamine ( <b>118</b> )	89
		Hydroxy-19,20-dihydroakuammicine ( <b>119</b> )	89
		<i>N</i> (4)-Demethylechitamine ( <b>120</b> )	89
		Picrinine ( <b>114</b> )	89
		Tubotaiwine ( <b>116</b> )	89
	Root-bark	Akuammicine ( <b>121</b> )	89, 90
		Akuammicine <i>N</i> (4)-methiodide ( <b>122</b> )	90
		Akuammicine <i>N</i> (4)-oxide ( <b>123</b> )	89, 90
		Echitamidine ( <b>124</b> )	90
		Echitamine ( <b>118</b> )	89, 90
		Hydroxy-19,20-dihydroakuammicine ( <b>119</b> )	89, 90

		<i>N</i> (4)-Demethylechitamine ( <b>120</b> )	89, 90	
		Tubotaiwine ( <b>116</b> )	89, 90	
		Ψ-Akuammigine ( <b>125</b> )	89	
<hr/>				
Peninsular Malaysia	Leaves	<i>5-Epi</i> -nareline ethyl ether ( <b>126</b> )	91	
		Nareline ethyl ether ( <b>127</b> )	91	
		Nareline methyl ether ( <b>128</b> )	91	
		Picrinine ( <b>114</b> )	91	
		Scholaricine ( <b>115</b> )	91	
		Scholarine <i>N</i> -oxide ( <b>129</b> )	91	
<hr/>				
India	Leaves	Akuammidine ( <b>130</b> )	92	
		Echitamidine ( <b>124</b> )	93	
		Echitamine ( <b>118</b> )	93	
		Nareline ( <b>113</b> )	92	
		Picalinal ( <b>131</b> )	92	
		Picrinine ( <b>114</b> )	92,93	
		Ψ-Akuammigine ( <b>125</b> )	92	
		Scholarine ( <b>132</b> )	94	
	Fruit pods	Nareline ( <b>113</b> )	95	
		<i>N</i> -Formylscholarine ( <b>133</b> )	95	
		Picrinine ( <b>114</b> )	95	
		Striactamine ( <b>134</b> )	95	
	Flowers	Picrinine ( <b>114</b> )	79	
		Strictamine ( <b>134</b> )	79	
		Tetrahydroalstonine ( <b>135</b> )	79	
	<hr/>			
	The Philippines	Leaves	19,20- <i>E</i> -Vallesamine ( <b>117</b> )	96
			20( <i>S</i> )-Tubotaiwine ( <b>116</b> )	86,88,96
20( <i>S</i> )-Tubotaiwine <i>N</i> -oxide ( <b>135</b> )			86,88	
6,7- <i>Seco</i> angustilobine B ( <b>136</b> )			86,88,96	
Angustilobine B acid ( <b>137</b> )			86,88	
Angustilobine B <i>N</i> -oxide ( <b>138</b> )			96	
Lagunamine (19-hydroxytubotaiwine) ( <b>139</b> )			86,88	
Losbanine (6,7- <i>seco-nor</i> -angustilobine B) ( <b>140</b> )			86,88	
Manilamine ( <b>141</b> )			96	
<i>N</i> (4)-Methylangustilobine B ( <b>142</b> )			96	
Bark		6,7- <i>Seco</i> angustilobine B ( <b>136</b> )	86	
		Acetylechitamine ( <b>143</b> )	86	
		Echitamine ( <b>118</b> )	86	
		Losbanine (6,7- <i>seco-nor</i> -angustilobine B) ( <b>140</b> )	86	
		<i>N</i> (4)-Demethylechitamine ( <i>norechitamine</i> ) ( <b>120</b> )	86	
		20( <i>S</i> )-Tubotaiwine ( <b>116</b> )	86	

Tubotaiwine *N*-oxide (**135**) 86

Taiwan	Leaves	19,20- <i>E</i> -Vallesamine ( <b>117</b> )	88
		19- <i>Episcolaricine</i> ( <b>144</b> )	88
		6,7- <i>Secoangustilobine B</i> ( <b>136</b> )	88
		Alschomine ( <b>111</b> )	88,97
		Isoalschomine ( <b>112</b> )	88,97
		Nareline ( <b>113</b> )	88,97
		Picralinal ( <b>131</b> )	88,97
		Picrinine ( <b>114</b> )	88,97
Indonesia	Leaves	19,20- <i>E</i> -Vallesamine ( <b>117</b> )	88
		19,20- <i>E</i> -Vallesamine <i>N</i> -oxide ( <b>145</b> )	88
		6,7- <i>Seco</i> -19,20 $\alpha$ -epoxyangustilobine B ( <b>146</b> )	88
		6,7- <i>Secoangustilobine B</i> ( <b>136</b> )	88
		Akuammidine ( <b>130</b> )	80,88
		Akuammidine- <i>N</i> -oxide ( <b>147</b> )	80
		Leuconolam ( <b>148</b> )	88
		<i>N</i> (1)-Methylburnamine ( <b>149</b> )	88
		<i>N</i> (4)-Methylscholoricine ( <b>150</b> )	88
		Picraline ( <b>151</b> )	88
		Scholaricine ( <b>115</b> )	88
		$\Psi$ -Akuammigine (pseudoakuammigine) ( <b>125</b> )	88
		$\Psi$ -Akuammigine <i>N</i> -oxide ( <b>152</b> )	88
		Voacristine ( <b>153</b> )	98
		Strictamine ( <b>154</b> )	98
		Nicotine ( <b>155</b> )	98
		Bark	Akuammicine <i>N</i> (4)-Oxide ( <b>123</b> )
	Akuammiginone ( <b>156</b> )		99
	Echitamidine <i>N</i> -oxide ( <b>157</b> )		99
	Echitamidine <i>N</i> -oxide 19- <i>O</i> - $\beta$ - <i>D</i> -glucopyranoside ( <b>158</b> )		99
Echitaminic acid ( <b>159</b> )	99		
<i>N</i> (4)-Demethylalstogustine ( <b>160</b> )	99		
<i>N</i> (4)-Demethylalstogustine <i>N</i> -oxide ( <b>161</b> )	99		
Pakistan	Leaves	19,20- <i>E</i> -Vallesamine ( <b>117</b> )	100
		19,20- <i>Z</i> -Vallesamine ( <b>162</b> )	100
		Alstonamine ( <b>163</b> )	101
		Rhazimanine ( <b>164</b> )	101
China	Leaves	19,20- <i>E</i> -Alstoscholarine ( <b>165</b> )	102
		19,20- <i>E</i> -Vallesamine ( <b>117</b> )	103,104

19,20-Z-Alstoscholarine ( <b>166</b> )	102
19- <i>Episcolaricine</i> ( <b>144</b> )	104
5-Methoxystrictamine ( <b>167</b> )	103,104
5-Oxo-17-deacetyl-1,2-dihydroakuammiline ( <b>168</b> )	104
Akuammidine ( <b>130</b> )	104
Leuconolam ( <b>148</b> )	104
Methyl (2 $\beta$ ,16 <i>R</i> ,19 <i>E</i> )-4,5-didehydro-1,2-dihydro-2-hydroxy-16-(hydroxymethyl)-akummilan-4-ium-17-oate chloride ( <b>169</b> )	104
<i>N</i> (1)-Methoxymethylpicrinine ( <b>170</b> )	103
<i>N</i> (1)-Methylburnamine ( <b>141</b> )	104
<i>N</i> (4)-Demetylechitamine (Norechitamine) ( <b>120</b> )	104
Picalinal ( <b>131</b> )	103,104
Picrinine ( <b>114</b> )	103,104
Rhazimanine ( <b>164</b> )	104
Scholsricine ( <b>115</b> )	103,104
Scholarisine A ( <b>171</b> )	78
17-Formyl-10-demethoxyvincorine <i>N</i> (4)-oxide ( <b>172</b> )	105
10-Methoxyalstiphyllanine H ( <b>173</b> )	105
10-Demethoxyvincorine <i>N</i> (4)-oxide ( <b>174</b> )	105
Melosline A ( <b>175</b> )	82
Melosline B ( <b>176</b> )	82
1-[2-[2-(Carboxymethyl)indole-3-yl]-3-ethylpyridinium hydroxide inner salt ( <b>177</b> )	82
Alstorisine A ( <b>178</b> )	106
Scholarisine H ( <b>179</b> )	107
Scholarisine I ( <b>180</b> )	107
Scholarisine J ( <b>181</b> )	107
Scholarisine K ( <b>182</b> )	107
Scholarisine L ( <b>183</b> )	107
Scholarisine M ( <b>184</b> )	107
Scholarisine N ( <b>185</b> )	107
Scholarisine O ( <b>186</b> )	107
Scholarisine T ( <b>187</b> )	108
Scholarisine U ( <b>188</b> )	108
Scholarisine V ( <b>189</b> )	108
Scholarisine W ( <b>190</b> )	108
Alstoscholarisine H ( <b>191</b> )	109
Alstoscholarisine I ( <b>192</b> )	109
Alstoscholarisine J ( <b>193</b> )	109
Alstoniascholarine A ( <b>194</b> )	83
Alstoniascholarine B ( <b>195</b> )	83
Alstoniascholarine C ( <b>196</b> )	83
Alstoniascholarine D ( <b>197</b> )	83
Alstoniascholarine E ( <b>198</b> )	83
Alstoniascholarine F ( <b>199</b> )	83
Alstoniascholarine G ( <b>200</b> )	83

	Alstoniascholarine H (201)	83
	Alstoniascholarine I (202)	83
	Alstoniascholarine J (203)	83
	Alstoniascholarine K (204)	83
	Alstoniascholarine L (205)	110
	Alstoniascholarine M (206)	110
	Alstoniascholarine N (207)	110
	Alstoniascholarine O (208)	110
	Alstoniascholarine P (209)	110
	Alstoniascholarine Q (210)	110
	Alstoniascholarine T (211)	111
	Alstoniascholarine U (212)	111
	Alstolactine A (213)	112
	Alstolactine B (214)	112
	Alstolactine C (215)	112
	Normavacurine-21-one (216)	84
	5-hydroxy-19,20- <i>E</i> -alschomine (217)	84
	5-hydroxy-19,20- <i>Z</i> -alschomine (218)	84
	Alistonitrine A (219)	113
Bark	19,20- <i>E</i> -Vallesamine (117)	114
	19- <i>Epi</i> -ajmalicine (220)	114
	19- <i>Epi</i> scholaricine (167)	114
	19 <i>Z</i> -16-Formyl-5 $\alpha$ -methoxystrictamine (221)	114
	20- <i>Epi</i> -19-oxodihydroakuammicine (Alstolucine F) (222)	114
	3- <i>Epi</i> -dihydrocorymine (223)	114
	5-Methoxystrictamine (168)	114
	Akuammidine (130)	114
	Echitamidine (124)	114
	Echitamine (118)	114
	Leuconoxine (224)	114
	<i>N</i> (4)-Demethylechitamine (120)	114
	Nareline (113)	114
	Picalinal (131)	114
	Picrinine (114)	114
	Scholarisine B (225)	114
	Scholarisine C (226)	114
	Scholarisine D (227)	114
	Scholarisine E (228)	114
	Scholarisine F (229)	114
	Scholarisine G (230)	114
Roots and bark	Alstonlarsine A (231)	85
	Alstonlarsine B (232)	85
	Alstonlarsine C (233)	85
	Alstonlarsine D (234)	85

---

Twigs	Melosline A ( <b>175</b> )	82
	Melosline B ( <b>176</b> )	82
	1-[2-[2-(Carboxymethyl)indole-3-yl]-3-ethylpyridinium hydroxide inner salt ( <b>177</b> )	82
Fruits	Scholarisine Q ( <b>235</b> )	115
	Scholarisine R ( <b>236</b> )	115

---

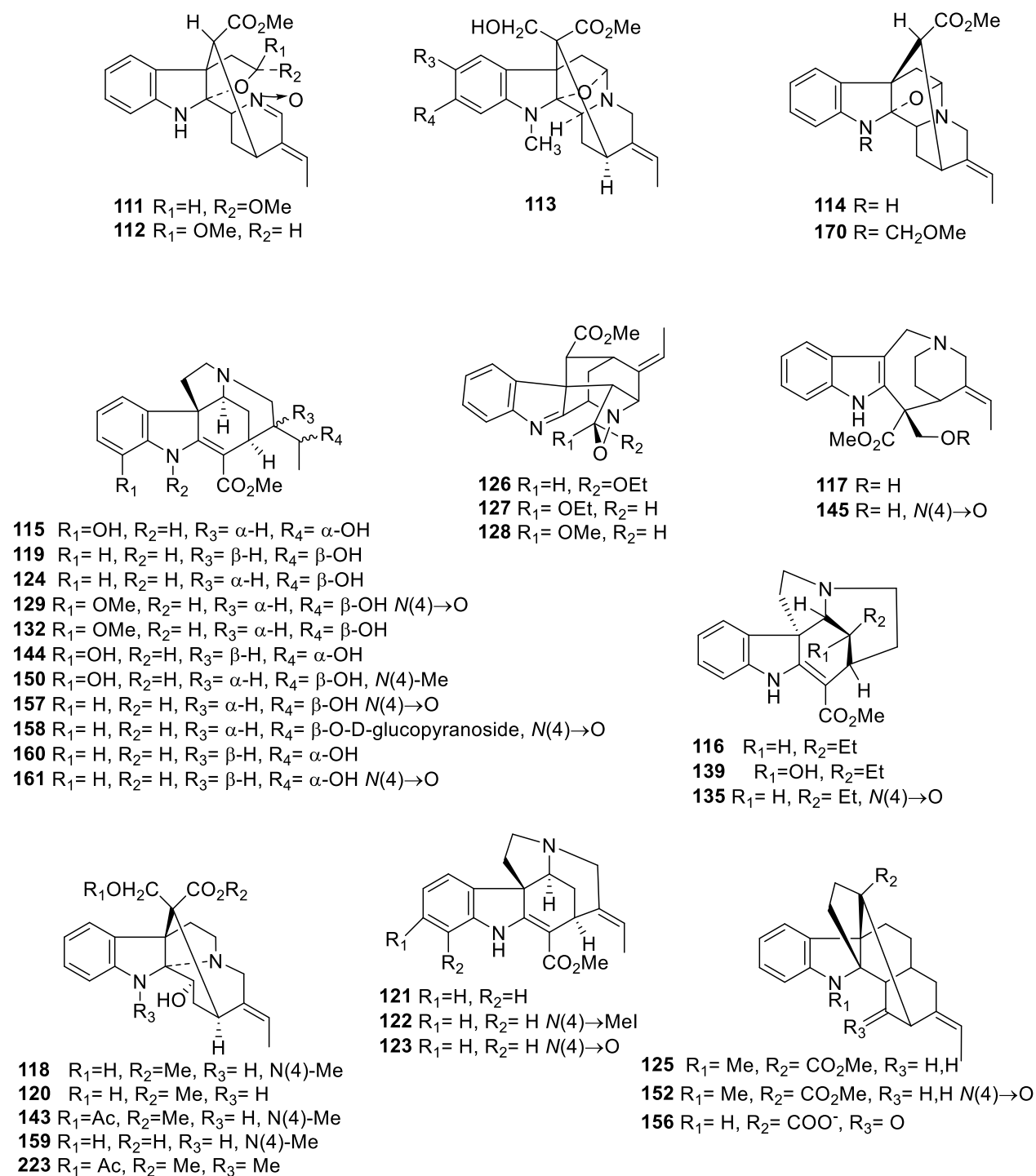


**Figure 1.5:** Alkaloids from *Alstonia scholaris*

continued next page...

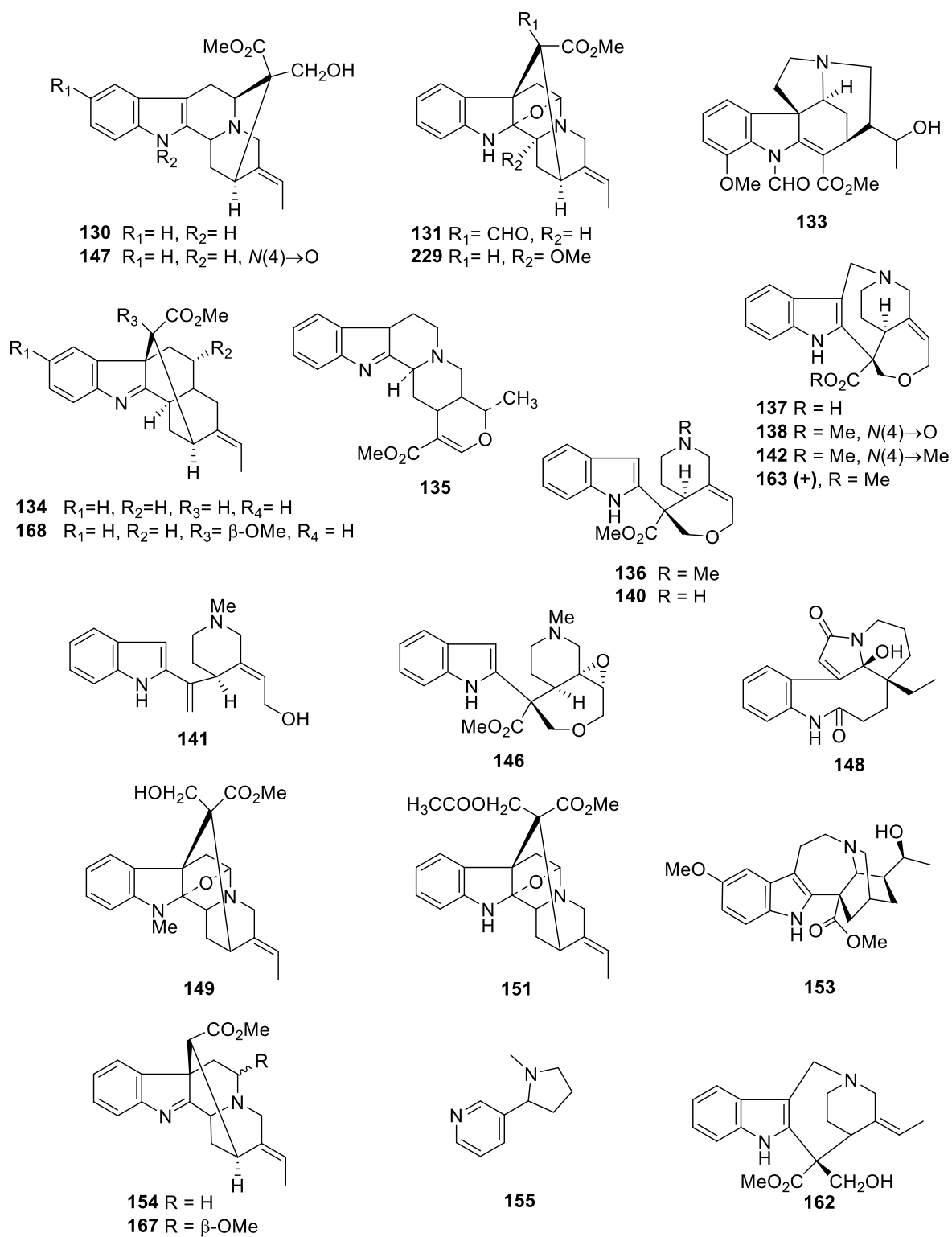


**Figure 1.5:** Alkaloids from *Alstonia scholaris*

continued next page...

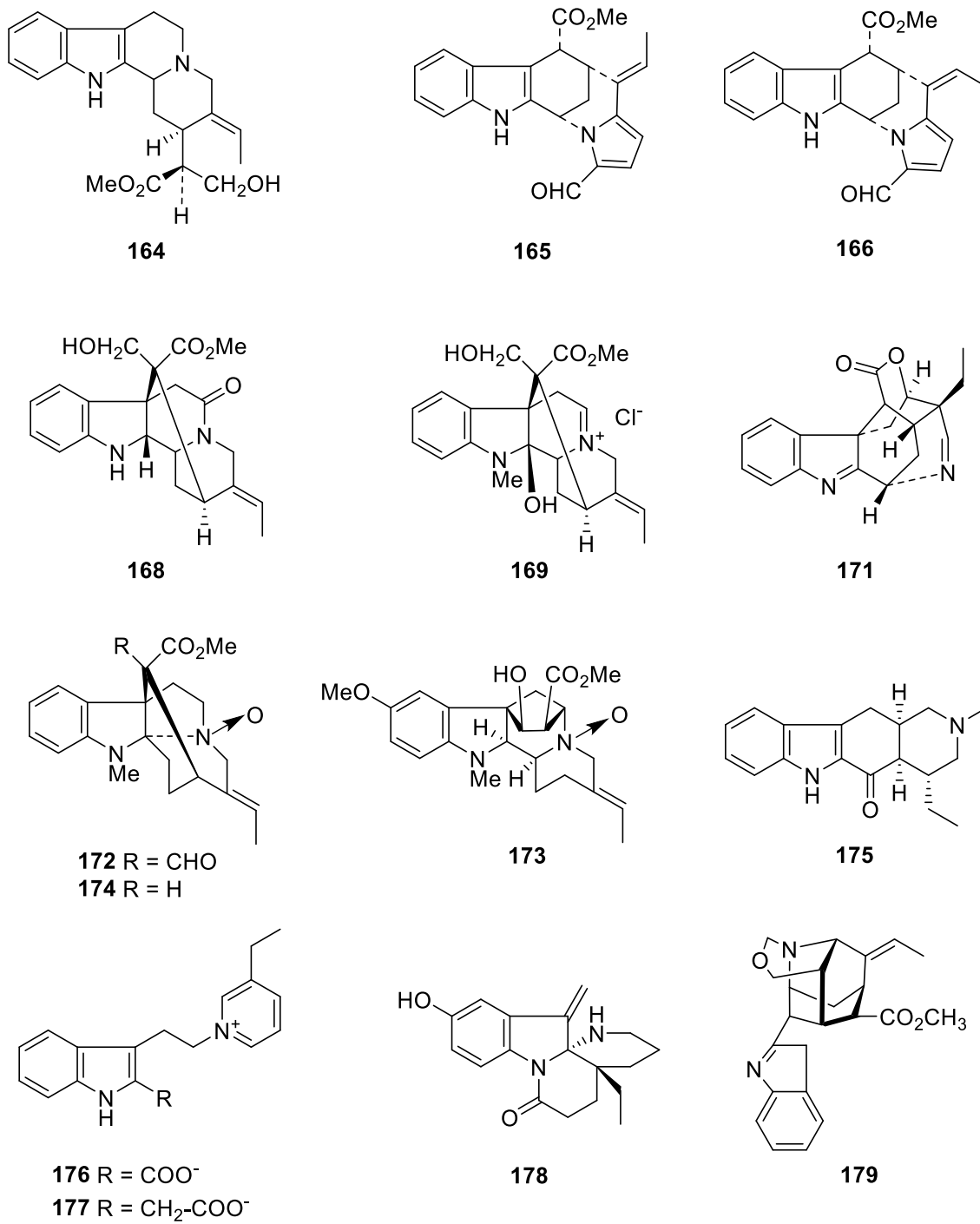


**Figure 1.5:** Alkaloids from *Alstonia scholaris*

continued next page...

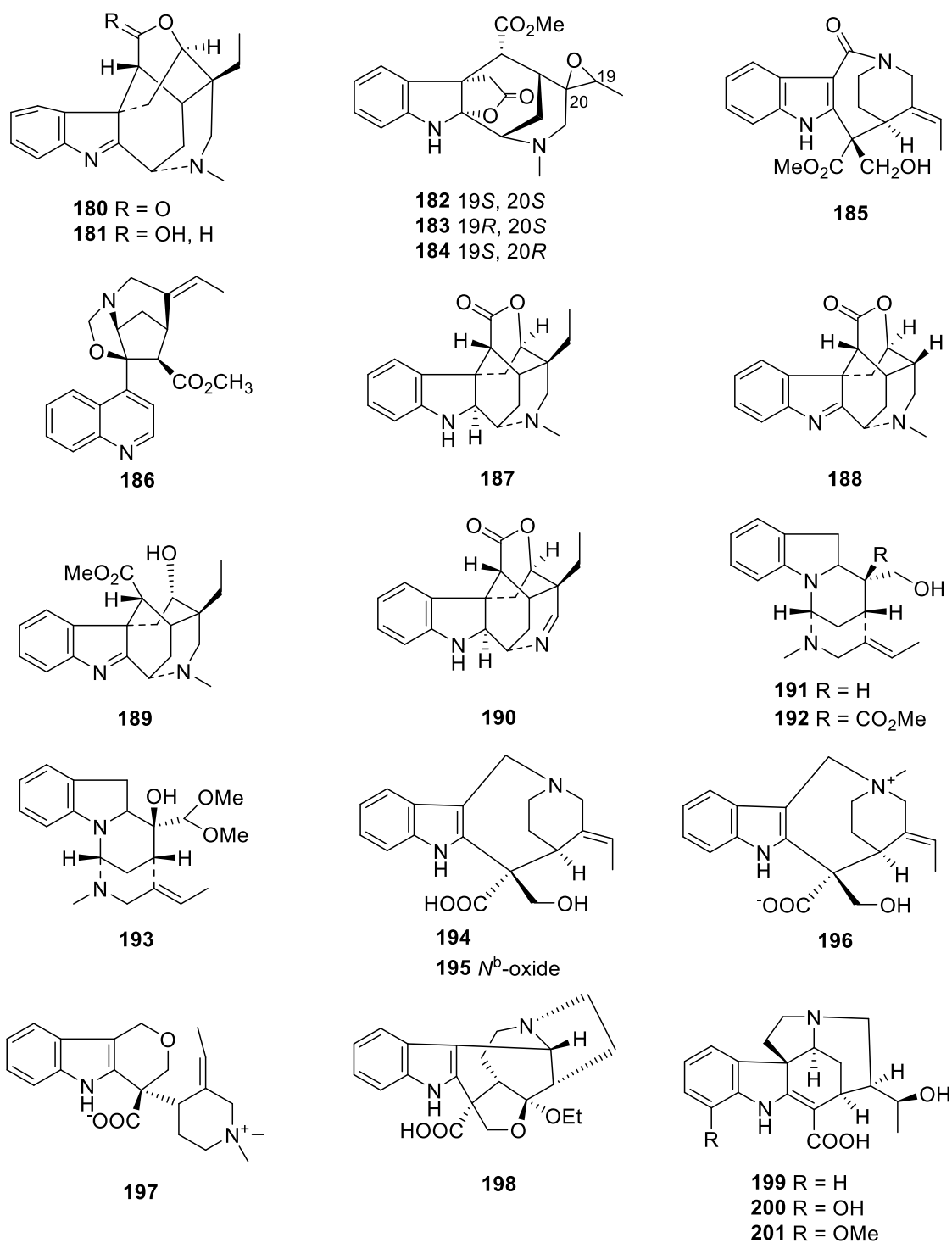


**Figure 1.5:** Alkaloids from *Alstonia scholaris*

continued next page...

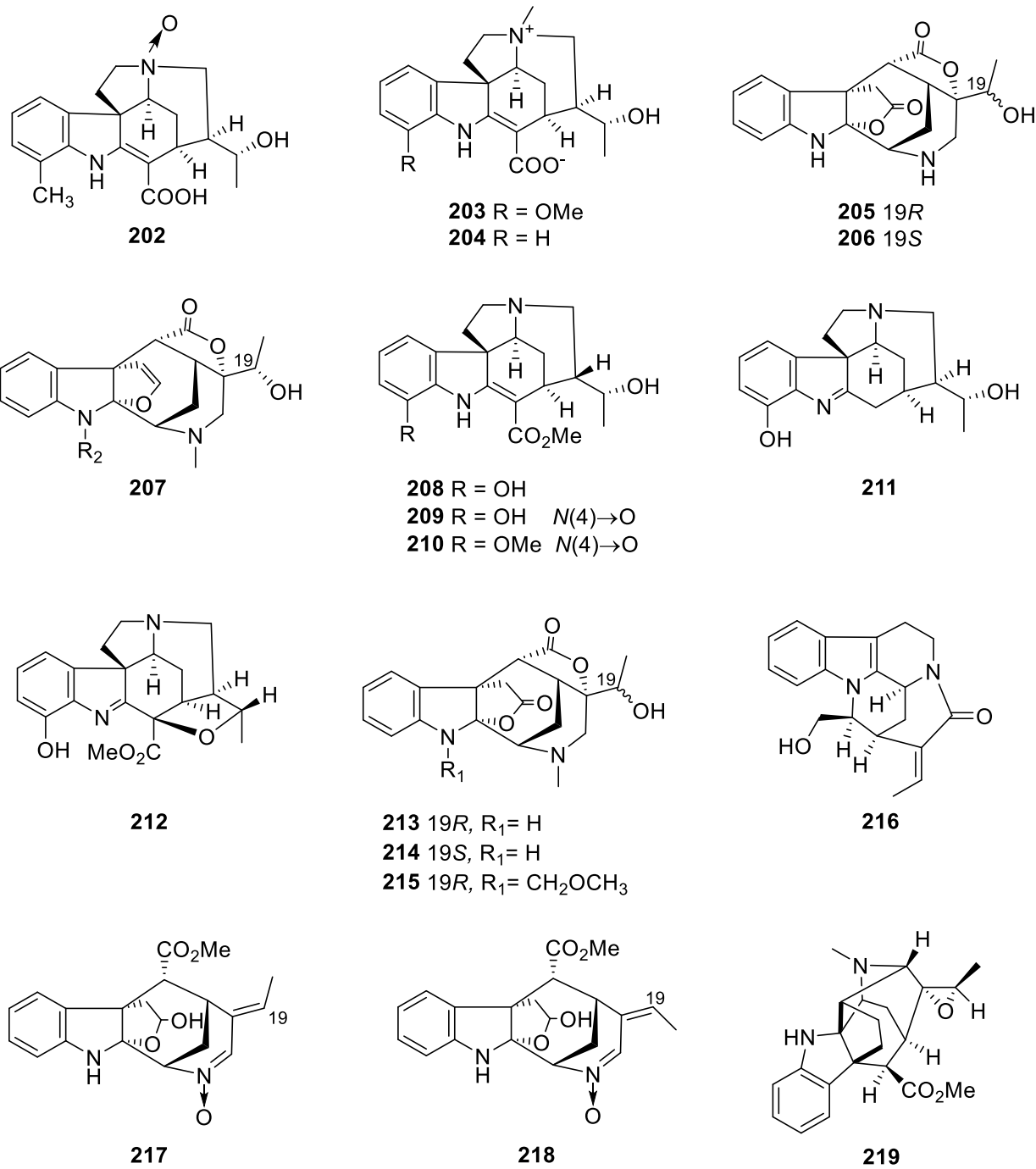


**Figure 1.5:** Alkaloids from *Alstonia scholaris*

continued next page...

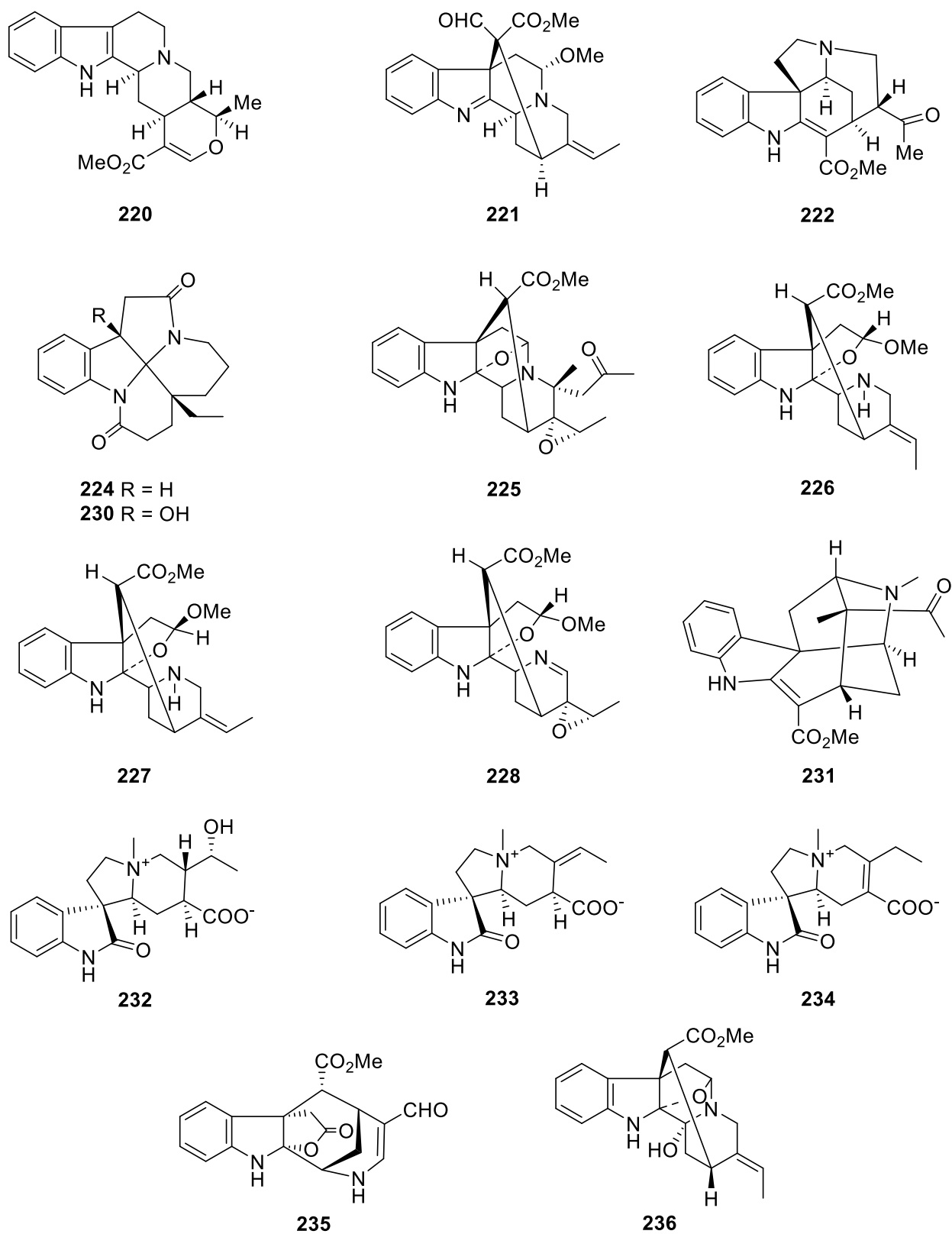


**Figure 1.5:** Alkaloids from *Alstonia scholaris*

Of the numerous alkaloids isolated from *A. scholaris*, many were reported to possess useful biological activity, including central nervous system depressant, antiplasmodial, anticancer, antibacterial, antifungal, and DRAK2 inhibitory activities, as summarised in **Table 1.4**. Therefore, *A. scholaris* represents a rich source of biologically active metabolites with potential to serve as lead compounds for drug discovery and development.

**Table 1.4** Biologically active *A. scholaris* alkaloids

<b>Compound</b>	<b>Reported bioactivity</b>	<b>Reference</b>
Picrinine ( <b>114</b> )	central nervous system depressant	79
Akuammidine ( <b>130</b> )	antiplasmodial activity	80
Akuammicine <i>N</i> -oxide ( <b>123</b> ) and <i>Nb</i> -demethylalstogustine ( <b>160</b> )	antiplasmodial activity	81
Melosline A ( <b>175</b> )	cytotoxicity against MCF-7 cancer cell line	82
Alstoniascholarines F ( <b>199</b> ) and J ( <b>203</b> )	antibacterial activity against <i>Pseudomonas aeruginosa</i>	83
Alstoniascholarines D ( <b>197</b> ), G ( <b>200</b> ) and J ( <b>203</b> )	antifungal activities against <i>Epidermophyton floccosum</i>	
Strictamine ( <b>134</b> ) and vallesamine <i>N</i> <sub>4</sub> -oxide ( <b>145</b> )	antibacterial activity against <i>Enterococcus faecalis</i>	84
Vallesamine ( <b>117</b> ) and nareline ( <b>113</b> )	antibacterial activity against <i>Pseudomonas aeruginosa</i>	
Nareline ( <b>113</b> )	antibacterial against <i>Klebsiella pneumonia</i>	
Alstonlarsine A ( <b>231</b> )	DRAK2 inhibitory activity	85

Many new and structurally intriguing alkaloids are continuously being discovered from different *A. scholaris* specimens collected from the different regions in Asia (**Table 1.3**). However, with regards to the *A. scholaris* occurring in Malaysia, there was only one phytochemical publication based on the leaf sample that was collected from the East Coast of Peninsular Malaysia (Selangor), which yielded akuammiline-type (**126-129**) and strychnan-type (**114,115**) indole alkaloids.<sup>91</sup> With geographical variation in mind, we postulated that *A. scholaris* collected from the West Coast of Peninsular Malaysia would yield different and potentially new alkaloids compared to the East Coast specimens. Therefore, the alkaloidal composition of the leaves, bark, and flowers of *A. scholaris* sampled from Selangor (West Coast of Peninsular Malaysia) were investigated in the present study, along with exploration of the biological activity of the pure alkaloids obtained.

## 1.8 Research Aim

The aim of the present research is to perform detailed phytochemical investigations on the alkaloidal composition of *Ficus schwarzii* and *Alstonia scholaris* with the aim to obtain alkaloids with new molecular structures and/or possessing useful biological activities.

The specific objectives of the present study are:

1. To obtain the crude alkaloid extracts from the leaves of *Ficus schwarzii* and the leaves, bark and flowers of *Alstonia scholaris* using the acid-base extraction method.
2. To isolate and purify the alkaloidal constituents of the leaves of *Ficus schwarzii* and the leaves, bark and flowers of *Alstonia scholaris* using various chromatographic methods including column chromatography, centrifugal thin layer chromatography and high-performance liquid chromatography.
3. To elucidate and characterize the 2D and 3D structures of the pure alkaloids obtained using various spectroscopic techniques (e.g., NMR, HRMS, UV and IR), chemical correlation and comparison of ECD spectra with those calculated by TDDFT.
4. To postulate the possible biogenetic pathways for new/ novel compounds.
5. To investigate the anticancer and vasorelaxant activity of the pure alkaloids obtained through collaborative efforts.

## CHAPTER TWO: ISOLATION AND STRUCTURE

### ELUCIDATION OF ALKALOIDS FROM *FICUS SCHWARZII*

The alkaloidal content of *Ficus schwarzii* was investigated for the first time in the present study. Appreciable presence of alkaloids was only detected in the leaves, but not the bark. A total of nine novel alkaloids were isolated and characterised from the alkaloid crude mixture of the leaves of *Ficus schwarzii*. Seven of these possess the 1,4-diarylbutanoid-phenylethylamine skeleton and were given the trivial names, schwarzinicines A–G (1–7). The remaining two alkaloids represent a pair of new diastereomeric 1-phenyl-3-aminotetralins, named schwarzificusines A and B (8 and 9), that are structurally related to the schwarzinicine alkaloids.

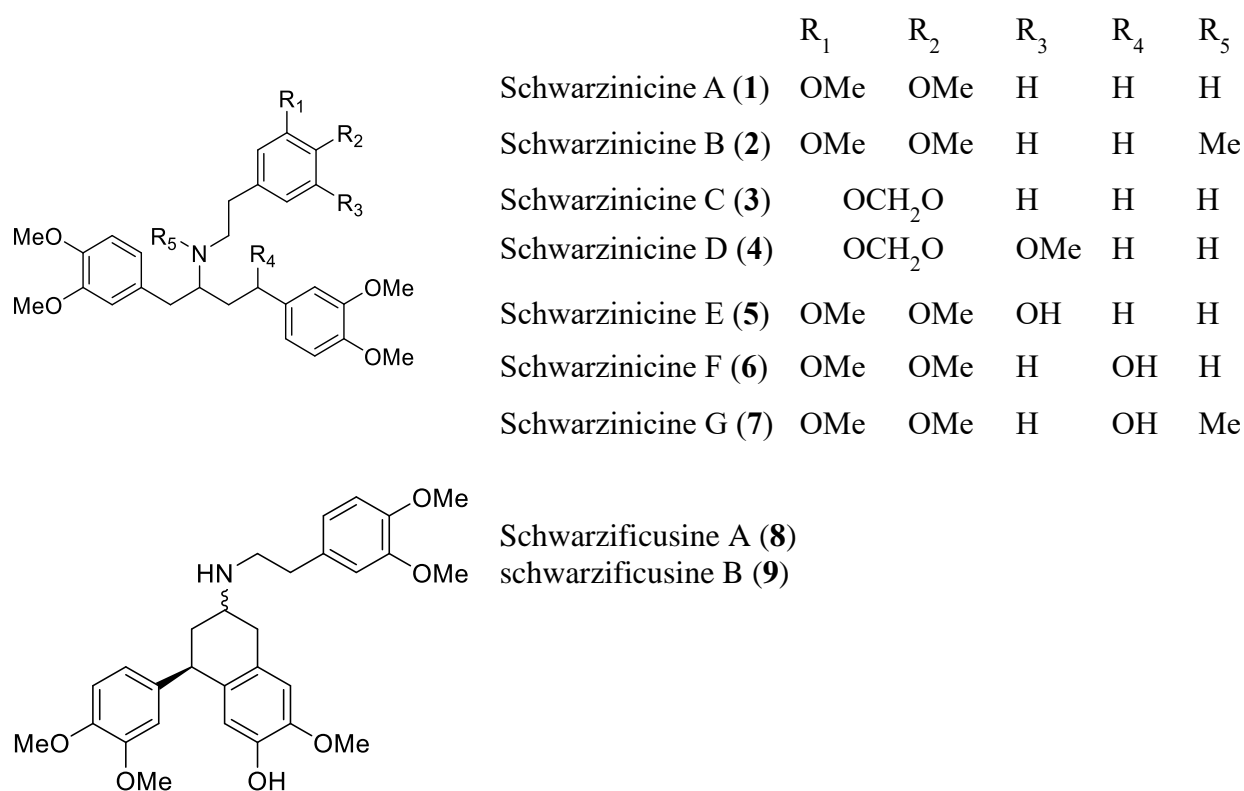


**Figure 2.0:** Alkaloids from *Ficus schwarzii*

## 2.1 Schwarzinicine A (1)

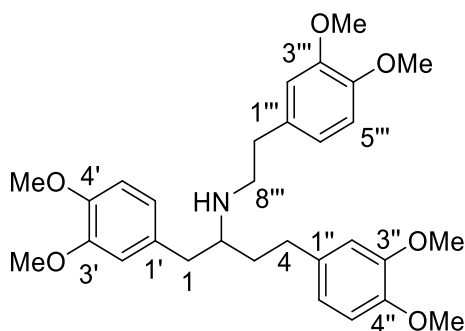


**Figure 2.1:** Schwarzinicine A (1)

Schwarzinicine A (1) was isolated as the most abundant alkaloid from the leaves of *F. schwarzii* as a light yellowish oil with a small specific optical rotation, i.e.,  $[\alpha]^{25}_{\text{D}} + 2$  ( $c$  1.17,  $\text{CHCl}_3$ ). The UV spectrum showed absorption maxima at 231 and 281 nm, characteristic of 3,4-dimethoxyphenyl chromophore.<sup>116</sup> The HR-DART-MS data revealed a molecular formula of  $\text{C}_{30}\text{H}_{39}\text{NO}_6$  based on the  $[\text{M}+\text{H}]^+$  peak detected at  $m/z$  510.2836. The  $^{13}\text{C}$  NMR spectrum of 1 (Table 2.1 and Figure 2.5) gave a total of 30 carbon resonances (three dioxygenated aryl rings, six methoxy carbons, five methylene carbons, and a methine carbon) in agreement with the molecular formula. 18 carbon peaks were found in the downfield region between  $\delta_{\text{C}}$  111 and 149 suggesting the presence of three sets of 3,4-dioxygenated phenyl groups based on their characteristic carbon shifts.<sup>46,117</sup> The six aromatic carbons with the most downfield resonances centred between  $\delta_{\text{C}}$  147 and 149 were due to six oxygenated aromatic carbons and were assigned to C-3'/3''/3''' and C-4'/4''/4'''. The three carbon signals at observed between  $\delta_{\text{C}}$  131 and 135 were readily assignable to the quaternary carbons at positions C-1'/1''/1'''. Similarly, the three resonances observed between  $\delta_{\text{C}}$  120 and 122 were due to C-6'/6''/6''' , while the remaining six aromatic resonances observed between  $\delta_{\text{C}}$  111 and 113 were attributed to C-2'/2''/2''' and C-5'/5''/5''' . In addition,

the six carbon resonances between  $\delta_C$  55.8 and 55.9 indicated the presence of six methoxy groups, thus confirming the presence of three sets of 3,4-dimethoxyphenyl moieties.

The  $^1\text{H}$  NMR spectrum of **1** (**Table 2.1** and **Figure 2.4**) showed the presence of nine aromatic protons, six methoxy groups, 11 aliphatic protons, and an NH group (indicated by the presence of a broad singlet at  $\delta_H$  1.98). The splitting patterns observed for the aromatic protons signals were consistent with the presence of three sets of 1,3,4-trisubstituted aryl rings, i.e., H-2'/2''/2''' (d,  $J = \sim 2$  Hz,  $\delta_H$  6.622, 6.663, and 6.67), H-5'/5''/5''' (d,  $J = \sim 8$  Hz,  $\delta_H$  6.717, 6.722, and 6.77), and H-6'/6''/6''' (dd,  $J = \sim 8$  and  $\sim 2$  Hz,  $\delta_H$  6.60, 6.615, and 6.657).

The HSQC and COSY spectra revealed the presence of  $\text{CH}_2\text{CHCH}_2\text{CH}_2$  and  $\text{CH}_2\text{CH}_2$  partial structures that correspond to the C-1–C-2–C-3–C-4 and C-7'''–C-8''' fragments in **1**, respectively (**Figure 2.2**). The HMBC data further confirmed the partial structures identified by the HSQC and COSY data (**Figure 2.2**). The three 3,4-dimethoxyphenyl groups were deduced to be connected to C-1, C-4 and C-7''' based on the three-bond correlations from H-1 to C-2' and C-6'; from H-2 to C-1'; from H-2' and H-6' to C-1; from H-2'' and H-6'' to C-4; from H-3 to C-1''; from H-7''' to C-2''' and C-6'''; from H-2''' and H-6''' to C-7'''; and from H-8''' to C-1''' (**Figure 2.2**). Additionally, the C-1–C-2–C-3–C-4 and C-7'''–C-8''' partial structures were deduced to be linked via the NH group based on the observed HMBC correlation from H-8''' to C-2. The full structure of **1** was thus established as shown in **Figure 2.1**. It is also worth mentioning that for unknown reasons, the NH absorption band of **1** was not particularly obvious around  $3322 - 3500\text{ cm}^{-1}$  in the IR spectrum. Therefore, to prove the existence of this NH group, **1** was *N*-methylated via a reductive amination method (NH reacted with formaldehyde and  $\text{NaBH}_3\text{CN}$  in the presence of AcOH) to furnish schwarzinicine B (**2**) (vide infra).

Due to severe overlapping of signals in the  $^1\text{H}$  and  $^{13}\text{C}$  spectra, the unambiguous assignments of some aromatic signals were not possible, and these interchangeable signals are indicated in **Table 2.1**. Finally, chiral HPLC analysis indicated schwarzinicine A (**1**) to be a scalemic mixture of the (+) and (-) enantiomers in a ratio of 1:4 (**Figure 2.3**).

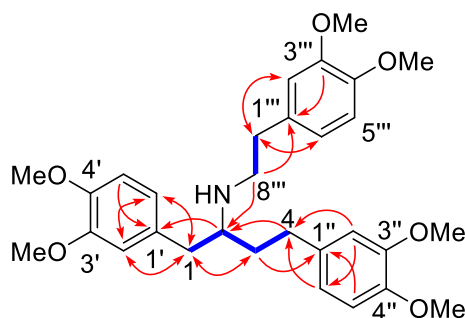
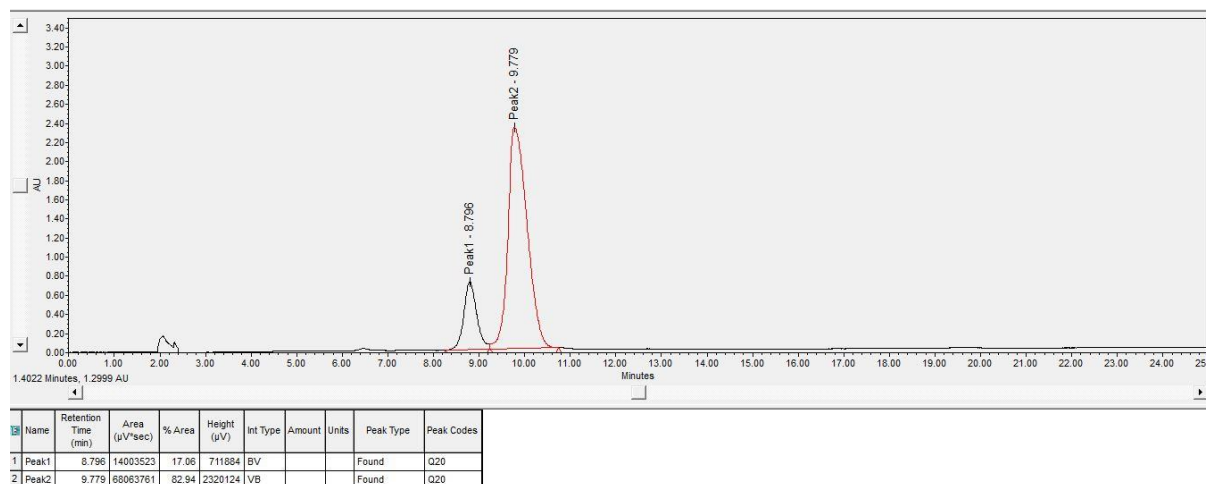


**Figure 2.2:** COSY (blue, bold) and selected HMBC (red arrows) correlations of schwarzinicine A (**1**)



Sample concentration (injection volume)	Column	Solvent system	Flow rate
2.0 mg/mL, (10.0 $\mu\text{L}$ )	Chiralpak IA column (4.6 $\times$ 150 mm)	hexane-EtOH-Et <sub>2</sub> NH, 80:20:0.1	1.0 mL/min

**Figure 2.3:** Chiral HPLC chromatogram of schwarzinicine A (**1**)

**Table 2.1:**  $^1\text{H}$  (600 MHz) and  $^{13}\text{C}$  (150 MHz) NMR spectroscopic data (in  $\text{CDCl}_3$  with TMS as internal reference) of schwarzinicine A (**1**)

Position	$\delta_{\text{H}}$ (mult., $J$ in Hz)	$\delta_{\text{C}}$
1	2.62, m 2.74, m	40.10
2	2.74, m	58.70
3	1.72, m 1.79, m	35.37
4	2.62, m	31.56
1'		131.50
2'	6.622, d (2)	112.25
3'		148.80 <sup>a</sup>
4'		147.17 <sup>b</sup>
5'	6.722, d (8.1) <sup>a</sup>	111.10 <sup>c</sup>
6'	6.60, dd (8.1, 2)	121.06
1''		134.77
2''	6.67, d (2)	111.64
3''		148.84 <sup>a</sup>
4''		147.44 <sup>b</sup>
5''	6.77, d (8.6)	111.22 <sup>c</sup>
6''	6.657, dd (8.6, 2)	120.07
1'''		132.13
2'''	6.663, d (1.8)	111.82
3'''		148.87 <sup>a</sup>
4'''		147.45 <sup>b</sup>
5'''	6.717, d (8.1) <sup>a</sup>	111.15 <sup>c</sup>
6'''	6.615, dd (8.1, 1.8)	120.43
7'''	2.67, m	35.75
8'''	2.77, m 2.90, m	48.36
3'-OMe	3.83, s <sup>b</sup>	55.77 <sup>d</sup>
4'-OMe	3.853, s <sup>b</sup>	55.77 <sup>d</sup>
3''-OMe	3.84, s <sup>b</sup>	55.81 <sup>d</sup>
4''-OMe	3.86, s <sup>b</sup>	55.81 <sup>d</sup>
3'''-OMe	3.82, s <sup>b</sup>	55.84 <sup>d</sup>
4'''-OMe	3.854, s <sup>b</sup>	55.93 <sup>d</sup>
NH	1.98, br s	

<sup>a-d</sup> Assignments may be interchanged within each column due to overlapping of signals

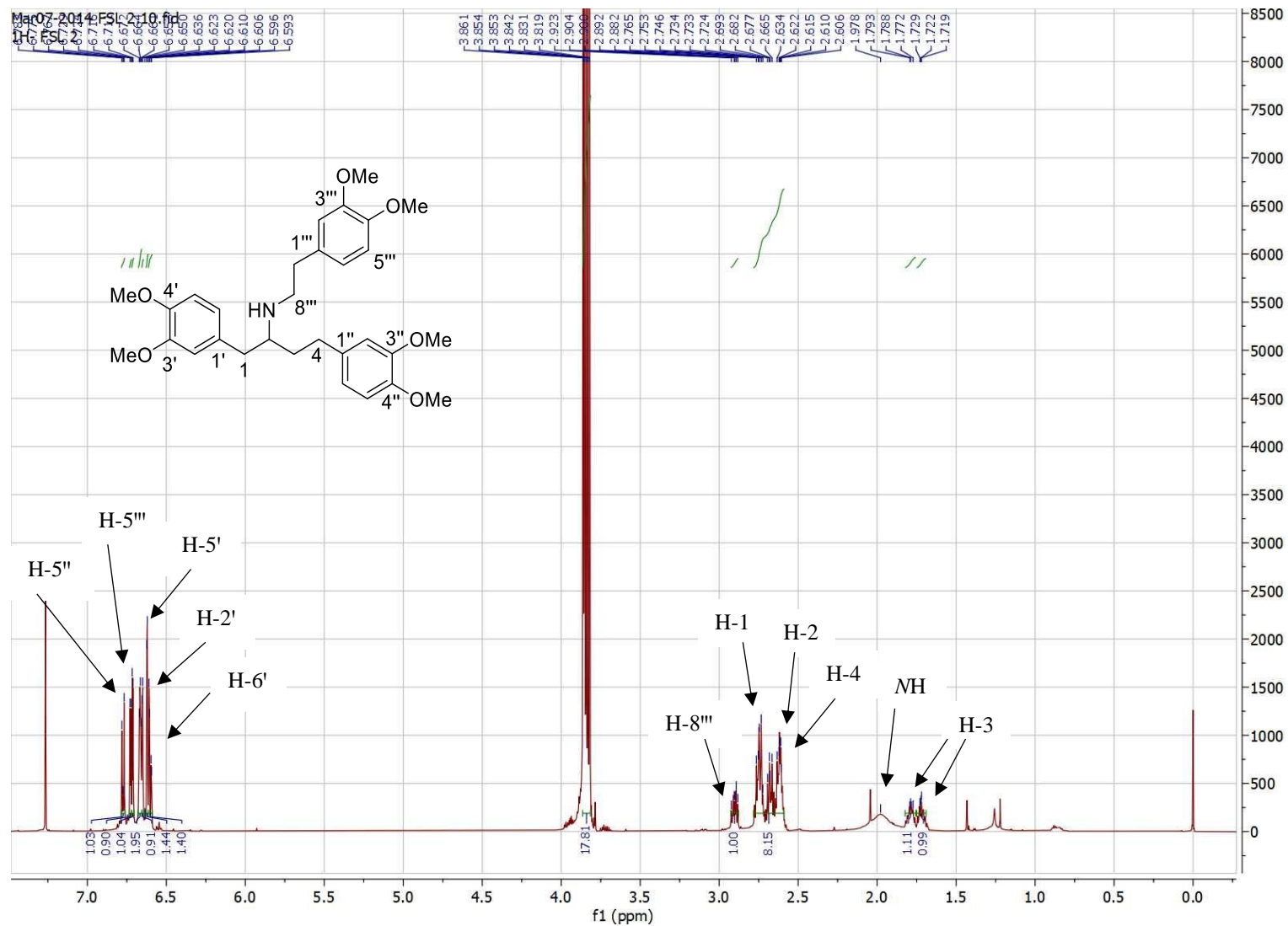
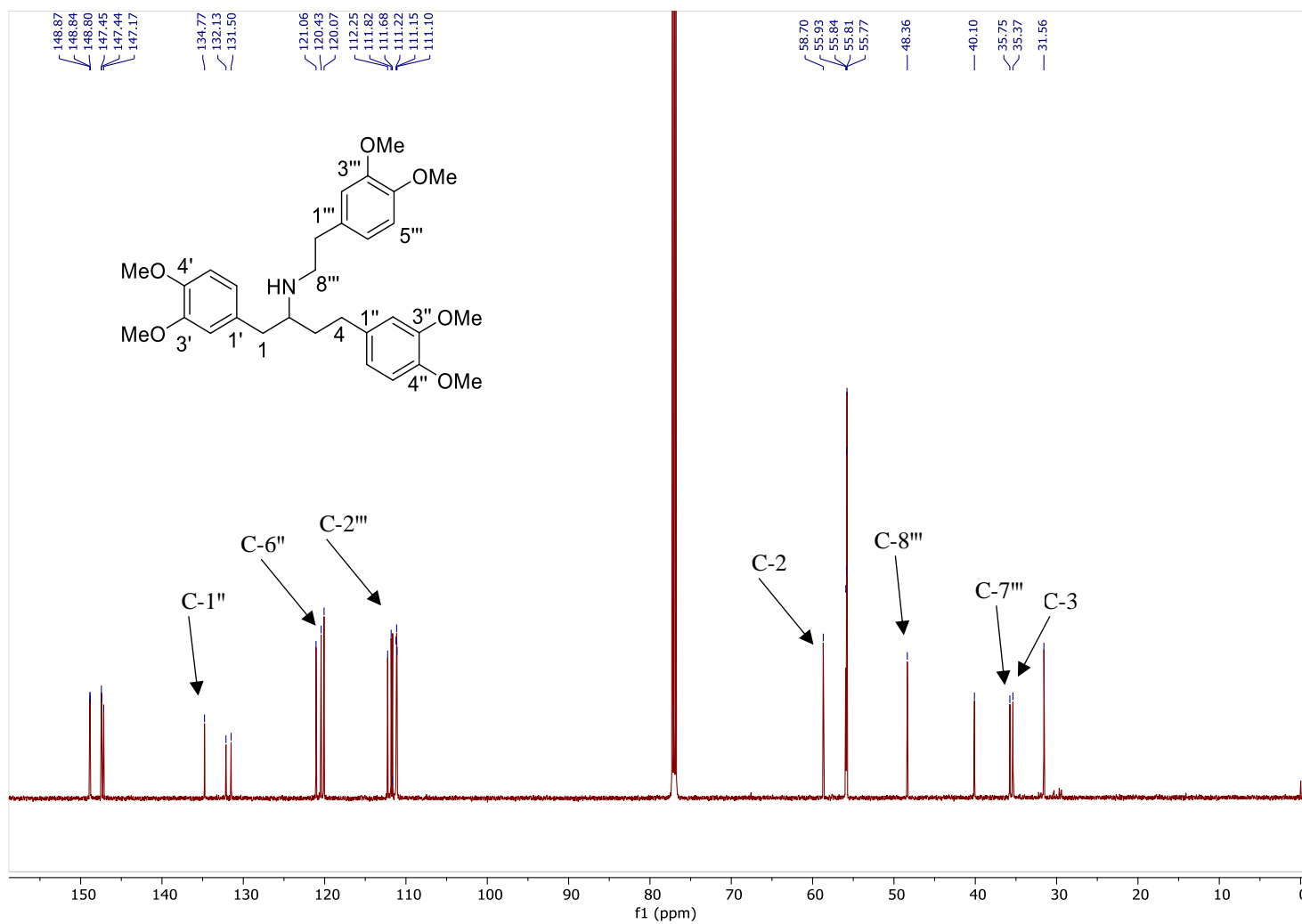
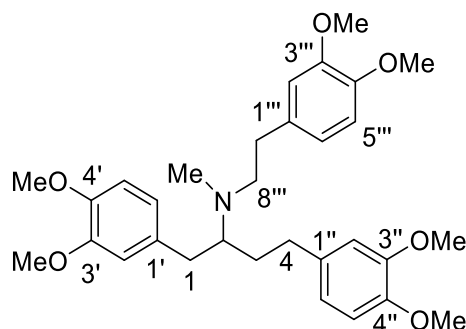


Figure 2.4: <sup>1</sup>H NMR spectrum of schwarzinicine A (1) (CDCl<sub>3</sub>, 600 MHz)



**Figure 2.5:**  $^{13}\text{C}$  NMR spectrum of schwarzinicine A (1) ( $\text{CDCl}_3$ , 150 MHz)

## 2.2 Schwarzinicine B (2)



**Figure 2.6:** Schwarzinicine B (2)

Schwarzinicine B (**2**) was isolated from the leaves of *F. schwarzii* as a light yellowish oil with  $[\alpha]_D^{25} +20$  ( $c$  1.01,  $\text{CHCl}_3$ ). The UV spectrum showed absorption maxima at 231 and 281 nm, similar to those of **1**. HR-DART-MS data showed a pseudo-molecular ion  $[\text{M}+\text{H}]^+$  peak at  $m/z$  524.2996, corresponding to the molecular formula  $\text{C}_{31}\text{H}_{41}\text{NO}_6$ . The NMR data of **2** were found to be similar to those of **1**, strongly suggesting that they are structurally closely related. Notably, the MH signal at  $\delta_{\text{H}}$  1.98 present in **1** was absent in **2**, replaced instead with an *N*-methyl signal observed at  $\delta_{\text{H}}$  2.38 and  $\delta_{\text{C}}$  36.84. This suggested that **2** is an *N*-methyl derivative of **1**.

Other than that, the  $^1\text{H}$  NMR spectrum (**Table 2.2** and **Figure 2.9**) showed nine aromatic protons, six aromatic methoxy groups and eleven aliphatic protons as in the case of **1**. The presence of three sets of 1,3,4-trisubstituted aryl rings as in the case of **1** were also supported by the splitting patterns observed for the aromatic proton signals: H-2'/2''/2''' ( $\delta_{\text{H}}$  6.62, 6.56, and 6.73), H-5'/5''/5''' (d,  $J = \sim 8$  Hz,  $\delta_{\text{H}}$  6.76, 6.73, and 6.79) and H-6'/6''/6''' (dd,  $J = \sim 8$  and  $\sim 2$  Hz,  $\delta_{\text{H}}$  6.65, 6.57, and 6.74). The  $^{13}\text{C}$  NMR spectrum (**Table 2.2** and **Figure 2.10**) indicated the presence of three dioxygenated-aryl rings, six methoxy carbons, an *N*-Me carbon,

five methylene carbons, and a methine carbon, in agreement with the molecular formula deduced from the HR-DART-MS measurements.

The HSQC and COSY data (**Figure 2.7**) showed the presence of CH<sub>2</sub>CH<sub>2</sub> and CH<sub>2</sub>CHCH<sub>2</sub>CH<sub>2</sub> partial structures, which corresponded to the C-7'''–C-8''' and C-1–C-2–C-3–C-4 fragments, respectively. The HMBC data further confirmed the partial structures identified by HSQC and COSY. The HMBC data allowed the three aryl rings to be linked to C-1, C-4 and C-7''' of the aliphatic backbone (**Figure 2.7**).

Assignments of some aromatic signals were not possible due to severe overlapping of signals in the <sup>1</sup>H and <sup>13</sup>C spectra, and these interchangeable signals are indicated in **Table 2.2**. Chiral HPLC analysis indicated schwarzinicine B (**2**) to be a single enantiomer (**Figure 2.8**).

The structure of **2** was also confirmed by its partial synthesis from **1**. The reductive methylation of **1** with formaldehyde and NaBH<sub>3</sub>CN in the presence of AcOH gave schwarzinicine B (**2**) in 54% yield. The spectroscopic data (<sup>1</sup>H, <sup>13</sup>C NMR, and UV) of the reaction product were indistinguishable from those of natural **2**.

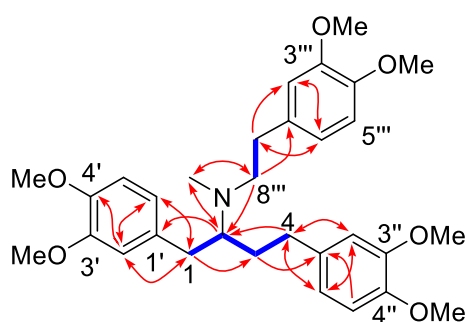
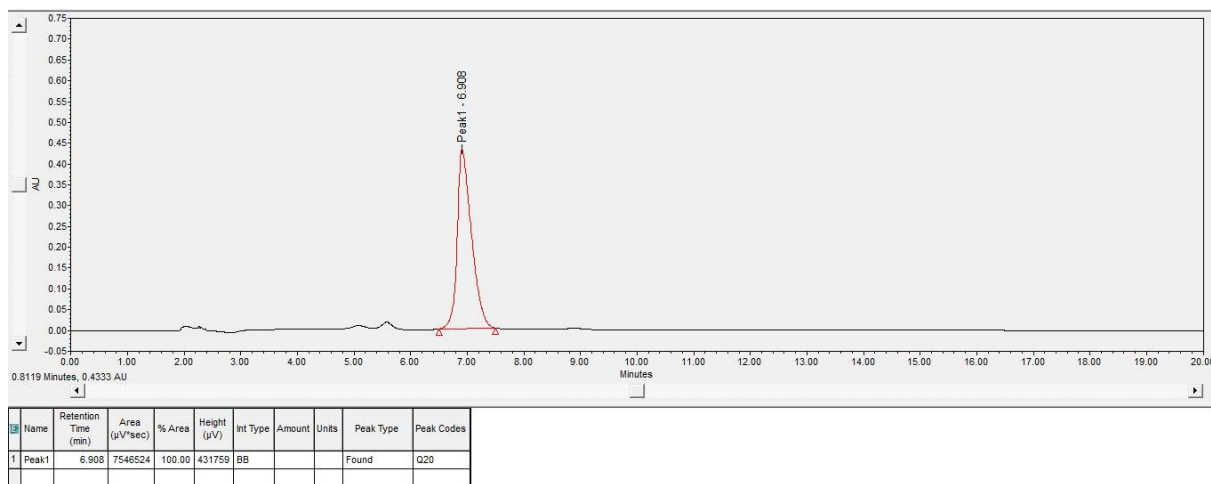


**Figure 2.7:** COSY (blue, bold) and selected HMBC (red arrows) correlations of schwarzinicine B (**2**)



Sample concentration (injection volume)	Column	Solvent system	Flow rate
3.7 mg/mL (5.0 μL)	Chiralpak IA column (4.6 × 150 mm)	hexane-EtOH-Et <sub>2</sub> NH, 80:20:0.1	1.0 mL/min

**Figure 2.8:** Chiral HPLC chromatogram of schwarzinicine B (2)

**Table 2.2:** <sup>1</sup>H (600 MHz) and <sup>13</sup>C (150 MHz) NMR spectroscopic data (in CDCl<sub>3</sub> with TMS as internal reference) of schwarzinicine B (**2**)

Position	$\delta_{\text{H}}$ (mult., <i>J</i> in Hz)	$\delta_{\text{C}}$
1	2.34, dd (13.4, 9.2) 2.89, dd (13.4, 4.3)	34.61
2	2.73, m	64.50
3	1.59, m 1.69, m	32.49 <sup>a</sup>
4	2.39, m 2.59, m	32.47 <sup>a</sup>
1'		133.39 <sup>b</sup>
2'	6.62, d (1.6)	112.35
3'		148.75 <sup>c</sup>
4'		147.10 <sup>d</sup>
5'	6.76, d (8.1)	111.06 <sup>e</sup>
6'	6.65, dd (8.1, 1.6)	121.06
1''		135.28
2''	6.56, m	111.73
3''		148.68 <sup>c</sup>
4''		147.28 <sup>d</sup>
5''	6.73, d (8.6)	111.12 <sup>e</sup>
6''	6.57, dd (8.6, 2)	120.10
1'''		133.35 <sup>b</sup>
2'''	6.73, m	112.18
3'''		148.61 <sup>c</sup>
4'''		146.90 <sup>d</sup>
5'''	6.79, d (7.9)	111.20 <sup>e</sup>
6'''	6.74, dd (7.9, 2)	120.59
7'''	2.71, m	34.90
8'''	2.65, m 2.77, m	55.70
3'-OMe	3.826, s	55.79 <sup>f</sup>
4'-OMe	3.833, s <sup>a</sup>	55.79 <sup>f</sup>
3''-OMe	3.80, s <sup>b</sup>	55.82 <sup>f</sup>
4''-OMe	3.85, s <sup>a</sup>	55.85 <sup>f</sup>
3'''-OMe	3.87, s <sup>b</sup>	55.86 <sup>f</sup>
4'''-OMe	3.85, s <sup>a</sup>	55.89 <sup>f</sup>
NMe	2.38, s	36.84

<sup>a-f</sup> Assignments may be interchanged within each column due to overlapping of signals

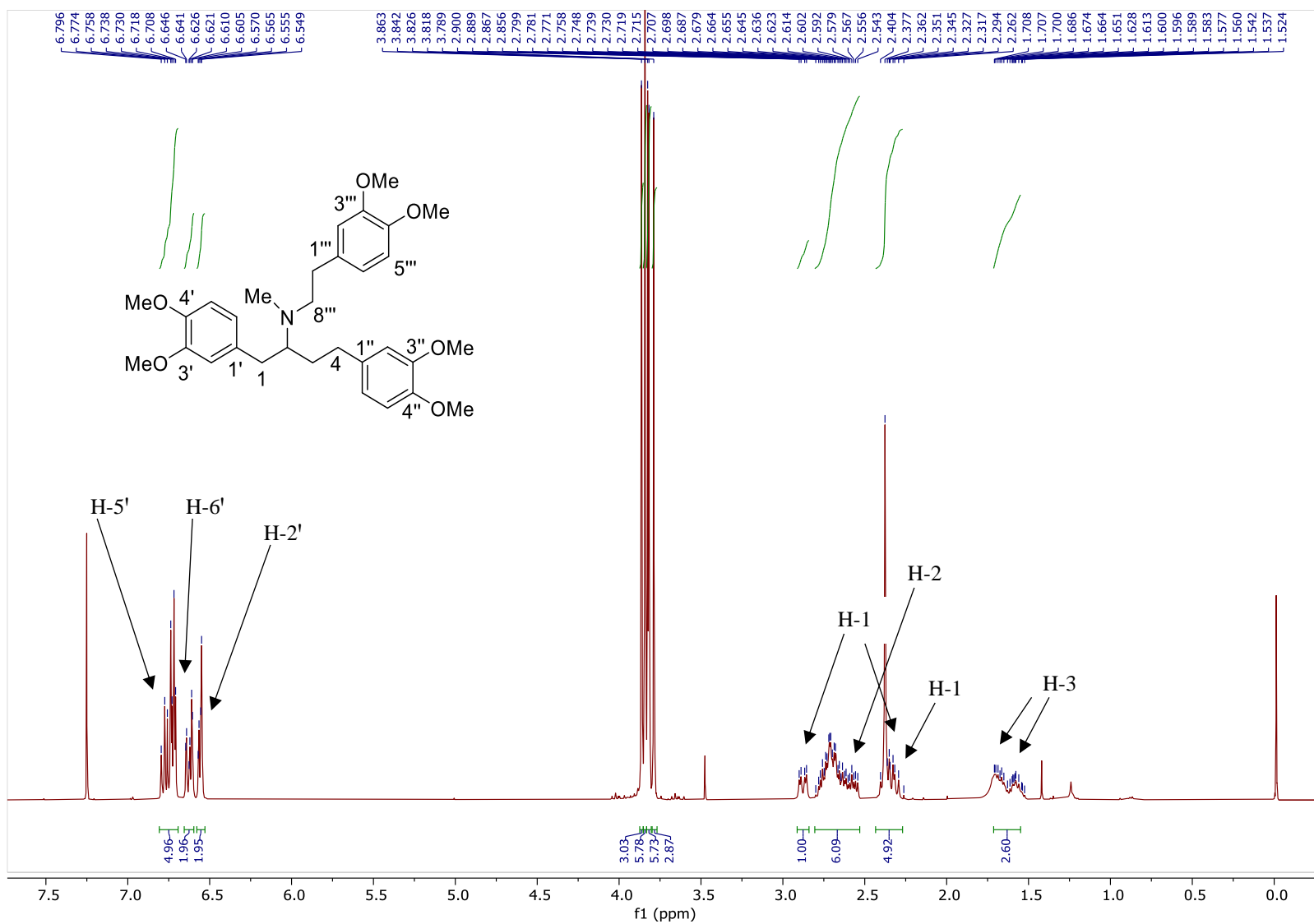


**Figure 2.9:**  $^1\text{H}$  NMR spectrum of schwarzinicine B (**2**) ( $\text{CDCl}_3$ , 600 MHz)



## 2.3 Schwarzinicine C (3)

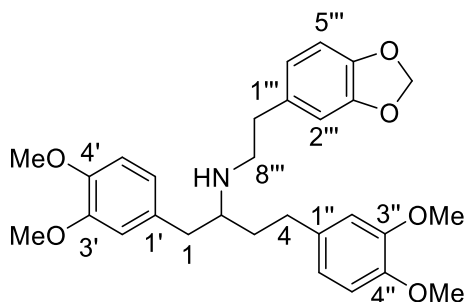


**Figure 2.11:** Schwarzinicine C (**3**)

Schwarzinicine C (**3**) was isolated as a light yellowish oil with  $[\alpha]_D^{25} -7$  ( $c$  0.48,  $\text{CHCl}_3$ ). The HR-DART-MS showed a pseudo-molecular ion  $[\text{M}+\text{H}]^+$  peak at  $m/z$  494.2505, corresponding to the molecular formula  $\text{C}_{29}\text{H}_{36}\text{NO}_6$ . The UV spectrum of **3** appeared to be very similar to that of **1** and **2**.

The  $^1\text{H}$  and  $^{13}\text{C}$  NMR data of **3** (Table 2.3, Figures 2.14 and 2.15) were generally similar to those of **1**, except that two of the six methoxy groups ( $3'''$ -OMe and  $4'''$ -OMe) present in **1**, were absent and replaced instead with a methylenedioxy group in **3** ( $\delta_{\text{C}}$  100.85,  $\delta_{\text{H}}$  5.91). This was consistent with the molecular mass of **3**, which was 16 mass units lower than that of **1**.

The HSQC and COSY data (Figure 2.12) showed the presence of  $\text{CH}_2\text{CH}_2$  and  $\text{CH}_2\text{CHCH}_2\text{CH}_2$  partial structures, which corresponded to the  $\text{C-}7'''$ – $\text{C-}8'''$  and  $\text{C-}1$ – $\text{C-}2$ – $\text{C-}3$ – $\text{C-}4$  fragments, respectively. The attachment of the methylenedioxy group placed at  $\text{C-}3'''$  and  $\text{C-}4'''$  in **3** was deduced based on the three-bond correlation observed from the H of the methylenedioxy group to  $\text{C-}3'''$  and  $\text{C-}4'''$  in HMBC spectrum (Figure 2.12). Schwarzinicine

C (3) was found to occur as a single enantiomer as inferred by chiral HPLC analysis (**Figure 2.13**).

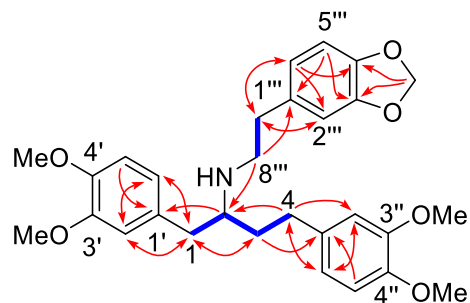
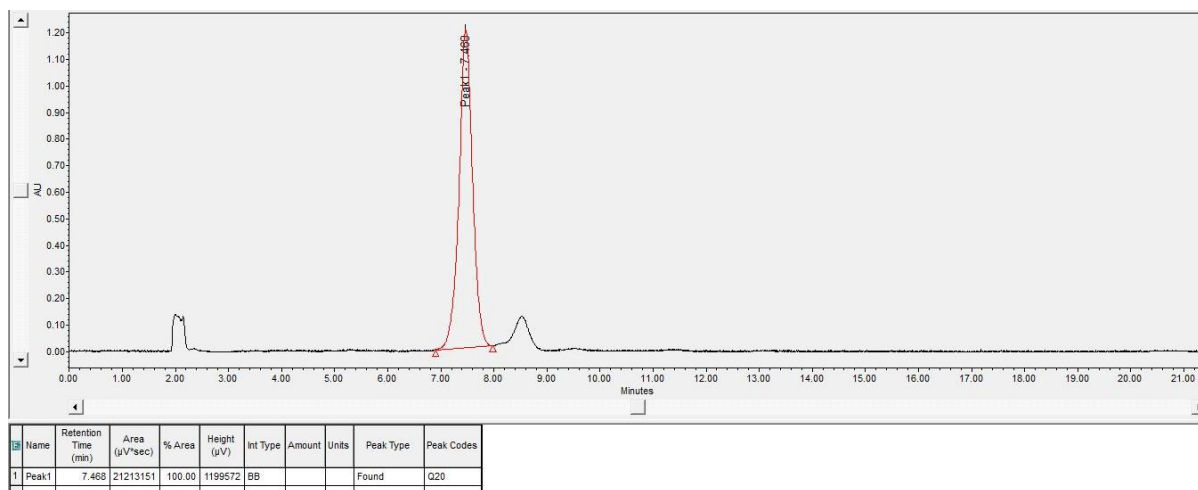


**Figure 2.12:** COSY (blue, bold) and selected HMBC (red arrows) correlations of schwarzinicine C (3)



Sample concentration (injection volume)	Column	Solvent system	Flow rate
1.6 mg/mL (10.0 µL)	Chiralpak IA column (4.6 × 150 mm)	hexane-EtOH-Et <sub>2</sub> NH <sub>3</sub> 90:10:0.1	1.0 mL/min

**Figure 2.13:** Chiral HPLC chromatogram of schwarzinicine C (3)

**Table 2.3:**  $^1\text{H}$  (600 MHz) and  $^{13}\text{C}$  (150 MHz) NMR spectroscopic data (in  $\text{CDCl}_3$  with TMS as internal reference) of schwarzinicine C (**3**)

Position	$\delta_{\text{H}}$ (mult., $J$ in Hz)	$\delta_{\text{C}}$
1	2.61, m 2.74, m	40.06
2	2.75, m	58.70
3	1.73, m 1.79, m	35.32
4	2.62, m	31.53
1'		131.40
2'	6.62, m	112.22
3'		148.82 <sup>a</sup>
4'		147.17 <sup>b</sup>
5'	6.74, d (8)	111.17 <sup>c</sup>
6'	6.63, dd (8, 2)	121.06
1''		134.74
2''	6.67, m	111.64
3''		148.84 <sup>a</sup>
4''		147.62 <sup>b</sup>
5''	6.78, d (8.6)	111.23 <sup>c</sup>
6''	6.68, m	120.07
1'''		133.25
2'''	6.58, d (1.4)	108.79
3'''		147.47
4'''		145.89
5'''	6.66, d (7.9)	108.12
6'''	6.53, dd (7.9, 1.4)	121.43
7'''	2.66, m	35.74
8'''	2.72, m 2.88, dt (11, 6.6)	48.35
3'-OMe	3.82, s <sup>a</sup>	55.77 <sup>d</sup>
4'-OMe	3.85, s <sup>a</sup>	55.81 <sup>d</sup>
3''-OMe	3.85, s <sup>a</sup>	55.82 <sup>d</sup>
4''-OMe	3.86, s <sup>a</sup>	55.92 <sup>d</sup>
OCH <sub>2</sub> O	5.91, s	100.85
NH	Not observed	

<sup>a-d</sup> Assignments may be interchanged within each column due to overlapping of signals

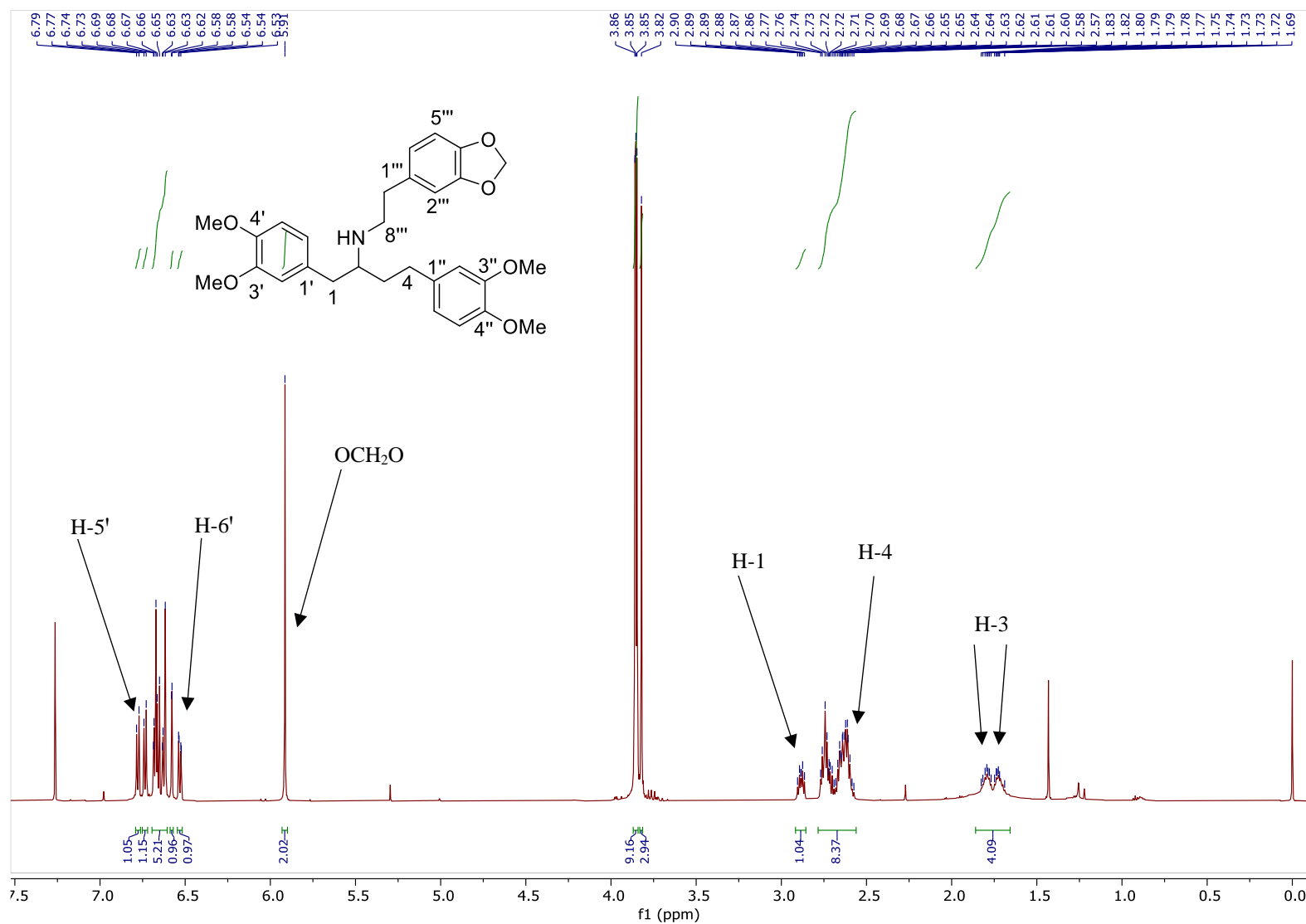


**Figure 2.14:** <sup>1</sup>H NMR spectrum of schwarzinicine c (**3**) (CDCl<sub>3</sub>, 600 MHz)

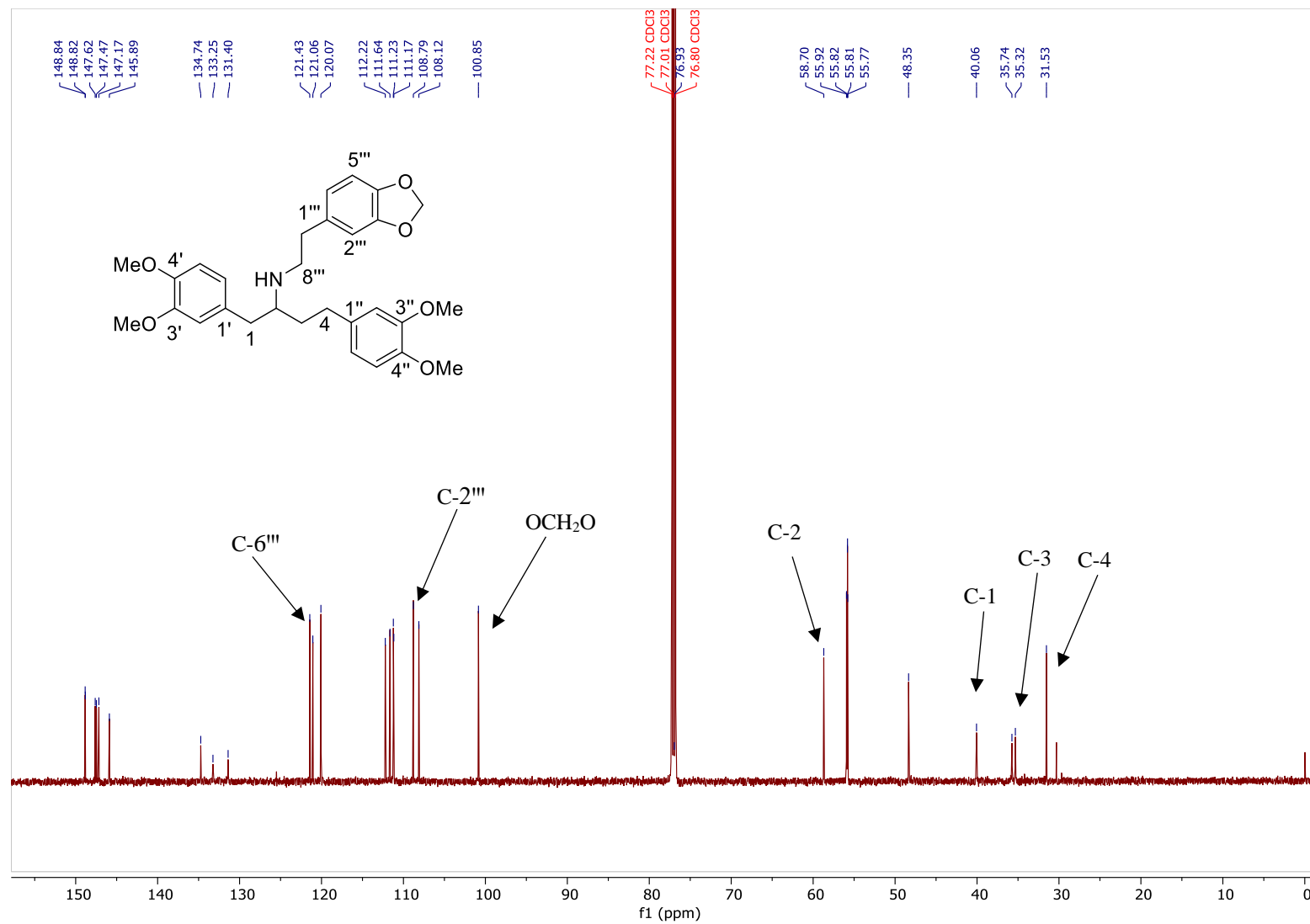


**Figure 2.15:** <sup>13</sup>C NMR spectrum of schwarzinicine C (**3**) (CDCl<sub>3</sub>, 150 MHz)

## 2.4 Schwarzinicine D (4)

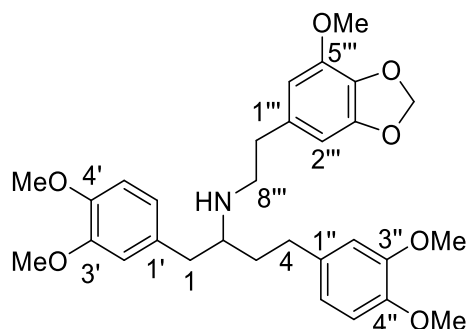


**Figure 2.16:** Schwarzinicine D (4)

Schwarzinicine D (4) was isolated as a light yellowish oil with  $[\alpha]_D^{+5}$  ( $c$  0.38,  $\text{CHCl}_3$ ). The UV spectrum showed absorption maxima (230 and 282 nm) as those of alkaloids 1 – 3. HR-DART-MS measurements revealed the molecular formula  $\text{C}_{30}\text{H}_{37}\text{NO}_7$  based on the  $[\text{M}+\text{H}]^+$  peak detected at  $m/z$  524.2645. The molecular mass of 4 is therefore 30 units higher compared to that of 3, suggesting the presence of an additional methoxy substitution in 4.

The  $^{13}\text{C}$  NMR spectrum of 4 (Table 2.4 and Figure 2.20) showed a general resemblance to that of 3, except that seven oxygenated aromatic carbon resonances were observed in 4, instead of six in 3. Similarly, the  $^1\text{H}$  NMR spectrum of 4 (Table 2.4 and Figure 2.19) was very similar to that of 3, except for the presence of an additional OMe singlet in 4 in place of the  $J = 7.9$  Hz doublet signal due to H-5''' in 3.

As with compounds 1 – 3, the  $\text{CH}_2\text{CHCH}_2\text{CH}_2$  and  $\text{CH}_2\text{CH}_2$  partial structures corresponding to the C-1–C-2–C-3–C-4 and C-7'''–C-8''' fragments in 4 respectively, were obtained from the HSQC and COSY data (Figure 2.17).

The additional OMe group was deduced to be located at C-5''' based on the HMBC correlation observed from MeO-5''' ( $\delta_{\text{H}}$  3.850) to C-5''' ( $\delta_{\text{C}}$  143.38) and the NOESY correlation

observed between MeO-5''' ( $\delta$  3.850) and H-6''' ( $\delta$  6.29) (Figure 2.17). The pair of distinct *meta*-coupled aromatic hydrogens observed at  $\delta$  6.28 and 6.29 ( $J = 1.2$  Hz) were assigned to H-2''' and H-6''' based on the three-bond correlations observed from H-2''' and H-6''' to C-7''' in the HMBC spectrum of **4** (Figure 2.17), which is consistent with a 1,3,4,5-tetrasubstituted phenyl moiety. These observations were also consistent with the NOEs observed for H-2'''/H-7''' and H-6'''/H-7''' in the NOESY spectrum. Schwarzizincine D (**4**) is therefore the 5'''-methoxy derivative of **3**. Finally, chiral HPLC analysis indicated schwarzizincine D (**4**) was isolated as a single enantiomer (Figure 2.18).

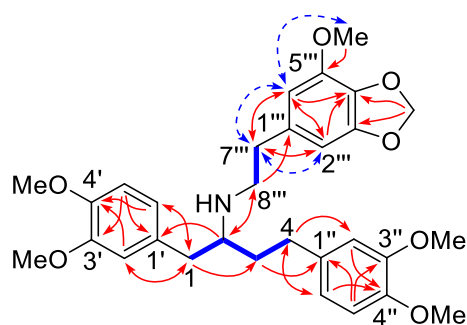
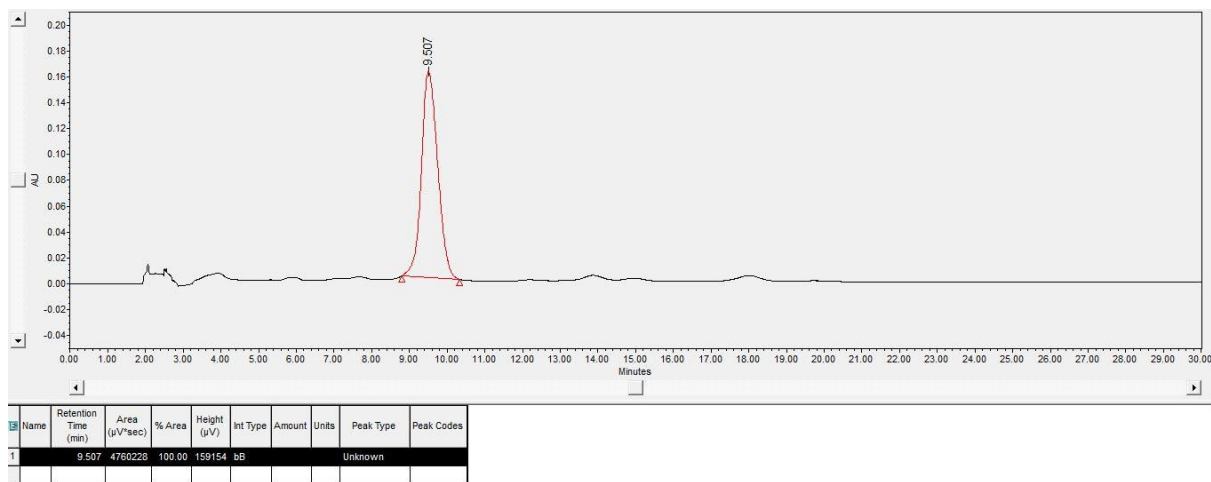


**Figure 2.17:** COSY (blue, bold), selected HMBC (red arrows) and NOESY (blue arrow) correlations of schwarzizincine D (**4**)



Sample concentration (injection volume)	Column	Solvent system	Flow rate
1.2 mg/mL (15.0 µL)	Chiralpak IA column (4.6 × 150 mm)	hexane-EtOH-Et <sub>2</sub> NH, 80:20:0.1	1.0 mL/min

**Figure 2.18:** Chiral HPLC chromatogram of schwarzinicine D (4)

**Table 2.4:** <sup>1</sup>H (600 MHz) and <sup>13</sup>C (150 MHz) NMR spectroscopic data (in CDCl<sub>3</sub> with TMS as internal reference) of schwarzinicine D (4)

Position	δ <sub>H</sub> (mult., <i>J</i> in Hz)	δ <sub>C</sub>
1	2.57, m 2.73, m	40.28
2	2.73, m	58.72
3	1.70, m 1.77, m	35.58
4	2.62, m	31.58
1'		131.56
2'	6.61, m	112.14
3'		148.77 <sup>a</sup>
4'		147.14 <sup>b</sup>
5'	6.78, d (8.6)	111.03 <sup>c</sup>
6'	6.61, m	121.03
1''		134.89
2''	6.67, m <sup>a</sup>	111.64
3''		148.82 <sup>a</sup>
4''		147.42 <sup>b</sup>
5''	6.78, d (8.6)	111.22 <sup>c</sup>
6''	6.68, m <sup>a</sup>	120.05
1'''		134.29
2'''	6.28, d (1.2) <sup>b</sup>	102.37
3'''		148.83 <sup>a</sup>
4'''		133.49
5'''	6.66, d (7.9)	143.38
6'''	6.29, d (1.2) <sup>b</sup>	107.82
7'''	2.62, m	36.44
8'''	2.74, m 2.88, dt (11, 6.5)	48.45
3'-OMe	3.820, s <sup>c</sup>	55.75 <sup>d</sup>
4'-OMe	3.856, s <sup>d</sup>	55.78 <sup>d</sup>
3''-OMe	3.846, s <sup>c</sup>	55.80 <sup>d</sup>
4''-OMe	3.863, s <sup>d</sup>	55.92 <sup>d</sup>
5'''-OMe	3.850, s	55.48 <sup>d</sup>
OCH <sub>2</sub> O	5.93, s	101.27
NH	1.53, br s	

<sup>a-d</sup> Assignments may be interchanged within each column due to overlapping of signals

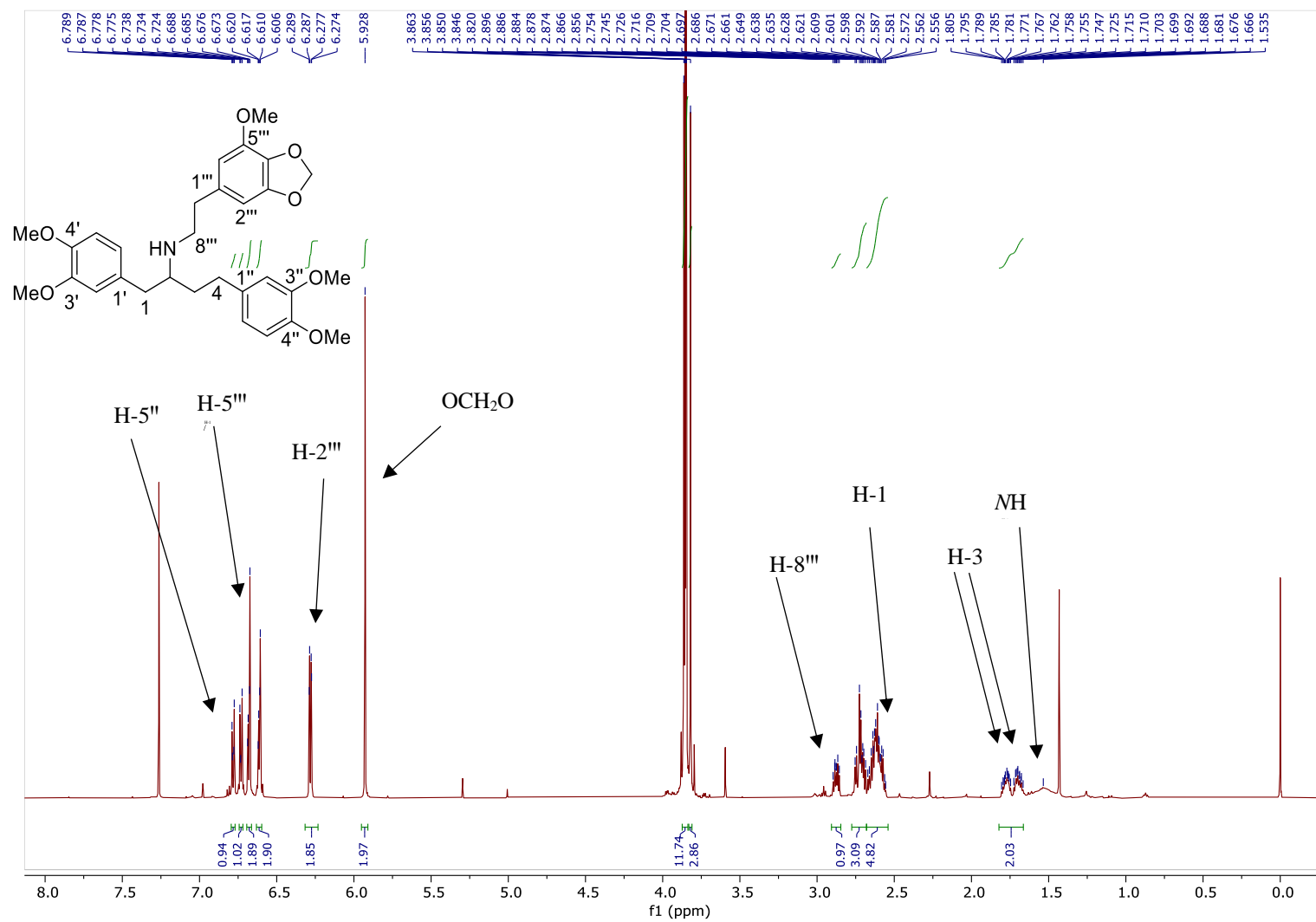


Figure 2.19: <sup>1</sup>H NMR spectrum of schwarzinicine D (4) (CDCl<sub>3</sub>, 600 MHz)

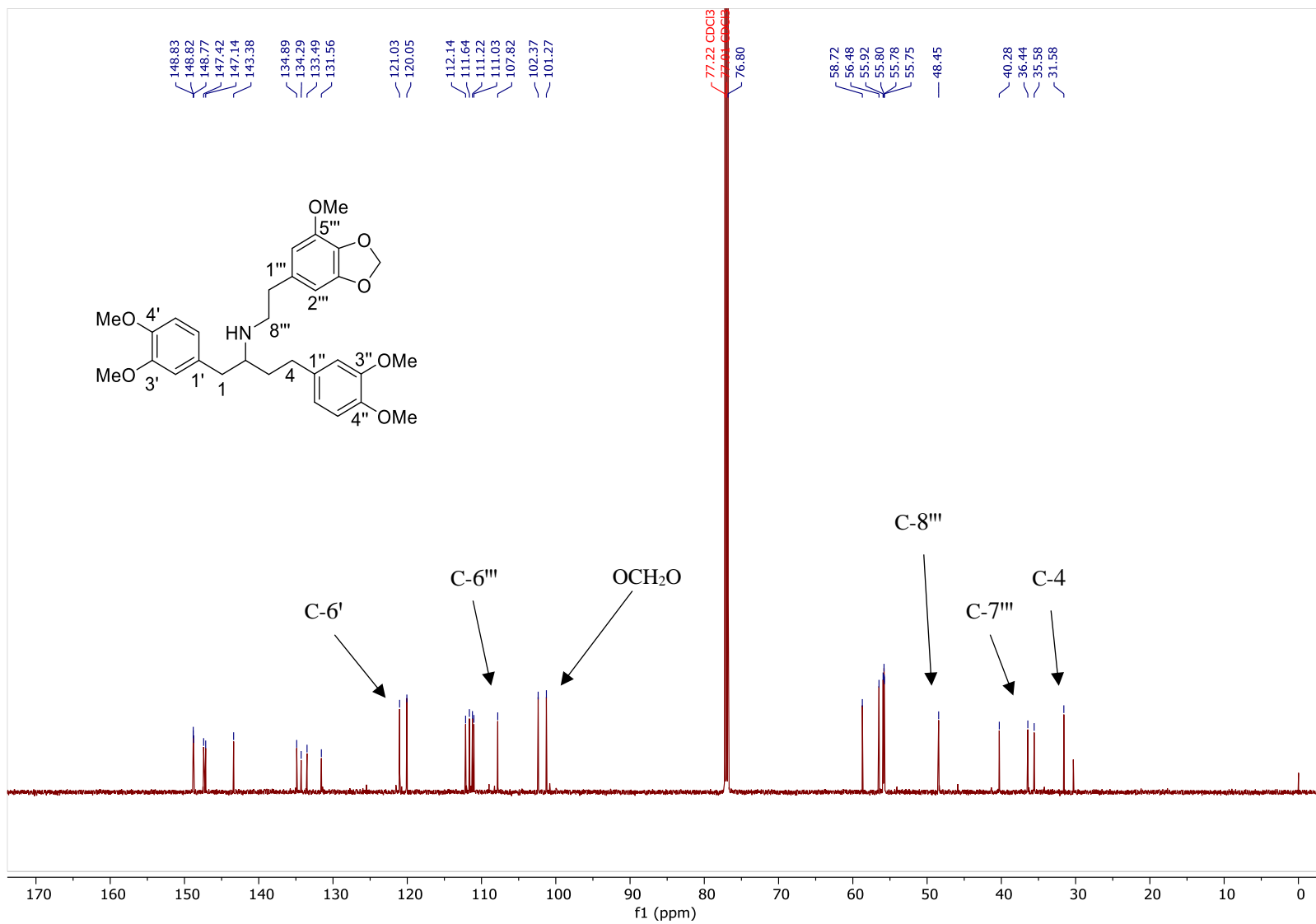
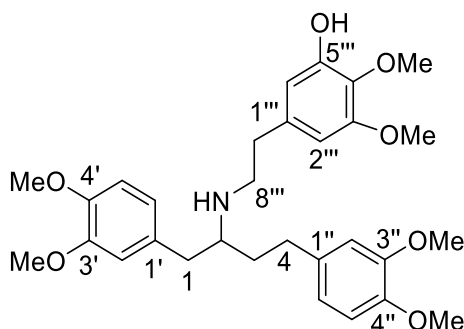


Figure 2.20: <sup>13</sup>C NMR spectrum of schwarzinicine D (4) (CDCl<sub>3</sub>, 150 MHz)

## 2.5 Schwarzinicine E (5)



**Figure 2.21:** Schwarzinicine E (5)

Schwarzinicine E (**5**) was isolated as a light yellowish oil with  $[\alpha]_D^{25} +3$  ( $c$  0.54,  $\text{CHCl}_3$ ). The UV spectrum of **5** was essentially similar to that of **1**. The HR-DART-MS measurements showed an  $[\text{M}+\text{H}]^+$  peak at  $m/z$  526.2777, which established the molecular formula as  $\text{C}_{30}\text{H}_{39}\text{NO}_7$ . The molecular mass of **5** is thus 16 mass units higher than that of **1**, suggesting the presence of an additional hydroxy substitution in **5**.

The  $^{13}\text{C}$  NMR spectrum of **5** (**Table 2.5** and **Figure 2.25**) showed a general resemblance to that of **1**, except that seven oxygenated aromatic carbon resonances were observed in **5**, instead of six in **1**. Similarly, the  $^1\text{H}$  NMR spectrum of **5** (**Table 2.5** and **Figure 2.24**) was very similar to that of **1**, except for the absence of the  $J = 8.1$  Hz doublet signal due to H-5''' in **1**. The HSQC and COSY data also revealed the  $\text{CH}_2\text{CHCH}_2\text{CH}_2$  and  $\text{CH}_2\text{CH}_2$  partial structures attributed to the C-1–C-2–C-3–C-4 and C-7'''–C-8''' fragments in **5**, respectively (**Figure 2.22**).

As in the case of **4**, a pair of distinct *meta*-coupled aromatic protons were observed at  $\delta_{\text{H}}$  6.24 and 6.38<sub>H</sub> ( $J = 1.6$  Hz), which were assigned to H-2''' and H-6''' based on the correlations from H-2''' and H-6''' to C-7''' and from H-7''' to C-2''' and C-6''' in the HMBC spectrum (**Figure 2.22**). This observation was consistent with the presence of a 1,3,4,5-tetrasubstituted phenyl

moiety. The two methoxy groups in this tetrasubstituted phenyl ring were determined to be attached to C-3''' and C-4''' based on the HMBC correlations from H-2''', H-6''', and 4'''-OMe to C-4'''; and from 3'''-OMe to C-3'''. The additional hydroxy group must therefore be located at C-5''', which is consistent with the NOEs observed for H-2'''/H-7''', H-6'''/H-7''', and H-2'''/MeO-3''' in the NOESY spectrum (**Figure 2.22**). Schwarzinicine E (**5**) is therefore the 5'''-hydroxy derivative of **1**. Finally, chiral HPLC analysis indicated schwarzinicine E (**5**) to be a single enantiomer (**Figure 2.23**).

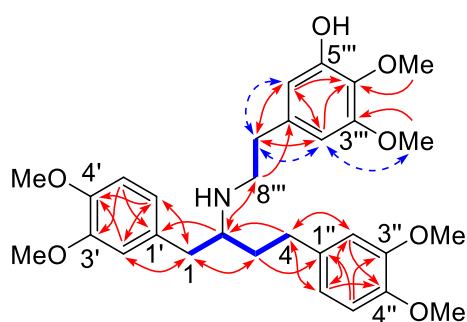
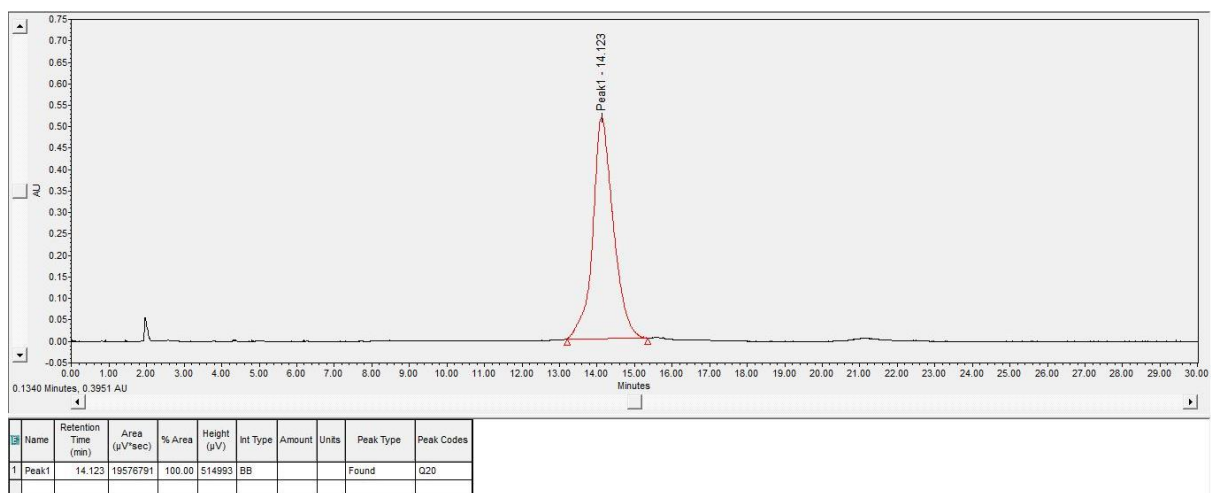


**Figure 2.22:** COSY (blue, bold), selected HMBC (red arrows) and NOESY (blue arrow) correlations of schwarzinicine E (**5**)



Sample concentration (injection volume)	Column	Solvent system	Flow rate
5.7 mg/mL (2.0 µL)	Chiralpak IA column (4.6 × 150 mm)	hexane-EtOH-Et <sub>2</sub> NH, 80:20:0.1	1.0 mL/min

**Figure 2.23:** Chiral HPLC chromatogram of schwarzinicine E (5)

**Table 2.5:**  $^1\text{H}$  (600 MHz) and  $^{13}\text{C}$  (150 MHz) NMR spectroscopic data (in  $\text{CDCl}_3$  with TMS as internal reference) of schwarzinicine E (**5**)

Position	$\delta_{\text{H}}$ (mult., $J$ in Hz)	$\delta_{\text{C}}$
1	2.62, m 2.71, m	40.22
2	2.74, m	58.62
3	1.70, m 1.75, m	35.42
4	2.60, m	31.57
1'		131.64
2'	6.63, m	112.28
3'		148.80 <sup>a</sup>
4'		147.15 <sup>b</sup>
5'	6.74, d (8.1)	111.15
6'	6.62, m	121.08
1''		134.84
2''	6.66, m	111.66
3''		148.84 <sup>a</sup>
4''		147.43 <sup>b</sup>
5''	6.77, d (8.6)	111.25
6''	6.65, m	120.08
1'''		136.00
2'''	6.24, d (1.6)	104.47
3'''		152.27
4'''		133.99
5'''		149.27
6'''	6.38, d (1.6)	108.12
7'''	2.63, m	36.48
8'''	2.76, m 2.87, dt (11, 7.0)	48.17
3'-OMe	3.82, s <sup>a</sup>	55.77 <sup>c</sup>
4'-OMe	3.85, s <sup>b</sup>	55.80 <sup>c</sup>
3''-OMe	3.84, s <sup>a</sup>	55.80 <sup>c</sup>
4''-OMe	3.85, s <sup>b</sup>	55.80 <sup>c</sup>
3'''-OMe	3.85, s	55.82 <sup>c</sup>
4'''-OMe	3.86, s <sup>b</sup>	55.93 <sup>c</sup>
NH	Not observed	

<sup>a-c</sup> Assignments may be interchanged within each column due to overlapping of signals

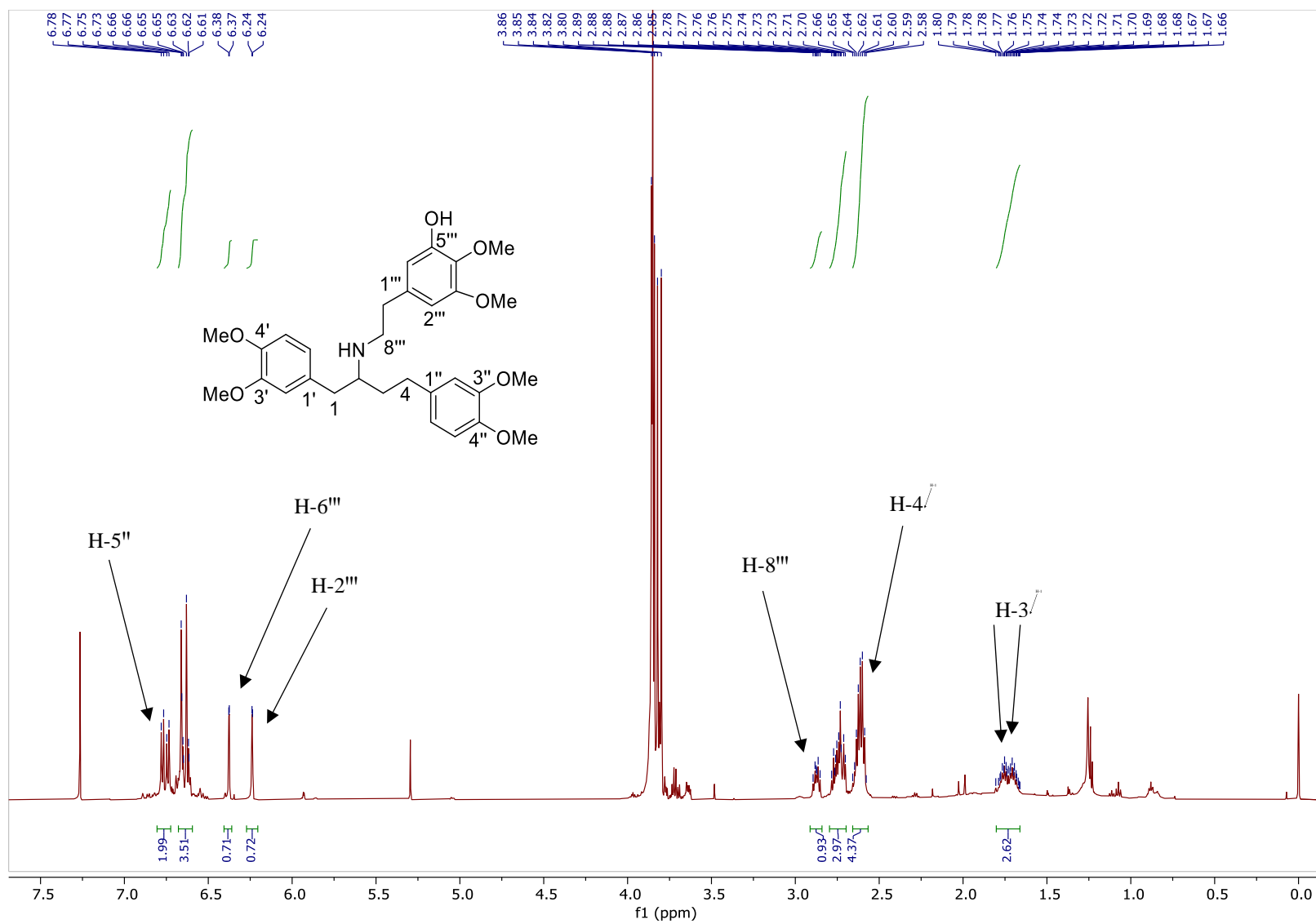
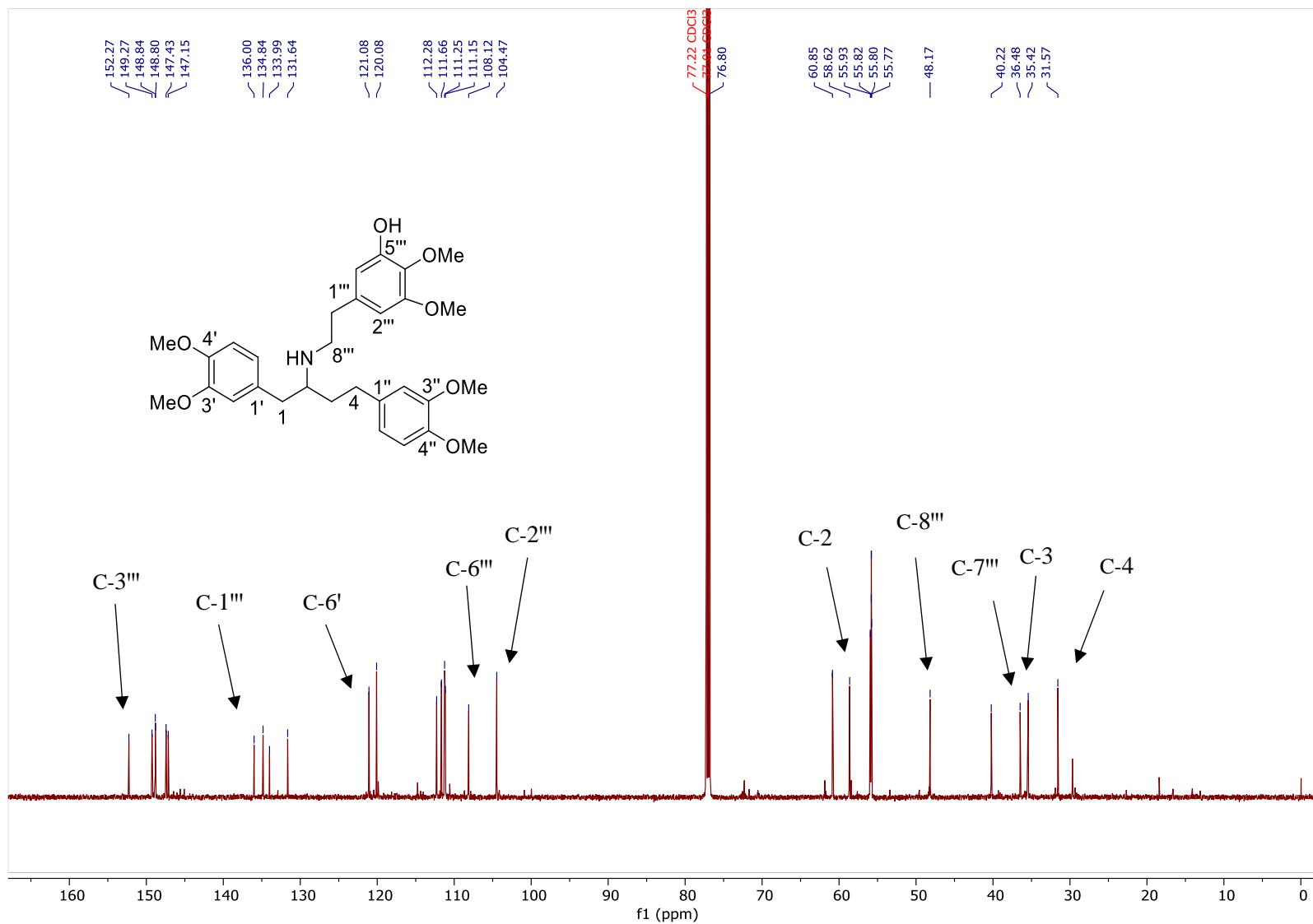
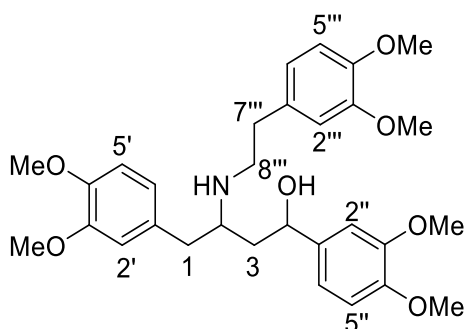


Figure 2.24: <sup>1</sup>H NMR spectrum of schwarzinicine E (5) (CDCl<sub>3</sub>, 600 MHz)



**Figure 2.25:** <sup>13</sup>C NMR spectrum of schwarzinicine E (5) (CDCl<sub>3</sub>, 150 MHz)

## 2.6 Schwarzinicine F (6)



**Figure 2.26:** Schwarzinicine F (6)

Schwarzinicine F (**6**) was isolated as a light yellowish oil with  $[\alpha]_D^{25} +25$  ( $c$  0.22,  $\text{CHCl}_3$ ). The UV spectrum of **6** was similar to those of **1** – **5**, indicating the presence of a similar chromophore. The HR-DART-MS measurements revealed the  $[\text{M}+\text{H}]^+$  peak at  $m/z$  526.2791, which analyzed for  $\text{C}_{30}\text{H}_{39}\text{NO}_7$ , indicating that **6** and **5** are isomers, i.e., **6** has an additional hydroxy substitution compared to **1**.

The  $^1\text{H}$  NMR spectrum of **6** (**Table 2.6** and **Figure 2.29**) showed the conspicuous presence of a deshielded methine signal at  $\delta$  5.07, which was absent in that of **1**. This, coupled with the observation that the number of aromatic proton signals present in the  $^1\text{H}$  NMR spectrum of **6** was the same as that in **1**, suggested that the hydroxy substitution in **6** occurred in the aliphatic backbone of the molecule. Additionally, the  $^{13}\text{C}$  NMR spectrum (**Table 2.6** and **Figure 2.30**) showed a deshielded resonance at  $\delta_{\text{C}}$  71.61, which was attributable to an oxymethine carbon based on the HSQC data. The three-bond correlations from the signal at  $\delta_{\text{H}}$  5.07 to C-2'' and C-6''; from H-2'' and H-6'' to the resonance at  $\delta_{\text{C}}$  71.61; from H-2 to C-4; and from H-4 to C-2, indicated the benzylic C-4 as the site of hydroxy substitution (**Figure 2.27**).

This is also consistent with the COSY spectrum, which revealed the presence of the  $\text{OCHCH}_2\text{CH}(\text{N})\text{CH}_2$  and  $\text{CH}_2\text{CH}_2$  partial structures corresponding to the C-4–C-3–C-2–C-1

and C-7'''–C-8''' fragments in **6**, respectively (**Figure 2.27**). Schwarzinicine F (**6**) is therefore the 4-hydroxy derivative of **1** and its planar structure was in full agreement with the HMBC data (**Figure 2.27**).

Chiral HPLC analysis of schwarzinicine F (**6**) established it as a single enantiomer (**Figure 2.28**). However, its relative configuration could not be determined via analysis of the NOESY data as the molecule displays high conformational flexibility. Stereochemical assignments based on derivatization of **6** was also precluded due to poor isolation yield. It was observed that **6** was less stable and prone to degradation in solution in comparison to compounds **1** – **5**, likely due to the presence of the relatively more reactive benzyl alcohol group in **6**.

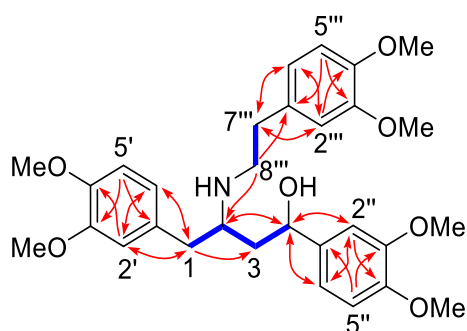
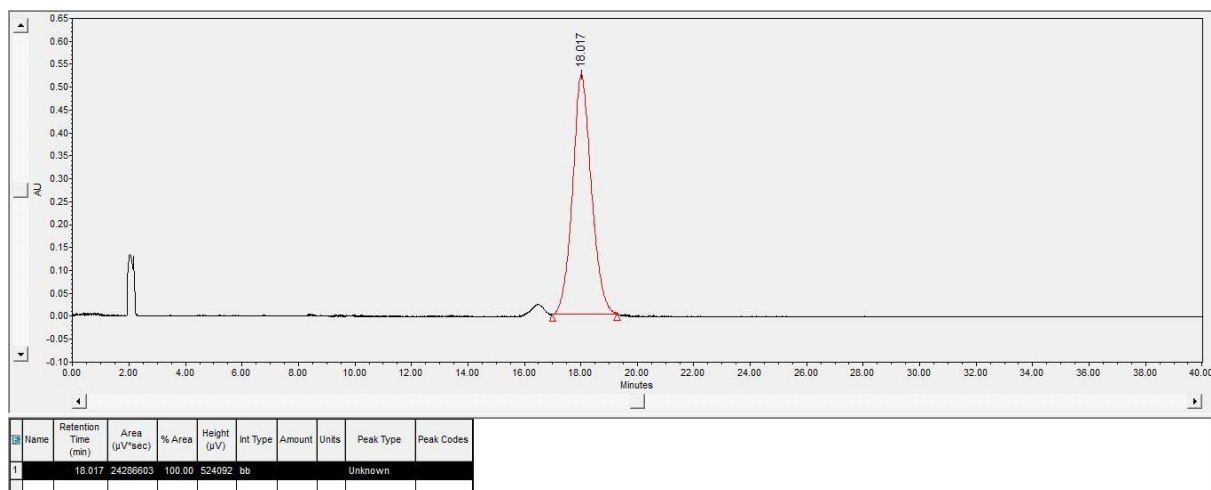


**Figure 2.27:** COSY (blue, bold) and selected HMBC (red arrows) correlations of schwarzinicine F (**6**)



Sample concentration (injection volume)	Column	Solvent system	Flow rate
1.2 mg/mL (20.0 μL)	Chiralpak IA column (4.6 × 150 mm)	hexane-EtOH-Et <sub>2</sub> NH, 90:10:0.1	1.0 mL/min

**Figure 2.28:** Chiral HPLC chromatogram of schwarzinicine F (6)

**Table 2.6:**  $^1\text{H}$  (600 MHz) and  $^{13}\text{C}$  (150 MHz) NMR spectroscopic data (in  $\text{CDCl}_3$  with TMS as internal reference) of schwarzinicine F (**6**).

Position	$\delta_{\text{H}}$ (mult., $J$ in Hz)	$\delta_{\text{C}}$
1	2.72, dd (13.7, 6.2) 2.82, dd (13.7, 7.9)	39.27
2	3.00, m	57.64
3	1.69, ddd (14.5, 5.8, 2.8) 1.96, ddd (14.5, 8.3, 3.2)	38.96
4	5.07, dd (8.3, 2.8)	71.61
1'		130.55
2'	6.56, d (1.8)	111.97
3'		148.96
4'		147.67 <sup>a</sup>
5'	6.70, d (8.1) <sup>a</sup>	111.15 <sup>b</sup>
6'	6.54, dd (8.1, 1.8)	120.92
1''		138.01
2''	6.90, br s	108.83
3''		148.83
4''		147.57
5''	6.82, m	110.92
6''	6.82, m	117.41
1'''		131.58
2'''	6.60, d (1.8)	111.72
3'''		148.96
4'''		147.75 <sup>a</sup>
5'''	6.74, dd (8.1) <sup>a</sup>	111.21 <sup>b</sup>
6'''	6.60, dd (8.1, 1.8)	120.45
7'''	2.65, m 2.99, m	35.68
8'''	2.78, m 3.00, m	48.41
3'-OMe	3.81, s <sup>b</sup>	55.80 <sup>c</sup>
4'-OMe	3.85, s <sup>b</sup>	55.81 <sup>c</sup>
3''-OMe	3.87, s <sup>b</sup>	55.81 <sup>c</sup>
4''-OMe	3.87, s <sup>b</sup>	55.81 <sup>c</sup>
3'''-OMe	3.87, s <sup>b</sup>	55.85 <sup>c</sup>
4'''-OMe	3.87, s <sup>b</sup>	55.93 <sup>c</sup>
NH	1.67, br s	

<sup>a-c</sup> Assignments may be interchanged within each column due to overlapping of signals

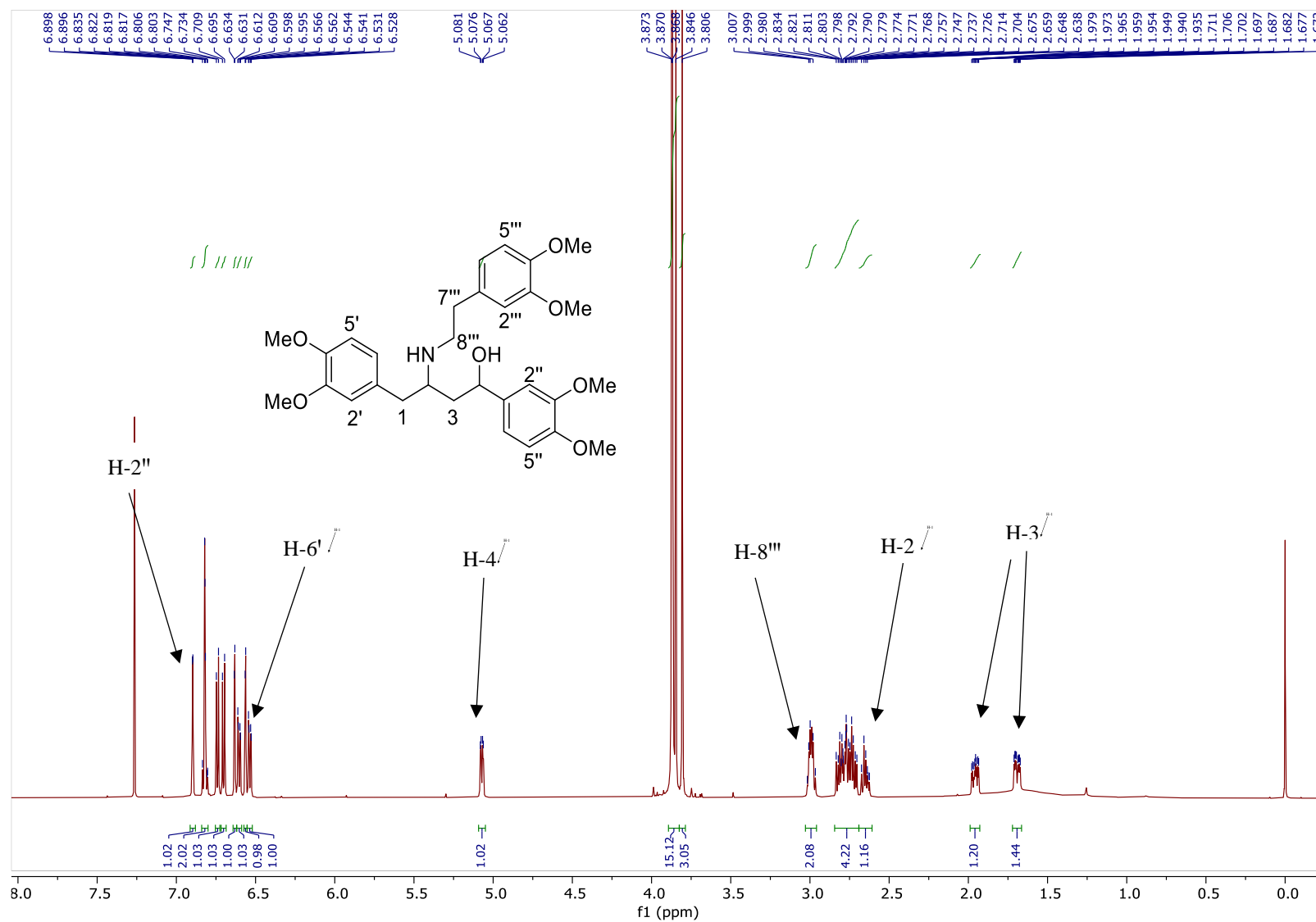


**Figure 2.29:**  $^1\text{H}$  NMR spectrum of schwarzinicine F (6) ( $\text{CDCl}_3$ , 600 MHz)

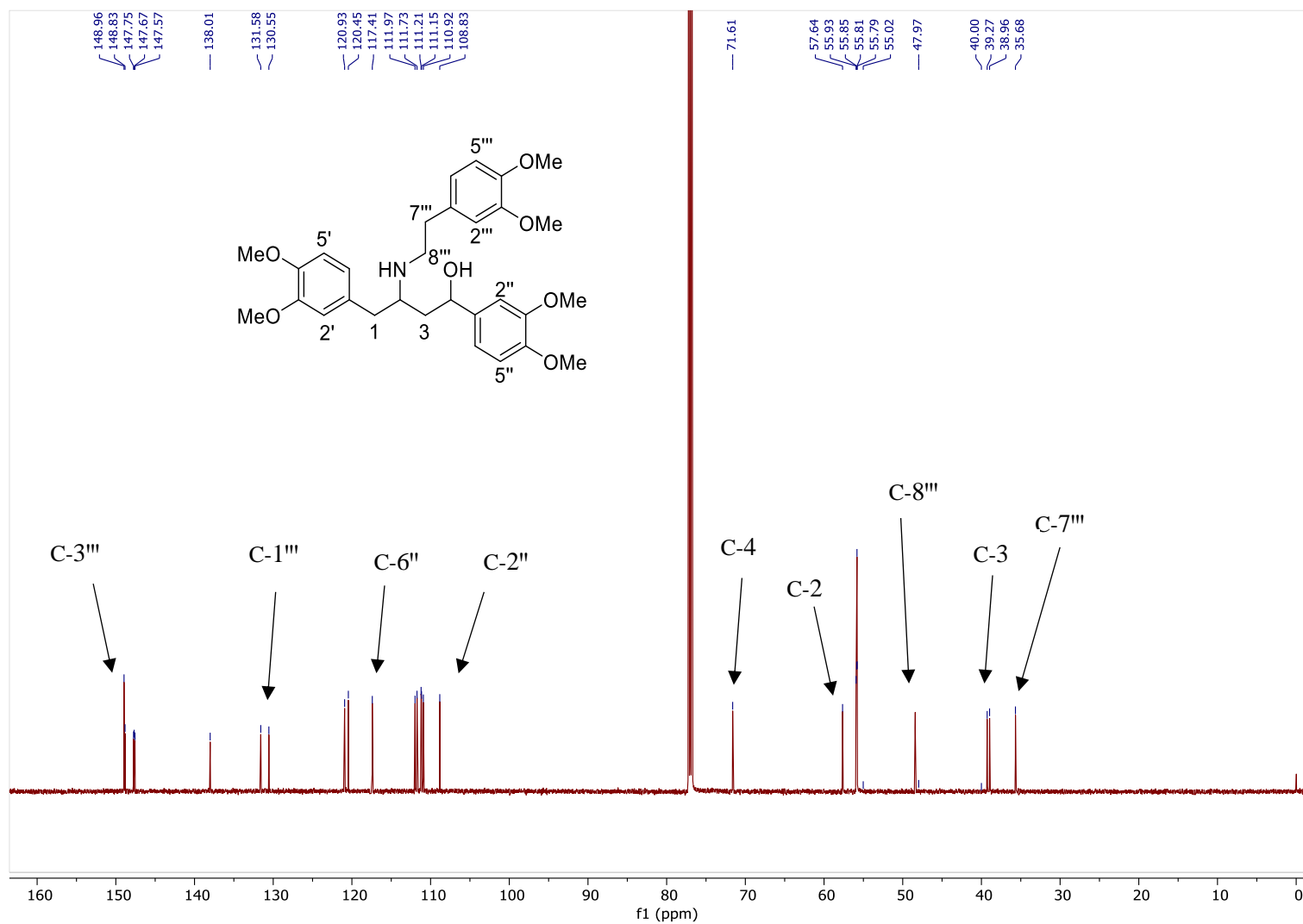
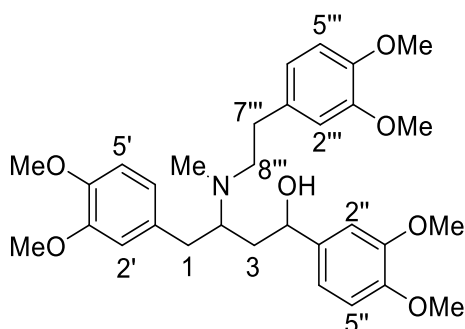


Figure 2.30: <sup>13</sup>C NMR spectrum of schwarzincine F (6) (CDCl<sub>3</sub>, 150 MHz)

## 2.7 Schwarzinicine G (7)



**Figure 2.31:** Schwarzinicine G (7)

Schwarzinicine G (**7**) was isolated as a light yellowish oil with  $[\alpha]_D^{25} -13$  ( $c$  0.35,  $\text{CHCl}_3$ ). The UV spectrum of **7** was similar to those of **1** – **6**, indicating the presence of a similar chromophore. The HR-DART-MS measurements revealed the molecular formula  $\text{C}_{31}\text{H}_{41}\text{NO}_7$  for **7** based on the  $[\text{M}+\text{H}]^+$  peak detected at  $m/z$  540.2966. This indicated that **7** is 14 mass units higher than **6**, suggesting the presence of an additional methyl substitution in **7** when compared to **6**. The HSQC and COSY data (**Figure 2.32**) showed the presence identical  $\text{CH}_2\text{CH}_2$  and  $\text{CH}_2\text{CHCH}_2\text{CH}_2$  partial structures present in **1** – **6**.

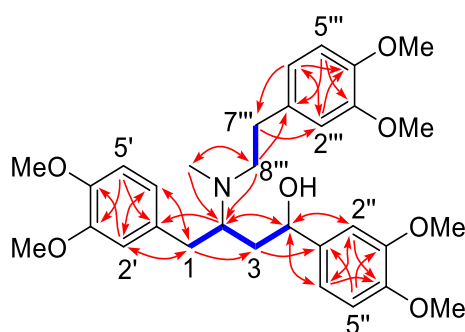
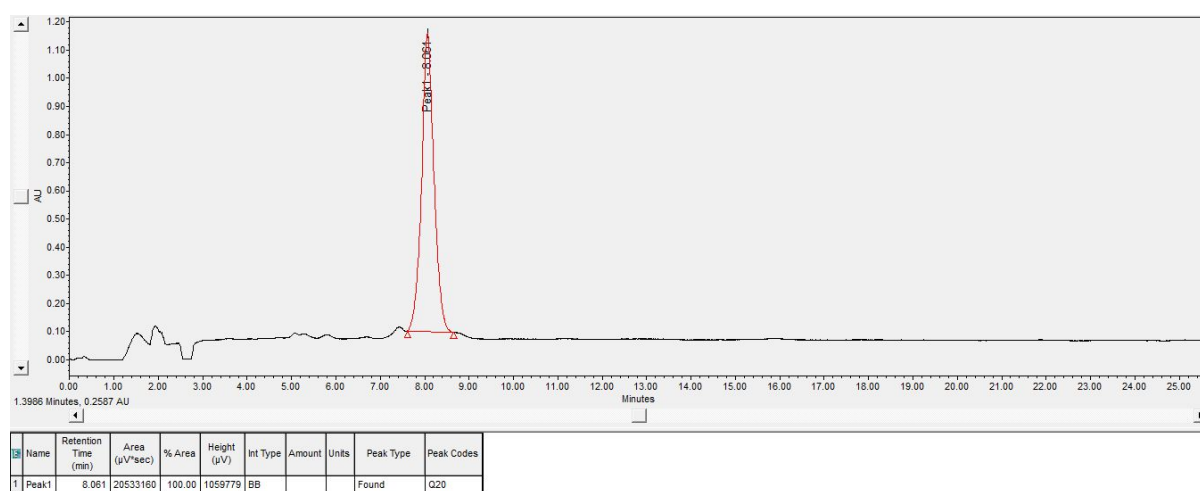


**Figure 2.32:** COSY (blue, bold) and selected HMBC (red arrows) correlations of schwarzinicine G (**7**)

The  $^{13}\text{C}$  and  $^1\text{H}$  NMR spectra of **7** (Table 2.7, Figures 2.34 and 2.35) largely resemble those of **6**, except for the presence of an additional *N*Me group ( $\delta_{\text{C}}$  36.48,  $\delta_{\text{H}}$  2.44) in **7**. Schwarzinicine G (**7**) is therefore deduced to be the *N*Me derivative of **6** and its planar structure was in complete agreement with the HMBC data (Figure 2.32).

Chiral HPLC analysis of schwarzinicine G (**7**) indicated it as a single enantiomer (Figure 2.33). As with the case of **6**, the stereochemical assignments of **7** could not be established due to high conformational flexibility, low isolation yield and degradation.



Sample concentration (injection volume)	Column	Solvent system	Flow rate
2.8 mg/mL (10.0 $\mu\text{L}$ )	Chiralpak IA column (4.6 $\times$ 150 mm)	hexane-EtOH-Et <sub>2</sub> NH, 80:20:0.1	1.0 mL/min

**Figure 2.33:** Chiral HPLC chromatogram of schwarzinicine G (**7**)

**Table 2.7:**  $^1\text{H}$  (600 MHz) and  $^{13}\text{C}$  (150 MHz) NMR spectroscopic data (in  $\text{CDCl}_3$  with TMS as internal reference) of schwarzinicine G (7)

Position	$\delta_{\text{H}}$ (mult., $J$ in Hz)	$\delta_{\text{C}}$
1	2.25, dd (13.5, 11.5) 2.83, m	32.49
2	2.83, m	62.43
3	1.61, br d (15) 2.12, ddd (15, 11.3, 4)	34.56
4	4.91, t (4)	72.16
1'		131.69
2'	6.36, d (1.7)	111.82
3'		148.79 <sup>a</sup>
4'		147.60 <sup>b</sup>
5'	6.70, d (8.1)	111.13
6'	6.44, dd (8.1, 1.7)	120.94
1''		137.72
2''	6.64, d (1.6)	108.47
3''		148.55 <sup>a</sup>
4''		147.24 <sup>b</sup>
5''	6.74, d (8.6)	110.67
6''	6.60, dd (8.6, 1.6)	117.17
1'''		132.42
2'''	6.73, m	112.07
3'''		149.00 <sup>a</sup>
4'''		147.28 <sup>b</sup>
5'''	6.83, d (8.1)	111.40
6'''	6.75, dd (8.1, 1.9)	120.57
7'''	2.77, m	34.71
8'''	2.57, m 2.91, m	55.88
3'-OMe	3.71, s <sup>a</sup>	55.59 <sup>c</sup>
4'-OMe	3.84, s <sup>b</sup>	55.92 <sup>c</sup>
3''-OMe	3.73, s <sup>a</sup>	55.74 <sup>c</sup>
4''-OMe	3.86, s <sup>b</sup>	55.88 <sup>c</sup>
3'''-OMe	3.90, s <sup>a</sup>	55.88 <sup>c</sup>
4'''-OMe	3.87, s <sup>b</sup>	55.96 <sup>c</sup>
NMe	2.44, s	37.48

<sup>a-c</sup> Assignments may be interchanged within each column due to overlapping of signals

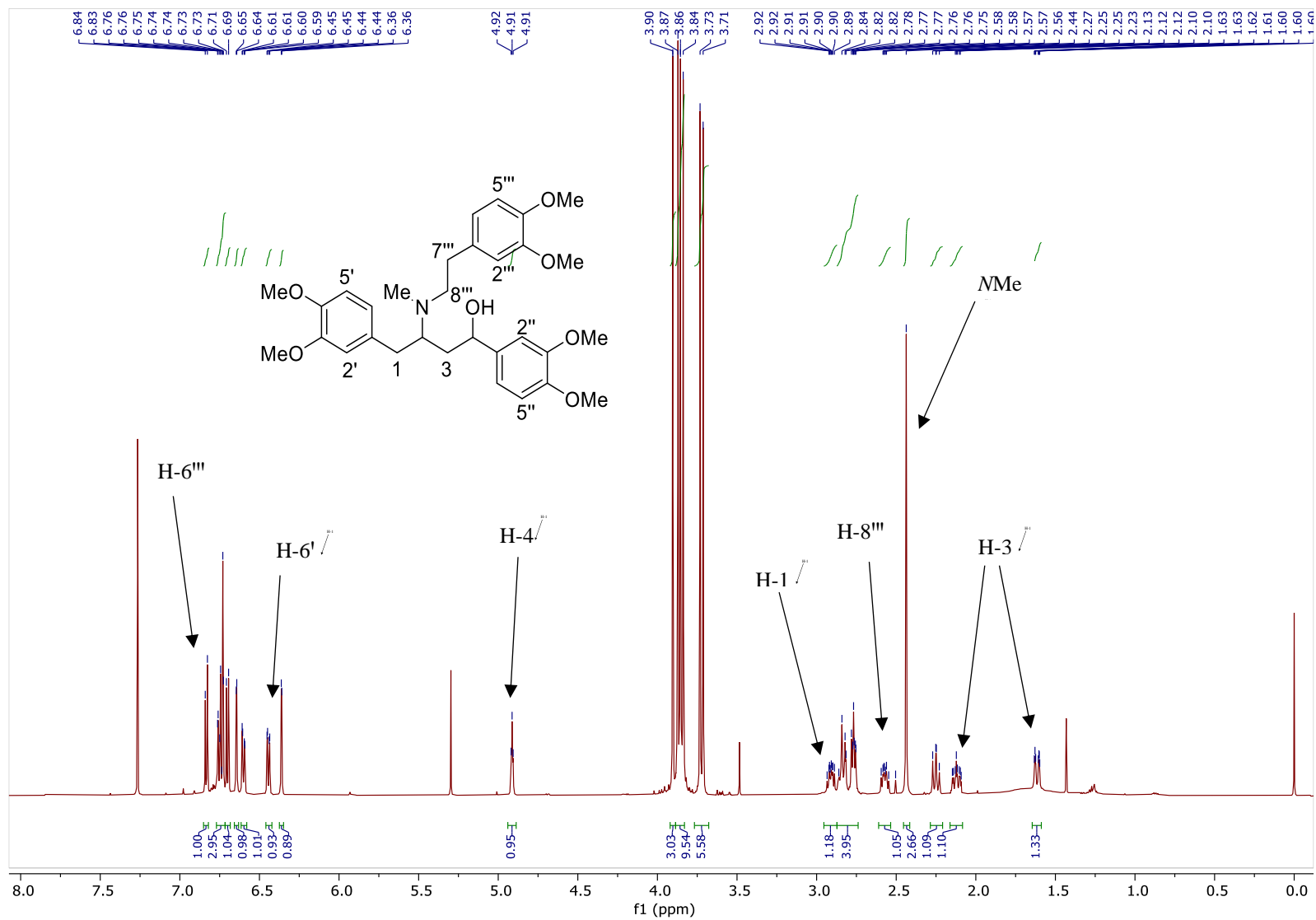


Figure 2.34:  $^1\text{H}$  NMR spectrum of schwarzinicine G (7) ( $\text{CDCl}_3$ , 600 MHz)

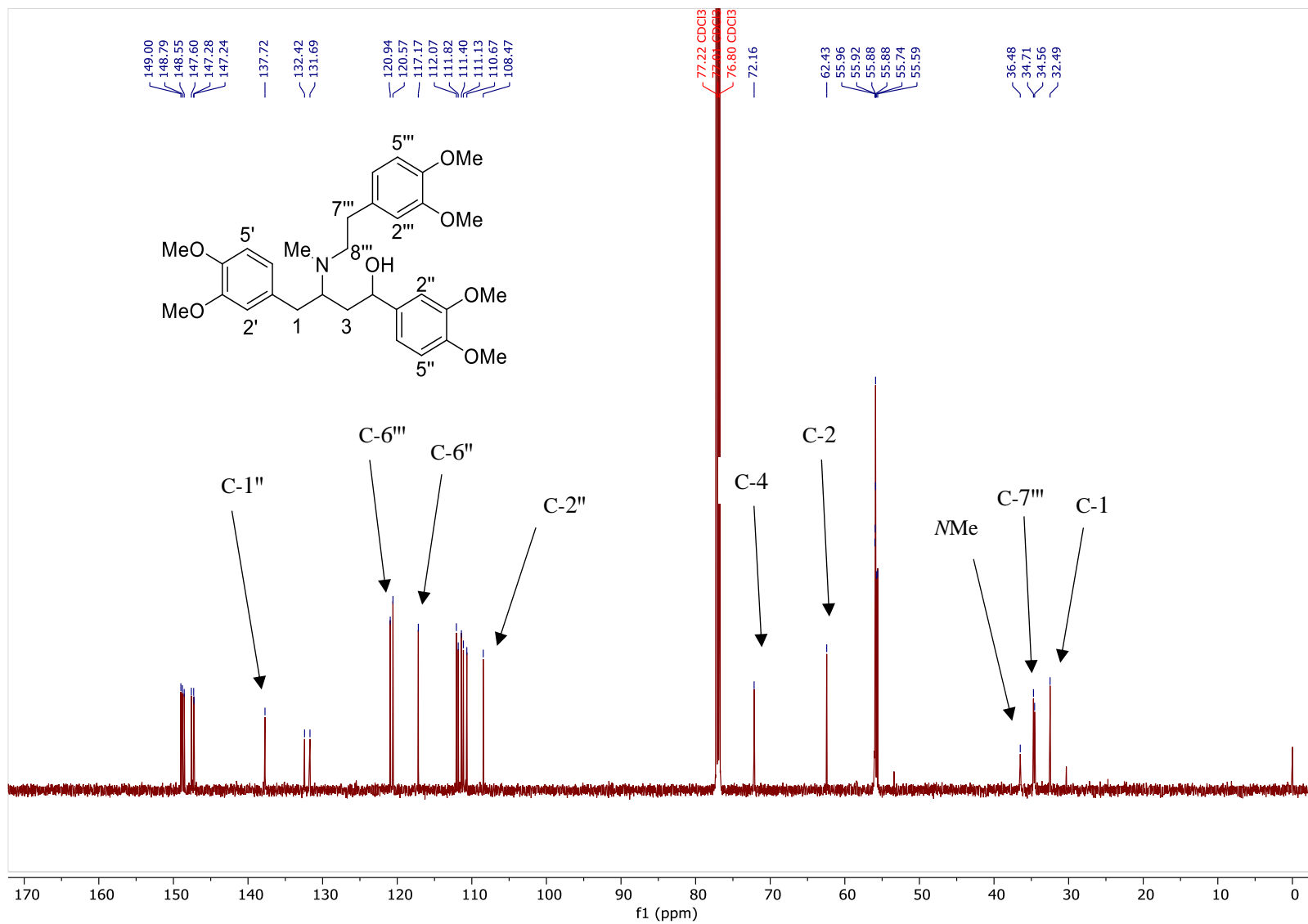
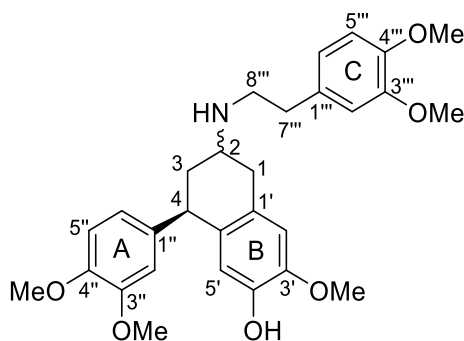


Figure 2.35: <sup>13</sup>C NMR spectrum of schwarzinicine G (7) (CDCl<sub>3</sub>, 150 MHz)

## 2.8 Schwarzificusine A and Schwarzificusine B (8 and 9)



**Figure 2.36:** Schwarzificusine A (**8**) and schwarzificusine B (**9**)

Schwarzificusine A (**8**) was obtained as a light yellowish oil with  $[\alpha]_D +14$  ( $c$  0.12,  $\text{CHCl}_3$ ). The UV spectrum showed absorption maxima at 230 and 281 nm, characteristic of a 3,4-dimethoxyphenyl chromophore. The IR spectrum showed the presence an absorption band  $3391\text{ cm}^{-1}$ , attributable to OH/NH function. The HR-DART-MS measurements revealed the  $[\text{M}+\text{H}]^+$  peak at  $m/z$  494.2544, which established the molecular formula of **8** as  $\text{C}_{29}\text{H}_{35}\text{NO}_6$ . The molecular formula also inferred the presence of an additional degree of unsaturation in the structure of **8** when compared to **1**.

The  $^{13}\text{C}$  NMR spectrum (**Table 2.8** and **Figure 2.40**) gave a total of 29 carbon resonances comprising five methyl carbons, four methylene carbons, ten methine carbons, six oxygenated aromatic carbons, and four aromatic quaternary carbons, in agreement with the molecular formula. Of the 29 resonances, 18 were found in the downfield region between  $\delta_{\text{C}}$  110 and 150, consistent with the presence of three aromatic rings in **8**. Additionally, the  $^{13}\text{C}$  spectrum also revealed the presence of five methoxy carbon resonances. The  $^1\text{H}$  NMR spectrum (**Table 2.8** and **Figure 2.39**) showed the presence of eight aromatic proton signals, six of which were due to two sets of 1,3,4-trisubstituted aryl rings, while the remaining two

aromatic singlet signals were due to a 1,2,4,5-tetrasubstituted aryl ring ( $\delta_C$  6.29 and 6.47). The  $^1H$  NMR also revealed the presence of five aromatic OMe groups.

The COSY data (**Figure 2.37**) revealed the presence of the  $CH_2CHCH_2CH$  and  $CH_2CH_2$  partial structures corresponding to the C-1–C-2–C-3–C-4 and C-7'''–C-8''' fragments in **8**, suggesting that **8** possesses a similar carbon framework to compounds **1** – **7** with a slight departure. The attachment of aryl ring A to C-4 was deduced from the three-bond correlations observed from H-3 to C-1''; from H-4 to C-6'' and C-2''; and from H-2'' and H-6'' to C-4 in the HMBC spectrum (**Figure 2.37**). Aryl ring B on the other hand was connected from C-1' to C-1 based on the three-bond correlations observed from H-1 to C-2' and C-6'; and from H-2' to C-1 and C-6', while the attachment from C-4 to C-6' was deduced based on the correlations observed from H-5' to C-1 and C-4. This indicated that aryl ring B is 1,2,4,5-tetrasubstituted, which is consistent with H-2' and H-5' being observed as singlet signals at  $\delta_H$  6.29 and 6.47, respectively. As with compounds **1** – **7**, the phenethylamine moiety was presumed to be branched from C-2. The five OMe groups were established to be attached to C-3', C-3'', C-5'', C-3''', and C-5''' based on the HMBC correlations observed from the OMe groups to the aromatic carbons they attached to. The remaining oxygenated aromatic C-4' was therefore deduced to be hydroxy substituted. The location of the hydroxyl group is also in agreement with the NOESY and 1D NOE difference data, which showed NOEs for 3'-OMe/H-2', H-1/H-2', 3''-OMe/H-2'', 4''-OMe/H-5'', 3'''-OMe/H-2''', and 4'''-OMe/H-5'''. In other words, the absence of NOE between H-5' and an aromatic methoxy group inferred that C-4' is the site of hydroxylation in **8**. The 2D structure proposed for compound **8** is entirely consistent with the HMBC data, and **8** is essentially a 4,6'-cyclic analogue of a 4'-O-demethyl derivative of schwarzinicine A (**1**).

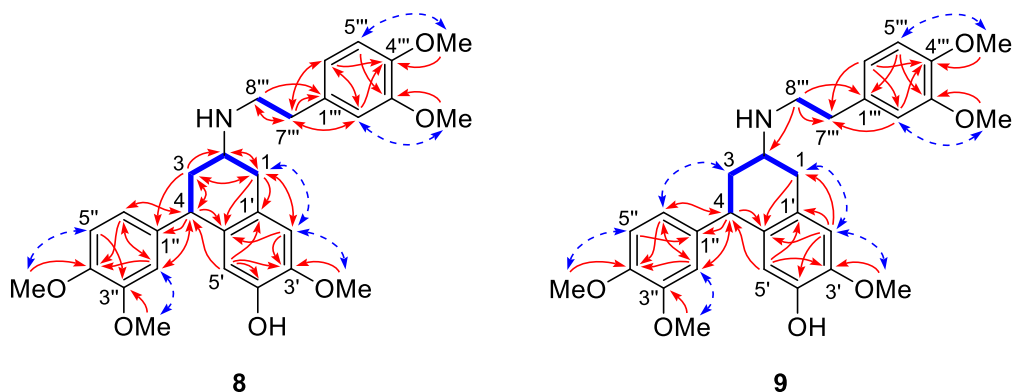


**Figure 2.37:** COSY (blue bold bonds), selected HMBC (red arrows) and selected NOE (blue arrows) correlations of schwarzificusines A and B (**8** and **9**)

Schwarzificusine B (**9**) was isolated as a light yellowish oil with  $[\alpha]_D +22$  ( $c$  0.21,  $\text{CHCl}_3$ ). The UV spectrum of **9** was similar to those of **1** – **8** indicating the presence of a similar chromophore. The IR spectrum showed the presence of OH ( $3421\text{ cm}^{-1}$ ) and NH ( $3270\text{ cm}^{-1}$ ) functions. The HR-DART-MS measurements established the molecular formula of **9** as  $\text{C}_{29}\text{H}_{35}\text{NO}_6$  based on the  $[\text{M}+\text{H}]^+$  peak detected at  $m/z$  494.2528, thus indicating that **9** is isomeric with **8**. Furthermore, the  $^{13}\text{C}$  and  $^1\text{H}$  NMR spectra of **9** (Table 2.8, Figures 2.41 and 2.42) were largely similar to those of **8**, except for the butanoid fragment at  $\text{CH}_2$ -1, CH-2, and  $\text{CH}_2$ -3.

The COSY data (Figure 2.37) of **9** revealed the presence of identical partial structures as in the case of **8**, i.e.,  $\text{CH}_2\text{CHCH}_2\text{CH}$  and  $\text{CH}_2\text{CH}_2$ . Additionally, detailed analysis of the HMBC and NOESY data of **9** also established a 2D structure that was identical to that of **8** (Figure 2.37). Since both schwarzificusines A and B (**8** and **9**) do not have identical NMR spectra, they were deduced to be diastereomeric.

Unfortunately, the relative configuration of both **8** and **9** could not be determined with certainty via analysis of the NOE data due to overlapping of some key signals. Furthermore,

due to low isolation yield and sample degradation, chiral HPLC analysis and stereochemical assignments based on derivatization were also precluded. Nonetheless, since the  $^1\text{H}$  and  $^{13}\text{C}$  NMR data for CH-4 for both **8** and **9** were remarkably similar (i.e.,  $\delta_{\text{H}}$  3.90 dd ( $J = 12.2, 5.2$  Hz),  $\delta_{\text{C}}$  45.00 for **8**;  $\delta_{\text{H}}$  3.91 dd ( $J = 12.1, 5.5$  Hz),  $\delta_{\text{C}}$  45.66 for **9**), the relative stereochemistry at C-4 for both compounds was deduced to be identical. The large coupling constant observed for H-4 ( $J = 12$  Hz) in both compounds indicated that H-4 is *trans*-diaxial to one of the two geminal protons at C-3 (**Figure 2.38**). In other words, the aryl ring A in **8** and **9** must be equatorially oriented at C-4 since H-4 is axially oriented. Therefore, as far as the relative stereochemistry is concerned, the point of difference between **8** and **9** is the configuration at C-2. This deduction is also consistent with the observations that the  $^1\text{H}$  and  $^{13}\text{C}$  NMR data of **8** and **9** (**Table 2.8**) are largely similar, except for the signals due to CH<sub>2</sub>-1, CH-2, and CH<sub>2</sub>-3. The two possible 3-D diastereomeric structures for schwarzifiscusines A and B (**8** and **9**) are shown in **Figure 2.38**.

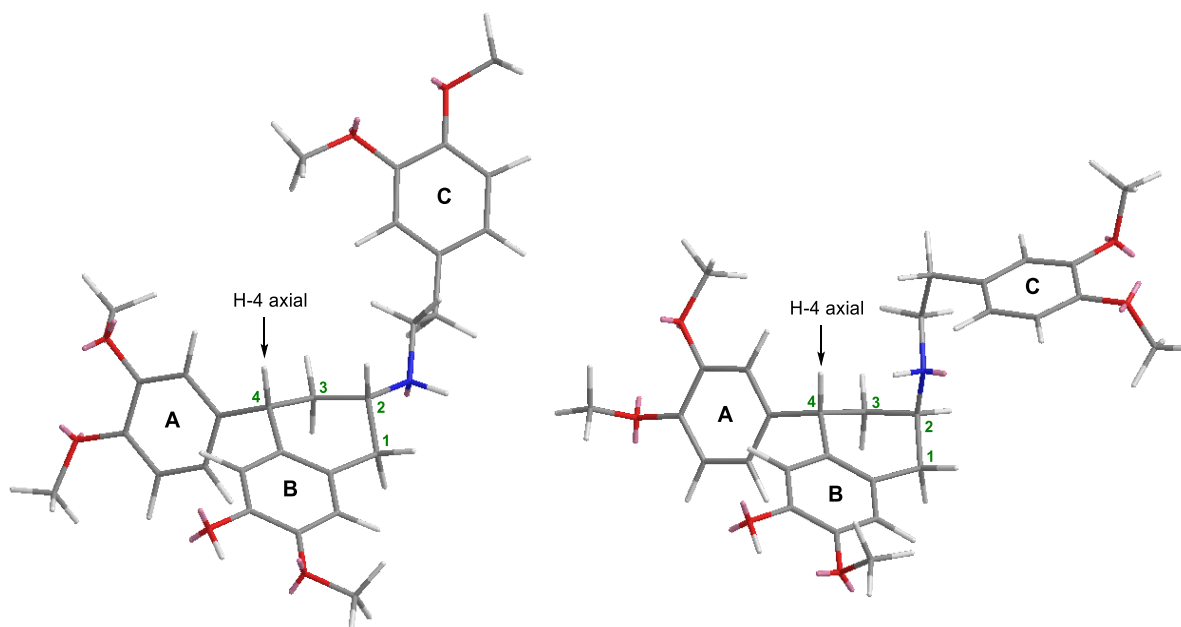


**Figure 2.38:** Diastereomeric structures proposed for **8** and **9**; stereochemistry shown is relative

**Table 2.8:**  $^1\text{H}$  (600 MHz) and  $^{13}\text{C}$  (150 MHz) NMR spectroscopic data (in  $\text{CDCl}_3$  with TMS as internal reference) of schwarzificusine A (**8**) and schwarzificusine B (**9**)

Position	Schwarzificusine A ( <b>8</b> )		Schwarzificusine B ( <b>9</b> )	
	$\delta_{\text{H}}$ (mult., $J$ in Hz)	$\delta_{\text{C}}$	$\delta_{\text{H}}$ (mult., $J$ in Hz)	$\delta_{\text{C}}$
1	3.12, m 3.39, m	32.39	2.72, m 3.01, m	37.17
2	3.54, m	55.23	3.04, m	54.27
3	2.26, q (12.0) 2.73, d (12.0)	35.94	1.68, m 2.29, d (11)	40.62
4	3.90, dd (12.0, 5.2) (axial)	45.00	3.91, dd (12.1, 5.5) (axial)	45.66
1'	-	123.48	-	126.65
2'	6.47, s	110.54	6.56, s	110.70
3'	-	144.29	-	145.08
4'	-	145.45	-	143.72
5'	6.29, s	114.69	6.33, s	114.80
6'	-	131.13	-	132.17 <sup>a</sup>
1''	-	136.73	-	138.70
2''	6.60, d (1.5)	111.52	6.62, d (1.9)	111.59
3''	-	148.99 <sup>a</sup>	-	148.96 <sup>b</sup>
4''	-	147.84 <sup>b</sup>	-	147.53 <sup>c</sup>
5''	6.61, d (8.2)	111.39 <sup>c</sup>	6.79, d (8.2)	111.37 <sup>d</sup>
6''	6.64, dd (8.2, 1.5)	120.58	6.71, dd (8.2, 1.9)	120.74
1'''	-	128.90	-	132.36 <sup>a</sup>
2'''	6.73, m	111.75	6.75, m	111.98
3'''	-	149.13 <sup>a</sup>	-	149.07 <sup>b</sup>
4'''	-	148.08 <sup>b</sup>	-	147.61 <sup>c</sup>
5'''	6.76, d (8.1)	111.19 <sup>c</sup>	6.81, d (7.9)	111.21 <sup>d</sup>
6'''	6.72, m	120.72	6.76, m	120.56
7'''	3.27, m	32.81	2.81, m	35.89
8'''	3.09, m 3.24, m	46.73	3.00, m	48.22
3'-OMe	3.73, s	55.75 <sup>d</sup>	3.85, s	55.84 <sup>e</sup>
3''-OMe	3.76, s	55.82 <sup>d</sup>	3.79, s	55.80 <sup>e</sup>
4''-OMe	3.77, s	55.96 <sup>d</sup>	3.86, s	55.87 <sup>e</sup>
3'''-OMe	3.83, s	55.85 <sup>d</sup>	3.87, s	55.92 <sup>e</sup>
4'''-OMe	3.85, s	55.91 <sup>d</sup>	3.86, s	55.92 <sup>e</sup>
NH	1.68, br s	-	1.57, br s	-
OH	5.39, br s	-	5.41, br s	-

<sup>a-c</sup> Assignments may be interchanged due to overlapping of signals

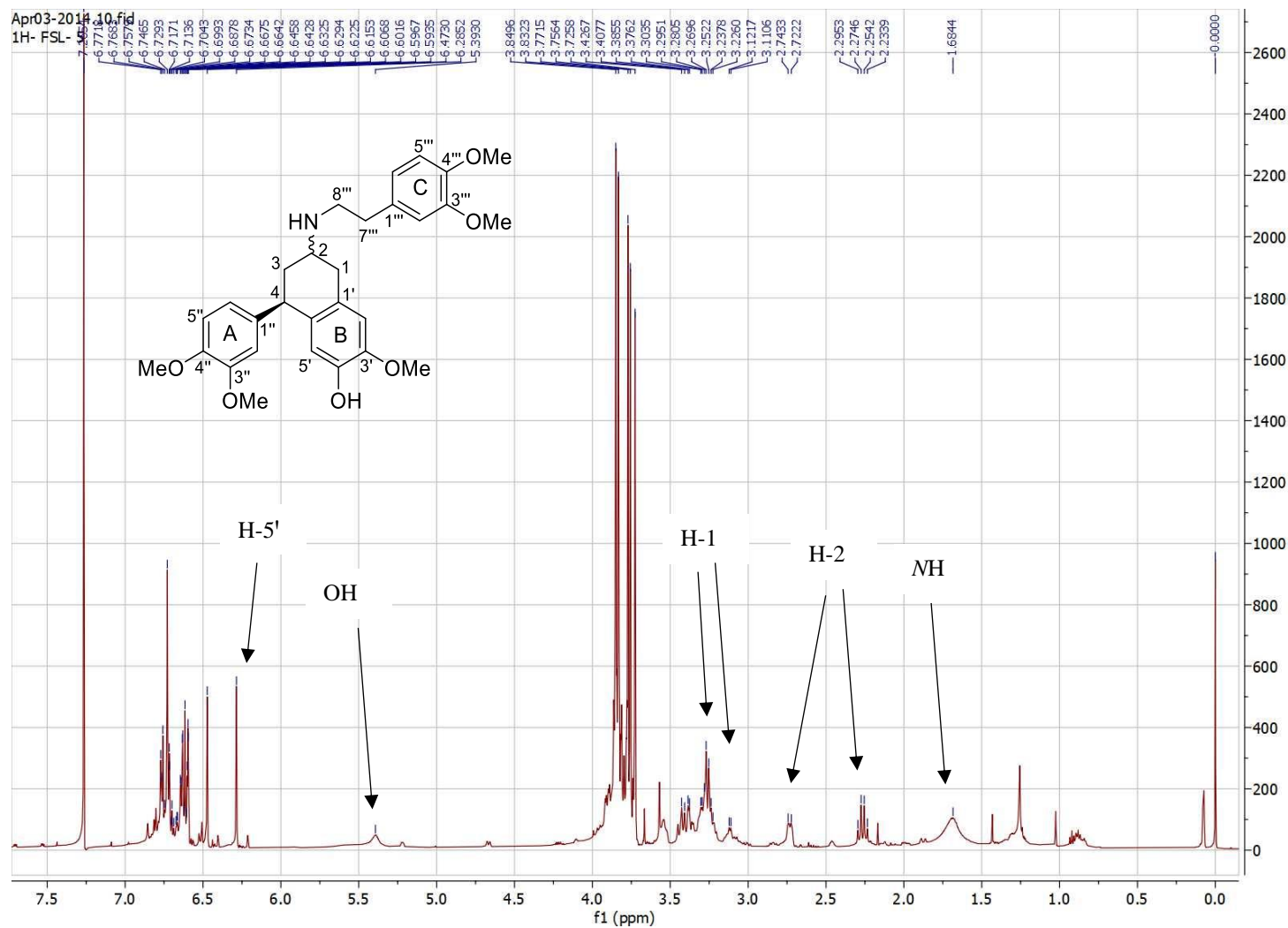


Figure 2.39:  $^1\text{H}$  NMR spectrum of schwarzificusine A (**8**) ( $\text{CDCl}_3$ , 600 MHz)

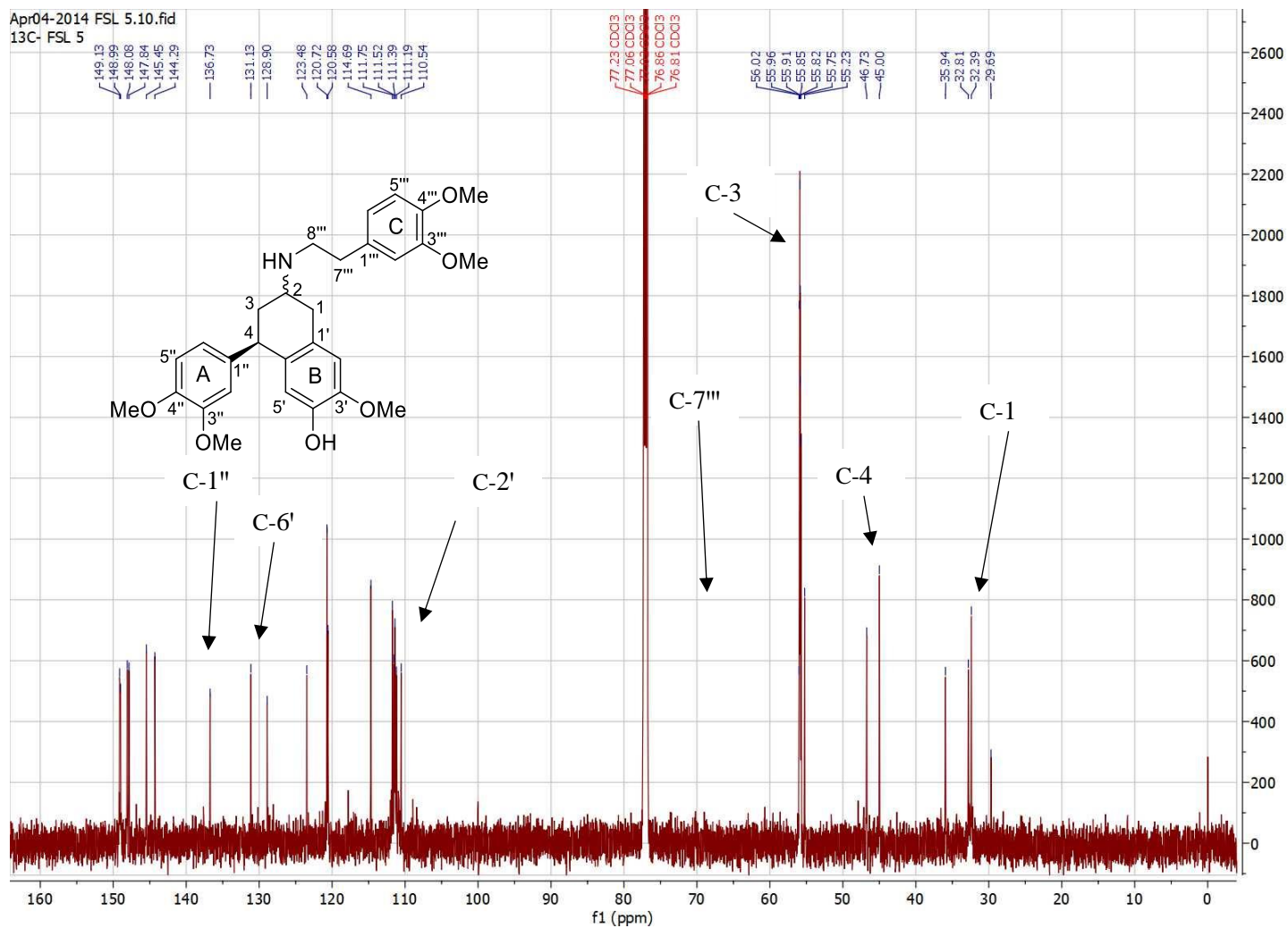
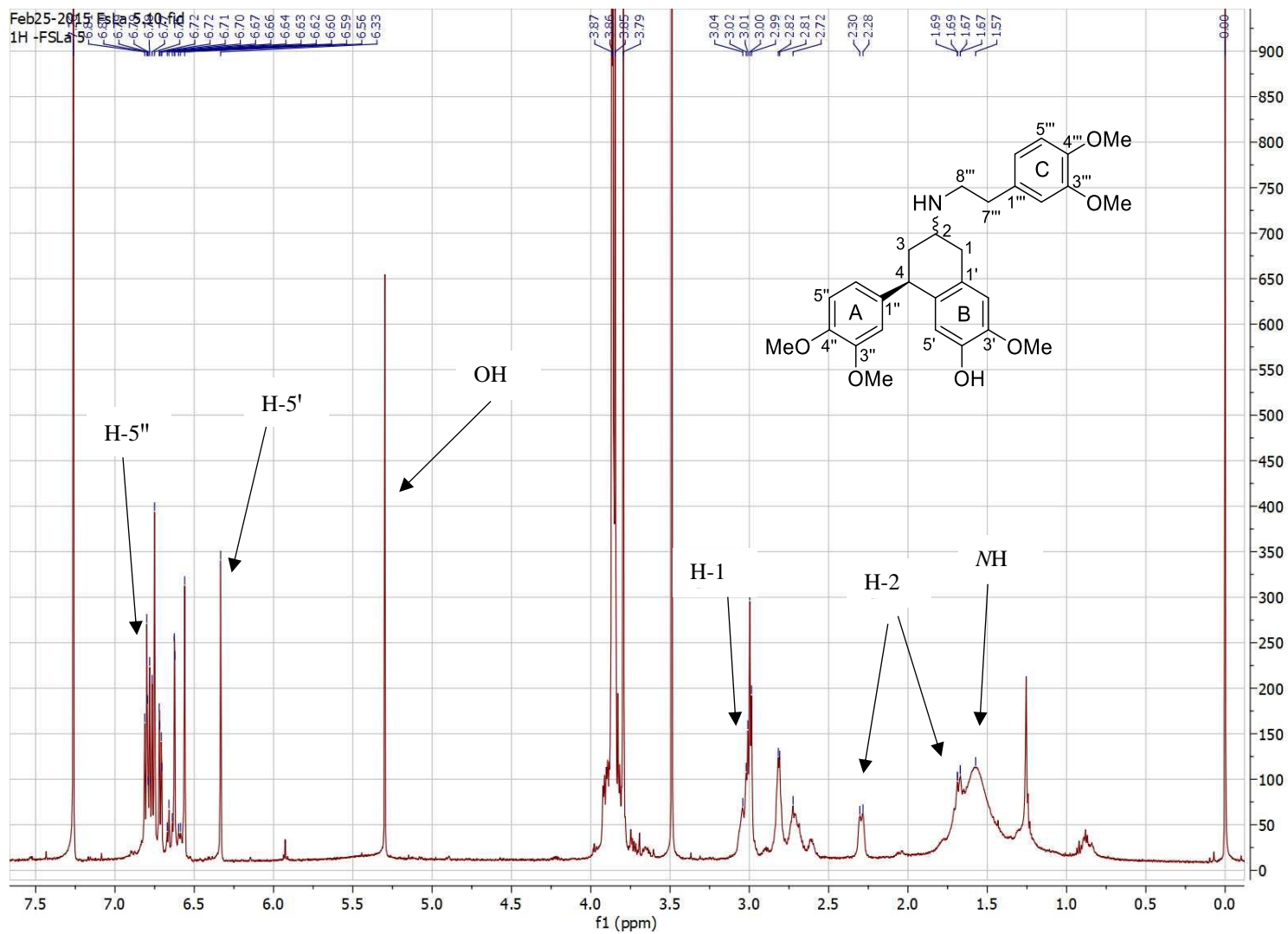
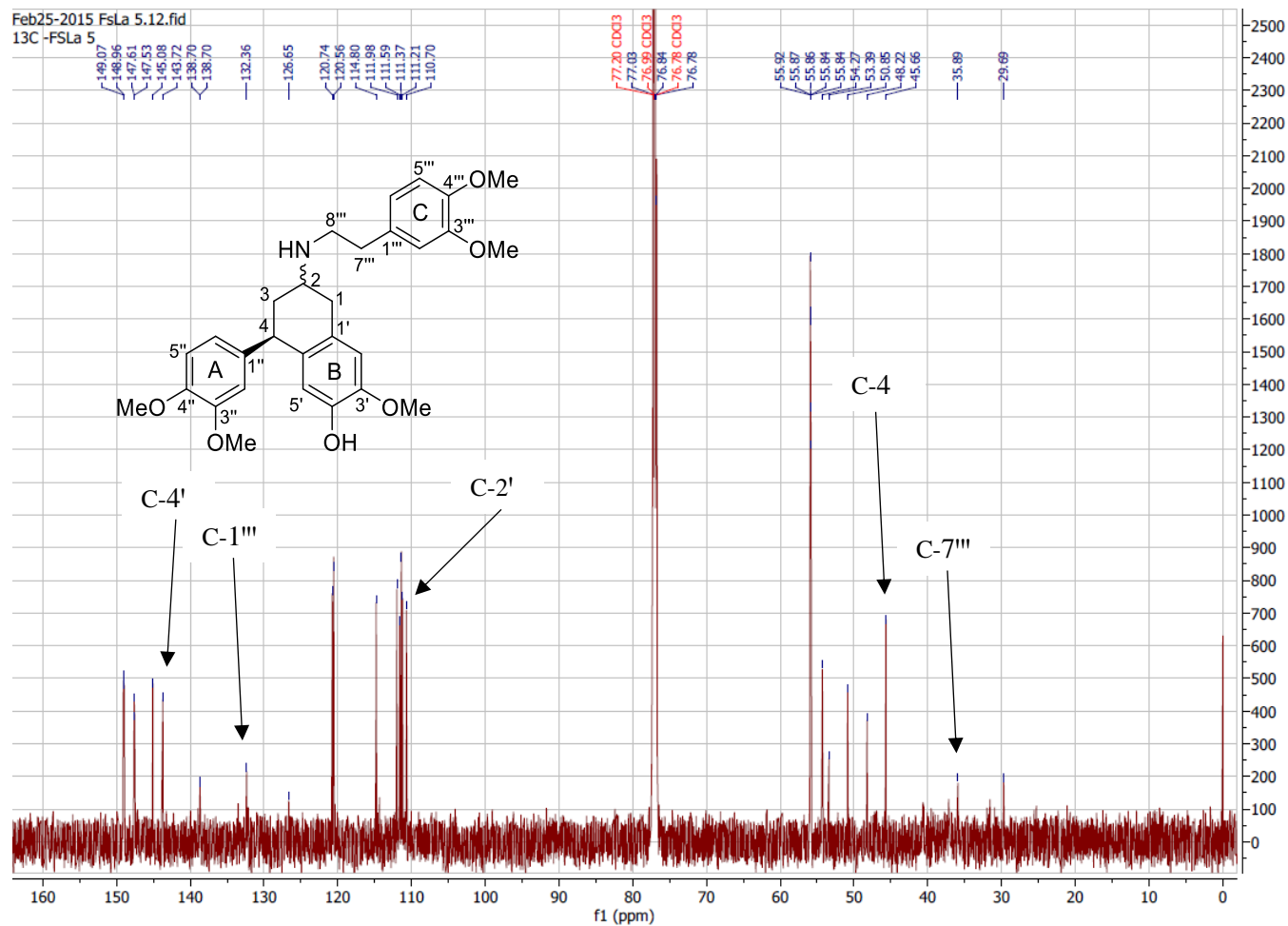


Figure 2.40:  $^{13}\text{C}$  NMR spectrum of schwarzificusine A (8) ( $\text{CDCl}_3$ , 150 MHz)



**Figure 2.41:**  $^1\text{H}$  NMR spectrum of schwarzificusine B (**9**) ( $\text{CDCl}_3$ , 600 MHz)



**Figure 2.42:**  $^{13}\text{C}$  NMR spectrum of schwarzificusine B (9) ( $\text{CDCl}_3$ , 150 MHz)

## 2.9 Proposed Biogenesis of Schwarzinicine and Schwarzificusine Alkaloids

The schwarzinicine alkaloids **1** – **7** represent the first examples of a 1,4-diarylbutanoid linked to a phenethylamine unit, and are possibly biosynthetically related to ficusnotins A–F, which were the first and only other plant-derived 1,4-diarylbutanoids to be reported from *Ficus nota*.<sup>54</sup> Based on the proposed biogenetic pathway reported previously for the ficusnotin compounds, the 1,4-diarylbutanoid core structure is possibly derived from *p*-coumaroyl-CoA, which following dimerization as well as multiple enzymatic modifications give rise to the 1,4-diarylbutanone compound, ficusnotin E (Figure 2.43).<sup>54</sup> Condensation between ficusnotin E (or *O*-demethyl ficusnotin E) and the appropriate arylethylamines via reductive amination furnishes the basic skeleton of the schwarzinicine alkaloids (**Figure 2.43**). Subsequent oxidation at the benzylic C-4 furnishes the reactive *p*-quinone methide cation intermediate. Trapping of the cation intermediate by a water molecule leads to the C-4 hydroxylated schwarzinicine alkaloids, i.e., schwarzinicines F and G (**6** and **7**).

On the other hand, schwarzificusines A and B (**8** and **9**) represent the second instance of naturally occurring compounds incorporating a 1-phenyl-3-aminotetralin core structure, the first being (±)-aspongamide A, which is an *N*-acetyldopamine trimer isolated from the insect *Aspongopus chinensis*.<sup>118</sup> However, based on the basic C-N skeleton present in the schwarzificusines, they are very likely derived from the schwarzinicine alkaloids. Starting from the *p*-quinone methide cation intermediate, intramolecular nucleophilic addition from C-2' to C-4 (via electrophilic aromatic substitution) will give rise to the tetralin ring system of schwarzificusines A and B (**8** and **9**) (**Figure 2.43**).

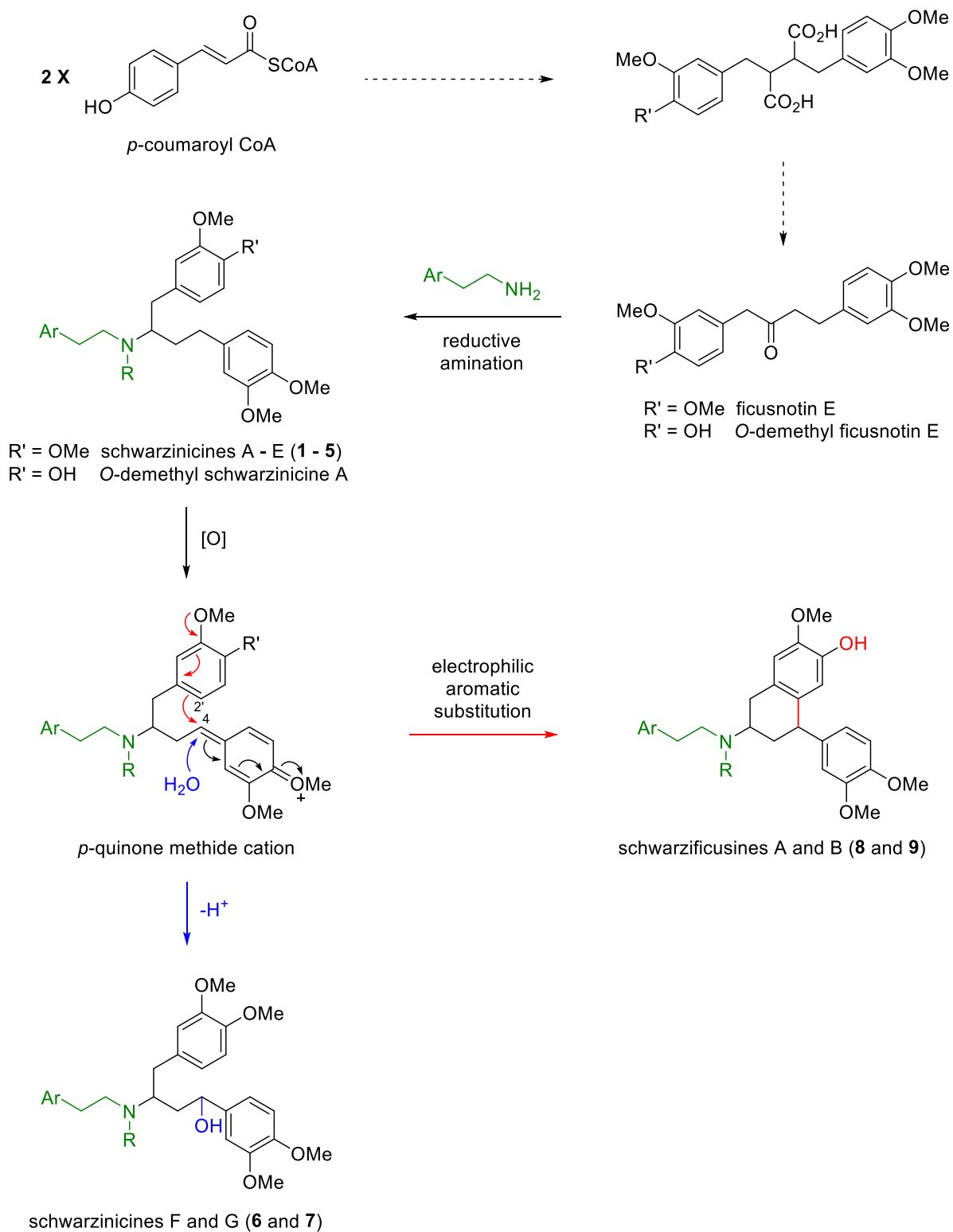


**Figure 2.43:** Plausible biogenetic pathways to schwarzinicine and schwarzificusine alkaloids

## CHAPTER THREE: ISOLATION AND STRUCTURE

### ELUCIDATION OF ALKALOIDS FROM *ALSTONIA SCHOLARIS*

Investigation of the alkaloidal content of the leaves, bark and flowers of *Alstonia scholaris* cultivated on the West Coast of Peninsular Malaysia provided a total of 17 alkaloids, of which five are new. These alkaloids can be classified into four main monoterpene indole alkaloid skeletal types, namely aspidospermatan (nine), corynanthean (five), strychnan (two) and vallesiachotaman (one).

Four of the nine aspidospermatan-type alkaloids isolated possess new or novel structure, namely alstoscholactine (**10**), alstolaxepine (**11**), *N*-formyllyunnanensine (**12**), and scholaphylline (**13**). The five known aspidospermatan-type alkaloids are 19,20-*E*-vallesamine (**14**), 19,20-*Z*-vallesamine (**15**), 19,20-*E*-vallesamine *N*-oxide (**16**), 6,7-*seco*angustilobine B (**17**), and 6,7-*seco*-19,20 $\alpha$ -epoxyangustilobine B (**18**). One of the six corynanthean-type alkaloids possesses a novel structure, namely alstobrogaline (**19**). The four known corynanthean-type alkaloids include tetrahydroalstonine (**20**), picrinine (**21**), 16*R*-19,20-*Z*-isositsirikine (**22**), and 16*R*-19,20-*E*-isositsirikine (**23**). Finally, scholaricine (**24**), and *N*-demethylalstogustine *N*-oxide (**25**) are known strychnan-type alkaloids, while *E/Z*-vallesiachotamine (**26**) is a pair of known vallesiachotaman-type alkaloids.

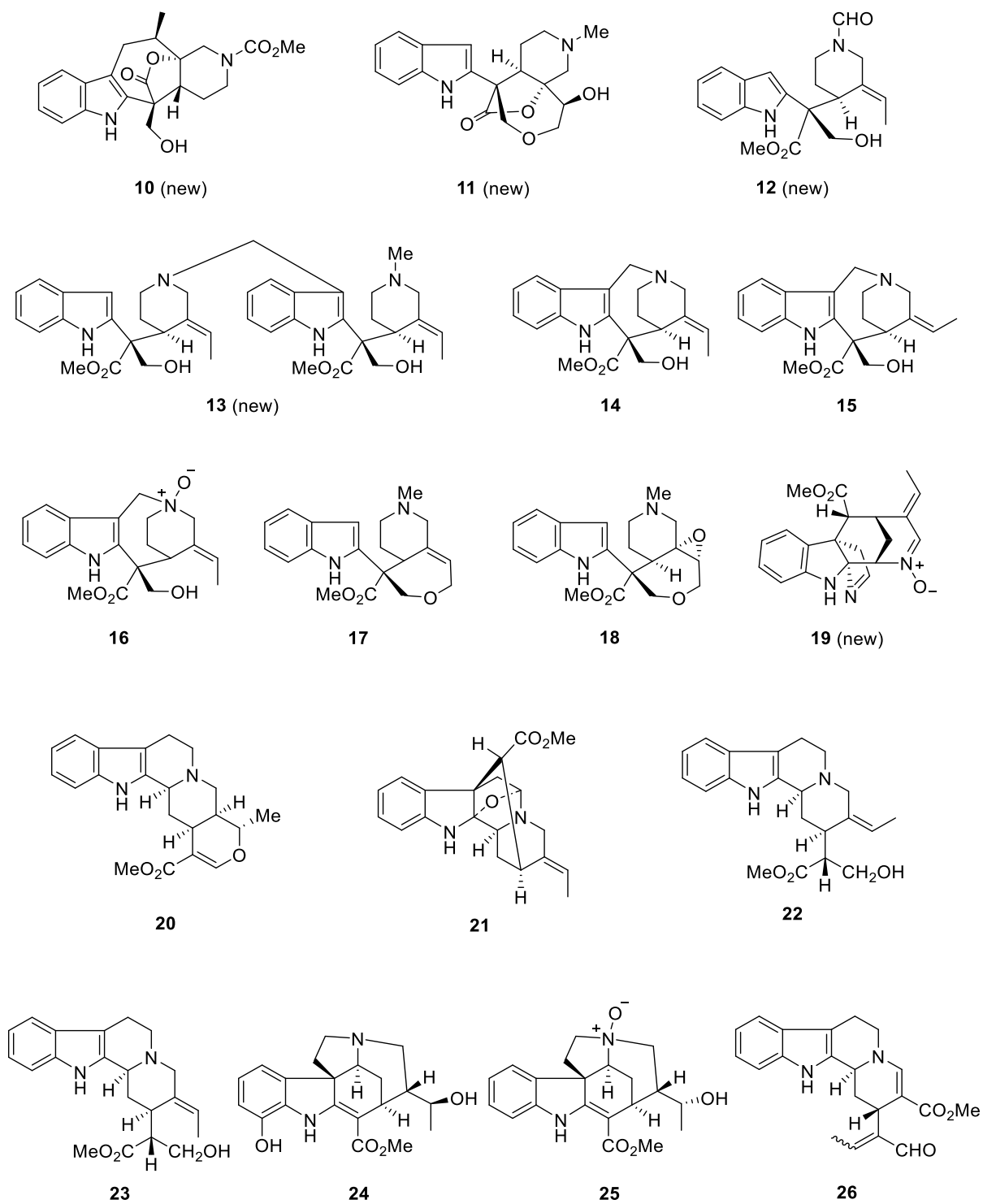


**Figure 3.1:** Alkaloids isolated from *Alstonia scholaris*

The bark of *A. scholaris* produced the highest number of alkaloids, 10 in total. This is followed by the leaf sample with eight alkaloids and three alkaloids were isolated from the flowers of *A. scholaris*. The following table summarises the source and yield of all the alkaloids isolated.

**Table 3.1:** Source and yield of alkaloids obtained from *A. scholaris*.

Alkaloid	Source	Mass (mg)		
		Bark	Leaves	Flowers
Alstoscholactine (10) (new)			8	
Alstolaxepine (11) (new)			33	
<i>N</i> -Formylyunnanensine (12) (new)		19		
Scholaphylline (13) (new)		4		
19,20- <i>E</i> -Vallesamine (14)		16	147	90
19,20- <i>Z</i> -Vallesamine (15)		7		
19,20- <i>E</i> -Vallesamine <i>N</i> -oxide (16)		8		
6,7- <i>Seco</i> angustilobine B (17)			33	
6,7- <i>Seco</i> -19,20 $\alpha$ -epoxyangustilobine B (18)		7		
Alstobrogaline (19) (new)			21	
Tetrahydroalstonine (20)				6
Picrinine (21)			32	34
16 <i>R</i> -19,20- <i>Z</i> -Isositsirikine (22)			7	
16 <i>R</i> -19,20- <i>E</i> -Isositsirikine (23)		10		
Scholaricine (24)			34	
<i>N</i> <sup>b</sup> -Demethylalstogustine <i>N</i> -oxide (25)		9		
<i>E/Z</i> -Vallesiachotamine (26)		8		

## 3.1 Aspidospermatan-type Alkaloids

### 3.1.1 Alstoscholactine (10)

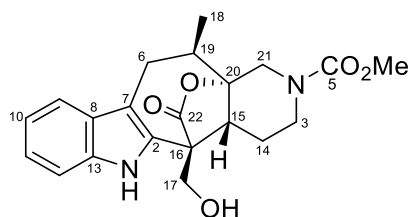


**Figure 3.2:** Alstoscholactine (**10**)

Alstoscholactine (**10**) was obtained from the leaf extract of *A. scholaris* as a light yellowish oil with  $[\alpha]_D^{25} +14$  ( $c$  1.04, CHCl<sub>3</sub>). The IR spectrum showed absorption bands due to the presence of hydroxyl (3403 cm<sup>-1</sup>),  $\gamma$ -lactone C=O (1761 cm<sup>-1</sup>), and carbamate C=O (1684 cm<sup>-1</sup>) functions. The UV spectrum showed absorption maxima at 222, 276 (sh), 283, 290 (sh) nm, which are characteristic of indole chromophore. The HR-DART-MS measurements determined the molecular formula of **10** as C<sub>21</sub>H<sub>24</sub>N<sub>2</sub>O<sub>5</sub> based on the [M+H]<sup>+</sup> peak detected at  $m/z$  385.17750.

In agreement with the molecular formula of **10**, the <sup>13</sup>C NMR spectrum (**Table 3.2** and **Figure 3.7**) showed a total of 21 carbons. The HSQC data subsequently showed that there were 11 aliphatic carbons (two CH<sub>3</sub>, five CH<sub>2</sub>, two CH, one quaternary and one oxygenated tertiary carbon), eight aromatic carbons (four CH, two quaternary, and two *N*-bearing tertiary carbons), a lactone carbonyl, and a carbamate carbonyl function. Eleven of the 21 carbons were observed as paired signals due to the presence of the NCO<sub>2</sub>Me group, displaying the *E/Z*-carbamate rotamer equilibrium.<sup>119</sup> The eight aromatic carbon resonances observed were assigned to the indole moiety on the basis of their characteristic carbon resonances,<sup>120</sup> and were supported by the HMBC and NOESY data (**Figures 3.3** and **3.4**). The most deshielded methylene carbon

shift at  $\delta_C$  61.7 (C-17) was characteristic of an oxymethylene, while the methylene carbon shifts at  $\delta_C$  41.3 (C-3) and 48.9/49.2 (C-21) were due to two aminomethylene groups associated with the  $NCO_2Me$  group. In addition, the pair of deshielded tertiary carbon shifts at  $\delta_C$  87.6/88.6 deduced oxygen substitution at this carbon, which on the basis of the HMBC correlations observed from H-6 and H-18 to C-20, was assigned to C-20.

Many of the signals in the  $^1H$  NMR spectrum of **10** appeared to be broadened as a result of interconversion of the carbamate rotamers.<sup>119,121</sup> Furthermore, the signals of H-3 $\alpha$ , H-3 $\beta$ , H-19, H-21 $\alpha$ , H-21 $\beta$ ,  $NCO_2Me$ , and  $NH$  were observed to be duplicated in a roughly 1:1 ratio. The  $^1H$  NMR spectrum (**Table 3.2** and **Figure 3.6**) along with the HSQC spectrum showed the presence of four contiguous aromatic hydrogens due to an indole moiety ( $\delta$  7.10 – 7.48), an indolic  $NH$  ( $\delta$  9.16), an isolated  $OCH_2$  ( $\delta_H$  4.19 and 4.43; d,  $J = 11.5$  Hz;  $\delta_C$  61.7), an isolated  $NCH_2$  ( $\delta_H$  3.50/3.70 and 3.94/4.05;  $\delta_C$  48.9/49.2), a  $CH_3$  group attaching to a methine carbon ( $\delta_H$  0.94, d,  $J = 6.7$  Hz;  $\delta_C$  15.7/15.9), and an  $NCO_2Me$  group ( $\delta_H$  3.73,  $\delta_C$  53.0;  $\delta_C$  156.1/156.2).

The COSY data (**Figure 3.3**) inferred the presence of the  $CH_2CH_2CH$  and  $CH_2CHCH_3$  partial structures due to the C-3–C-14–C-15 and C-6–C-19–C-18 fragments, respectively, present in **10**. The COSY data also confirmed the presence of two isolated  $CH_2$  groups at C-17 (oxymethylene) and C-21 (aminomethylene). The HMBC correlations from H-6 to C-2, C-7, and C-8 (**Figure 3.3**) revealed the attachment of the C-6–C-19–C-18 fragment to C-7 of the indole moiety. Additionally, the HMBC correlations from H-6 and H-18 to C-20 suggested that C-19 was linked to C-20, which was then connected to the isolated aminomethylene C-21 based on the HMBC correlations from H-21 to C-19 and C-20. The HMBC correlation from H-21 to C-15 indicated that the C-3–C-14–C-15 fragment was attached to C-20. The HMBC correlations from H-21 to C-3 and C-5; and from H-3 to C-5, deduced that both C-3 and C-21 were connected via the nitrogen atom of the carbamate group. Finally, the HMBC correlations

from H-15 to C-2, C-16, and C-22, as well as from H-17 to C-2, C-15, C-16, and C-22, were used to infer the attachments of C-2 (indole), C-15 (tertiary carbon), and C-17 (CH<sub>2</sub>OH) to C-16, in which the lactone function is branched from.

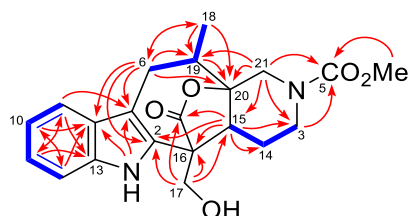


**Figure 3.3:** COSY (blue, bold) and selected HMBC (red arrows) correlations of alstoscholactine (**10**)

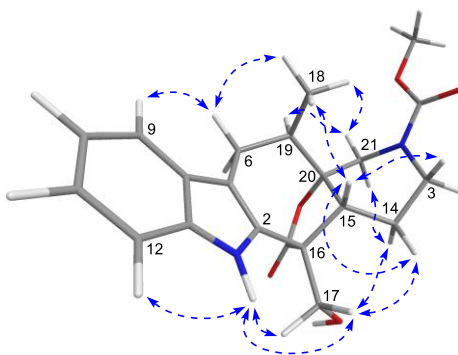


**Figure 3.4:** Selected NOESY correlations of alstoscholactine (**10**)

The planar structure elucidated so far is in good agreement with the NOESY data, which were useful to assign the relative configurations of all the stereocenters present in **10** (**Figure 3.4**). The dispositions of both Me-18 and H-15 were inferred to be  $\beta$  based on the NOEs observed for Me-18/H-6 $\beta$ , H-9/H-6 $\beta$ , and Me-18/H-15. These observations, combined with the restricted conformation of the structure of alstoscholactine (**10**), deduced that an  $\alpha$ -oriented

lactone function was the only possibility. Furthermore, the NOEs observed for H-14 $\alpha$ /H-21 $\alpha$  and H-15/H-3 $\beta$  showed that the carbamate-bearing piperidine moiety possesses a boat conformation. The relative configuration of **10** was thus deduced to be 15*R*,16*S*,19*R*,20*S*. Finally, comparison of the experimental ECD data with those obtained from time-dependent density functional theory (TDDFT) calculations (**Figure 3.5**) established the absolute configuration of **10** as 15*R*,16*S*,19*R*,20*S*.

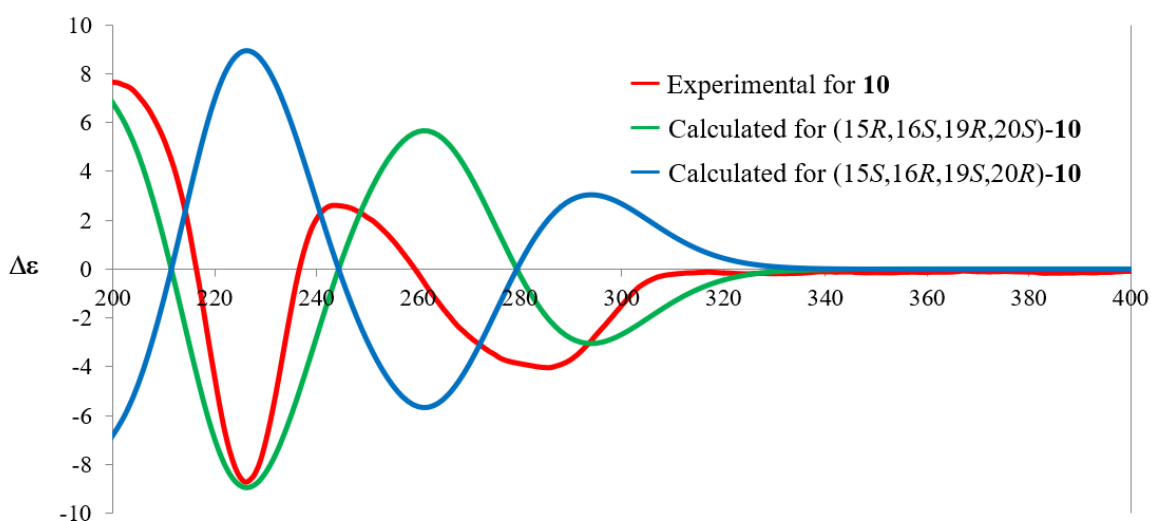


**Figure 3.5:** Experimental and calculated ECD spectra of alstoscholactine (**10**)

Alstoscholactine (**10**) represents the first member of a new class of rearranged stemmadenine alkaloids presenting an unprecedented C-6–C-19 connectivity among naturally occurring monoterpenoid indole alkaloids.

In addition, the synthesis of alstoscholactine (**10**) from 19,20-*E*-vallesamine (**14**) indicate both the alkaloids originated from the same precursor and provides additional sample for bioactivity.

**Table 3.2:**  $^1\text{H}$  (600 MHz) and  $^{13}\text{C}$  (150 MHz) NMR spectroscopic data (in  $\text{CDCl}_3$  with TMS as internal reference) of alstoscholactine (**10**)

Position	$\delta_{\text{H}}$ (mult., $J$ in Hz)	$\delta_{\text{C}}$
2		132.9
3 $\alpha$	3.60, m; 3.80 m <sup>a</sup>	41.3
3 $\beta$	2.99, t (11); 3.18 br t (11) <sup>a</sup>	
5		156.1, 156.2 <sup>a</sup>
6 $\alpha$	3.05, dd (16, 4.4)	25.4, 25.7 <sup>a</sup>
6 $\beta$	2.82, dd (16, 3)	
7		109.7
8		129.0
9	7.48, d (8)	118.0
10	7.10, t (8)	119.6
11	7.15, t (8)	122.1
12	7.32, d (8)	111.3
13		134.9
14 $\alpha$	1.77, m	22.1, 22.4 <sup>a</sup>
14 $\beta$	1.91, m	
15	2.68, m	41.8, 42.2 <sup>a</sup>
16		51.0, 51.8 <sup>a</sup>
17	4.19, br s	61.7
17'	4.43, d (11.5)	
18	0.94, d (6.7)	15.7, 15.9 <sup>a</sup>
18'		
19	2.38, m; 2.50 m <sup>a</sup>	40.2, 40.6 <sup>a</sup>
20		87.6, 88.6 <sup>a</sup>
21 $\alpha$	3.94, d (15); 4.05 d (15) <sup>a</sup>	48.9, 49.2 <sup>a</sup>
21 $\beta$	3.50, d (15); 3.70 m <sup>a</sup>	
22		174.6, 174.8 <sup>a</sup>
NH	9.16, br s; 9.19 br s <sup>a</sup>	
<u>NCOOMe</u>	3.72, s; 3.74 s <sup>a</sup>	52.9
17-OH	3.36, br s	

<sup>a</sup> Duplication of signals due to carbamate rotamers.

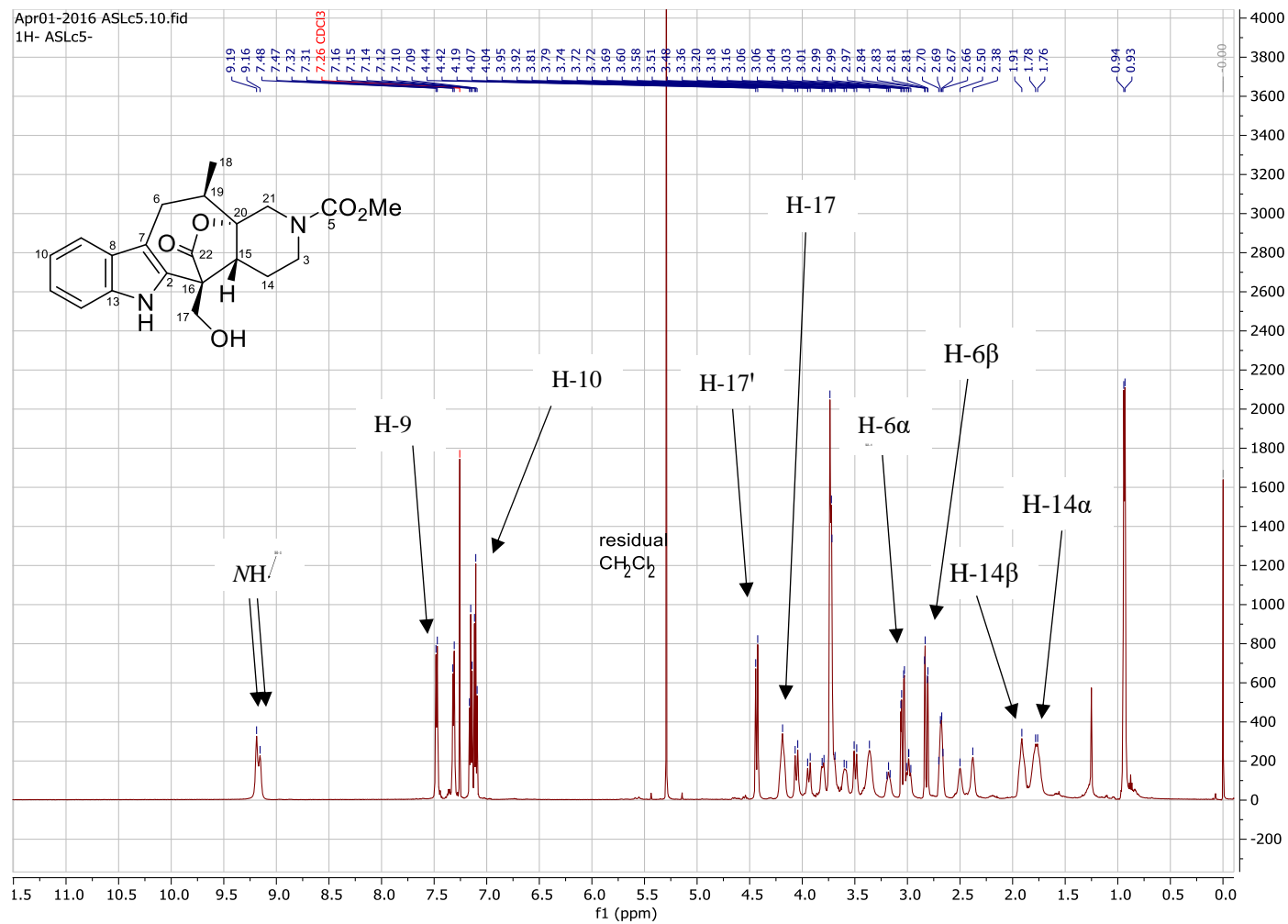


**Figure 3.6:** <sup>1</sup>H NMR spectrum of alstoscholactine (**10**) (CDCl<sub>3</sub>, 600 MHz)

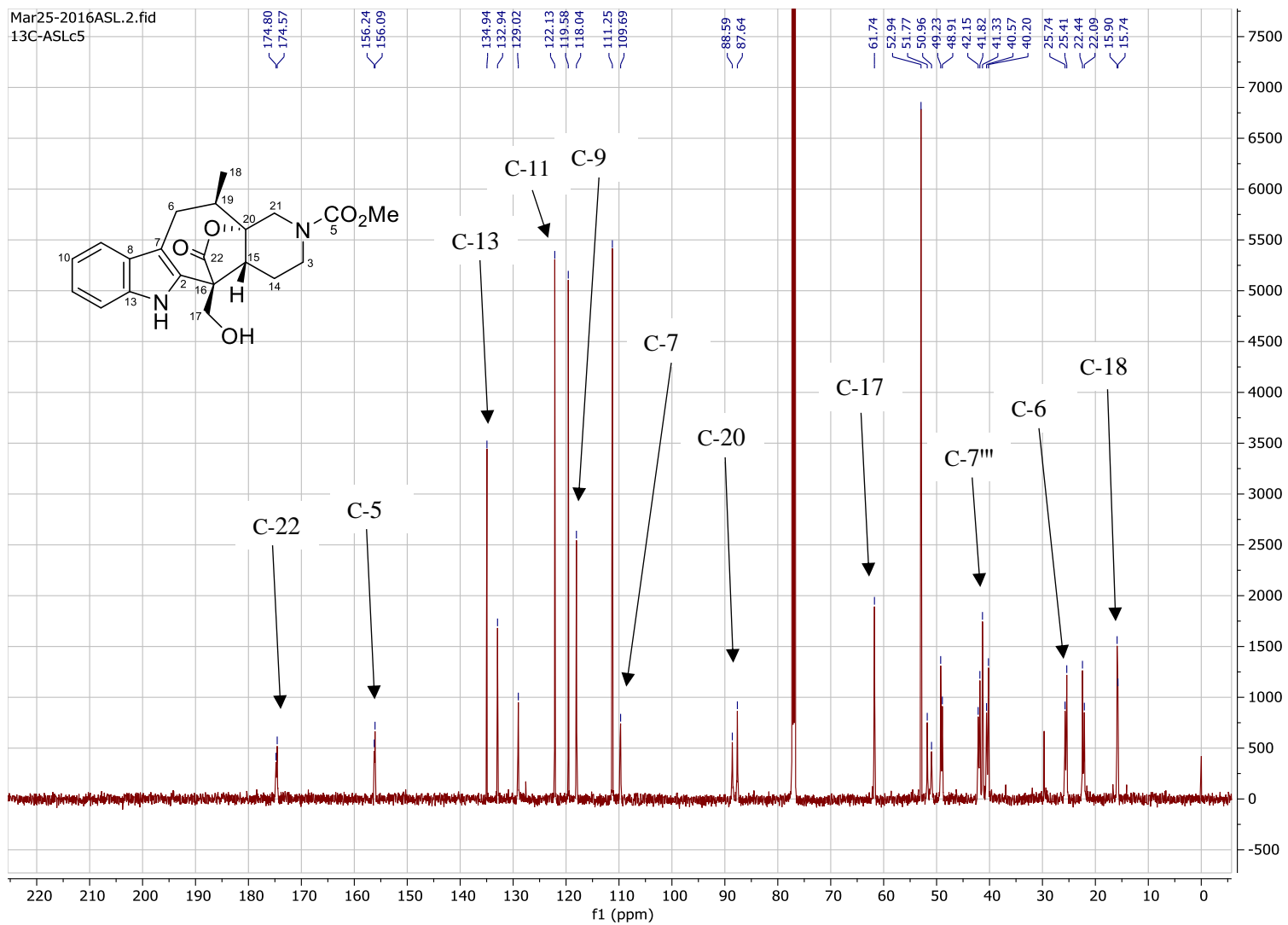


**Figure 3.7:**  $^{13}\text{C}$  NMR spectrum of alstoscholactine (**10**) ( $\text{CDCl}_3$ , 150 MHz)

### 3.1.2 Alstolaxepine (11)

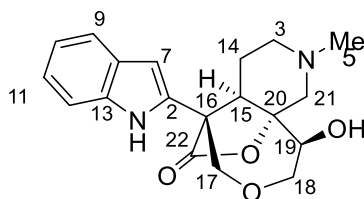


**Figure 3.8:** Alstolaxepine (**11**)

Alstolaxepine (**11**) was initially obtained as a light yellowish oil with  $[\alpha]_D^{25} -12$  ( $c$  0.67,  $\text{CHCl}_3$ ). It was subsequently crystallised as light orange needles with melting point 109–112 °C. The IR spectrum showed bands at 3343 and 1774  $\text{cm}^{-1}$  due to OH/NH and  $\gamma$ -lactone C=O functions. The UV spectrum showed absorption maxima at 217, 271, 279, and 289 nm, indicating the presence of indole chromophore. HR-DART-MS measurements determined the molecular formula of **11** as  $\text{C}_{19}\text{H}_{22}\text{N}_2\text{O}_4$  based on the  $[\text{M}+\text{H}]^+$  peak detected at  $m/z$  343.16440.

The  $^1\text{H}$  NMR spectrum (**Table 3.3** and **Figure 3.12**) revealed four aromatic signals at  $\delta$  7.10 – 7.55 due to an indole moiety, an NH signal at  $\delta_{\text{H}}$  9.15, an NMe signal at  $\delta_{\text{H}}$  2.45, and a relatively shielded aromatic signal at  $\delta_{\text{H}}$  6.38. The signal at  $\delta$  6.38 was readily assigned to H-7 on the basis of the correlations observed from H-7 to C-9 and C-13 in the HMBC spectrum. This suggested that **11** belongs to the 6,7-*seco* class of monoterpene indole alkaloid. Furthermore, the chemical shifts of the five aromatic hydrogens and the indolic NH ( $\delta_{\text{H}}$  9.15) are very similar to those of 6,7-*seco*angustilobine B (**17**) and its derivative alkaloids.<sup>120,122</sup> The  $^{13}\text{C}$  NMR spectrum (**Table 3.3** and **Figure 3.13**) revealed the presence of 19 carbon resonances, while the HSQC spectrum revealed the presence of 10 aliphatic carbons (one  $\text{CH}_3$ , five  $\text{CH}_2$ , two CH, one quaternary and one oxygenated tertiary carbon), eight aromatic carbons (five CH,

one quaternary, and two *N*-bearing tertiary carbons), and one lactone carbonyl carbon ( $\delta_C$  179.5). The resonances of one tertiary carbon ( $\delta_C$  80.5), one CH ( $\delta_C$  78.7,  $\delta_H$  4.04), and two CH<sub>2</sub> carbons ( $\delta_C$  76.1,  $\delta_H$  4.10 and 4.24;  $\delta_C$  69.9,  $\delta_H$  3.64 and 4.02) suggested oxygenation at these carbons.

The COSY data (**Figure 3.9**) revealed the presence of the *N*CH<sub>2</sub>CH<sub>2</sub>CH, *N*CH<sub>2</sub>, and CH<sub>2</sub>CH partial structures due to the *N*-C-3-C-14-C-15, *N*-C-21, and C-18-C-19 fragments, respectively, present in **11**. The partial structures disclosed so far were linked based on detailed HMBC data analysis (**Figure 3.9**). The *N*-C-3-C-14-C-15 fragment was attached to C-20 on the basis of the HMBC correlation observed from H-14 to C-20, while the attachment between C-3 and the isolated methylene C-21 through *N*-4 was deduced on the basis of the HMBC correlations observed from H-3 to C-21; from Me-5 to C-3 and C-21; and from H-21 to C-3 and C-5. The piperidine ring was established by connecting C-21 to C-20 on the basis of the correlations observed from H-21 to C-20 and C-15 in the HMBC spectrum. The C-18-C-19 fragment was attached to C-20 on the basis of the HMBC correlations from H-19 to C-15 and C-21 and from H-18 to C-20. The connection between C-17 and C-18 through an ether bridge was deduced based on the correlations observed from H-17 to C-18; and from H-18 to C-17 in the HMBC spectrum. The oxepane ring was established by connecting C-15 to C-16 and C-16 to C-17, as deduced based on the HMBC correlations observed from H-15 to C-17; and from H-17 to C-2, C-15, and C-16. The C-22  $\gamma$ -lactone carbonyl carbon was established to be attached to C-16 on the basis of the correlation from H-17 to C-22 observed in the HMBC spectrum. Finally, construction of the planar structure of **11** was completed by the HMBC correlations observed from H-15 and H-17 to C-2, which revealed the linkage between C-2 and C-16.

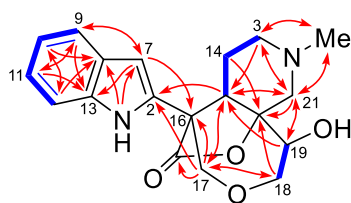


**Figure 3.9:** COSY (blue, bold) and selected HMBC (red arrows) correlations of alstolaxepine (11)

The relative configurations at the stereocenters present in **11** were established based on the NOESY data, as well as the NOE difference data, whereby the signals of H-3 $\beta$ , H-14 $\alpha$ , H-14 $\beta$ , H-18 $\alpha$ , H-21 $\alpha$ , and H-21 $\beta$  were irradiated (**Figure 3.10**). The H-3 $\alpha$ /H-21 $\alpha$ , H-3 $\alpha$ /H-15, and H-15/H-21 $\alpha$  NOEs suggested a chair conformation for the piperidine ring, with H-3 $\alpha$ , H-15, and H-21 $\alpha$  adopting axial orientation. The H-14 $\beta$ /H-17 $\beta$  and H-14 $\beta$ /H-18 $\beta$  NOEs dictated that the lactone group was  $\alpha$ -oriented, while the C-17–O–C-18–C-19 fragment  $\beta$ -oriented. Based on these observations, the relative configurations at C-15, C-16, and C-20 were established as *R*, *S*, and *R*, respectively. On the basis of the clear NOE observed between H-19 and H-21 $\beta$ , the relative configuration at C-19 was inferred to be *S*, where the hydroxyl group is  $\beta$ -oriented. This inference was consistent with the absence of the H-14 $\beta$ /H-19 NOE.

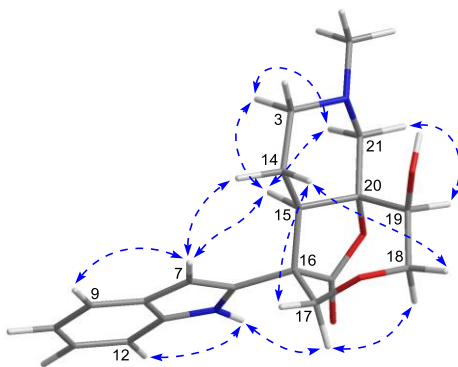


**Figure 3.10:** Selected NOESY correlations of alstolaxepine (11)

Since suitable crystals were at hand, the absolute configuration of **11** was confirmed by X-ray diffraction analysis (**Figure 3.11**). The X-ray structure also showed the presence of a hydrogen bond connecting 19-OH ( $\delta_{\text{H}}$  7.63 br s) and N-4.

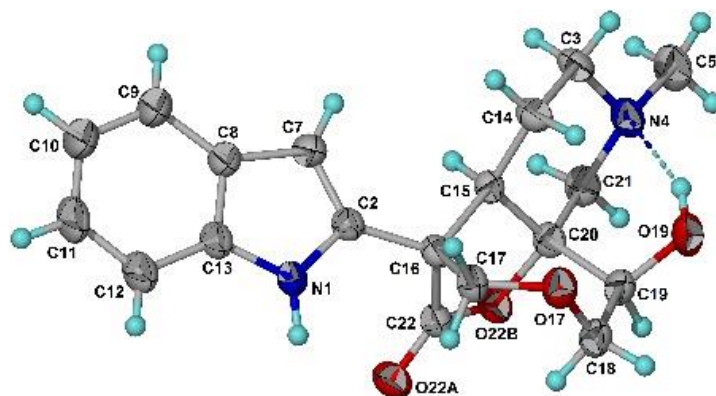


**Figure 3.11:** X-ray crystal structure of alstolaxepine (**11**)

Alstolaxepine (**11**) represents a new 6,7-*seco*-angustilobine B-type alkaloid incorporating a  $\gamma$ -lactone-bridged oxepane ring (i.e., 3,7-dioxabicyclo[4.2.1]nonan-8-one), which is unprecedented among natural products.

**Table 3.3:**  $^1\text{H}$  (600 MHz) and  $^{13}\text{C}$  (150 MHz) NMR spectroscopic data (in  $\text{CDCl}_3$  with TMS as internal reference) of alstolaxepine (**11**)

Position	$\delta_{\text{H}}$ (mult., $J$ in Hz)	$\delta_{\text{C}}$
2		134.9
3 $\alpha$	2.34, td (12, 3)	55.7
3 $\beta$	3.20, br d (12)	
5	2.45, s	45.2
7	6.38, dd (2, 1)	99.3
8		127.7
9	7.55, br d (8)	120.3
10	7.10, td (8, 1)	120.2
11	7.18, td (8, 1)	122.4
12	7.37, br d (8)	111.3
13		135.7
14 $\alpha$	2.18, br d (13)	22.1
14 $\beta$	3.04, qd (13, 4.3)	
15	2.62, dd (13.5, 2.4)	53.9
16		51.4
17 $\beta$	4.10, d (12.3)	76.1
17 $\alpha$	4.24, d (12.3)	
18 $\alpha$	3.64, dd (14.2, 1.2)	69.9
18 $\beta$	4.02, dd (14.2, 2.4)	
19	4.04, m	78.7
20		80.5
21 $\alpha$	2.56, d (10.1)	64.3
21 $\beta$	3.44, d (10.1)	
22		179.5
NH	9.15, br s	
19-OH	7.63, br s	

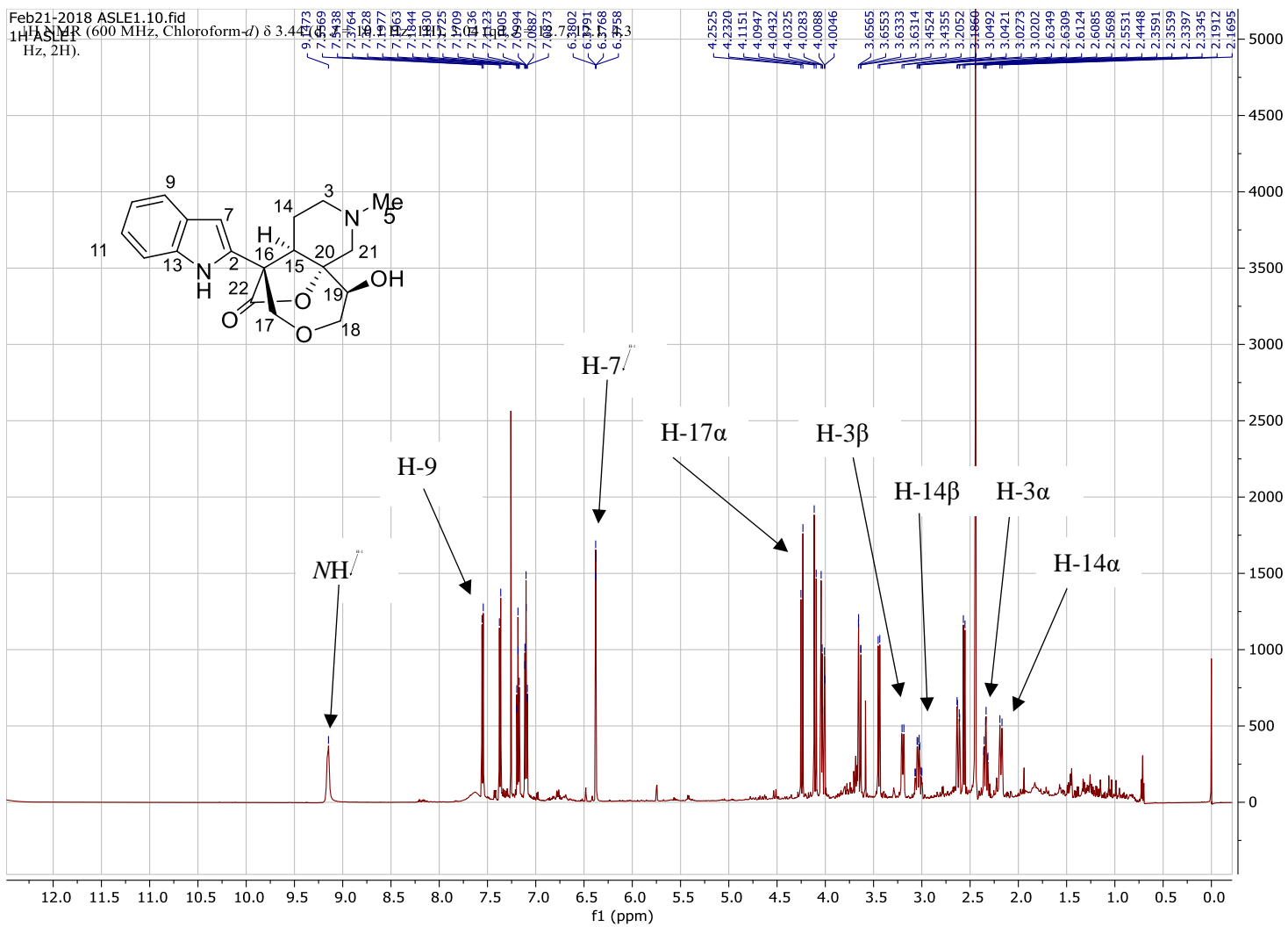


**Figure 3.12:** <sup>1</sup>H NMR spectrum of alstolaxepine (**11**) (CDCl<sub>3</sub>, 600 MHz)

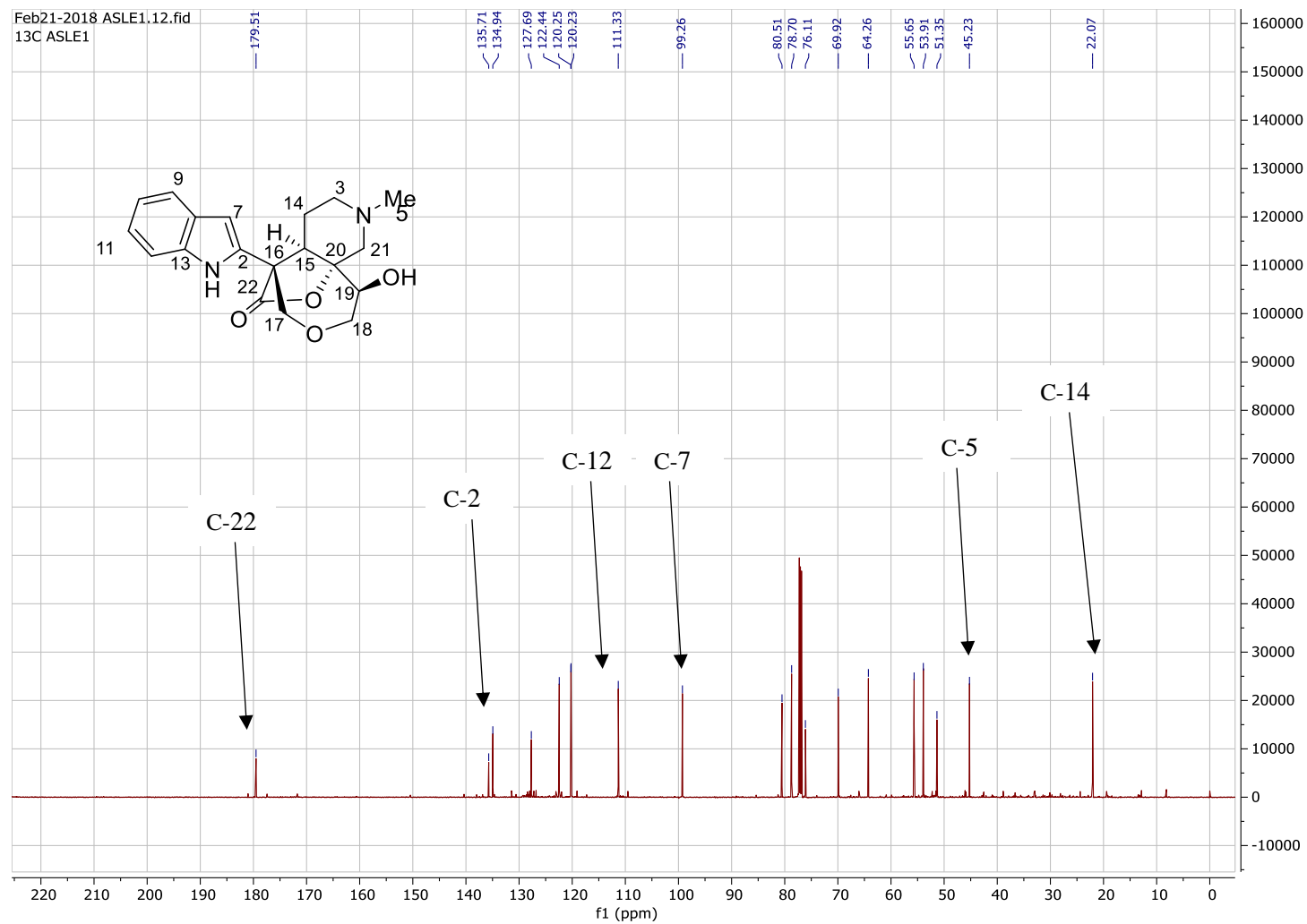


**Figure 3.13:**  $^{13}\text{C}$  NMR spectrum of alstolaxepine (**11**) ( $\text{CDCl}_3$ , 150 MHz)

### 3.1.3 *N*-Formylyunnanensine (**12**)

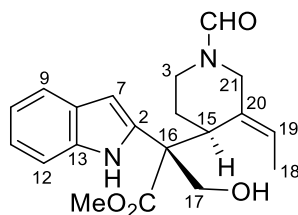


**Figure 3.14:** *N*-Formylyunnanensine (**12**)

*N*-Formylyunnanensine (**12**) was obtained from the bark of *A. scholaris* as a light yellowish oil with  $[\alpha]_D^{25} +23$  ( $c$  0.91,  $\text{CHCl}_3$ ). The IR spectrum showed absorption bands due to the presence of OH/NH ( $3304$  and  $3408\text{ cm}^{-1}$ ), ester C=O ( $1726\text{ cm}^{-1}$ ) and amide C=O ( $1647\text{ cm}^{-1}$ ) functions, while the UV spectrum showed absorption maxima ( $218$ ,  $281$ , and  $290\text{ nm}$ ) characteristic of indole chromophore. The HR-DART-MS showed a  $[\text{M}+\text{H}]^+$  peak at  $m/z$  358.18047, which deduced the molecular formula of  $\text{C}_{20}\text{H}_{24}\text{N}_2\text{O}_4$ . On first inspection, all the signals present in the  $^1\text{H}$  and  $^{13}\text{C}$  NMR spectra of **12** (**Figures 3.17** and **3.18**) appeared to be duplicated in a ratio of 1:1. This suggested the presence of two nearly identical molecules equilibrating in a 1:1 ratio in  $\text{CDCl}_3$  solution or a dimeric compound constituting identical monomeric halves.

Detailed analysis of  $^{13}\text{C}$  NMR spectrum (**Table 3.4** and **Figure 3.18**) revealed 20 pairs of carbon resonances. The HSQC data subsequently showed the presence of eight pairs of aliphatic carbons (two pairs of  $\text{CH}_3$ , four pairs of  $\text{CH}_2$ , one pair of  $\text{CH}$ , and one pair of quaternary carbons), eight pairs of aromatic carbons (five pairs of  $\text{CH}$ , one pair of quaternary, and two pairs of *N*-bearing tertiary carbons), two pairs of olefinic carbons (one pair of  $\text{CH}$  and one pair of quaternary carbons), a pair of ester carbonyl, and a pair of formyl carbons. When the  $^{13}\text{C}$  NMR data were considered along with the MS data, **12** was deduced to be a mixture of two interconvertible isomers that are nearly identical in structures (e.g., rotamers).

The most deshielded pair of aliphatic methylene carbon resonances at  $\delta_C$  66.05/66.57 (C-17) was characteristic of an oxymethylene. The ten pairs aromatic and olefinic carbon resonances observed in the range of  $\delta_C$  101.84 – 136.24 could be readily assigned to the indole moiety (C-2, C-7 – C-13) and ethylidene group (C-19, C-20) based on their characteristic carbon shifts, cf., yunnanensine.<sup>123</sup> The pair of ester carbonyl carbon resonances at  $\delta_C$  174.25 and 174.31 along with the pair of methoxy resonances at  $\delta_C$  53.03 and 53.04 suggested the presence of a CO<sub>2</sub>Me group, which was supported by the three-bond correlations observed from the methoxy resonances ( $\delta_H$  3.86 and 3.88) to the ester carbonyl carbon resonances in the HMBC spectrum. The pair of formyl carbon resonances observed at  $\delta_C$  160.36 and 160.64 ( $\delta_H$  7.73 and 7.80) suggested the presence of a formamide group, thus suggesting that the duplication of signals observed in the <sup>1</sup>H and <sup>13</sup>C NMR was the result of the *E/Z*-formamide rotamer equilibrium.

The <sup>1</sup>H NMR spectrum (**Table 3.4** and **Figure 3.17**) showed the presence of four pairs of aromatic signals ( $\delta_H$  7.11 – 7.57) due to the four contiguous hydrogens of the two indole moiety, a pair isolated aromatic signals at  $\delta_H$  6.44 and 6.48 (H-7), a pair of indolic NH signals at  $\delta_H$  9.97 and 9.91, a pair of duplicated AB doublets of an isolated oxymethylene group ( $\delta_H$  4.25 – 4.40, *J* = 11.3 Hz, CH<sub>2</sub>-17), a pair of isolated a pair of methoxy signals at  $\delta_H$  3.86 and 3.88 (CO<sub>2</sub>Me), and a pair of signals due to the ethylidene moiety ( $\delta_H$  5.70/5.78, quartet × 2, H-19;  $\delta_H$  1.63/1.68, doublet × 2, H-18).

The COSY data (**Figure 3.15**) inferred the presence of the CHCHCHCH, NCH<sub>2</sub>CH<sub>2</sub>CH, and =CHCH<sub>3</sub> partial structures due to the C-9–C-10–C-11–C-12, N–C-3–C-14–C-15, and C-19–C-18 fragments in **12**, respectively. The C-9–C-10–C-11–C-12 fragment was connected to C-8 and C-13 based on the HMBC correlations observed from H-9 to C-13; from H-11 to C-13; and from H-12 to C-8 (**Figure 3.15**). Additionally, the C-7–C-2 fragment was connected to

C-8 and the indolic nitrogen atom based on the HMBC correlations from H-7 to C-2, C-8, and C-9; and from H-9 to C-7. The presence of the indolic NH was confirmed by the correlations from NH to C-8 and C-13. The HMBC correlations from H-21 to C15 and C-20 confirmed the presence of the isolated aminomethylene group at C-20. The H-21 to C-20 correlation in addition to the H-14 to C-16 correlation also confirmed the attachment of the *N*-C-3-C-14-C-15 fragment to C-16 and C-20. The C-19-C-18 ethylidene fragment was determined to be attached to C-20 based on the correlations from H-18 to C-20 and from H-19 to C-15 and C-21. The attachment the quaternary C-16 to the indolic C-2 was supported by the correlation from H-15 to C-2. Finally, the HMBC correlations from H-17 and H-15 to the ester carbonyl carbon indicated the attachment of CO<sub>2</sub>Me group at C-16. The structural features revealed thus so far are characteristic of those of yunnanensine.<sup>123</sup> Finally, the correlations observed from the formyl H-5 to C-3 and C-21; and from H-3 and H-21 to the formyl carbonyl carbon ( $\delta_C$  160.36 and 160.64) in the HMBC spectrum established the presence of the *N*-formyl (formamide) moiety at the piperidine ring nitrogen atom. The planar structure of **12** was thus established as shown in **Figure 3.14**.

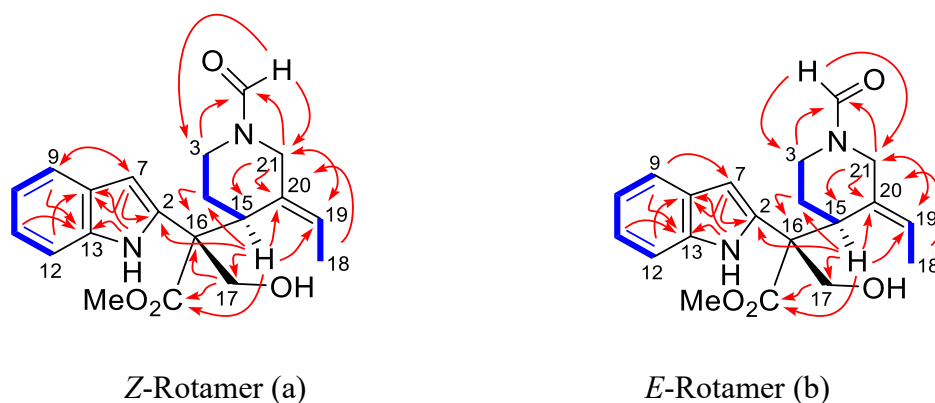


**Figure 3.15:** COSY (blue, bold) and selected HMBC (red arrows) correlations of *N*-formilyunnanensine (**12**)

The NOESY data further confirmed the presence of the two rotamers of **12** (**Figure 3.16**). Based on the molecular models, the NOE observed between H-5a ( $\delta_H$  7.73) and H-21a'

( $\delta_{\text{H}}$  3.40, equatorial) indicated the *Z*-formamide rotamer, in which H-5a was oriented on the same side and in close proximity with H-21a' (**Figure 3.16**). On the other hand, the NOE observed between H-5b ( $\delta_{\text{H}}$  7.80) and H-3b' ( $\delta_{\text{H}}$  3.09, equatorial) indicated the *E*-formamide rotamer, in which H-5b was oriented on the same side and in close proximity with H-3b'. Further inspection of the molecular models revealed that the formyl C=O group in **12** was in close proximity with H-3a' ( $\delta_{\text{H}}$  3.51) in the *Z*-formamide rotamer, but was in close proximity with H-21b' ( $\delta_{\text{H}}$  4.17) in the *E*-formamide rotamer (**Figure 3.16**). These observations are entirely consistent with H-3a' in the *Z*-rotamer and H-21b' in the *E*-rotamer being unusually deshielded as a result of anisotropic effect of the carbonyl function (**Figure 3.16**). Alkaloid **12** was therefore established as the *N*-formyl derivative of yunnanensine, an alkaloid that was first reported from *Ervatamia yunnanensis*.<sup>123</sup>

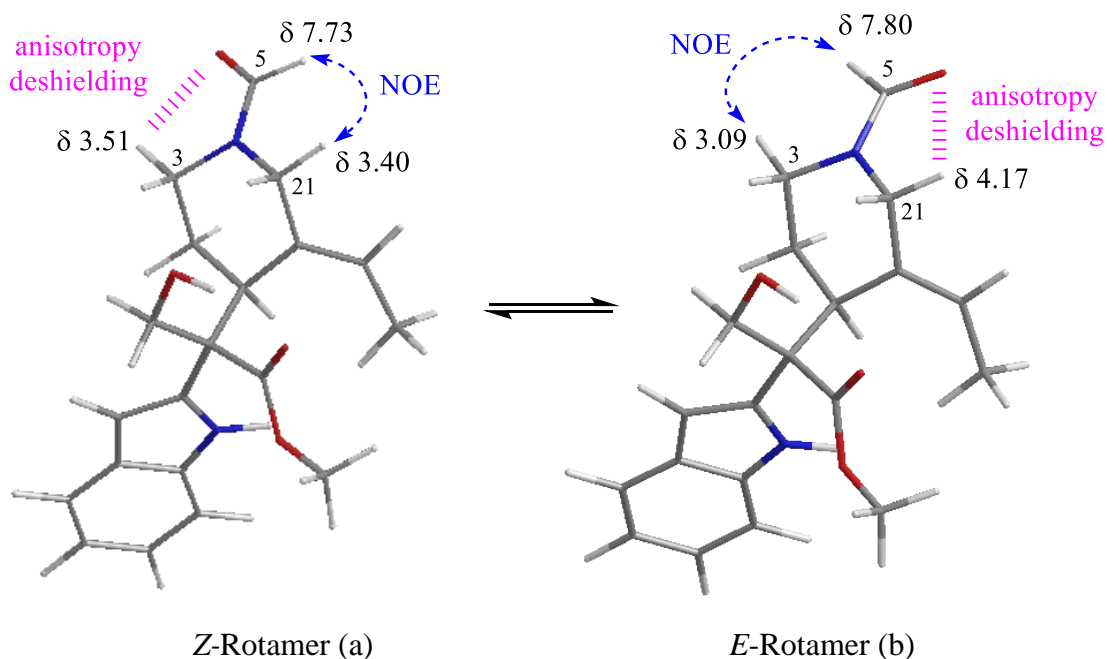


**Figure 3.16:** Selected NOESY correlations of *N*-formilyunnanensine (**12**) rotamers

**Table 3.4:**  $^1\text{H}$  (600 MHz) and  $^{13}\text{C}$  (150 MHz) NMR spectroscopic data (in  $\text{CDCl}_3$  with TMS as internal reference) of *N*-formyllynnanensine (**12**)

Position	<i>Z</i> -Rotamer (a)		<i>E</i> -Rotamer (b)		
	$\delta_{\text{H}}$ (mult., <i>J</i> in Hz)	$\delta_{\text{C}}$	Position	$\delta_{\text{H}}$ (mult., <i>J</i> in Hz)	$\delta_{\text{C}}$
2a	-	134.72	2b	-	134.47
3a (ax)	2.85, ddd (13.3, 9.6, 3.8)	37.24	3b (ax)	2.92, ddd (13.2, 9.4, 3.5)	42.23
3a' (eq)	3.51, m		3b' (eq)	3.09, m	
5a	7.73, s	160.64	5b	7.80, s	160.36
7a	6.44, dd (1.9, 0.6)	101.84	7b	6.48, dd (1.9, 0.6)	102.03
8a	-	127.46	8b	-	127.55
9a	7.57, d (8)	120.37	9b	7.57, d (8)	120.50
10a	7.11, t (8) <sup>a</sup>	120.30	10b	7.12, t (8) <sup>a</sup>	120.30
11a	7.19, t (8) <sup>b</sup>	122.35 <sup>c</sup>	11b	7.20, t (8) <sup>b</sup>	122.42 <sup>c</sup>
12a	7.40, d (8) <sup>d</sup>	111.34	12b	7.42, d (8) <sup>d</sup>	111.52
13a	-	136.18 <sup>e</sup>	13b	-	136.24 <sup>e</sup>
14a	1.69, m	26.00	14b	1.73, m	27.75
14a'	1.87, m		14b'	1.92, m	
15a	3.43, m	40.20	15b	3.49, m	40.28
16a	-	58.48	16b	-	58.16
17a	4.25, d (11.3)	66.57	17b	4.25, d (11.3)	66.05
17a'	4.39, d (11.3)		17b'	4.40, d (11.3)	
18a	1.68, dd (7, 1.3)	14.16	18b	1.63, dd (7, 1.6)	14.05
19a	5.70, q (7)	128.16	19b	5.78, q (7)	129.33
20a	-	132.16	20b	-	130.69
21a (ax)	3.14, d (14)	51.69	21b (ax)	3.05, d (14)	47.14
21a' (eq)	3.40, d (14)		21b' (eq)	4.17, d (14)	
<u>CO<sub>2</sub>Me</u> (a)	3.86, s <sup>f</sup>	53.03 <sup>g</sup>	<u>CO<sub>2</sub>Me</u> (b)	3.88, s <sup>f</sup>	53.04 <sup>g</sup>
<u>CO<sub>2</sub>Me</u> (a)	-	174.31 <sup>h</sup>	<u>CO<sub>2</sub>Me</u> (b)	-	174.35 <sup>h</sup>
NH (a)	9.97, br s	-	NH (b)	9.91, br s	-
OH (a)	2.33, br s	-	OH (b)	2.33, br s	-

<sup>a-h</sup> Signals are interchangeable within each row (between the two rotamers)

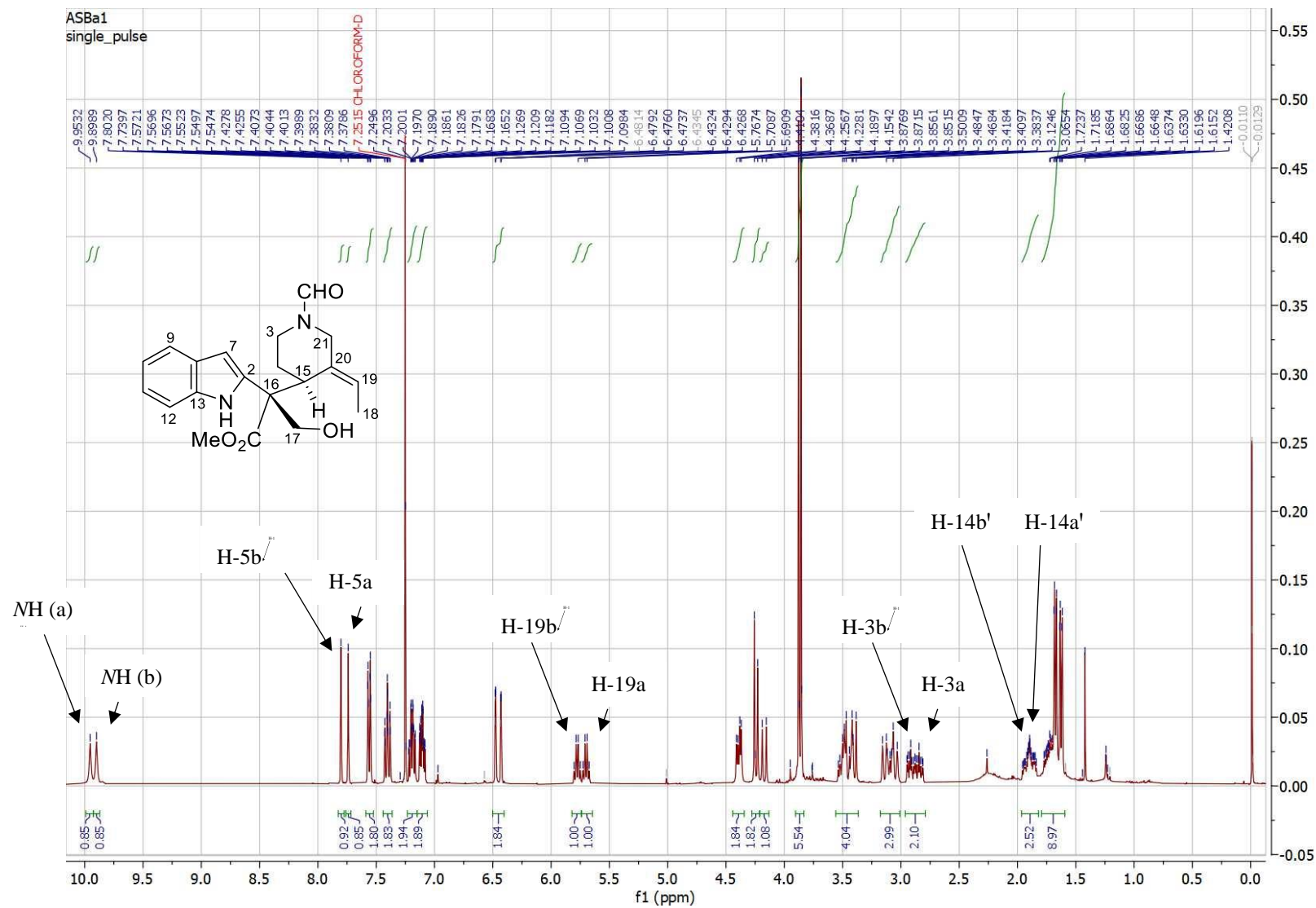
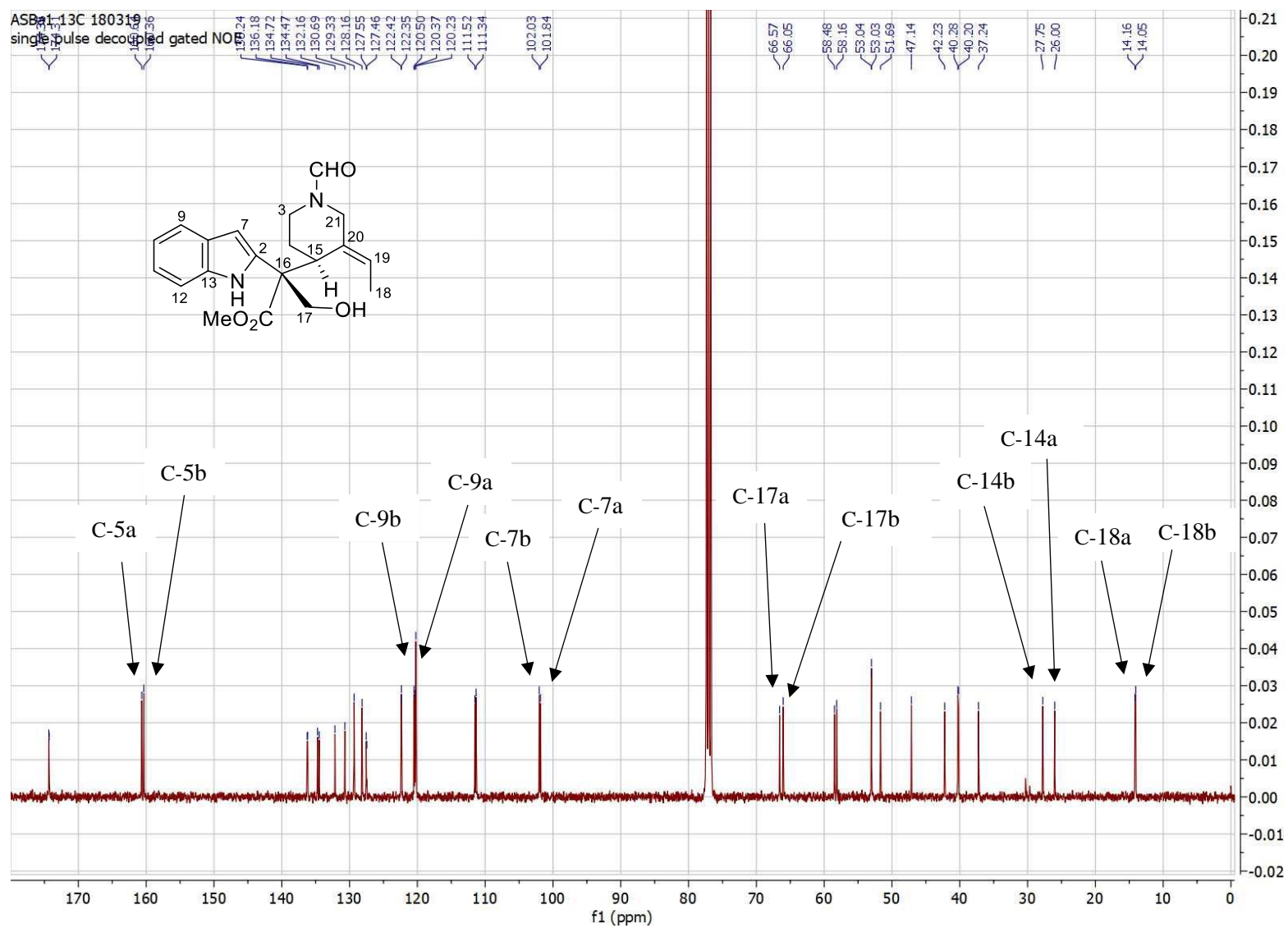
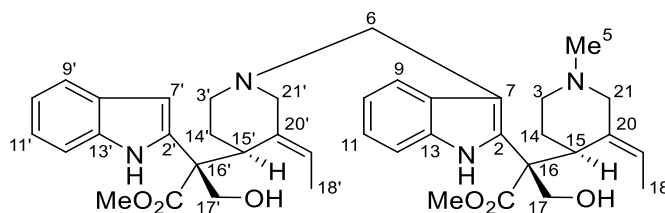


Figure 3.17: <sup>1</sup>H NMR spectrum of *N*-formilyunnanensine (12) (CDCl<sub>3</sub>, 600 MHz)



**Figure 3.18:** <sup>13</sup>C NMR spectrum of *N*-formilyunnanensine (**12**) (CDCl<sub>3</sub>, 150 MHz)

### 3.1.4 Scholaphylline (13)



**Figure 3.19:** Scholaphylline (**13**)

Scholaphylline (**13**) was isolated as a light yellowish oil from bark of *A. scholaris* with  $[\alpha]_D^{25} -39$  (*c* 0.51,  $\text{CHCl}_3$ ). The UV spectrum showed absorption maxima characteristic of indole chromophore (219 and 283 nm), while the IR spectrum indicated the presence of OH/NH ( $3403\text{ cm}^{-1}$ ) and ester C=O ( $1718\text{ cm}^{-1}$ ) functions. The HR-ESI-MS showed an  $[\text{M}+\text{H}]^+$  peak at *m/z* 683.3821, establishing the molecular formula of **13** as  $\text{C}_{40}\text{H}_{50}\text{N}_4\text{O}_6$ . The MS data suggested **13** to be a dimeric monoterpene indole alkaloid, although its  $^1\text{H}$  and  $^{13}\text{C}$  NMR spectra (**Table 3.5**, **Figures 3.22** and **3.23**) resembled those of **12** and yunnanensine, providing an early indication that **13** was composed of yunnanensine-like monomeric units.

The  $^{13}\text{C}$  NMR spectrum of **13** (**Table 3.5** and **Figure 3.23**) showed a total of 40 carbon resonances in agreement with the molecular formula. The HSQC data subsequently revealed that there were five methyl, nine methylene, thirteen methine, eleven quaternary, and two carbonyl carbons. There were eighteen carbon resonances observed between  $\delta_{\text{C}}$  100 and 140, which could be readily assigned to two indole moieties (C-2, C-7–C13, C-2', C-7'–C-13') and two ethylidene groups (C-19, C-20, C-19', and C-20'). Additionally, the two  $\text{CH}_3$  carbon resonances (C-18 and C-18') were observed at  $\delta_{\text{C}}$  14.08 and 14.22, while the two  $\text{CO}_2\text{Me}$  resonances were observed at  $\delta_{\text{C}}$  175.95, 174.77, 52.95, and 52.87. Detailed inspection of the  $^{13}\text{C}$  NMR spectrum revealed that the *N*-methyl and isolated aminomethylene groups observed at observed at  $\delta_{\text{C}}$  45.63 ( $\delta_{\text{H}}$  1.85) and  $\delta_{\text{C}}$  52.92 ( $\delta_{\text{H}}$  2.90, 3.71), respectively, were the only groups that did not appear in pairs in the structure of **13**.

The  $^1\text{H}$  NMR spectrum of **13** (Table 3.5 and Figure 3.22) showed the presence of eight aromatic hydrogen signals in the range of  $\delta_{\text{H}}$  6.70 – 7.52, which were attributed to two unsubstituted indole moieties. Additionally, a broad singlet was observed at  $\delta_{\text{H}}$  6.51, which is characteristic of the indolic H-7 (cf., H-7 of **12**). Broad singlets due to the two indolic NH groups were also observed at  $\delta_{\text{H}}$  10.28 and 10.00. The presence of two CO<sub>2</sub>Me groups were observed at  $\delta_{\text{H}}$  3.81 and 3.83, while the two ethylidene side chains were indicated by the signals observed at  $\delta_{\text{H}}$  5.56, 5.72, 1.68, and 1.61.

The COSY data readily revealed two sets of partial structures characteristic of yunnanensine structure, i.e.,  $2 \times \text{CHCHCHCH}$ ,  $2 \times \text{CH}_2\text{CH}_2\text{CH}$ , and  $2 \times \text{C}=\text{CHCH}_3$  (ethylidene) (Figure 3.20). These fragments, along with  $2 \times \text{CO}_2\text{Me}$ ,  $2 \times \text{CH}_2\text{OH}$ , and  $2 \times \text{CH}_2\text{N}$ , were deduced to constitute two units of yunnanensine-like structures based on the HMBC data (Figure 3.20). The lone *N*-methyl group ( $\delta_{\text{C}}$  45.63;  $\delta_{\text{H}}$  1.85) was deduced to be part of the piperidine moiety in monomer I based on the three-bond correlations observed from H-5 to C-3 and C-21. Finally, the lone aminomethylene group ( $\delta_{\text{C}}$  52.92;  $\delta_{\text{H}}$  2.90, 3.71) was established as the bridge that connects C-7 and N-4' from the two yunnanensine-like monomers (I and II) based on the HMBC correlations observed from H-6 to C-2, C-7, C-8, C-3', and C-21'. The structure proposed for **13** is also entirely consistent with the NOESY data (Figure 3.21). For instance, the NOE observed between H-6 and H-9 further confirmed that CH<sub>2</sub>-6 is the point of connection between the two monomeric units.

Based on the structures of the monomeric units, scholaphylline (**13**) can be classified under the *Strychnos-Strychnos* class of bisindoles, and represents the first member of the *secostemmadenine-secovallesamine*-type bisindole.<sup>124,125</sup>

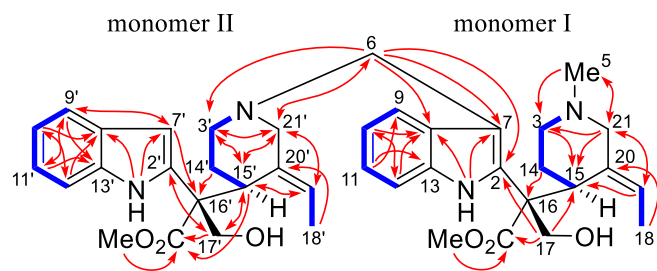


**Figure 3.20:** COSY (blue, bold) and selected HMBC (red arrows) of scholaphylline (13)

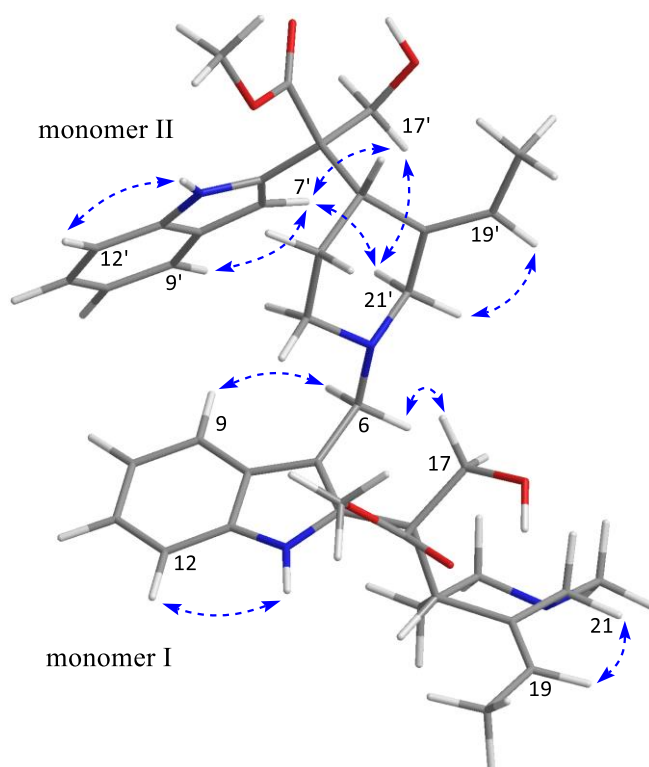


**Figure 3.21:** Selected NOESY correlations of scholaphylline (13)

**Table 3.5:**  $^1\text{H}$  (700 MHz) and  $^{13}\text{C}$  (175 MHz) NMR spectroscopic data (in  $\text{CDCl}_3$  with TMS as internal reference) of scholaphylline (**13**)

Position	$\delta_{\text{H}}$ (mult., $J$ in Hz)	$\delta_{\text{C}}$	Position	$\delta_{\text{H}}$ (mult., $J$ in Hz)	$\delta_{\text{C}}$
2	-	132.67	2'	-	135.07
3	1.60, m	52.07	3'	1.16, m	47.37
	2.44, d (11.0)			2.27, d (11.9)	
5 (Me)	1.85, s	45.63			
6	2.90, m	52.92			
	3.71, d (13.5)				
7	-	108.19	7'	6.51, br s	102.13
8	-	129.53	8'	-	127.52
9	6.70, br d (8)	117.68	9'	7.65, d (8)	120.31
10	6.97, t (7.5)	119.49	10'	7.19, t (7.5)	120.20
11	7.12, t (7.5)	121.69	11'	7.32, t (7.5)	122.32
12	7.31, d (8)	110.94	12'	7.52, d (8)	111.45
13	-	134.34	13'	-	136.22
14	1.71, m	27.54	14'	1.69, m	27.20
	1.71, m			1.43, m	
15	3.15, br d (5)	39.15	15'	3.21, d (6.5)	38.95
16	-	60.97	16'	-	57.92
17	4.23, d (12.3)	64.74	17'	4.25, d (11.4)	66.20
	4.33, d (12.4)			4.37, d (11.4)	
18	1.61, dd (6.9, 1.2)	14.22	18'	1.68, dd (6.9, 1.5)	14.08
19	5.56, q (6.9)	126.46	19'	5.72, q (6.9)	126.76
20	-	134.34	20'	-	133.11
21	1.87, m	62.03	21'	2.67, d (11.4) <sup>a</sup>	61.49
	2.68, d (11.1) <sup>a</sup>			2.95, d (11.9)	
<u>CO<sub>2</sub>Me</u>	3.81, s	52.87 <sup>b</sup>	<u>CO<sub>2</sub>Me'</u>	3.83, s	52.95 <sup>b</sup>
<u>CO<sub>2</sub>Me</u>	-	175.95	<u>CO<sub>2</sub>Me'</u>	-	174.77
NH	10.28, br s	-	NH'	10.00, br s	-

<sup>a-b</sup> Assignments may be interchanged within each row due to partial overlapping of signals

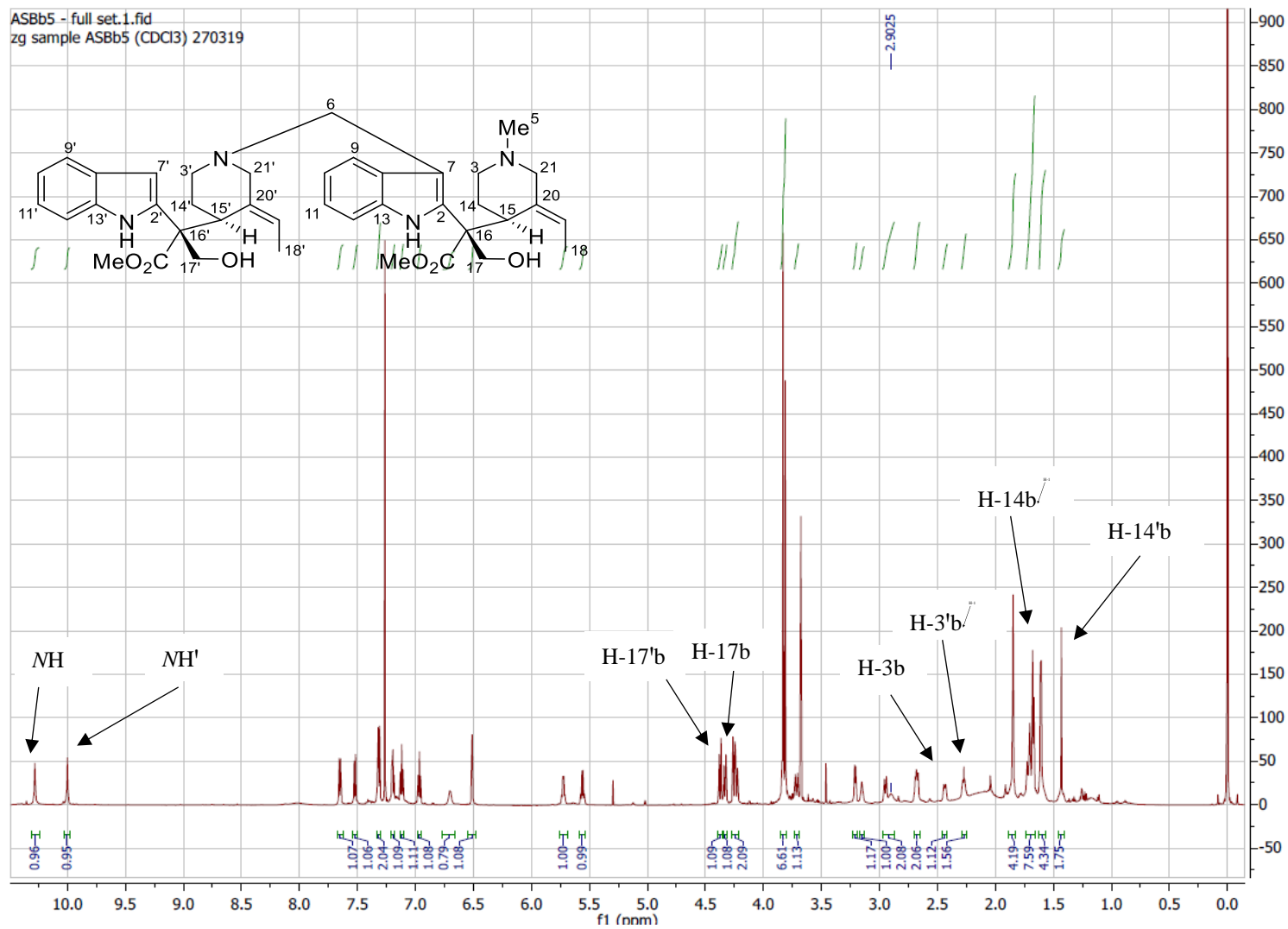
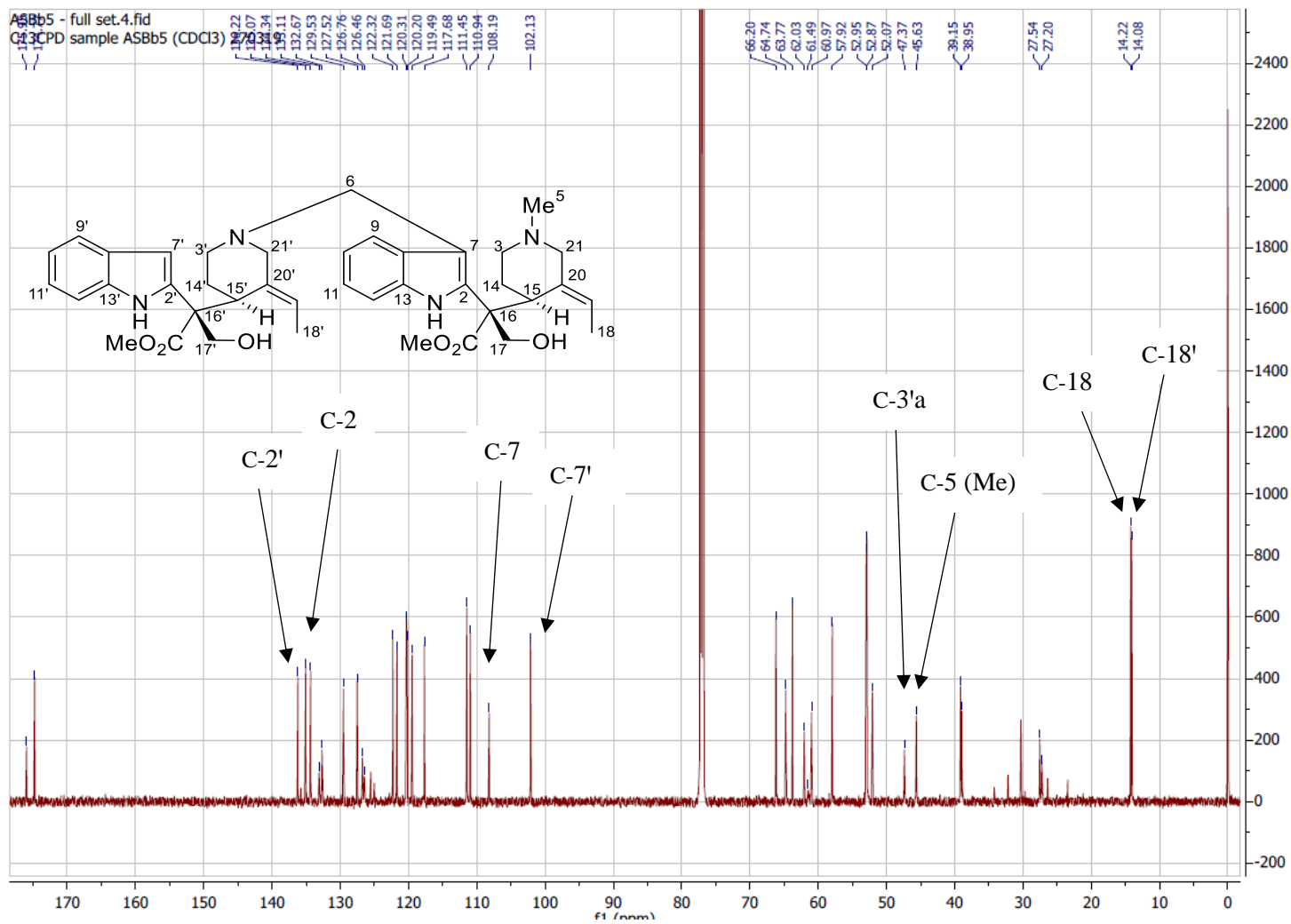


Figure 3.22: <sup>1</sup>H NMR spectrum of scholaphylline (**13**) (CDCl<sub>3</sub>, 700 MHz)



**Figure 3.23:**  $^{13}\text{C}$  NMR spectrum of scholaphylline (**13**) ( $\text{CDCl}_3$ , 175 MHz)

### 3.1.5 19,20-*E*-Vallesamine (14), 19,20-*Z*-vallesamine (15), 19,20-*E*-vallesamine *N*-oxide (16), 6,7-*seco*angustilobine B (17), and 6,7-*seco*-19,20 $\alpha$ -epoxyangustilobine B (18)

Five known aspidospermatan-type alkaloids, *viz.*, 19,20-*E*-vallesamine (14),<sup>100</sup> 19,20-*Z*-vallesamine (15),<sup>100</sup> 19,20-*E*-vallesamine *N*-oxide (16),<sup>88</sup> 6,7-*seco*angustilobine B (17),<sup>86,88</sup> and 6,7-*seco*-19,20 $\alpha$ -epoxyangustilobine B (18)<sup>88</sup> were also isolated. The <sup>1</sup>H and <sup>13</sup>C NMR spectra of these compounds are shown in **Figures 3.24 – 3.33**, and while the NMR spectroscopic data are summarized in **Tables 3.6 – 3.8**. Other data are given in Chapter 4 (Experimental).

**Table 3.6:** <sup>1</sup>H (600 MHz) and <sup>13</sup>C (150 MHz) NMR spectroscopic data (in CDCl<sub>3</sub> with TMS as internal reference) of 19,20-*E*-vallesamine (14)

Position	$\delta_{\text{H}}$ (mult., <i>J</i> in Hz)	$\delta_{\text{C}}$
2	-	133.5
3	2.86, m	47.5
	2.86, m	
6	4.78, d (17.1)	50.9
	4.07, d (17.1)	
7	-	108.7
8	-	128.2
9	7.48, d (8.0)	118.3
10	7.07, br t (8.0)	119.0
11	7.17, td (8.0, 0.8)	122.2
12	7.30, d (8.0)	110.7
13	-	135.3
14	2.32, m	24.1
	1.86, td (13, 4)	
15	3.62, dd (11.8, 4)	36.3
16	-	58.7
17	4.19, d (11)	70.3
	3.79, d (11)	
18	1.73, d (6.9)	14.1
19	5.53, q (6.9)	124.2
20	-	133.0
21	3.59, m	52.9
	3.71, m	
NH	9.57, br s	-
CO <sub>2</sub> Me	3.74, s	53.9
CO <sub>2</sub> Me	-	175.3

**Table 3.7:**  $^1\text{H}$  (700 MHz) and  $^{13}\text{C}$  (150 MHz) NMR spectroscopic data (in  $\text{CDCl}_3$  with TMS as internal reference) of 19,20-*Z*-vallesamine (**15**) and 19,20-*E*-vallesamine *N*-oxide (**16**)

Position	15		16	
	$\delta_{\text{H}}$ (mult., <i>J</i> in Hz)	$\delta_{\text{C}}$	$\delta_{\text{H}}$ (mult., <i>J</i> in Hz)	$\delta_{\text{C}}$
2	-	134.74	-	133.8
3	3.01, m 2.90, m	47.30	3.50, m 3.45, m	64.5
6	4.95, d (17) 4.08, d (17)	48.25	4.88, d (16) 5.30, d (16)	69.8
7		101.40	-	104.6
8		130.59	-	127.4
9	7.48, d (8)	117.78	7.55, d (7)	118.0
10	7.09, t (8)	120.29	7.07, t (7)	120.1
11	7.19, t (8)	123.21	7.18, t (7)	123.1
12	7.31, d (8)	111.23	7.27, d (7)	111.0
13		134.81	-	134.6
14	2.28, m 2.04, td (12.5, 7.2)	20.44	2.19, m 2.32, m	23.4
15	3.67, m	34.60	3.66, dd (12, 3)	33.5
16		58.44	-	58.4
17	3.85, d (10.6) 4.23, d (10.6)	69.93	3.87, d (10) 4.28, d (10)	69.8
18	1.74, d (7)	14.32	1.72, m	14.3
19	5.58, q (7)	124.60	5.55, m	129.2
20		127.20	-	127.4
21	3.67, m 3.63, m	51.45	3.84, d (16) 4.59, d (16)	72.2
NH	9.93, br s	-	10.53, br s	-
<u>CO<sub>2</sub>Me</u>	3.75, s	53.37	3.73, s	53.2
<u>CO<sub>2</sub>Me</u>	-	173.18	-	173.3

**Table 3.8:**  $^1\text{H}$  (700 MHz) and  $^{13}\text{C}$  (175 MHz) NMR spectroscopic data (in  $\text{CDCl}_3$  with TMS as internal reference) of 6,7-*seco*angustilobine B (**17**) and 6,7-*seco*-19,20 $\alpha$ -epoxyangustilobine B (**18**)

Position	17		18	
	$\delta_{\text{H}}$ (mult., $J$ in Hz)	$\delta_{\text{C}}$	$\delta_{\text{H}}$ (mult., $J$ in Hz)	$\delta_{\text{C}}$
2	-	135.88	-	134.0
3	2.08, td (12, 3) 2.77, d (12.0)	56.63	1.96, td (12, 2.9) 2.86, br d (12)	56.2
7	6.26, s	100.47	6.19, dd (2.2, 0.9)	100.6
8		127.85	-	127.8
9	7.55, d (8)	120.53	7.54, d (8)	120.5
10	7.10, t (8)	120.10	7.10, td (8, 1)	120.2
11	7.15, t (8)	122.19	7.18, td (8, 1)	122.5
12	7.32, d (8)	111.08	7.34, d (8)	111.0
13	-	136.04	-	135.7
14	1.00, dd (12, 3) 1.48, qd (12, 3)	29.05	1.17, m 1.60, m	26.6
15	3.22, d (12)	46.65	3.16, d (12.9)	46.0
16		56.66	-	53.2
17	4.10, d (11.8) 4.78, d (11.8)	70.82	3.73, d (12.4) 4.75, dd (12.4, 1.6)	70.3
18	4.22, d (17) 4.33, dd (17, 3)	69.32	3.96, d (14.4) 4.37, dd (14.4, 3.3)	67.2
19	5.55, t (3)	123.65	2.97, d (3.3)	63.0
20	-	137.67	-	63.0
21	2.80, d (11) 3.16, d (11)	67.15	2.34, dd (10.7, 1.6) 2.60, d (10.7)	66.0
NH	8.80, s		8.33, br s	
$\text{CO}_2\text{Me}$	3.70, s	52.88	3.79, s	53.2
$\underline{\text{C}}\text{O}_2\text{Me}$		173.82		173.1
N-Me	2.25, s	45.54	2.28, s	45.7

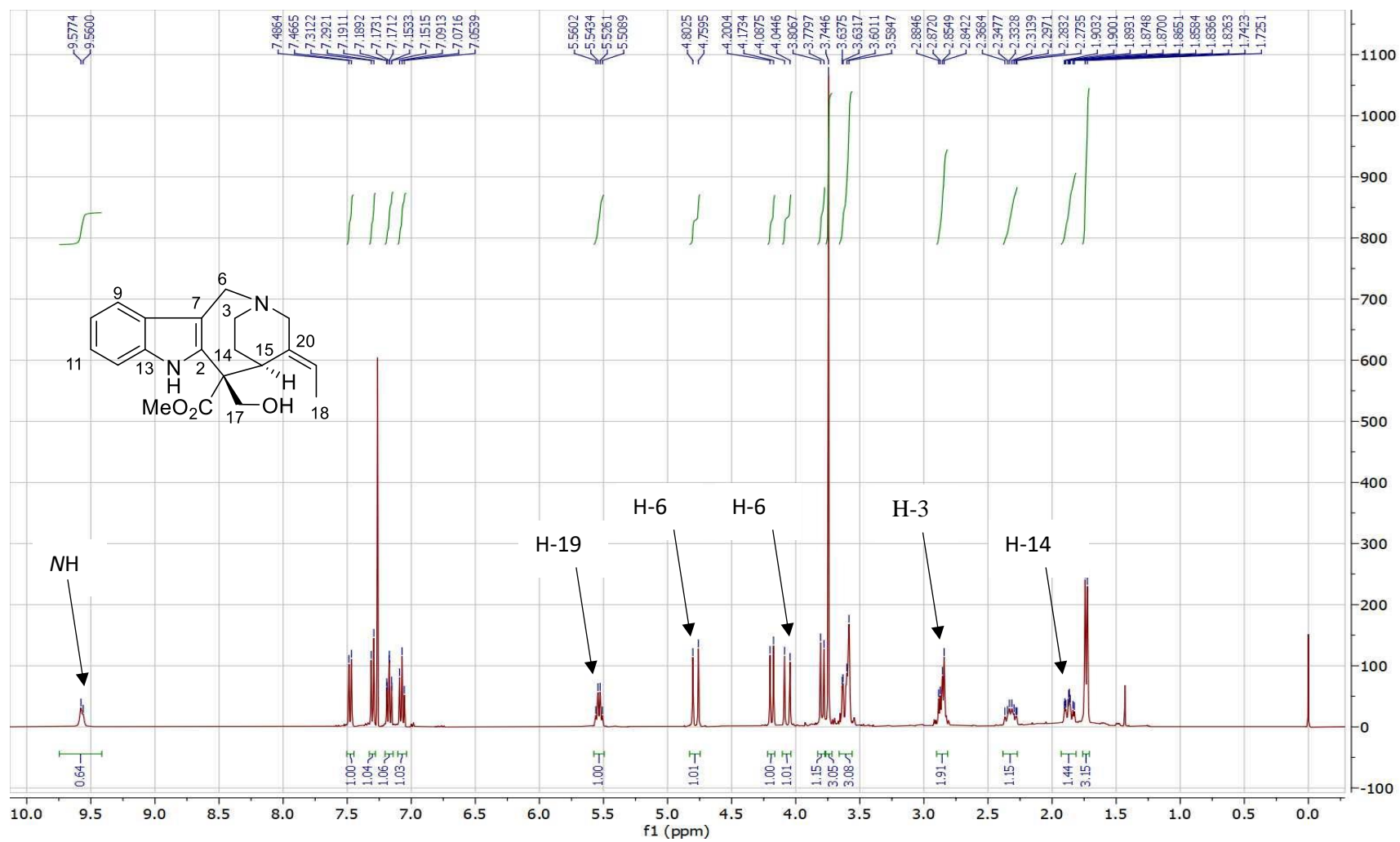


Figure 3.24: <sup>1</sup>H NMR spectrum of 19,20-*E*-vallesamine (**14**) (CDCl<sub>3</sub>, 600 MHz)

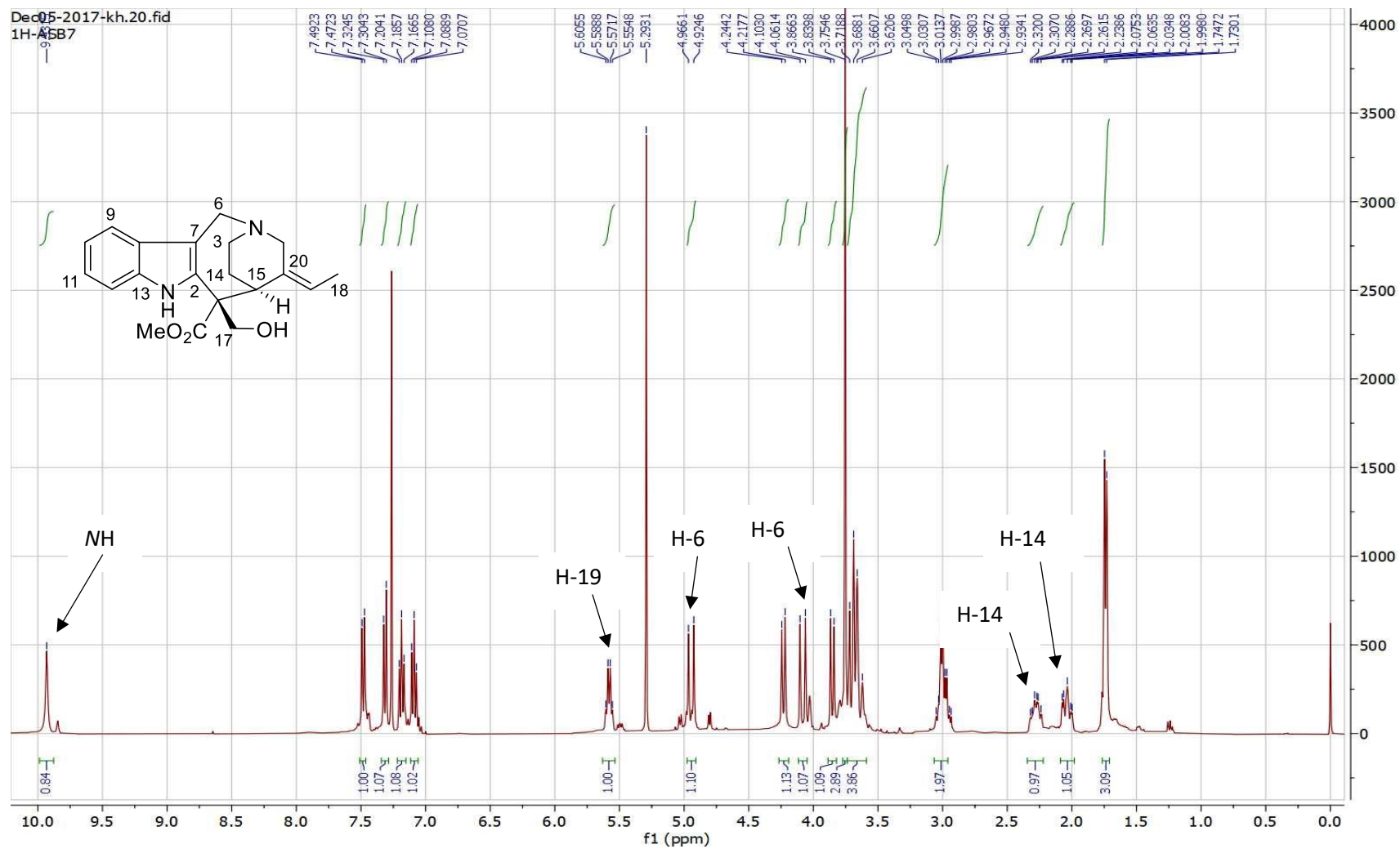


Figure 3.25: <sup>1</sup>H NMR spectrum of 19,20-Z-vallesamine (15) (CDCl<sub>3</sub>, 600 MHz)

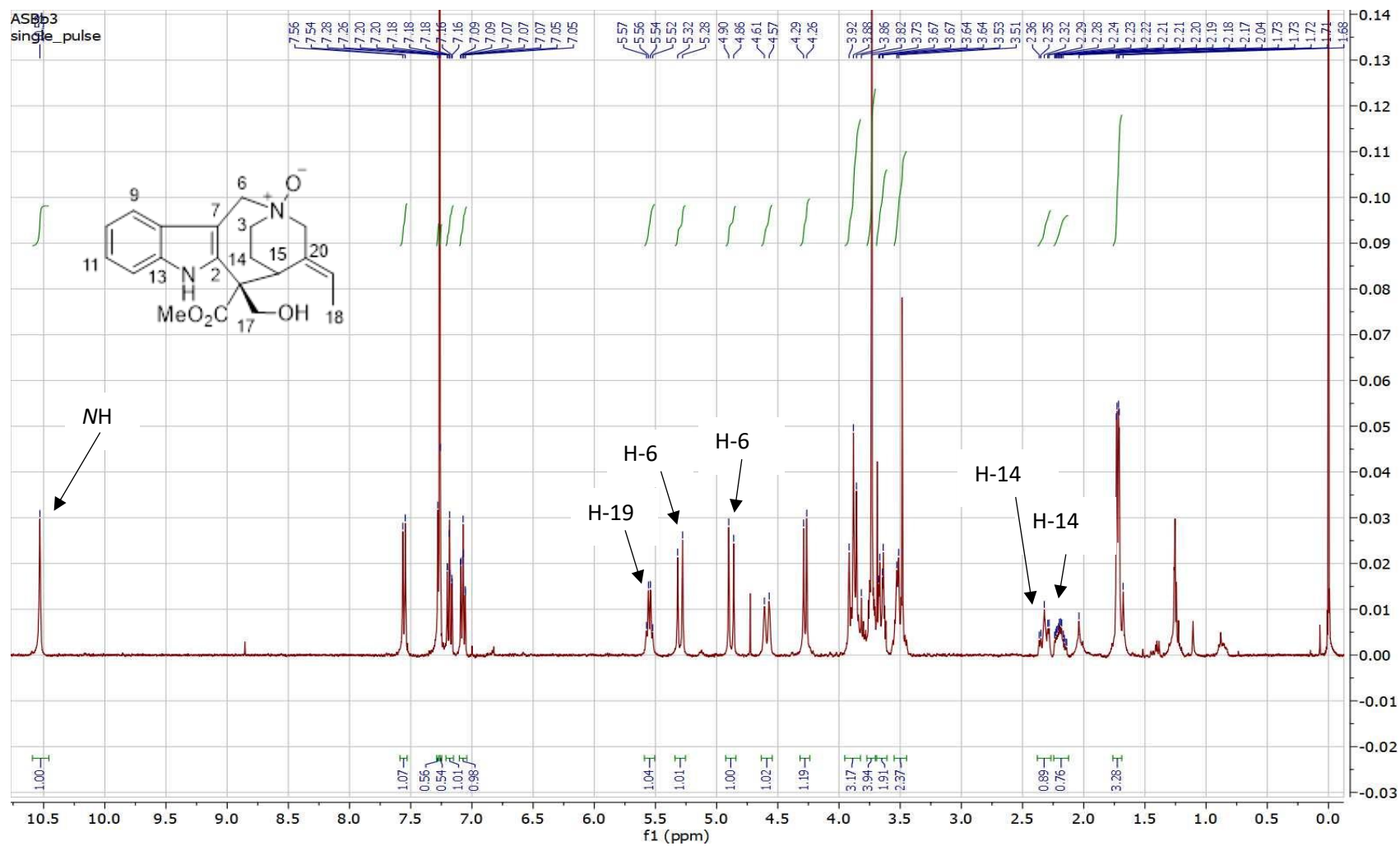


Figure 3.26: <sup>1</sup>H NMR spectrum of 19,20-*E*-vallesamine *N*-oxide (**16**) (CDCl<sub>3</sub>, 600 MHz)

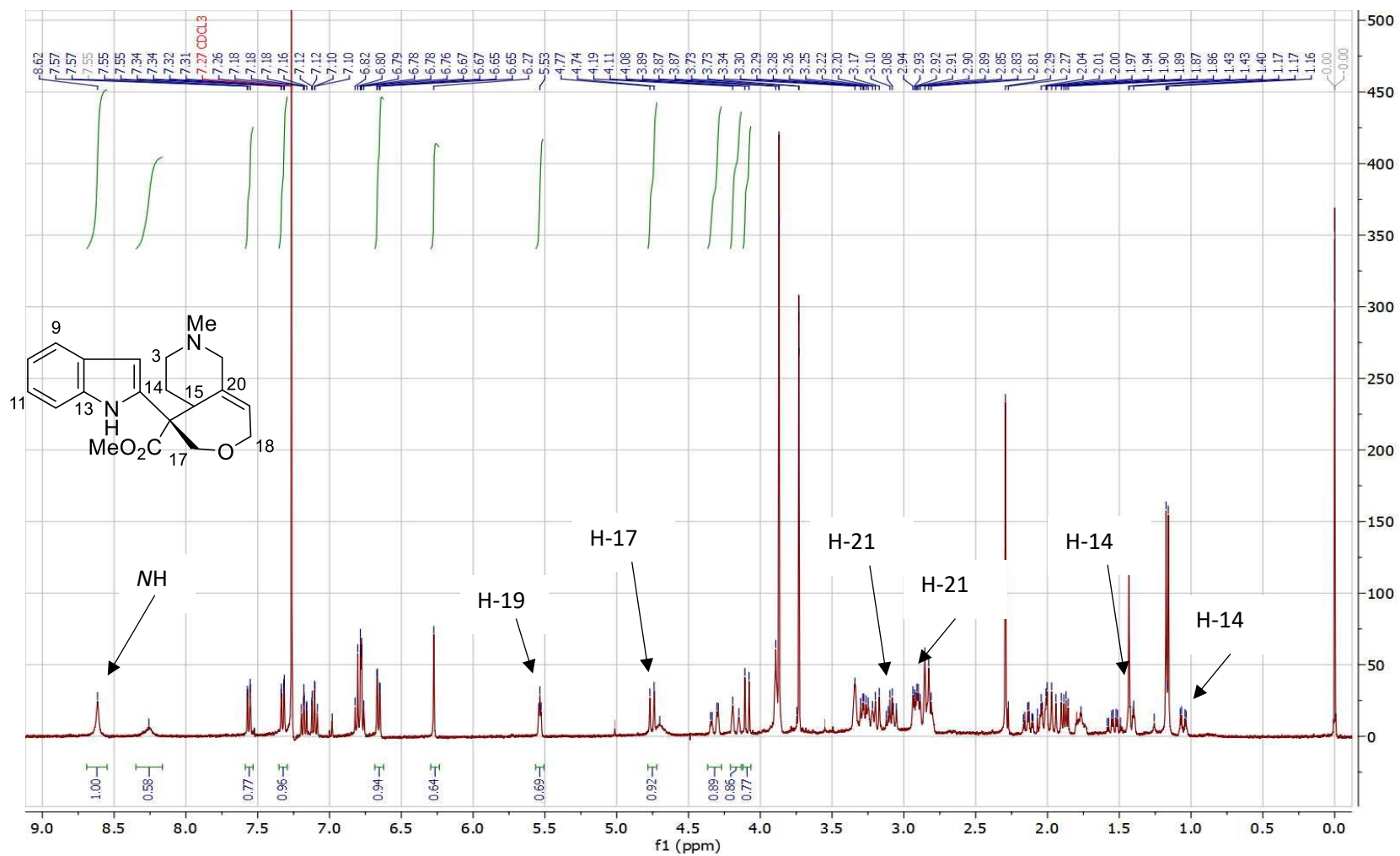


Figure 3.27:  $^1\text{H}$  NMR spectrum of 6,7-secoangustilobine B (17) ( $\text{CDCl}_3$ , 600 MHz)

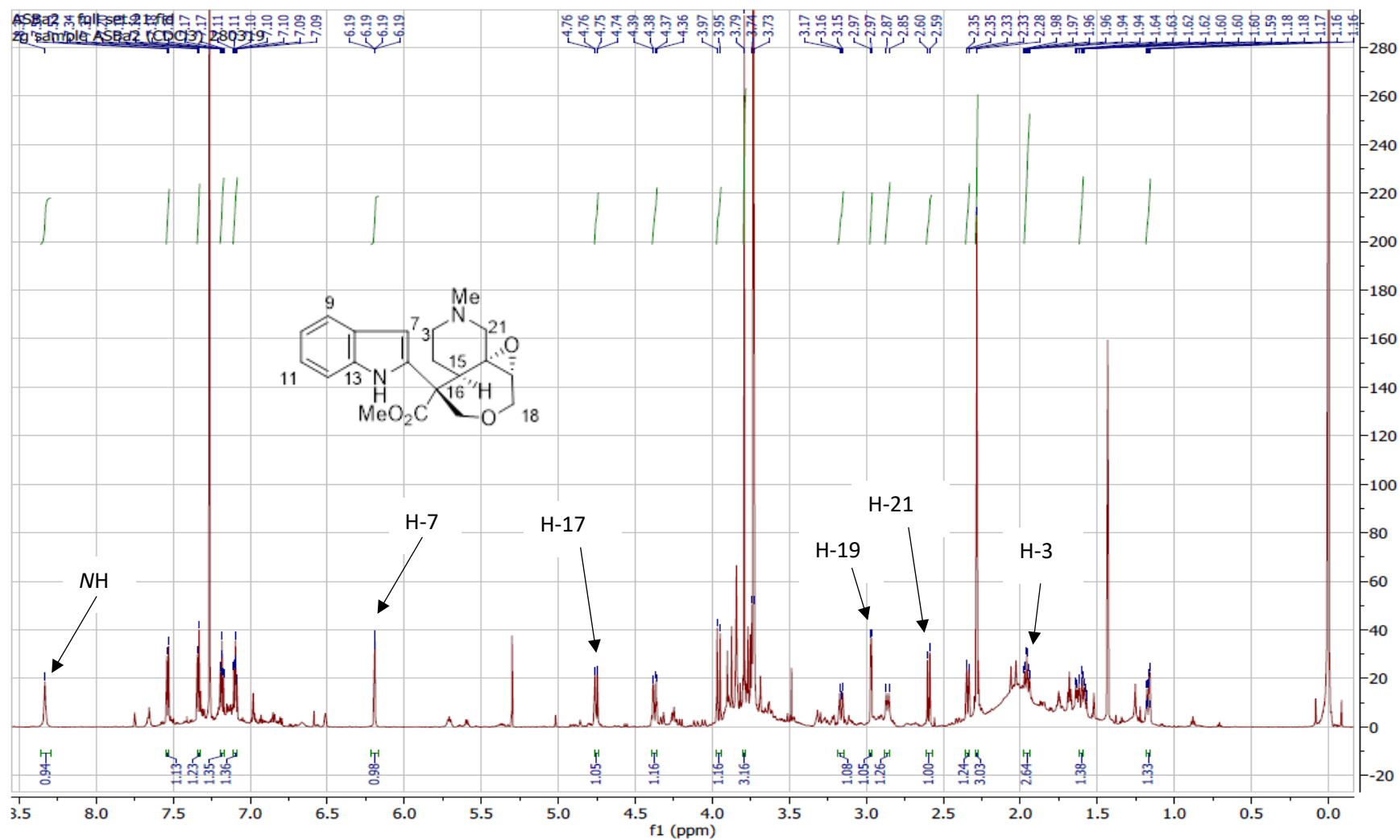


Figure 3.28:  $^1\text{H}$  NMR spectrum of 6,7-*seco*-19,20 $\alpha$ -epoxyangustilobine B (**18**) ( $\text{CDCl}_3$ , 600 MHz)

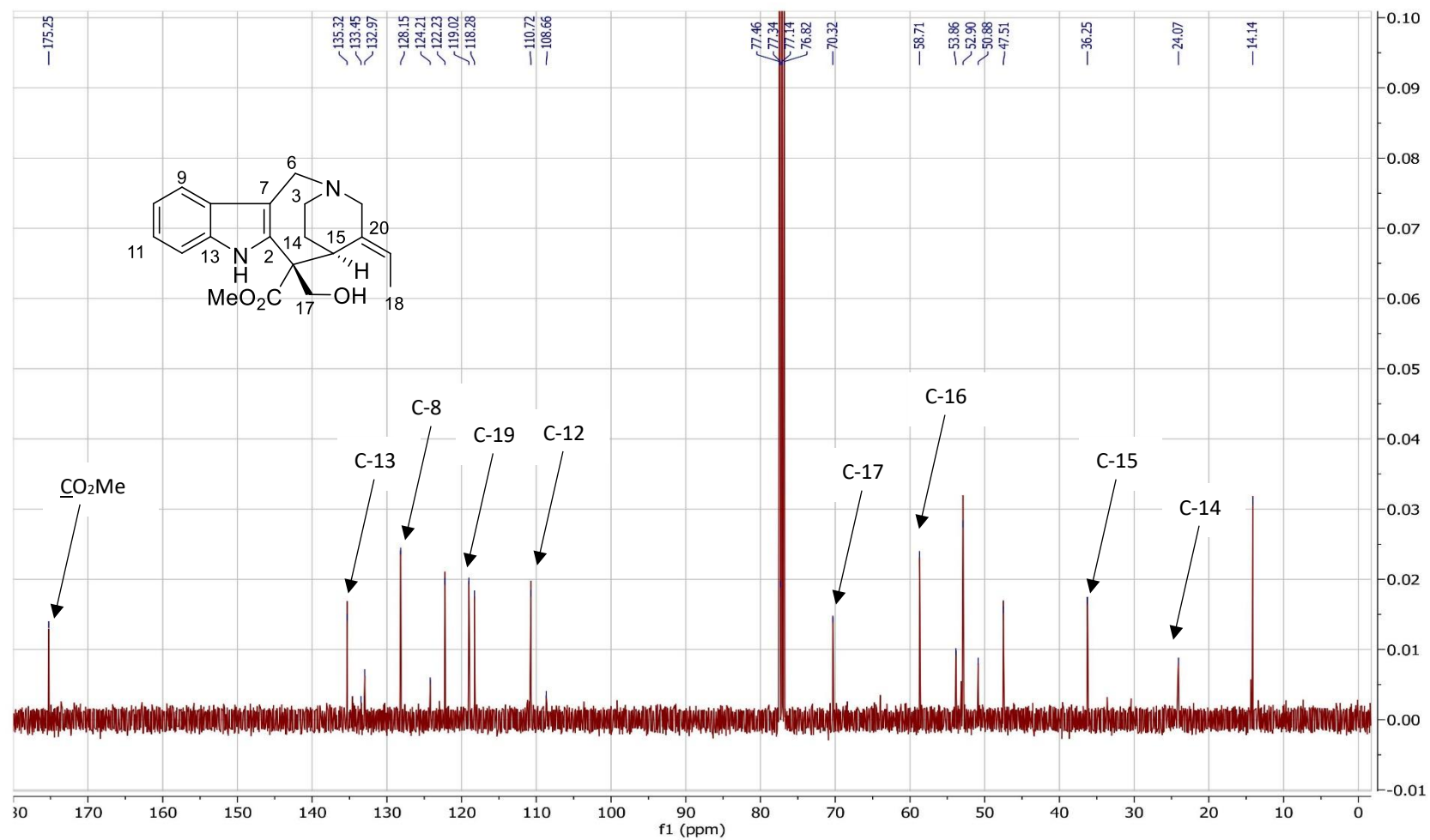
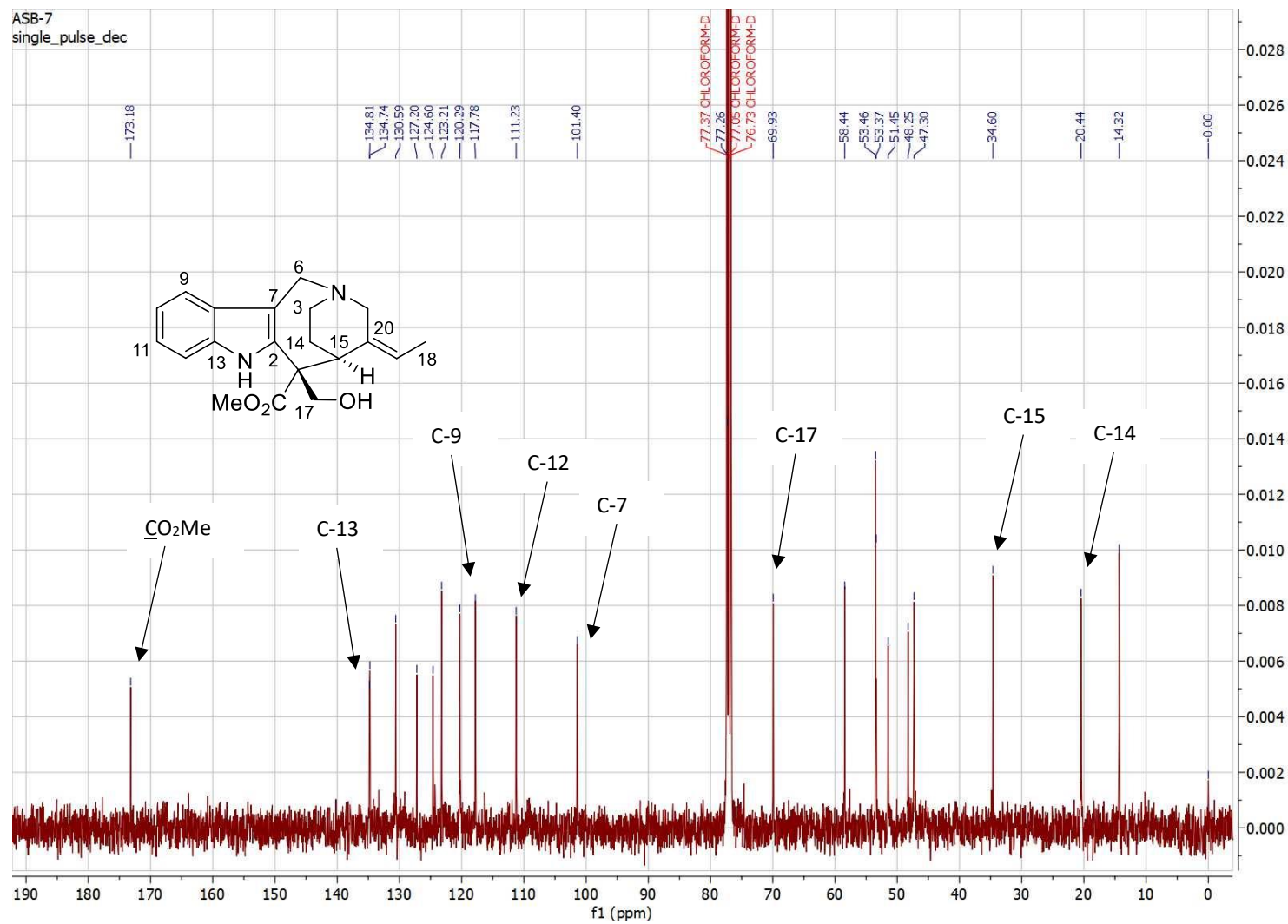


Figure 3.29: <sup>13</sup>C NMR spectrum of 19,20-*E*-vallesamine (14) (CDCl<sub>3</sub>, 150 MHz)



**Figure 3.30:** <sup>13</sup>C NMR spectrum of 19,20-Z-vallesamine (15) (CDCl<sub>3</sub>, 150 MHz)

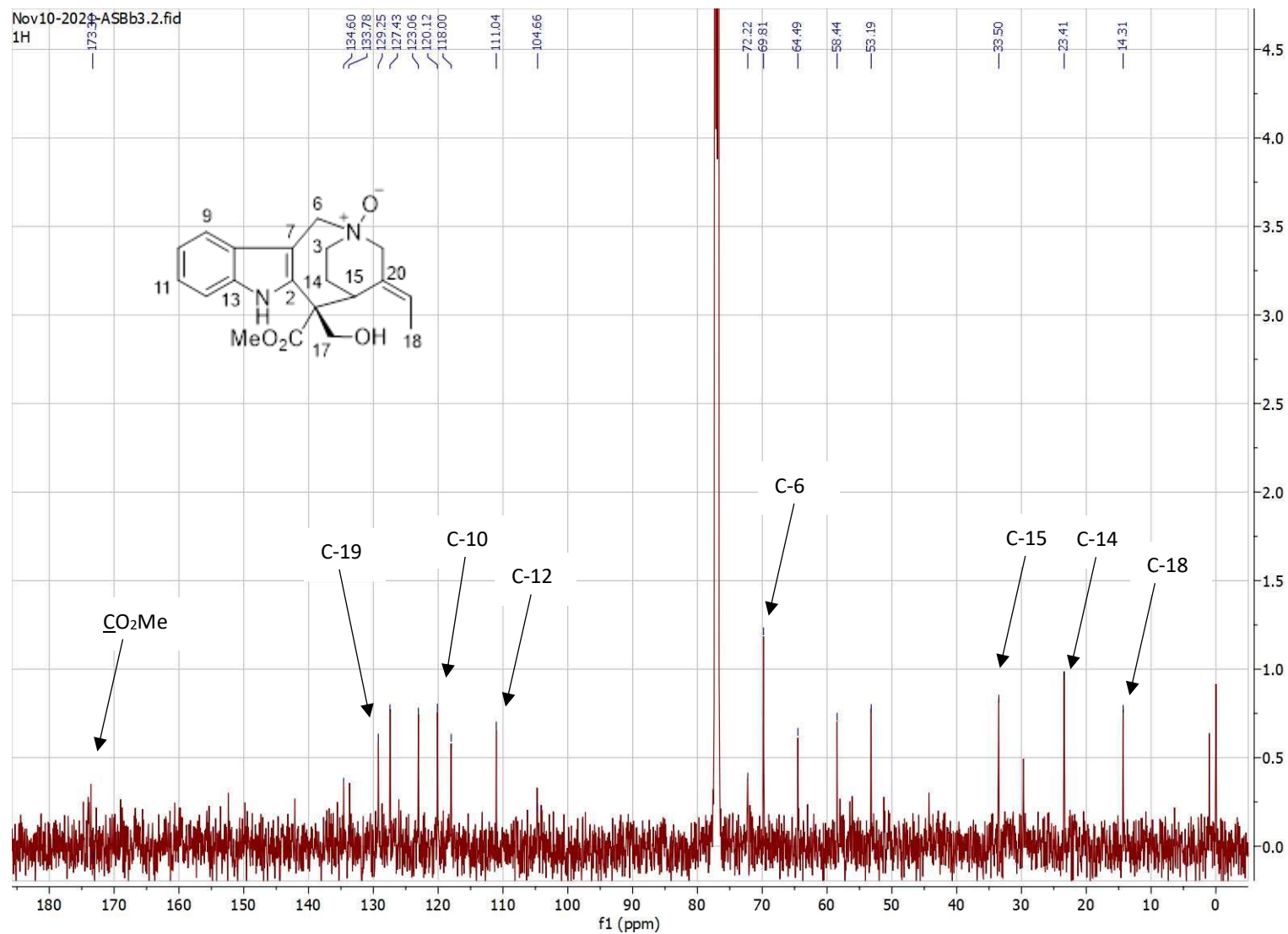


Figure 3.31: <sup>13</sup>C NMR spectrum of 19,20-*E*-vallesamine *N*-oxide (**16**) (CDCl<sub>3</sub>, 150 MHz)

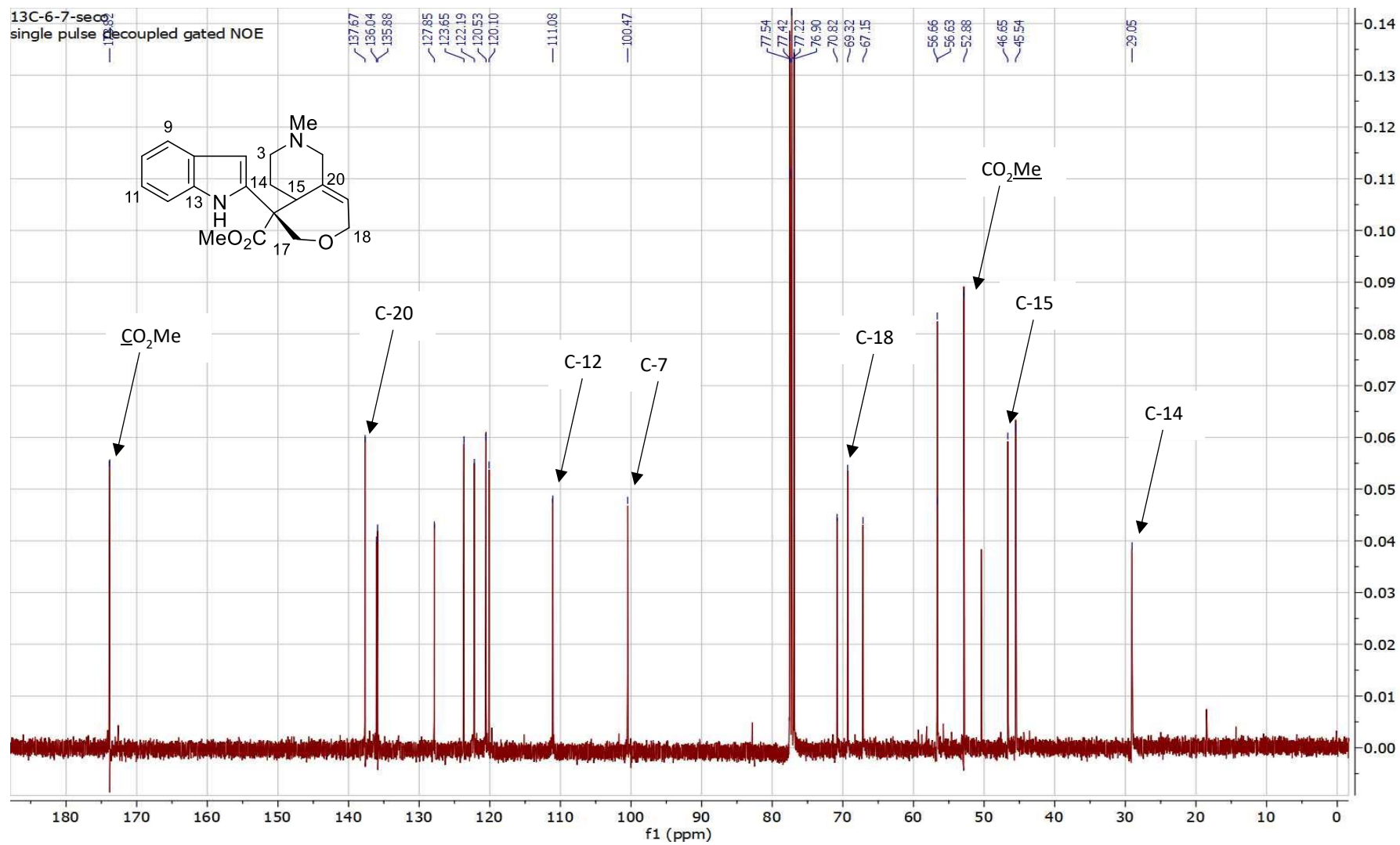


Figure 3.32: <sup>13</sup>C NMR spectrum of 6,7-secangustilobine B (17) (CDCl<sub>3</sub>, 150 MHz)

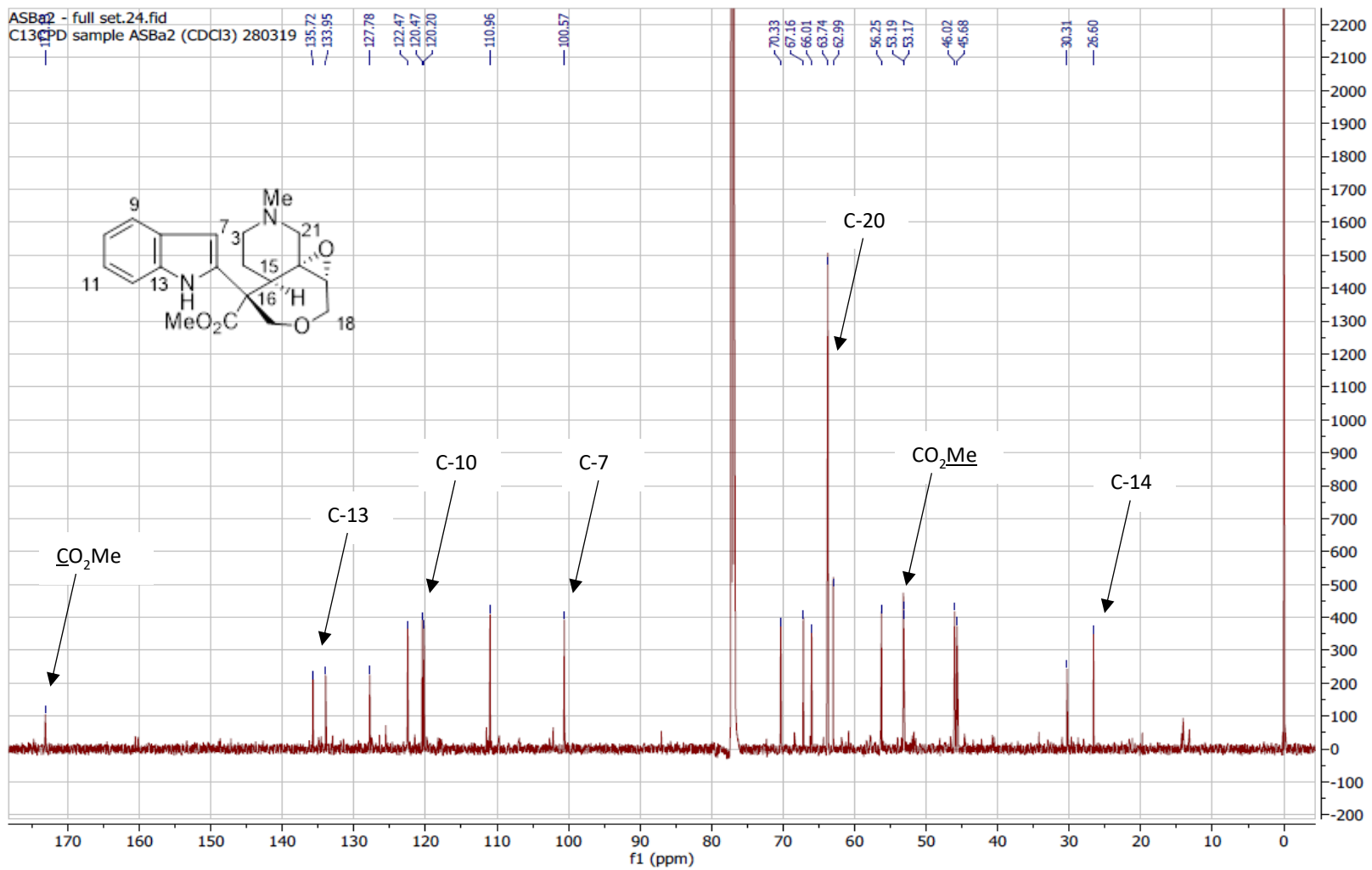
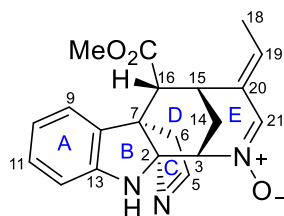


Figure 3.33:  $^{13}\text{C}$  NMR spectrum of 6,7-*seco*-19,20 $\alpha$ -epoxyangustilobine B (**18**) ( $\text{CDCl}_3$ , 150 MHz)

## 3.2 Corynanthean-type Alkaloids

### 3.2.1 Alstobrogaline (19)



**Figure 3.34:** Structure of alstobrogaline (**19**)

Alstobrogaline (**19**) was obtained as a light yellowish oil and then crystallized from  $\text{CHCl}_3$  to form light orange block crystals, mp 187 °C (decomposed),  $[\alpha]_D^{25} +93$  ( $c$  0.10,  $\text{CHCl}_3$ ). The IR spectrum revealed NH ( $3249\text{ cm}^{-1}$ ) and ester carbonyl ( $1739\text{ cm}^{-1}$ ) absorption bands, while the UV spectrum revealed absorption maxima (235 and 290 nm) characteristic of dihydroindole chromophore. The HR-DART-MS measurements established the molecular formula of **19** as  $\text{C}_{20}\text{H}_{21}\text{N}_3\text{O}_3$  based on the  $[\text{M}+\text{H}]^+$  peak detected at  $m/z$  352.1674. Notably, the molecular formula revealed 12 degrees of unsaturation and the existence of a third nitrogen atom, which is uncommon among the monoterpenoid indole alkaloids.

The  $^1\text{H}$  NMR spectrum (**Table 3.9** and **Figure 3.38**) showed the presence of signals due to four aromatic hydrogens ( $\delta_{\text{H}}$  6.73–7.10), an ester methyl at  $\delta_{\text{H}}$  3.73 (s), an indolic NH at  $\delta_{\text{H}}$  4.92 (br s), and an ethylidene side chain ( $\delta_{\text{H}}$  1.75, d, 3H;  $\delta_{\text{H}}$  5.84, q, 2H;  $J = 7.5$  Hz). Additionally, two unusually deshielded signals at  $\delta_{\text{H}}$  7.29 (br s) and 7.69 (s) were also observed. Consistent with the molecular formula established by HRMS measurements, the  $^{13}\text{C}$  NMR spectrum (**Table 3.9** and **Figure 3.39**) showed 20 carbon resonances, while the HSQC data indicated 11 downfield resonances (seven  $sp^2$  CH, one  $N$ -bearing  $sp^2$  tertiary carbon, two  $sp^2$  quaternary carbons, and one ester C=O) and nine upfield resonances (two  $\text{CH}_3$ , two  $sp^3$   $\text{CH}_2$ ,

three  $sp^3$  CH, one  $sp^3$  quaternary carbon, and one significantly deshielded non-H-bearing  $sp^3$  carbon at  $\delta_c$  98.8). The downfield resonances corresponding to the indolic benzene ring ( $\delta_c$  111.3, 120.5, 123.0, 129.0, 136.3, and 145.7) and ethylidene side chain ( $\delta_c$  130.0, 132.3, and 14.4) were readily assigned based on comparison with other indole alkaloids with a dihydroindole chromophore and an ethylidene unit, and these assignments were corroborated by the HMBC and NOESY data (**Figures 3.35** and **3.36**).

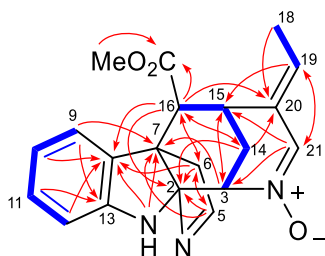


**Figure 3.35:** COSY (blue, bold) and selected HMBC (red arrows) correlations of alstobrogaline (**19**)

The COSY data revealed the presence of the CHCHCHCH, NCHCH<sub>2</sub>CHCH, and =CHCH<sub>3</sub> partial structures corresponding to the C-9–C-10–C-11–C-12, N–C-3–C-14–C-15–C-16, and C-18–C-19 fragments in **19**, respectively (**Figure 3.35**). The C-9–C-10–C-11–C-12 fragment was attributed to the four contiguous aromatic hydrogens of the unsubstituted dihydroindole moiety. This was confirmed by the HMBC data which showed correlations from H-9 to C-7 and C-13; from H-12 to C-8; and from MH to C-7 and C-8. The N–C-3–C-14–C-15–C-16 fragment was linked to C-2 and C-7 on the basis of the correlations observed from H-3 to C-7; from H-14 to C-2; and from H-16 to C-2, C-6, and C-8 in the HMBC spectrum (**Figure 3.35**). Construction of the six-membered ring D in **19** is thus completed. Additionally,

the CO<sub>2</sub>Me moiety and its connection to C-16 was revealed by the correlations observed from H-16 and OMe ( $\delta$  3.73) to the carbonyl carbon at  $\delta_C$  171.9 in the HMBC spectrum.

The C-18–C-19 fragment was assigned to the ethylidene side chain by the three-bond correlation observed from H-18 to C-20 in the HMBC spectrum. The attachments of C-15 and C-21 ( $\delta_C$  138.1) to C-20 were indicated by the correlations observed from H-19 to C-15 and C-21; and from H-21 ( $\delta_H$  7.29) to C-15, C-19, and C-20 in the HMBC spectrum. On the other hand, C-21 was linked to C-3 via *N*-4 based on the HMBC correlation observed from H-21 to C-3. Construction of the six-membered ring E in **19** is thus completed. The presence of the nitrono moiety at the *N*-4–C-21 fragment was consistent with the unusually deshielded chemical shifts observed for CH-21, i.e.,  $\delta_C$  138.1 and  $\delta_H$  7.29.<sup>97</sup> The five-membered ring C in **19** was finally assembled by connecting C-2 to C-5 via an *N* atom, and C-6 to C-7, based on the correlations observed from H-6 to C-2, C-5, C-8, and C-16; and from H-5 to C-2, C-6, and C-7 in the HMBC spectrum. The unusually deshielded chemical shifts observed for CH-5 ( $\delta_C$  167.9 and  $\delta_H$  7.69) is consistent with the presence of the aldimine group (CH-5=N). On the other hand, C-2 has a chemical shift ( $\delta_C$  98.8) that was indicative of an aminal carbon. The planar structure proposed for **19** is in complete agreement with the HMBC data (**Figure 3.35**).

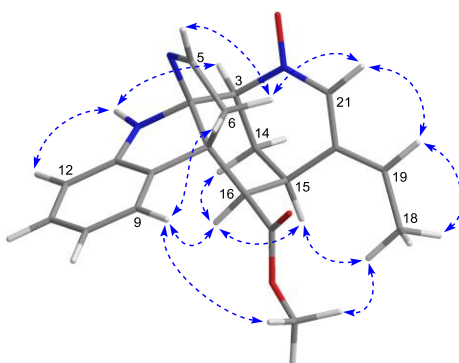


**Figure 3.36:** Selected NOESY correlations of alstobrogaline (**19**)

The relative configurations at the various stereocenters were deduced from the NOESY data (**Figure 3.36**). The NOE observed for H-16/H-14' indicated a 1,3-diaxial relationship for H-16 and H-14', whereas the NOEs observed for H-3/NH and H-15/H-16 indicated that both H-3 and H-15 are equatorially oriented. These observations also inferred that ring D adopted a chair conformation, while the C-3–N-4 and C-15–C-20 bonds are axial. Furthermore, the NOE observed for H-6/H-21 required ring C and the N-4–C-21–C-20 fragment to be located on the same face of ring D. Taken together, the configurations at C-2, C-3, C-7, C-15, and C-16 were determined to be *rel*-(2*S*,3*S*,7*R*,15*R*,16*R*). Finally, the geometry of the C-19–C-20 double bond was deduced to be *E* based on the NOE observed for H-19/H-21. Since suitable crystals of **19** were obtained, X-ray diffraction analysis was carried out, which confirmed the absolute configurations at all stereocenters as 2*S*,3*S*,7*R*,15*R*,16*R* (**Figure 3.37**).

Alstobrogaline (**19**) represents a novel and unusual monoterpene indole alkaloid incorporating a third *N* atom, and possessing an aldimine as well as a nitron function. To the best of knowledge, following the isolation of two 4,5-*seco*-picrinine-type alkaloids (i.e., alschomine and isoalschomine) [6], compound **19** represents the third instance in which a monoterpene indole alkaloid incorporates a nitron function.

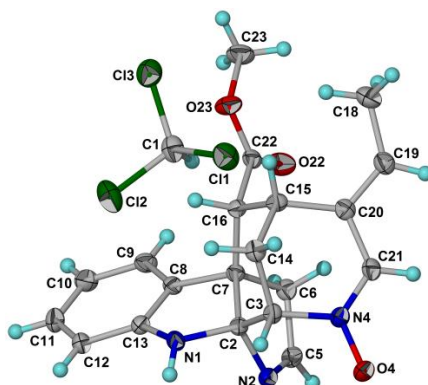


**Figure 3.37:** X-ray crystal structure of alstobrogaline (**19**) [Flack parameter,  $x = -0.02(2)$ ].

**Table 3.9:**  $^1\text{H}$  (600 MHz) and  $^{13}\text{C}$  (150 MHz) NMR spectroscopic data (in  $\text{CDCl}_3$  with TMS as internal reference) of alstobrogaline (**19**)

Position	$\delta_{\text{H}}$ (mult., $J$ in Hz)	$\delta_{\text{C}}$
2		98.8
3	4.55, t (3) (equatorial)	69.2
5	7.69, br s	167.9
6	3.25, m 3.25, m	47.4
7		50.6
8		136.3
9	6.99, d (7.5)	123.0
10	6.75, t (7.5)	120.5
11	7.10, t (7.5)	129.0
12	6.73, d (7.5)	111.3
13		145.7
14	2.24, dt (13.6, 3) (equatorial)	28.8
14'	2.46, dt (13.6, 3) (axial)	
15	3.34, m (equatorial)	27.5
16	2.81, d (3.6) (axial)	52.6
18	1.75, d (7.5)	14.4
19	5.84, q (7.5)	132.3
20		130.0
21	7.29, s	138.1
<u>CO<sub>2</sub>Me</u>		171.9
CO <sub>2</sub> Me	3.73, s	51.9
NH	4.92, br s	

Mar13-2017 ASLD 2.10.fid  
1H- ASLD-2

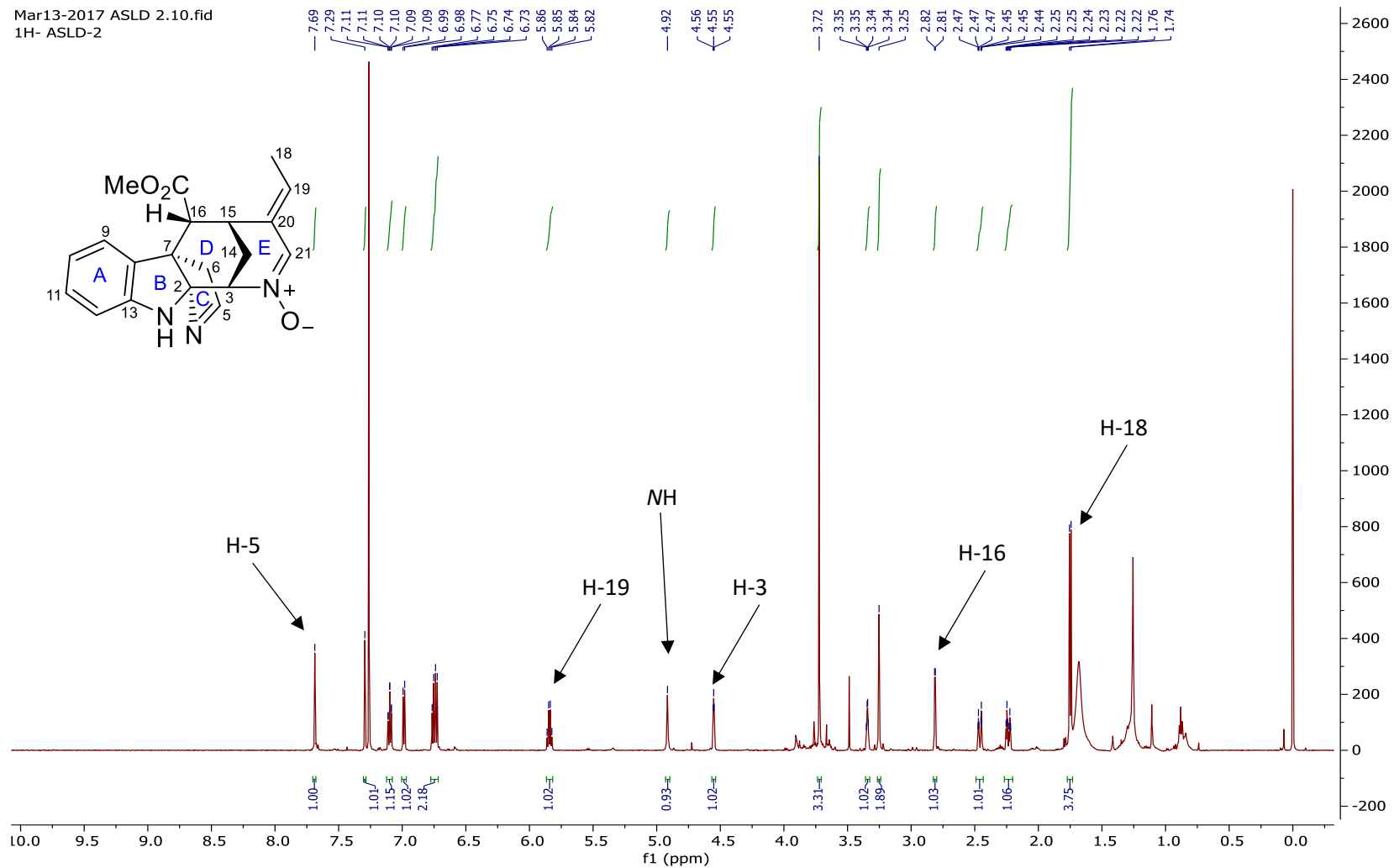


Figure 3.38: <sup>1</sup>H NMR spectrum of alstobrogaline (19) (CDCl<sub>3</sub>, 600 MHz)

Mar13-2017 ASLD 2.12.fid  
13C- ASLD-2

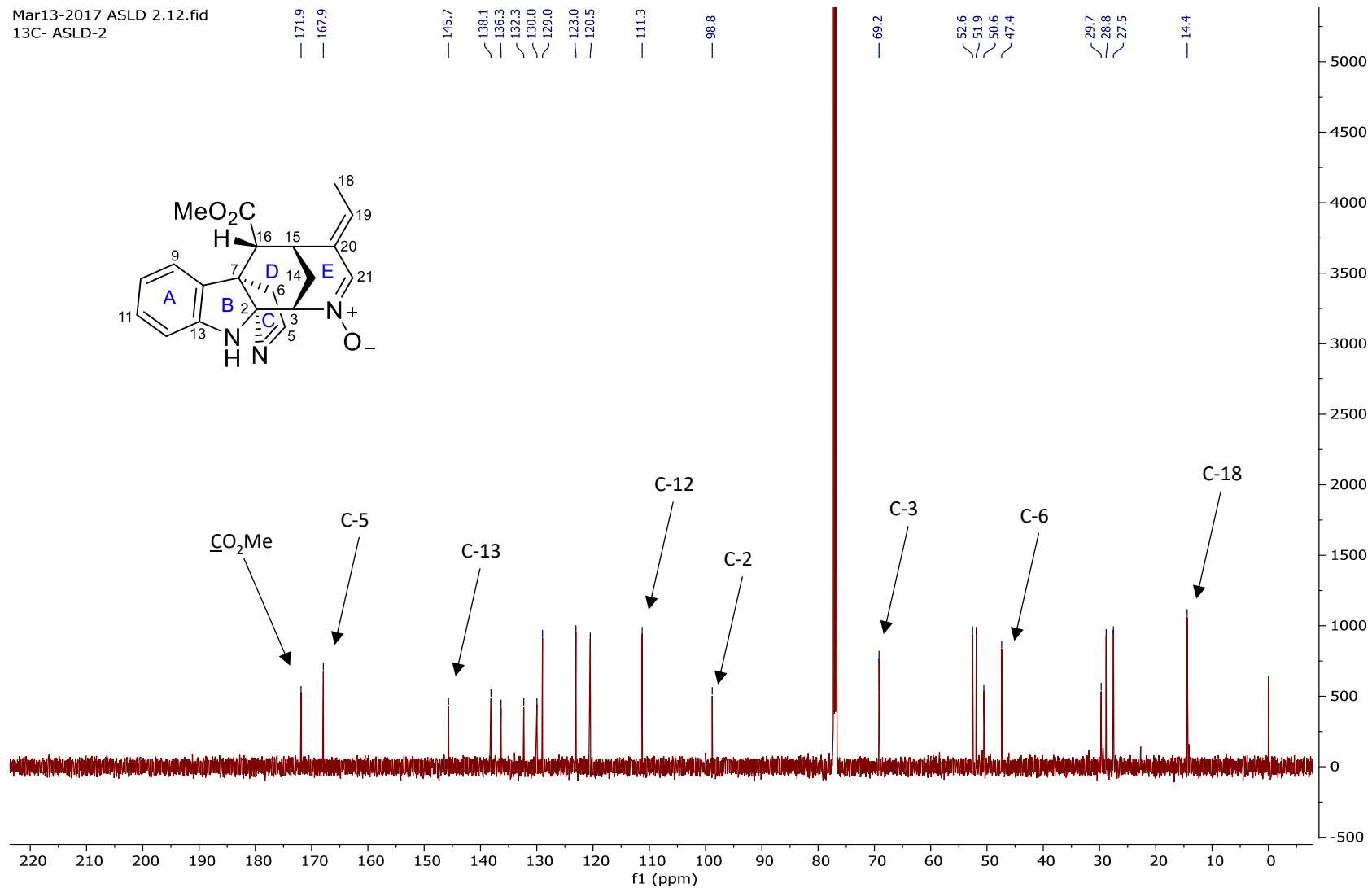


Figure 3.39: <sup>13</sup>C NMR spectrum of alstobrogaline (19) (CDCl<sub>3</sub>, 150 MHz)

### 3.2.2 Tetrahydroalstonine (20), picrinine (21), 16*R*-19,20-*Z*-isositsirikine (22) and 16*R*-19,20-*E*-isositsirikine (23)

Five known corynanthean-type alkaloids, *viz.*, tetrahydroalstonine (**20**),<sup>79</sup> picrinine (**21**),<sup>89,91</sup> 16*R*-19,20-*Z*-isositsirikine (**22**)<sup>126</sup> and 16*R*-19,20-*E*-isositsirikine (**23**),<sup>126</sup> were also isolated. The <sup>1</sup>H and <sup>13</sup>C NMR spectra of these compounds are shown in **Figures 3.40 – 3.47**, while the NMR spectroscopic data are summarized in **Tables 3.10 – 3.11**. Other data are given in Chapter 4 (Experimental).

**Table 3.10:** <sup>1</sup>H (600 MHz) and <sup>13</sup>C (150 MHz) NMR spectroscopic data (in CDCl<sub>3</sub> with TMS as internal reference) of tetrahydroalstonine (**20**) and picrinine (**21**)

Position	<b>20</b>		<b>21</b>	
	$\delta_{\text{H}}$ (mult., <i>J</i> in Hz)	$\delta_{\text{C}}$	$\delta_{\text{H}}$ (mult., <i>J</i> in Hz)	$\delta_{\text{C}}$
2	-	134.52	-	106.30
3	3.35, d (12)	59.81	3.60, d (4.6)	51.75
5	2.56, m	53.54	4.83, d (2.1)	87.31
	2.96, m			
6	2.71, m	21.74	3.42, d (13.7)	40.47
	2.93, m		2.26, dd (13.6, 2.5)	
7	-	108.08		51.14
8	-	127.18		135.12
9	7.28, d (8)	118.02	7.14, d (7.5)	125.05
10	7.07, t (8)	119.37	6.79, t (7.5)	120.74
11	7.12, t (8)	121.36	7.08, t (7.5)	127.94
12	7.45, d (8)	110.77	6.75, d (7.5)	110.57
13	-	135.98	-	147.54
14	2.50, dt (12, 3.4)	34.24	2.14, dt (14.1, 14.0)	25.94
	1.54, q (12)		1.87, d (14.0)	
15	2.76, m	31.36	3.28, s	31.02
16	-	109.51	2.44, d (3.4)	51.96
17	7.56, s	155.72	-	172.42
18	1.40, d (6.2)	18.50	1.49, dd (7.0, 2.0)	12.72
19	4.50, dq (12.3, 6.2)	72.45	5.41, q (7.0)	120.44
20	1.70, m	38.43	-	136.03
21	2.73, m	56.29	3.76, d (17.5)	46.31
	3.11, dd (12.3, 2)		3.10, d (17.5)	
CO <sub>2</sub> Me	3.75, s	51.10	3.65, s	51.44
CO <sub>2</sub> Me	-	167.97	-	
NH	7.83, s	-	4.87, br s	

**Table 3.11:**  $^1\text{H}$  (600 MHz) and  $^{13}\text{C}$  (150 MHz) NMR spectroscopic data (in  $\text{CDCl}_3$  with TMS as internal reference) of 16*R*-19,20-*Z*-isositsirikine (**22**) and 16*R*-19,20-*E*-isositsirikine (**23**)

Position	<b>22</b>		<b>23</b>	
	$\delta_{\text{H}}$ (mult., <i>J</i> in Hz)	$\delta_{\text{C}}$	$\delta_{\text{H}}$ (mult., <i>J</i> in Hz)	$\delta_{\text{C}}$
2	-	134.23	-	133.97
3	3.61, d (10.3)	58.48	4.32, br s	52.73
5	2.72, m	52.27	3.14 <sup>a</sup> , m	51.40
	3.19, m		3.29, dd (13.0, 5.0)	
6	2.75, m	21.10	2.64, dd (13.0, 5.0)	17.65
	2.99, m		2.94, d (13.0)	
7	-	108.21	-	107.79
8	-	127.35	-	127.68
9	7.46, d (7.8)	118.15	7.48, d (8)	117.97
10	7.08, m	118.69	7.11, t (8)	119.49
11	7.13, m	119.45	7.17, t (8)	121.54
12	7.31, m	110.87	7.39, d (8)	111.32
13	-	136.11	-	136.17
14	2.15, dt (12.6, 4.3)	34.22	2.23 <sup>b</sup> , m	30.39
	1.69, m		2.23 <sup>b</sup> , m	
15	2.61, d (15.6)	40.94	3.14 <sup>a</sup> , m	32.57
16	2.99, m	49.07	2.52, ddd (12.2, 7.9, 5.0)	49.61
17	3.90, dd (11, 7.7)	62.56	3.55, m	62.13
	3.81, dd (11, 4.8)		3.50, m	
18	1.71, d (6.7)	13.17	1.68, dd (7.0, 1.8)	13.31
19	5.46, q (6.7)	121.49	5.64, q (7.0)	123.45
20	-	134.19	-	133.55
21	2.89, d (12.6)	54.42	3.55, m	52.29
	3.79, m		2.94, d (12.1)	
<u>CO<sub>2</sub>Me</u>	3.73, s	51.92	3.82, s	52.29
<u>CO<sub>2</sub>Me</u>	-	175.07	-	175.56
NH	7.95, s	-	8.67, br s	-

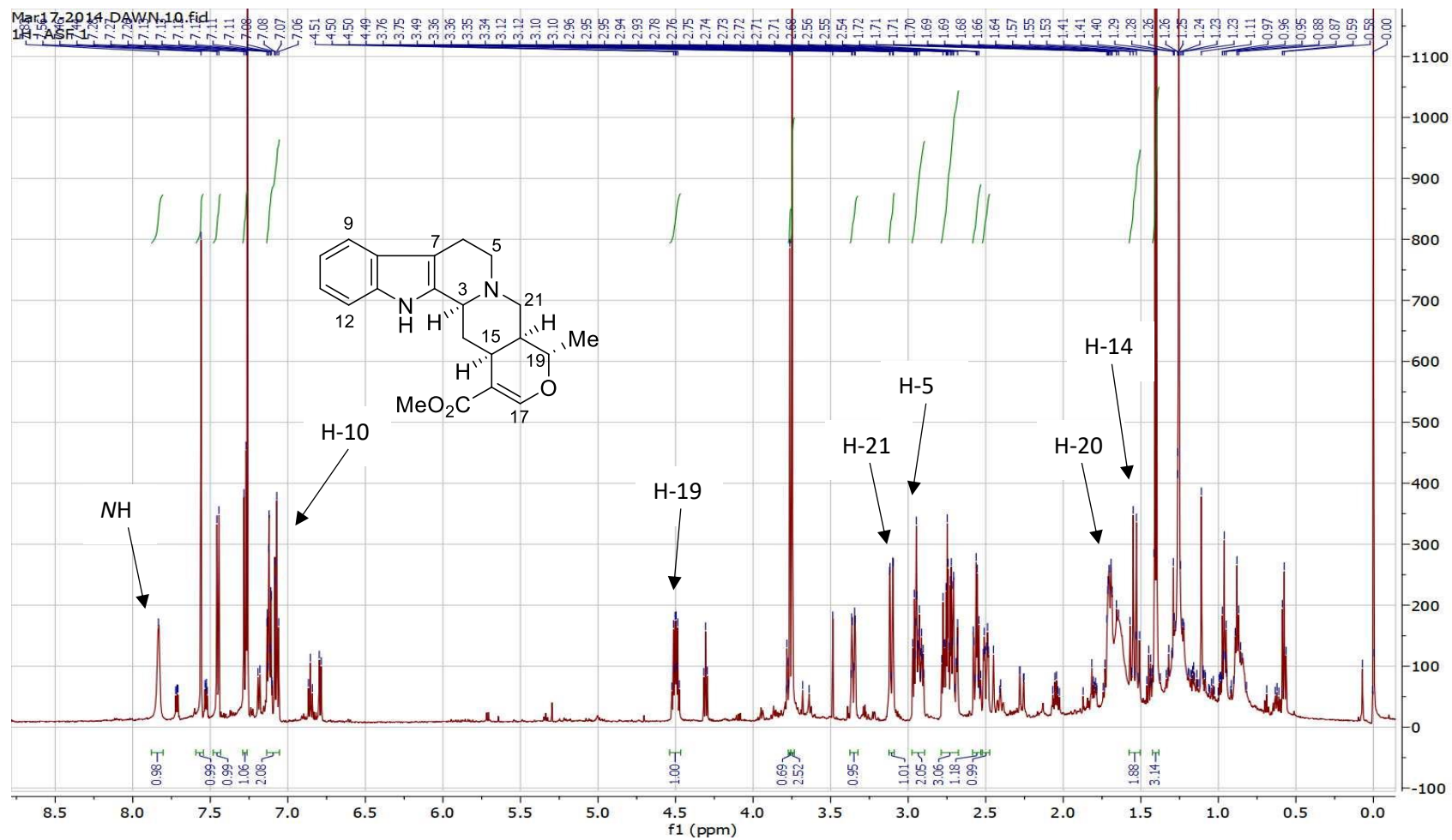


Figure 3.40:  $^1\text{H}$  NMR spectrum of tetrahydroalstonine (**20**) ( $\text{CDCl}_3$ , 600 MHz)

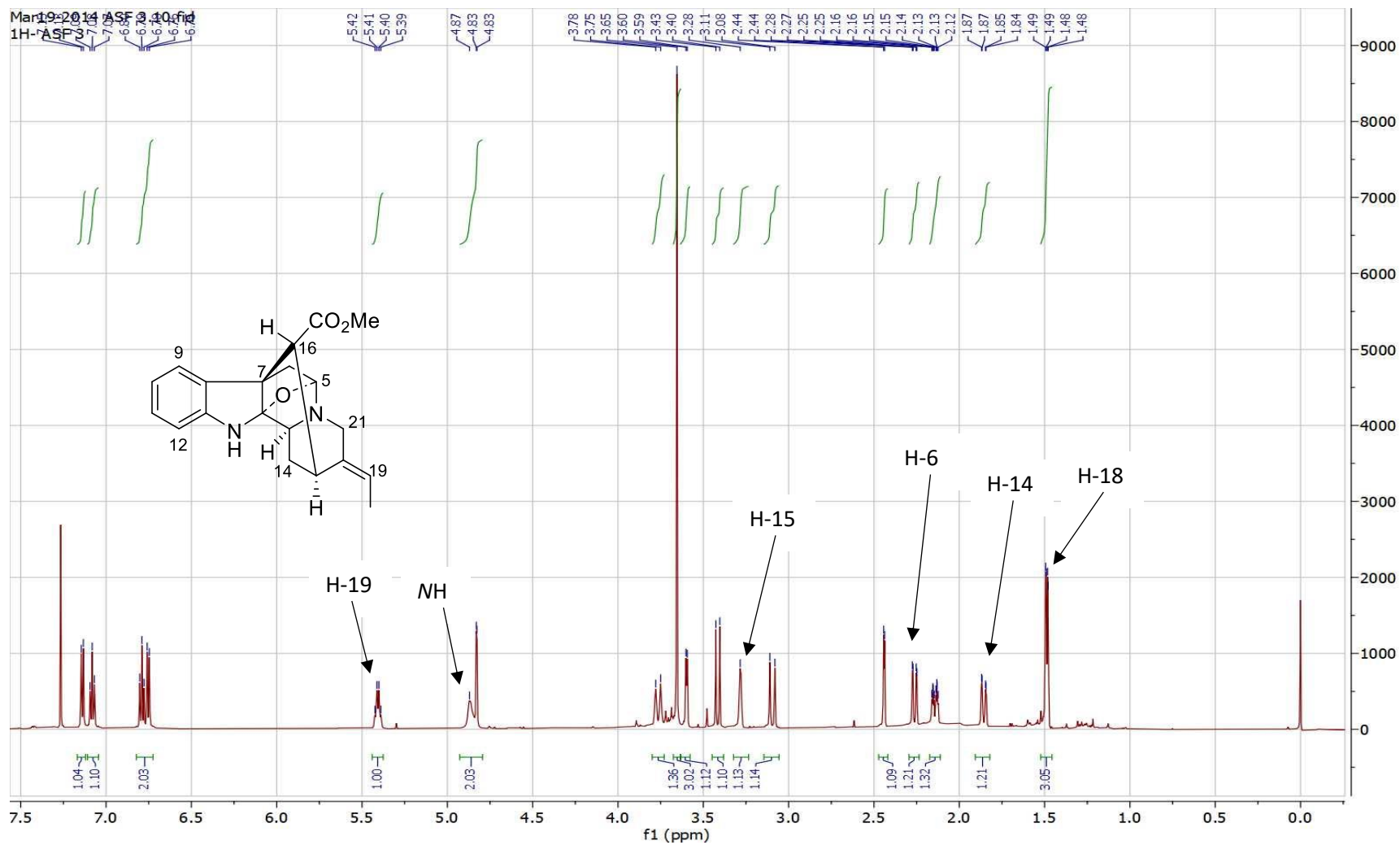
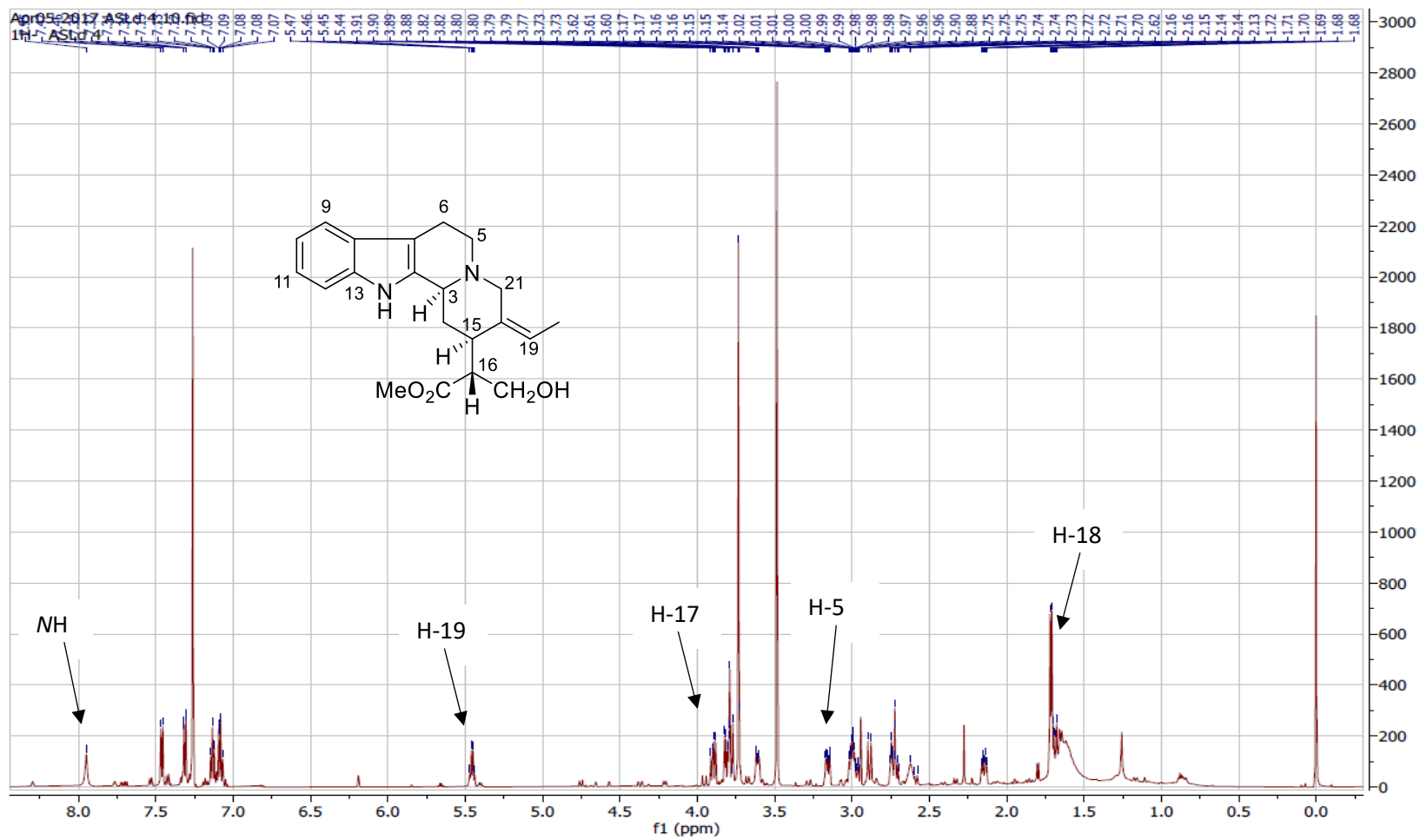
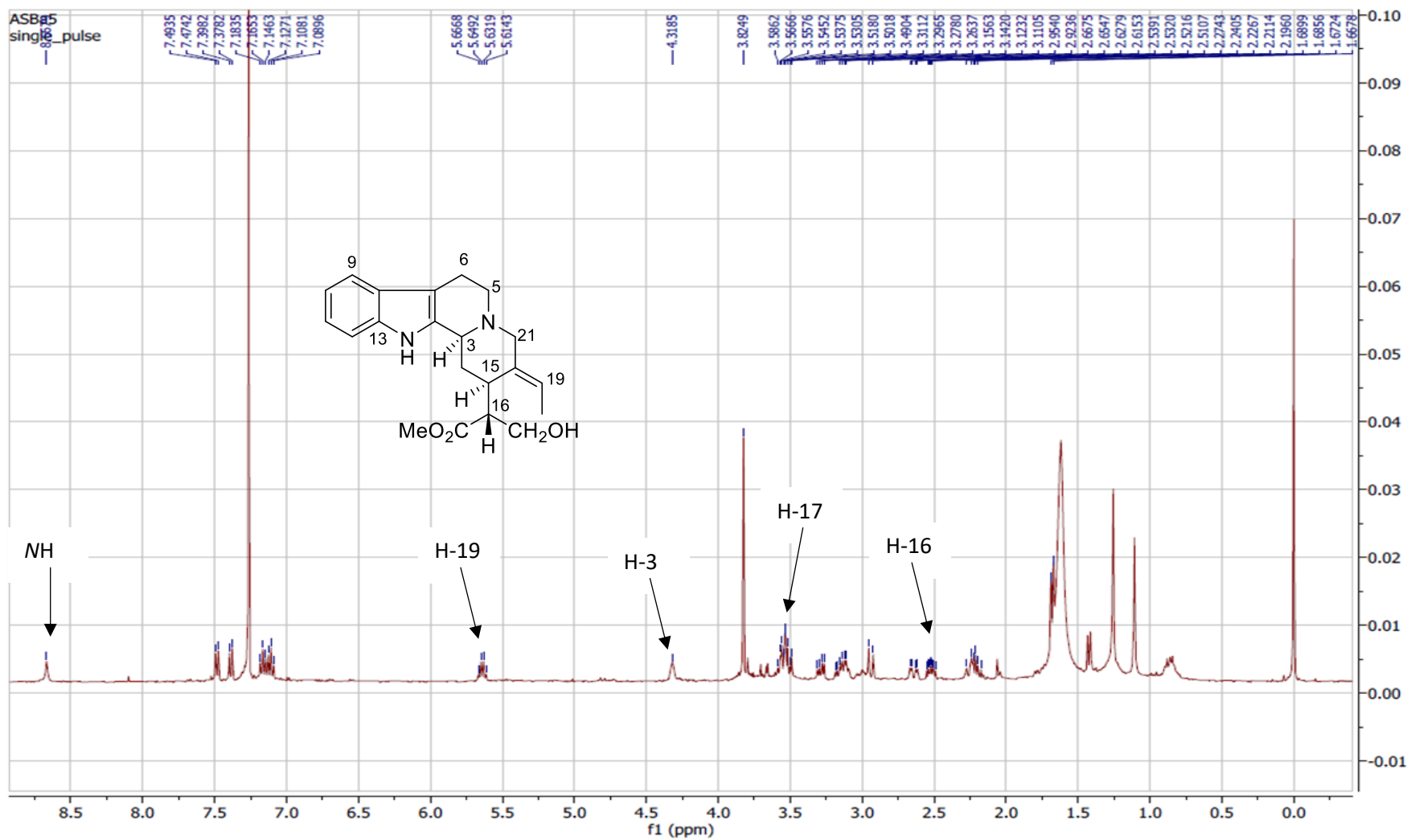


Figure 3.41:  $^1\text{H}$  NMR spectrum of picrinine (**21**) ( $\text{CDCl}_3$ , 600 MHz)



**Figure 3.42:**  $^1\text{H}$  NMR spectrum of 16*R*-19,20-*Z*-isositsirikine (**22**) ( $\text{CDCl}_3$ , 600 MHz)



**Figure 3.43:**  $^1\text{H}$  NMR spectrum of 16*R*-19,20-*E*-isositsirikine (**23**) ( $\text{CDCl}_3$ , 600 MHz)

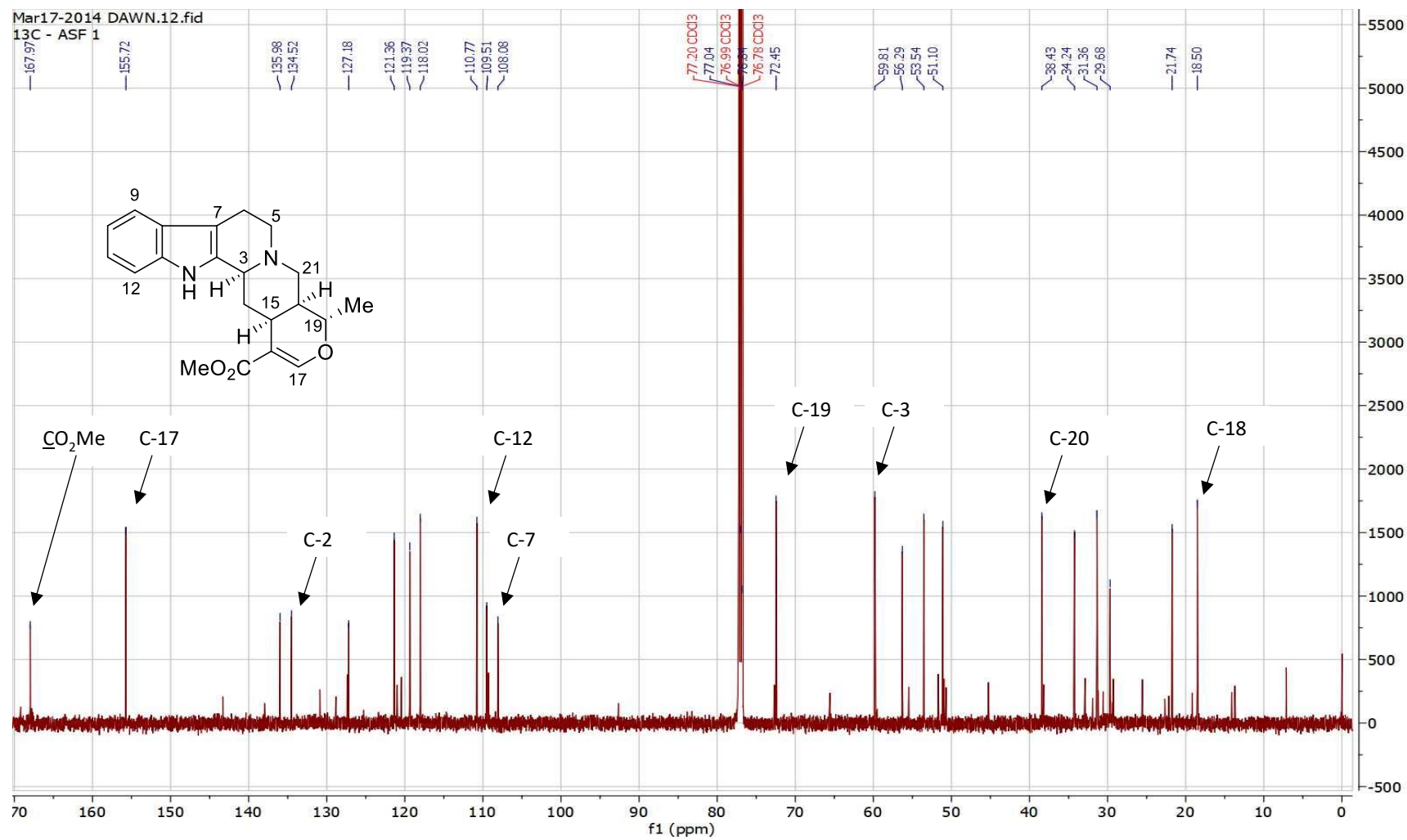


Figure 3.44:  $^{13}\text{C}$  NMR spectrum of tetrahydroalstonine (**20**) ( $\text{CDCl}_3$ , 150 MHz)

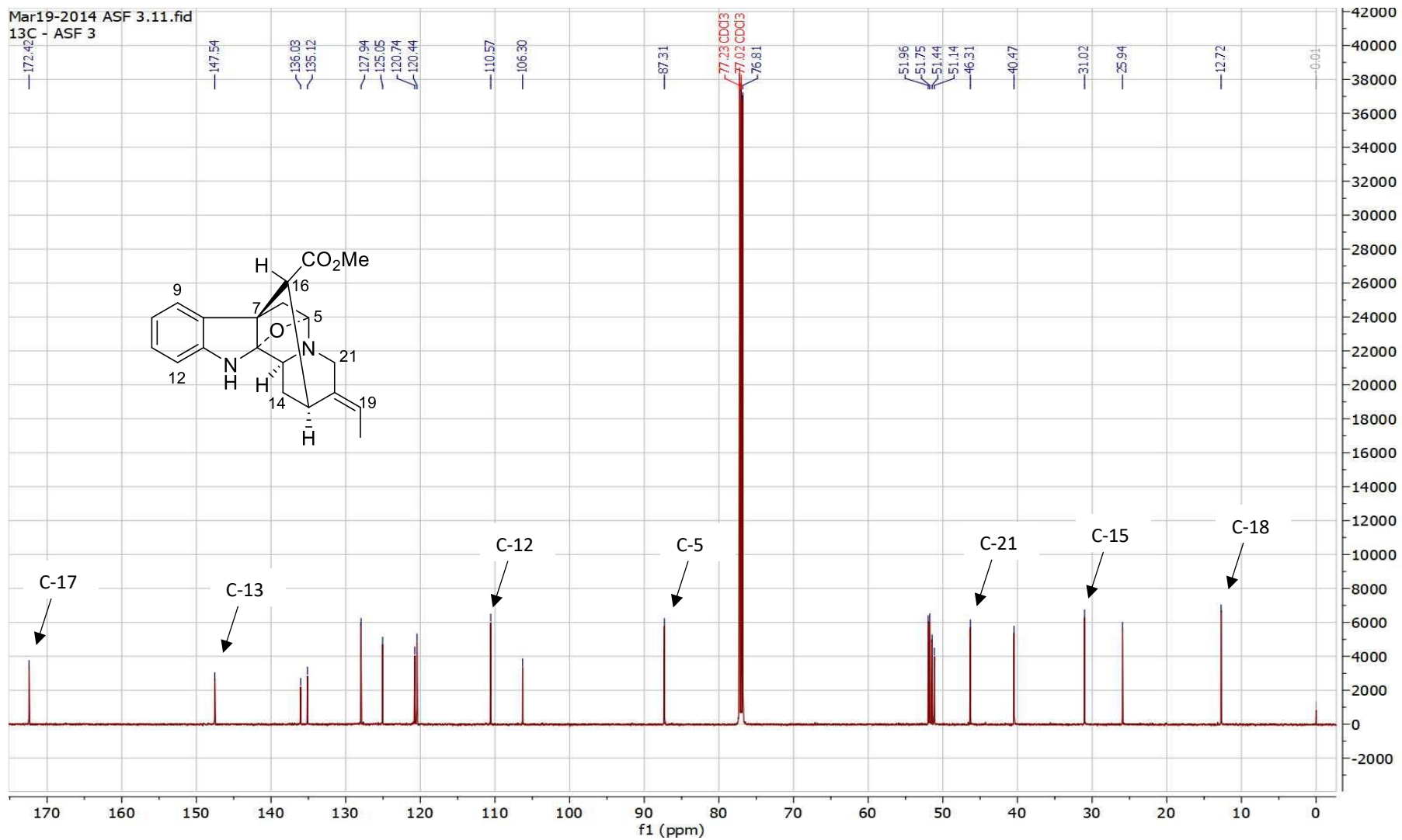
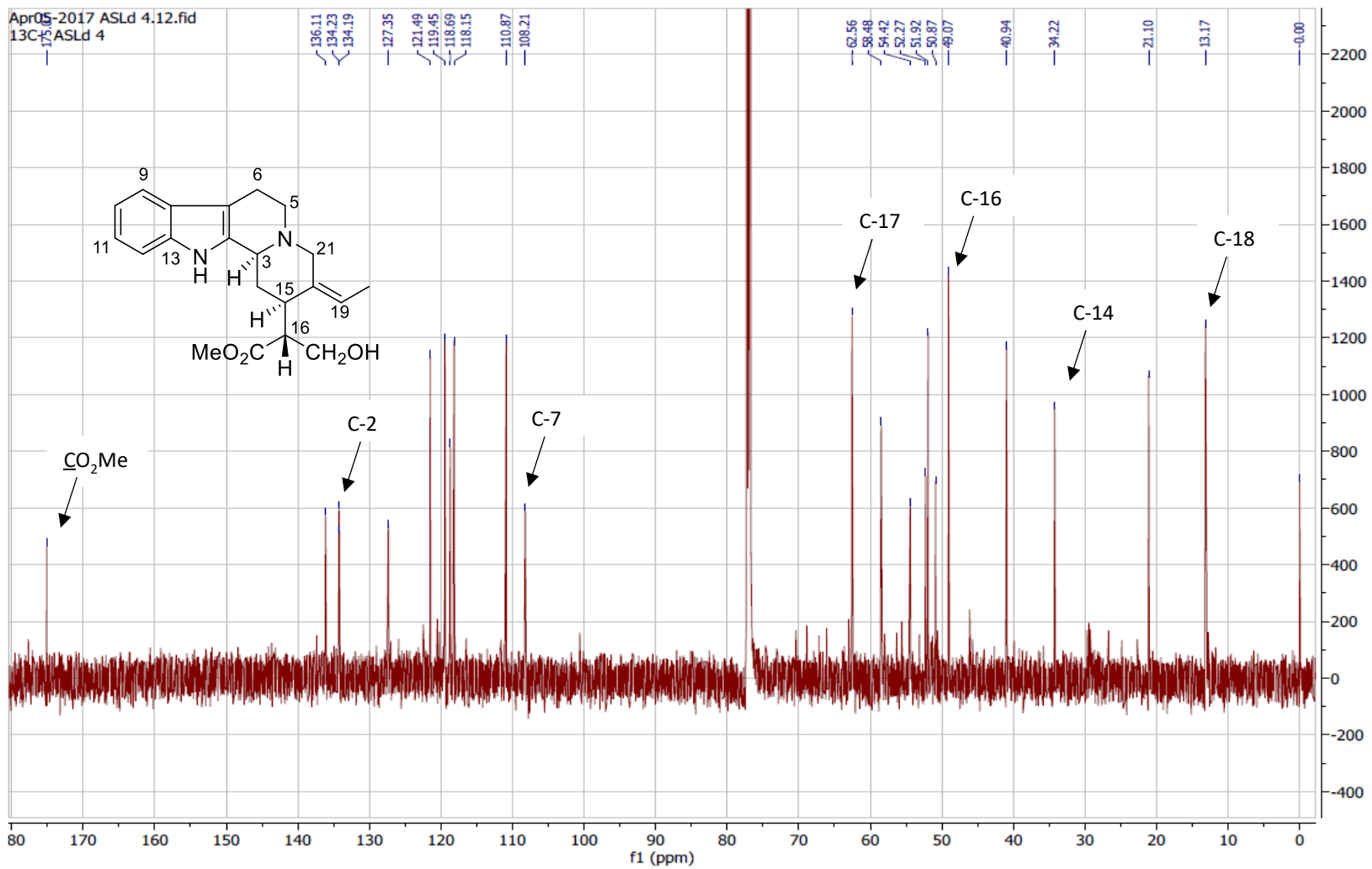
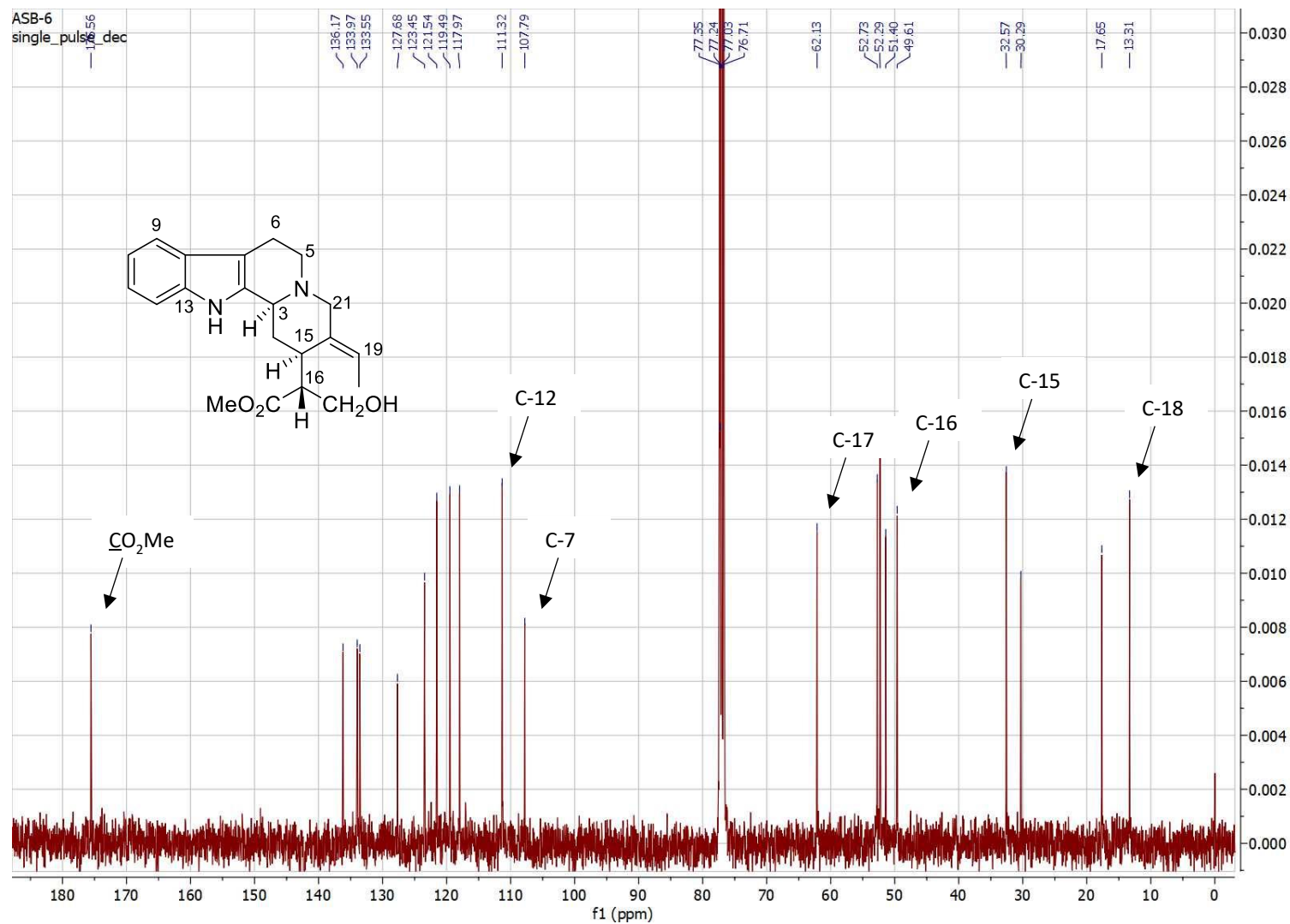


Figure 3.45: <sup>13</sup>C NMR spectrum of picrinine (21) (CDCl<sub>3</sub>, 150 MHz)



**Figure 3.46:** <sup>13</sup>C NMR spectrum of 16R-19,20-Z-isositsirikine (**22**) (CDCl<sub>3</sub>, 150 MHz)



**Figure 3.47:** <sup>13</sup>C NMR spectrum of 16R-19,20-E-isositsirikine (**23**) (CDCl<sub>3</sub>, 150 MHz)

### 3.3 Strychnan-type Alkaloids

#### 3.3.1 Scholaricine (24) and *N*-demethylalstogustine *N*-oxide (25)

Two known strychnan-type alkaloids, *viz.*, scholaricine (**24**)<sup>88,91</sup> and *N*-demethylalstogustine *N*-oxide (**25**),<sup>99</sup> were also isolated. The <sup>1</sup>H and <sup>13</sup>C NMR spectra of these compounds are shown in **Figures 3.48 – 3.51**, while the NMR spectroscopic data are summarized in **Table 3.12**. Other data are given in Chapter 4 (Experimental).

**Table 3.12:** <sup>1</sup>H (600 MHz) and <sup>13</sup>C (150 MHz) NMR spectroscopic data (in CDCl<sub>3</sub> with TMS as internal reference) of scholaricine (**24**) and *N*-demethylalstogustine *N*-oxide (**25**)

Position	<b>24</b>		<b>25</b>	
	$\delta_{\text{H}}$ (mult., <i>J</i> in Hz)	$\delta_{\text{C}}$	$\delta_{\text{H}}$ (mult., <i>J</i> in Hz)	$\delta_{\text{C}}$
2	-	170.90	-	166.67
3	4.09, s	60.89	4.35, t (3.0)	75.53
5	2.92, dd (11.9, 7.3) 3.27, m	53.34	3.71, td (12.0, 8.3, 1.0) 3.60, dd (12.0, 8.0)	68.02
6	1.97, dd (13.0, 6.9) 2.85, td (13.0, 7.3)	42.39	2.19, ddd (14.5, 8.0, 1.0) 2.60, ddd (14.5, 12.0, 8.0)	39.37
7		56.86	-	53.18
8		135.81	-	133.02
9	6.74, m	111.34	7.25, d (7.5)	119.87
10	6.80, t (7.6)	122.56	6.96, td (7.5, 1.0)	121.84
11	6.74, m	116.0	7.20, td (7.5, 1.0)	128.84
12		141.52	6.86, d (7.5)	110.52
13		131.52	-	144.08
14	1.44, m 2.09, m	30.38	1.24, d (14.0) 3.29, ddd (14.0, 5.0, 3.0)	23.55
15	3.38, d (3.7)	28.31	3.45, m	24.93
16		96.61	-	103.63
18	1.17, (6.1)	19.73	1.39, d (6.4)	20.21
19	3.27, m	68.14	4.22, qd (6.4, 2.7)	69.09
20	1.85, m	45.17	1.86, m	41.20
21	2.09, m 3.10, dd (11.9, 4.8)	47.84	3.50, d (13.5) 3.88, dd (13.5, 6.6)	65.01
CO <sub>2</sub> Me	3.88, s	52.14	3.80, s	51.63
CO <sub>2</sub> Me		168.96	-	167.43
NH	8.66 s	-	8.67, s	-

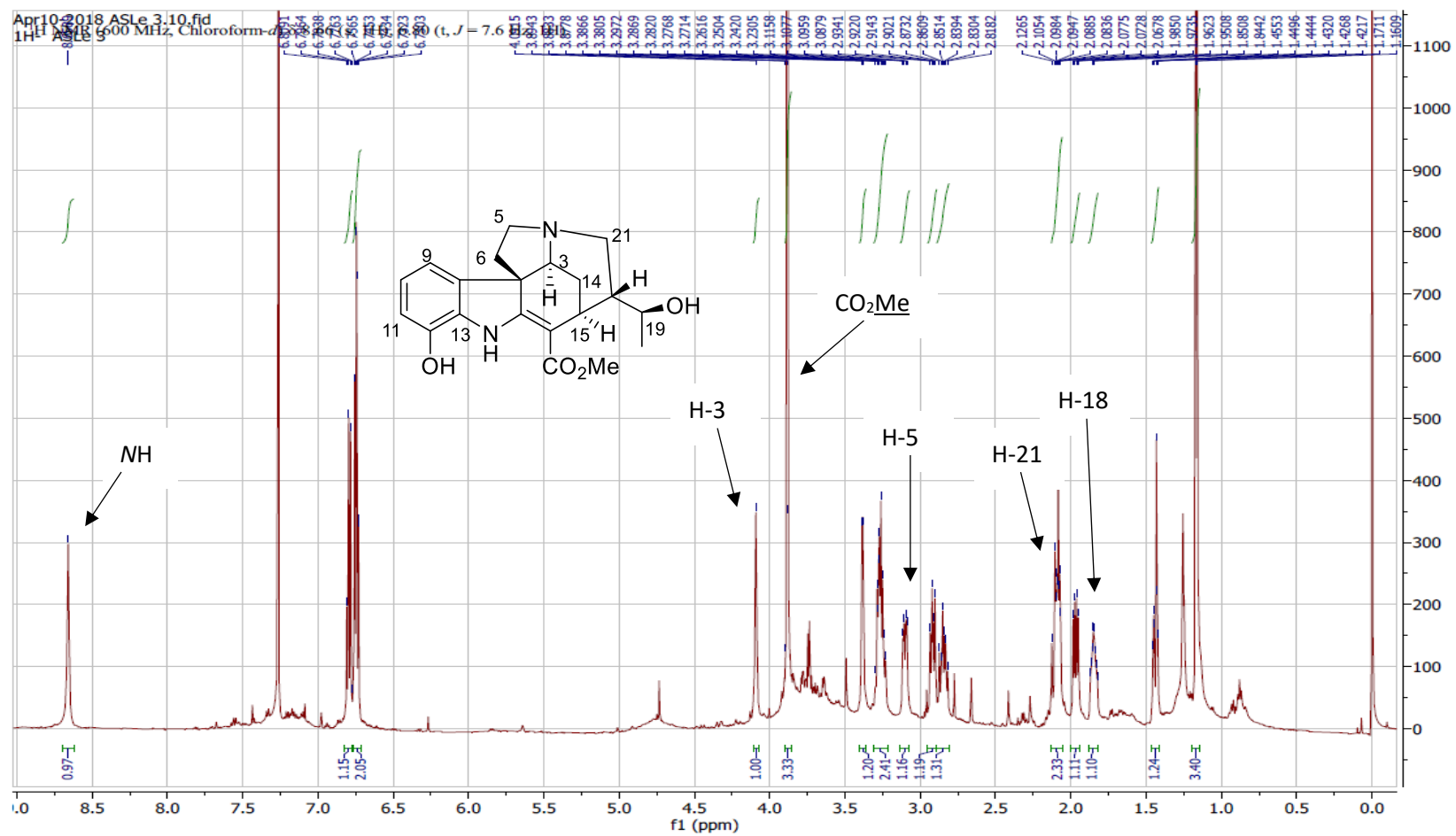


Figure 3.48: <sup>1</sup>H NMR spectrum of scholaricine (24) (CDCl<sub>3</sub>, 600 MHz)

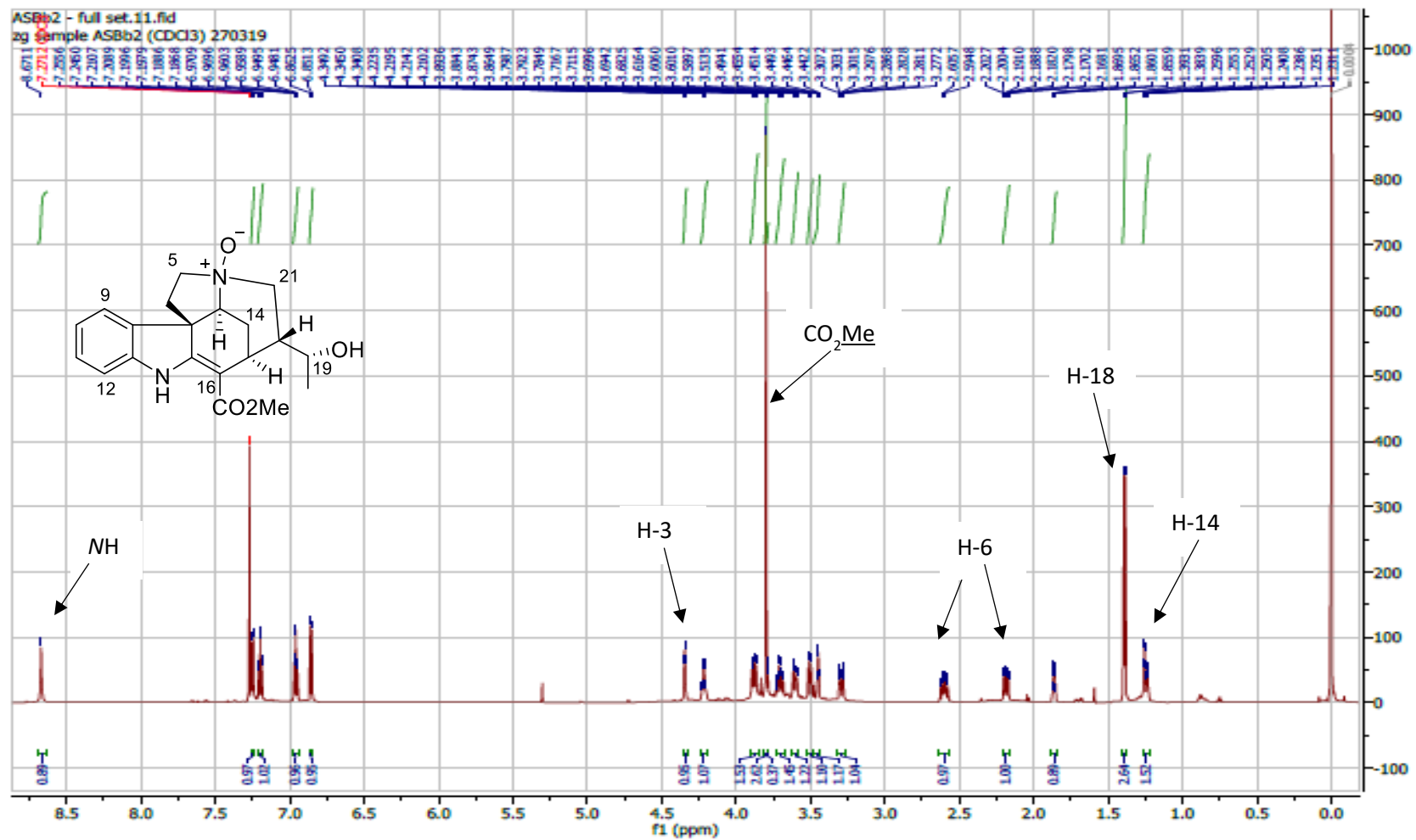


Figure 3.49: <sup>1</sup>H NMR spectrum of *N*-demethylalstogustine *N*-oxide (25) (CDCl<sub>3</sub>, 600 MHz)

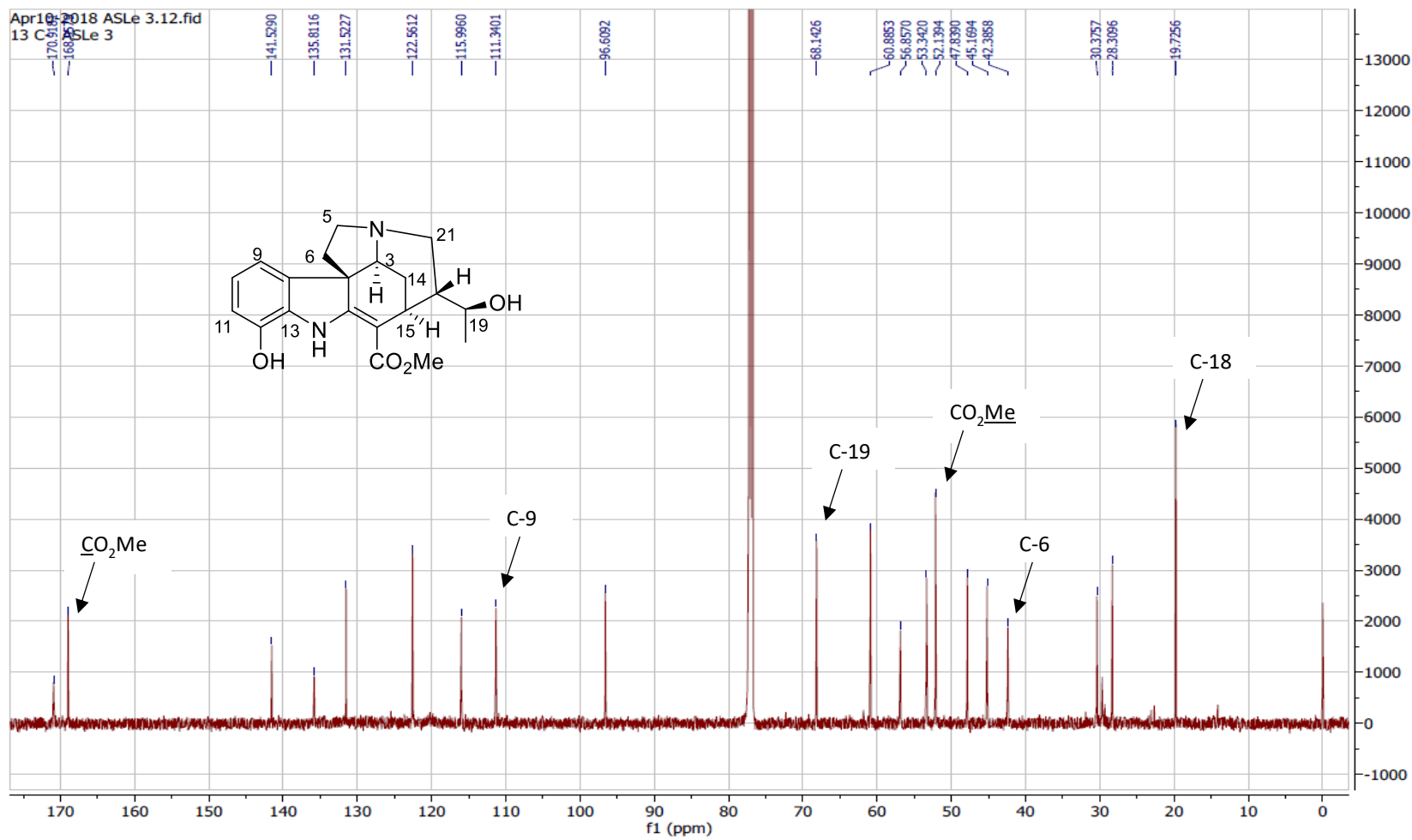
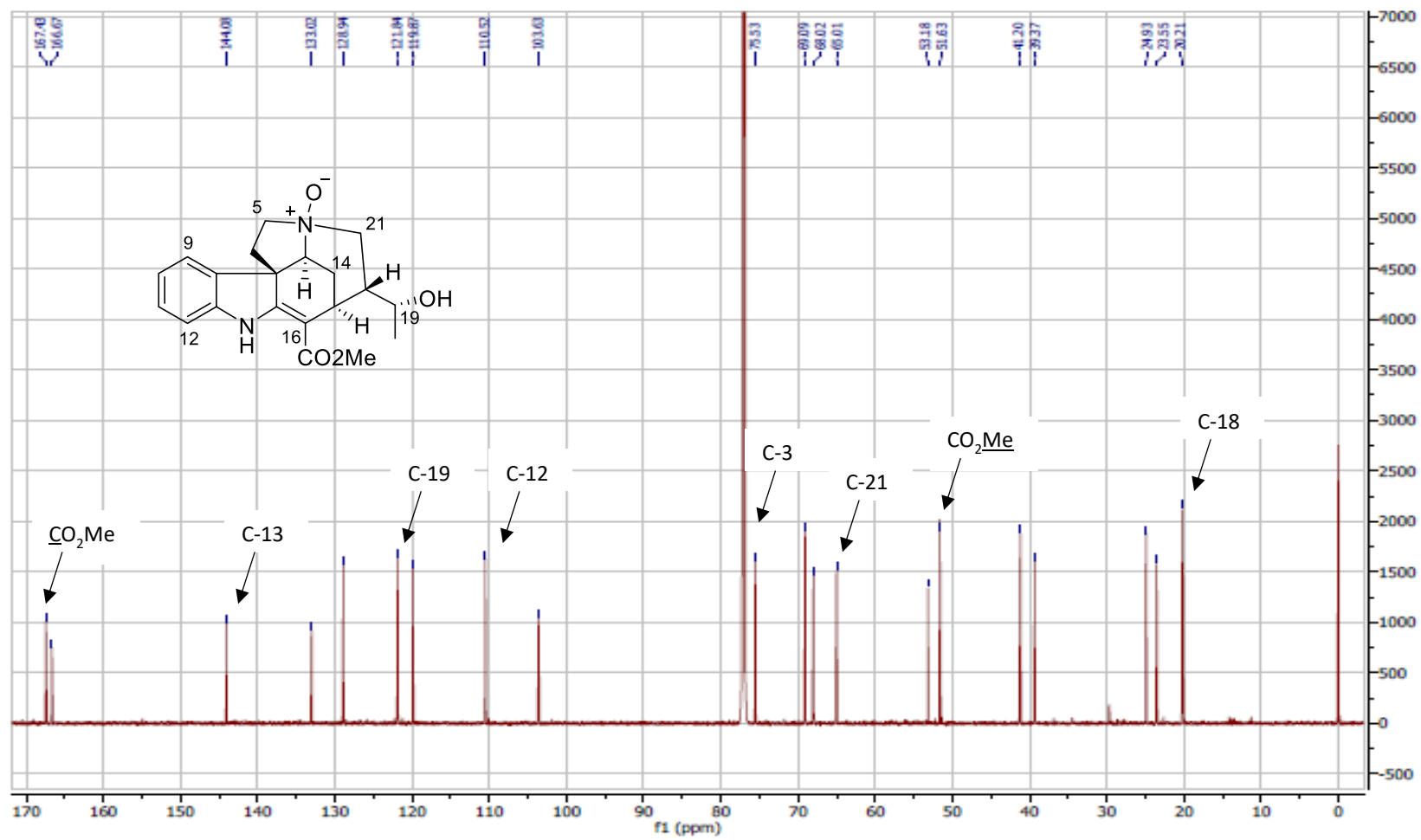


Figure 3.50: <sup>13</sup>C NMR spectrum of scholaricine (**24**) (CDCl<sub>3</sub>, 150 MHz)



**Figure 3.51:** <sup>13</sup>C NMR spectrum of *N*-demethylalstogustine *N*-oxide (**25**) (CDCl<sub>3</sub>, 150 MHz)

## 3.4 Vallesiachotaman-type Alkaloids

### 3.4.1 *E/Z*-Vallesiachotamine (26)

A pair of known vallesiachotaman-type alkaloids, *viz.*, *E/Z*-vallesiachotamine (26), were obtained as an inseparable mixture.<sup>127,128</sup> The <sup>1</sup>H and <sup>13</sup>C NMR spectra are shown in **Figure 3.52** and **Figure 3.53**, while the NMR spectroscopic data are summarized in **Table 3.13**. Other data are given in Chapter 4 (Experimental).

**Table 3.13:** <sup>1</sup>H (600 MHz) and <sup>13</sup>C (150 MHz) NMR spectroscopic data (in CDCl<sub>3</sub> with TMS as internal reference) of *E/Z*-vallesiachotamine (26)

Position	<i>E</i> -vallesiachotamine		<i>Z</i> -vallesiachotamine	
	$\delta_{\text{H}}$ (mult., <i>J</i> in Hz)	$\delta_{\text{C}}$	$\delta_{\text{H}}$ (mult., <i>J</i> in Hz)	$\delta_{\text{C}}$
2	-	132.13	-	132.47
3	4.25, d (12.3)	47.71	4.47, d (12.5)	49.32
5	3.59, m	50.90	3.59, m	51.08
	3.72, m		3.72, m	
6	2.80, m	21.96	2.80, m	22.05
	2.92, m		2.92, m	
7	-	108.39	-	108.49
8	-	136.28	-	136.28
9	7.47, d (8.6)	118.00	7.47, d (8.6)	118.11
10	7.11, m	119.68	7.11, m	119.73
11	7.16, m	122.05	7.16, m	122.06
12	7.30, m	111.02	7.30, m	111.05
13	-	126.78	-	126.78
14	1.79, m	32.76	1.92, ddd (13.4, 11.6, 6.2)	34.10
	2.24, ddd (13.3, 3.5, 1.7)		2.18, m	
15	4.02, m	30.86	4.02, m	28.40
16	-	93.71	-	94.17
17	7.76, s	147.46	7.68, s	147.77
18	2.18, d (7.3)	13.06	2.09, d (7.3)	15.05
19	6.55, q (7.3)	146.94	6.67, q (7.3)	152.81
20	-	143.14	-	146.42
21	10.27, s	190.71	9.36, s	195.88
CO <sub>2</sub> Me	3.64, s	50.68	3.64, s	50.73
<u>CO</u> <sub>2</sub> Me	-	168.18	-	168.38
NH	8.21, br s	-	8.15, br s	-

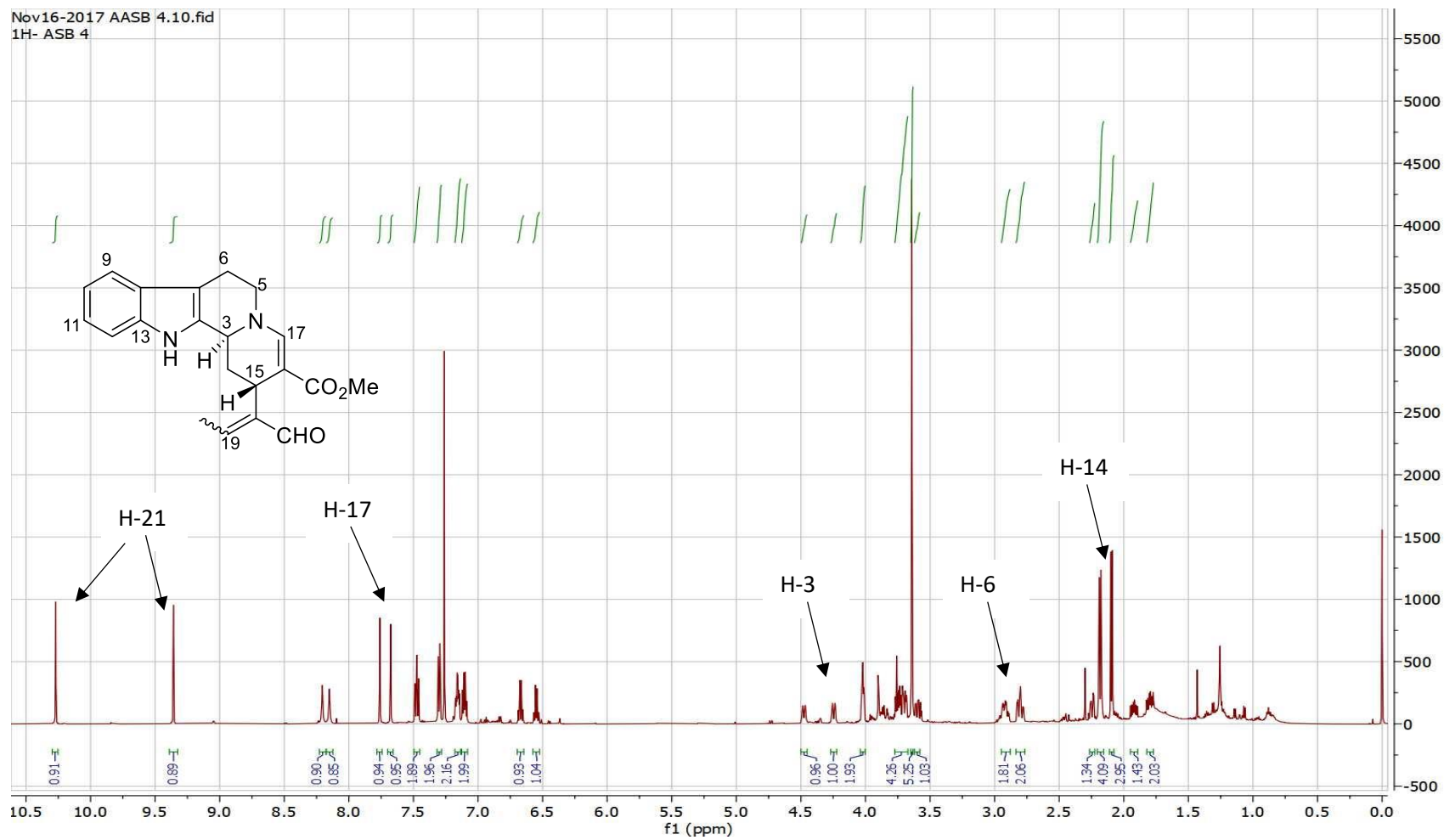


Figure 3.52: <sup>1</sup>H NMR spectrum of *E/Z*-vallesiachotamine (**26**) (CDCl<sub>3</sub>, 600 MHz)

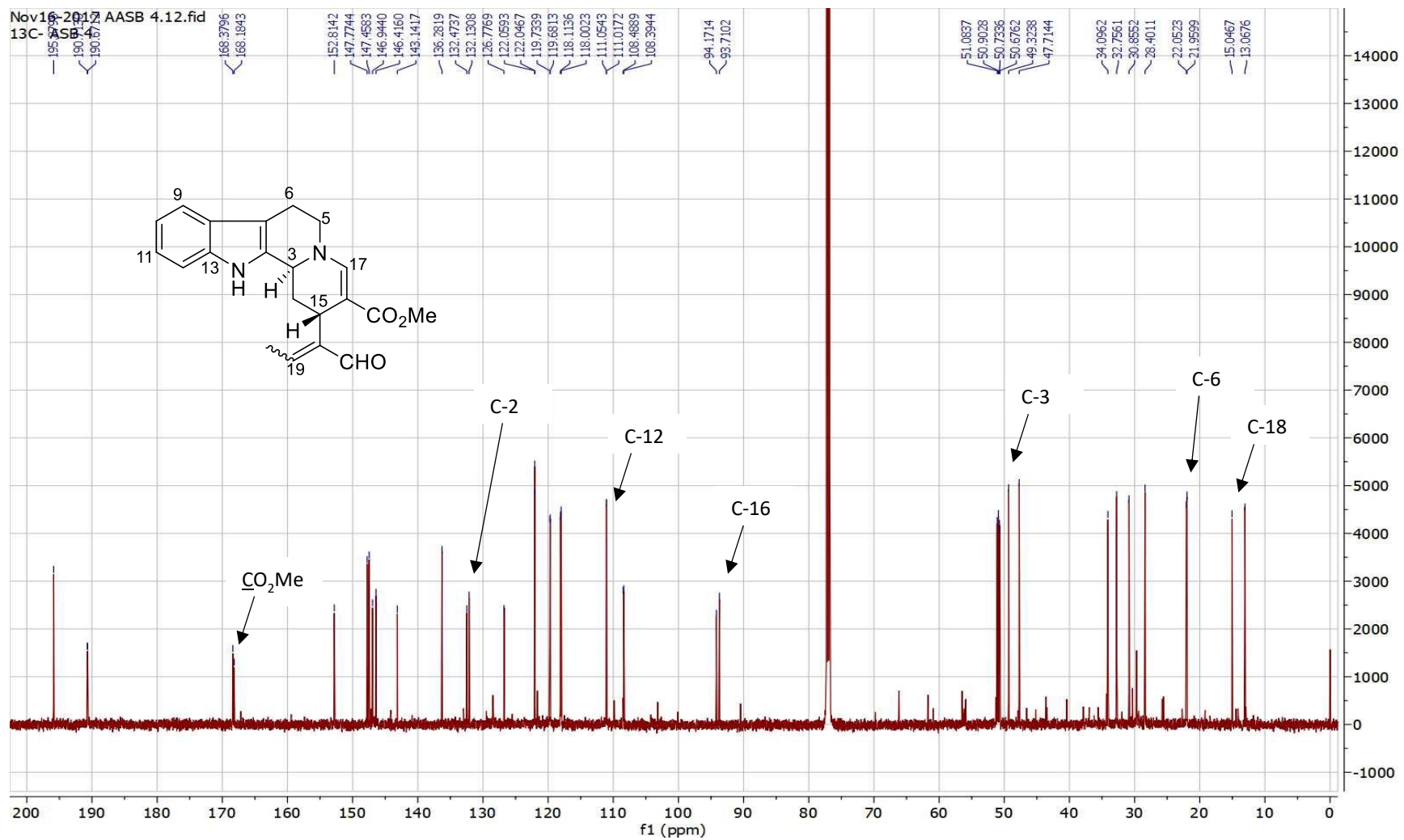


Figure 3.53: <sup>13</sup>C NMR spectrum of *E/Z*-vallesiachotamine (26) (CDCl<sub>3</sub>, 150 MHz)

### 3.5 Proposed Biogenesis of Alstoscholactine (10), Alstolaxepine (11), *N*-Formilyunnanensine (12), Scholaphylline (13), and Alstobrogaline (19)

Stemmadenine, which is involved in the biosynthesis of many indole alkaloids,<sup>129</sup> is postulated to be an upstream precursor of alkaloids **10**, **11**, **12**, and **13** (**Figure 3.54**). The biogenetic link between stemmadenine, 19*E*-vallesamine (**14**), and 6,7-*seco*angustilobine B (**17**), has previously been reported to require the critical intermediacy of the iminium ion intermediate **(i)** (**Figure 3.54**).<sup>129–131</sup> Both 19*E*-vallesamine (**14**) and 6,7-*seco*angustilobine B (**17**) were also obtained in the current investigation. As such, the same iminium ion **(i)** was postulated as the common biogenetic link to alstoscholactine (**10**), alstolaxepine (**11**), *N*-formilyunnanensine (**12**), and scholaphylline (**13**) (**Figure 3.54**).

Hydration of the *N*-4 iminium ion and hydrolysis of the CO<sub>2</sub>Me group in **i** furnish the carboxyl-carbinolamine intermediate **(ii)**. The carbinolamine group is then converted to the NCO<sub>2</sub>Me group via oxidation and esterification reactions. A subsequent nucleophilic addition of the 19,20-double bond onto the conjugated imine at C-6 forged the cycloheptane ring C present in **10**. The resulting C-20 tertiary carbocation is then trapped by the carboxyl group to furnish the  $\gamma$ -lactone bridge and thus completed the construction of the structure of alstoscholactine (**10**) (**Figure 3.54**).

The iminium ion intermediate **(i)** can also be converted to 6,7-*seco*angustilobine B (**17**), which on epoxidation of the 19,20-double bond, followed by hydrolysis of the CO<sub>2</sub>Me group, give the carboxyl-epoxide intermediate **(iii)**. Subsequent intramolecular nucleophilic attack of the carboxyl group onto C-20 with concomitant epoxide ring-opening provide the final structure of alstolaxepine (**11**) (**Figure 3.54**).

Alternatively, double hydration of intermediate (i) gives the diol intermediate (iv). Following that, a fragmentation step occurs resulting in the expulsion of C-6 as a formaldehyde molecule to produce carbinolamine (v), which is subsequently oxidized to yield *N*-formilyunnanensine (12) (Figure 3.54).

The diol intermediate (iv) can alternatively undergo a double formaldehyde expulsion leading to the loss of both C-5 and C-6 to provide yunnanensine, one of the two monomers required to biosynthesize 13. A selective reduction of the iminium ion at C-5 in (i) gives enamine (vi), which is the second required monomeric half. Finally, a nucleophilic conjugate addition from N-4 of yunnanensine to C-6 of enamine (vi) yields scholaphylline (13) (Figure 3.54).

Since alstobrogaline (19) is a corynanthe-derived alkaloid, it follows a different biogenetic pathway. One plausible biogenetic pathway to 19 is shown in Figure 3.55, starting from an akuammiline-type precursor such as strictamine. Firstly, strictamine undergoes an oxidation to the C-5–N-4 iminium ion (vii), which following hydrolytic cleavage gives the amine-aldehyde (viii). Subsequently, transamination of the aldehyde in (viii) gives a primary amine, which then performs a nucleophilic addition onto the imine C-2 to give the pentacyclic aminal (xi). Finally, oxidation of 5 gives the desired alkaloid, alstobrogaline (19), which incorporates an aldimine and a nitron function at C-5 and C-21, respectively.

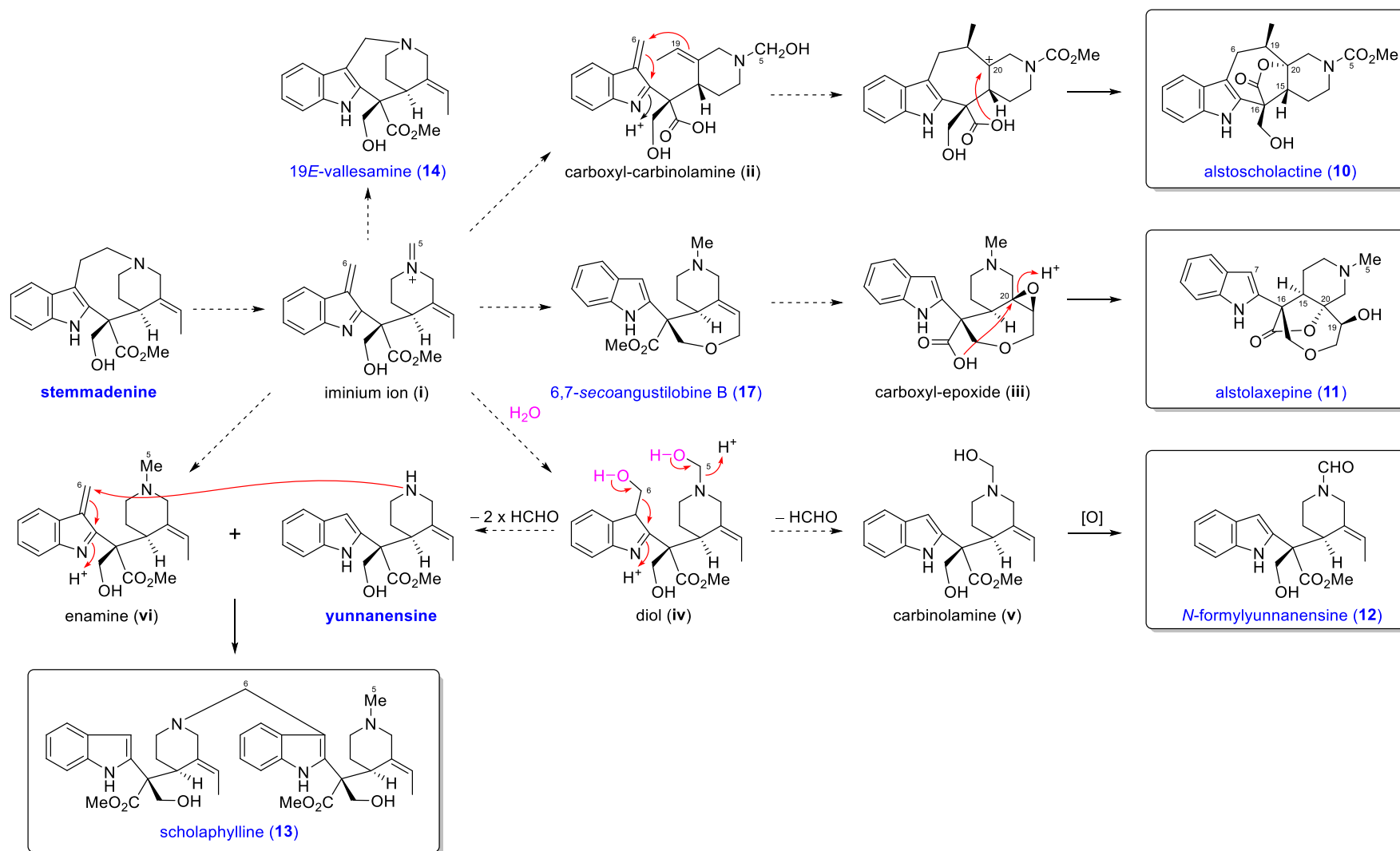


**Figure 3.54:** Plausible biogenetic pathways to alstoscholactine (10), alstolaxepine (11), *N*-formylyunnanensine (12), and scholaphylline (13)

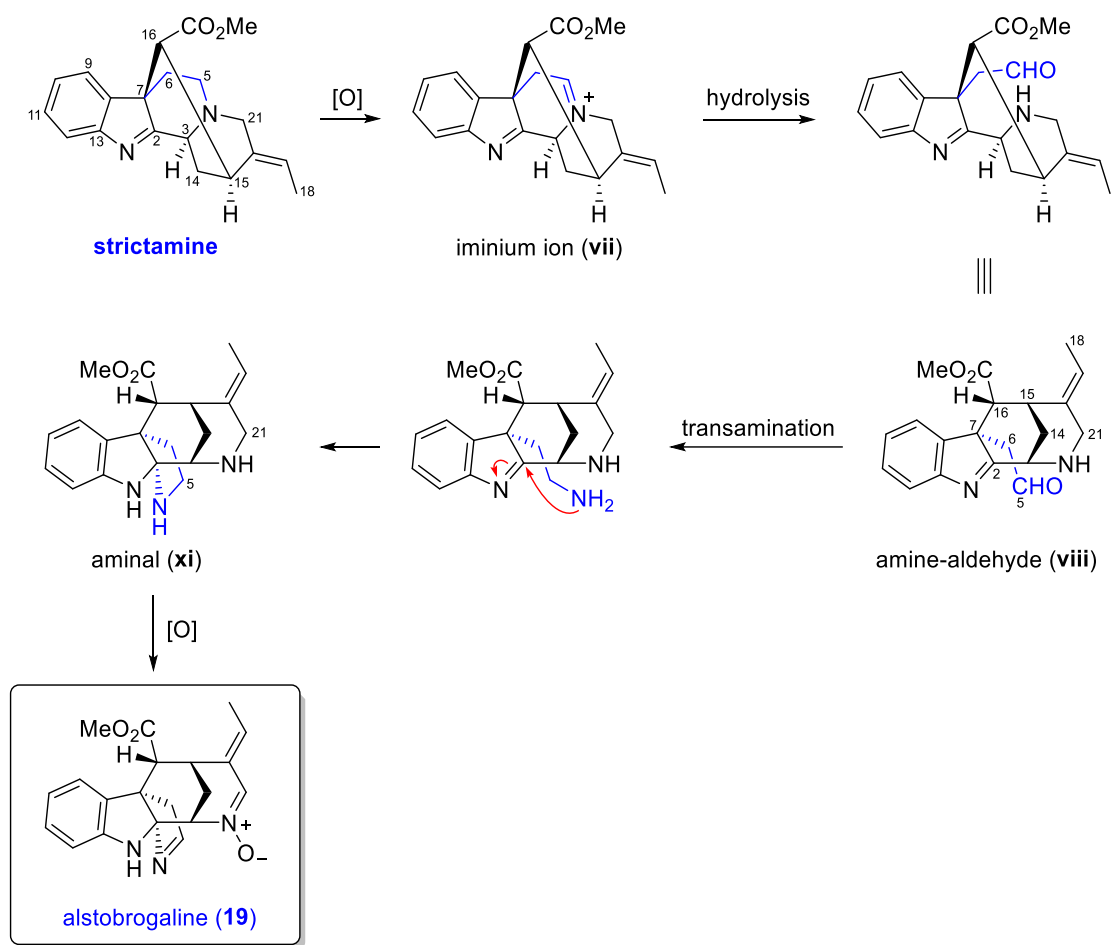


**Figure 3.55:** Plausible biogenetic pathway to alstobrogaline (19)

## CHAPTER FOUR: EXPERIMENTAL

### 4.1 Spectroscopic Techniques

Spectroscopic techniques including nuclear magnetic resonance (NMR) spectroscopy, infrared (IR) spectroscopy, ultraviolet-visible (UV-vis) spectroscopy, high-resolution mass spectrometry (MS), electronic circular dichroism (ECD) spectroscopy, and measurement of optical rotations were used to elucidate the structures of the alkaloids isolated from the present study.

#### 4.1.1 NMR spectroscopy

One-dimensional (1D) NMR ( $^1\text{H}$  and  $^{13}\text{C}$ ) and two-dimensional (2D) NMR (COSY, HSQC, HMBC, and NOESY) spectra were recorded on a Bruker 400, 600 or 700 MHz spectrometer. Chemical shifts ( $\delta$ ) were recorded in ppm and coupling constants ( $J$ ) in Hz. The alkaloids were dissolved in  $\text{CDCl}_3$  with tetramethylsilane (TMS) added as an internal standard ( $\delta = 0$ ).

#### 4.1.2 IR spectroscopy

IR spectra of the alkaloids were recorded on a PerkinElmer Spectrum 400 FT-IR/FT-FIR spectrophotometer and were processed using the built-in *Spectrum* interface. Total of 16 scans acquired for each sample, including the background scan.

### 4.1.3 UV-vis spectroscopy

UV spectra of the alkaloids were recorded on a Shimadzu UV-3101PC spectrophotometer or PerkinElmer Lambda 35UV/Vis spectrophotometer. The samples were dissolved in MeOH or MeCN with known concentration (0.01mg/ml – 0.04mg/ml) and scanned for the range of 200 – 400 nm. Molar absorptivity ( $\epsilon$ ) was calculated according to the Beer-Lambert Law:

$$A = \epsilon \times c \times l$$

where  $A$  is the UV absorbance,  $c$  is the concentration (mg/ml) of the solute,  $l$  is the length of the cell

### 4.1.4 High-resolution MS

High-resolution direct analysis in real time mass spectrometry (HR-DART-MS) measurements were obtained on a JEOL Accu TOF-DART mass spectrometer. High-resolution electrospray ionisation mass spectrometry (HR-ESI-MS) measurements were performed on a MicroTOF QIII Bruker Daltonic using an ESI positive ionization with the following settings capillary voltage: 3500 V; nebulizer pressure: 3.5 bar; drying gas: 10 L/min at 250°C. The mass range was at  $m/z$  50 – 1000.

### 4.1.5 Optical rotations

Optical rotations were determined on a JASCO P-1020 automatic digital polarimeter. The solution samples were prepared by dissolving the alkaloids in 2 ml of  $\text{CHCl}_3$ . Specific optical rotation  $[\alpha]$  was calculated from the angle of rotation using the following equation:

$$[\alpha]_D^{25^\circ} = \frac{100\alpha}{c \times l}$$

where  $\alpha$  is the angle of rotation,  $c$  is the concentration in g/100 ml, and  $l$  is the length in dm

### 4.1.6 ECD spectroscopy

ECD spectra were measured using a Jasco J-815 Circular Dichroism Spectrometer. The experimental parameters, spectral processing and smoothening were performed using the built in *Spectra Manager* interface. The samples were dissolved in MeOH or MeCN and scanned for the range of 190 – 400 nm.

## 4.2 Plant materials, Extraction, and Isolation of Alkaloids

### 4.2.1 Source and authentication of plant materials

The plant materials were collected from two areas in Selangor and were identified by Dr. Yong Kien Thai from Institute of Biological Sciences, University of Malaya, Malaysia. Voucher specimens are deposited at the Herbarium, University of Malaya (UM) (**Table 4.1**).

**Table 4.1:** Source and authentication of plant materials

Species	Herbarium Specimen Number	Locality	Date of Collection
<i>Ficus schwarzii</i>	KLU48248	Ulu Gombak	July 2013
Koord.			
<i>Alstonia scholaris</i>	KLU47983	Semenyih	June 2013
(L.) R. Br.			

### 4.2.2 Plant processing and extraction

Fresh leaves of *Ficus schwarzii* were collected and processed to ensure stems and twigs were removed. The fresh leaves were air dried and ground to produce 21.6 kg dried material. Similarly, the leaves, bark, and flowers of *Alstonia scholaris* were collected, processed and air dried, to give 6.3 kg, 5.6 kg, and 1.0 kg of dried materials, respectively.

The general procedure for solvent extraction of the plant material, followed by acid-base extraction to give the crude alkaloid extract are described as follows. The ground plant material was extracted with 95% EtOH (overnight) for four times at room temperature. The ethanolic extract was concentrated in vacuo and subsequently added into 3% tartaric acid solution. This allowed the basic alkaloids in the ethanolic extract to be converted to the

aqueous-soluble alkaloid tartrate salts, while the non-alkaloid substances remained insoluble in the acidic aqueous solution. The insoluble substances in the acidic solution were removed via filtration through kieselguhr. Concentrated NH<sub>3</sub> solution was subsequently added to the acidic filtrate until pH 10 was achieved. The liberated alkaloids were extracted three times with chloroform. The combined chloroform layer was washed with distilled water three times to remove the ammonia residual, dried over anhydrous Na<sub>2</sub>SO<sub>4</sub>, and concentrated to give the crude alkaloid mixture. Subsequently, the crude alkaloids were subjected to various chromatographic methods to isolate pure compounds.

**Table 4.2:** Mass of dried plant materials and crude alkaloid

<b>Species</b>	<b>Sample</b>	<b>Mass of Dried Material, (kg)</b>	<b>Mass of Crude Alkaloid, (g)</b>
<i>Ficus schwarzii</i>	Leaves	21.6	4.4
	Leaves	6.3	26.0
<i>Alstonia scholaris</i>	Bark	5.6	19.0
	Flowers	1.0	1.6

## **4.2.3 Chromatographic methods**

### **4.2.3.1 Column chromatography**

Column chromatography was utilized to initially fractionate the crude alkaloidal mixture into smaller and simpler fractions. The neck section just above the stopcock of the glass column was plugged with cotton to prevent silica gel from leaking out during elution. Silica gel 60 (Merck 9385, 0.040 – 0.063 mm) was made into slurry with an eluting solvent pre-determined by TLC profiling. The amount of silica gel used was approximately based on a mass ratio of silica gel to crude mixture of 50 g : 1 g. The silica gel slurry was packed in the column and allowed to equilibrate for 15 minutes before loading of sample. Sodium sulphate anhydrous was added as a layer on top of the silica bed to serve as a protective layer as well as to remove traces of water from the eluent or sample that are loaded into the column for separation. Chloroform was used as an eluent for the solvent system with decreasing hexane gradient followed by increasing methanol gradient. Thin layer chromatography (TLC) was used to follow the progress of the fractionation process as well as to examine the composition of each fraction. Fractions that have similar TLC profiles would be combined. Fractions with mass significantly greater than 1 g were further chromatographed using column chromatography, while fractions with smaller mass (<1 g) were separated further using preparative centrifugal TLC.

#### **4.2.3.2 Preparative centrifugal thin layer chromatography (CTLC)**

Preparative centrifugal TLC was performed using a Chromatotron. A round chromatographic plate measuring 24 cm in diameter was used to carry out preparative centrifugal TLC. To prepare the chromatographic plate, the edge of the glass plate was secured with cellophane tape to form a mold. Silica gel 60 PF<sub>254</sub> containing gypsum (Merck 7759) was added to cold distilled water and shaken to produce a slurry. The well shaken homogeneous slurry was then quickly poured onto the glass plate to form a layer of wet silica gel and allowed to set. To obtain an even setting, the circular glass plate was rotated while the slurry was being poured. The plate was left to air-dry and subsequently dried in an oven at 100°C for approximately 12 hours. The activated chromatographic plate was then shaved with an appropriate steel blade to produce a thin layer of silica coating of the desired thickness (1, 2, or 4 mm). A plate with 1 mm thickness of silica coating was used to separate a sample with mass up to ~300 mg, 2 mm thickness for a sample mass up to ~600 mg, and 4 mm thickness for a sample mass up to ~1.2 g. The shaved plate was mounted onto a Chromatotron before sample was loaded. The sample was first dissolved in a minimum volume of a suitable solvent (usually chloroform) and loaded at the centre of the plate while the plate was spinning to form a thin band of sample. Elution was carried with appropriate solvent system (usually chloroform-, ethyl acetate-, or diethyl ether-based solvent). The fractions collected were concentrated by rotary-evaporation, examined by TLC and combined where appropriate.

#### 4.2.3.3 Thin layer chromatography (TLC)

TLC was used to identify alkaloid presence (with Dragendorff's reagent), monitor progress of separation for CC and CTLC, examine degree of separation, and reveal complexity of a mixture. It was also used in conjunction with CC and CTLC to determine the suitable initial composition of solvent used as eluent for chromatographic fractionation ( $R_f$  of 0.2 – 0.3 was appropriate). A labeled TLC plate (5 × 10 cm, 0.25 mm thick aluminium pre-coated plate of silica gel 60 F254) was used to spot the separated fractions using a fine glass spotter. The loaded TLC plate was then placed in a glass jar saturated with the appropriate solvent system. The jar was closed tightly and left aside for the TLC plate to develop until the solvent front reached approximately 1 cm from the top end of the plate. The TLC plate was removed from the jar, the solvent front marked, and the plate examined under UV light (254 nm) to outline the spots appeared in each fraction. Subsequently, the TLC plate was sprayed with Dragendorff's reagent to check for orange staining spots, which indicated alkaloid presence.

#### 4.2.3.4 High performance liquid chromatography (HPLC)

High-Performance Liquid Chromatography (HPLC) was used in the present study to analyse the enantiomeric compositions of compounds **1** – **7** on a chiral-phase column. HPLC analysis was performed on a Waters liquid chromatograph equipped with a Waters 600 controller and a Waters 2489 tunable absorbance detector and manual collector. Analyses were performed using a Chiralpak IA column (4.6 × 150 mm) at room temperature. The alkaloids were first dissolved in EtOH before injection. The eluent flow rate was set at 1.0 mL/min, while the eluents used are listed as follow: hexane-EtOH-Et<sub>2</sub>NH, 80:20:0.1 for **1** (2.0 mg/mL, 10.0 μL), **2** (3.7 mg/mL, 5.0 μL), **4** (1.2 mg/mL, 15.0 μL), **5** (5.7 mg/mL, 2.0 μL), and **7** (2.8 mg/mL,

10.0  $\mu\text{L}$ ); hexane-EtOH-Et<sub>2</sub>NH, 90:10:0.1 for **3** (1.6 mg/mL, 10.0  $\mu\text{L}$ ), and **6** (1.2 mg/mL, 20.0  $\mu\text{L}$ ).

### 4.3 Spray reagent (Dragendorff's reagent)

Dragendorff's reagent was used to detect the presence of alkaloids. Developed TLC plates were sprayed with Dragendorff's reagent and the presence of alkaloids was indicated if when the spots turned orange. The change in colour is due to the chemicals that made up the reagent: bismuth nitrate and potassium iodide which in the presence of alkaloids under acidic conditions will produce the ion pair of  $[\text{BiI}_4]^-$  and  $[\text{HNR}_3]^+$ , that is generally orange in colour. The intensity of the colour could provide a rough indication of the amount of alkaloids present.

Preparation of Dragendorff's solution:

The stock solution was prepared by mixing the equal portions of *Solution A* (0.85 g of bismuth nitrate was dissolved in 40 mL of distilled water and 10 mL of glacial acetic acid) and *Solution B* (20 g of potassium iodide was dissolved in 50 mL of distilled water). Before use, 10 mL of the stock solution was mixed with 20 mL of glacial acetic acid and top-up to 100 mL using distilled water.

### 4.4 Isolation of compounds 1 – 9 from the leaves of *F. schwarzii*

4.4 g of the crude alkaloid mixture was initially fractionated by column chromatography ( $\text{SiO}_2$ ,  $\text{CHCl}_3$ -MeOH, with increasing percentage of MeOH) followed by repeated chromatography of the partially resolved fractions using column chromatography or preparative centrifugal thin layer chromatography. The solvent systems used for preparative centrifugal thin layer chromatography were  $\text{CHCl}_3$ -hexane ( $\text{NH}_3$ -saturated),  $\text{Et}_2\text{O}$ -hexane ( $\text{NH}_3$ -saturated),  $\text{CHCl}_3$ -

MeOH (NH<sub>3</sub>-saturated), and Et<sub>2</sub>O-MeOH (NH<sub>3</sub>-saturated). The yields of the compounds obtained were as follows: **1** (389 mg), **2** (197 mg), **3** (9 mg), **4** (7 mg), **5** (17 mg), **6** (4 mg), **7** (7 mg), **8** (5 mg), and **9** (5 mg).

#### **4.5 Conversion of schwarzinicine A (1) to schwarzinicine B (2) via N-methylation**

To a stirring solution of **1** (19.9 mg, 0.039 mmol) in MeOH (4 mL) was added 37% aq. formaldehyde (0.1 mL, 1.34 mmol, 34 equiv) and NaBH<sub>3</sub>CN (37.0 mg, 0.59 mmol, 15 equiv). The mixture was stirred at room temperature for 1 h before addition of AcOH (0.4 mL, 6.99 mmol, 175 equiv). The solution was stirred further for 23 h before addition of 1 M NaOH solution (8 mL). The resulting mixture was then extracted with CH<sub>2</sub>Cl<sub>2</sub> (3 × 10 mL). The organic phase was washed with brine and dried with Na<sub>2</sub>SO<sub>4</sub> anhydrous before concentrated *in vacuo*. The crude product was purified by preparative centrifugal thin layer chromatography with Et<sub>2</sub>O-hexane (4:1) as eluent to furnish **2** as a light yellowish oil (11.1 mg, 0.021 mmol, 54%).

## **4.6 Isolation of compounds 10 – 27 from *Alstonia scholaris***

### **4.6.1 Isolation of compounds 10, 11, 14, 17, 19, 21 – 23, and 25 from the leaves of *A. scholaris***

26 g of the crude alkaloid mixture was initially fractionated by column chromatography (SiO<sub>2</sub>, CHCl<sub>3</sub>-MeOH, with increasing percentage of MeOH) followed by repeated chromatography of the partially resolved fractions using column chromatography or preparative centrifugal thin layer chromatography. The solvent systems used for preparative centrifugal thin layer chromatography were CHCl<sub>3</sub>-hexane (NH<sub>3</sub>-saturated), Et<sub>2</sub>O-hexane (NH<sub>3</sub>-saturated), CHCl<sub>3</sub>-MeOH (NH<sub>3</sub>-saturated), and Et<sub>2</sub>O-MeOH (NH<sub>3</sub>-saturated). The yields of the compounds obtained were as follows: **10** (8 mg), **11** (33 mg), **14** (147 mg), **17** (33 mg), **19** (21 mg), **21** (32 mg), **22** (29 mg), **23** (7 mg), and **25** (34 mg).

### **4.6.2 Isolation of compounds 12 – 16, 18, 24, 26, and 27 from the bark of *A. scholaris***

19 g of the crude alkaloid mixture was initially fractionated by column chromatography (SiO<sub>2</sub>, CHCl<sub>3</sub>-MeOH, with increasing percentage of MeOH) followed by repeated chromatography of the partially resolved fractions using column chromatography or preparative centrifugal thin layer chromatography. The solvent systems used for preparative centrifugal thin layer chromatography were CHCl<sub>3</sub>-hexane (NH<sub>3</sub>-saturated), Et<sub>2</sub>O-hexane (NH<sub>3</sub>-saturated), CHCl<sub>3</sub>-MeOH (NH<sub>3</sub>-saturated), and Et<sub>2</sub>O-MeOH (NH<sub>3</sub>-saturated). The yields of the compounds obtained were as follows: **12** (19 mg), **13** (4 mg), **14** (16 mg), **15** (7 mg), **16** (8 mg), **18** (7 mg), **24** (10 mg), **26** (4 mg), and **27** (8 mg).

#### 4.6.3 Isolation of compounds **14**, **20**, and **21** from the flowers of *A. scholaris*

1.6 g of the crude alkaloid mixture was initially fractionated by column chromatography (SiO<sub>2</sub>, CHCl<sub>3</sub>-MeOH, with increasing percentage of MeOH) followed by repeated chromatography of the partially resolved fractions using preparative centrifugal thin layer chromatography. The solvent systems used for preparative centrifugal thin layer chromatography were CHCl<sub>3</sub>-hexane (NH<sub>3</sub>-saturated), Et<sub>2</sub>O-hexane (NH<sub>3</sub>-saturated), CHCl<sub>3</sub>-MeOH (NH<sub>3</sub>-saturated), and Et<sub>2</sub>O-MeOH (NH<sub>3</sub>-saturated). The yields of the compounds obtained were as follows: **14** (90 mg), **20** (6 mg), and **21** (34mg).

#### 4.7 Transformation of 19,20-*E*-vallesamine (**14**) to alstoscholactine (**10**)

To a stirred solution of 19,20-*E*-vallesamine (17 mg, 0.04 mmol) in CH<sub>2</sub>Cl<sub>2</sub> (4 mL) was added K<sub>2</sub>CO<sub>3</sub> (36.6 mg, 0.26 mmol, 6 equiv) and methyl chloroformate (6.1 μL, 0.08 mmol, 2 equiv). The resulting mixture was stirred at room temperature for 30 min. The reaction mixture then was concentrated *in vacuo*. The resulting residue was purified by preparative centrifugal thin layer chromatography using an eluent system of CHCl<sub>3</sub> (NH<sub>3</sub>-saturated) to yield **10** as a light yellowish oil (9.7 mg, 63%).

## 4.8 Summary of Physical Data

### 4.8.1 Alkaloids of *Ficus schwarzi*

#### 4.8.1.1 Physical data for compound 1

Name	: <b>Schwarzinicine A</b>
Yield	: 389 mg (0.0018 %)
Physical description	: Light yellowish oil
$[\alpha]_D$	: +2 ( <i>c</i> 1.17, CHCl <sub>3</sub> )
HR-DART-MS	: <i>m/z</i> 510.2836 [M + H] <sup>+</sup> (calcd for C <sub>30</sub> H <sub>39</sub> NO <sub>6</sub> + H, 510.2856)
IR $\nu_{\max}$ (cm <sup>-1</sup> )	: 2923, 2851, 1516, 1463, 1261, 1236, 1140, and 1028
UV (MeCN) $\lambda_{\max}$ (log $\epsilon$ )	: 231 (4.05), 281 (3.63) nm
<sup>1</sup> H and <sup>13</sup> C NMR data	: <b>Table 2.1</b>

#### 4.8.1.2 Physical data for compound 2

Name	: <b>Schwarzinicine B</b>
Yield	: 197 mg (0.00091 %)
Physical description	: Light yellowish oil
$[\alpha]_D$	: +20 ( <i>c</i> 1.01, CHCl <sub>3</sub> )
HR-DART-MS	: <i>m/z</i> 524.2996 [M + H] <sup>+</sup> (calcd for C <sub>31</sub> H <sub>41</sub> NO <sub>6</sub> + H, 524.3012)
IR $\nu_{\max}$ (cm <sup>-1</sup> )	: 2934, 2851, 1516, 1463, 1262, 1236, 1141, and 1028
UV (MeCN) $\lambda_{\max}$ (log $\epsilon$ )	: 231 (4.22), 281 (3.79) nm
<sup>1</sup> H and <sup>13</sup> C NMR data	: <b>Table 2.2</b>

#### 4.8.1.3 Physical data for compound 3

Name	:	<b>Schwarzinicine C</b>
Yield	:	9 mg (0.000042 %)
Physical description	:	Light yellowish oil
$[\alpha]_D$	:	-7 ( <i>c</i> 0.48, CHCl <sub>3</sub> )
HR-DART-MS	:	<i>m/z</i> 494.2505 [M + H] <sup>+</sup> (calcd for C <sub>29</sub> H <sub>36</sub> NO <sub>6</sub> + H, 494.2543)
IR $\nu_{\max}$ (cm <sup>-1</sup> )	:	2919, 2834, 1514, 1440, 1234, 1138, and 1026
UV (MeCN) $\lambda_{\max}$ (log $\epsilon$ )	:	231 (4.04), 281 (3.44) nm
<sup>1</sup> H and <sup>13</sup> C NMR data	:	<b>Table 2.3</b>

#### 4.8.1.4 Physical data for compound 4

Name	:	<b>Schwarzinicine D</b>
Yield	:	7 mg (0.000032 %)
Physical description	:	Light yellowish oil
$[\alpha]_D$	:	+5 ( <i>c</i> 0.38, CHCl <sub>3</sub> )
HR-DART-MS	:	<i>m/z</i> 524.2645 [M + H] <sup>+</sup> (calcd for C <sub>30</sub> H <sub>37</sub> NO <sub>7</sub> + H, 524.2643)
IR $\nu_{\max}$ (cm <sup>-1</sup> )	:	2935, 2836, 1514, 1451, 1261, 1236, 1136, and 1029
UV (MeCN) $\lambda_{\max}$ (log $\epsilon$ )	:	230 (4.14), 282 (3.63) nm
<sup>1</sup> H and <sup>13</sup> C NMR data	:	<b>Table 2.4</b>

#### 4.8.1.5 Physical data for compound 5

Name	:	<b>Schwarzinicine E</b>
Yield	:	17 mg (0.000079 %)
Physical description	:	Light yellowish oil
$[\alpha]_D$	:	+3 (CHCl <sub>3</sub> , <i>c</i> 0.54)
HR-DART-MS	:	<i>m/z</i> 526.2777 [M + H] <sup>+</sup> (calcd for C <sub>30</sub> H <sub>39</sub> NO <sub>7</sub> + H, 526.2799)
IR $\nu_{\max}$ (cm <sup>-1</sup> )	:	2932, 2836, 1512, 1451, 1261, 1235, 1138, and 1025
UV (MeCN) $\lambda_{\max}$ (log $\epsilon$ )	:	230 (3.62), 279 (3.08) nm
<sup>1</sup> H and <sup>13</sup> C NMR data	:	<b>Table 2.5</b>

#### 4.8.1.6 Physical data for compound 6

Name	:	<b>Schwarzinicine F</b>
Yield	:	4 mg (0.000019 %)
Physical description	:	Light yellowish oil
$[\alpha]_D$	:	+25 ( <i>c</i> 0.22, CHCl <sub>3</sub> )
HR-DART-MS	:	<i>m/z</i> 526.2791 [M + H] <sup>+</sup> (calcd for C <sub>30</sub> H <sub>39</sub> NO <sub>7</sub> + H, 526.2799)
IR $\nu_{\max}$ (cm <sup>-1</sup> )	:	2935, 2835, 1513, 1463, 1258, 1233, 1138, and 1025
UV (MeCN) $\lambda_{\max}$ (log $\epsilon$ )	:	230 (4.05), 281 (3.62) nm
<sup>1</sup> H and <sup>13</sup> C NMR data	:	<b>Table 2.6</b>

#### 4.8.1.7 Physical data for compound 7

Name	:	<b>Schwarzinicine G</b>
Yield	:	7 mg (0.000032 %)
Physical description	:	Light yellowish oil
$[\alpha]_D$	:	-13 ( <i>c</i> 0.35, CHCl <sub>3</sub> )
HR-DART-MS	:	<i>m/z</i> 540.2966 [M + H] <sup>+</sup> (calcd for C <sub>31</sub> H <sub>41</sub> NO <sub>7</sub> + H, 540.2956)
IR $\nu_{\max}$ (cm <sup>-1</sup> )	:	2936, 2835, 1515, 1464, 1261, 1235, 1140, and 1028
UV (MeCN) $\lambda_{\max}$ (log $\epsilon$ )	:	231 (4.28), 281 (3.86) nm
<sup>1</sup> H and <sup>13</sup> C NMR data	:	<b>Table 2.7</b>

#### 4.8.1.8 Physical data for compound 8

Name	:	<b>Schwarzificusine A</b>
Yield	:	5 mg (0.000023 %)
Physical description	:	Light yellowish oil
$[\alpha]_D$	:	+14 ( <i>c</i> 0.12, CHCl <sub>3</sub> )
HR-DART-MS	:	<i>m/z</i> 494.2544 [M + H] <sup>+</sup> (calcd for C <sub>29</sub> H <sub>35</sub> NO <sub>6</sub> + H, 494.2543)
IR $\nu_{\max}$ (cm <sup>-1</sup> )	:	3391, 3004, 2959, 1594, 1514, 1140, and 1026
UV (MeCN) $\lambda_{\max}$ (log $\epsilon$ )	:	230 (3.92), 281 (3.09) nm
<sup>1</sup> H and <sup>13</sup> C NMR data	:	<b>Table 2.8</b>

#### 4.8.1.9 Physical data for compound 9

Name	:	<b>Schwarzificusine B</b>
Yield	:	5 mg (0.000023 %)
Physical description	:	Light yellowish oil
$[\alpha]_D$	:	+22 ( <i>c</i> 0.21, CHCl <sub>3</sub> )
HR-DART-MS	:	<i>m/z</i> 494.2528 [M + H] <sup>+</sup> (calcd for C <sub>29</sub> H <sub>35</sub> NO <sub>6</sub> + H, 494.2543)
IR $\nu_{\max}$ (cm <sup>-1</sup> )	:	3421, 3270, 3001, 2931, 1591, 1510, 1137, and 1027
UV (MeCN) $\lambda_{\max}$ (log $\epsilon$ )	:	230 (3.85), 279 (3.51) nm
<sup>1</sup> H and <sup>13</sup> C NMR data	:	<b>Table 2.8</b>

#### 4.8.2 Alkaloids of *Alstonia scholaris*

##### 4.8.2.1 Physical data for compound 10

Name	:	<b>Alstoscholactine</b>
Yield	:	Leaves: 8 mg (0.00013 %)
Physical description	:	Light yellowish oil
$[\alpha]_D$	:	+14 ( <i>c</i> 1.04, CHCl <sub>3</sub> )
HR-DART-MS	:	<i>m/z</i> 385.1760 [M+H] <sup>+</sup> (calcd for C <sub>21</sub> H <sub>24</sub> N <sub>2</sub> O <sub>5</sub> + H, 385.1764)
IR $\nu_{\max}$ (cm <sup>-1</sup> )	:	3403, 1761, and 1684
UV (MeCN) $\lambda_{\max}$ (log $\epsilon$ )	:	222 (4.30), 276 (3.75), 283 (3.79), and 290 (3.74) nm
<sup>1</sup> H and <sup>13</sup> C NMR data	:	<b>Table 3.2</b>

#### 4.8.2.2 Physical data for compound 11

Name	:	<b>Alstolaxepine</b>
Yield	:	Leaves: 33 mg (0.00052 %)
Physical description	:	Light yellowish oil
$[\alpha]_D$	:	-12 ( <i>c</i> 0.67, CHCl <sub>3</sub> )
Melting point (°C)	:	109 – 112
HR-DART-MS	:	<i>m/z</i> 343.1644 [M+H] <sup>+</sup> (calcd for C <sub>19</sub> H <sub>22</sub> N <sub>2</sub> O <sub>4</sub> + H, 343.1658)
IR $\nu_{\max}$ (cm <sup>-1</sup> )	:	3343 and 1774
UV (MeCN) $\lambda_{\max}$ (log $\epsilon$ )	:	217 (4.44), 271 (3.85), 279 (3.83), and 289 (3.72) nm
<sup>1</sup> H and <sup>13</sup> C NMR data	:	<b>Table 3.3</b>

#### 4.8.2.3 Physical data for compound 12

Name	:	<b><i>N</i>-Formylyunnanensine</b>
Yield	:	Bark: 19 mg (0.00034 %)
Physical description	:	Light yellowish oil
$[\alpha]_D$	:	+23 ( <i>c</i> 0.91, CHCl <sub>3</sub> )
HR-DART-MS	:	<i>m/z</i> 357.18047 [M+H] <sup>+</sup> (calcd for C <sub>20</sub> H <sub>25</sub> N <sub>2</sub> O <sub>4</sub> + H, 357.18143)
IR $\nu_{\max}$ (cm <sup>-1</sup> )	:	3408, 3304, 1726, and 1647
UV (MeCN) $\lambda_{\max}$ (log $\epsilon$ )	:	218 (4.30), 281 (3.65), and 290 (3.56) nm
<sup>1</sup> H and <sup>13</sup> C NMR data	:	<b>Table 3.4</b>

#### 4.8.2.4 Physical data for compound 13

Name	:	<b>Scholaphylline</b>
Yield	:	Bark: 4 mg (0.000071 %)
Physical description	:	Light yellowish oil
$[\alpha]_D$	:	-39 ( <i>c</i> 0.51, CHCl <sub>3</sub> )
HR-ESI-MS	:	<i>m/z</i> 683.3821 [M+H] <sup>+</sup> (calcd for C <sub>40</sub> H <sub>50</sub> N <sub>4</sub> O <sub>6</sub> + H, 683.3803)
IR $\nu_{\max}$ (cm <sup>-1</sup> )	:	3403, and 1718
UV (MeCN) $\lambda_{\max}$ (log $\epsilon$ )	:	219 (4.57) and 283 (4.00) nm
<sup>1</sup> H and <sup>13</sup> C NMR data	:	<b>Table 3.5</b>

#### 4.8.2.5 Physical data for compound 14

Name	:	<b>19,20-<i>E</i>-Vallesamine</b>
Yield	:	Bark: 16 mg (0.00029 %) Leaves: 147 mg (0.0023 %) Flowers: 90 mg (0.009 %)
Physical description	:	Light yellowish oil
$[\alpha]_D$	:	+11 ( <i>c</i> 0.2, CHCl <sub>3</sub> )
HR-DART-MS	:	<i>m/z</i> 341.18535 [M+H] <sup>+</sup> (calcd for C <sub>20</sub> H <sub>24</sub> N <sub>2</sub> O <sub>3</sub> + H, 341.1860)
IR $\nu_{\max}$ (cm <sup>-1</sup> )	:	3355 and 1723
UV (MeCN) $\lambda_{\max}$ (log $\epsilon$ )	:	222 (4.21) and 284 (3.63) nm
<sup>1</sup> H and <sup>13</sup> C NMR data	:	<b>Table 3.6</b>

#### 4.8.2.6 Physical data for compound 15

Name	:	<b>19,20-Z-Vallesamine</b>
Yield	:	Bark: 7 mg (0.00013 %)
Physical description	:	Light yellowish oil
$[\alpha]_D$	:	-60 ( <i>c</i> 1.4, CHCl <sub>3</sub> )
HR-DART-MS	:	<i>m/z</i> 341.18554 [M+H] <sup>+</sup> (calcd for C <sub>20</sub> H <sub>24</sub> N <sub>2</sub> O <sub>3</sub> + H, 341.1860)
IR $\nu_{\max}$ (cm <sup>-1</sup> )	:	3368 and 1722
UV (MeCN) $\lambda_{\max}$ (log $\epsilon$ )	:	220 (4.36) and 284 (3.73) nm
<sup>1</sup> H and <sup>13</sup> C NMR data	:	<b>Table 3.7</b>

#### 4.8.2.7 Physical data for compound 16

Name	:	<b>19,20-E-Vallesamine N-oxide</b>
Yield	:	Bark: 8 mg (0.00014 %)
$[\alpha]_D$	:	+8 ( <i>c</i> 0.35, CHCl <sub>3</sub> )
Physical description	:	Light yellowish oil
HR-ESI-MS	:	<i>m/z</i> 357.1844 [M+H] <sup>+</sup> (calcd for C <sub>20</sub> H <sub>24</sub> N <sub>2</sub> O <sub>4</sub> + H, 357.1809)
IR $\nu_{\max}$ (cm <sup>-1</sup> )	:	3324 and 1726
UV (MeCN) $\lambda_{\max}$ (log $\epsilon$ )	:	217 (4.31) and 282 (3.67) nm
<sup>1</sup> H and <sup>13</sup> C NMR data	:	<b>Table 3.7</b>

#### 4.8.2.8 Physical data for compound 17

Name	:	<b>6,7-<i>Seco</i>angustilobine B</b>
Yield	:	Leaves: 33 mg (0.00052 %)
Physical description	:	Light yellowish oil
$[\alpha]_D$	:	+98 ( <i>c</i> 0.39, CHCl <sub>3</sub> )
HR-DART-MS	:	<i>m/z</i> 341.18495 [M+H] <sup>+</sup> (calcd for C <sub>20</sub> H <sub>24</sub> N <sub>2</sub> O <sub>3</sub> + H, 341.18652)
IR $\nu_{\max}$ (cm <sup>-1</sup> )	:	3365 and 1726
UV (MeCN) $\lambda_{\max}$ (log $\epsilon$ )	:	219 (4.34), 273 (3.86), 282 (3.86), and 289 (3.78) nm
<sup>1</sup> H and <sup>13</sup> C NMR data	:	<b>Table 3.8</b>

#### 4.8.2.9 Physical data for compound 18

Name	:	<b>6,7-<i>Seco</i>-19,20<math>\alpha</math>-epoxyangustilobine B</b>
Yield	:	Bark: 7 mg (0.00013 %)
Physical description	:	Light yellowish oil
$[\alpha]_D$	:	-14 ( <i>c</i> 0.28, CHCl <sub>3</sub> )
IR $\nu_{\max}$ (cm <sup>-1</sup> )	:	3353, 1726, and 1652
UV (MeCN) $\lambda_{\max}$ (log $\epsilon$ )	:	217 (4.22), 280 (3.56), and 289 (3.45) nm
<sup>1</sup> H and <sup>13</sup> C NMR data	:	<b>Table 3.8</b>

#### 4.8.2.10 Physical data for compound 19

Name	:	<b>Alstobrogaline</b>
Yield	:	Leaves: 21 mg (0.00033 %)
Physical description	:	Light yellowish oil
Melting point (°C)	:	187 (decomposed)
$[\alpha]_D$	:	+93 ( <i>c</i> 0.10, CHCl <sub>3</sub> )
HR-DART-MS	:	<i>m/z</i> 352.1674 [M+H] <sup>+</sup> (calcd for C <sub>20</sub> H <sub>21</sub> N <sub>3</sub> O <sub>3</sub> + H, 352.1661)
IR $\nu_{\max}$ (cm <sup>-1</sup> )	:	3249, and 1739
UV (MeCN) $\lambda_{\max}$ (log $\epsilon$ )	:	235 (3.69) and 290 (3.89) nm
<sup>1</sup> H and <sup>13</sup> C NMR data	:	<b>Table 3.9</b>

#### 4.8.2.11 Physical data for compound 20

Name	:	<b>Tetrahydroalstonine</b>
Yield	:	Flowers: 6 mg (0.0006 %)
Physical description	:	Light yellowish oil
HR-ESI-MS	:	<i>m/z</i> 339.20646 [M+H] <sup>+</sup> (calcd for C <sub>21</sub> H <sub>26</sub> N <sub>2</sub> O <sub>2</sub> + H, 339.20646)
IR $\nu_{\max}$ (cm <sup>-1</sup> )	:	3353 and 1700
UV (MeCN) $\lambda_{\max}$ (log $\epsilon$ )	:	228 (4.21), 250 (3.74), 284 (3.57), and 291 (3.57) nm
<sup>1</sup> H and <sup>13</sup> C NMR data	:	<b>Table 3.10</b>

#### 4.8.2.12 Physical data for compound 21

Name : **Picrinine**

Yield : Leaves: 32 mg (0.00051 %)  
Flowers: 34 mg (0.0034 %)

Physical description : Light yellowish oil

HR-ESI-MS :  $m/z$  339.17254 [M+H]<sup>+</sup> (calcd for C<sub>20</sub>H<sub>22</sub>N<sub>2</sub>O<sub>3</sub> + H, 339.17087)

IR  $\nu_{\max}$  (cm<sup>-1</sup>) : 3346 and 1734

UV (MeCN)  $\lambda_{\max}$  (log  $\epsilon$ ) : 228 (3.93), 259 (3.31), and 289 (3.57) nm

<sup>1</sup>H and <sup>13</sup>C NMR data : **Table 3.10**

#### 4.8.2.13 Physical data for compound 22

Name : **16R-19,20-Z-Isositsirikine**

Yield : Leaves: 7 mg (0.00011 %)

Physical description : Light yellowish oil

<sup>1</sup>H and <sup>13</sup>C NMR data : **Table 3.11**

#### 4.8.2.14 Physical data for compound 23

Name	:	<b>16R-19,20-E-Isositsirikine</b>
Yield	:	Bark: 10 mg (0.00018 %)
Physical description	:	Light yellowish oil
$[\alpha]_D$	:	-16 ( <i>c</i> 0.22, MeOH)
HR-DART-MS	:	$m/z$ 355.20339 $[M+H]^+$ (calcd for $C_{21}H_{26}N_2O_3 + H$ , 355.2016)
IR $\nu_{max}$ (cm <sup>-1</sup> )	:	3379, 2830, 2785, 1726, and 1630
UV (MeCN) $\lambda_{max}$ (log $\epsilon$ )	:	218 (3.88), 282 (3.66), and 290 (3.11) nm
<sup>1</sup> H and <sup>13</sup> C NMR data	:	<b>Table 3.11</b>

#### 4.8.2.15 Physical data for compound 24

Name	:	<b>Scholaricine</b>
Yield	:	Leaves: 34 mg (0.00054 %)
Physical description	:	Light yellowish oil
UV (MeCN) $\lambda_{max}$ (log $\epsilon$ )	:	215 (4.27), 236 (4.15), 290 (3.69), and 339 (4.13) nm
<sup>1</sup> H and <sup>13</sup> C NMR data	:	<b>Table 3.12</b>

#### 4.8.2.16 Physical data for compound 25

Name	:	<b>N<sup>b</sup>-Demethylalstogustine N-oxide</b>
Yield	:	Bark: 9 mg (0.00016 %)
Physical description	:	Light yellowish oil
$[\alpha]_D$	:	-346 ( <i>c</i> 0.43, CHCl <sub>3</sub> )
HR-ESI-MS	:	<i>m/z</i> 357.1831 [M+H] <sup>+</sup> (calcd for C <sub>20</sub> H <sub>24</sub> N <sub>2</sub> O <sub>4</sub> + H, 357.1809)
IR $\nu_{\max}$ (cm <sup>-1</sup> )	:	3351, 3236, 1676, and 1603
UV (MeCN) $\lambda_{\max}$ (log $\epsilon$ )	:	223 (3.93), 291 (3.75), and 326 (3.80) nm
<sup>1</sup> H and <sup>13</sup> C NMR data	:	<b>Table 3.12</b>

#### 4.8.2.17 Physical data for compound 26

Name	:	<b><i>E/Z</i>-Vallesiachotamine</b>
Yield	:	Bark: 8 mg (0.00014 %)
Physical description	:	Light yellowish oil
Mass spectrum	:	<i>m/z</i> 351.17028 [M+H] <sup>+</sup> (calcd for C <sub>21</sub> H <sub>23</sub> N <sub>2</sub> O <sub>3</sub> + H, 351.17087)
IR $\nu_{\max}$ (cm <sup>-1</sup> )	:	1738 and 2856
UV (MeCN) $\lambda_{\max}$ (log $\epsilon$ )	:	223 (4.27) 289 (4.07) nm
<sup>1</sup> H and <sup>13</sup> C NMR data	:	<b>Table 3.13</b>

## CHAPTER FIVE: CONCLUDING REMARKS

The main aim of the present study was to perform phytochemical investigations of the alkaloidal composition of the leaves of *Ficus schwarzii* and the leaves, stem-bark and flowers of the West Coast *Alstonia scholaris*.

A total of nine new alkaloids, namely schwarinicines A–G (**1–7**) and schwarzificusines A and B (**8** and **9**), were isolated and characterised from the leaves of *Ficus schwarzii*. The schwarzinicine alkaloids (**1–7**) represent the first examples of 1,4-diarylbutanoid-phenethylamine conjugates obtained as natural products,<sup>132</sup> while schwarzificusines A and B (**8** and **9**) represent rare naturally occurring compounds incorporating a 1-phenyl-3-aminotetralin core structure. The schwarzificusines are postulated to be structurally related to the schwarzinicine alkaloids.

A total of 17 monoterpenoid indole alkaloids were isolated and characterised from the leaves, stem-bark, and flowers of *Alstonia scholaris*. Five of these, namely alstoscholactine (**10**), alstolaxepine (**11**), *N*-formilyunnanensine (**12**), scholaphylline (**13**), and alstobrogaline (**19**), were determined to be new compounds. Alkaloids **10**, **11**, and **19** possess novel ring systems. Alkaloid **10** represents a rearranged stemmadenine alkaloid with an unprecedented C-6-C-19 connectivity, while alkaloid **11** represents a 6,7-*seco*-angustilobine B-type alkaloid incorporating a rare  $\gamma$ -lactone-bridged oxepane ring system.<sup>133</sup> While alkaloid **12** is the *N*-formyl derivative of the known alkaloid yunnanensine, and alkaloid **13** represents the first member of the *secostemmadenine-secovallesamine*-type bisindole. Alkaloid **19** represents a novel and unusual monoterpenoid indole alkaloid incorporating a third *N* atom, and possessing an aldimine as well as a nitron function.<sup>134</sup>

Although it is outside the scope of this thesis, it is desirable to evaluate the biological activities of the new alkaloids discovered from this research. The following sections summarise some of the most notable findings based on the work carried out by other research groups.

In collaboration with Professor Ting Kang Nee's research group (School of Pharmacy, University of Nottingham Malaysia), the vasorelaxant activity of schwarzinicines A–D (**1–4**) in rat isolated aortic rings was evaluated.<sup>132</sup> Schwarzinicines A–D (**1–4**) were found to induce a pronounced concentration-dependent relaxation in rat isolated aortic rings (endothelium-intact) pre-contracted with 0.1  $\mu\text{M}$  phenylephrine. Dobutamine, which is a phenylalkylamine compound and a known vasorelaxant agent, was used as a positive control. The maximum relaxation magnitude produced by all the four compounds ( $E_{\text{max}}$  106% – 120%) was significantly greater than that of dobutamine ( $E_{\text{max}}$  92%), while the potency of all the compounds tested was comparable at  $\text{EC}_{50}$  range between 0.96 and 2.5  $\mu\text{M}$  (**Figure 5.1**).

**Table 5.1:** Vasorelaxant activity of schwarzinicines A–D (**1–4**) against phenylephrine-Induced Contraction.

Compound	<i>n</i>	$\text{EC}_{50}^{\text{a}}$ ( $\mu\text{M}$ )	$E_{\text{max}}^{\text{a}}$ (%)
<b>1</b>	6	$2.01 \pm 0.67$	$119.3 \pm 3.6^*$
<b>2</b>	5	$0.96 \pm 0.25$	$106.0 \pm 1.5^*$
<b>3</b>	6	$1.88 \pm 0.64$	$120.4 \pm 4.2^*$
<b>4</b>	6	$2.10 \pm 0.35$	$116.1 \pm 3.6^*$
Dobutamine (positive control)	5	$2.50 \pm 1.11$	$92.0 \pm 5.0$

<sup>a</sup>Each value represents mean  $\pm$  standard error of the mean (SEM) of *n* number of animals.

\*Significantly different from dobutamine ( $p < 0.05$ ).

In collaboration with Professor Leong Chee Onn's research group (School of Pharmacy, International Medical University), the antiproliferative activity of alstoscholactine (**10**), alstolaxepine (**11**), *N*-Formyllyunnanensine (**12**), scholaphylline (**13**), and alstobrogaline (**19**) was evaluated against selected breast cancer cell lines (MDA-MB-231, MDA-MB-468, and MCF7) and a normal breast cell line (MCF10A). Alkaloids **10**, **11**, and **12** were shown to possess no appreciable cytotoxic activity against all the cell lines tested ( $IC_{50} > 40 \mu M$ ). Scholaphylline (**13**) was weakly cytotoxic against MDA-MB-231 ( $IC_{50} = 32.0 \pm 2.2 \mu M$ ) and MDA-MB-468 ( $IC_{50} = 34.1 \pm 3.3 \mu M$ ) cell lines, while alstobrogaline (**19**)<sup>134</sup> were weakly cytotoxic against MDA-MB-231 ( $IC_{50} = 25.3 \pm 0.4 \mu M$ ), MDA-MB-468 ( $IC_{50} = 35.5 \pm 1.1 \mu M$ ), and MCF7 ( $IC_{50} = 24.1 \pm 1.7 \mu M$ ) cell lines (**Table 5.2**).

**Table 5.2:** Antiproliferative activity of scholaphylline (**13**) and alstobrogaline (**19**).

Compound	$IC_{50}^a$ ( $\mu M$ )			
	MDA-MB-231	MDA-MB-468	MCF7	MCF10A
<b>13</b>	$32.0 \pm 2.2$	$34.14 \pm 3.3$	$64.7 \pm 2.8$	$92.6 \pm 9.2$
<b>19</b>	$25.3 \pm 0.4$	$35.5 \pm 1.1$	$24.1 \pm 1.7$	$92.4 \pm 1.8$
Cisplatin (positive control)	$6.2 \pm 0.1$	$7.1 \pm 0.1$	$9.0 \pm 0.4$	$6.3 \pm 0.2$

<sup>a</sup>Results are presented as means  $\pm$  SEM at three independent experiments.

## REFERENCES

1. Geetha, T. S.; Geetha N. *Int. J. PharmTech Res.* **2014**, *6* (2), 521–529.
2. Rahmat, E.; Kang, Y. *J. Plant Biotechnol.* **2019**, *46* (3), 143–157.
3. Dixon, R. A. *Nature* **2001**, *411* (6839), 843–847.
4. Oksman-Caldentey, K. M.; Inzé, D. *Trends Plant Sci.* **2004**, *9* (9), 433–440.
5. Jain, C.; Khatana, S.; Vijayvergia R. *International Journal of Pharmaceutical Sciences and Research.* **2019**, *10* (2), 494–504.
6. Sarker, S. D.; Nahar L. *Chemistry For Pharmacy Students*; John Wiley & Sons Ltd: West Sussex, 2007; pp 283 - 287.
7. Rao, R. S.; Ravishankar, G. A. *Biotechnol. Adv.* **2002**, *20* (2), 101–113.
8. Fernand, S.; Thakur, G. S.; Sharma, R.; Sanodiya, B. S.; Baghel, R.; Thakur, R.; Singh, B. N.; Savita, A.; Dubey, A.; Sikarwar, L.; Jaiswal, P.; Prasad, G. B. K. S.; Bisen, P. S. *African J. Biotechnol.* **2013**, *12* (20), 2900–2907.
9. Verpoorte, R., Alfermann. A. W. *Secondary Metabolism. In Metabolic Engineering of Plant Secondary Metabolism*; Kluwer Academic Publishers: Dordrecht, 2000; pp 1 - 29.
10. Buckingham, J.; Baggaley, K.H.; Roberts, A. D.; Szabó, L. F. *Dictionary of Alkaloids with CD-ROM*; CRC Press Web, 2010; pp 3-17.
11. Verpoorte, R.; Memelink, J. *Curr. Opin. Biotechnol.* **2002**, *13* (2), 181–187.
12. Facchini, P. J.; Bird, D. A.; St-Pierre, B. *Trends Plant Sci.* **2004**, *9* (3), 116–122.
13. Pelletier, S. W. *The Nature and Definition of an Alkaloid. In Alkaloids: Chemical and Biological Perspectives, Volume 1*; Wiley-Interscience: New York, 1983; p 398.
14. Hesse, M. *Alkaloids: Nature's Curse or Blessing?*, 1st ed.; VHCA and WILEY-VCH: Zurich, 2002; 1 – 5.
15. Aniszewski, T. *Alkaloids: Chemistry, Biology, Ecology and Applications*, 2nd ed.; Elsevier: Helsinki, 2015; pp 3 – 17.
16. Bruneton, J. *Pharmacognosy*, 2nd ed.; Lavoisier Publishing Inc.: Paris, 2001; 999-1011.
17. Ku, W. F.; Tan, S. J.; Low, Y. Y.; Komiyama, K.; Kam, T. S. *Phytochemistry* **2011**, *72* (17), 2212–2218.
18. Waller, G. R.; Nowacki, E. K. *Alkaloid Biology and Metabolism in Plants*; Springer

- US: Boston, MA, 1978; pp 17 – 29.
19. Roberts, M. F. *Alkaloids: Biochemistry, Ecology, and Medicinal Applications*, 1st ed.; Plenum Press: New York, 2013; pp 63 – 84.
  20. Koshino, H.; Lee, I.; Kim, J.-P.; Kim, W.; Uzawa, J.; Yoo, I. *Tetrahedron Lett.* **1996**, *37* (26), 4549–4550.
  21. Waring, P.; Beaver, J. *Gen. Pharmacol.* **1996**, *27* (8), 1311–1316.
  22. Aniszewski, T. *Alkaloids - Secrets of Life*; Elsevier Science & Technology: Helsinki, 2007; 45 – 63.
  23. Costa, T. O. G.; Morales, R. A. V.; Brito, J. P.; Gordo, M.; Pinto, A. C.; Bloch, C. *Toxicon* **2005**, *46* (4), 371–375.
  24. Kashman, Y.; Hirsh, S.; McConnell, O. J.; Ohtani, I.; Kusumi, T.; Kakisawa, H. *J. Am. Chem. Soc.* **1989**, *111* (24), 8925–8926.
  25. Ohtani, I.; Kusumi, T.; Kakisawa, H.; Kashman, Y.; Hirsh, S. *J. Am. Chem. Soc.* **1992**, *114* (22), 8479–8483.
  26. Wang, C. M.; Yeh, K. L.; Tsai, S. J.; Jhan, Y. L.; Chou, C. H. *Molecules* **2017**, *22* (12), 1–13.
  27. Amirkia, V.; Heinrich, M. *Phytochem. Lett.* **2014**, *10*, xlviii–53.
  28. Cordell, G. A.; Funayama, S. *Alkaloids*; Elsevier, 2015; pp 1–20.
  29. Cordell, G. A.; Funayama, S. *Alkaloids*; Elsevier, 2015; pp 63–102.
  30. Datwyler, S. L.; Weiblen, G. D. *Am. J. Bot.* **2004**, *91* (5), 767–777.
  31. Harrison, R. D. *Bioscience* **2005**, *55* (12), 1053.
  32. Weiblen, G. D. *Am. J. Bot.* **2000**, *87* (9), 1342–1357.
  33. Chaware, G. K.; Kumar, V.; Kumar, S.; Kumar, P. *Int. J. Fruit Sci.* **2020**, *20* (S2), S969–S986.
  34. Babu, K.; Gokul Shankar, S.; Rai, S. *Turk. J. Botany* **2010**, *34* (3), 215–224.
  35. Oyeleke, S. B.; Dauda, B. E. N.; Boye, O. A. *African J. Biotechnol.* **2008**, *7* (10), 1414–1417.
  36. Ahmad, S.; Rao, H.; Akhtar, M.; Ahmad, I.; Hayat, M. M.; Iqbal, Z.; Nisar-ur-Rahman. *J. Med. Plant Res.* **2011**, *5* (28), 6393–6400.
  37. Kapoor, L. D. *CRC Handbook of Ayurvedic Medicinal Plants*; CRC Press, 2018.

38. Mawa, S.; Husain, K.; Jantan, I. *Evidence-based Complementary and Alternative Medicine*. 2013.
39. Khan, A. S.: *Springer International Publishing*, 2017, 235–253.
40. Singh, D.; Singh, B.; Goel, R. K. *J. Ethnopharmacol.* **2011**, *134* (3), 565–583.
41. Yap, V. A.; Loong, B. J.; Ting, K. N.; Loh, S. H. S.; Yong, K. T.; Low, Y. Y.; Kam, T. S.; Lim, K. H. *Phytochemistry* **2015**, *109*, 96–102.
42. Venkatachalam, S. R.; Mulchandani, N. B. *Naturwissenschaften* **1982**, *69* (6), 287–288.
43. Peraza-Sánchez, S. R.; Chai, H. B.; Young, G. S.; Santisuk, T.; Reutrakul, V.; Farnsworth, N. R.; Cordell, G. A.; Pezzuto, J. M.; Kinghorn, A. D. *Planta Med.* **2002**, *68* (2), 186–188.
44. Shi, Z. F.; Lei, C.; Yu, B. W.; Wang, H. Y.; Hou, A. J. *Chem. Biodivers.* **2016**, *13* (4), 445–450.
45. Subramaniam, G.; Ang, K. K. H.; Ng, S.; Buss, A. D.; Butler, M. S. *Phytochem. Lett.* **2009**, *2* (2), 88–90.
46. Yap, V. A.; Qazzaz, M. E.; Raja, V. J.; Bradshaw, T. D.; Loh, H.-S.; Sim, K.-S.; Yong, K.-T.; Low, Y.-Y.; Lim, K.-H. *Phytochem. Lett.* **2016**, *15*, 136–141.
47. Zhang, H. J.; Tamez, P. A.; Aydogmus, Z.; Tan, G. T.; Saikawa, Y.; Hashimoto, K.; Nakata, M.; Hung, N. Van; Xuan, L. T.; Cuong, N. M.; Soejarto, D. D.; Pezzuto, J. M.; Fong, H. H. S. *Planta Med.* **2002**, *68* (12), 1088–1091.
48. Al-Khdhairawi, A. A. Q.; Krishnan, P.; Mai, C. W.; Chung, F. F. L.; Leong, C. O.; Yong, K. T.; Chong, K. W.; Low, Y. Y.; Kam, T. S.; Lim, K. H. *J. Nat. Prod.* **2017**, *80* (10), 2734–2740.
49. Kubo, M.; Yatsuzuka, W.; Matsushima, S.; Harada, K.; Inoue, Y.; Miyamoto, H.; Matsumoto, M.; Fukuyama, Y. *Chem. Pharm. Bull. (Tokyo)*. **2016**, *64* (7), 957–960.
50. Wu, P.-L.; Rao, K. V.; Su, C.-H.; Kuoh, C.-S.; Wu, T.-S. *Heterocycles* **2002**, *57* (12), 2401–2408.
51. Damu, A. G.; Kuo, P. C.; Shi, L. S.; Li, C. Y.; Kuoh, C. S.; Wu, P. L.; Wu, T. S. *J. Nat. Prod.* **2005**, *68* (7), 1071–1075.
52. Damu, A. G.; Kuo, P. C.; Shi, L. S.; Li, C. Y.; Su, C. R.; Wu, T. S. *Planta Med.* **2009**, *75* (10), 1152–1156.
53. Ueda, J. Y.; Takagi, M.; Shin-ya, K. *J. Nat. Prod.* **2009**, *72* (12), 2181–2183.

54. Latayada, F. S.; Uy, M. M.; Akihara, Y.; Ohta, E.; Nehira, T.; Ômura, H.; Ohta, S. *Phytochemistry* **2017**, *141*, 98–104.
55. Wan, C.; Chen, C.; Li, M.; Yang, Y.; Chen, M.; Chen, J. *Plants* **2017**, *6* (4), 44.
56. Khan, I.; Rali, T.; Sticher, O. *Planta Med.* **1993**, *59* (3), 286.
57. Johns, S. R.; Russel, J. H.; Heffernan, M. L. *Tetrahedron Lett.* **1965**, *6* (24), 1987–1991.
58. Chemler, S. R. *Curr. Bioact. Compd.* **2009**, *5* (1), 2–19.
59. Mandhare, A. A.; Dhulap, S. A.; Dhulap, A. S.; Biradar, S. C. *Chem. informatics* **2015**, *1* (1:5), 1–15.
60. Cordell, G. A.; Quinn-Beattie, M. Lou; Farnsworth, N. R. *Phyther. Res.* **2001**, *15* (3), 183–205.
61. Shi, Z. F.; Lei, C.; Yu, B. W.; Wang, H. Y.; Hou, A.-J. *Chem. Biodivers.* **2016**, *13* (4), 445–450.
62. Ueda, J.; Takagi, M.; Shin-ya, K. *J. Nat. Prod.* **2009**, *72* (12), 2181–2183.
63. Damu, A. G.; Kuo, P. C.; Shi, L. S.; Li, C. Y.; Kuoh, C. S.; Wu, P. L.; Wu, T. S. *J. Nat. Prod.* **2005**, *68* (7), 1071–1075.
64. Badron, U. H.; Talip, N.; Mohamad, A. L.; Affenddi, A. E. A.; Juhari, A. A. A. *Trop. life Sci. Res.* **2014**, *25* (2), 111–125.
65. Berg, C. C.; Corner, E. J. H. *Flora Malesiana Series I - Seed Plants.* **2005**, *17* (2), 1–730.
66. Berg, C. C.; Culmsee, H. *Blumea J. Plant Taxon. Plant Geogr.* **2011**, *56* (3), 265–269.
67. Abubakar, I. B.; Lim, K. H.; Loh, H. S. *Nat. Prod. Res.* **2015**, *29* (22), 2137–2140.
68. Kiew, R.; Chung, R. C.; Saw, L. .; Soepadmo, E.; Boyce, P; *Flora of Peninsular Malaysia Series II- Seed Plants.* 2011; 25–26.
69. Gasson, P.; Sidiyasa, K. *Kew Bull.* **2000**, *55* (2), 507.
70. Khyade, M. S.; Kasote, D. M.; Vaikos, N. P. *J. Ethnopharmacol.* **2014**, *153* (1), 1–18.
71. Olajide, O. A.; Awe, S. O.; Makinde, J. M.; Ekhelar, A. I.; Olusola, A.; Morebise, O.; Okpako, D. T. *J. Ethnopharmacol.* **2000**, *71* (1–2), 179–186.
72. Ernesto, F., Orazio, T.-S. *Modern Alkaloids. Structure, Isolation, Synthesis and Biology*; Wiley-VCH, 2007; pp 111 - 138.

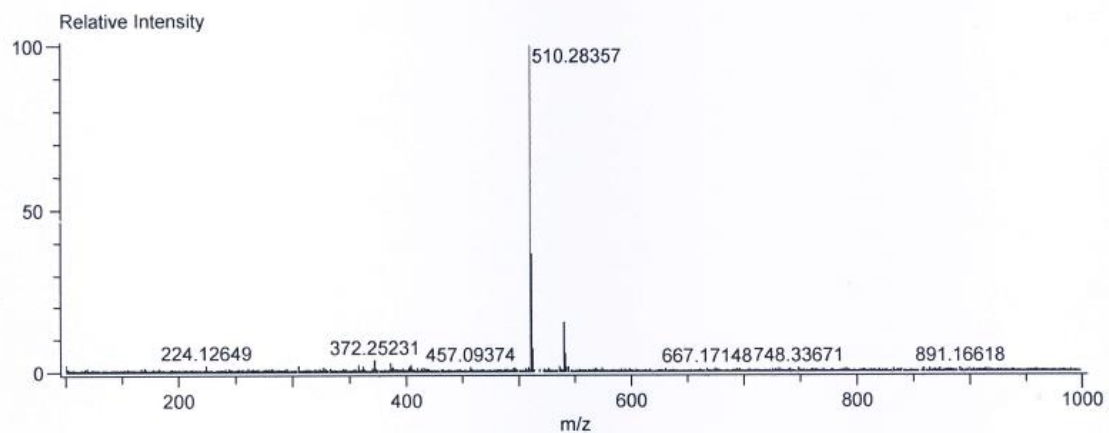
73. Seigler, D. S. *Indole Alkaloids: Plant Secondary Metabolism*; Springer US: Boston, 1998; pp 628–654.
74. Lim, K. H. *Biologically Active Indole and Bisindole Alkaloids from Kopsia and Tabernaemontana*, University of Malaya, 2008.
75. Pratyush, K.; Misra, C. S.; James, J.; Lipin Dev, M. S.; Veettil, A. K. T.; Thankamani, V. *J. Pharm. Sci. Res.* **2011**, *3* (8), 1394–1403.
76. Kalaria, P.; Gheewala, P.; Chakraborty, M.; Kamath, J. *Int. J. Res. Ayurveda Pharm.* **2012**, *3* (3), 367–371.
77. Oktavia, R.; Misfadhila, S.; Rivai, H. *World Journal Of Pharmacy And Pharmaceutical Sciences.* **2020**, *9* (8), 334–354.
78. Cai, X. H.; Tan, Q. G.; Liu, Y. P.; Feng, T.; Du, Z. Z.; Li, W. Q.; Luo, X. D. *Org. Lett.* **2008**, *10* (4), 577–580.
79. Dutta, S.; Bhattacharya, S.; Ray, A. *Planta Med.* **1976**, *30* (05), 86–89.
80. Hirasawa, Y.; Miyama, S.; Kawahara, N.; Goda, Y.; Rahman, A.; Ekasari, W.; Widyawaruyanti, A.; Indrayanto, G.; Zaini, N. C.; Morita, H. *Heterocycles* **2009**, *79* (C), 1107–1112.
81. Salim, A. A.; Garson, M. J.; Craik, D. J. *J. Nat. Prod.* **2004**, *67* (9), 1591–1594.
82. Kuok, C. F.; Zhang, J.; Kuok, C. F.; Zhang, Q. W.; Fan, C. L.; Fan, R. Z.; Zhang, D. M.; Zhang, X. Q.; Ye, W. C. *Tetrahedron Lett.* **2017**, *58* (28), 2740–2742.
83. Qin, X. J.; Zhao, Y. L.; Lunga, P. K.; Yang, X. W.; Song, C. W.; Cheng, G. G.; Liu, L.; Chen, Y. Y.; Liu, Y. P.; Luo, X. D. *Tetrahedron* **2015**, *71* (25), 4372–4378.
84. Liu, L.; Chen, Y. Y.; Qin, X. J.; Wang, B.; Jin, Q.; Liu, Y. P.; Luo, X. D. *Fitoterapia* **2015**, *105*, 160–164.
85. Zhu, X. X.; Fan, Y. Y.; Xu, L.; Liu, Q. F.; Wu, J. P.; Li, J. Y.; Li, J.; Gao, K.; Yue, J. M. *Org. Lett.* **2019**, *21* (5), 1471–1474.
86. Yamauchi, T.; Abe, F.; Padolina, W. G.; Dayrit, F. M. A. *Phytochemistry* **1990**, *29* (10), 3321–3325.
87. Liu, Y. P.; Lai, R.; Yao, Y. G.; Zhang, Z. K.; Pu, E. T.; Cai, X. H.; Luo, X. D. *Org. Lett.* **2013**, *15* (19), 4940–4943.
88. Yamauchi, T.; Abe, F.; Chen, R. fu; Nonaka, G. I.; Santisuk, T.; Padolina, W. G. *Phytochemistry* **1990**, *29* (11), 3547–3552.
89. Boonchuay, W.; Court, W. E. *Planta Med.* **1976**, *29* (04), 380–390.

90. Warank, F.; Court, W. E.; *Phytochemistry*. **1976**, *15*, 821.
91. Kam, T. S.; Nyeoh, K. T.; Sim, K. M.; Yoganathan, K. *Phytochemistry*. **1997**, *45* (6), 1303–1305.
92. Morita, Y.; Hesse, M.; Schmid, H.; Banerji, A.; Banerji, J.; Chatterjee, A.; Oberhänsli, W. E. *Helv. Chim. Acta* **1977**, *60* (4), 1419–1434.
93. Chatterjee, A.; Mukherjee, B.; Ray, A. B.; Das, B. *Tetrahedron Lett.* **1965**, *41*, 3633–3637.
94. Banerji, A.; Siddhanta, A. K. *Phytochemistry* **1981**, *20* (3), 540–542.
95. Jain, L.; Pandey, M. B.; Singh, S.; Singh, A. K.; Pandey, V. B. *Nat. Prod. Res.* **2009**, *23* (17), 1599–1602.
96. Macabeo, A. P. G.; Krohn, K.; Gehle, D.; Read, R. W.; Brophy, J. J.; Cordell, G. A.; Franzblau, S. G.; Aguinaldo, A. M. *Phytochemistry* **2005**, *66* (10), 1158–1162.
97. Abe, F.; Chen, R. fu; Yamauchi, T.; Nobuhiro, M.; Ueda, I. *Chem. Pharm. Bull.* **1989**, *37*, 887–890.
98. Hamdiani, S.; Al-As'Ari, M.; Satriani, A. R.; Hadi, S. *AIP Conf. Proc.* **2018**, 2023.
99. Salim, A. A.; Garson, M. J.; Craik, D. J. *J. Nat. Prod.* **2004**, *67* (9), 1591–1594.
100. Atta-Ur-Rahman, A.; Alvi, K. A.; Abbas, S. A.; Voelter, W. *Heterocycles* **1987**, *26* (2), 413–419.
101. Atta-Ur-Rahman, A.; Alvi, K. A. *Phytochemistry* **1987**, *26* (7), 2139–2142.
102. Cai, X. H.; Du, Z. Z.; Luo, X. D. *Org. Lett.* **2007**, *9* (9), 1817–1820.
103. Wang, F.; Ren, F. C.; Liu, J. K. *Phytochemistry* **2009**, *70* (5), 650–654.
104. Zhou, H.; He, H. P.; Kong, N. C.; Wang, Y. H.; Liu, X. D.; Hao, X. J. *Helv. Chim. Acta* **2006**, *89* (3), 515–519.
105. Hu, J.; Mao, X.; Shi, X.; Jin, N.; Shi, J. *Chem. Nat. Compd.* **2018**, *54* (5), 934–937.
106. Chen, Y. Y.; Yang, J.; Yang, X. W.; Khan, A.; Liu, L.; Wang, B.; Zhao, Y. L.; Liu, Y. P.; Ding, Z. T.; Luo, X. D. *Tetrahedron Lett.* **2016**, *57* (16), 1754–1757.
107. Yang, X. W.; Luo, X. D.; Lunga, P. K.; Zhao, Y. L.; Qin, X. J.; Chen, Y. Y.; Liu, L.; Li, X. N.; Liu, Y. P. *Tetrahedron* **2015**, *71* (22), 3694–3698.
108. Yu, H. F.; Huang, W. Y.; Ding, C. F.; Wei, X.; Zhang, L. C.; Qin, X. J.; Ma, H. X.; Yang, Z. F.; Liu, Y. P.; Zhang, R. P.; Wang, X. H.; Luo, X. D. *Tetrahedron Lett.* **2018**,

- 59 (31), 2975–2978.
109. Pan, Z.; Qin, X. J.; Liu, Y. P.; Wu, T.; Luo, X. D.; Xia, C. *Org. Lett.* **2016**, *18* (4), 654–657.
  110. Qin, X. J.; Zhao, Y. L.; Song, C. W.; Wang, B.; Chen, Y. Y.; Liu, L.; Li, Q.; Li, D.; Liu, Y. P.; Luo, X. D. *Nat. Products Bioprospect.* **2015**, *5* (4), 185–193.
  111. Wei, X.; Qin, X. J.; Jin, Q.; Yu, H. F.; Ding, C. F.; Khan, A.; Liu, Y. P.; Xia, C.; Luo, X. D. *Tetrahedron Lett.* **2020**, *61* (21), 151894.
  112. Yang, X. W.; Qin, X. J.; Zhao, Y. L.; Lunga, P. K.; Li, X. N.; Jiang, S. Z.; Cheng, G. G.; Liu, Y. P.; Luo, X. D. *Tetrahedron Lett.* **2014**, *55* (33), 4593–4596.
  113. Zhu, G. Y.; Yao, X. J.; Liu, L.; Bai, L. P.; Jiang, Z. H. *Org. Lett.* **2014**, *16* (4), 1080–1083.
  114. Feng, T.; Cai, X. H.; Zhao, P. J.; Du, Z. Z.; Li, W. Q.; Luo, X. D. *Planta Med.* **2009**, *75* (14), 1537–1541.
  115. Wang, B.; Dai, Z.; Yang, X. W.; Liu, Y. P.; Khan, A.; Yang, Z. F.; Huang, W. Y.; Wang, X. H.; Zhao, X. D.; Luo, X. D. *Phytomedicine* **2018**, *48*, 170–178.
  116. Martinez, J. C. V.; Cuca, L. E. S.; Santana, A. J. M.; Pombo-Villar, E.; Golding, B. T. *Phytochemistry* **1985**, *24* (7), 1612–1614.
  117. Zacchino, S. A.; Badano, H. J. *Nat. Prod.* **1985**, *48* (5), 830–832.
  118. Yan, Y.; Ai, J.; Shi, Y.; Zuo, Z.; Hou, B.; Luo, J.; Cheng, Y. **2014**, 1–4.
  119. Dugave, C.; Demange, L. *Chem. Rev.* **2003**, *103* (7), 2475–2532.
  120. Zeches, M.; Ravao, T.; Richard, B.; Massiot, G.; Men-olivier, L. Le; Verpoorte, R. J. *Nat. Prod.* **1987**, *50* (4), 714–720.
  121. Akhmedov, N. G.; Myshakin, E. M.; Hall, C. D. *Magn. Reson. Chem.* **2004**, *42* (1), 39–48.
  122. Lim, J. L.; Sim, K. S.; Yong, K. T.; Loong, B. J.; Ting, K. N.; Lim, S. H.; Low, Y. Y.; Kam, T. S. *Phytochemistry* **2015**, *117*, 317–324.
  123. Luo, X. G.; Chen, H. S.; Liang, S.; Huang, M.; Xuan, W. D.; Jin, L. *Chinese Chem. Lett.* **2007**, *18* (6), 697–699.
  124. Kam, T. S.; Choo, Y. M. *The Alkaloids: Chemistry and Biology*; Elsevier 2006; pp 181–337.

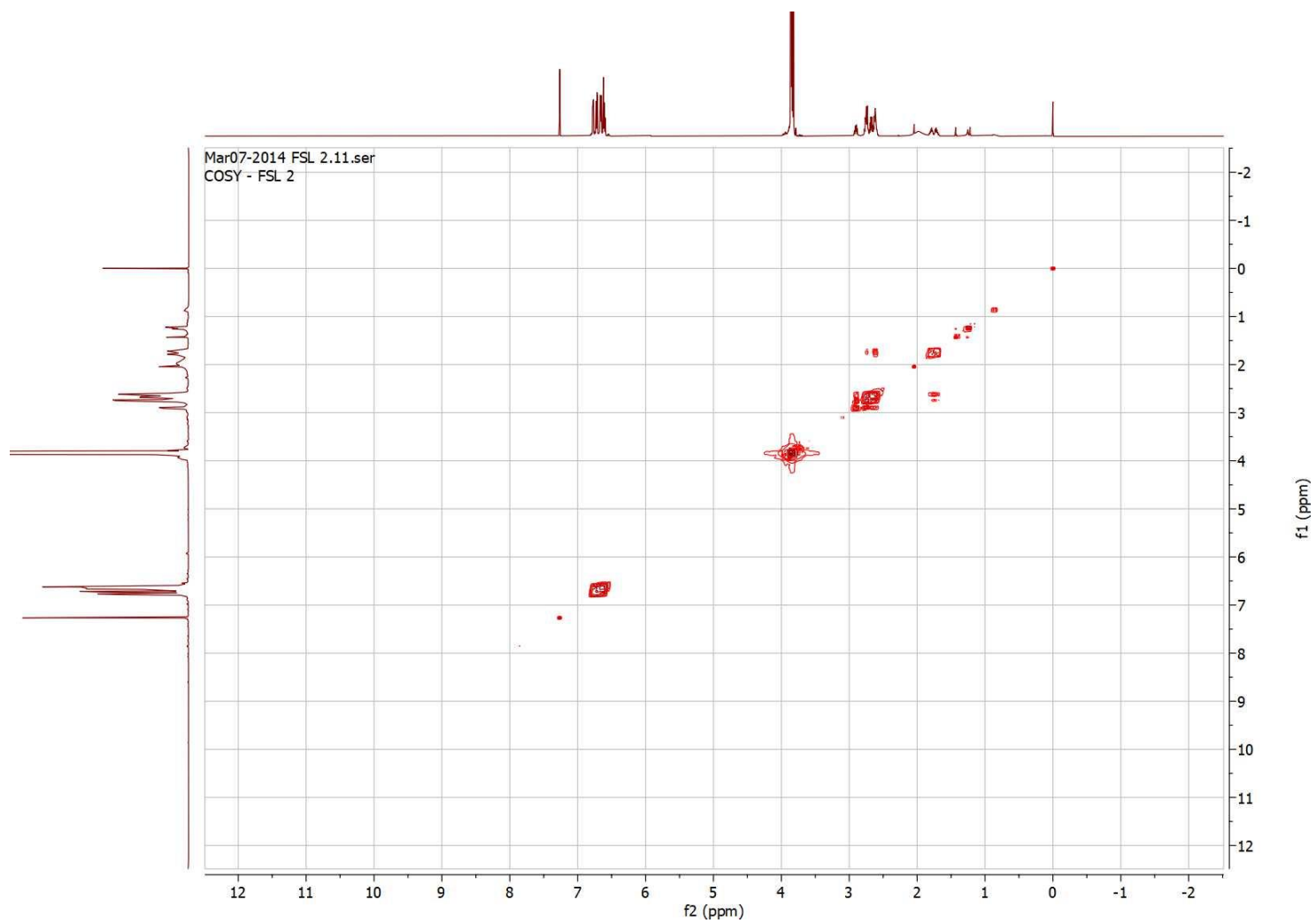
125. Kitajima, M.; Takayama, H. *The Alkaloids: Chemistry and Biology*; Academic Press: San Diego, 2016; pp 232 - 311.
126. Kohl, W.; Witte, B.; Sheldrick, W.; Höfle, G. *Planta Med.* **1984**, *50* (03), 242–244.
127. Spitzner, D.; Zaubitzer, T.; Shi, Y. J.; Wenkert, E. *J. Org. Chem.* **1988**, *53* (10), 2274–2278.
128. Paul, J. H. A.; Maxwell, A. R.; Reynolds, W. F. *J. Nat. Prod.* **2003**, *66* (6), 752–754.
129. Szabó, L. F. *Arkivoc* **2008**, *2008* (3), 167–181.
130. Lim, K. H.; Low, Y. Y.; Kam, T. S. *Tetrahedron Lett.* **2006**, *47* (29), 5037–5039.
131. Koyama, K.; Hirasawa, Y.; Zaima, K.; Hoe, T. C.; Chan, K. L.; Morita, H. *Bioorganic Med. Chem.* **2008**, *16* (13), 6483–6488.
132. Krishnan, P.; Lee, F.; Yap, V. A.; Low, Y.; Kam, T.; Yong, K. T.; Ting, K. N.; Lim, K. H. *J. Nat. Prod.* **2019**, *83*(1), 152 - 158.
133. Krishnan, P.; Lee, F. K.; Chong, K. W.; Mai, C. W.; Muhamad, A.; Lim, S. H.; Low, Y. Y.; Ting, K. N.; Lim, K. H. *Org. Lett.* **2018**, *20* (24), 8014–8018.
134. Krishnan, P.; Mai, C. W.; Yong, K. T.; Low, Y. Y.; Lim, K. H. *Tetrahedron Lett.* **2019**, *60* (11), 789–791.

## APPENDICES

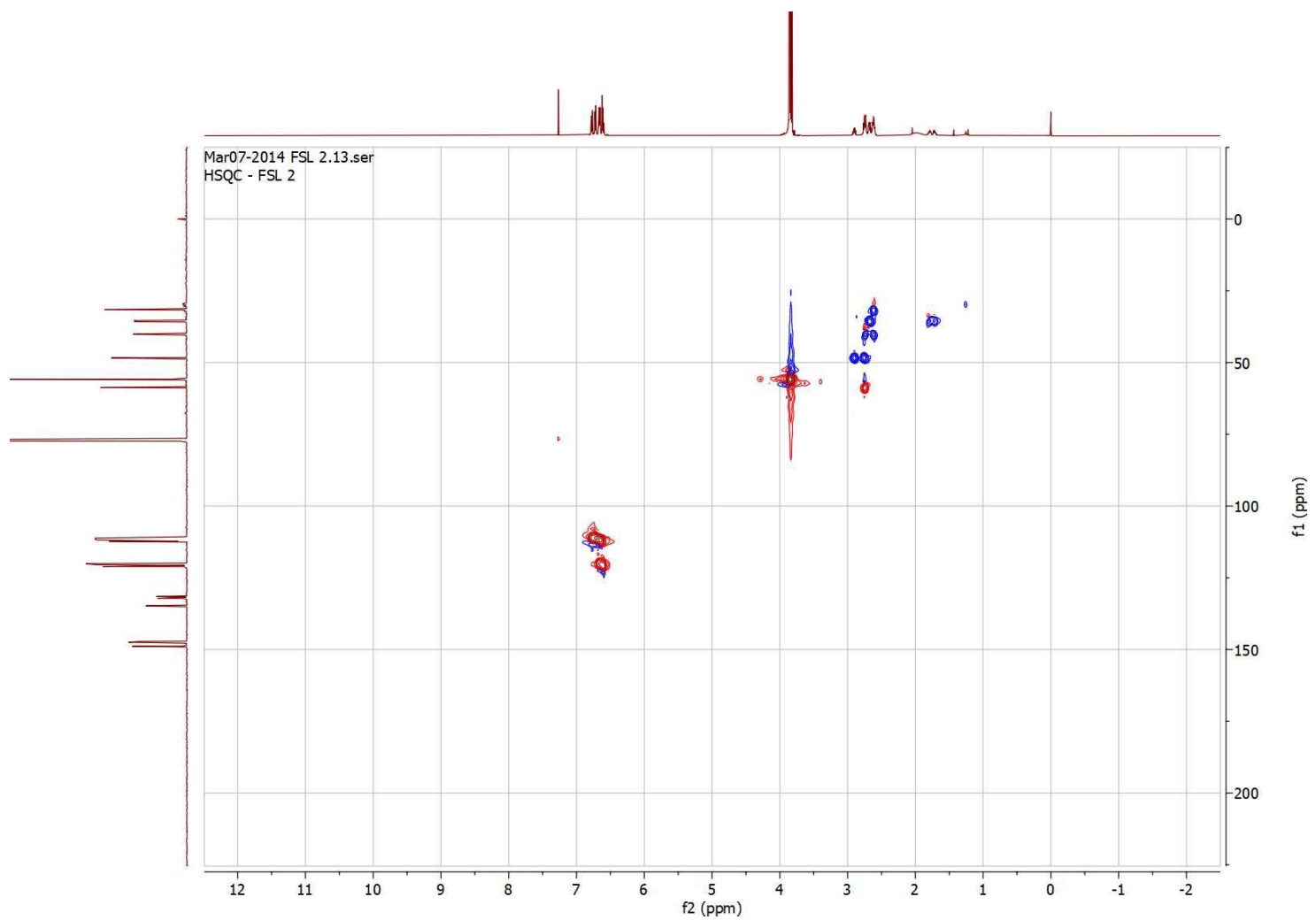


Mass	Intensity	Calc. Mass	Mass Difference (mmu)	Mass Difference (ppm)	Possible Formula	Unsaturation Number
510.28357	63543.72	510.28288	0.68	1.34	$^{12}\text{C}_{27}\text{H}_{42}\text{O}_9$	7.0
		510.28556	-2.00	-3.91	$^{12}\text{C}_{30}\text{H}_{40}\text{N}_1\text{O}_6$	11.5
		510.27969	3.88	7.60	$^{12}\text{C}_{37}\text{H}_{36}\text{N}_1\text{O}_1$	20.5
		510.28824	-4.68	-9.16	$^{12}\text{C}_{33}\text{H}_{38}\text{N}_2\text{O}_3$	16.0
		510.27701	6.56	12.85	$^{12}\text{C}_{34}\text{H}_{38}\text{O}_4$	16.0

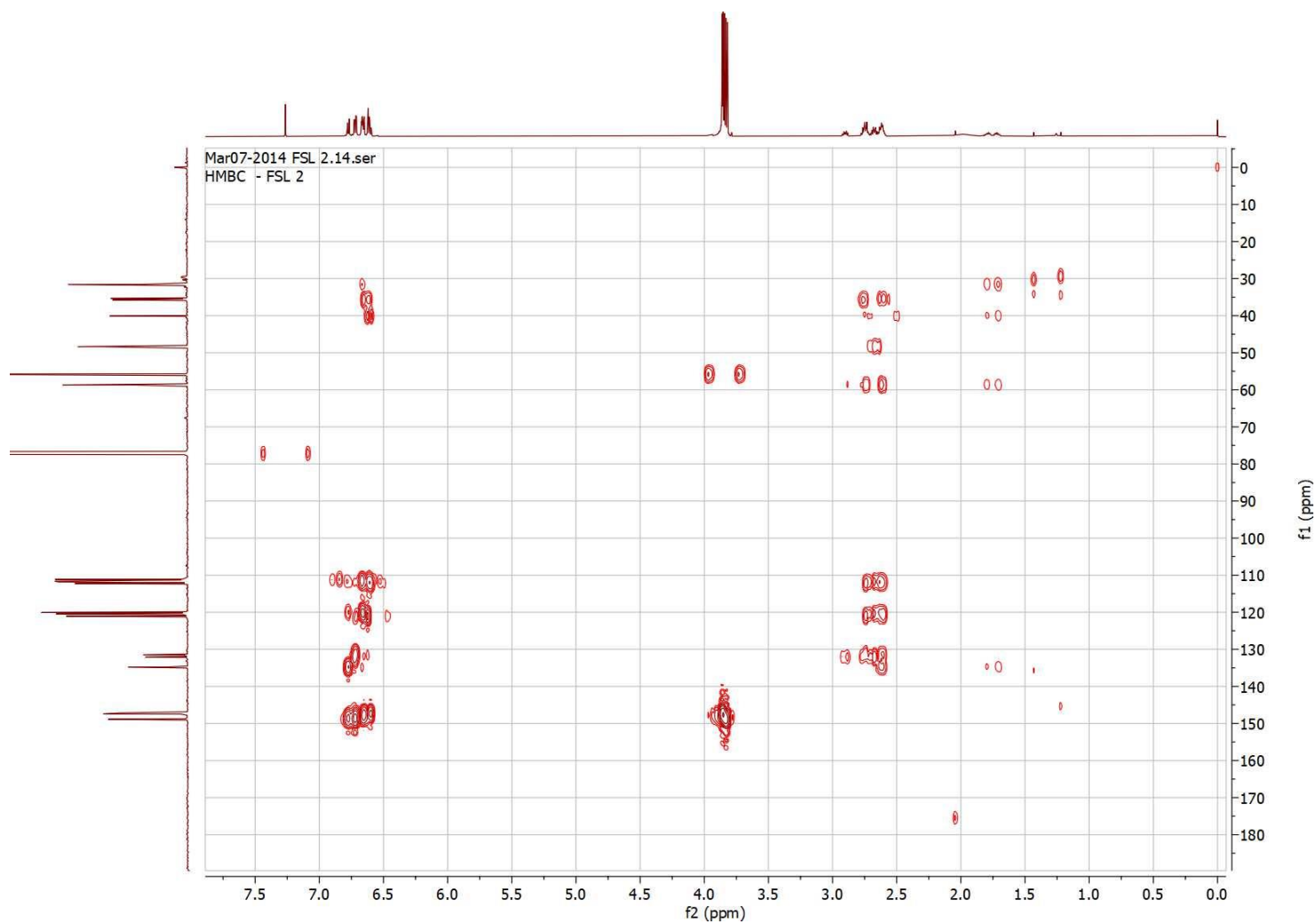
**Appendix 1: HR-DART-MS of schwarzinicine A (1)**



**Appendix 2:** COSY Spectrum of schwarzinicine A (1)



**Appendix 3: HSQC Spectrum of schwarzinicine A (1)**

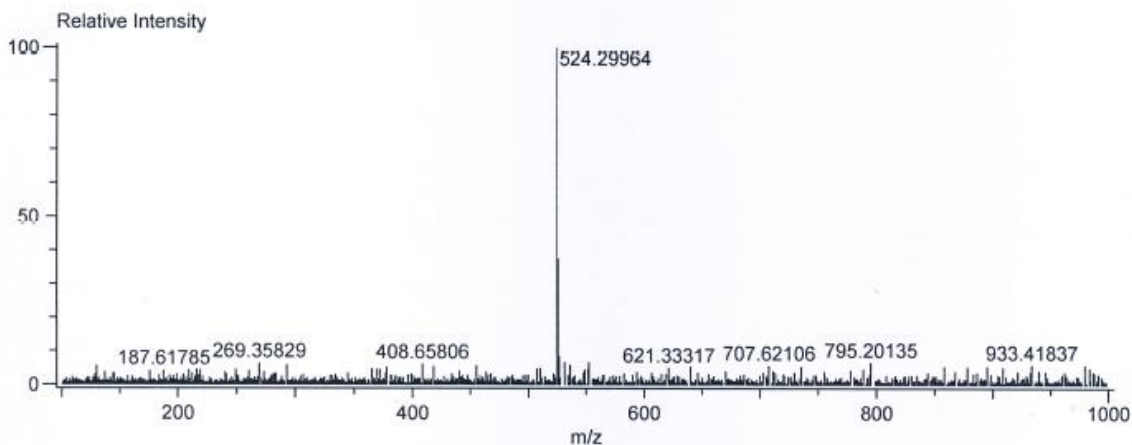


Appendix 4: HMBC Spectrum of schwarzinicine A (1)

Data:FSL3  
 Sample Name:  
 Description:  
 Ionization Mode:ESI+  
 History:Determine m/z[Peak Detect[Centroid,30,Area];Correct Base[0.5%]];Correct Ba...

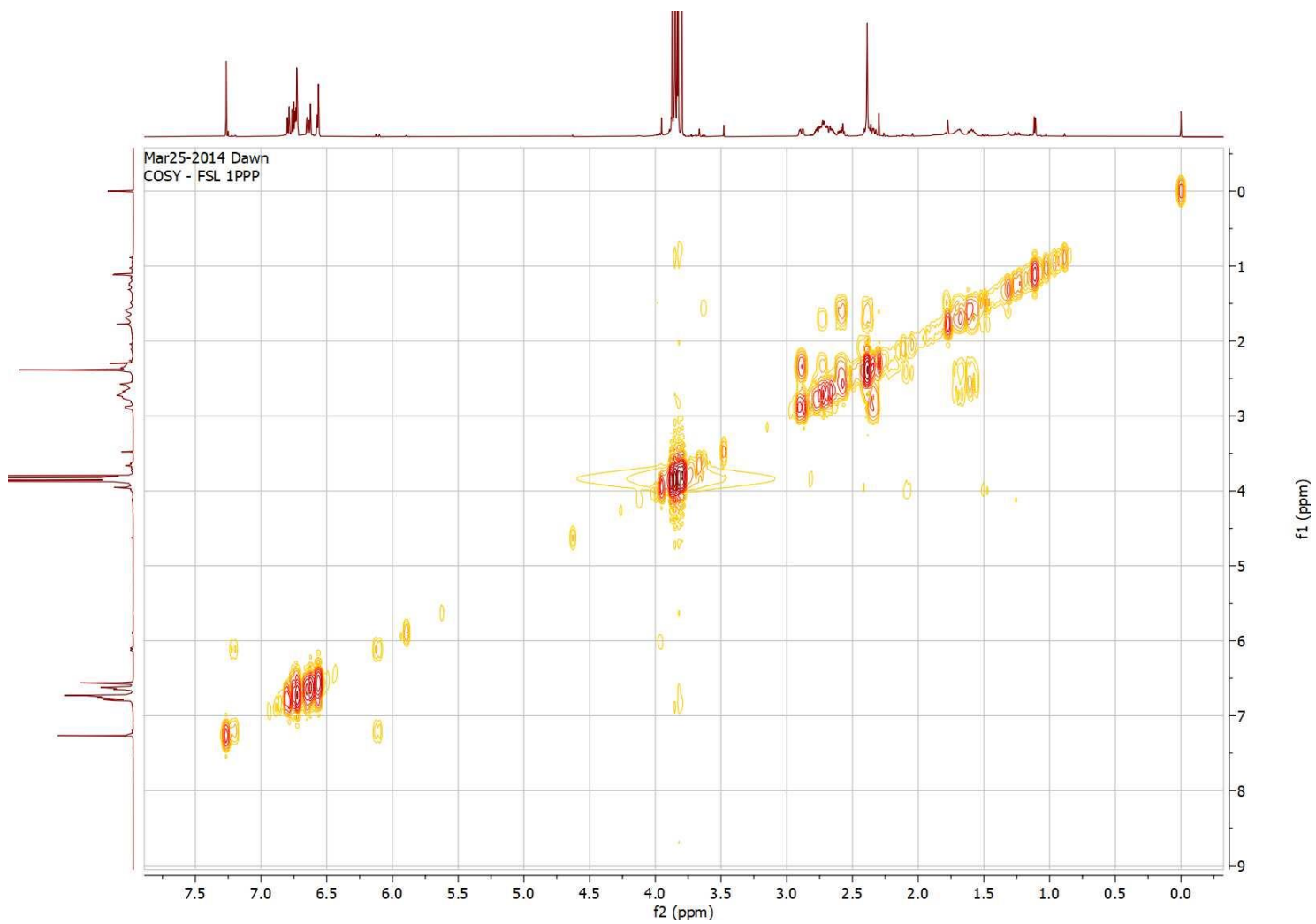
Acquired:3/19/2014 4:16:45 PM  
 Operator:AccuTOF  
 Mass Calibration data:Calibration  
 Created:3/19/2014 4:21:15 PM  
 Created by:AccuTOF

Charge number:1 Tolerance:15.00(ppm), 5.00 .. 15.00(mmu) Unsaturation Number:0.0 .. 25.0 (Fracio...  
 Element:<sup>12</sup>C:0 .. 60, <sup>1</sup>H:10 .. 60, <sup>14</sup>N:0 .. 5, <sup>23</sup>Na:0 .. 0, <sup>16</sup>O:0 .. 15

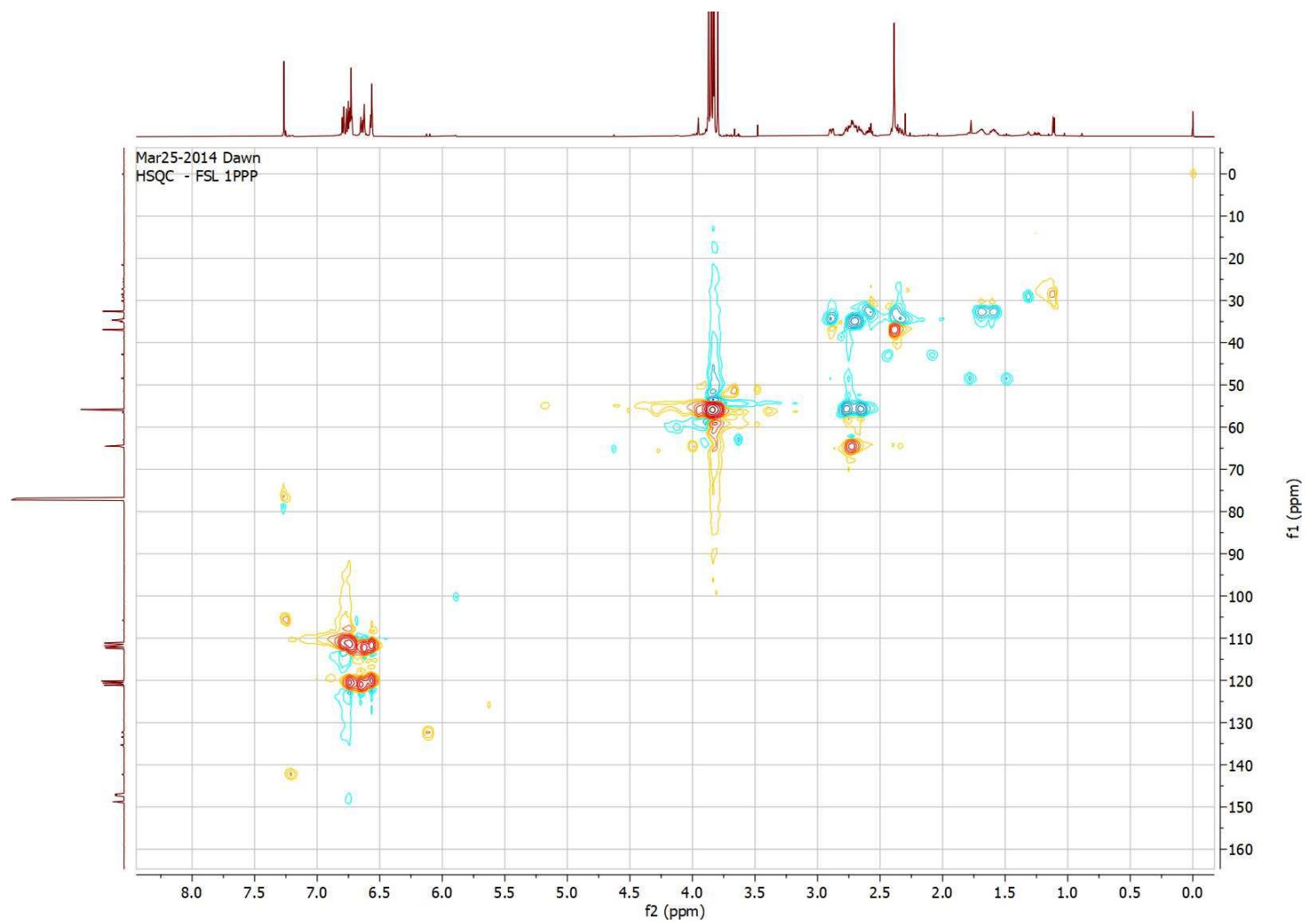


Mass	Intensity	Calc. Mass	Mass Difference (mmu)	Mass Difference (ppm)	Possible Formula	Unsaturation Number
524.29964	16388.18	524.29987	-0.23	-0.43	<sup>12</sup> C <sub>29</sub> <sup>1</sup> H <sub>40</sub> <sup>14</sup> N <sub>4</sub> <sup>16</sup> O <sub>5</sub>	12.0
		524.29853	1.11	2.12	<sup>12</sup> C <sub>28</sub> <sup>1</sup> H <sub>44</sub> <sup>16</sup> O <sub>9</sub>	7.0
		524.30121	-1.57	-2.99	<sup>12</sup> C <sub>31</sub> <sup>1</sup> H <sub>42</sub> <sup>14</sup> N <sub>1</sub> <sup>16</sup> O <sub>6</sub>	11.5
		524.29719	2.45	4.68	<sup>12</sup> C <sub>26</sub> <sup>1</sup> H <sub>42</sub> <sup>14</sup> N <sub>3</sub> <sup>16</sup> O <sub>8</sub>	7.5
		524.30255	-2.91	-5.54	<sup>12</sup> C <sub>32</sub> <sup>1</sup> H <sub>38</sub> <sup>14</sup> N <sub>5</sub> <sup>16</sup> O <sub>2</sub>	16.5
		524.30389	-4.25	-8.10	<sup>12</sup> C <sub>34</sub> <sup>1</sup> H <sub>40</sub> <sup>14</sup> N <sub>2</sub> <sup>16</sup> O <sub>3</sub>	16.0
		524.29534	4.30	8.21	<sup>12</sup> C <sub>38</sub> <sup>1</sup> H <sub>38</sub> <sup>14</sup> N <sub>1</sub> <sup>16</sup> O <sub>1</sub>	20.5
		524.29451	5.13	9.79	<sup>12</sup> C <sub>23</sub> <sup>1</sup> H <sub>44</sub> <sup>14</sup> N <sub>2</sub> <sup>16</sup> O <sub>11</sub>	3.0
		524.29400	5.65	10.77	<sup>12</sup> C <sub>36</sub> <sup>1</sup> H <sub>38</sub> <sup>14</sup> N <sub>4</sub>	21.0
		524.30574	-6.10	-11.63	<sup>12</sup> C <sub>22</sub> <sup>1</sup> H <sub>44</sub> <sup>14</sup> N <sub>4</sub> <sup>16</sup> O <sub>10</sub>	3.0
		524.29317	6.48	12.35	<sup>12</sup> C <sub>21</sub> <sup>1</sup> H <sub>42</sub> <sup>14</sup> N <sub>5</sub> <sup>16</sup> O <sub>10</sub>	3.5
		524.30657	-6.93	-13.21	<sup>12</sup> C <sub>37</sub> <sup>1</sup> H <sub>38</sub> <sup>14</sup> N <sub>3</sub>	20.5
		524.29266	6.99	13.32	<sup>12</sup> C <sub>35</sub> <sup>1</sup> H <sub>40</sub> <sup>16</sup> O <sub>4</sub>	16.0
524.30708	-7.44	-14.19	<sup>12</sup> C <sub>24</sub> <sup>1</sup> H <sub>46</sub> <sup>14</sup> N <sub>1</sub> <sup>16</sup> O <sub>11</sub>	2.5		

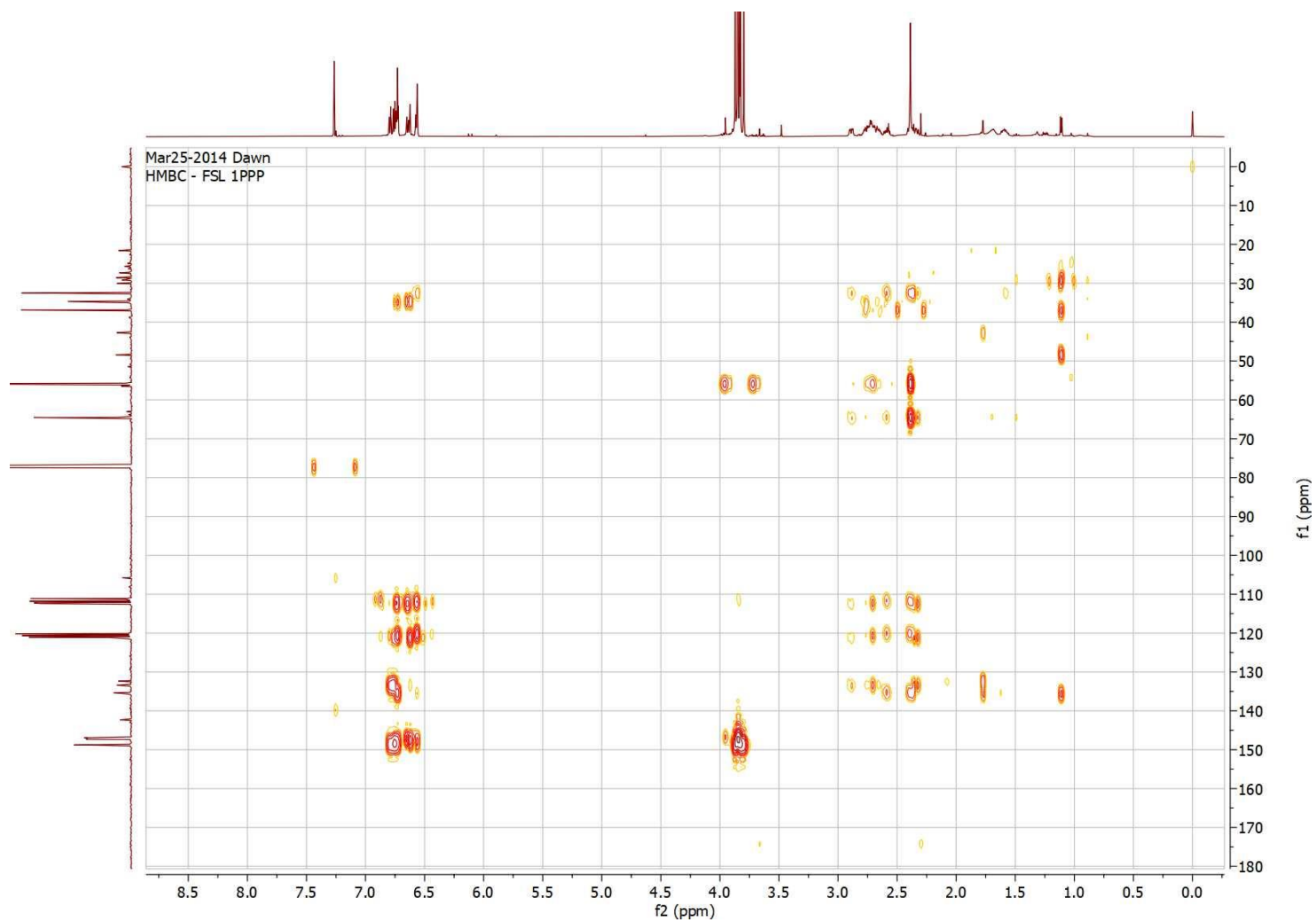
## Appendix 5: HR-DART-MS of schwarzinicine B (2)



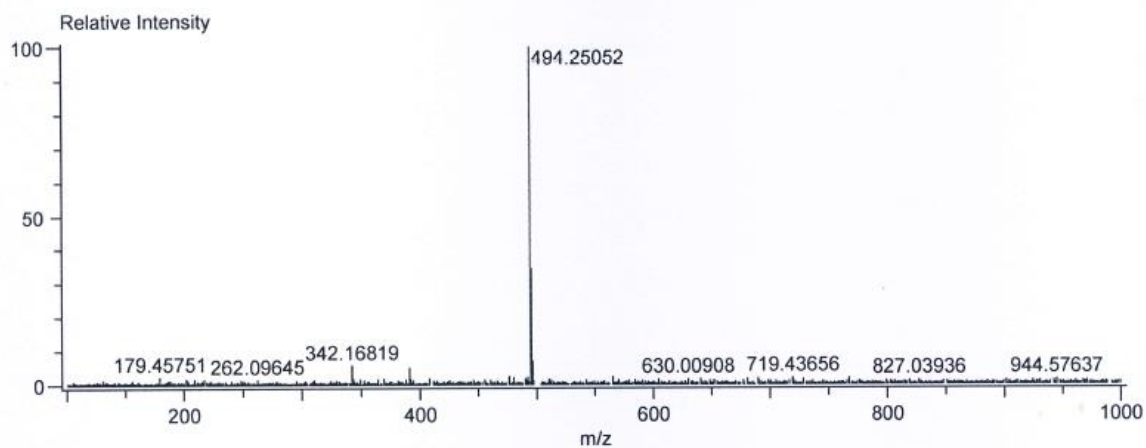
**Appendix 6: COSY Spectrum of schwarzinicine B (2)**



**Appendix 7: HSQC Spectrum of schwarzinicine B (2)**

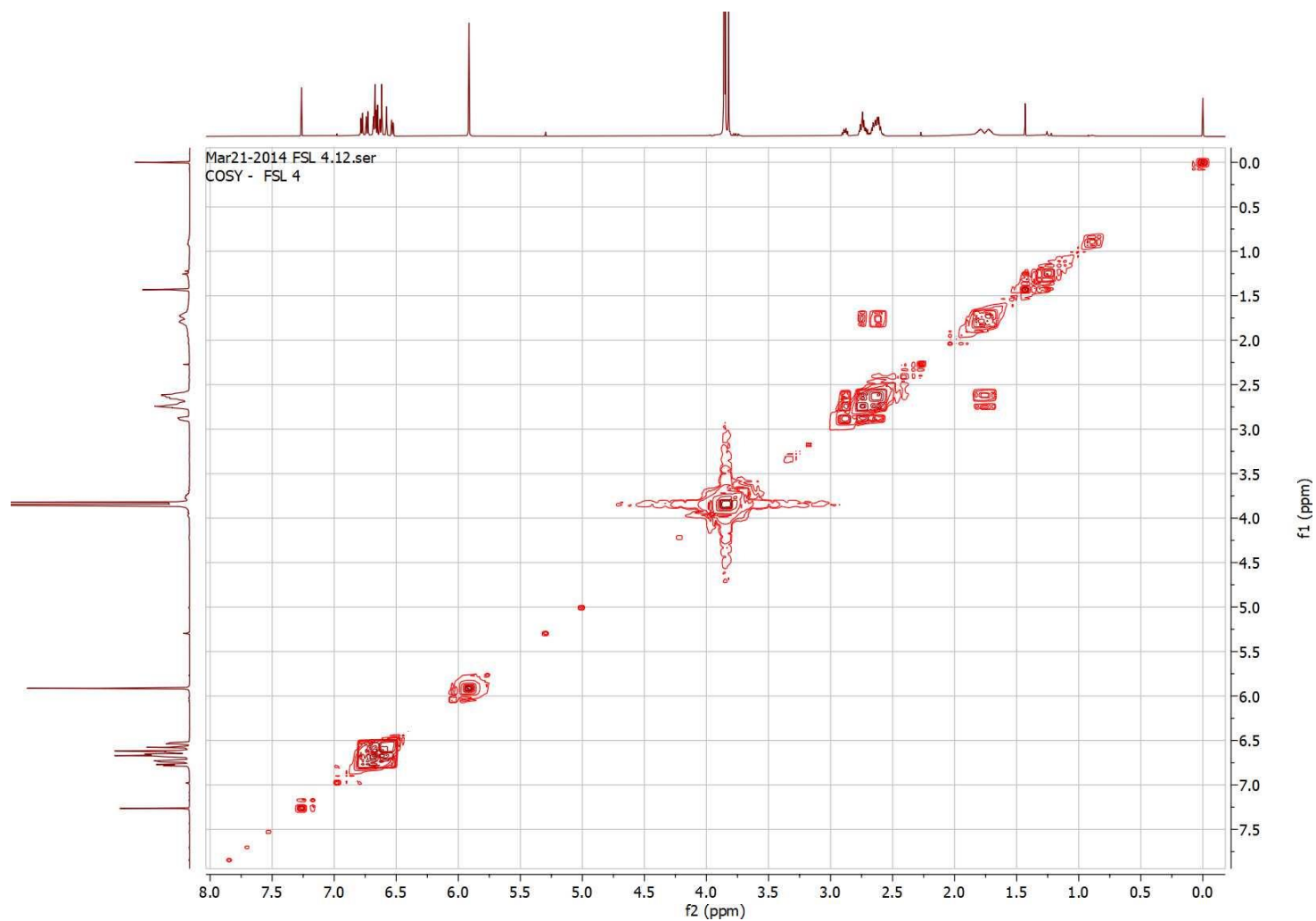


**Appendix 8: HMBC Spectrum of schwarzinicine B (2)**



Mass	Intensity	Calc. Mass	Mass Difference (mmu)	Mass Difference (ppm)	Possible Formula	Unsaturation Number
494.25052	59451.88	494.25024	0.29	0.58	<sup>12</sup> C <sub>24</sub> <sup>1</sup> H <sub>36</sub> <sup>14</sup> N <sub>3</sub> <sup>16</sup> O <sub>8</sub>	8.5
		494.25158	-1.06	-2.14	<sup>12</sup> C <sub>26</sub> <sup>1</sup> H <sub>38</sub> <sup>16</sup> O <sub>9</sub>	8.0
		494.24839	2.14	4.32	<sup>12</sup> C <sub>36</sub> <sup>1</sup> H <sub>32</sub> <sup>14</sup> N <sub>1</sub> <sup>16</sup> O <sub>1</sub>	21.5
		494.25292	-2.39	-4.85	<sup>12</sup> C <sub>27</sub> <sup>1</sup> H <sub>34</sub> <sup>14</sup> N <sub>4</sub> <sup>16</sup> O <sub>5</sub>	13.0
		494.24756	2.97	6.00	<sup>12</sup> C <sub>21</sub> <sup>1</sup> H <sub>38</sub> <sup>14</sup> N <sub>2</sub> <sup>16</sup> O <sub>11</sub>	4.0
		494.24705	3.48	7.04	<sup>12</sup> C <sub>34</sub> <sup>1</sup> H <sub>30</sub> <sup>14</sup> N <sub>4</sub>	22.0
		494.25426	-3.74	-7.56	<sup>12</sup> C <sub>29</sub> <sup>1</sup> H <sub>36</sub> <sup>14</sup> N <sub>1</sub> <sup>16</sup> O <sub>6</sub>	12.5
		494.24622	4.31	8.72	<sup>12</sup> C <sub>19</sub> <sup>1</sup> H <sub>36</sub> <sup>14</sup> N <sub>5</sub> <sup>16</sup> O <sub>10</sub>	4.5
		494.24571	4.82	9.74	<sup>12</sup> C <sub>33</sub> <sup>1</sup> H <sub>34</sub> <sup>16</sup> O <sub>4</sub>	17.0
		494.25560	-5.08	-10.27	<sup>12</sup> C <sub>30</sub> <sup>1</sup> H <sub>32</sub> <sup>14</sup> N <sub>5</sub> <sup>16</sup> O <sub>2</sub>	17.5
		494.24437	6.16	12.46	<sup>12</sup> C <sub>31</sub> <sup>1</sup> H <sub>32</sub> <sup>14</sup> N <sub>3</sub> <sup>16</sup> O <sub>3</sub>	17.5
		494.25694	-6.42	-12.98	<sup>12</sup> C <sub>32</sub> <sup>1</sup> H <sub>34</sub> <sup>14</sup> N <sub>2</sub> <sup>16</sup> O <sub>3</sub>	17.0
494.24354	6.99	14.14	<sup>12</sup> C <sub>16</sub> <sup>1</sup> H <sub>38</sub> <sup>14</sup> N <sub>4</sub> <sup>16</sup> O <sub>13</sub>	0.0		

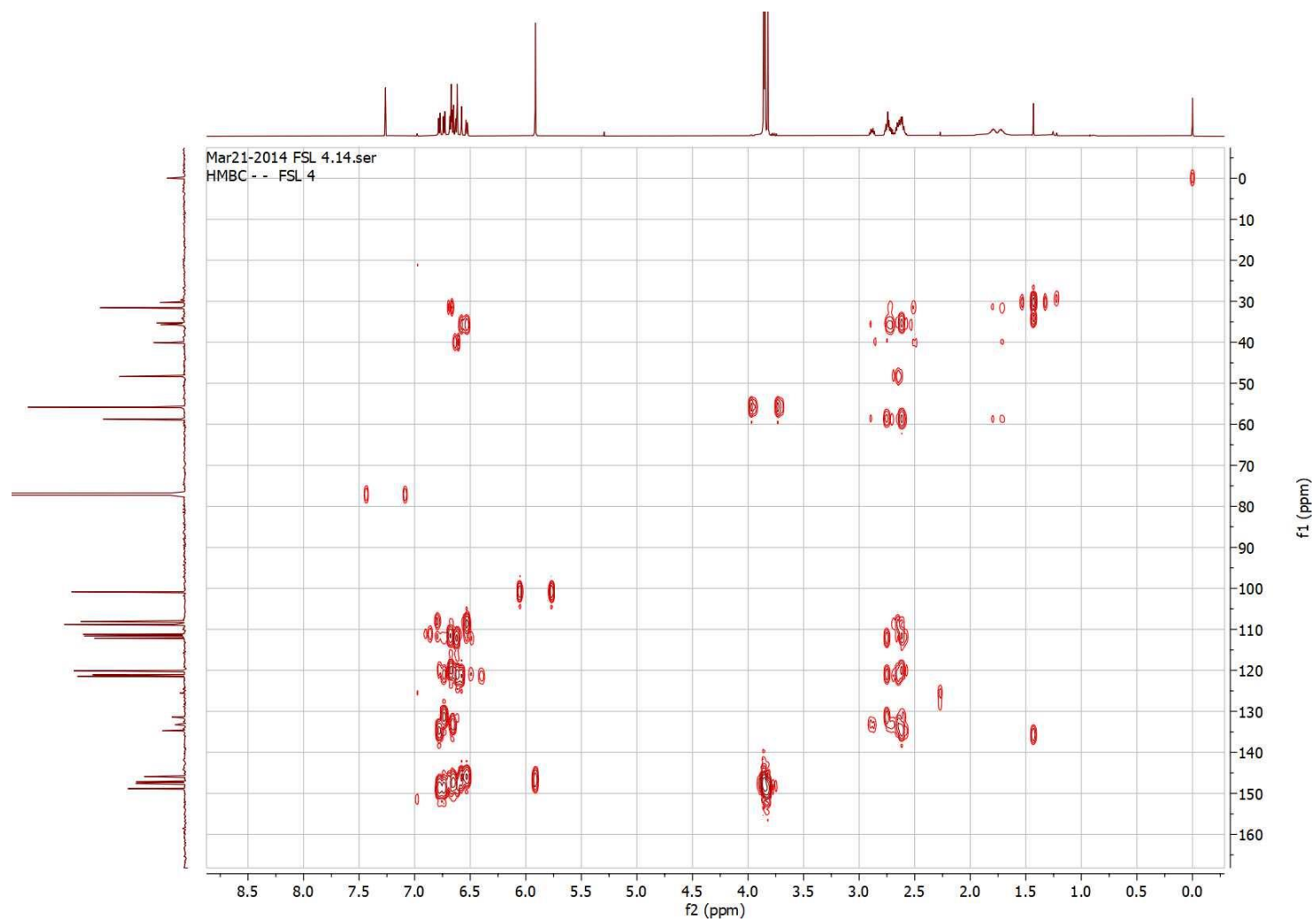
### Appendix 9: HR-DART-MS of schwarzinicine C (3)



**Appendix 10: COSY Spectrum of schwarzinicine C (3)**

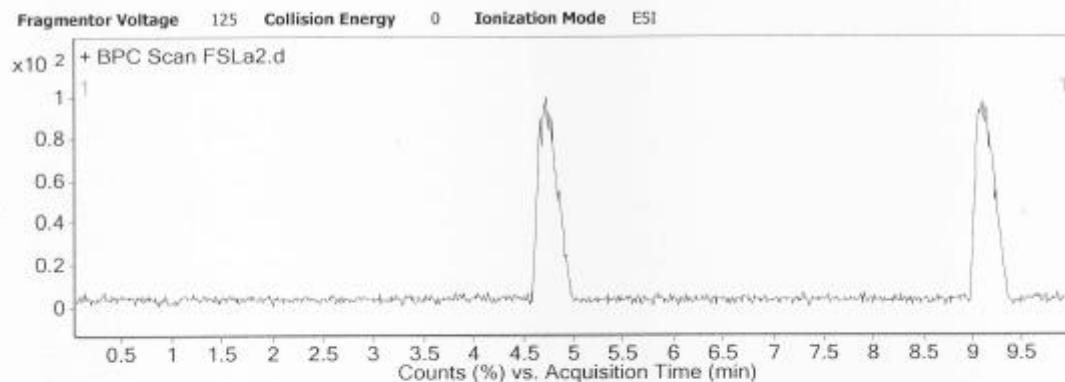


**Appendix 11:** HSQC Spectrum of schwarzinicine C (3)

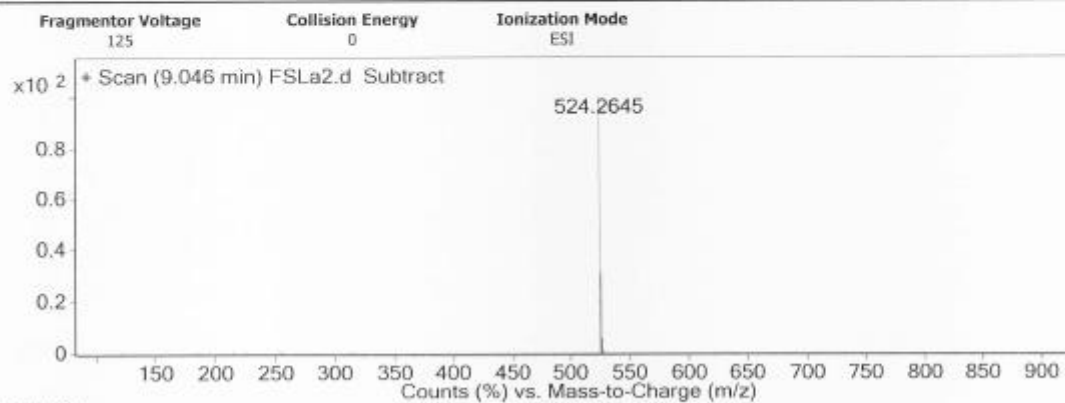


**Appendix 12: HMBC Spectrum of schwarzinicine C (3)**

### User Chromatograms



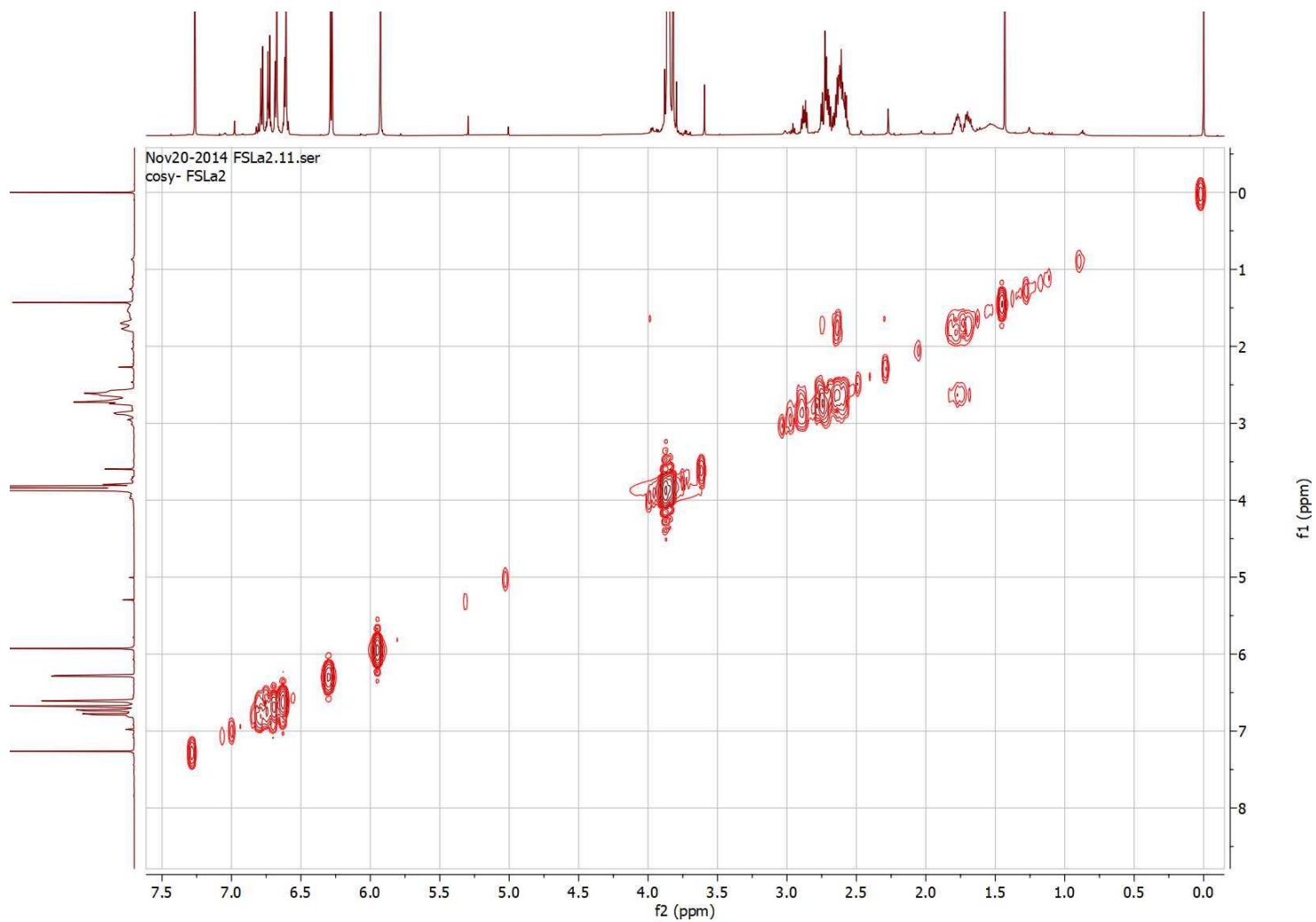
### User Spectra



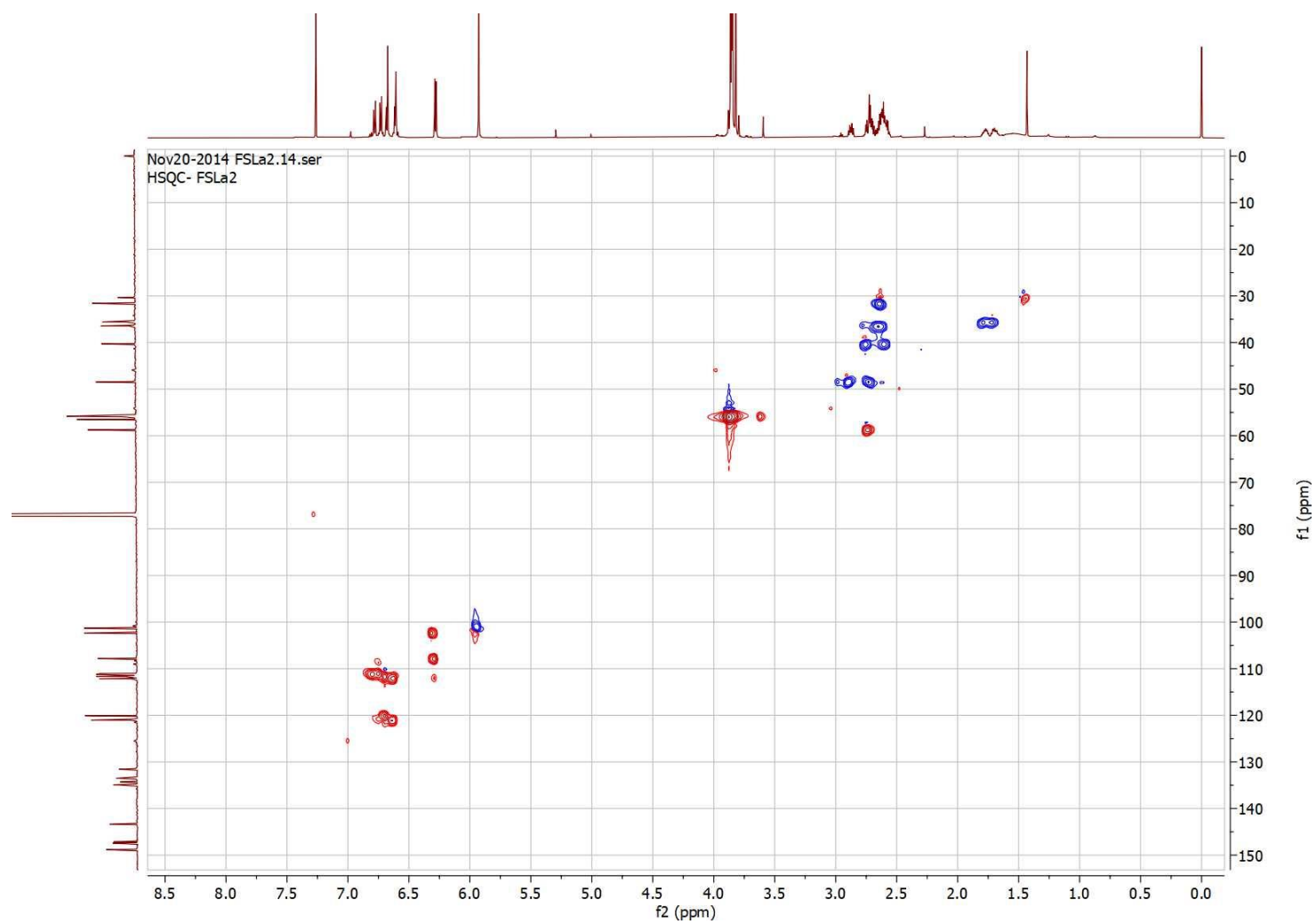
#### Peak List

m/z	z	Abund	Formula	Ion
524.2645	1	196242.2	C <sub>30</sub> H <sub>38</sub> N <sub>07</sub>	(M+H) <sup>+</sup>
525.2675	1	61110.1	C <sub>30</sub> H <sub>38</sub> N <sub>07</sub>	(M+H) <sup>+</sup>
526.2723	1	11060	C <sub>30</sub> H <sub>38</sub> N <sub>07</sub>	(M+H) <sup>+</sup>

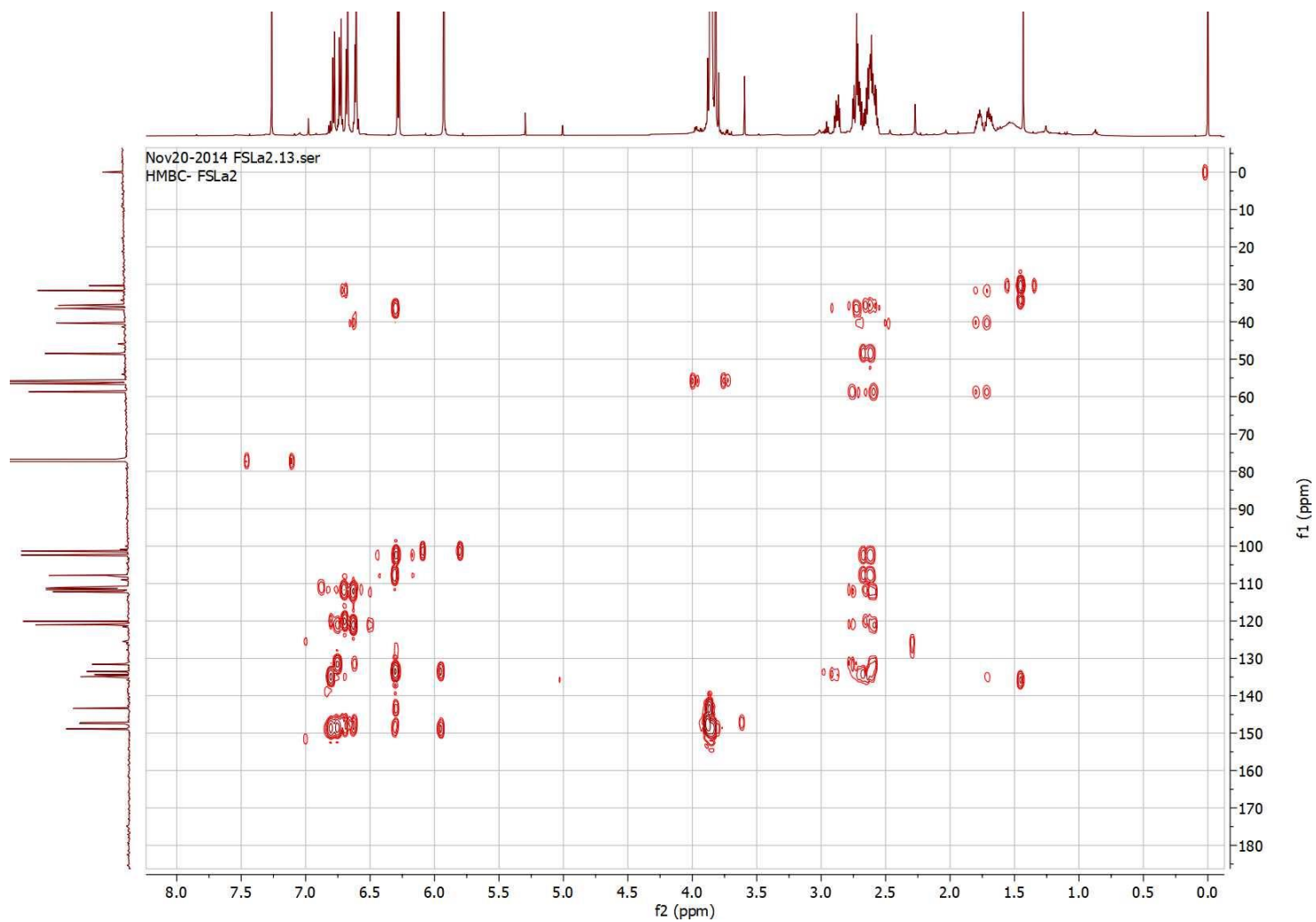
Appendix 13: HR-DART-MS of schwarzinicine D (4)



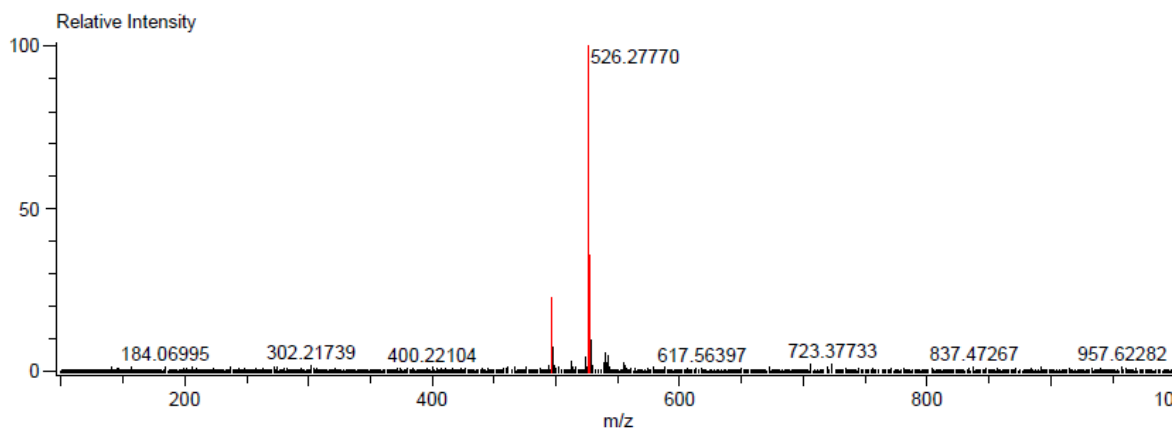
Appendix 14: COSY Spectrum of schwarzinicine D (4)



**Appendix 15:** HSQC Spectrum of schwarzinicine D (4)

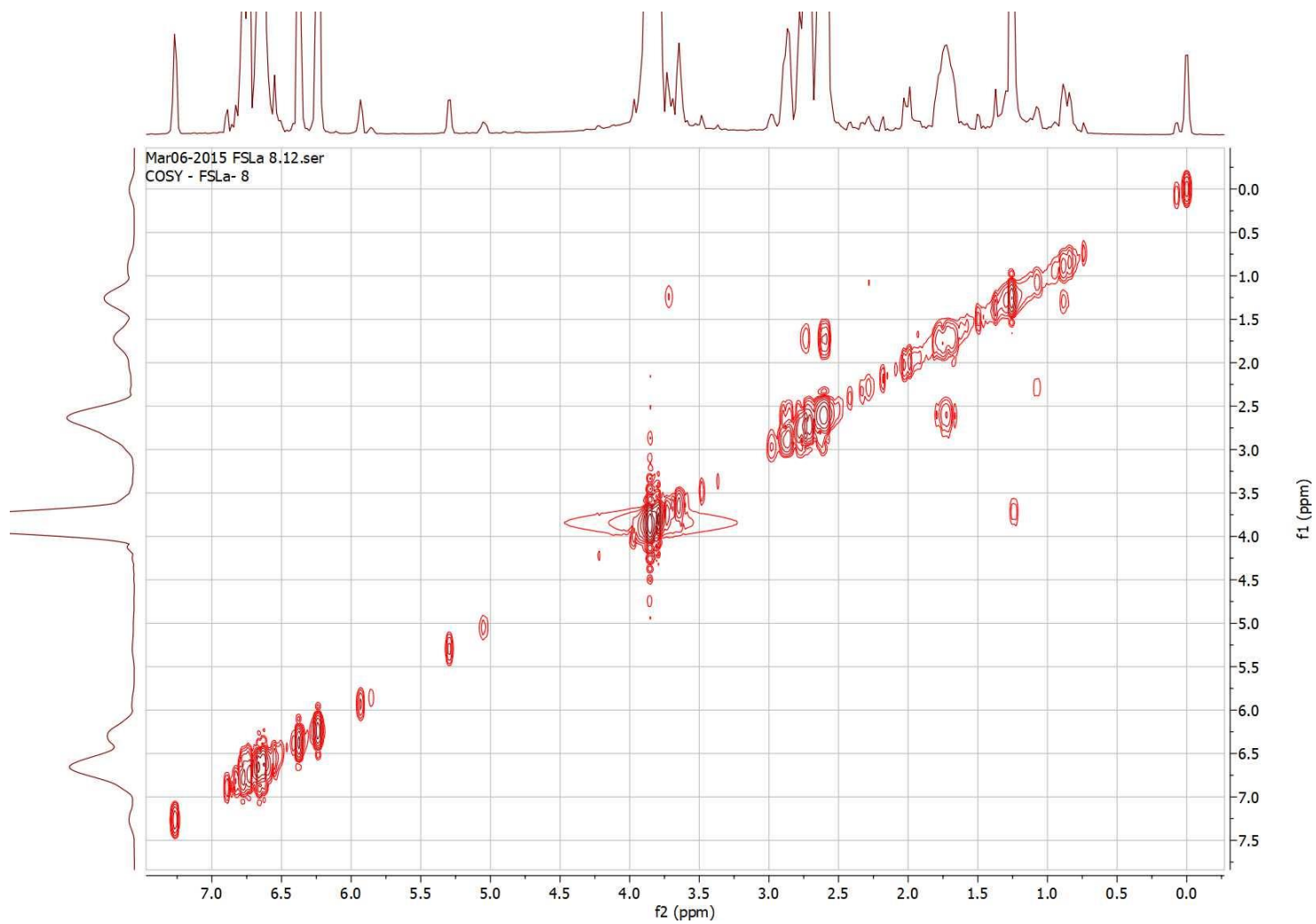


**Appendix 16: HMBC Spectrum of schwarzinicine D (4)**

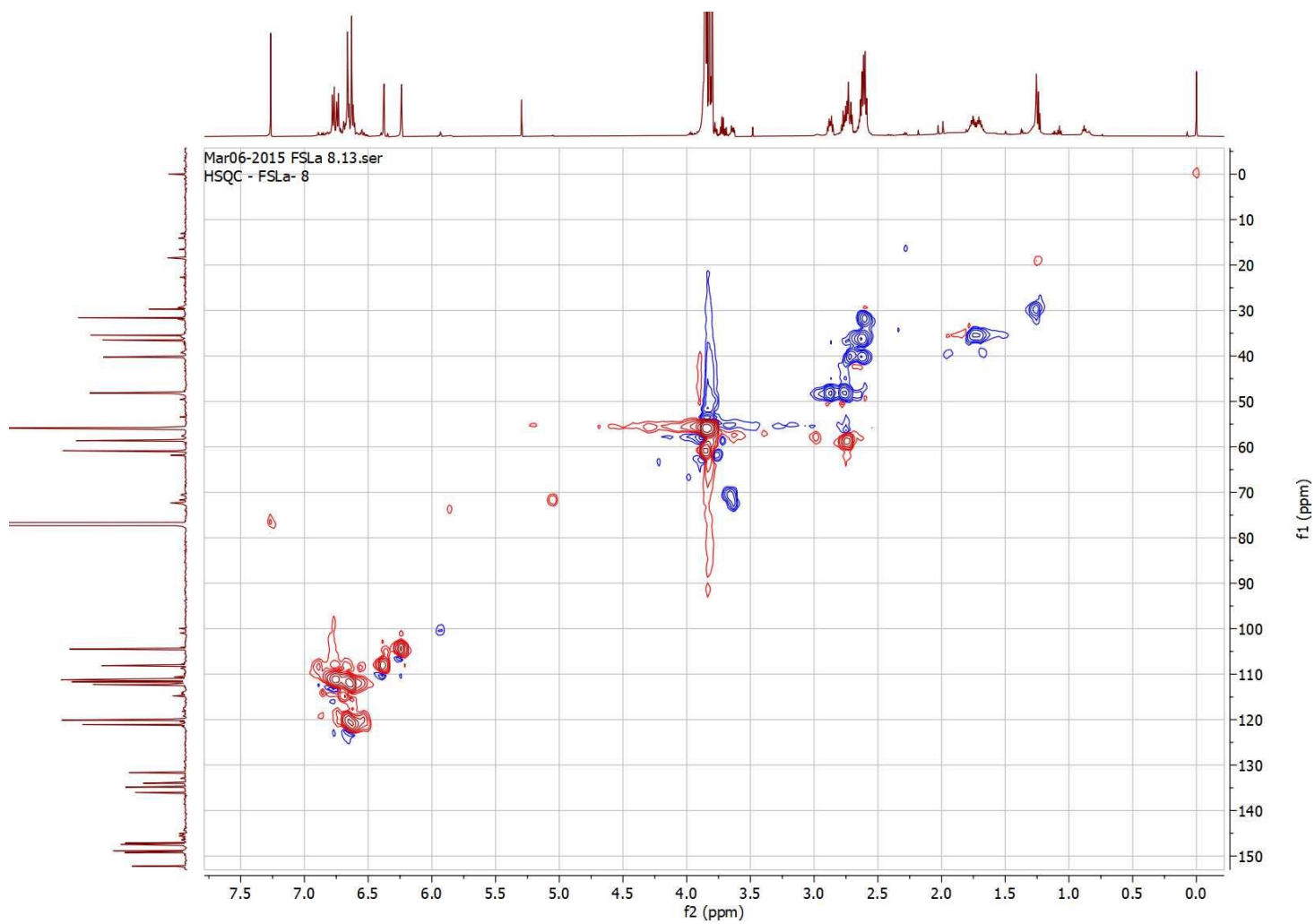


Mass	Intensity	Calc. Mass	Mass Difference (mmu)	Mass Difference (ppm)	Possible Formula	Unsaturation Number		
496.26898	17086.62	496.26857	0.41	0.83	<sup>12</sup> C <sub>27</sub> <sup>1</sup> H <sub>38</sub> <sup>14</sup> N <sub>4</sub> <sup>16</sup> O <sub>5</sub>	12.0		
		496.26991	-0.93	-1.88	<sup>12</sup> C <sub>29</sub> <sup>1</sup> H <sub>38</sub> <sup>14</sup> N <sub>1</sub> <sup>16</sup> O <sub>8</sub>	11.5		
		496.26723	1.75	3.52	<sup>12</sup> C <sub>26</sub> <sup>1</sup> H <sub>40</sub> <sup>16</sup> O <sub>9</sub>	7.0		
		496.27125	-2.27	-4.57	<sup>12</sup> C <sub>30</sub> <sup>1</sup> H <sub>34</sub> <sup>14</sup> N <sub>5</sub> <sup>16</sup> O <sub>2</sub>	16.5		
		496.26589	3.09	6.23	<sup>12</sup> C <sub>24</sub> <sup>1</sup> H <sub>38</sub> <sup>14</sup> N <sub>3</sub> <sup>16</sup> O <sub>8</sub>	7.5		
		496.27259	-3.61	-7.28	<sup>12</sup> C <sub>32</sub> <sup>1</sup> H <sub>36</sub> <sup>14</sup> N <sub>2</sub> <sup>16</sup> O <sub>3</sub>	16.0		
		496.26404	4.94	9.96	<sup>12</sup> C <sub>36</sub> <sup>1</sup> H <sub>34</sub> <sup>14</sup> N <sub>1</sub> <sup>16</sup> O <sub>1</sub>	20.5		
		496.27444	-5.46	-11.01	<sup>12</sup> C <sub>20</sub> <sup>1</sup> H <sub>40</sub> <sup>14</sup> N <sub>4</sub> <sup>16</sup> O <sub>10</sub>	3.0		
		496.26321	5.77	11.63	<sup>12</sup> C <sub>21</sub> <sup>1</sup> H <sub>40</sub> <sup>14</sup> N <sub>2</sub> <sup>16</sup> O <sub>11</sub>	3.0		
		496.26270	6.28	12.66	<sup>12</sup> C <sub>34</sub> <sup>1</sup> H <sub>32</sub> <sup>14</sup> N <sub>4</sub>	21.0		
		496.27527	-6.29	-12.68	<sup>12</sup> C <sub>35</sub> <sup>1</sup> H <sub>34</sub> <sup>14</sup> N <sub>3</sub>	20.5		
		496.27578	-6.81	-13.71	<sup>12</sup> C <sub>22</sub> <sup>1</sup> H <sub>42</sub> <sup>14</sup> N <sub>1</sub> <sup>16</sup> O <sub>11</sub>	2.5		
		496.26187	7.11	14.33	<sup>12</sup> C <sub>19</sub> <sup>1</sup> H <sub>38</sub> <sup>14</sup> N <sub>5</sub> <sup>16</sup> O <sub>10</sub>	3.5		
526.27770	75709.04	526.27780	-0.09	-0.18	<sup>12</sup> C <sub>27</sub> <sup>1</sup> H <sub>42</sub> <sup>16</sup> O <sub>10</sub>	7.0		
		526.27645	1.25	2.38	<sup>12</sup> C <sub>25</sub> <sup>1</sup> H <sub>40</sub> <sup>14</sup> N <sub>3</sub> <sup>16</sup> O <sub>9</sub>	7.5		
		526.27913	-1.43	-2.72	<sup>12</sup> C <sub>28</sub> <sup>1</sup> H <sub>38</sub> <sup>14</sup> N <sub>4</sub> <sup>16</sup> O <sub>8</sub>	12.0		
		526.28048	-2.77	-5.27	<sup>12</sup> C <sub>30</sub> <sup>1</sup> H <sub>40</sub> <sup>14</sup> N <sub>1</sub> <sup>16</sup> O <sub>7</sub>	11.5		
		526.27460	3.10	5.89	<sup>12</sup> C <sub>37</sub> <sup>1</sup> H <sub>36</sub> <sup>14</sup> N <sub>1</sub> <sup>16</sup> O <sub>2</sub>	20.5		
		526.27377	3.93	7.47	<sup>12</sup> C <sub>22</sub> <sup>1</sup> H <sub>42</sub> <sup>14</sup> N <sub>2</sub> <sup>16</sup> O <sub>12</sub>	3.0		
		526.28181	-4.11	-7.81	<sup>12</sup> C <sub>31</sub> <sup>1</sup> H <sub>36</sub> <sup>14</sup> N <sub>5</sub> <sup>16</sup> O <sub>3</sub>	16.5		
		526.27326	4.44	8.44	<sup>12</sup> C <sub>35</sub> <sup>1</sup> H <sub>34</sub> <sup>14</sup> N <sub>4</sub> <sup>16</sup> O <sub>1</sub>	21.0		
		526.27243	5.27	10.02	<sup>12</sup> C <sub>20</sub> <sup>1</sup> H <sub>40</sub> <sup>14</sup> N <sub>5</sub> <sup>16</sup> O <sub>11</sub>	3.5		
		526.28316	-5.45	-10.36	<sup>12</sup> C <sub>33</sub> <sup>1</sup> H <sub>38</sub> <sup>14</sup> N <sub>2</sub> <sup>16</sup> O <sub>4</sub>	16.0		
		526.27192	5.78	10.98	<sup>12</sup> C <sub>34</sub> <sup>1</sup> H <sub>38</sub> <sup>16</sup> O <sub>5</sub>	16.0		
		526.27058	7.12	13.54	<sup>12</sup> C <sub>32</sub> <sup>1</sup> H <sub>36</sub> <sup>14</sup> N <sub>3</sub> <sup>16</sup> O <sub>4</sub>	16.5		
		526.28501	-7.30	-13.88	<sup>12</sup> C <sub>21</sub> <sup>1</sup> H <sub>42</sub> <sup>14</sup> N <sub>4</sub> <sup>16</sup> O <sub>11</sub>	3.0		
		527.28329	26939.37	527.28243	0.86	1.63	<sup>12</sup> C <sub>37</sub> <sup>1</sup> H <sub>37</sub> <sup>14</sup> N <sub>1</sub> <sup>16</sup> O <sub>2</sub>	20.0
		527.28428		-0.99	-1.88	<sup>12</sup> C <sub>25</sub> <sup>1</sup> H <sub>41</sub> <sup>14</sup> N <sub>3</sub> <sup>16</sup> O <sub>9</sub>	7.0	
527.28160	1.69	3.21		<sup>12</sup> C <sub>22</sub> <sup>1</sup> H <sub>43</sub> <sup>14</sup> N <sub>2</sub> <sup>16</sup> O <sub>12</sub>	2.5			
527.28109	2.20	4.18		<sup>12</sup> C <sub>35</sub> <sup>1</sup> H <sub>35</sub> <sup>14</sup> N <sub>4</sub> <sup>16</sup> O <sub>1</sub>	20.5			

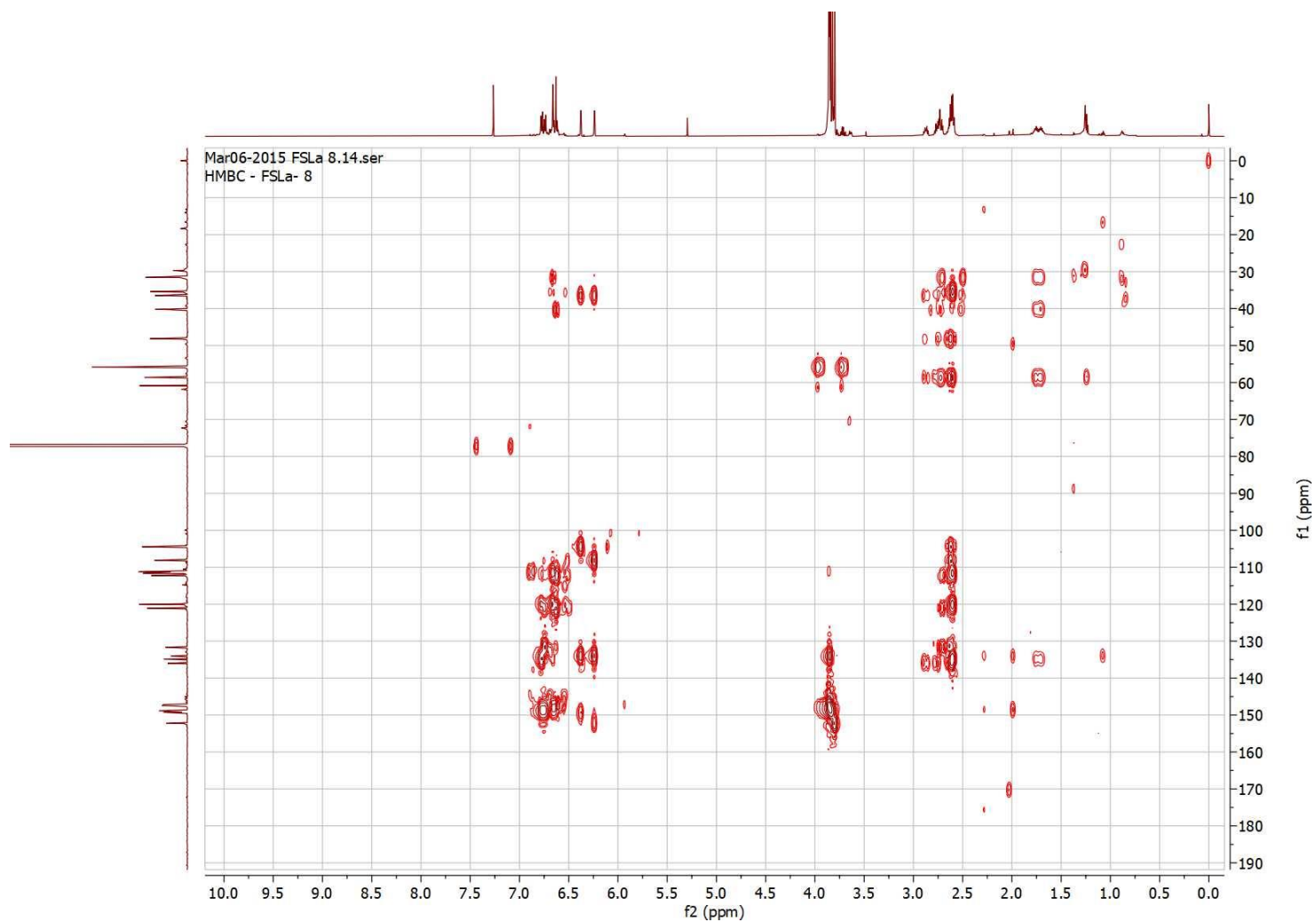
**Appendix 17: HR-DART-MS of schwarzinicine E (5)**



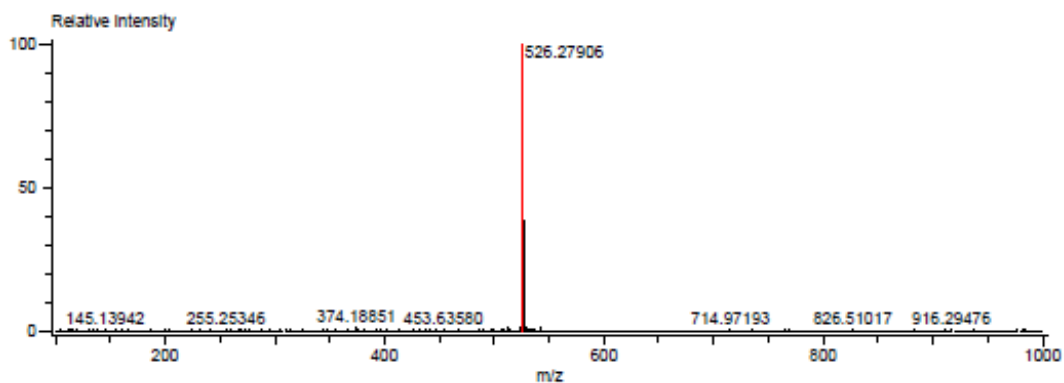
**Appendix 18: COSY Spectrum of schwarzinicine E (5)**



**Appendix 19:** HSQC Spectrum of schwarzinicine E (5)

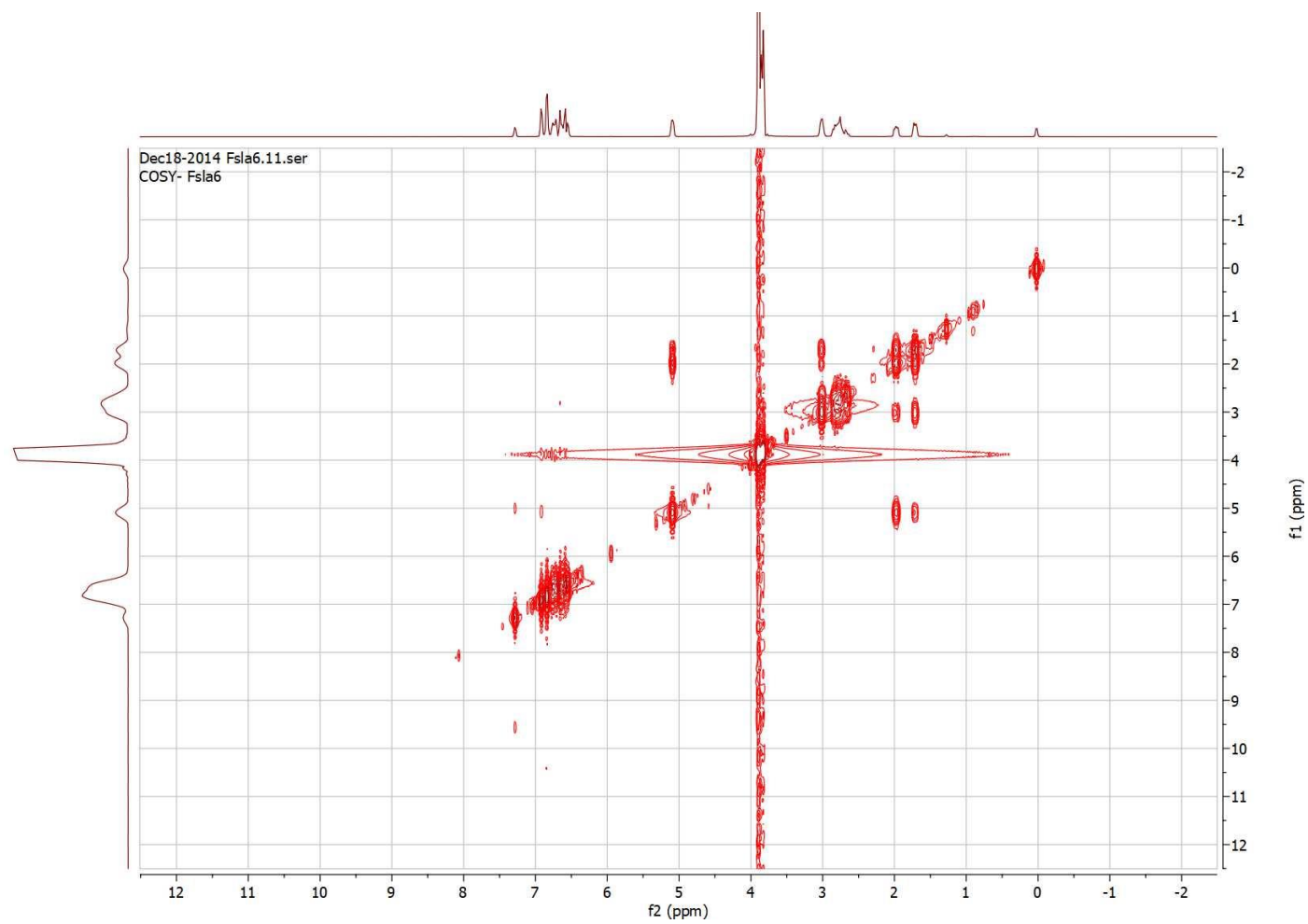


**Appendix 20:** HMBC Spectrum of schwarzinicine E (5)

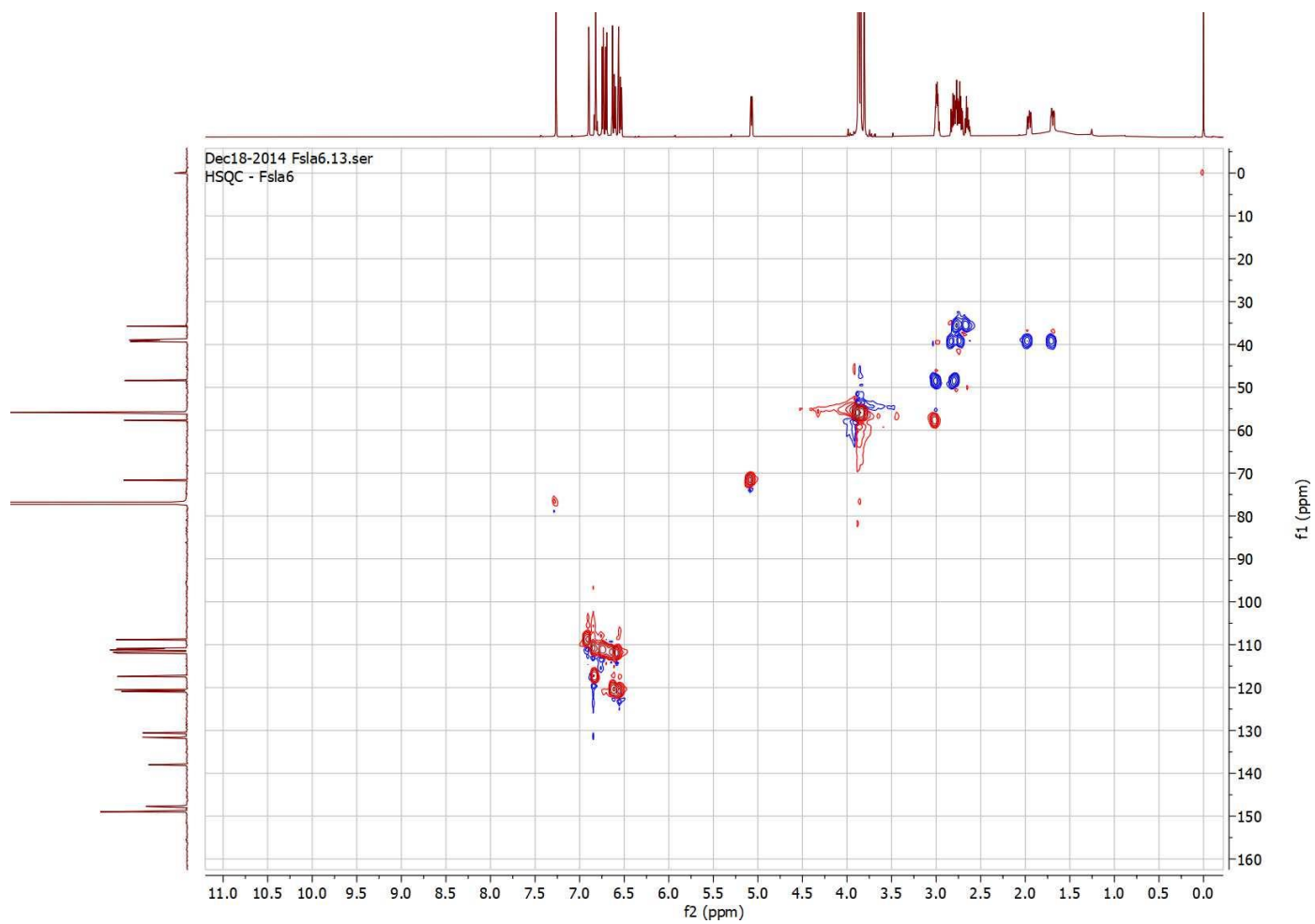


Mass	Intensity	Calc. Mass	Mass Difference (mmu)	Mass Difference (ppm)	Possible Formula	Unsaturation Number
526.27906	177640.58	526.27913	-0.07	-0.14	<sup>12</sup> C <sub>28</sub> <sup>1</sup> H <sub>36</sub> <sup>14</sup> N <sub>4</sub> <sup>16</sup> O <sub>8</sub>	12.0
		526.27780	1.26	2.40	<sup>12</sup> C <sub>27</sub> <sup>1</sup> H <sub>42</sub> <sup>16</sup> O <sub>10</sub>	7.0
		526.28048	-1.42	-2.69	<sup>12</sup> C <sub>30</sub> <sup>1</sup> H <sub>40</sub> <sup>14</sup> N <sub>1</sub> <sup>16</sup> O <sub>7</sub>	11.5
		526.27645	2.61	4.95	<sup>12</sup> C <sub>28</sub> <sup>1</sup> H <sub>40</sub> <sup>14</sup> N <sub>3</sub> <sup>16</sup> O <sub>8</sub>	7.5
		526.28181	-2.75	-5.23	<sup>12</sup> C <sub>31</sub> <sup>1</sup> H <sub>36</sub> <sup>14</sup> N <sub>5</sub> <sup>16</sup> O <sub>3</sub>	16.5
		526.28316	-4.10	-7.78	<sup>12</sup> C <sub>33</sub> <sup>1</sup> H <sub>36</sub> <sup>14</sup> N <sub>2</sub> <sup>16</sup> O <sub>4</sub>	16.0
		526.27460	4.46	8.47	<sup>12</sup> C <sub>27</sub> <sup>1</sup> H <sub>36</sub> <sup>14</sup> N <sub>1</sub> <sup>16</sup> O <sub>2</sub>	20.5
		526.27377	5.29	10.04	<sup>12</sup> C <sub>22</sub> <sup>1</sup> H <sub>42</sub> <sup>14</sup> N <sub>2</sub> <sup>16</sup> O <sub>12</sub>	3.0
		526.27326	5.80	11.02	<sup>12</sup> C <sub>28</sub> <sup>1</sup> H <sub>34</sub> <sup>14</sup> N <sub>4</sub> <sup>16</sup> O <sub>1</sub>	21.0
		526.28501	-5.95	-11.30	<sup>12</sup> C <sub>21</sub> <sup>1</sup> H <sub>42</sub> <sup>14</sup> N <sub>4</sub> <sup>16</sup> O <sub>11</sub>	3.0
		526.27243	6.63	12.60	<sup>12</sup> C <sub>30</sub> <sup>1</sup> H <sub>40</sub> <sup>14</sup> N <sub>6</sub> <sup>16</sup> O <sub>11</sub>	3.5
		526.28584	-6.78	-12.88	<sup>12</sup> C <sub>36</sub> <sup>1</sup> H <sub>36</sub> <sup>14</sup> N <sub>3</sub> <sup>16</sup> O <sub>1</sub>	20.5
		526.27192	7.14	13.56	<sup>12</sup> C <sub>34</sub> <sup>1</sup> H <sub>36</sub> <sup>16</sup> O <sub>5</sub>	16.0
		526.28635	-7.29	-13.85	<sup>12</sup> C <sub>23</sub> <sup>1</sup> H <sub>44</sub> <sup>14</sup> N <sub>1</sub> <sup>16</sup> O <sub>12</sub>	2.5

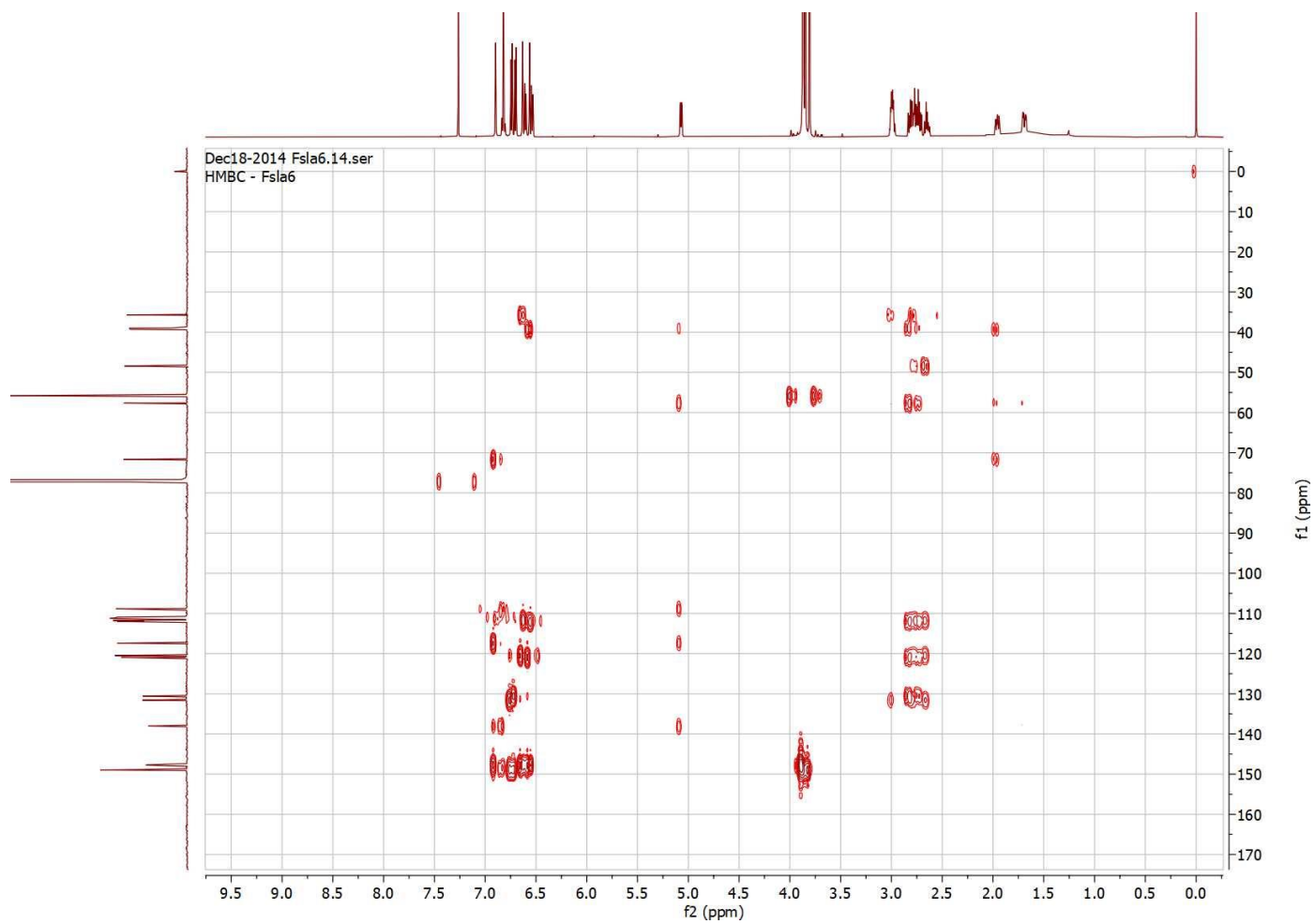
**Appendix 21: HR-DART-MS of schwarzinicine F (6)**



**Appendix 22: COSY Spectrum of schwarzinicine F (6)**

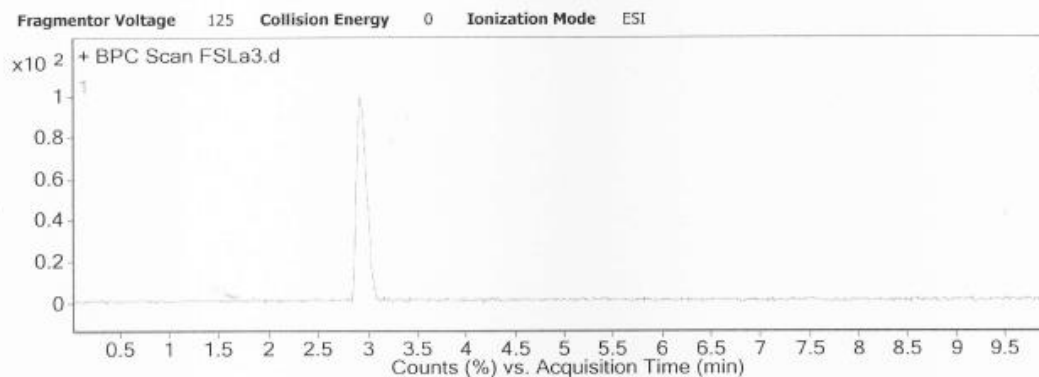


**Appendix 23: HSQC Spectrum of schwarzinicine F (6)**

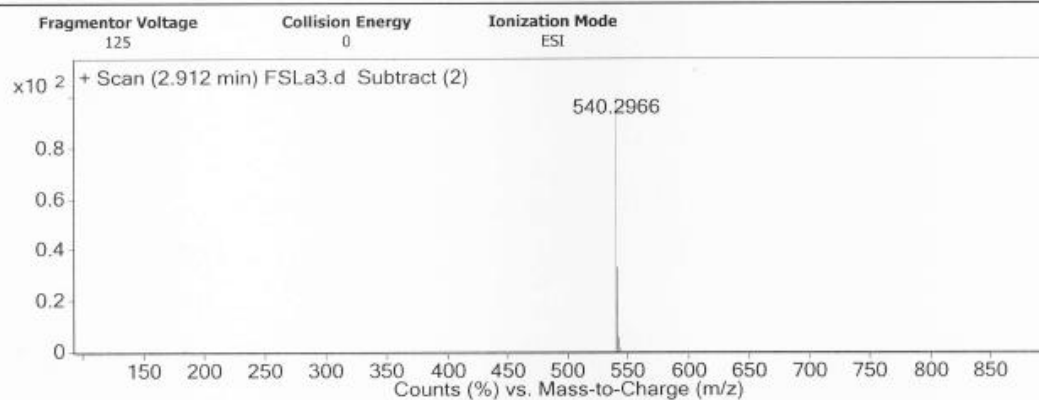


**Appendix 24:** HMBC Spectrum of schwarzinicine F (6)

### User Chromatograms



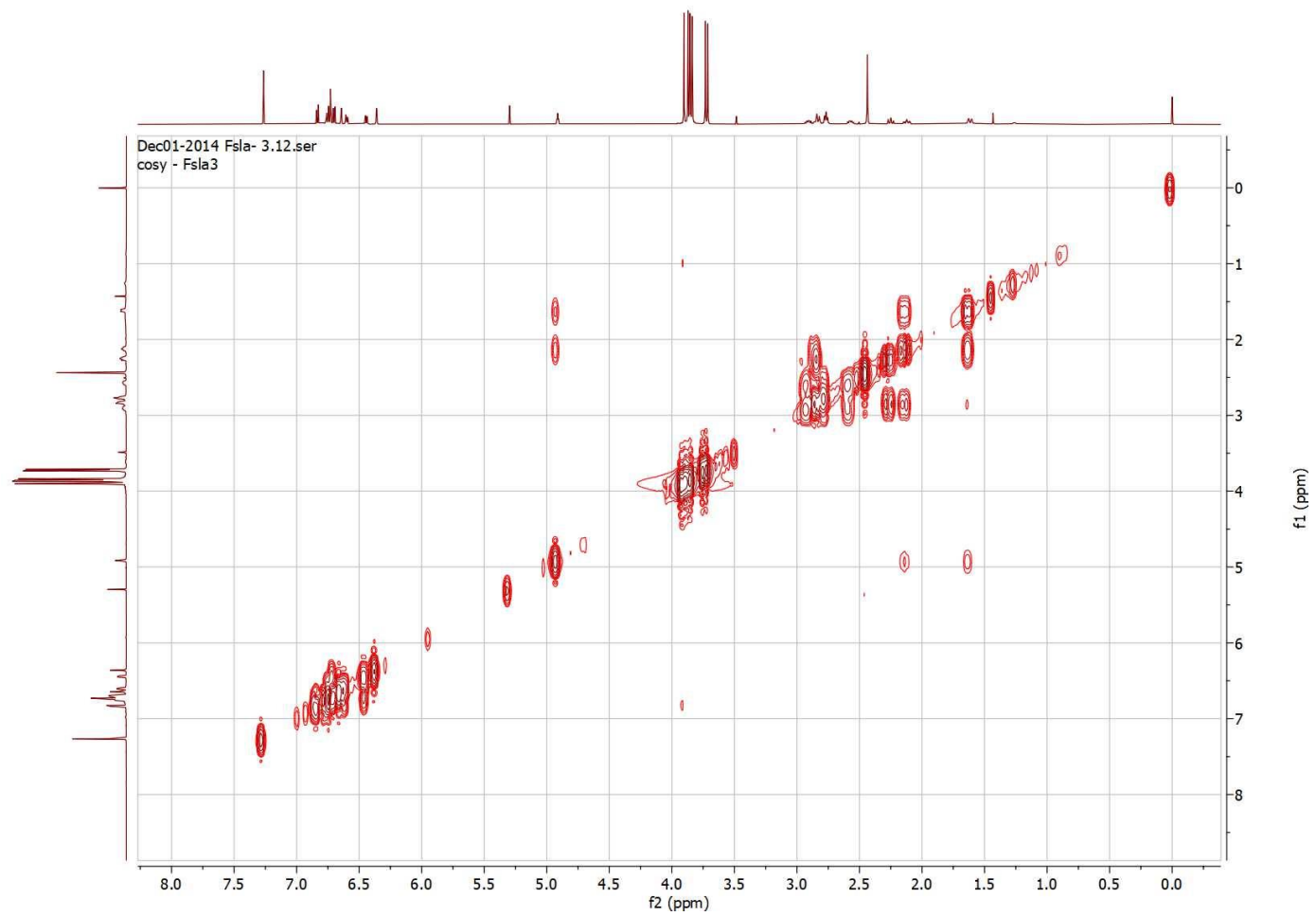
### User Spectra



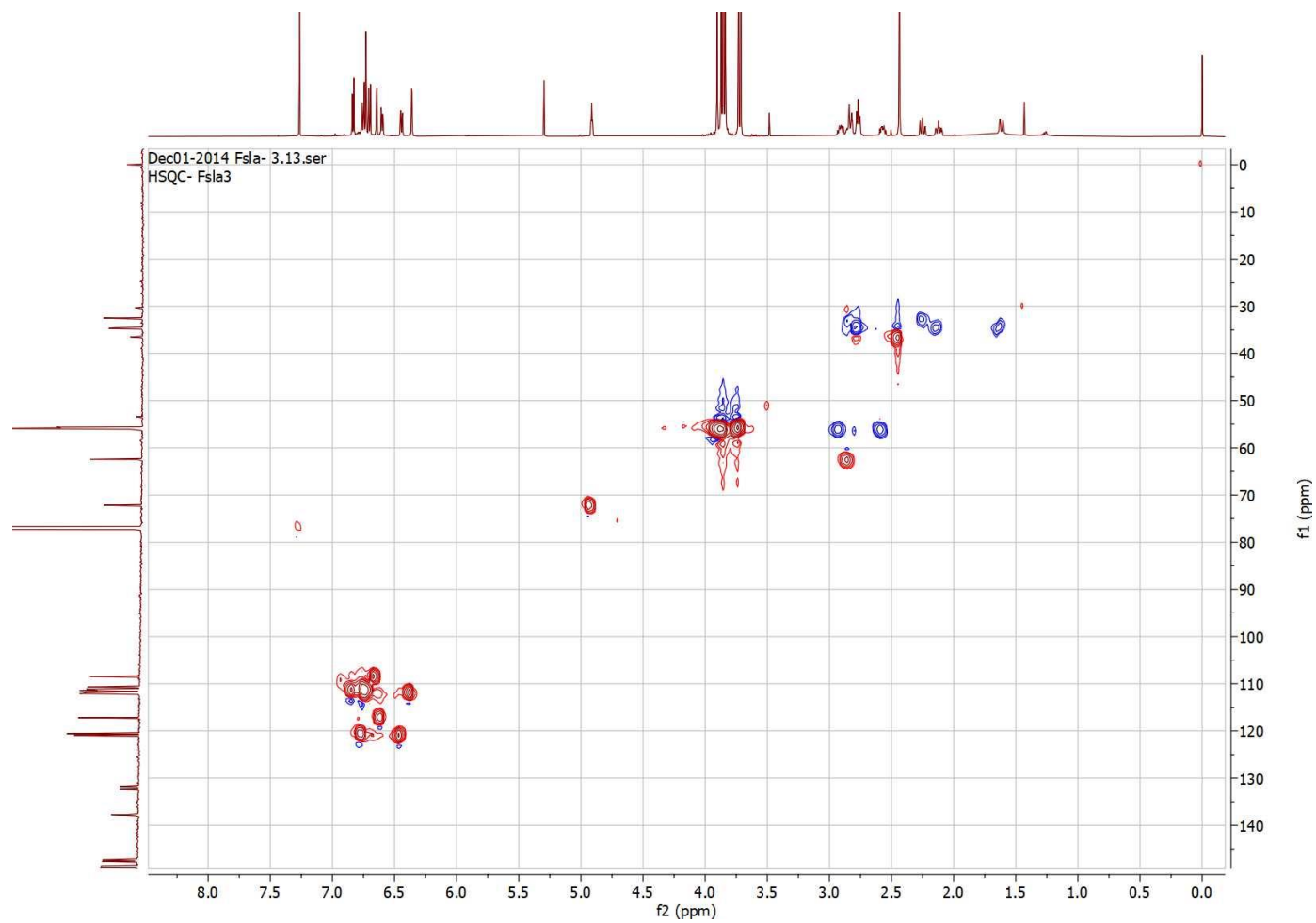
#### Peak List

<i>m/z</i>	<i>z</i>	Abund	Formula	Ion
540.2966	1	434050	C <sub>32</sub> H <sub>38</sub> N <sub>5</sub> O <sub>3</sub>	(M+H) <sup>+</sup>
541.299	1	142524.4	C <sub>32</sub> H <sub>38</sub> N <sub>5</sub> O <sub>3</sub>	(M+H) <sup>+</sup>
542.3021	1	25443.1	C <sub>32</sub> H <sub>38</sub> N <sub>5</sub> O <sub>3</sub>	(M+H) <sup>+</sup>

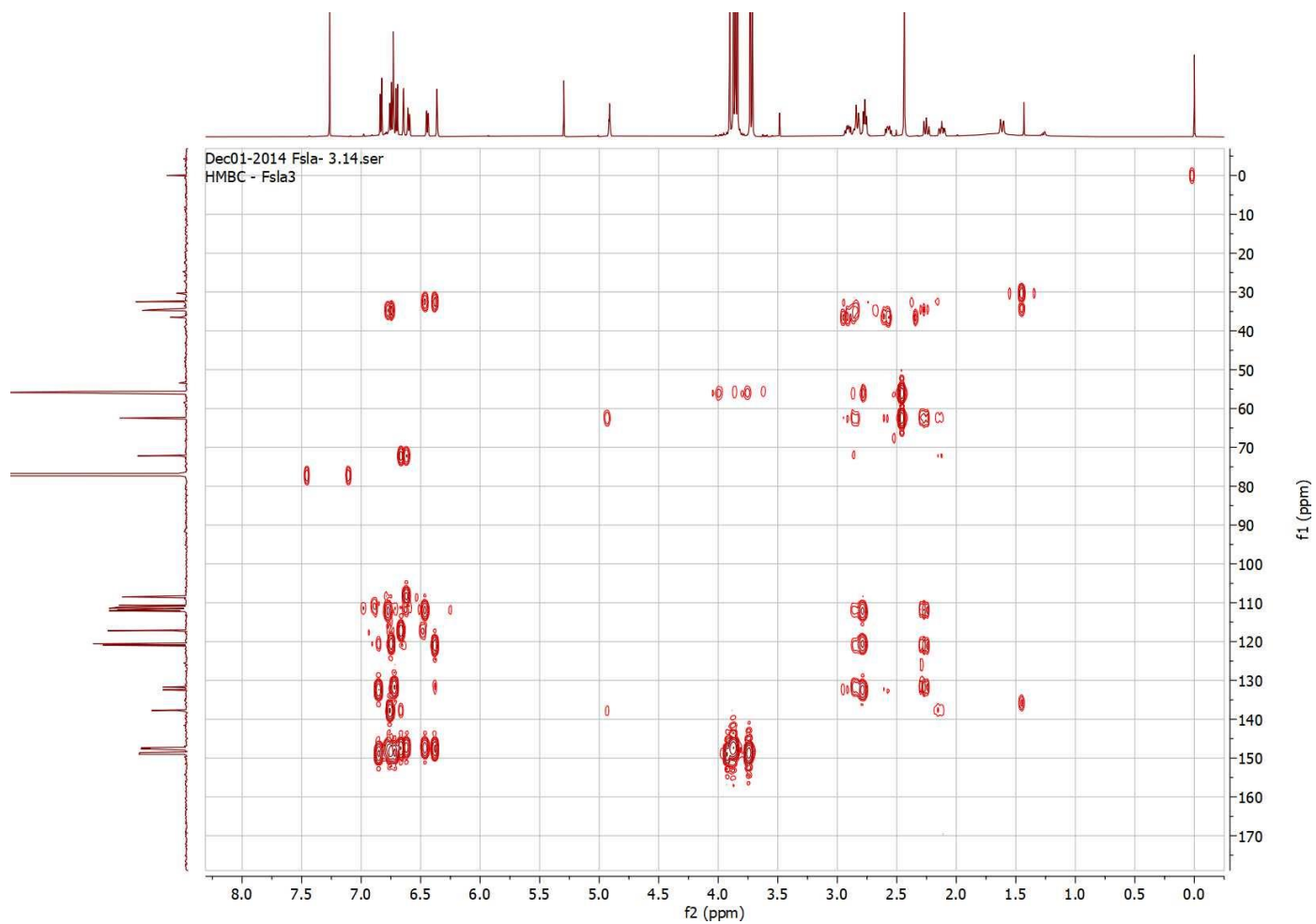
### Appendix 25: HR-DART-MS of schwarzinicine G (7)



**Appendix 26:** COSY Spectrum of schwarzinicine G (7)

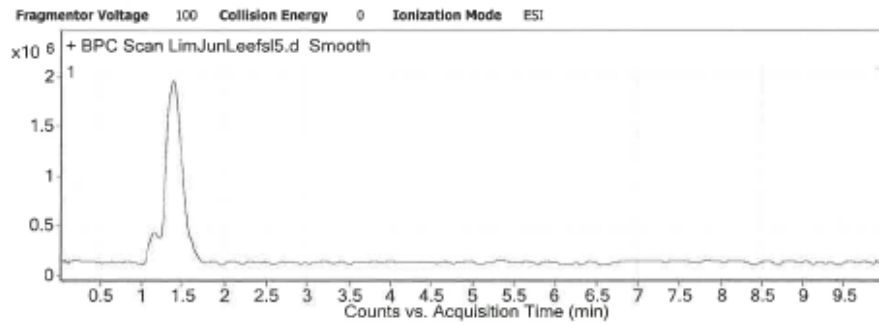


**Appendix 27:** HSQC Spectrum of schwarzinicine G (7)

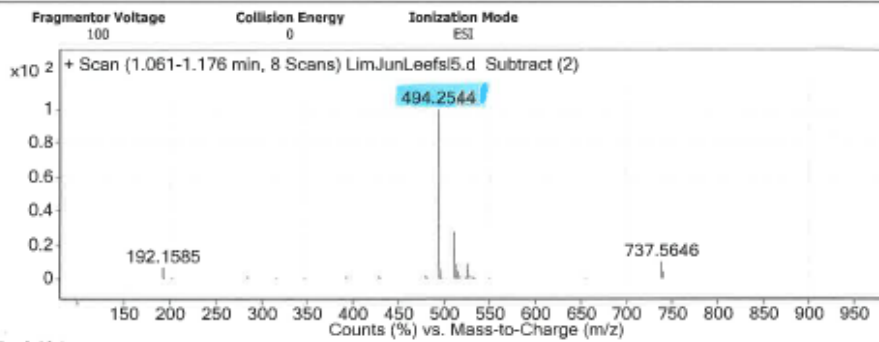


**Appendix 28:** HMBC Spectrum of schwarzinicine G (7)

## User Chromatograms



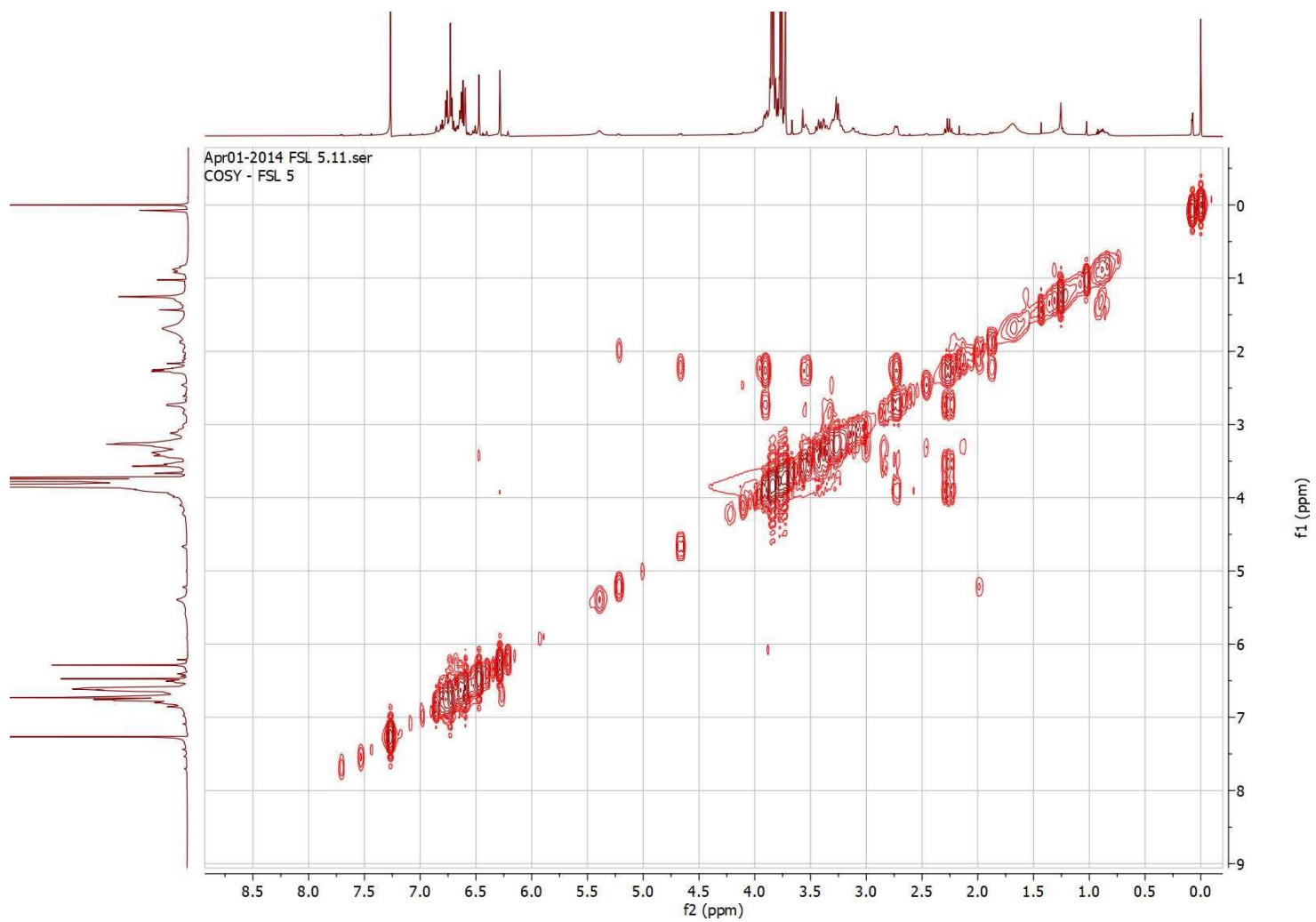
## User Spectra



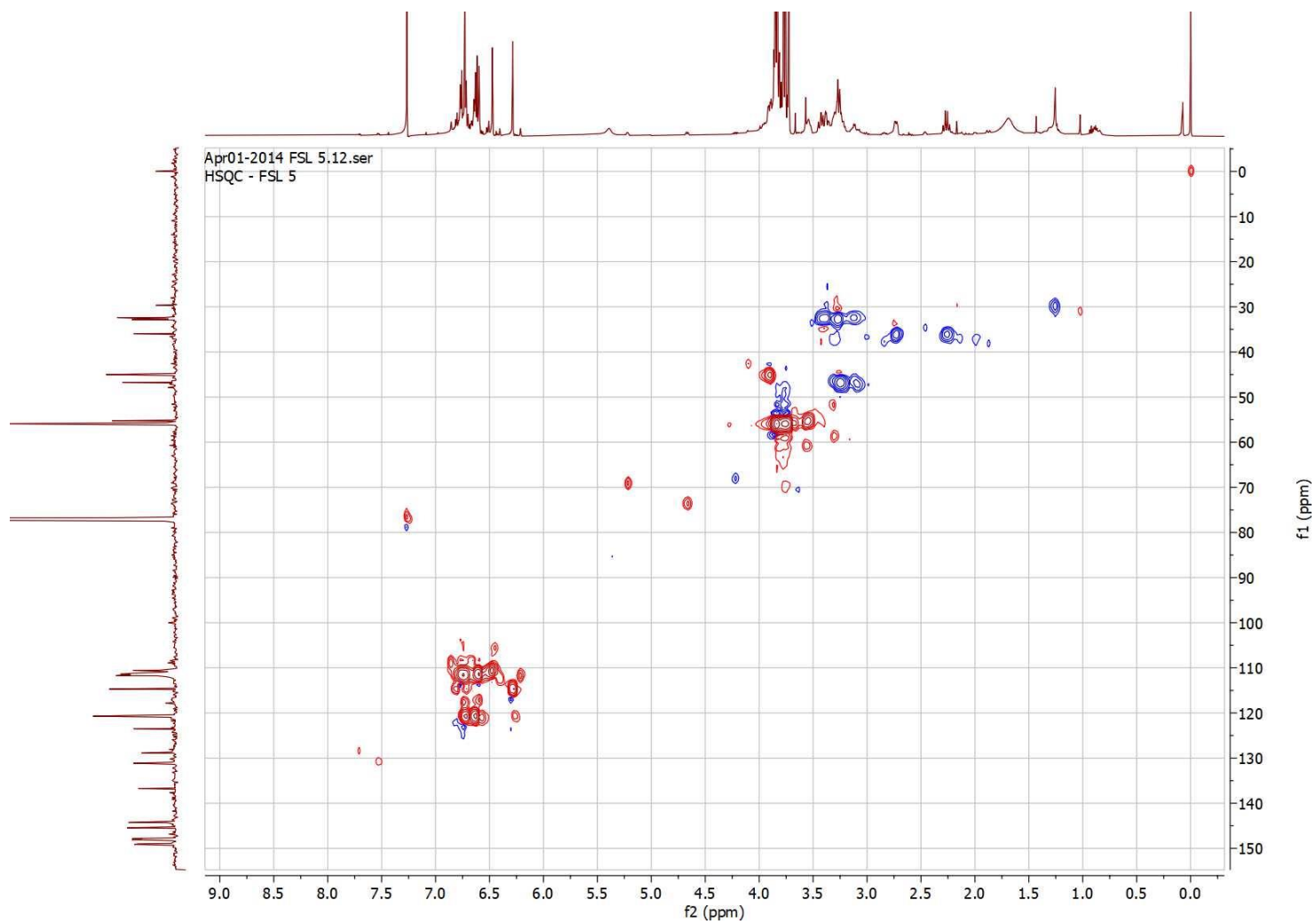
### Peak List

m/z	z	Abund
192.1585		23895.6
494.2544	1	360565
495.2574	1	109888.4
496.2604	1	22501.3
511.3963		39513.9
512.2645	1	100226.7
513.2676	1	30236.5
526.2796		31417.1
737.5646		35730.1

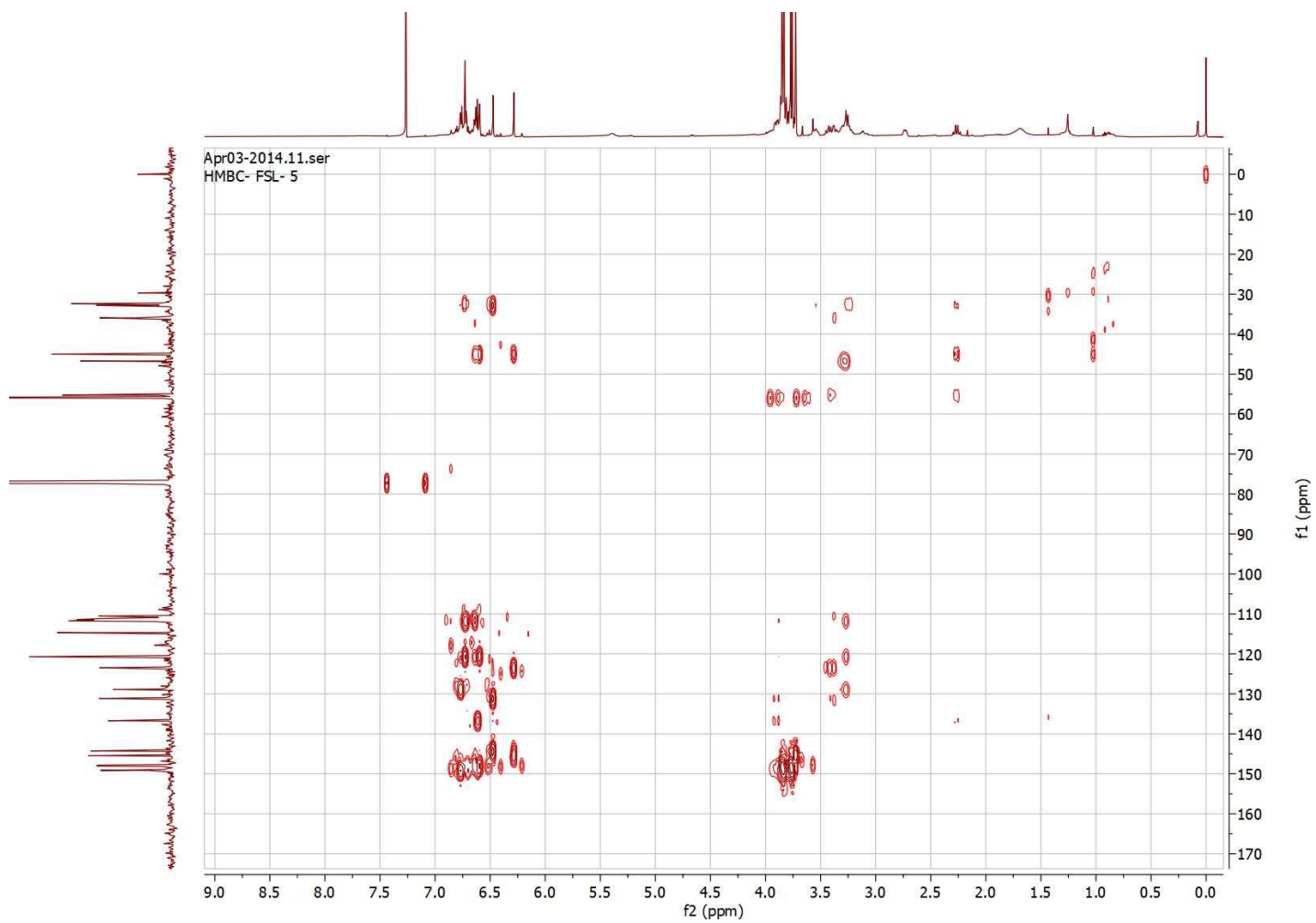
## Appendix 29: HR-DART-MS of schwarzificusine A (8)



**Appendix 30: COSY of schwarzificusine A (8)**

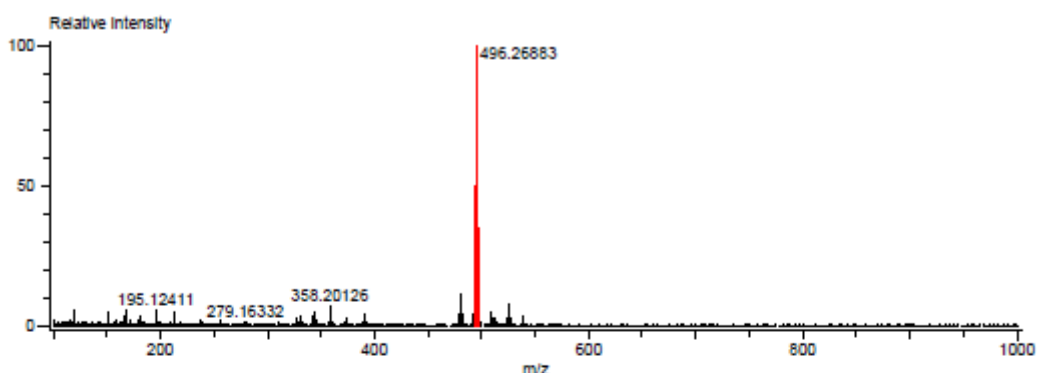


Appendix 31: HSQC of schwarzificusine A (8)



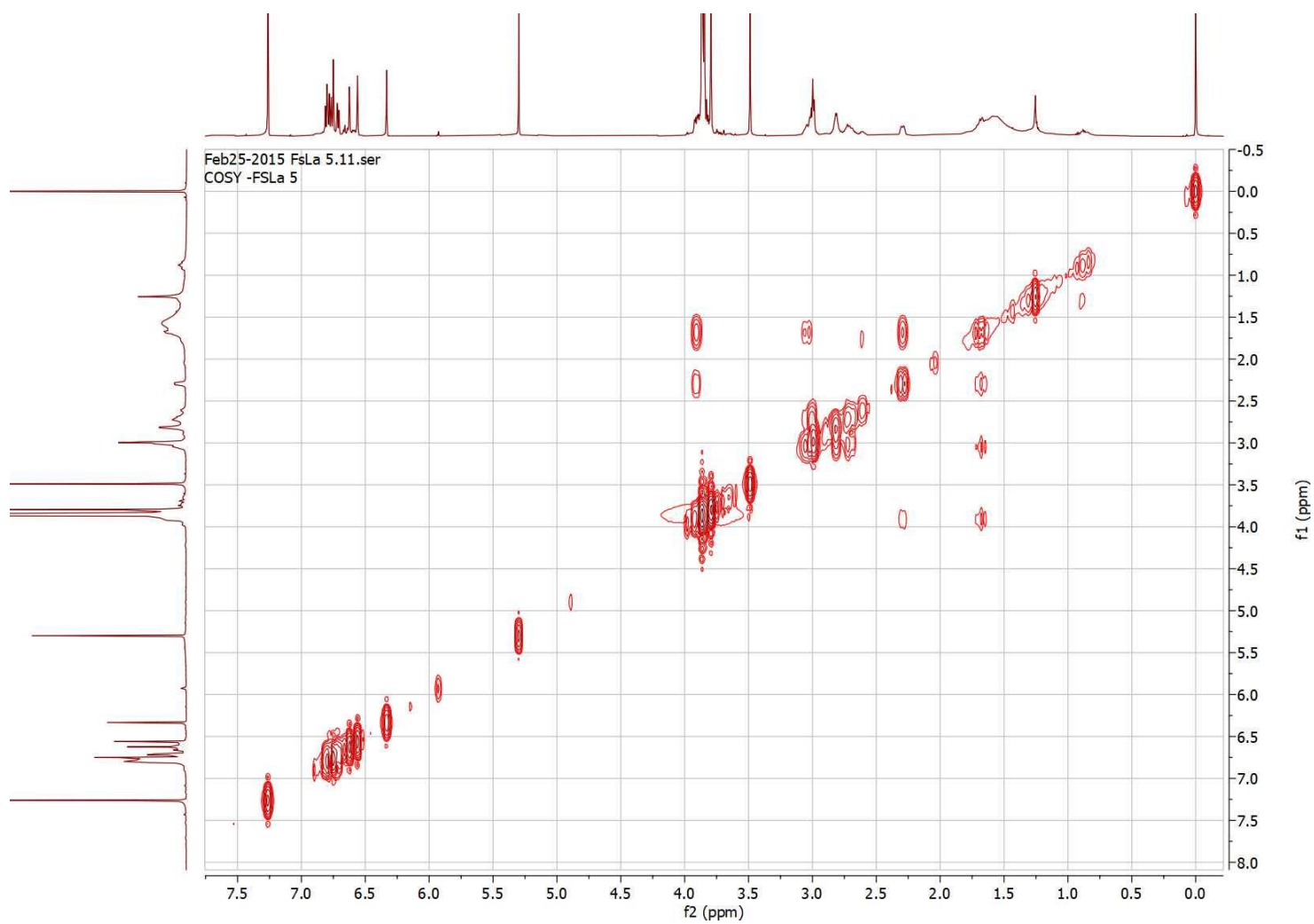
**Appendix 32: HMBC of schwarzificusine A (8)**



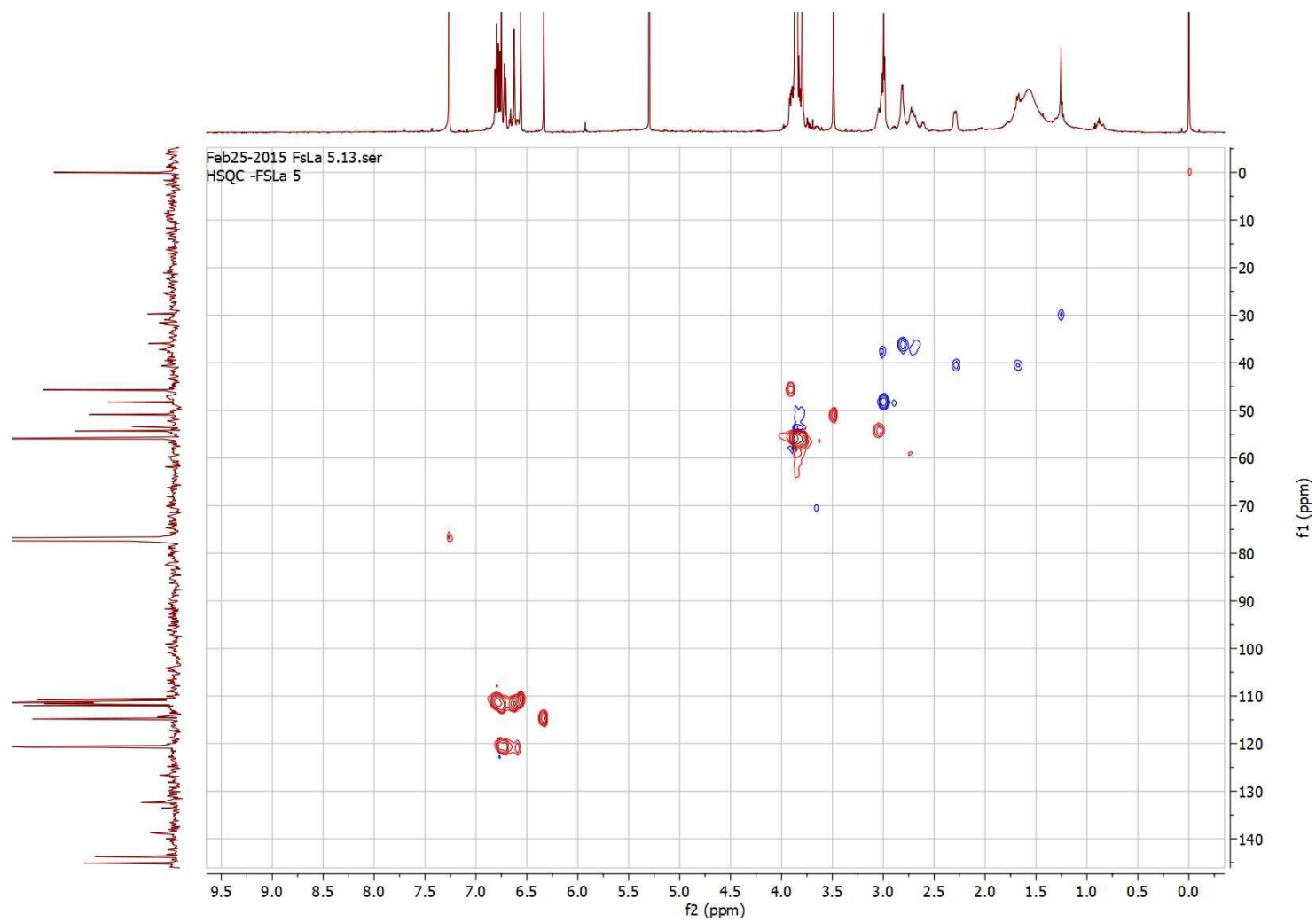


Mass	Intensity	Calc. Mass	Mass Difference (mmu)	Mass Difference (ppm)	Possible Formula	Unsaturation Number
494.25283	43453.27	494.25292	-0.09	-0.18	$^{12}\text{C}_{27}\text{H}_{34}^{14}\text{N}_4^{16}\text{O}_5$	13.0
		494.25158	1.25	2.53	$^{12}\text{C}_{26}\text{H}_{33}^{16}\text{O}_9$	8.0
		494.25426	-1.43	-2.89	$^{12}\text{C}_{29}\text{H}_{36}^{14}\text{N}_1^{16}\text{O}_6$	12.5
		494.25024	2.59	5.25	$^{12}\text{C}_{24}\text{H}_{36}^{14}\text{N}_5^{16}\text{O}_5$	8.5
		494.25560	-2.77	-5.60	$^{12}\text{C}_{30}\text{H}_{32}^{14}\text{N}_5^{16}\text{O}_2$	17.5
		494.25694	-4.11	-8.32	$^{12}\text{C}_{32}\text{H}_{34}^{14}\text{N}_2^{16}\text{O}_3$	17.0
		494.24839	4.44	8.99	$^{12}\text{C}_{36}\text{H}_{32}^{14}\text{N}_1^{16}\text{O}_1$	21.5
		494.24756	5.27	10.67	$^{12}\text{C}_{21}\text{H}_{36}^{14}\text{N}_2^{16}\text{O}_{11}$	4.0
		494.24705	5.79	11.71	$^{12}\text{C}_{34}\text{H}_{30}^{14}\text{N}_4$	22.0
		494.25879	-5.96	-12.06	$^{12}\text{C}_{20}\text{H}_{36}^{14}\text{N}_4^{16}\text{O}_{10}$	4.0
		494.24622	6.62	13.38	$^{12}\text{C}_{19}\text{H}_{36}^{14}\text{N}_5^{16}\text{O}_{10}$	4.5
		494.25962	-6.79	-13.74	$^{12}\text{C}_{36}\text{H}_{32}^{14}\text{N}_3$	21.5
		494.24571	7.12	14.41	$^{12}\text{C}_{33}\text{H}_{34}^{16}\text{O}_4$	17.0
		494.26013	-7.30	-14.78	$^{12}\text{C}_{22}\text{H}_{40}^{14}\text{N}_1^{16}\text{O}_{11}$	3.5
496.26883	86920.73	496.26857	0.26	0.52	$^{12}\text{C}_{27}\text{H}_{36}^{14}\text{N}_4^{16}\text{O}_5$	12.0
		496.26991	-1.08	-2.18	$^{12}\text{C}_{29}\text{H}_{36}^{14}\text{N}_1^{16}\text{O}_6$	11.5
		496.26723	1.60	3.22	$^{12}\text{C}_{26}\text{H}_{40}^{16}\text{O}_9$	7.0
		496.27125	-2.42	-4.88	$^{12}\text{C}_{30}\text{H}_{34}^{14}\text{N}_5^{16}\text{O}_2$	16.5
		496.26589	2.94	5.92	$^{12}\text{C}_{24}\text{H}_{36}^{14}\text{N}_3^{16}\text{O}_6$	7.5
		496.27259	-3.76	-7.58	$^{12}\text{C}_{32}\text{H}_{36}^{14}\text{N}_2^{16}\text{O}_3$	16.0
		496.26404	4.79	9.65	$^{12}\text{C}_{36}\text{H}_{34}^{14}\text{N}_1^{16}\text{O}_1$	20.5
		496.27444	-5.61	-11.31	$^{12}\text{C}_{20}\text{H}_{40}^{14}\text{N}_4^{16}\text{O}_{10}$	3.0
		496.26321	5.62	11.33	$^{12}\text{C}_{21}\text{H}_{40}^{14}\text{N}_2^{16}\text{O}_{11}$	3.0
		496.26270	6.13	12.36	$^{12}\text{C}_{34}\text{H}_{32}^{14}\text{N}_4$	21.0
		496.27527	-6.44	-12.96	$^{12}\text{C}_{36}\text{H}_{34}^{14}\text{N}_3$	20.5
		496.27578	-6.96	-14.02	$^{12}\text{C}_{22}\text{H}_{42}^{14}\text{N}_1^{16}\text{O}_{11}$	2.5
		496.26187	6.96	14.03	$^{12}\text{C}_{19}\text{H}_{36}^{14}\text{N}_5^{16}\text{O}_{10}$	3.5
		497.27352	30204.13	497.27371	-0.19	-0.38
497.27506	-1.53			-3.08	$^{12}\text{C}_{26}\text{H}_{41}^{16}\text{O}_9$	6.5
497.27186	1.66			3.34	$^{12}\text{C}_{36}\text{H}_{35}^{14}\text{N}_1^{16}\text{O}_1$	20.0
497.27103	2.49			5.01	$^{12}\text{C}_{21}\text{H}_{41}^{14}\text{N}_2^{16}\text{O}_{11}$	2.5
497.27639	-2.87			-5.77	$^{12}\text{C}_{27}\text{H}_{37}^{14}\text{N}_4^{16}\text{O}_5$	11.5
497.27052	3.00			6.04	$^{12}\text{C}_{34}\text{H}_{33}^{14}\text{N}_4$	20.5

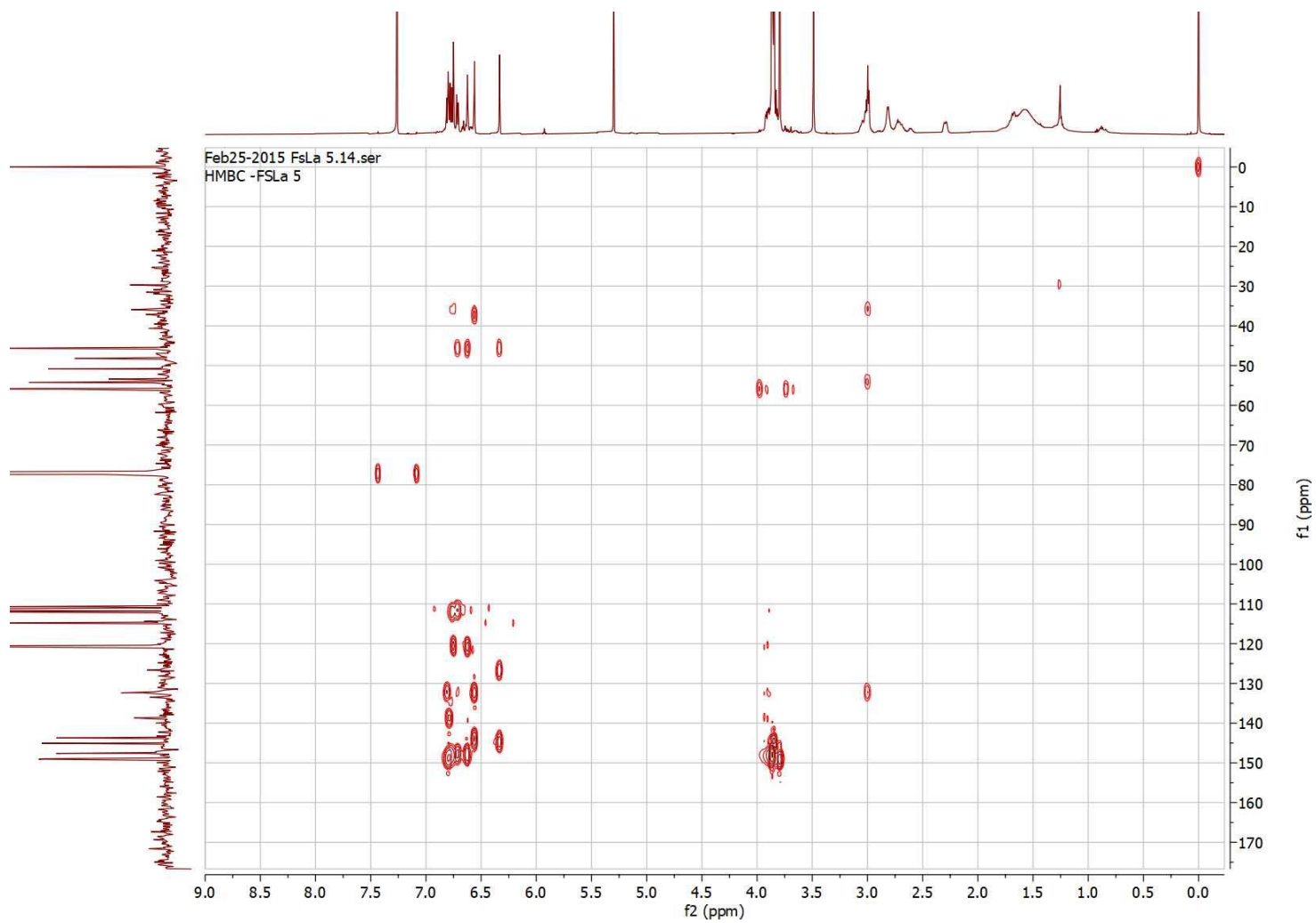
Appendix 34: HR-DART-MS of schwarzificusine B (9)



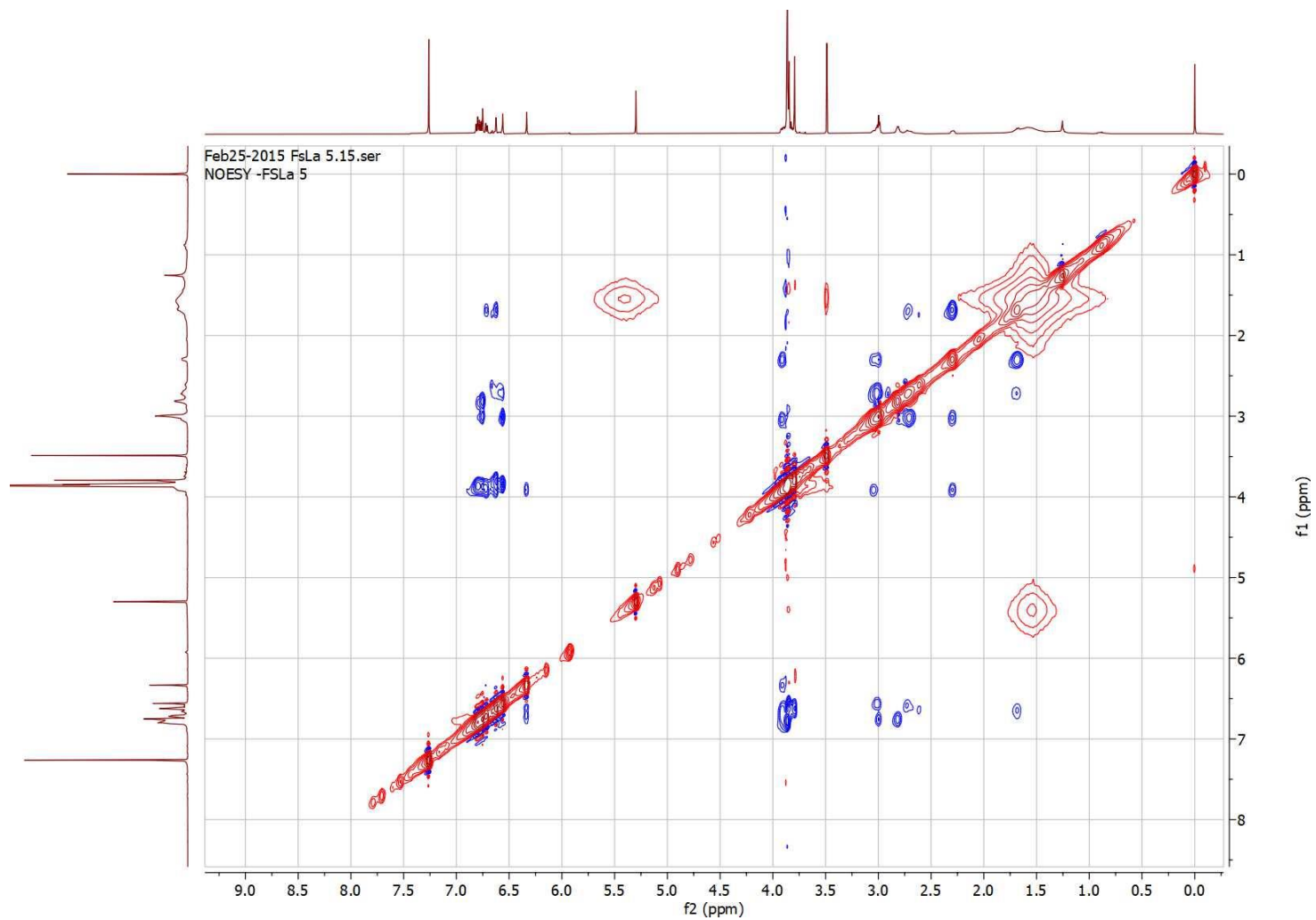
**Appendix 35: COSY of schwarzificusine B (9)**



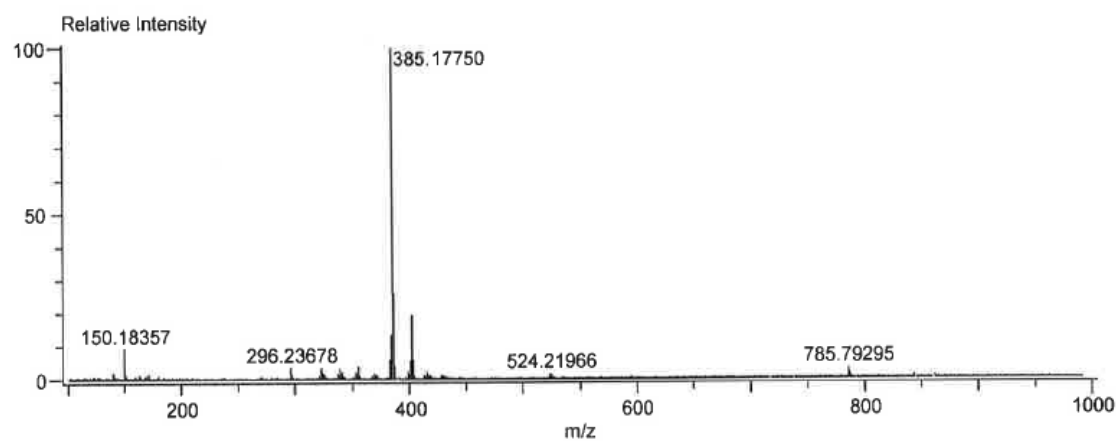
**Appendix 36: HSQC of schwarzificusine B (9)**



**Appendix 37: HMBC of schwarzificusine B (9)**

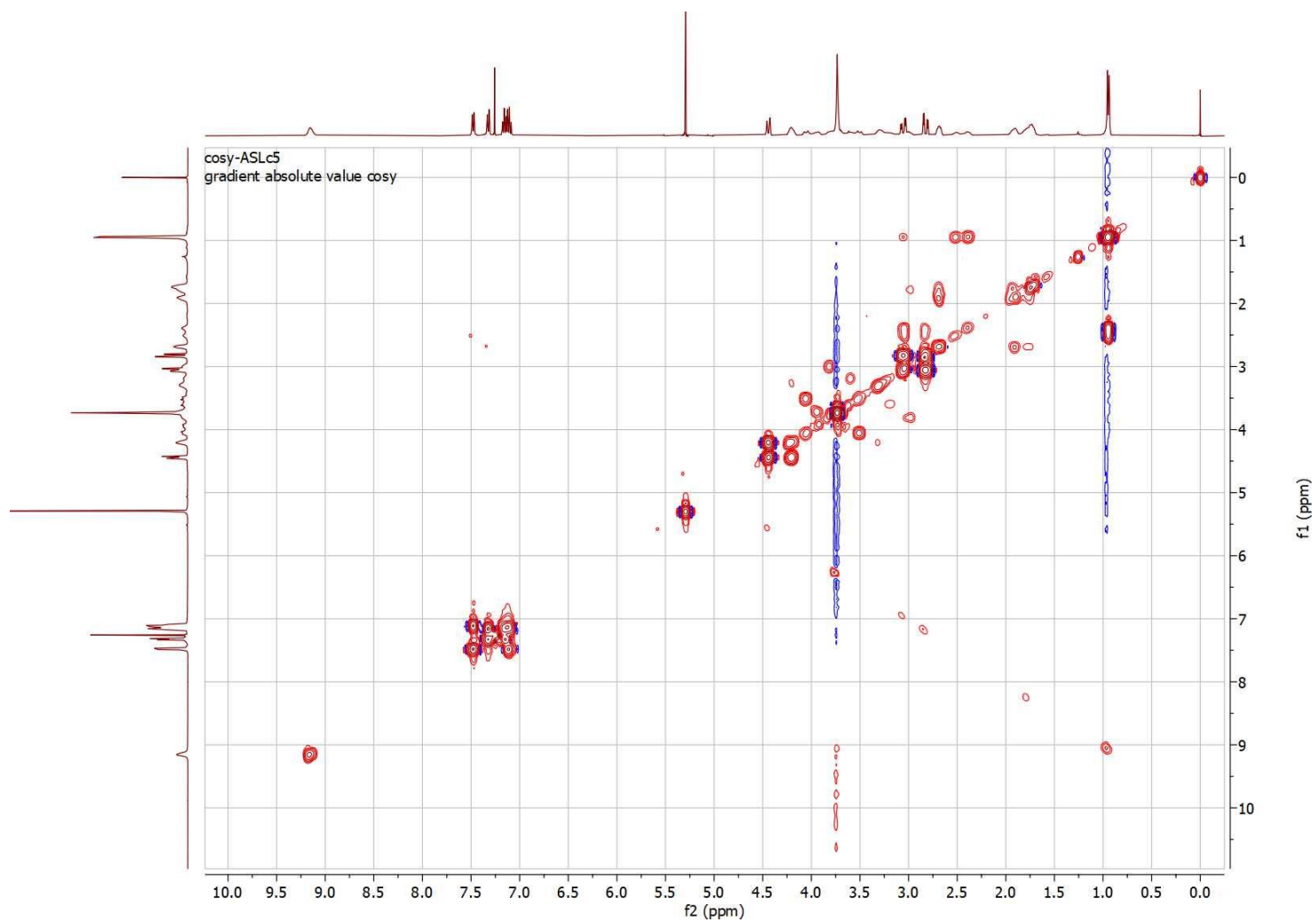


**Appendix 38: NOESY of schwarzificusine B (9)**

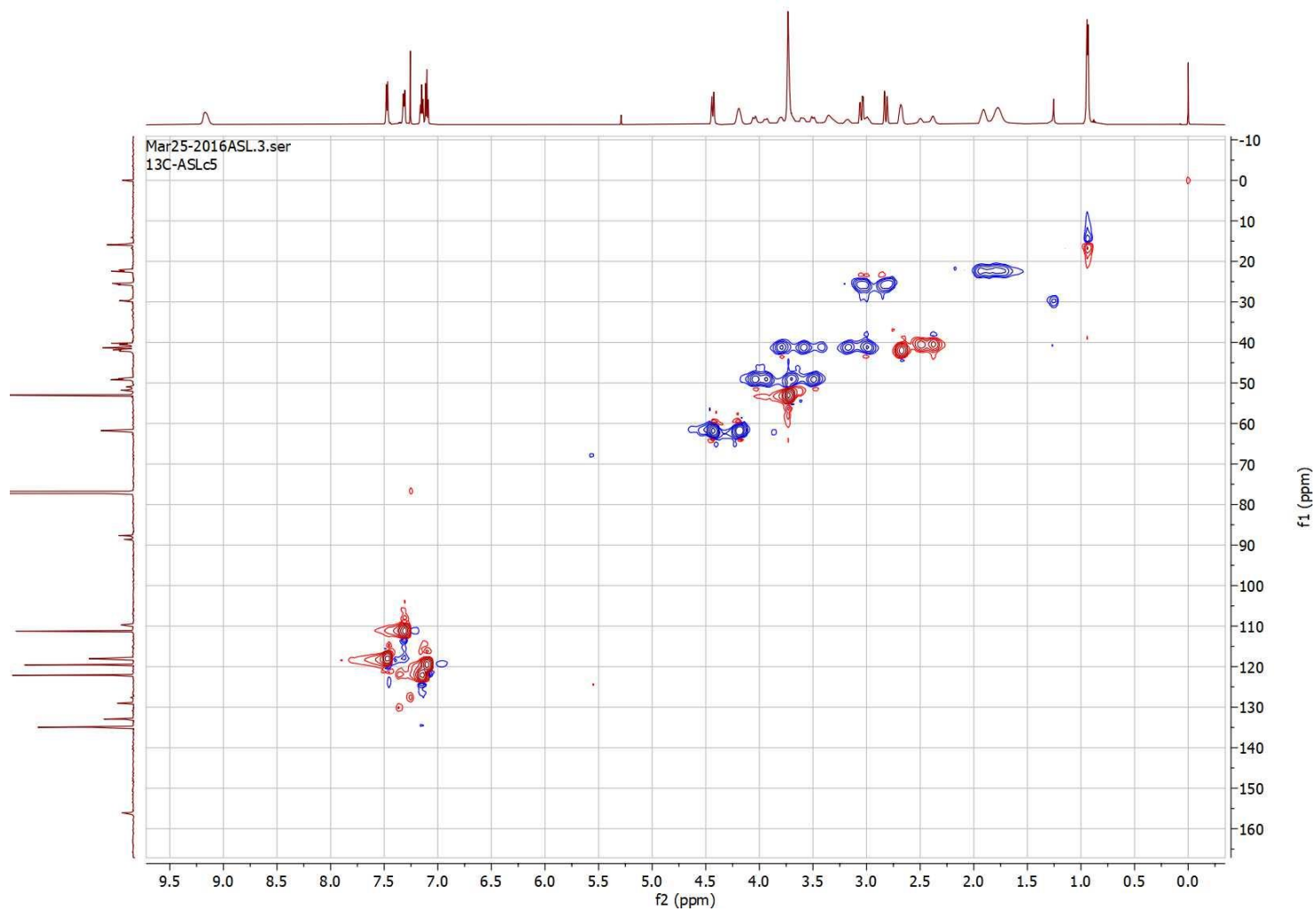


Mass	Intensity	Calc. Mass	Mass Difference (mmu)	Mass Difference (ppm)	Possible Formula
385.17750	109586.75	385.17635	1.15	2.99	$^{12}\text{C}_{21}\text{H}_{25}\text{N}_2\text{O}_5$
		385.17903	-1.53	-3.97	$^{12}\text{C}_{24}\text{H}_{23}\text{N}_3\text{O}_2$

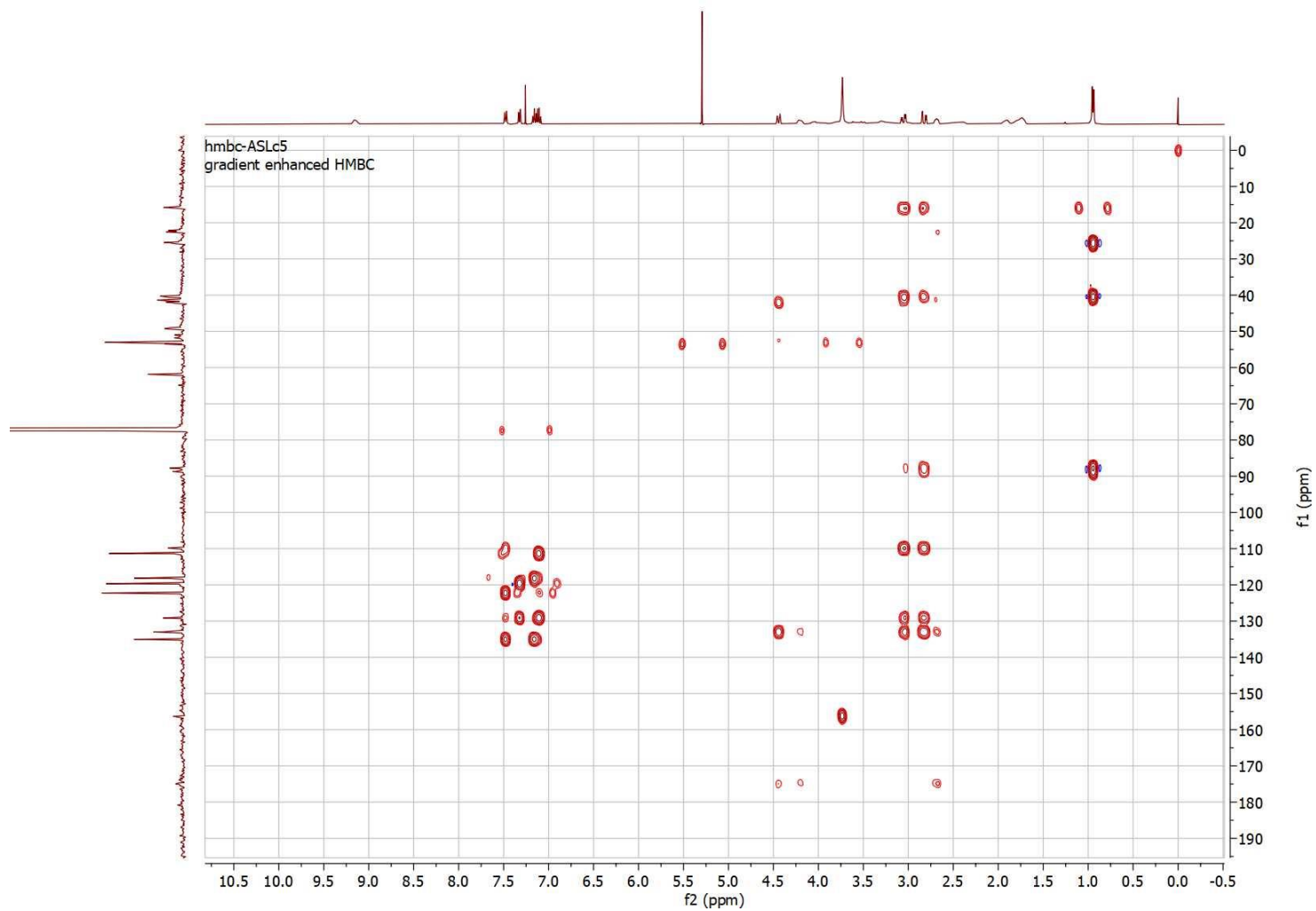
**Appendix 39: HR-DART-MS of alstoscholactine (10)**



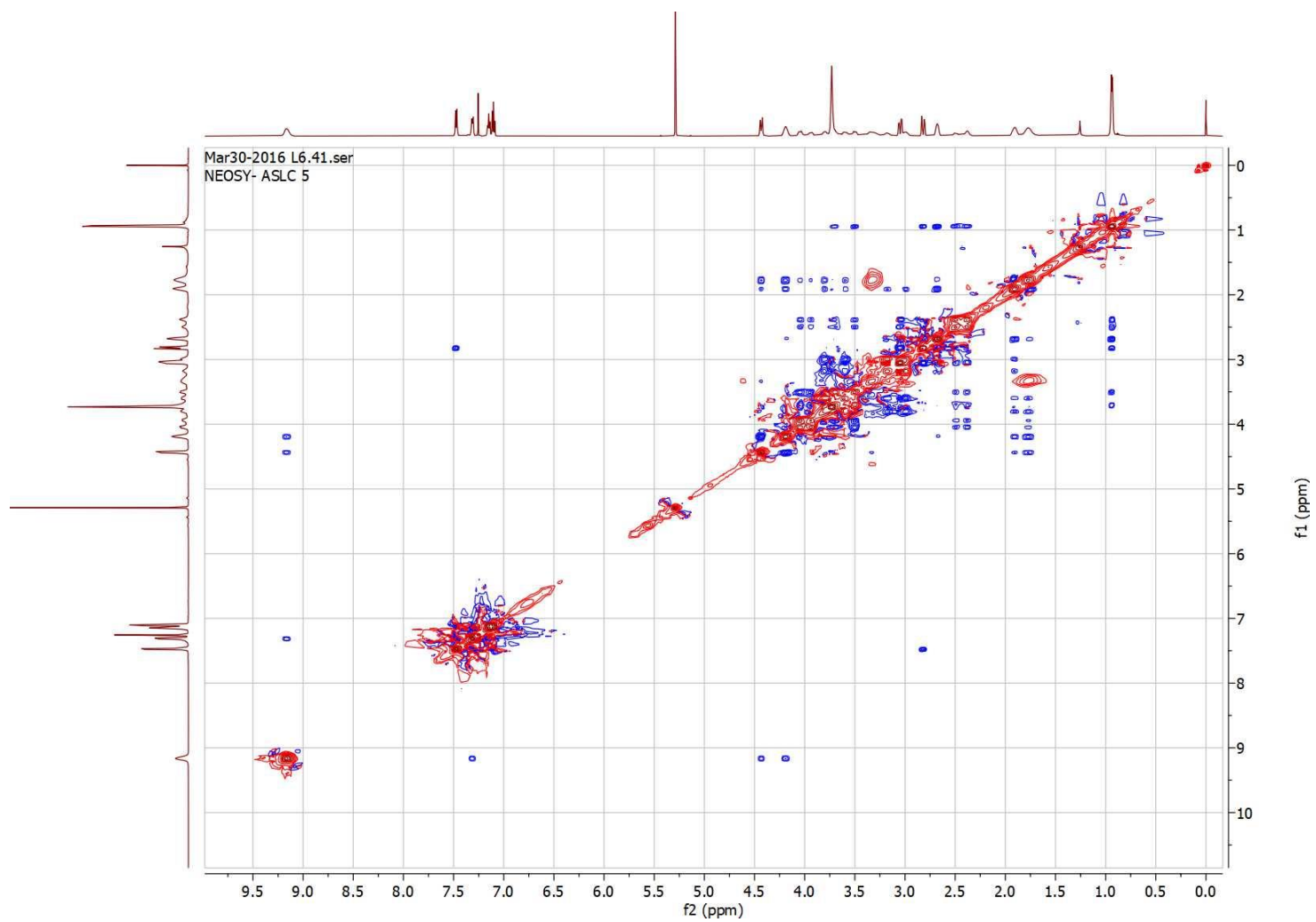
**Appendix 40: COSY of alstoscholactine (10)**



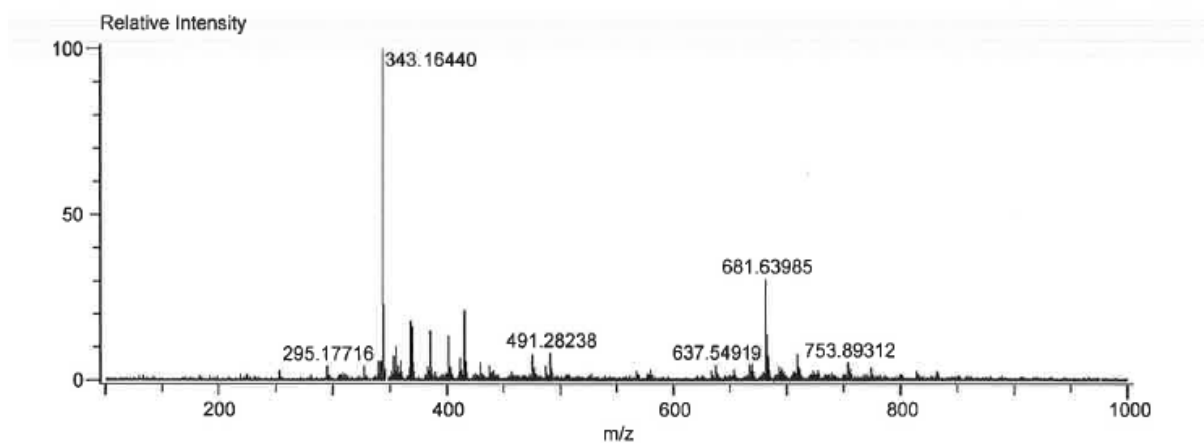
**Appendix 41: HSQC of alstoscholactone (10)**



**Appendix 42: HMBC of alstoscholactine (10)**

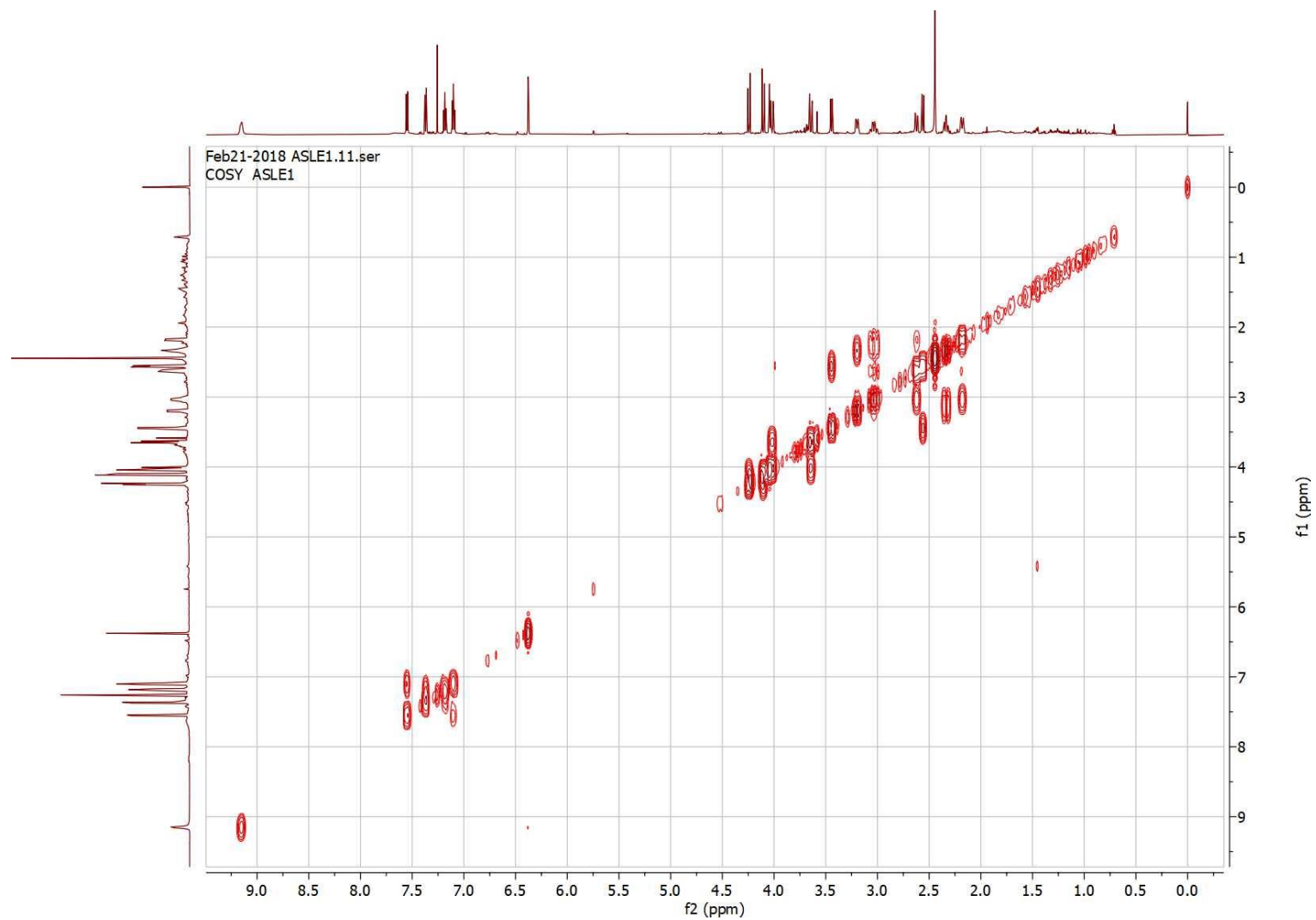


**Appendix 43: NOESY of alstoscholactine (10)**

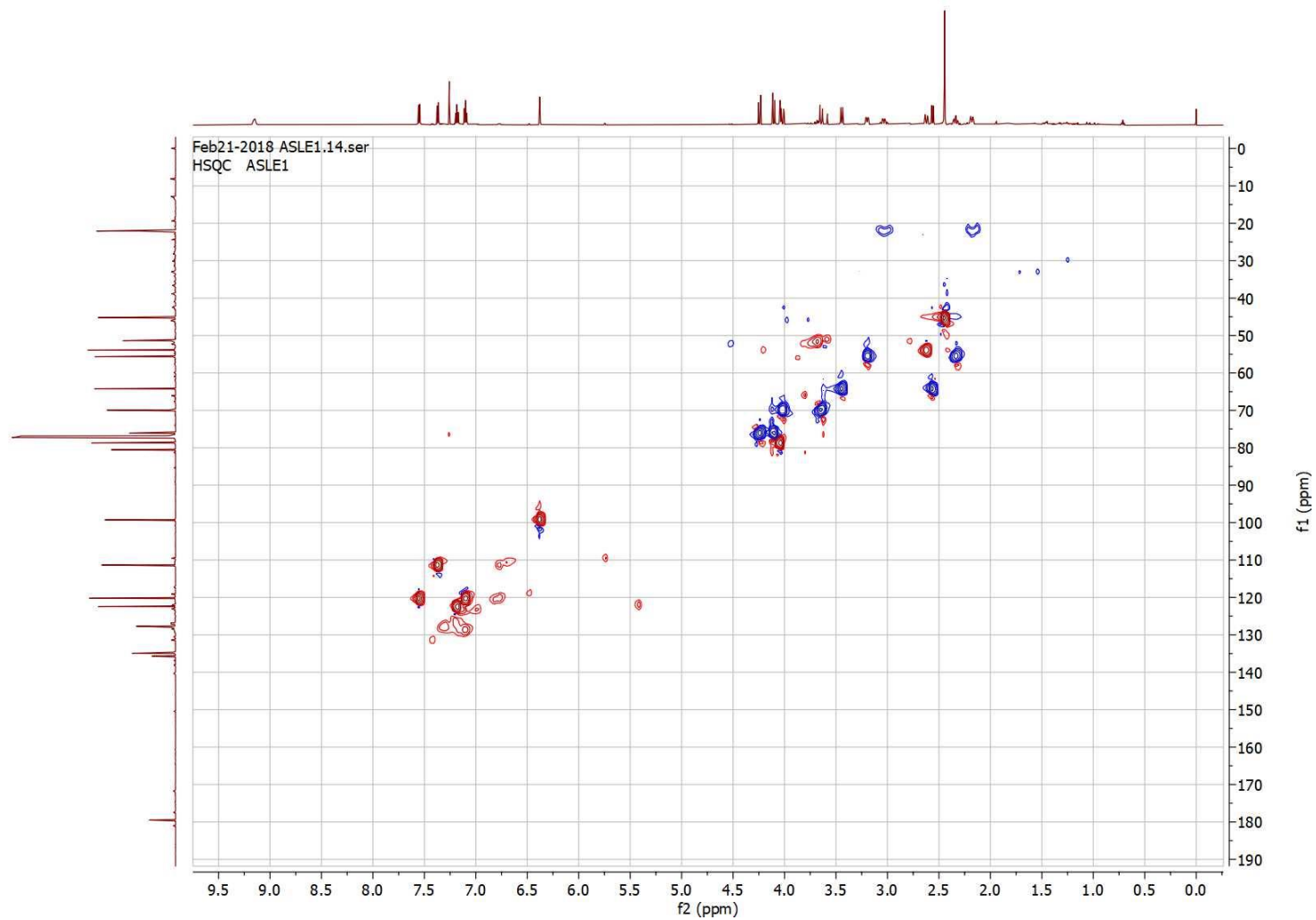


Mass	Intensity	Calc. Mass	Mass Difference (mmu)	Mass Difference (ppm)	Possible Formula
343.16440	48547.25	343.16444	-0.04	-0.11	$^{12}\text{C}_{17}^1\text{H}_{21}^{14}\text{N}_5^{16}\text{O}_3$
		343.16310	1.30	3.79	$^{12}\text{C}_{16}^1\text{H}_{25}^{14}\text{N}_1^{16}\text{O}_7$
		343.16578	-1.38	-4.02	$^{12}\text{C}_{19}^1\text{H}_{23}^{14}\text{N}_2^{16}\text{O}_4$
		343.16176	2.64	7.70	$^{12}\text{C}_{14}^1\text{H}_{23}^{14}\text{N}_4^{16}\text{O}_5$
		343.16846	-4.06	-11.83	$^{12}\text{C}_{22}^1\text{H}_{21}^{14}\text{N}_3^{16}\text{O}_1$
		343.16980	-5.40	-15.74	$^{12}\text{C}_{24}^1\text{H}_{23}^{16}\text{O}_2$
343.17031	-5.91	-17.22	$^{12}\text{C}_{10}^1\text{H}_{25}^{14}\text{N}_5^{16}\text{O}_8$		

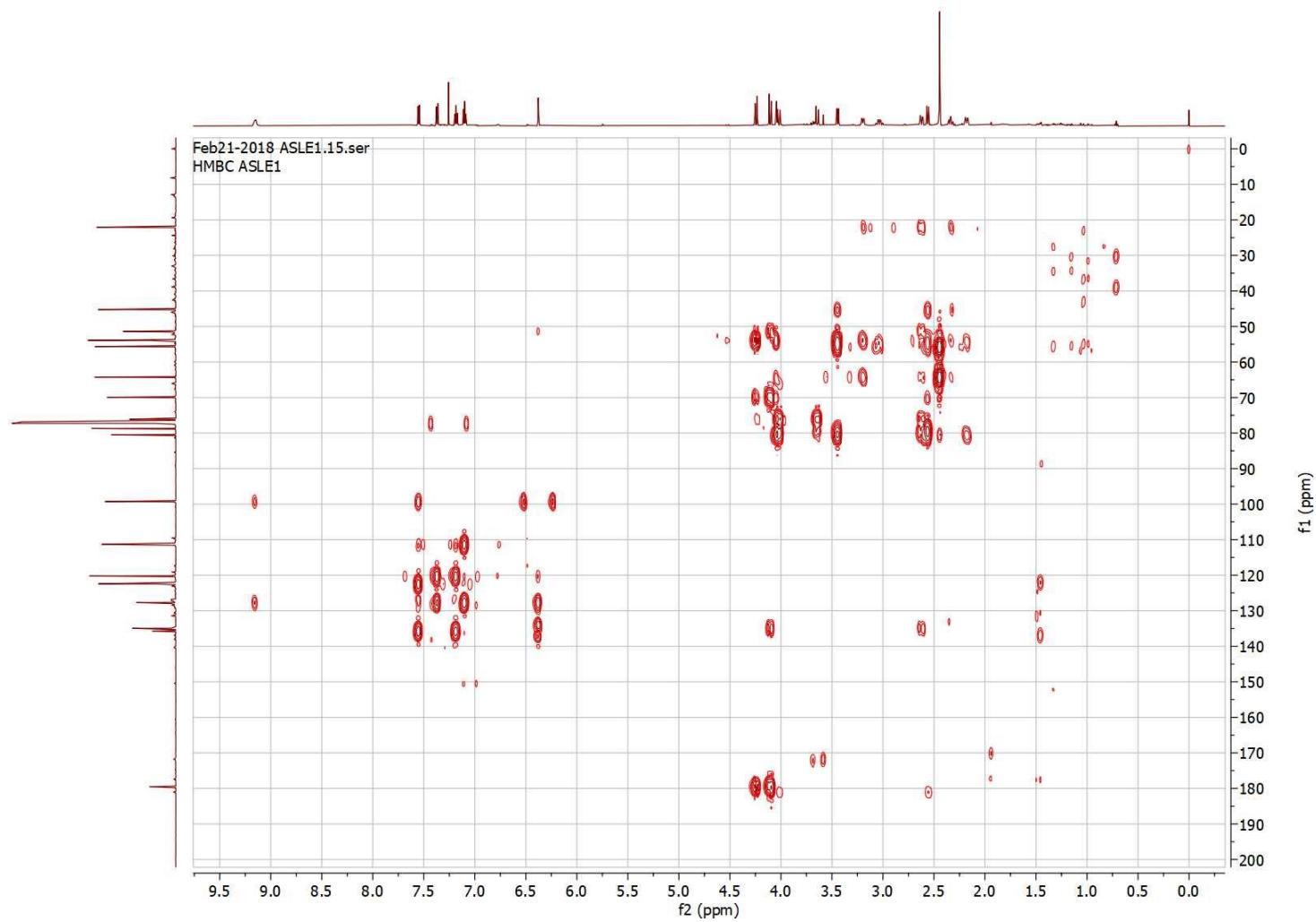
**Appendix 44:** HR-DART-MS of alstolaxepine (**11**)



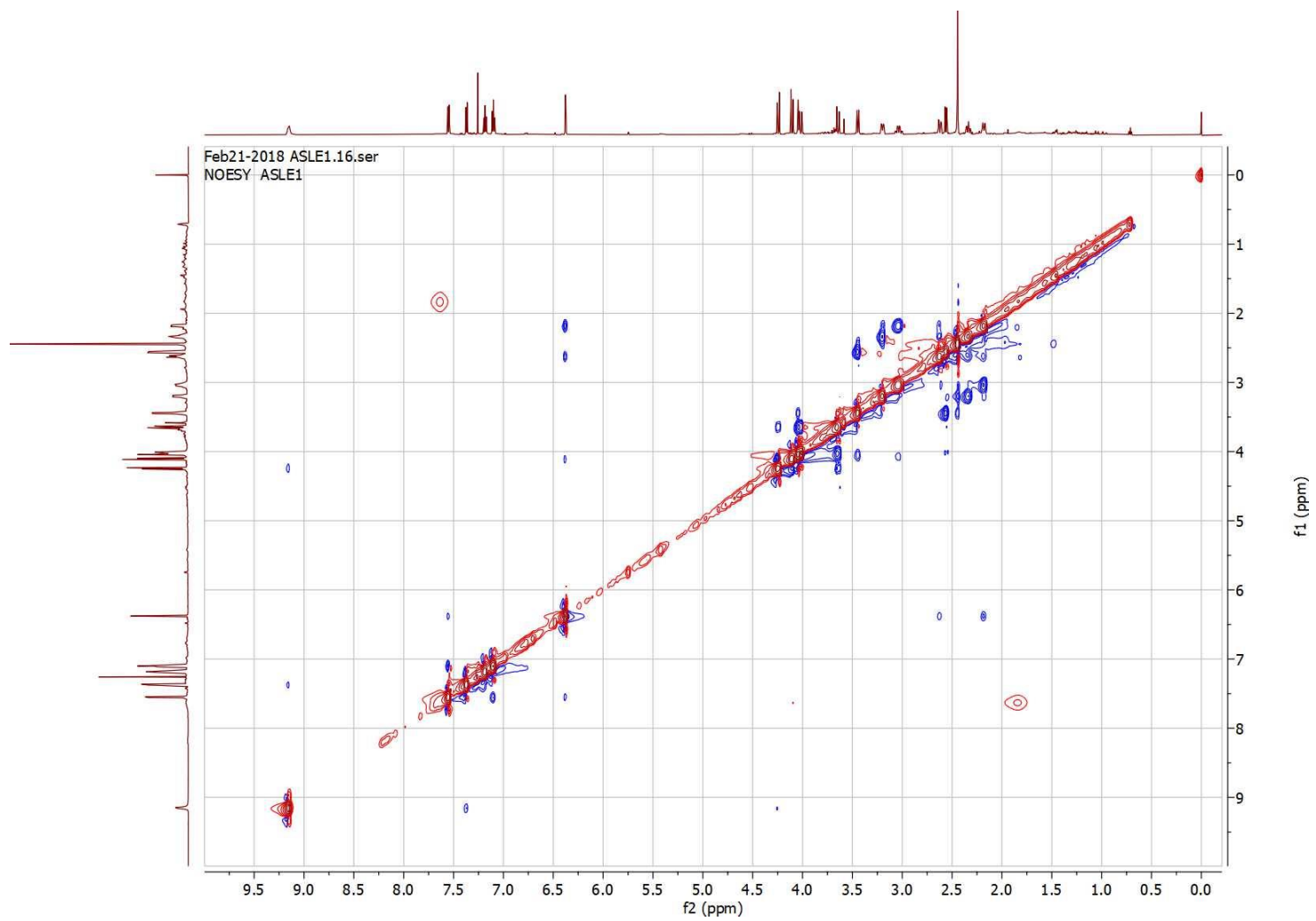
**Appendix 45: COSY of alstolaxepine (11)**



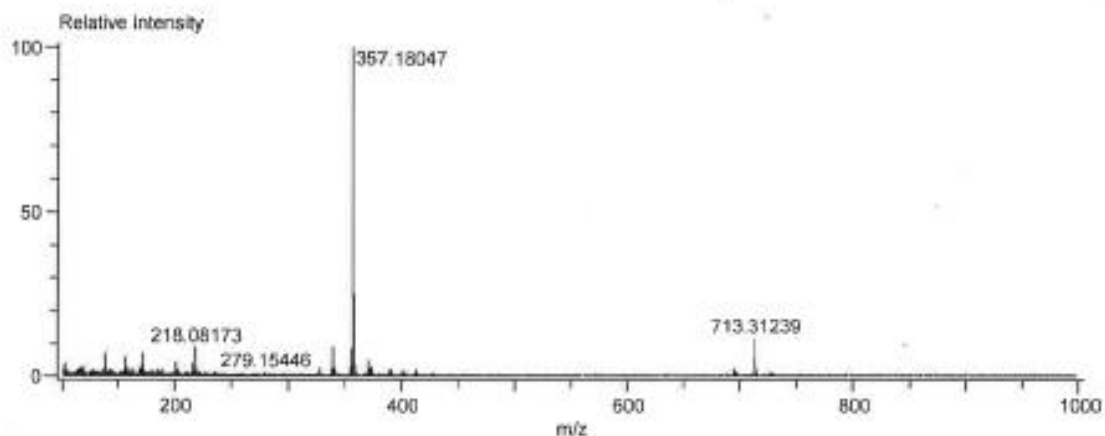
**Appendix 46: HSQC of alstolaxepine (11)**



**Appendix 47: HMBC of alstolaxepine (11)**

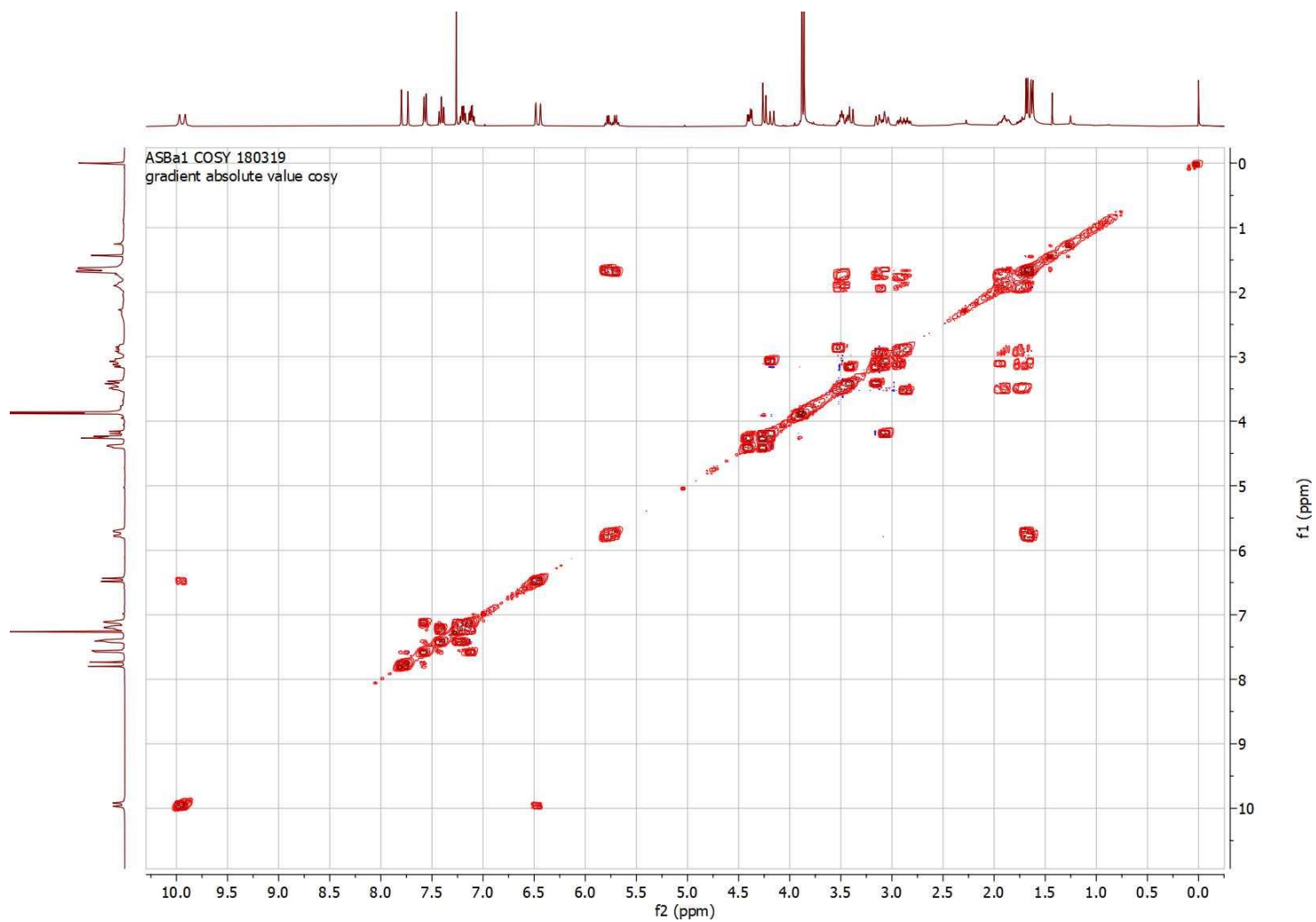


Appendix 48: NOESY of alstolaxepine (11)

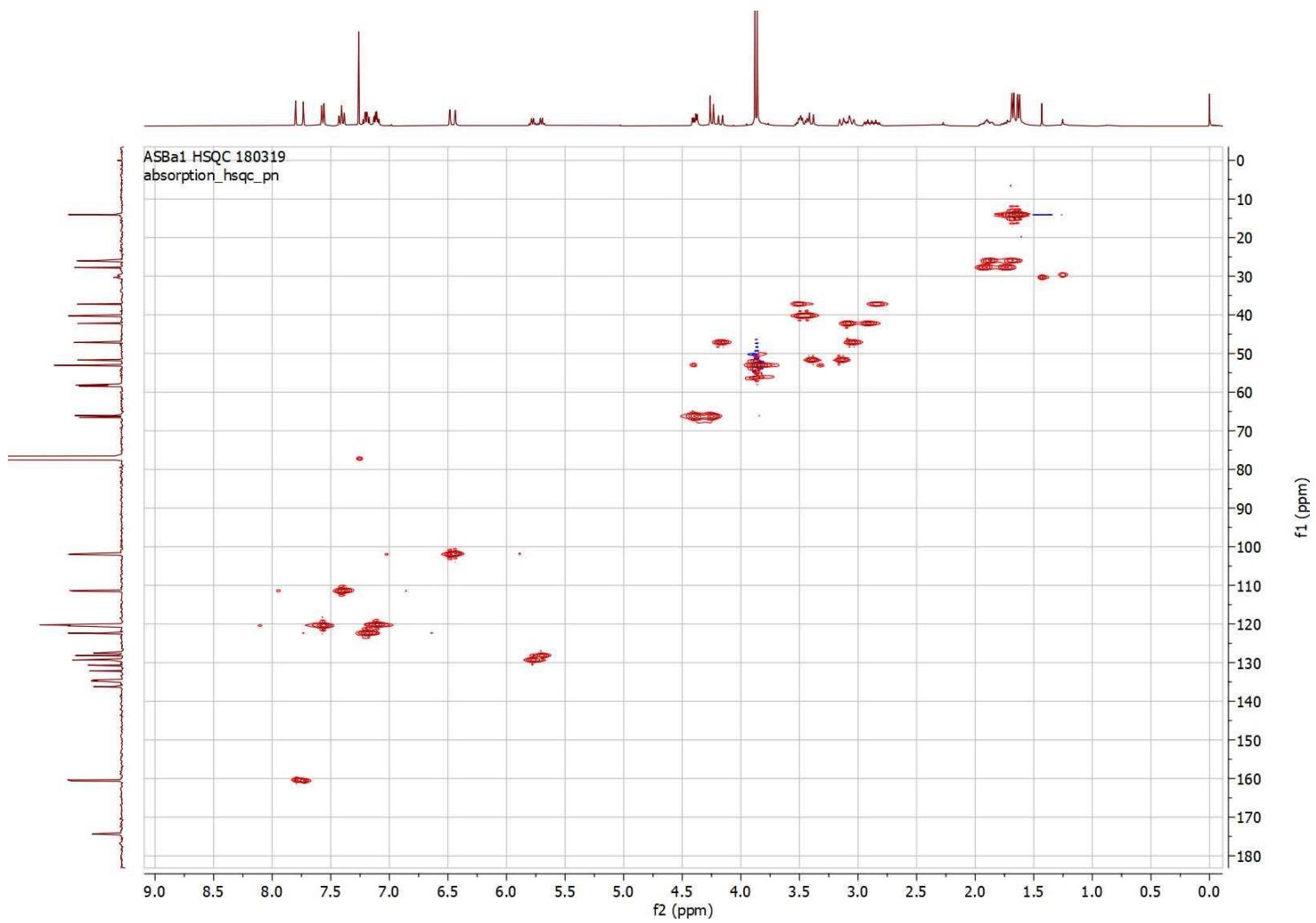


Mass	Intensity	Calc. Mass	Mass Difference (mmu)	Mass Difference (ppm)	Possible Formula
357.18047	115270.25	357.18059	-0.12	-0.33	<sup>12</sup> C <sub>3</sub> <sup>1</sup> H <sub>16</sub> <sup>14</sup> N <sub>17</sub> <sup>16</sup> O <sub>4</sub>
		357.18009	0.38	1.08	<sup>12</sup> C <sub>18</sub> <sup>1</sup> H <sub>21</sub> <sup>14</sup> N <sub>5</sub> <sup>16</sup> O <sub>5</sub>
		357.18143	-0.96	-2.68	<sup>12</sup> C <sub>22</sub> <sup>1</sup> H <sub>22</sub> <sup>14</sup> N <sub>2</sub> <sup>16</sup> O <sub>4</sub>
		357.17925	1.22	3.43	<sup>12</sup> C <sub>1</sub> <sup>1</sup> H <sub>17</sub> <sup>14</sup> N <sub>20</sub> <sup>16</sup> O <sub>3</sub>
		357.18193	-1.46	-4.09	<sup>12</sup> C <sub>5</sub> <sup>1</sup> H <sub>21</sub> <sup>14</sup> N <sub>14</sub> <sup>16</sup> O <sub>5</sub>
		357.17875	1.72	4.82	<sup>12</sup> C <sub>17</sub> <sup>1</sup> H <sub>21</sub> <sup>14</sup> N <sub>1</sub> <sup>16</sup> O <sub>7</sub>
		357.17875	1.73	4.84	<sup>12</sup> C <sub>16</sub> <sup>1</sup> H <sub>21</sub> <sup>14</sup> N <sub>6</sub> <sup>16</sup> O <sub>2</sub>
		357.18277	-2.30	-6.43	<sup>12</sup> C <sub>21</sub> <sup>1</sup> H <sub>21</sub> <sup>14</sup> N <sub>6</sub>
		357.18327	-2.80	-7.83	<sup>12</sup> C <sub>5</sub> <sup>1</sup> H <sub>17</sub> <sup>14</sup> N <sub>16</sub> <sup>16</sup> O <sub>1</sub>
		357.18328	-2.80	-7.85	<sup>12</sup> C <sub>7</sub> <sup>1</sup> H <sub>23</sub> <sup>14</sup> N <sub>1</sub> <sup>16</sup> O <sub>5</sub>
		357.17741	3.06	8.58	<sup>12</sup> C <sub>15</sub> <sup>1</sup> H <sub>25</sub> <sup>14</sup> N <sub>4</sub> <sup>16</sup> O <sub>5</sub>
		357.17740	3.07	8.59	<sup>12</sup> C <sub>14</sub> <sup>1</sup> H <sub>19</sub> <sup>14</sup> N <sub>11</sub> <sup>16</sup> O <sub>3</sub>
		357.18411	-3.64	-10.18	<sup>12</sup> C <sub>23</sub> <sup>1</sup> H <sub>23</sub> <sup>14</sup> N <sub>5</sub> <sup>16</sup> O <sub>1</sub>
		357.18461	-4.14	-11.59	<sup>12</sup> C <sub>8</sub> <sup>1</sup> H <sub>16</sub> <sup>14</sup> N <sub>10</sub> <sup>16</sup> O <sub>3</sub>
		357.18462	-4.15	-11.81	<sup>12</sup> C <sub>6</sub> <sup>1</sup> H <sub>25</sub> <sup>14</sup> N <sub>6</sub> <sup>16</sup> O <sub>7</sub>
		357.17607	4.40	12.33	<sup>12</sup> C <sub>14</sub> <sup>1</sup> H <sub>29</sub> <sup>16</sup> O <sub>10</sub>
		357.17607	4.41	12.34	<sup>12</sup> C <sub>13</sub> <sup>1</sup> H <sub>23</sub> <sup>14</sup> N <sub>1</sub> <sup>16</sup> O <sub>5</sub>
		357.17606	4.41	12.35	<sup>12</sup> C <sub>12</sub> <sup>1</sup> H <sub>17</sub> <sup>14</sup> N <sub>14</sub>
		357.18545	-4.98	-13.94	<sup>12</sup> C <sub>25</sub> <sup>1</sup> H <sub>25</sub> <sup>16</sup> O <sub>2</sub>
		357.18596	-5.48	-15.35	<sup>12</sup> C <sub>13</sub> <sup>1</sup> H <sub>21</sub> <sup>14</sup> N <sub>12</sub> <sup>16</sup> O <sub>3</sub>
		357.18596	-5.49	-15.37	<sup>12</sup> C <sub>11</sub> <sup>1</sup> H <sub>27</sub> <sup>14</sup> N <sub>6</sub> <sup>16</sup> O <sub>8</sub>
		357.17473	5.74	16.08	<sup>12</sup> C <sub>12</sub> <sup>1</sup> H <sub>27</sub> <sup>14</sup> N <sub>5</sub> <sup>16</sup> O <sub>5</sub>
		357.17472	5.75	16.10	<sup>12</sup> C <sub>11</sub> <sup>1</sup> H <sub>21</sub> <sup>14</sup> N <sub>10</sub> <sup>16</sup> O <sub>4</sub>
		357.18730	-6.83	-19.11	<sup>12</sup> C <sub>12</sub> <sup>1</sup> H <sub>23</sub> <sup>14</sup> N <sub>6</sub> <sup>16</sup> O <sub>4</sub>
357.18730	-6.83	-19.12	<sup>12</sup> C <sub>13</sub> <sup>1</sup> H <sub>29</sub> <sup>14</sup> N <sub>2</sub> <sup>16</sup> O <sub>9</sub>		
357.17339	7.09	19.84	<sup>12</sup> C <sub>10</sub> <sup>1</sup> H <sub>25</sub> <sup>14</sup> N <sub>6</sub> <sup>16</sup> O <sub>8</sub>		
357.17338	7.09	19.86	<sup>12</sup> C <sub>9</sub> <sup>1</sup> H <sub>19</sub> <sup>14</sup> N <sub>13</sub> <sup>16</sup> O <sub>3</sub>		
713.31239	13205.93	713.31245	-0.06	-0.09	<sup>12</sup> C <sub>30</sub> <sup>1</sup> H <sub>43</sub> <sup>14</sup> N <sub>17</sub> <sup>16</sup> O <sub>18</sub>
		713.31195	0.44	0.62	<sup>12</sup> C <sub>31</sub> <sup>1</sup> H <sub>47</sub> <sup>14</sup> N <sub>8</sub> <sup>16</sup> O <sub>14</sub>
		713.31194	0.45	0.62	<sup>12</sup> C <sub>20</sub> <sup>1</sup> H <sub>41</sub> <sup>14</sup> N <sub>12</sub> <sup>16</sup> O <sub>9</sub>
		713.31194	0.45	0.63	<sup>12</sup> C <sub>29</sub> <sup>1</sup> H <sub>35</sub> <sup>14</sup> N <sub>19</sub> <sup>16</sup> O <sub>4</sub>
		713.31328	-0.88	-1.25	<sup>12</sup> C <sub>31</sub> <sup>1</sup> H <sub>37</sub> <sup>14</sup> N <sub>15</sub> <sup>16</sup> O <sub>5</sub>
		713.31329	-0.90	-1.26	<sup>12</sup> C <sub>32</sub> <sup>1</sup> H <sub>43</sub> <sup>14</sup> N <sub>6</sub> <sup>16</sup> O <sub>10</sub>
713.31329	-0.90	-1.26	<sup>12</sup> C <sub>33</sub> <sup>1</sup> H <sub>49</sub> <sup>14</sup> N <sub>2</sub> <sup>16</sup> O <sub>15</sub>		

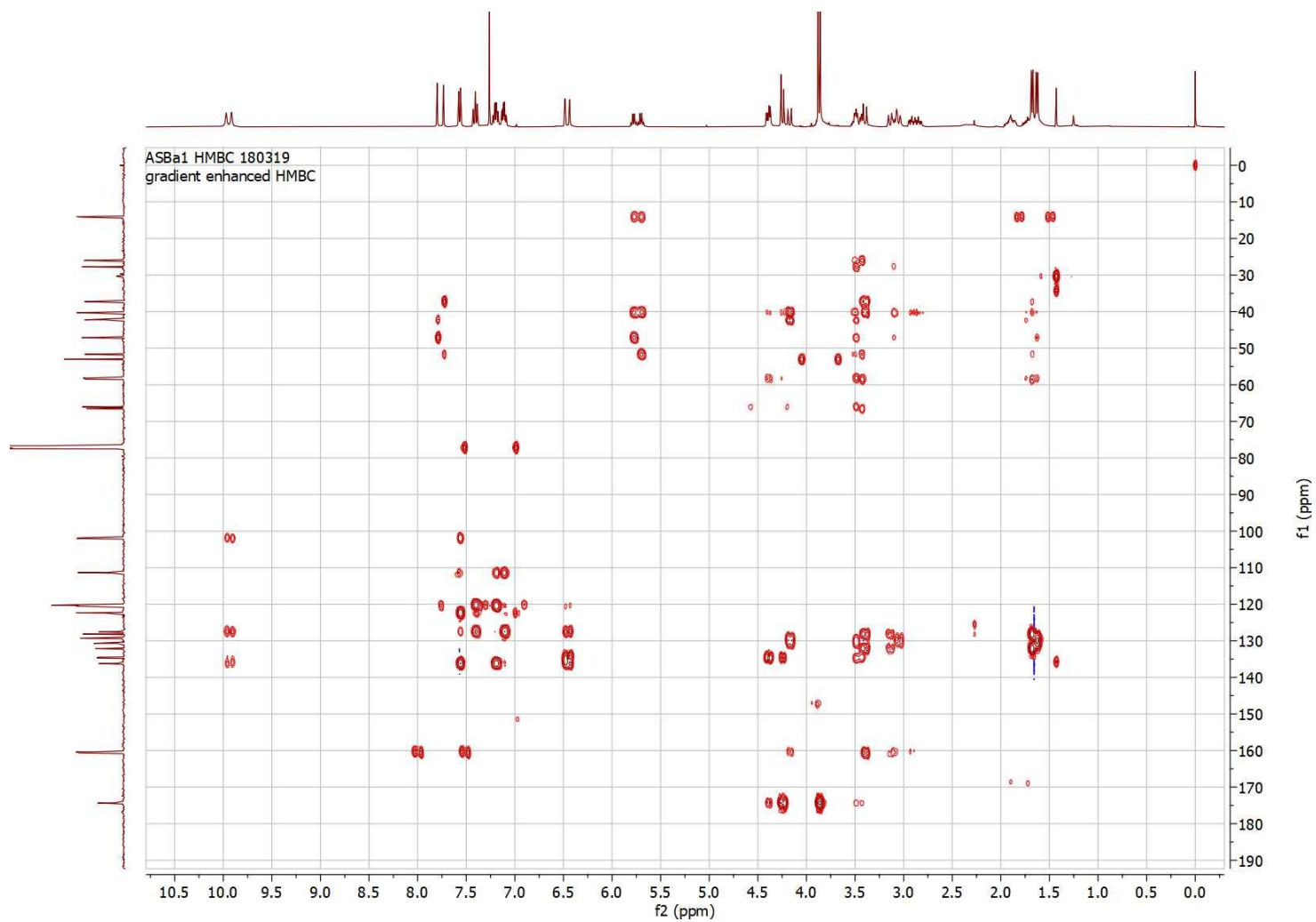
Appendix 49: HR-DART-MS of *N*-formyllynnanensine (12)



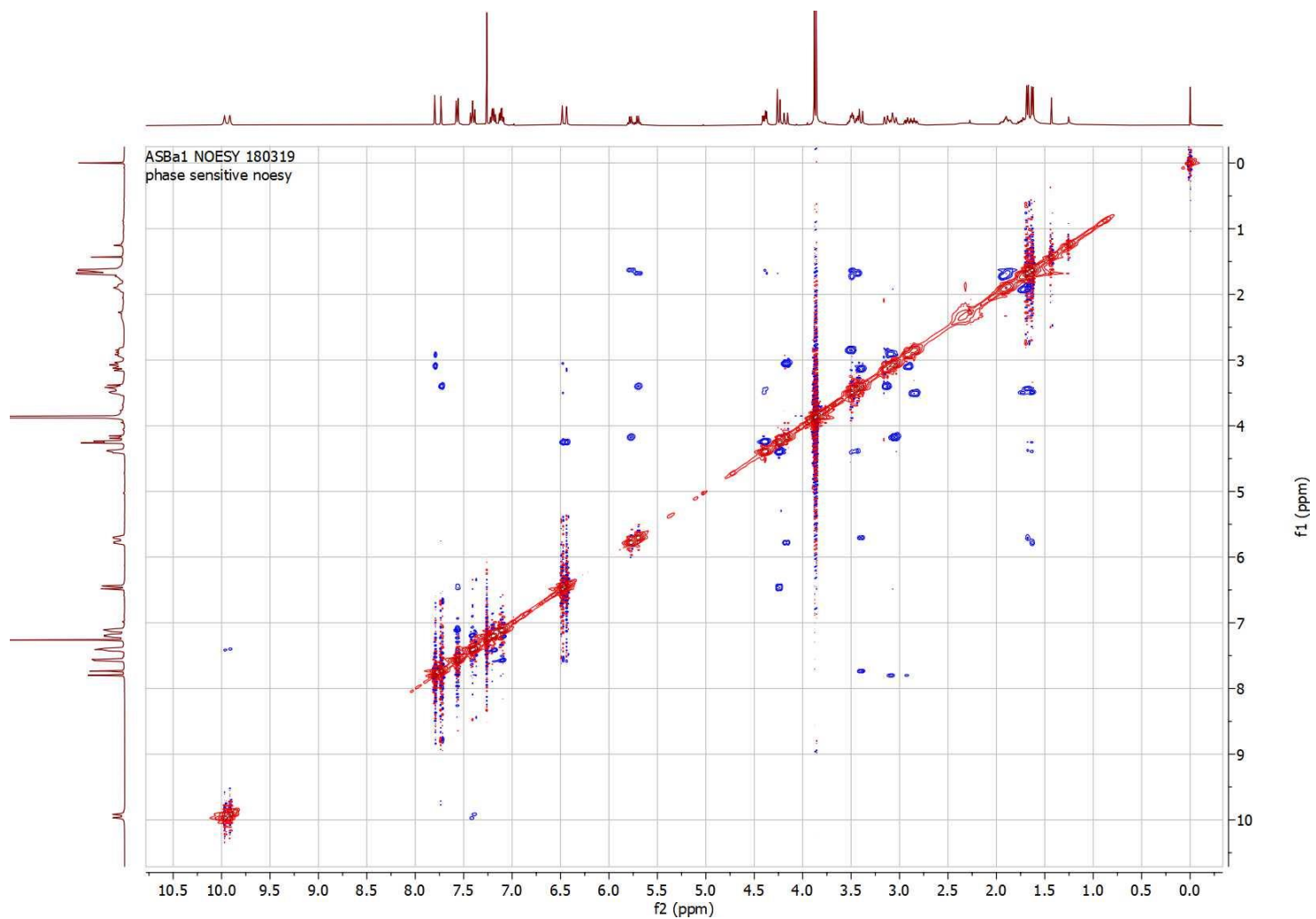
**Appendix 50:** COSY of *N*-formilyunnanensine (**12**)



**Appendix 51:** HSQC of *N*-formylyunnanensine (**12**)

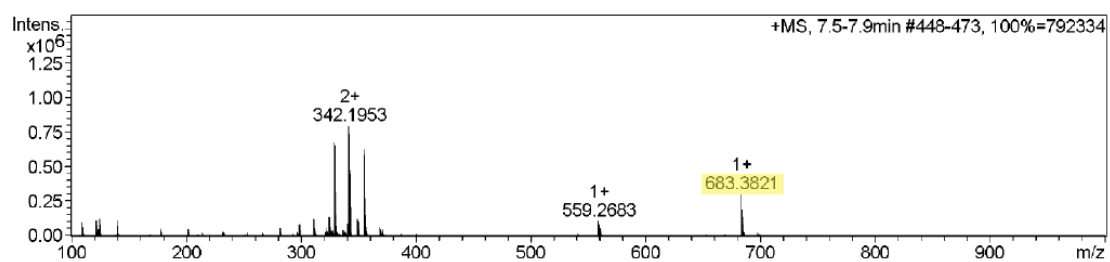


**Appendix 52:** HMBC of *N*-formilyunnanensine (**12**)

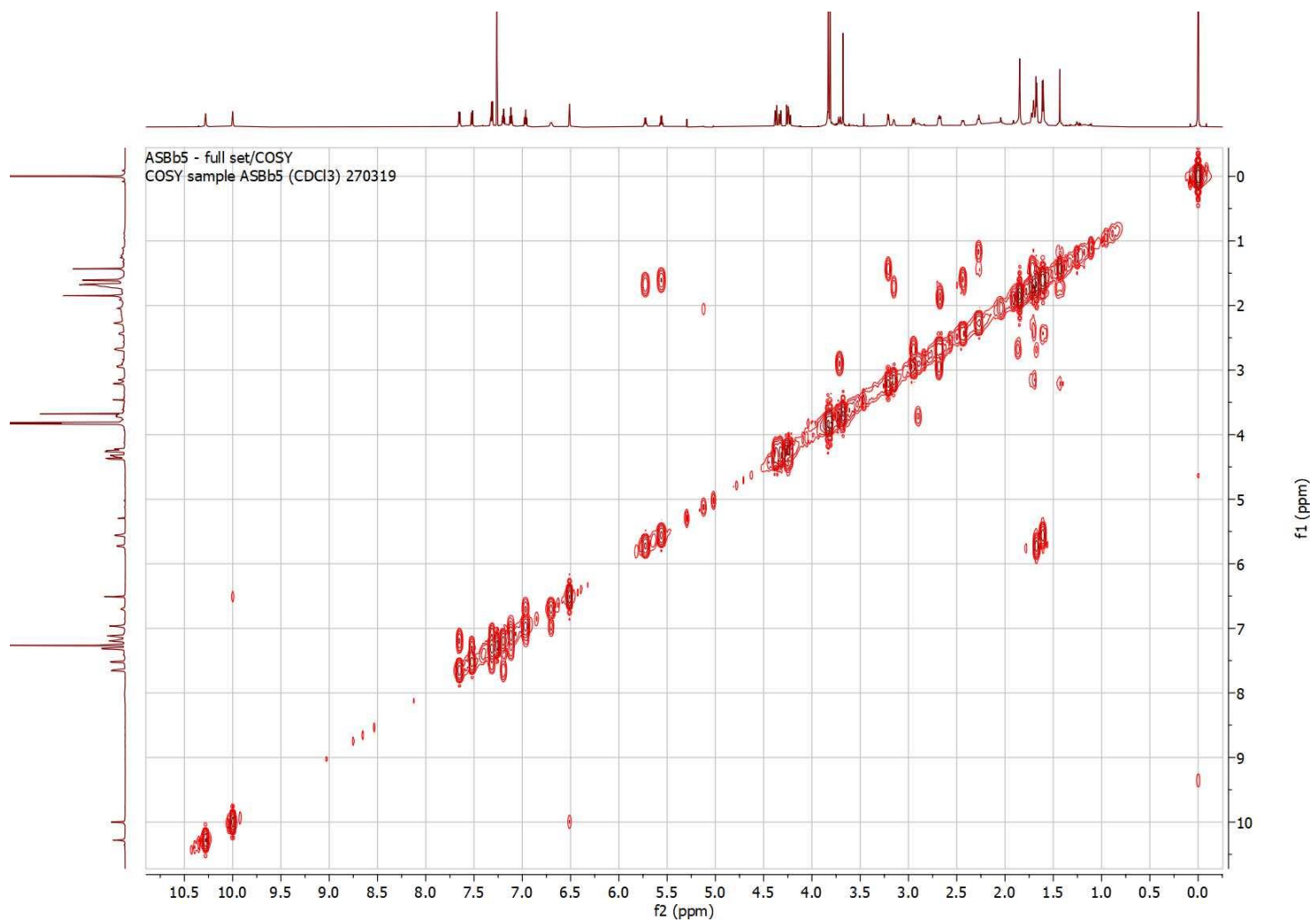


**Appendix 53:** NOESY of *N*-formylunnannensine (**12**)

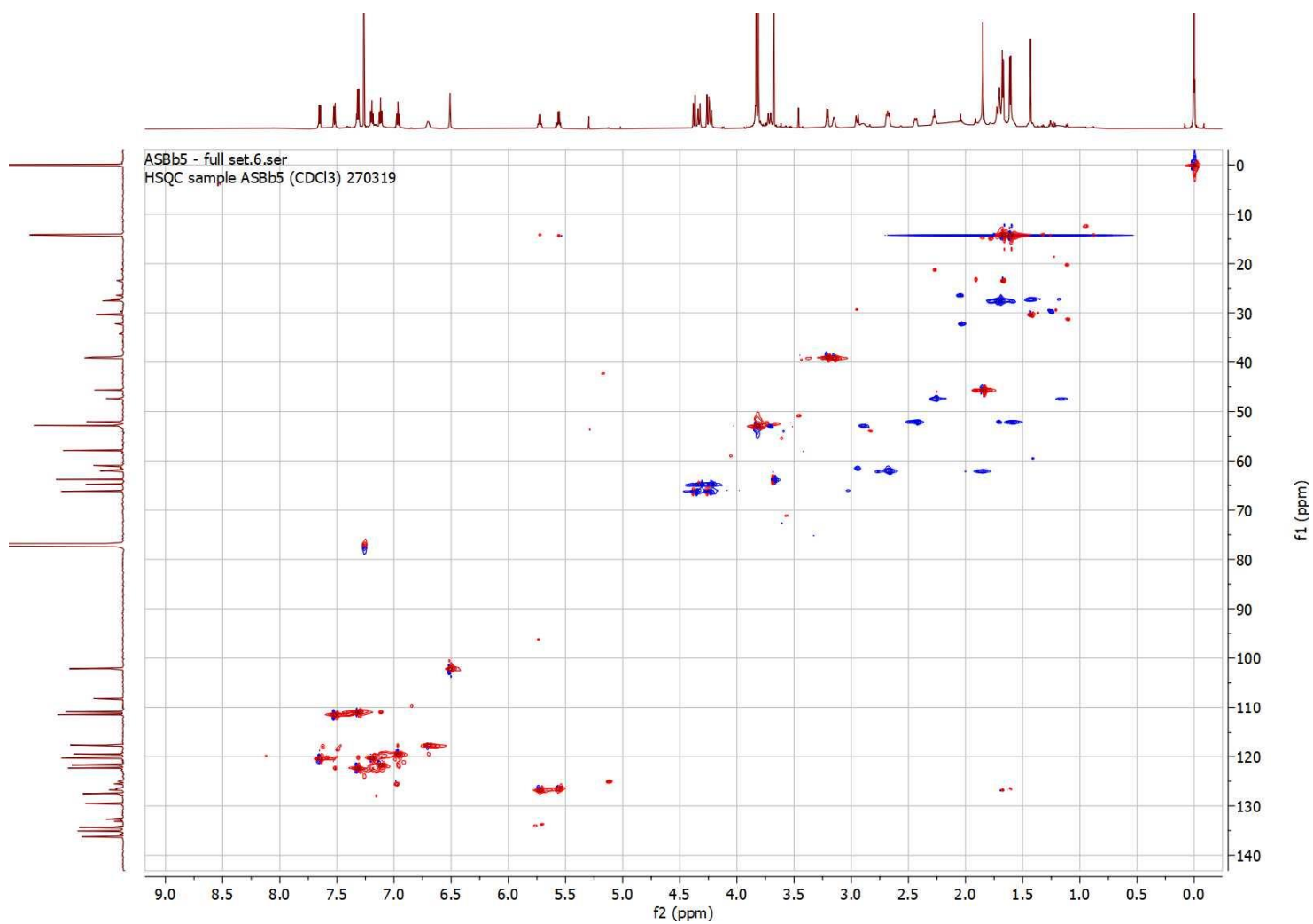
ASBb5



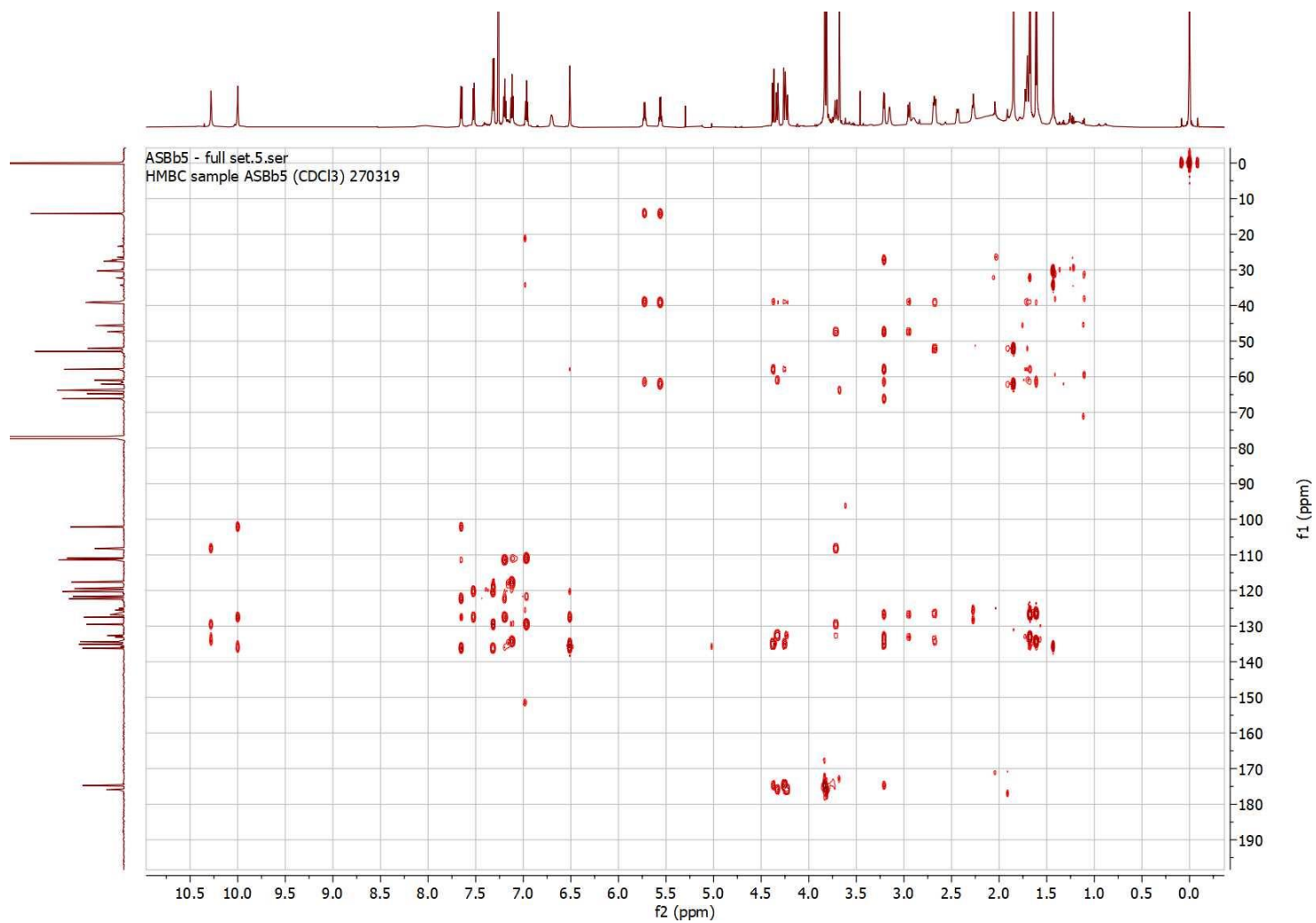
**Appendix 54: HR-ESI-MS of scholaphylline (13)**



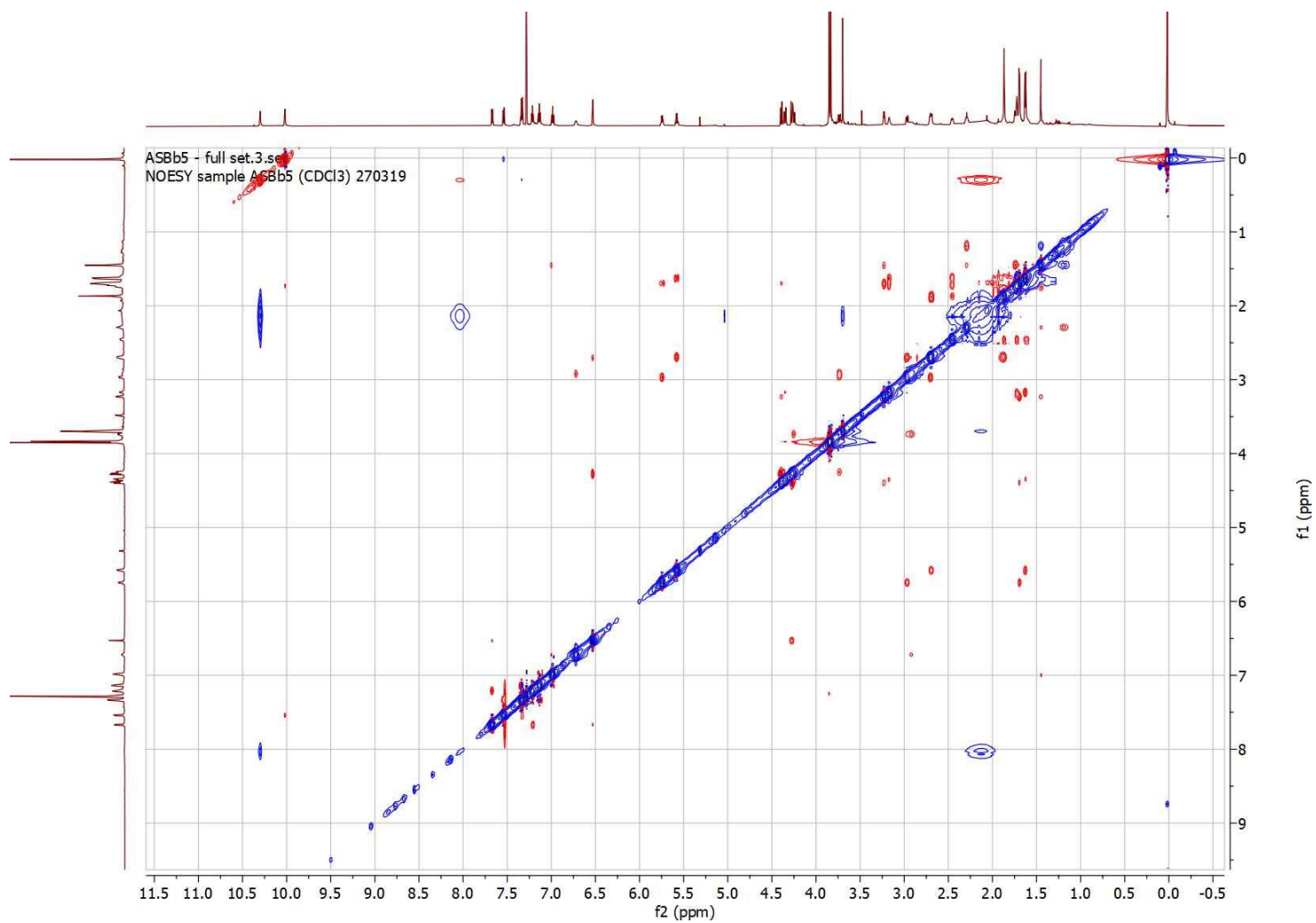
**Appendix 55: COSY of scholaphylline (13)**



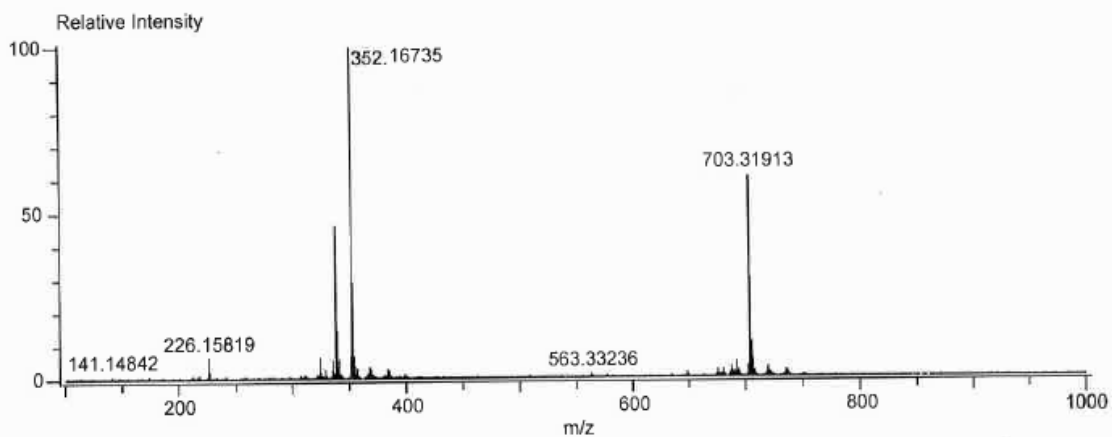
**Appendix 56: HSQC of scholaphylline (13)**



**Appendix 57: HMBC of scholaphylline (13)**

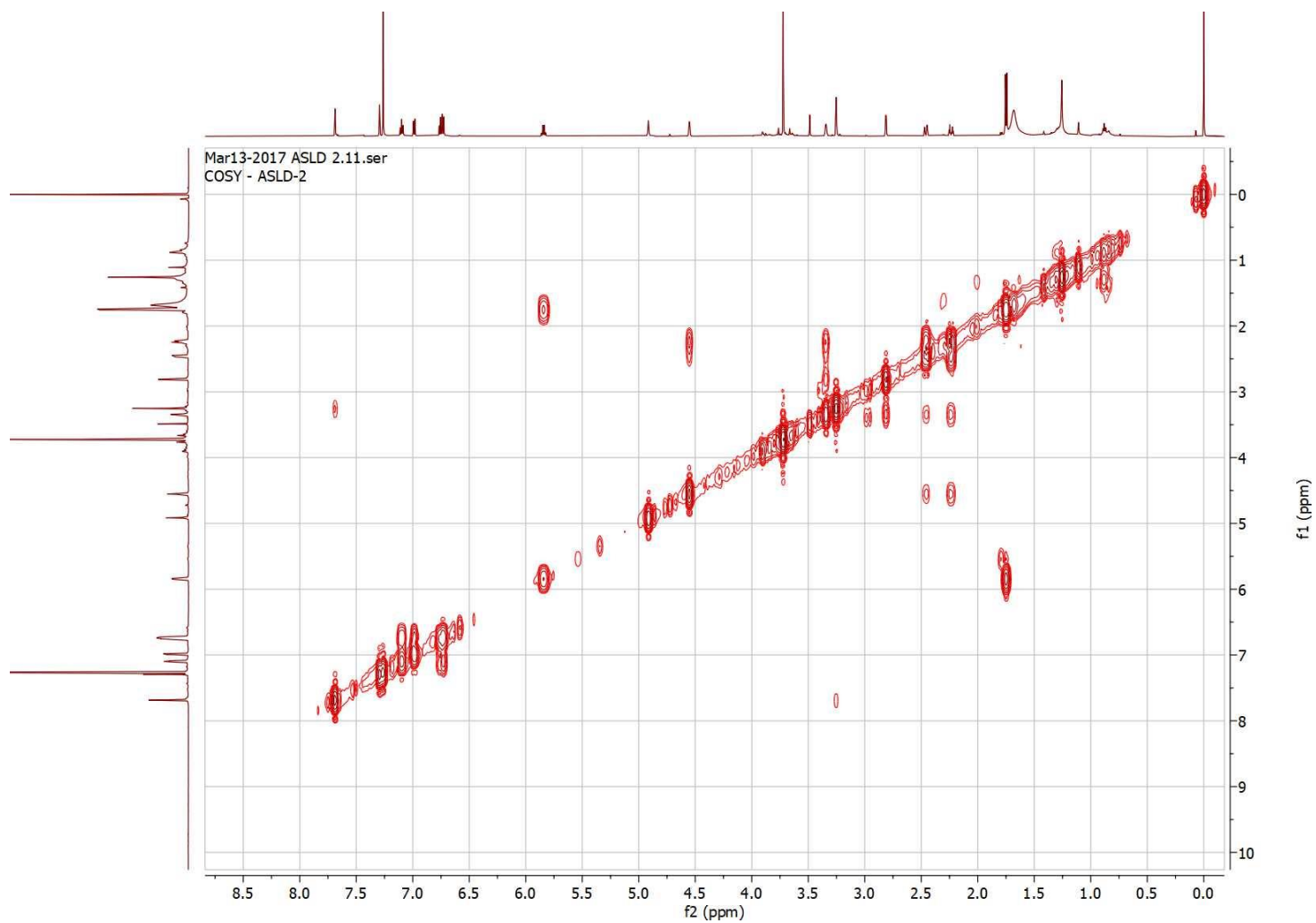


**Appendix 58: NOESY of scholaphylline (13)**

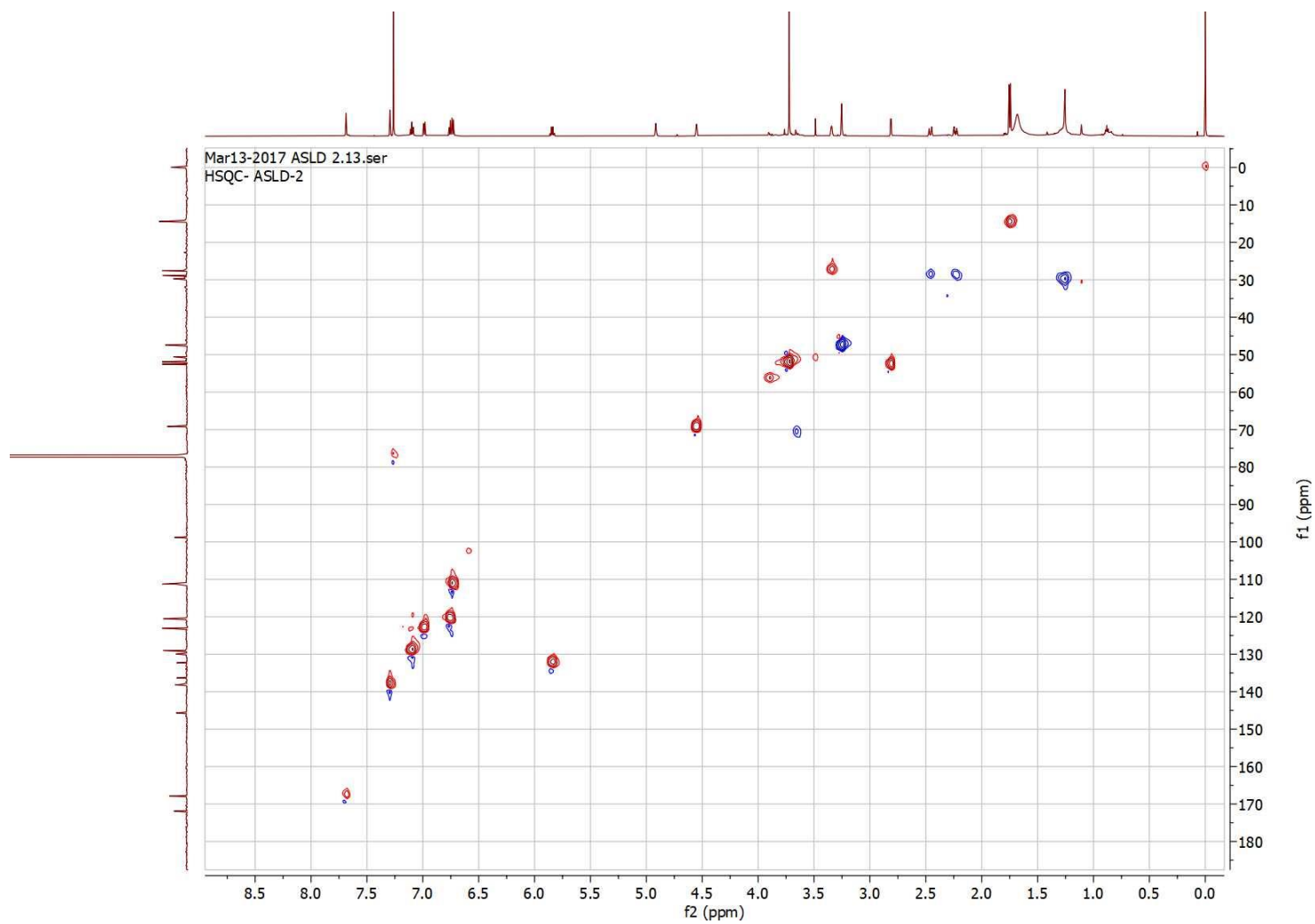


Mass	Intensity	Calc. Mass	Mass Difference (mmu)	Mass Difference (ppm)	Possible Formula
352.16735	169010.75	352.16746	-0.11	-0.30	$^{12}\text{C}_{22}\text{H}_{24}\text{N}_3\text{O}_4$
		352.16612	1.24	3.51	$^{12}\text{C}_{20}\text{H}_{22}\text{N}_3\text{O}_3$
		352.16880	-1.44	-4.10	$^{12}\text{C}_{23}\text{H}_{20}\text{N}_4$
		352.17014	-2.79	-7.92	$^{12}\text{C}_{25}\text{H}_{22}\text{N}_1\text{O}_1$

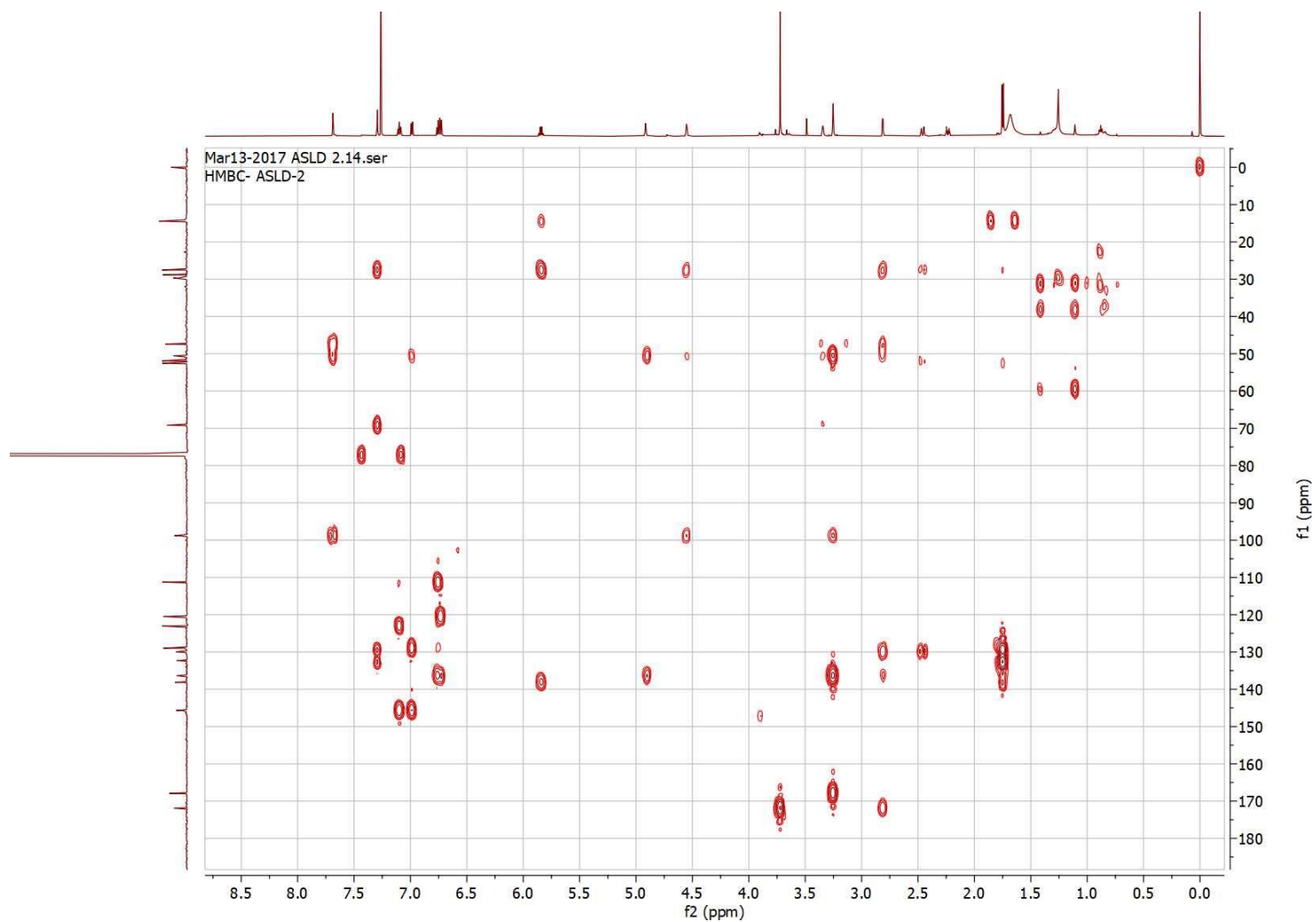
**Appendix 59:** HR-DART-MS of alstobrogaline (**19**)



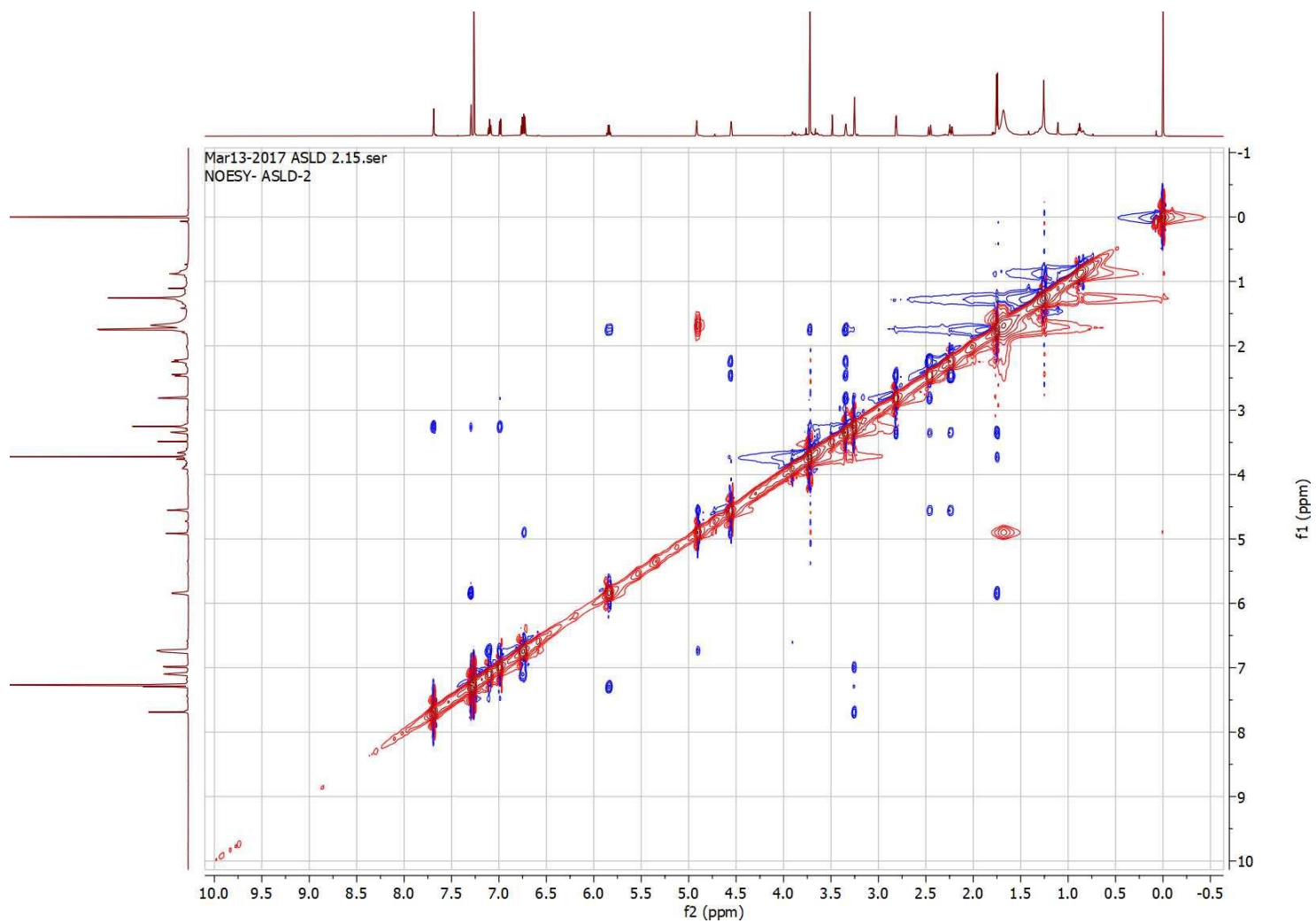
**Appendix 60:** COSY of alstobrogaline (**19**)



**Appendix 61: HSQC of alstobrogaline (19)**



Appendix 62: HMBC of alstobrogaline (19)



Appendix 63: NOESY of alstobrogaline (19)

## Schwarzinincines A–G, 1,4-Diarylbutanoid–Phenethylamine Conjugates from the Leaves of *Ficus schwarzii*

Premanand Krishnan, Fong-Kai Lee, Veronica Alicia Yap, Yun-Yee Low, Toh-Seok Kam, Kien-Thai Yong, Kang-Nee Ting, and Kuan-Hon Lim\*

Cite This: <https://dx.doi.org/10.1021/acs.jnatprod.9b01160>

Read Online

ACCESS |

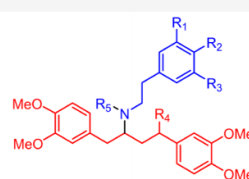
Metrics & More

Article Recommendations

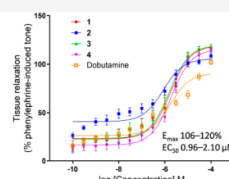
Supporting Information



*Ficus schwarzii*



Schwarzinincines A–G (1–7)



Vasorelaxant activity

**ABSTRACT:** Schwarzinincines A–G (1–7), representing the first examples of 1,4-diarylbutanoid–phenethylamine conjugates, were isolated from the leaves of *Ficus schwarzii*. The structures of these compounds were determined by detailed analysis of their MS, 1D and 2D NMR data. Compounds 1–4 exhibited pronounced vasorelaxant effects in the rat isolated aorta ( $E_{\max}$  106–120%;  $EC_{50}$  0.96–2.10  $\mu$ M). However, compounds 1 and 2 showed no cytotoxic effects against A549, MCF-7, and HCT 116 human cancer cells ( $IC_{50}$  > 10  $\mu$ M).

The genus *Ficus*, belonging to the Ficeae tribe of the family Moraceae, comprises more than 750 species distributed in the tropical and subtropical regions of the world, with about 100 of the species occurring in Malaysia.<sup>1</sup> A number of *Ficus* species were reported to possess multiple ethnomedicinal uses including for the treatment of diarrhea, dysentery, skin diseases, diabetes, inflammation, ulcers, and cancer-related diseases.<sup>2</sup> To date, only eight *Ficus* species have been reported for their alkaloidal content, namely, *F. hispida*,<sup>3–6</sup> *F. fistulosa*,<sup>7–9</sup> *F. fistulosa* var. *tengerensis*,<sup>10</sup> *F. septica*,<sup>11–14</sup> *F. nota*,<sup>15</sup> *F. hirta*,<sup>16</sup> *F. pachyrhachis*,<sup>17</sup> and *F. pantoniana*,<sup>18</sup> suggesting that plants of this genus are still largely under-investigated. This prompted us to explore *Ficus* species that occur in Peninsular Malaysia for alkaloids that possess interesting structures and/or useful biological activities. In addition to our previous investigations into the alkaloidal contents of *F. hispida*,<sup>3</sup> *F. fistulosa*,<sup>7</sup> and *F. fistulosa* var. *tengerensis*,<sup>10</sup> we also investigated *Ficus schwarzii* Koord., a tree that can grow up to 15 m in height and is widely distributed in southern Myanmar, Thailand, Peninsular Malaysia, Sumatra, and Borneo.<sup>19</sup> Herein, we report the isolation and structure elucidation of seven new 1,4-diarylbutanoid–phenethylamine conjugates, namely, schwarzinincines A–G (1–7) (Figure 1), from the leaves of *F. schwarzii*. The vasorelaxant effects of schwarzinincines A–D (1–4) in rat isolated aorta and cytotoxic effects of schwarzinincines A and B (1 and 4) against three human cancer cell lines are also reported.

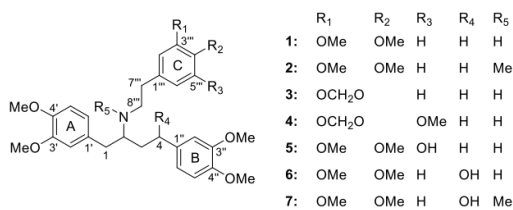


Figure 1. Structures of compounds 1–7.

### RESULTS AND DISCUSSION

Schwarzinincine A (1) was isolated as the most abundant alkaloid as a light yellowish oil with  $[\alpha]_D^{25} +2$  ( $CHCl_3$ ,  $c$  1.17). The UV spectrum showed absorption maxima at 231 and 281 nm, which were consistent with the presence of 3,4-dimethoxyphenyl groups.<sup>20</sup> HRMS measurements revealed a  $[M + H]^+$  peak at  $m/z$  510.2836, which established the molecular formula as  $C_{30}H_{39}NO_6$ . The <sup>13</sup>C NMR spectrum (Table 1) gave a total of 30 carbon resonances, while the

Received: November 21, 2019

Table 1.  $^{13}\text{C}$  NMR (150 MHz) Spectroscopic Data of 1–7 in  $\text{CDCl}_3$  ( $\delta$  in ppm)

position	1	2	3	4	5	6	7
1	40.10	34.61	40.06	40.28	40.22	39.27	32.49
2	58.70	64.50	58.70	58.72	58.62	57.64	62.43
3	35.37	32.49 <sup>a</sup>	35.32	35.58	35.42	38.96	34.56
4	31.56	32.47 <sup>a</sup>	31.53	31.58	31.57	71.61	72.16
1'	131.50	133.39 <sup>b</sup>	131.40	131.56	131.64	130.55	131.69
2'	112.25	112.35	112.22	112.14	112.28	111.97	111.82
3'	148.80 <sup>d</sup>	148.75 <sup>c</sup>	148.82 <sup>d</sup>	148.77 <sup>a</sup>	148.80 <sup>d</sup>	148.96	148.79 <sup>d</sup>
4'	147.17 <sup>b</sup>	147.10 <sup>d</sup>	147.17 <sup>b</sup>	147.14 <sup>b</sup>	147.15 <sup>b</sup>	147.67 <sup>a</sup>	147.60 <sup>b</sup>
5'	111.10 <sup>c</sup>	111.06 <sup>c</sup>	111.17 <sup>c</sup>	111.03 <sup>c</sup>	111.15	111.15 <sup>b</sup>	111.13
6'	121.06	121.06	121.06	121.03	121.08	120.92	120.94
1''	134.77	135.28	134.74	134.89	134.84	138.01	137.72
2''	111.64	111.73	111.64	111.64	111.66	108.83	108.47
3''	148.84 <sup>a</sup>	148.68 <sup>c</sup>	148.84 <sup>a</sup>	148.82 <sup>a</sup>	148.84 <sup>a</sup>	148.83	148.55 <sup>d</sup>
4''	147.44 <sup>b</sup>	147.28 <sup>d</sup>	147.62 <sup>b</sup>	147.42 <sup>b</sup>	147.43 <sup>b</sup>	147.57	147.24 <sup>b</sup>
5''	111.22 <sup>c</sup>	111.12 <sup>c</sup>	111.23 <sup>c</sup>	111.22 <sup>c</sup>	111.25	110.92	110.67
6''	120.07	120.10	120.07	120.05	120.08	117.41	117.17
1'''	132.13	133.35 <sup>b</sup>	133.25	134.29	136.00	131.58	132.42
2'''	111.82	112.18	108.79	102.37	104.47	111.72	112.07
3'''	148.87 <sup>a</sup>	148.61 <sup>c</sup>	147.47	148.83 <sup>a</sup>	152.27	148.96	149.00 <sup>d</sup>
4'''	147.45 <sup>b</sup>	146.90 <sup>d</sup>	145.89	133.49	133.99	147.75 <sup>a</sup>	147.28 <sup>b</sup>
5'''	111.15 <sup>c</sup>	111.20 <sup>c</sup>	108.12	143.38	149.27	111.21 <sup>b</sup>	111.40
6'''	120.43	120.59	121.43	107.82	108.12	120.45	120.57
7'''	35.75	34.90	35.74	36.44	36.48	35.68	34.71
8'''	48.36	55.70	48.35	48.45	48.17	48.41	55.88
MeO-3'	55.77 <sup>d</sup>	55.79 <sup>f</sup>	55.77 <sup>d</sup>	55.75 <sup>d</sup>	55.77 <sup>c</sup>	55.80 <sup>e</sup>	55.59 <sup>c</sup>
MeO-4'	55.77 <sup>d</sup>	55.79 <sup>f</sup>	55.81 <sup>d</sup>	55.78 <sup>d</sup>	55.80 <sup>c</sup>	55.81 <sup>c</sup>	55.92 <sup>c</sup>
MeO-3''	55.81 <sup>d</sup>	55.82 <sup>f</sup>	55.82 <sup>d</sup>	55.80 <sup>d</sup>	55.80 <sup>c</sup>	55.81 <sup>c</sup>	55.74 <sup>c</sup>
MeO-4''	55.81 <sup>d</sup>	55.85 <sup>f</sup>	55.92 <sup>d</sup>	55.92 <sup>d</sup>	55.80 <sup>c</sup>	55.81 <sup>c</sup>	55.88 <sup>c</sup>
MeO-3'''	55.84 <sup>d</sup>	55.86 <sup>f</sup>			55.82 <sup>c</sup>	55.85 <sup>c</sup>	55.88 <sup>c</sup>
MeO-4'''	55.93 <sup>d</sup>	55.89 <sup>f</sup>			55.93 <sup>c</sup>	55.93 <sup>c</sup>	55.96 <sup>c</sup>
MeO-5'''				56.48 <sup>d</sup>			
NMe		36.84					36.48
OCH <sub>2</sub> O			100.85	101.27			

<sup>a–f</sup>Assignments may be interchanged within each column due to severe or partial overlapped of signals.

HSQC spectrum showed the presence of 18 aromatic carbons (nine methine, three quaternary, and six oxygenated carbons) and 12 aliphatic carbons (one methine, five methylene, and six methoxy carbons). Since there are only six oxygen atoms in the molecular formula of **1**, the six methoxy groups must be attached to the six oxygenated aromatic carbons. The 18 aromatic carbon resonances were readily assigned to three sets of 3,4-dimethoxyphenyl groups based on their characteristic carbon shifts,<sup>7,21</sup> and these assignments were corroborated by the HMBC data (Figure 2). The  $^1\text{H}$  NMR spectrum (Table 2) showed the presence of nine aromatic hydrogens, six methoxy groups, 11 aliphatic hydrogens, and an NH group ( $\delta_{\text{H}}$  1.98, br s). The splitting patterns observed for the aromatic hydrogen signals were consistent with the presence of three sets of 3,4-dimethoxyphenyl rings: H-2'/2''/2''' (d with  $J \approx 2$  Hz at  $\delta_{\text{H}}$  6.622, 6.663, and 6.67), H-5'/5''/5''' (d with  $J \approx 8$  Hz at  $\delta_{\text{H}}$  6.717, 6.722, and 6.77), and H-6'/6''/6''' (dd with  $J \approx 8$  and 2 Hz at  $\delta_{\text{H}}$  6.60, 6.615, and 6.657).

The COSY spectrum showed the presence of two partial structures, namely,  $\text{CH}_2\text{CHCH}_2\text{CH}_2$  and  $\text{CH}_2\text{CH}_2$ , which were attributed to the C-1–C-2–C-3–C-4 and C-7'''–C-8''' fragments in **1**, respectively (Figure 2). The attachments of the three 3,4-dimethoxyphenyl moieties to C-1, C-4, and C-7''' were firmly established based on the three-bond correlations from H-1 to C-2', C-6'; from H-2 to C-1'; from H-2' and H-6'

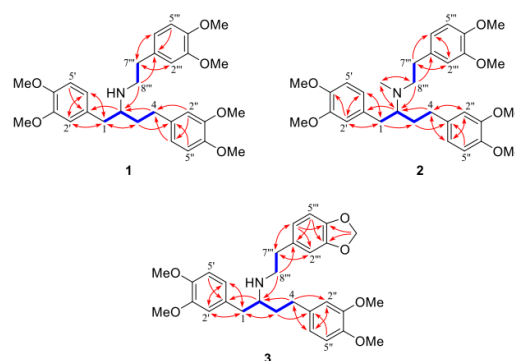


Figure 2.  $^1\text{H}$ – $^1\text{H}$  COSY (blue, bold) and selected HMBC (red arrows) correlations of 1–3.

to C-1; from H-2'' and H-6'' to C-4; from H-3 to C-1''; from H-7''' to C-2'', C-6''; from H-2''' and H-6''' to C-7'''; and from H-8''' to C-1''' (Figure 2). Furthermore, the three-bond correlation observed from H-8''' to C-2 indicated linking of the C-1–C-2–C-3–C-4 and C-7'''–C-8''' fragments via an NH group, thus establishing the full structure of **1** as shown in

B

<https://dx.doi.org/10.1021/acs.jnatprod.9b01160>  
J. Nat. Prod. XXXX, XXX, XXX–XXX

Table 2.  $^1\text{H}$  NMR (600 MHz) Spectroscopic Data of 1–7 in  $\text{CDCl}_3$  ( $\delta$  in ppm,  $J$  in Hz)

position	1	2	3	4	5	6	7
1	2.62, m	2.34, dd (13.4, 9.2)	2.61, m	2.57, m	2.62, m	2.72, dd (13.7, 6.2)	2.25, dd (13.5, 11.5)
	2.74, m	2.89, dd (13.4, 4.3)	2.74, m	2.73, m	2.71, m	2.82, dd (13.7, 7.9)	2.83, m
2	2.74, m	2.73, m	2.75, m	2.73, m	2.74, m	3.00, m	2.83, m
3	1.72, m	1.59, m	1.73, m	1.70, m	1.70, m	1.69, ddd (14.5, 5.8, 2.8)	1.61, br d (15)
	1.79, m	1.69, m	1.79, m	1.77, m	1.75, m	1.96, ddd (14.5, 8.3, 3.2)	2.12, ddd (15, 11.3, 4)
4	2.62, m	2.39, m	2.62, m	2.62, m	2.60, m	5.07, dd (8.3, 2.8)	4.91, t (3.6)
		2.59, m					
2'	6.622, d (2)	6.62 (1.6)	6.62, m	6.61, m	6.63, m	6.56, d (1.8)	6.36, d (1.7)
5'	6.722, d (8.1) <sup>a</sup>	6.76, d (8.1)	6.74, d (8)	6.78, d (8.6)	6.74, d (8.1)	6.70, d (8.1) <sup>a</sup>	6.70, d (8.1)
6'	6.60, dd (8.1, 2)	6.65, dd (8.1, 1.6)	6.63, dd (8, 2)	6.61, m	6.62, m	6.54, dd (8.1, 1.8)	6.44, dd (8.1, 1.7)
2''	6.67, d (2)	6.56, m	6.67, m	6.67, m <sup>a</sup>	6.66, m	6.90, br s	6.64, d (1.6)
5''	6.77, d (8.6)	6.73, d (8.6)	6.78, d (8.6)	6.78, d (8.6)	6.77, d (8.6)	6.82, m	6.74, d (8.6)
6''	6.657, dd (8.6, 2)	6.57, dd (8.6, 2)	6.68, m	6.68, m <sup>a</sup>	6.65, m	6.82, m	6.60, dd (8.6, 1.6)
2'''	6.663, d (1.8)	6.73, m	6.58, d (1.4)	6.28, d (1.2) <sup>b</sup>	6.24, d (1.6)	6.63, d (1.8)	6.73, m
5'''	6.717, d (8.1) <sup>a</sup>	6.79, d (7.9)	6.66, d (7.9)			6.74, dd (8.1) <sup>a</sup>	6.83, d (8.1)
6'''	6.615, dd (8.1, 1.8)	6.74, dd (7.9, 2)	6.53, dd (7.9, 1.4)	6.29, d (1.2) <sup>b</sup>	6.38, d (1.6)	6.60, dd (8.1, 1.8)	6.75, dd (8.1, 1.9)
7'''	2.67, m	2.71 m	2.66, m	2.62, m	2.63, m	2.65, m	2.77, m
						2.99, m	
8'''	2.77, m	2.65, m	2.72, m	2.74, m	2.76, m	2.78, m	2.57, m
	2.90, m	2.77, m	2.88, dt (11, 6.6)	2.88, dt (11, 6.5)	2.87, dt (11, 7.0)	3.00, m	2.91, m
MeO-3'	3.83, s <sup>b</sup>	3.826, s	3.82, s <sup>a</sup>	3.820, s <sup>c</sup>	3.82, s <sup>a</sup>	3.81, s <sup>b</sup>	3.71, s <sup>a</sup>
MeO-4'	3.853, s <sup>b</sup>	3.833, s <sup>a</sup>	3.85, s <sup>a</sup>	3.856, s <sup>d</sup>	3.85, s <sup>b</sup>	3.85, s <sup>b</sup>	3.84, s <sup>b</sup>
MeO-3''	3.84, s <sup>b</sup>	3.80, s <sup>b</sup>	3.85, s <sup>a</sup>	3.846, s <sup>c</sup>	3.84, s <sup>a</sup>	3.87, s <sup>b</sup>	3.73, s <sup>a</sup>
MeO-4''	3.86, s <sup>b</sup>	3.85, s <sup>a</sup>	3.86, s <sup>a</sup>	3.863, s <sup>d</sup>	3.85, s <sup>b</sup>	3.87, s <sup>b</sup>	3.86, s <sup>b</sup>
MeO-3'''	3.82, s <sup>b</sup>	3.87, s <sup>b</sup>			3.80, s	3.87, s <sup>b</sup>	3.90, s <sup>a</sup>
MeO-4'''	3.854, s <sup>b</sup>	3.85, s <sup>a</sup>			3.86, s <sup>b</sup>	3.87, s <sup>b</sup>	3.87, s <sup>b</sup>
MeO-5'''				3.850, s			
NH	1.98, br s		not observed	1.53, br s	not observed	1.67, br s	
NMe		2.38, s					2.44, s
OCH <sub>2</sub> O			5.91, s	5.93, s			

<sup>a-c</sup>Assignments may be interchanged within each column due to severe or partial overlapped of signals.

Figure 1. However, for unknown reasons, the NH stretching band in the IR spectrum of **1** was not evident. The presence of this NH group was confirmed by an *N*-methylation reaction (vide infra).

Schwarzincine B (**2**) was isolated as a light yellowish oil with  $[\alpha]_D^{25} +20$  ( $\text{CHCl}_3$ ,  $c$  1.01). The UV spectrum (231 and 281 nm) was similar to that of **1**. The HRMS data showed the presence of a  $[\text{M} + \text{H}]^+$  peak at  $m/z$  524.3006 (corresponding to the molecular formula  $\text{C}_{31}\text{H}_{41}\text{NO}_6$ ), which was 14 mass units higher than that of **1**, suggesting an additional methyl substitution compared to **1**. Furthermore, the  $^{13}\text{C}$  and  $^1\text{H}$  NMR spectra of **2** (Tables 1 and 2, respectively) were largely similar to those of **1**, except for the presence of the NMe group ( $\delta_{\text{C}}$  36.84,  $\delta_{\text{H}}$  2.38) in **2** in place of the NH signal in **1**. Schwarzincine B (**2**) was therefore assigned as the NMe derivative of **1**. The structure proposed of **2** was in full agreement with the HMBC data (Figure 2). The structure of **2** was also confirmed by its partial synthesis from **1**. The reductive methylation of **1** with formaldehyde and  $\text{NaBH}_3\text{CN}$  in the presence of AcOH gave schwarzincine B (**2**) in 54% yield. The spectroscopic data ( $^1\text{H}$  and  $^{13}\text{C}$  NMR, UV) of the reaction product were indistinguishable from those of natural **2**.

Schwarzincine C (**3**) was isolated as a light yellowish oil with  $[\alpha]_D^{25} -7$  ( $\text{CHCl}_3$ ,  $c$  0.48). The HRMS data ( $[\text{M} + \text{H}]^+$   $m/z$  494.2550) gave the molecular formula  $\text{C}_{29}\text{H}_{33}\text{NO}_6$ . The UV spectrum of **3** was similar to that of **1**. The  $^{13}\text{C}$  and  $^1\text{H}$  NMR spectra (Tables 1 and 2) of **3** showed a general resemblance to those of **1**, except that two of the six methoxy groups present were replaced by a methylenedioxy group in **3** ( $\delta_{\text{C}}$  100.85,  $\delta_{\text{H}}$  5.91). This was consistent with the molecular mass of **3**, which was 16 mass units lower than that of **1**. The attachment of the methylenedioxy group at C-3''' and C-4''' was indicated by the three-bond correlations observed from  $\text{OCH}_2\text{O}$  to C-3''' and C-4''' in the HMBC spectrum (Figure 2). The proposed structure of **3** was in full agreement with the 2D NMR data (Figure 2).

Schwarzincine D (**4**) was isolated as a light yellowish oil with  $[\alpha]_D^{25} +5$  ( $\text{CHCl}_3$ ,  $c$  0.38). The UV spectrum showed similar absorption maxima (230 and 282 nm) to those of **1**. The HRMS data showed a  $[\text{M} + \text{H}]^+$  peak at  $m/z$  524.2645 (corresponding to the molecular formula  $\text{C}_{30}\text{H}_{37}\text{NO}_7$ ), which was 30 mass units higher than that of **3**, suggesting the presence of an additional methoxy substitution in **4** when compared to **3**. The  $^{13}\text{C}$  NMR spectrum of **4** (Table 1) showed a general resemblance to that of **3**, except that seven oxygenated aromatic carbon resonances were observed in **4**,

instead of six in **3**. Similarly, the  $^1\text{H}$  NMR spectrum of **4** (Table 2) was very similar to that of **3**, except for the presence of an additional methoxy singlet in **4** in place of the aromatic doublet ( $J = 7.9$  Hz) due to H-5''' in **3**. The attachment of the methoxy group at C-5''' was deduced based on the HMBC three-bond correlation from MeO-5''' ( $\delta_{\text{H}}$  3.850) to C-5''' ( $\delta_{\text{C}}$  143.38) and the NOESY correlation between MeO-5''' ( $\delta$  3.850) and H-6''' ( $\delta_{\text{H}}$  6.29) (Figure 3). The pair of *meta*-

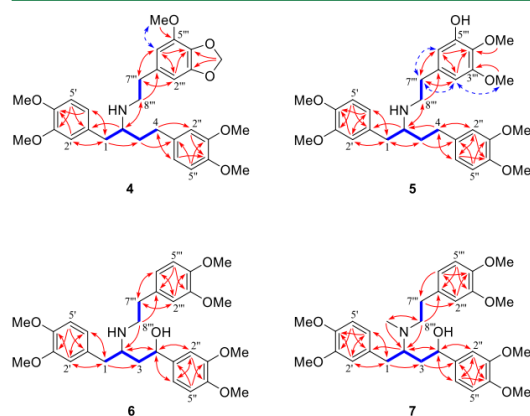


**Figure 3.**  $^1\text{H}$ – $^1\text{H}$  COSY (blue, bold), selected HMBC (red arrows), and NOE (blue arrows) correlations of **4**–**7**.

coupled aromatic hydrogens observed at  $\delta$  6.28 and 6.29 ( $J = 1.2$  Hz), which were assigned to H-2''' and H-6''' based on the correlations from H-2''' and H-6''' to C-7''' and from H-7''' to C-2''' and C-6''' (Figure 3) in the HMBC spectrum, were consistent with the splitting patterns shown by a 1,3,4,5-tetrasubstituted phenyl moiety (ring C). Schwarzinicine D (**4**) was therefore established as the 5'''-methoxy derivative of **3**.

Schwarzinicine E (**5**) was isolated as a light yellowish oil with  $[\alpha]_{\text{D}}^{25} +3$  ( $\text{CHCl}_3$ ,  $c$  0.54). The UV spectrum of **5** was essentially the same as that of **1**. The HRMS data showed a  $[\text{M} + \text{H}]^+$  peak at  $m/z$  526.2777 (corresponding to the molecular formula  $\text{C}_{30}\text{H}_{39}\text{NO}_7$ ), which was 16 mass units higher than that of **1**, suggesting the presence of an additional hydroxy substitution in **5** when compared to **1**. The  $^{13}\text{C}$  and  $^1\text{H}$  NMR spectra of **5** (Table 1) showed a general resemblance to those of **1**, except that the methine resonances in **1** ( $\delta_{\text{C}}$  111.15;  $\delta_{\text{H}}$  6.717 d ( $J = 8.1$  Hz)) were replaced by an oxygenated aromatic carbon resonance in **5** ( $\delta_{\text{C}}$  149.27). As in the case of **4**, a pair of *meta*-coupled aromatic hydrogens was observed at  $\delta_{\text{H}}$  6.24 and 6.38 ( $J = 1.6$  Hz), which were assigned to H-2''' and H-6''' based on the correlations from H-2''' and H-6''' to C-7''' and from H-7''' to C-2''' and C-6''' (Figure 3) in the HMBC spectrum, indicating the presence of a 1,3,4,5-tetrasubstituted phenyl moiety (ring C). The two methoxy groups in ring C were determined to be attached to C-3''' and C-4''' based on the HMBC data (three-bond correlations from H-2''' to C-3''' and C-4''' and from MeO-3''' to C-3''' and MeO-4''' to C-4''' and from MeO-3''' to C-3'''). The additional hydroxy group must therefore be located at C-5''' which was consistent with the NOEs observed for H-2'''/H-7''', H-6'''/H-7''', and H-2'''/MeO-2''' (Figure 3). Schwarzinicine E (**5**) was therefore assigned as the 5'''-hydroxy derivative of **1**.

Schwarzinicine F (**6**) was isolated as a light yellowish oil with  $[\alpha]_{\text{D}}^{25} +25$  ( $\text{CHCl}_3$ ,  $c$  0.22). The UV spectrum of **6** was

similar to that of **1**. HRMS measurements revealed the  $[\text{M} + \text{H}]^+$  peak at  $m/z$  526.2791, which analyzed for  $\text{C}_{30}\text{H}_{39}\text{NO}_7 + \text{H}$ , indicating that **6** and **5** are isomers. The  $^1\text{H}$  NMR spectrum of **6** (Table 2) showed the presence of a conspicuous deshielded methine signal at  $\delta_{\text{H}}$  5.07, which was absent in that of **1**. This, coupled with the observation that the number of aromatic hydrogen signals present in the  $^1\text{H}$  NMR spectrum of **6** was the same as that in **1**, suggested that the hydroxy substitution in **6** occurred in the aliphatic backbone of the molecule. Additionally, the  $^{13}\text{C}$  NMR spectrum (Table 1) showed a deshielded resonance at  $\delta_{\text{C}}$  71.61, which was attributable to an oxymethine carbon based on the HSQC data. The three-bond correlations from the signal at  $\delta_{\text{H}}$  5.07 to C-2'' and C-6''; from H-2'' and H-6'' to the resonance at  $\delta_{\text{C}}$  71.61; from H-2 to C-4; and from H-4 to C-2 indicated the benzylic C-4 as the site of hydroxy substitution (Figure 3). This is also consistent with the COSY spectrum, which revealed the presence of  $\text{OCHCH}_2\text{CH}(\text{N})\text{CH}_2$  and  $\text{CH}_2\text{CH}_2$  partial structures corresponding to the C-4–C-3–C-2–C-1 and C-7'''–C-8''' fragments in **6**, respectively (Figure 3). Schwarzinicine F (**6**) was therefore assigned as the 4-hydroxy derivative of **1**, and its planar structure was in full agreement with the HMBC data obtained (Figure 3).

Schwarzinicine G (**7**) was isolated as a light yellowish oil with  $[\alpha]_{\text{D}}^{25} -13$  ( $\text{CHCl}_3$ ,  $c$  0.35). The UV spectrum of **7** was similar to that of **1**. HRMS measurements revealed the molecular formula,  $\text{C}_{31}\text{H}_{41}\text{NO}_7$ , based on the  $[\text{M} + \text{H}]^+$  peak detected at  $m/z$  540.2966, which was 14 mass units higher than that of **6**, suggesting an additional methyl group substitution in **7** when compared to **6**. Furthermore, the  $^{13}\text{C}$  and  $^1\text{H}$  NMR spectra of **7** (Tables 1 and 2, respectively) were largely similar to those of **6**, except for the presence of an additional NMe group ( $\delta_{\text{C}}$  36.48,  $\delta_{\text{H}}$  2.44) in **7**. Schwarzinicine G (**7**) was therefore determined as the NMe derivative of **6**, and its planar structure was in complete agreement with the HMBC data obtained (Figure 3).

The relative configurations of both **6** and **7** could not be determined via analysis of the NOE data, as the molecules display high conformational flexibility. Additionally, stereochemical assignments based on derivatization of **6** and **7** were precluded due to their low isolation yields, instability, and decomposition. It was observed that both **6** and **7** were relatively unstable in solution when compared to **1**–**5**, possibly due to the presence of the labile benzyl alcohol moiety.

The schwarzinicine alkaloids **1**–**7** represent the first examples of a 1,4-diarylbutanoid linked to a phenethylamine unit and are possibly related to ficusnotins A–F, which were the first and only other plant-derived 1,4-diarylbutanoids to be reported.<sup>15</sup> Interestingly, chiral-phase HPLC analyses of the schwarzinicine alkaloids revealed schwarzinicine A (**1**) to be a scalemic mixture (4:1 ratio), while schwarzinicines B–G (**2**–**7**) were obtained as pure enantiomers. It is worth noting that ficusnotins B, C, and F (**8**, **9**, and **10**) were previously reported as racemic mixtures (Figure 4).<sup>15</sup>

The vasorelaxant activities of schwarzinicines A–D (**1**–**4**) were evaluated in rat isolated aortic rings (endothelium-intact) precontracted with 0.1  $\mu\text{M}$  phenylephrine. Dobutamine, which is a phenylalkylamine compound and a known vasorelaxant agent, was used as a positive control. Compounds **1**–**4** were found to exhibit pronounced vasorelaxation in a concentration-dependent manner (Table 3 and Figure 5). The maximum relaxation magnitude ( $E_{\text{max}}$ ) produced by all the four compounds was significantly greater than that of dobutamine.

D

<https://dx.doi.org/10.1021/acs.jnatprod.9b01160>  
J. Nat. Prod. XXXX, XXX, XXX–XXX

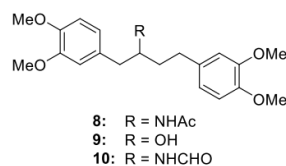


Figure 4. Structures of ficusnotins B (8), C (9), and F (10).

Table 3. Vasorelaxant Activity of Compounds 1–4 against Phenylephrine-Induced Contraction

compound	n	EC <sub>50</sub> <sup>a</sup> (μM)	E <sub>max</sub> <sup>a</sup> (%)
1	6	2.01 ± 0.67	119.3 ± 3.6 <sup>b</sup>
2	5	0.96 ± 0.25	106.0 ± 1.5 <sup>b</sup>
3	6	1.88 ± 0.64	120.4 ± 4.2 <sup>b</sup>
4	6	2.10 ± 0.35	116.1 ± 3.6 <sup>b</sup>
dobutamine	5	2.50 ± 1.11	92.0 ± 5.0

<sup>a</sup>Each value represents the mean ± standard error of the mean (SEM) of n number of animals. <sup>b</sup>Significantly different from dobutamine (*p* < 0.05).

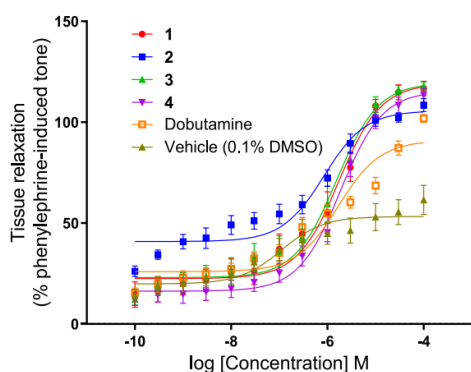


Figure 5. Vasorelaxant effects of 1–4 and dobutamine against phenylephrine-induced contractions in rat isolated aortic rings. Each point represents the mean ± SEM of n number of animals.

The potency of all the compounds tested was comparable at an EC<sub>50</sub> range between 0.96 and 2.10 μM. The comparable activity shown by schwarzinicines A, C, and D (1, 3, and 4) suggested that minor variations in substituents or substitution patterns on the aryl ring C have little effect on activity.

Additionally, the cytotoxic effects of schwarzinicines A and B (1 and 2) were assessed against three human cancer cell lines (A549, MCF-7, and HCT 116) via the neutral red (NR) uptake assay. Both the compounds were essentially non-cytotoxic toward these cell lines (IC<sub>50</sub> > 10 μM).

## EXPERIMENTAL SECTION

**General Experimental Procedures.** Optical rotations were determined on a JASCO P-1020 automatic digital polarimeter. UV spectra were obtained on a PerkinElmer Lambda 25 UV–vis spectrophotometer. IR spectra were recorded on a PerkinElmer Spectrum RX1 FT-IR and 400 FT-IR/FT-FIR spectrometers. <sup>1</sup>H and <sup>13</sup>C NMR spectra were recorded in CDCl<sub>3</sub> using tetramethylsilane as internal standard on a Bruker 600 MHz NMR spectrometer. HRDARTMS were obtained on a JEOL Accu TOF-DART mass spectrometer. HPLC was performed on a Waters ACQUITY Arc System UHPLC and a Waters 2998 photodiode array detector.

**Plant Material.** The leaves of *Ficus schwarzi* were collected in July 2013 from Ulu Gombak, Selangor, Malaysia, and identified by K. T. Yong (Institute of Biological Sciences, University of Malaya, Malaysia). Herbarium voucher specimens (KLU48248) are deposited at the Herbarium, University of Malaya.

**Extraction and Isolation.** The ground dried leaves of *F. schwarzi* (21.6 kg) were extracted with 95% EtOH at room temperature four times. The ethanolic extract was concentrated in vacuo to give approximately 5 kg of dried material, which was subsequently added into a 3% tartaric acid solution. The insoluble substances in the acidic solution were removed via filtration through kieselguhr. Concentrated NH<sub>3</sub> solution was then added to the filtrate until pH 10 was achieved. The liberated alkaloids were extracted three times with CHCl<sub>3</sub>, washed with water, dried over anhydrous Na<sub>2</sub>SO<sub>4</sub>, and concentrated to give 4.4 g of crude alkaloid mixture. The crude alkaloid mixture was initially fractionated by column chromatography (silica gel, CHCl<sub>3</sub>/MeOH, with increasing percentages of MeOH) followed by repeated chromatography of the partially resolved fractions using column chromatography or preparative radial chromatography. The solvent systems used for preparative radial chromatography were CHCl<sub>3</sub>/hexane (NH<sub>3</sub>-saturated), Et<sub>2</sub>O/hexane (NH<sub>3</sub>-saturated), CHCl<sub>3</sub>/MeOH (NH<sub>3</sub>-saturated), and Et<sub>2</sub>O/MeOH (NH<sub>3</sub>-saturated). The yields of the compounds obtained were as follows: 1 (389 mg), 2 (197 mg), 3 (9 mg), 4 (7 mg), 5 (17 mg), 6 (4 mg), and 7 (7 mg).

**Schwarzincine A (1):** light yellowish oil; [α]<sub>D</sub><sup>25</sup> +2 (CHCl<sub>3</sub>, *c* 1.17); UV (CH<sub>3</sub>CN) λ<sub>max</sub> (log ε) 231 (4.05), 281 (3.63) nm; IR ν<sub>max</sub> 2923, 2851, 1515, 1463, 1261, 1236, 1140, 1028 cm<sup>-1</sup>; <sup>13</sup>C and <sup>1</sup>H NMR data, see Tables 1 and 2; HRDARTMS *m/z* 510.2836 [M + H]<sup>+</sup> (calcd for C<sub>30</sub>H<sub>39</sub>NO<sub>6</sub> + H, 510.2850).

**Schwarzincine B (2):** light yellowish oil; [α]<sub>D</sub><sup>25</sup> +20 (CHCl<sub>3</sub>, *c* 1.01); UV (CH<sub>3</sub>CN) λ<sub>max</sub> (log ε) 231 (4.22), 281 (3.79) nm; IR ν<sub>max</sub> 2934, 2851, 1516, 1463, 1262, 1236, 1141, 1028 cm<sup>-1</sup>; <sup>13</sup>C and <sup>1</sup>H NMR data, see Tables 1 and 2; HRDARTMS *m/z* 524.3006 [M + H]<sup>+</sup> (calcd for C<sub>31</sub>H<sub>41</sub>NO<sub>6</sub> + H, 524.3007).

**Schwarzincine C (3):** light yellowish oil; [α]<sub>D</sub><sup>25</sup> -7 (CHCl<sub>3</sub>, *c* 0.48); UV (CH<sub>3</sub>CN) λ<sub>max</sub> (log ε) 231 (4.04), 281 (3.44) nm; IR ν<sub>max</sub> 2919, 2834, 1514, 1440, 1234, 1138, 1026 cm<sup>-1</sup>; <sup>13</sup>C and <sup>1</sup>H NMR data, see Tables 1 and 2; HRDARTMS *m/z* 494.2550 [M + H]<sup>+</sup> (calcd for C<sub>29</sub>H<sub>36</sub>NO<sub>6</sub> + H, 494.2537).

**Schwarzincine D (4):** light yellowish oil; [α]<sub>D</sub><sup>25</sup> +5 (CHCl<sub>3</sub>, *c* 0.38); UV (CH<sub>3</sub>CN) λ<sub>max</sub> (log ε) 230 (4.14), 282 (3.63) nm; IR ν<sub>max</sub> 2935, 2836, 1514, 1451, 1261, 1236, 1136, 1029 cm<sup>-1</sup>; <sup>13</sup>C and <sup>1</sup>H NMR data, see Tables 1 and 2; HRDARTMS *m/z* 524.2645 [M + H]<sup>+</sup> (calcd for C<sub>30</sub>H<sub>37</sub>NO<sub>7</sub> + H, 524.2643).

**Schwarzincine E (5):** light yellowish oil; [α]<sub>D</sub><sup>25</sup> +3 (CHCl<sub>3</sub>, *c* 0.54); UV (CH<sub>3</sub>CN) λ<sub>max</sub> (log ε) 230 (3.62), 279 (3.08) nm; IR ν<sub>max</sub> 2932, 2836, 1512, 1451, 1261, 1235, 1138, 1025 cm<sup>-1</sup>; <sup>13</sup>C and <sup>1</sup>H NMR data, see Tables 1 and 2; HRDARTMS *m/z* 526.2777 [M + H]<sup>+</sup> (calcd for C<sub>30</sub>H<sub>39</sub>NO<sub>7</sub> + H, 526.2799).

**Schwarzincine F (6):** light yellowish oil; [α]<sub>D</sub><sup>25</sup> +25 (CHCl<sub>3</sub>, *c* 0.22); UV (CH<sub>3</sub>CN) λ<sub>max</sub> (log ε) 230 (4.05), 281 (3.62) nm; IR ν<sub>max</sub> 2935, 2835, 1513, 1463, 1258, 1233, 1138, 1025 cm<sup>-1</sup>; <sup>13</sup>C and <sup>1</sup>H NMR data, see Tables 1 and 2; HRDARTMS *m/z* 526.2791 [M + H]<sup>+</sup> (calcd for C<sub>30</sub>H<sub>39</sub>NO<sub>7</sub> + H, 526.2799).

**Schwarzincine G (7):** light yellowish oil; [α]<sub>D</sub><sup>25</sup> -13 (CHCl<sub>3</sub>, *c* 0.35); UV (CH<sub>3</sub>CN) λ<sub>max</sub> (log ε) 231 (4.28), 281 (3.86) nm; IR ν<sub>max</sub> 2936, 2835, 1515, 1464, 1261, 1235, 1140, 1028 cm<sup>-1</sup>; <sup>13</sup>C and <sup>1</sup>H NMR data, see Tables 1 and 2; HRDARTMS *m/z* 540.2966 [M + H]<sup>+</sup> (calcd for C<sub>31</sub>H<sub>41</sub>NO<sub>7</sub> + H, 540.2956).

**Chiral-Phase HPLC Analyses of 1–7.** Analyses were carried out using a Chiralpak IA (4.6 × 150 mm) column, packed with amylose tris(3,5-dimethylphenylcarbamate) immobilized on 5 μm silica gel, at ambient temperature. The compounds were first dissolved in EtOH prior to injection. The flow rate of the eluting solvent was set at 1.0 mL/min, while the eluting solvents used are listed as follows: hexane/EtOH/Et<sub>2</sub>NH, 80:20:0.1 for 1 (2.0 mg/mL, 10.0 μL), 2 (3.7 mg/mL, 5.0 μL), 4 (1.2 mg/mL, 15.0 μL), 5 (5.7 mg/mL, 2.0 μL), and 7 (2.8 mg/mL, 10.0 μL); hexane/EtOH/Et<sub>2</sub>NH, 90:10:0.1 for 3 (1.6 mg/mL, 10.0 μL) and 6 (1.2 mg/mL, 20.0 μL).

E

<https://dx.doi.org/10.1021/acs.jnatprod.9b01160>  
J. Nat. Prod. XXXX, XXX, XXX–XXX

**N-Methylation of Schwarzincine A (1) to Schwarzincine B (2).** To a stirring solution of **1** (19.9 mg, 0.039 mmol) in MeOH (4 mL) was added 37% aqueous formaldehyde (0.1 mL, 1.34 mmol, 34 equiv) and NaBH<sub>3</sub>CN (37.0 mg, 0.59 mmol, 15 equiv). The mixture was stirred at room temperature for 1 h before addition of AcOH (0.4 mL, 6.99 mmol, 175 equiv). The solution was stirred further for 23 h before addition of 1 M NaOH solution (8 mL). The resulting mixture was then extracted with CH<sub>2</sub>Cl<sub>2</sub> (3 × 10 mL). The organic phase was washed with brine and dried with anhydrous Na<sub>2</sub>SO<sub>4</sub> before concentrated in vacuo. The crude product was purified by preparative radial chromatography with Et<sub>2</sub>O/hexane (4:1) as eluent to furnish **2** as a light yellowish oil (11.1 mg, 0.021 mmol, 54%).

**Measurement of Aorta Relaxation.**<sup>22</sup> Adult male Sprague–Dawley rats (2–3 months old, 300–420 g) were euthanized with CO<sub>2</sub>. Ethical approval was obtained from the University of Nottingham's Animal Welfare and Ethical Review Body (AWERB ref: UNMC12). The entire thoracic aorta was immediately excised, cut into segments of 4 mm length, and transferred into Krebs-Ringer bicarbonate solution. Each segment was suspended by a glass rod in a glass organ bath chamber containing 10 mL of Krebs-Ringer bicarbonate solution at 37 °C and aerated with 5% CO<sub>2</sub> in 95% O<sub>2</sub>. The tissue was allowed to equilibrate for 15 min in the solution before a tension (2 g) was applied. The tissue with the loaded tension was allowed to equilibrate for 30 min prior to stimulation with 60 mM KCl solution twice to test for tissue viability. Each aortic ring was then contracted with phenylephrine (0.1 μM). When the phenylephrine-induced contraction reached a stable tone, each compound (**1**–**4** or dobutamine) was added into the bath cumulatively from 0.1 nM to 0.1 mM.

**Cytotoxicity Assay.** Cell viability was assessed by the NR uptake assay on A549, MCF-7, and HCT 116 human cancer cell lines performed according to the method described previously.<sup>3</sup> Vinblastine was used as a positive control (IC<sub>50</sub> 10.0, 1.0, and 0.5 nM, respectively).

**Data Analysis and Statistics.** A force transducer (MLTF050/ST, ADInstruments, US) and a PowerLab data acquisition system (LabChart v7.3.4) were used to measure and record the change in tension in the study. The raw data were analyzed using GraphPad Prism. The relaxation responses were calculated as percentage inhibition of phenylephrine-induced contraction. Maximum response (*E*<sub>max</sub>) and EC<sub>50</sub> values were obtained, where EC<sub>50</sub> is the concentration of the compound that produces 50% of its maximum response (*E*<sub>max</sub>). The data were expressed as means ± SEM of *n* number of animals. Statistical analysis was done using unpaired *t* tests (two-tailed) with dobutamine as the control. Results were considered to be statistically significant if *p* < 0.05.

## ■ ASSOCIATED CONTENT

### Supporting Information

The Supporting Information is available free of charge at <https://pubs.acs.org/doi/10.1021/acs.jnatprod.9b01160>.

<sup>1</sup>H NMR, <sup>13</sup>C NMR, and chiral-phase HPLC chromatograms of compounds **1**–**7** (PDF)

## ■ AUTHOR INFORMATION

### Corresponding Author

**Kuan-Hon Lim** – University of Nottingham Malaysia, Semenyih, Malaysia; [orcid.org/0000-0003-1462-3324](https://orcid.org/0000-0003-1462-3324); Phone: +603-89248208; Email: [KuanHon.Lim@nottingham.edu.my](mailto:KuanHon.Lim@nottingham.edu.my); Fax: +603-89248018

### Other Authors

**Premanand Krishnan** – University of Nottingham Malaysia, Semenyih, Malaysia

**Fong-Kai Lee** – University of Nottingham Malaysia, Semenyih, Malaysia

**Veronica Alicia Yap** – University of Nottingham Malaysia, Semenyih, Malaysia

**Yun-Yee Low** – University of Malaya, Kuala Lumpur, Malaysia; [orcid.org/0000-0002-7429-4238](https://orcid.org/0000-0002-7429-4238)

**Toh-Seok Kam** – University of Malaya, Kuala Lumpur, Malaysia; [orcid.org/0000-0002-4910-6434](https://orcid.org/0000-0002-4910-6434)

**Kien-Thai Yong** – University of Malaya, Kuala Lumpur, Malaysia

**Kang-Nee Ting** – University of Nottingham Malaysia, Semenyih, Malaysia

Complete contact information is available at: <https://pubs.acs.org/10.1021/acs.jnatprod.9b01160>

## Notes

The authors declare no competing financial interest.

## ■ ACKNOWLEDGMENTS

The authors are grateful to MOHE Malaysia (FRGS/1/2017/STG01/UNIM/02/3 and FRGS/1/2017/SKK10/UNIM/01/1) for financial support.

## ■ REFERENCES

- (1) Berg, C. C.; Corner, E. J. H. In *Flora Malesiana, Series I-Seed Plants, Moraceae, Ficus*; Nooteboom, H. P., Ed.; Nationaal Herbarium Nederland: Leiden, 2005; Vol. 17/2, pp 1–702.
- (2) Lansky, E. P.; Paavilainen, H. M.; Pawlus, A. D.; Newman, R. A. *J. Ethnopharmacol.* **2008**, *119*, 195–213.
- (3) Yap, V. A.; Loong, B.-J.; Ting, K.-N.; Loh, S. H.-S.; Yong, K.-T.; Low, Y.-Y.; Kam, T.-S.; Lim, K.-H. *Phytochemistry* **2015**, *109*, 96–102.
- (4) Venkatachalam, S. R.; Mulchandani, N. B. *Naturwissenschaften* **1982**, *69*, 287–288.
- (5) Peraza-Sánchez, S. R.; Chai, H.-B.; Shin, Y. G.; Santisuk, T.; Reutrakul, V.; Farnsworth, N. R.; Cordell, G. A.; Pezzuto, J. M.; Kinghorn, A. D. *Planta Med.* **2002**, *68*, 186–188.
- (6) Shi, Z.-F.; Lei, C.; Yu, B.-W.; Wang, H.-Y.; Hou, A.-J. *Chem. Biodiversity* **2016**, *13*, 445–450.
- (7) Yap, V. A.; Qazzaz, M. E.; Raja, V. J.; Bradshaw, T. D.; Loh, H.-S.; Sim, K.-S.; Yong, K.-T.; Low, Y.-Y.; Lim, K.-H. *Phytochem. Lett.* **2016**, *15*, 136–141.
- (8) Subramaniam, G.; Ang, K. K. H.; Ng, S.; Buss, A. D.; Butler, M. S. *Phytochem. Lett.* **2009**, *2*, 88–90.
- (9) Zhang, H.-J.; Tamez, P. A.; Aydogmus, Z.; Tan, G. T.; Saikawa, Y.; Hashimoto, K.; Nakata, M.; Hung, N. V.; Xuan, L. T.; Cuong, N. M.; Soejarto, D. D.; Pezzuto, J. M.; Fong, H. H. S. *Planta Med.* **2002**, *68*, 1088–1091.
- (10) Al-Khdhairawi, A. A. Q.; Krishnan, P.; Mai, C.-W.; Chung, F. F.-L.; Leong, C.-O.; Yong, K.-T.; Chong, K.-W.; Low, Y.-Y.; Kam, T.-S.; Lim, K.-H. *J. Nat. Prod.* **2017**, *80*, 2734–2740.
- (11) Kubo, M.; Yatsuzuka, W.; Matsushima, S.; Harada, K.; Inoue, Y.; Miyamoto, H.; Matsumoto, M.; Fukuyama, Y. *Chem. Pharm. Bull.* **2016**, *64*, 957–960.
- (12) Ueda, J. Y.; Takagi, M.; Shin-Ya, K. *J. Nat. Prod.* **2009**, *72*, 2181–2183.
- (13) Damu, A. G.; Kuo, P.-C.; Shi, L.-S.; Li, C.-Y.; Kuoh, C.-S.; Wu, P.-L.; Wu, T.-S. *J. Nat. Prod.* **2005**, *68*, 1071–1075.
- (14) Damu, A.; Kuo, P.-C.; Shi, L.-S.; Li, C.-Y.; Su, C.-R.; Wu, T.-S. *Planta Med.* **2009**, *75*, 1152–1156.
- (15) Latayada, F. S.; Uy, M. M.; Akihara, Y.; Ohta, E.; Nehira, T.; Omura, H.; Ohta, S. *Phytochemistry* **2017**, *141*, 98–104.
- (16) Wan, C.; Chen, C.; Li, M.; Yang, Y.; Chen, M.; Chen, J. *Plants* **2017**, *6*, 1–9.
- (17) Khan, I.; Rali, T.; Sticher, O. *Planta Med.* **1993**, *59*, 286.

F

<https://dx.doi.org/10.1021/acs.jnatprod.9b01160>  
J. Nat. Prod. XXXX, XXX, XXX–XXX

- (18) Johns, S. R.; Russel, J. H.; Heffernan, M. L. *Tetrahedron Lett.* **1965**, *6*, 1987–1991.
- (19) Berg, C. C.; Culmsee, H. *Blumea J. Plant Taxon. Plant Geogr.* **2011**, *56*, 265–269.
- (20) Martinez, J. C.; Cuca, L. E.; Santana, M. A. J.; Pombo-Villar, E.; Golding, B. T. *Phytochemistry* **1985**, *24*, 1612–1614.
- (21) Zacchino, S. A.; Badano, H. J. *Nat. Prod.* **1985**, *48*, 830–832.
- (22) Loong, B.-J.; Tan, J.-H.; Lim, K.-H.; Mbaki, Y.; Ting, K.-N. *Naunyn-Schmiedeberg's Arch. Pharmacol.* **2015**, *388*, 1061–1067.

# Alstoscholactine and Alstolaxepine, Monoterpenoid Indole Alkaloids with $\gamma$ -Lactone-Bridged Cycloheptane and Oxepane Moieties from *Alstonia scholaris*

Premanand Krishnan,<sup>†</sup> Fong-Kai Lee,<sup>†</sup> Kam-Weng Chong,<sup>‡</sup> Chun-Wai Mai,<sup>§,||</sup> Azira Muhamad,<sup>¶</sup> Siew-Huah Lim,<sup>‡</sup> Yun-Yee Low,<sup>‡</sup> Kang-Nee Ting,<sup>‡</sup> and Kuan-Hon Lim<sup>\*,†,||</sup>

<sup>†</sup>School of Pharmacy and <sup>‡</sup>Department of Biomedical Sciences, University of Nottingham Malaysia Campus, Jalan Broga, 43500 Semenyih, Selangor, Malaysia

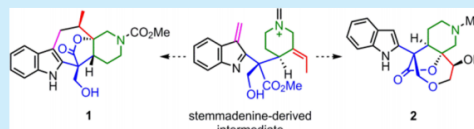
<sup>§</sup>School of Pharmacy and <sup>||</sup>Center for Cancer and Stem Cell Research, International Medical University, Bukit Jalil, 57000 Kuala Lumpur, Malaysia

<sup>‡</sup>Department of Chemistry, Faculty of Science, University of Malaya, 50603 Kuala Lumpur, Malaysia

<sup>¶</sup>Malaysia Genome Institute, Jalan Bangi, 43000 Kajang, Selangor, Malaysia

## S Supporting Information

**ABSTRACT:** Two new monoterpenoid indole alkaloids, alstoscholactine (**1**) and alstolaxepine (**2**), were isolated from *Alstonia scholaris*. Compound **1** represents a rearranged stemmadenine alkaloid with an unprecedented C-6–C-19 connectivity, whereas compound **2** represents a 6,7-*seco*-angustilobine B-type alkaloid incorporating a rare  $\gamma$ -lactone-bridged oxepane ring system. Their structures and absolute configurations were determined by spectroscopic analyses. Compound **1** was successfully semisynthesized from 19*E*-vallesamine. Compound **2** induced marked vasorelaxation in rat isolated aortic rings precontracted with phenylephrine.



*Alstonia scholaris* (L.) R. Br., which is widely distributed in South and Southeast Asia, is often cultivated for its ornamental and medicinal values.<sup>1</sup> The different plant parts of *A. scholaris* are used in traditional medicine in China, India, and Southeast Asia for the treatment of various diseases.<sup>2–4</sup> Recent *in vivo* and *in vitro* studies revealed that the extracts of *A. scholaris* possess antihypertensive and vasorelaxant effects in rats.<sup>5,6</sup> It is notable that *A. scholaris* is a prolific producer of monoterpenoid indole alkaloids, many of which possess unique polycyclic skeletons and/or useful biological activities. A number of these alkaloids have therefore fascinated chemists to make them their synthetic targets.<sup>7</sup> It was also previously noted that the alkaloidal composition of *A. scholaris* is affected by geographical variation.<sup>8</sup> Although many phytochemical studies have been conducted on the samples of *A. scholaris* collected from different regions,<sup>2,8</sup> there was only one report on the Malaysian leaf sample (collected from the east coast of Peninsular Malaysia), from which six akuammiline- and strychnan-type indole alkaloids were identified.<sup>4</sup> In the present study, the leaf sample of *A. scholaris* cultivated on the west coast of Peninsular Malaysia was investigated. As a result, two new monoterpenoid indole alkaloids, namely, alstoscholactine (**1**) and alstolaxepine (**2**), characterized by previously unknown polycyclic structures were isolated (Figure 1). Herein, we report the isolation, structure determination, biological activity, and possible biogenetic pathways of compounds **1** and **2**.

Alstoscholactine (**1**) was obtained from the basic fraction of the ethanolic extract as a light yellowish oil,  $[\alpha]_D^{25} +14$  (*c* 1.04,

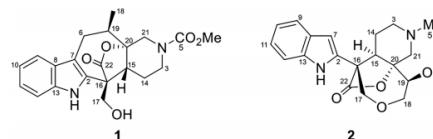


Figure 1. Structures of alkaloids **1** and **2**.

$\text{CHCl}_3$ ). The IR spectrum showed absorption bands at 3403, 1761, and 1684  $\text{cm}^{-1}$  due to the presence of OH/NH,  $\gamma$ -lactone carbonyl, and carbamate carbonyl functions, respectively. The UV spectrum showed characteristic indole absorption maxima at 222, 276 (sh), 283, and 290 (sh) nm. HRMS measurements established the molecular formula as  $\text{C}_{21}\text{H}_{24}\text{N}_2\text{O}_5$ .<sup>9</sup>

In agreement with the molecular formula of **1**, the <sup>13</sup>C NMR data (Table 1) indicated a total of 21 carbons, whereas the HSQC data revealed the presence of 11 aliphatic carbons (two methyl, five methylene, two methine, one quaternary, and one oxygenated tertiary carbon), eight aromatic carbons (four methine, two quaternary, and two N-bearing tertiary carbons), and two carbonyl carbons due to a lactone and a carbamate group. Of the 21 carbons, 11 were observed as paired signals due to the presence of the *E/Z*-carbamate rotamers<sup>10</sup> associated with the  $\text{NCO}_2\text{Me}$  group. The eight aromatic carbon resonances

Received: November 9, 2018

Published: December 13, 2018

Table 1.  $^1\text{H}$  NMR (600 MHz) and  $^{13}\text{C}$  NMR (150 MHz) Data for **1** and **2** in  $\text{CDCl}_3$ 

C/H	1		2	
	$\delta_{\text{C}}$	$\delta_{\text{H}}$	$\delta_{\text{C}}$	$\delta_{\text{H}}$
2	132.9		134.9	
3 $\alpha$	41.3	3.60 m, 3.80 m <sup>a</sup>	55.7	2.34 td (12, 3)
3 $\beta$		2.99 t (11), 3.18 br t (11) <sup>a</sup>		3.20 br d (12)
5	156.1, 156.2 <sup>a</sup>		45.2	2.45 s (N-Me)
6 $\alpha$	25.4, 25.7 <sup>a</sup>	3.05 dd (16, 4.4)		
6 $\beta$		2.82 dd (16, 3)		
7	109.7		99.3	6.38 dd (2, 1)
8	129.0		127.7	
9	118.0	7.48 d (8)	120.3	7.55 br d (8)
10	119.6	7.10 t (8)	120.2	7.10 td (8, 1)
11	122.1	7.15 t (8)	122.4	7.18 td (8, 1)
12	111.3	7.32 d (8)	111.3	7.37 br d (8)
13	134.9		135.7	
14 $\alpha$	22.1, 22.4 <sup>a</sup>	1.77 m	22.1	2.18 br d (13)
14 $\beta$		1.91 m		3.04 qd (13, 4.3)
15	41.8, 42.2 <sup>a</sup>	2.68 m	53.9	2.62 dd (13.5, 2.4)
16	51.0, 51.8 <sup>a</sup>		51.4	
17	61.7	4.19 br s	76.1	4.10 d (12.3) ( $\beta$ )
17'		4.43 d (11.5)		4.24 d (12.3) ( $\alpha$ )
18	15.7, 15.9 <sup>a</sup>	0.94 d (6.7)	69.9	3.64 dd (14.2, 1.2) ( $\alpha$ )
18'				4.02 dd (14.2, 2.4) ( $\beta$ )
19	40.2, 40.6 <sup>a</sup>	2.38 m, 2.50 m <sup>a</sup>	78.7	4.04 m
20	87.6, 88.6 <sup>a</sup>		80.5	
21 $\alpha$	48.9, 49.2 <sup>a</sup>	3.94 d (15), 4.05 d (15) <sup>a</sup>	64.3	2.56 d (10.1)
21 $\beta$		3.50 d (15), 3.70 m <sup>a</sup>		3.44 d (10.1)
22	174.6, 174.8 <sup>a</sup>		179.5	
NH		9.16 br s, 9.19 br s <sup>a</sup>		9.15 br s
NCOOMe	52.9	3.72 s, 3.74 s <sup>a</sup>		
NCOOMe	156.1, 156.2 <sup>a</sup>			
OH		3.36 br s (17-OH)		7.63 br s (19-OH)

<sup>a</sup>Duplication of signals due to carbamate rotamers.

could be readily assigned to the indole moiety based on their characteristic carbon shifts,<sup>11</sup> and these assignments were corroborated by the HMBC and NOESY data (Figures 2 and

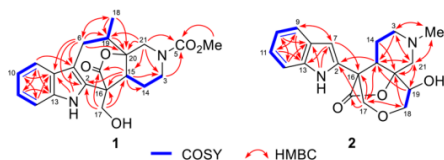


Figure 2. COSY and selected HMBCs of **1** and **2**.

3, respectively). The most deshielded methylene carbon resonance at  $\delta_{\text{C}}$  61.7 (C-17) was characteristic of an oxy-

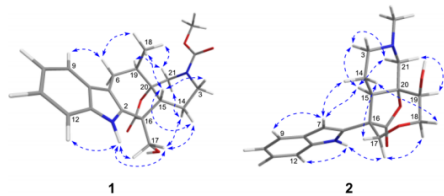


Figure 3. Selected NOEs of **1** and **2**.

methylene group, whereas the methylene carbon resonances at  $\delta_{\text{C}}$  41.3 (C-3) and 48.9/49.2 (C-21) were attributed to two aminomethylene groups associated with the carbamate function ( $\text{NCO}_2\text{Me}$ ). Additionally, the pair of deshielded tertiary carbon resonances observed at  $\delta_{\text{C}}$  87.6/88.6 indicated oxygen substitution at this carbon, which was assigned to C-20, based on the HMBC correlations from H-6 and H-18 to C-20.

Due to interconversion of the carbamate rotamers,<sup>10,12</sup> many of the signals in the  $^1\text{H}$  NMR spectrum of **1** appeared to be broadened, and H-3 $\alpha$ , H-3 $\beta$ , H-19, H-21 $\alpha$ , H-21 $\beta$ , NCOOMe, and NH were observed as duplicated signals in approximately 1:1 ratio.<sup>13</sup> The  $^1\text{H}$  NMR data (Table 1) with the aid of the HSQC data showed signals due to four contiguous aromatic hydrogens of an indole moiety ( $\delta$  7.10–7.48), an indolic NH ( $\delta$  9.16/9.19), an isolated oxymethylene ( $\delta_{\text{H}}$  4.19 and 4.43;  $d, J = 11.5$  Hz;  $\delta_{\text{C}}$  61.7), an isolated aminomethylene ( $\delta_{\text{H}}$  3.50/3.70 and 3.94/4.05;  $\delta_{\text{C}}$  48.9/49.2), a methine-bearing methyl group ( $\delta_{\text{H}}$  0.94,  $d, J = 6.7$  Hz;  $\delta_{\text{C}}$  15.7/15.9), and a  $\text{NCO}_2\text{Me}$  group ( $\delta_{\text{H}}$  3.72,  $\delta_{\text{C}}$  52.9;  $\delta_{\text{C}}$  156.1/156.2).

The COSY data (Figure 2) revealed two partial structures, namely,  $\text{CH}_2\text{CH}_2\text{CH}$  and  $\text{CH}_2\text{CHCH}_3$ , which were attributed to the C-3–C-14–C-15 and C-6–C-19–C-18 fragments in **1**, respectively. The COSY data also confirmed the presence of two isolated methylene groups at C-17 (oxymethylene) and C-21 (aminomethylene). The attachment of the C-6–C-19–C-18 fragment to C-7 of the indole moiety was indicated by the HMBC correlations observed from H-6 to C-2, C-7, and C-8

(Figure 2). On the other hand, the three-bond correlations from H-6 and H-18 to C-20 indicated linkage of C-19 to C-20, which was in turn linked to the isolated aminomethylene C-21 by the correlations observed from H-21 to C-19 and C-20. The attachment of the C-3–C-14–C-15 fragment to C-20 was indicated by the observed three-bond correlation from H-21 to C-15. Both C-3 and C-21 were deduced to be linked via the carbamate N atom based on the observed three-bond correlations from H-21 to C-3 and C-5 and from H-3 to C-5. Finally, the attachments of C-2 (indole), C-15, and C-17 to the lactone-bearing C-16 were inferred by the HMBC correlations from H-15 to C-2, C-16, and C-22 and from H-17 to C-2, C-15, C-16, and C-22.

The structure unraveled thus far is consistent with the NOESY data, which established the relative configurations at the various stereocenters in **1** (Figure 3). The  $\beta$  disposition of Me-18 was inferred by the NOEs observed for Me-18/H-6 $\beta$  and H-9/H-6 $\beta$ , whereas the NOE observed for Me-18/H-15 required H-15 to be  $\beta$ -oriented. These NOEs, coupled with the rigid ring system of alstoscholactine (**1**), dictated an  $\alpha$ -disposition for the lactone function. Additionally, the NOEs observed for H-14 $\alpha$ /H-21 $\alpha$  and H-15/H-3 $\beta$  indicated that the carbamate-containing piperidine ring adopts a boat conformation. The relative configuration of **1** was therefore determined as 15*R*,16*S*,19*R*,20*S*, which was also established as the absolute configuration by comparison of the experimental and calculated ECD spectra (Figure 4).

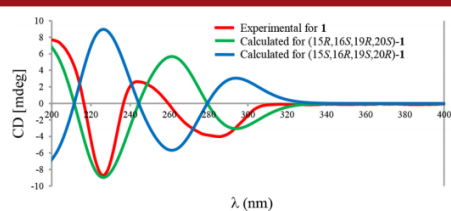


Figure 4. Experimental and calculated ECD spectra of **1**.

Alstoscholactine (**1**) represents the first member of a new class of rearranged stemmadenine alkaloids presenting an unprecedented C-6–C-19 connectivity among naturally occurring monoterpene indole alkaloids. However, a search of the literature revealed that the basic skeleton of **1** has previously been encountered in the product of a reaction between 19*E*-vallesamine (**3**) and benzyl chloroformate.<sup>14</sup> Inspired by this transformation, we successfully carried out a semisynthesis of **1** by reacting **3** with methyl chloroformate (2 equiv) in the presence of  $K_2CO_3$  (5 equiv), which gave a single major product **1** in 61% yield. The structure was confirmed by comparison of its NMR data, HRMS,  $[\alpha]_D$ , ECD, and TLC with those of the authentic material.

Alstolaxepine (**2**) was obtained as a light yellowish oil and subsequently crystallized from dichloromethane as light orange needles, mp 109–112 °C, with  $[\alpha]_D^{25} -12$  (*c* 0.67,  $CHCl_3$ ). The IR spectrum showed the presence of OH/NH (3343  $cm^{-1}$ ) and  $\gamma$ -lactone carbonyl (1774  $cm^{-1}$ ) functions, whereas the UV spectrum ( $\lambda_{max}$  217, 271, 279, and 289 nm) indicated the presence of an indole chromophore. HRMS measurements established the molecular formula as  $C_{19}H_{22}N_2O_4$ .<sup>15</sup>

The  $^1H$  NMR data (Table 1) showed the presence of four aromatic signals at  $\delta$  7.10–7.55 due to the four contiguous hydrogens of an indole moiety, an indolic NH at  $\delta$  9.15, an *N*-Me

at  $\delta$  2.45, and a shielded aromatic signal at  $\delta$  6.38. The latter signal was assigned to H-7 based on the HMBC correlations from H-7 to C-9 and C-13, which inferred that **2** is a 6,7-*seco*-monoterpene indole alkaloid. In fact, signals due to the five aromatic hydrogens as well as the indolic NH closely resemble those of 6,7-*seco*-angustilobine B (**4**) and related alkaloids.<sup>11,16</sup> The  $^{13}C$  NMR data (Table 1) accounted for a total of 19 carbon resonances, and the HSQC data revealed the presence of 10 aliphatic carbons (one methyl, five methylene, two methine, one quaternary, and one oxygenated tertiary carbon), eight aromatic carbons (five methine, one quaternary, and two *N*-bearing tertiary carbons), and one carbonyl carbon due to a lactone function ( $\delta_C$  179.5). The resonances of one tertiary, one methine, and two methylene carbons observed at  $\delta_C$  80.5, 78.7 ( $\delta_H$  4.04), 76.1 ( $\delta_H$  4.10 and 4.24), and 69.9 ( $\delta_H$  3.64 and 4.02), respectively, indicated oxygen substitution at these carbons.

The COSY data showed the presence of  $NCH_2CH_2CH$ ,  $NCH_2$ , and  $CH_2CH$  partial structures corresponding to the *N*-C-3–C-14–C-15, *N*-C-21, and C-18–C-19 fragments in **2**, respectively (Figure 2). The partial structures revealed thus far were connected via detailed analysis of the HMBC data (Figure 2). The *N*-C-3–C-14–C-15 fragment was deduced to be attached to C-20 based on the observed three-bond correlation from H-14 to C-20, whereas the connection from C-3 to the isolated methylene C-21 via *N*-4 was established based on the three-bond correlations from H-3 to C-21, from Me-5 to C-3 and C-21, and from H-21 to C-3 and C-5. The piperidine ring was constructed by linking C-21 to C-20 based on the observed HMBC correlations from H-21 to C-20 and C-15. The C-18–C-19 fragment was readily linked to C-20 based on the correlations from H-19 to C-15 and C-21 and from H-18 to C-20. The connection between C-18 and C-17 via an ether linkage was indicated by the HMBC correlations from H-17 to C-18 and from H-18 to C-17. The oxepane ring was constructed by linking C-17 to C-16 and C-16 to C-15, as indicated by the HMBC correlations from H-17 to C-2, C-15, and C-16 and from H-15 to C-17. The location of the  $\gamma$ -lactone carbonyl (C-22) was determined to be at C-16 based on the HMBC correlation from H-17 to C-22. Finally, the correlations from H-15 and H-17 to C-2 established the connection between C-2 and C-16, which completed the assembly of the 2D structure of **2**.

The relative configurations at the various stereocenters were deduced based on the NOESY spectrum and NOE difference data (H-3 $\beta$ , H-14 $\alpha$ , H-14 $\beta$ , H-18 $\alpha$ , H-21 $\alpha$ , and H-21 $\beta$  were irradiated) (Figure 3). The NOEs observed for H-3 $\alpha$ /H-21 $\alpha$ , H-3 $\alpha$ /H-15, and H-15/H-21 $\alpha$  indicated that the piperidine ring adopts a chair conformation with H-3 $\alpha$ , H-15, and H-21 $\alpha$  being axially oriented. On the other hand, the NOEs observed for H-14 $\beta$ /H-17 $\beta$  and H-14 $\beta$ /H-18 $\beta$  required the lactone function to be  $\alpha$ -disposed, whereas the C-17–O–C-18–C-19 fragment  $\beta$ -disposed. Taken together, the relative configurations at C-15, C-16, and C-20 were deduced to be *R*, *S*, and *R*, respectively. The relative configuration at the hydroxymethine C-19 was deduced to be *S* ( $\beta$ -OH) based on the strong NOE observed between H-19 and H-21 $\beta$ . This was also in agreement with the conspicuous absence of NOE between H-14 $\beta$  and H-19. Finally, the structure and absolute configuration of **2** were confirmed by X-ray diffraction analysis (CCDC 1877737, Figure 5). Interestingly, the X-ray structure revealed the presence of a H-bond between 19-OH ( $\delta_H$  7.63 br s) and *N*-4.

Alstolaxepine (**2**) represents a new 6,7-*seco*-angustilobine B-type alkaloid incorporating a  $\gamma$ -lactone-bridged oxepane ring

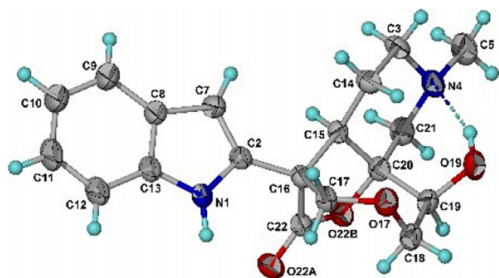
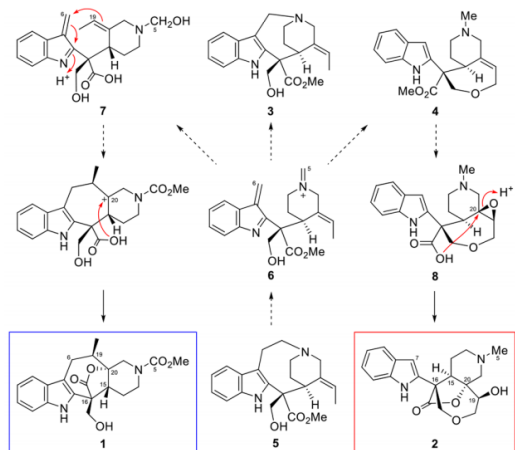


Figure 5. X-ray crystal structure of **2** [Flack parameter,  $x = -0.05(14)$ ; Hooft parameter,  $y = -0.10(7)$ ].

(i.e., 3,7-dioxabicyclo[4.2.1]nonan-8-one), which is unprecedented among natural products.

Stemmadenine (**5**), which plays an important role in the biosynthesis of many indole alkaloids,<sup>17</sup> is postulated to be an upstream precursor of **1** and **2**. The biogenetic relationship among 19*E*-vallesamine (**3**), 5,6-*seco*-angustilobine B (**4**), and **5** have previously been reported to involve the crucial intermediacy of the 5,6-*seco*-stemmadenine iminium ion intermediate **6** (Scheme 1).<sup>17–19</sup> Both **3** and **4** were also

#### Scheme 1. Possible Biogenetic Pathways to **1** and **2**



isolated in the present study. Possible biogenetic pathways to both **1** and **2** could be traced back to the same iminium ion **6** (Scheme 1). Hydration of the N-4 iminium ion and hydrolysis of the methyl ester function in **6** furnished a carboxyl–carbinolamine intermediate **7**. The carbinolamine group would then be converted to the NCO<sub>2</sub>Me via oxidation and esterification reactions. A subsequent nucleophilic addition of the 19,20 double bond onto the conjugated imine at C-6 forged the cycloheptane ring C in **1**. The resulting C-20 tertiary carbocation was then trapped by the carboxyl group to furnish the  $\gamma$ -lactone bridge and thus completed the construction of the structure of **1**. Alternatively, the iminium ion intermediate **6** was converted to 6,7-*seco*-angustilobine B (**4**), which on epoxidation of the 19,20 double bond, followed by hydrolysis of the methyl ester, gave the carboxyl–epoxide intermediate **8**. Subsequent intramolecular nucleophilic attack of the carboxyl group onto C-

20 with concomitant epoxide ring opening provided the final structure of **2**. The proposed pathways to **1** and **2** are consistent with the relative configurations established for their structures.

Both **1** and **2** showed no appreciable cytotoxic activity when tested against a panel of five breast cancer cell lines (MDA-MB-231, MDA-MB-468, MCF7, SKBR3, and T47D; IC<sub>50</sub> > 25  $\mu$ M).<sup>20</sup> However, **2** was found to induce marked concentration-dependent vasorelaxation effects in rat isolated aortic rings precontracted with phenylephrine with EC<sub>50</sub> = 6.58  $\pm$  3.66  $\mu$ M and  $E_{\max}$  = 93.9  $\pm$  4.3% (cf. verapamil, EC<sub>50</sub> = 0.55  $\pm$  0.19  $\mu$ M and  $E_{\max}$  = 106.4  $\pm$  3.4%) (Figure 6).<sup>21</sup>

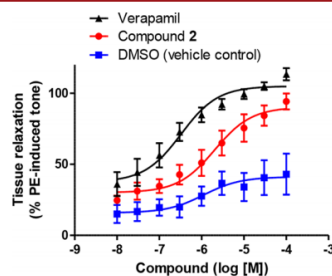


Figure 6. Dose–response curves of **2** and verapamil (positive control) on endothelium-intact aortic rings precontracted with phenylephrine (0.1  $\mu$ M). Data are expressed as the mean  $\pm$  SEM ( $n = 5$  or 6).

#### ■ ASSOCIATED CONTENT

##### Supporting Information

The Supporting Information is available free of charge on the ACS Publications website at DOI: 10.1021/acs.orglett.8b03592.

Experimental procedures, NMR, and HRMS data of **1** and **2**; computational data for **1**; X-ray crystal data and structure refinement parameters for **2** (PDF)

#### Accession Codes

CCDC 1877737 contains the supplementary crystallographic data for this paper. These data can be obtained free of charge via [www.ccdc.cam.ac.uk/data\\_request/cif](http://www.ccdc.cam.ac.uk/data_request/cif), or by emailing [data\\_request@ccdc.cam.ac.uk](mailto:data_request@ccdc.cam.ac.uk), or by contacting The Cambridge Crystallographic Data Centre, 12 Union Road, Cambridge CB2 1EZ, UK; fax: +44 1223 336033.

#### ■ AUTHOR INFORMATION

##### Corresponding Author

\*E-mail: [kuanhon.lim@nottingham.edu.my](mailto:kuanhon.lim@nottingham.edu.my)

##### ORCID

Yun-Yee Low: 0000-0002-7429-4238

Kuan-Hon Lim: 0000-0003-1462-3324

##### Notes

The authors declare no competing financial interest.

#### ■ DEDICATION

Dedicated to Professor Toh-Seok Kam on the occasion of his 70th birthday.

#### ■ REFERENCES

(1) Zhu, G. Y.; Yao, X. J.; Liu, L.; Bai, L. P.; Jiang, Z. H. *Org. Lett.* **2014**, *16*, 1080–1083.

- (2) Khyade, M. S.; Kasote, D. M.; Vaikos, N. P. *J. Ethnopharmacol.* **2014**, *153*, 1–18.
- (3) Cai, X. H.; Du, Z. Z.; Luo, X. D. *Org. Lett.* **2007**, *9*, 1817–1820.
- (4) Kam, T. S.; Nyeoh, K. T.; Sim, K. M.; Yoganathan, K. *Phytochemistry* **1997**, *45*, 1303–1305.
- (5) Bello, I.; Usman, N. S.; Mahmud, R.; Asmawi, M. Z. *J. Ethnopharmacol.* **2015**, *175*, 422–431.
- (6) Idris, B.; Asmawi, M. Z.; Nasiba, U. S.; Mahmud, R.; Abubakar, K. *Int. J. Pharmacol.* **2015**, *11*, 327–334.
- (7) (a) Smith, J. M.; Moreno, J.; Boal, B. W.; Garg, N. K. *J. Org. Chem.* **2015**, *80*, 8954–8967. (b) Wang, D.; Hou, M.; Ji, Y.; Gao, S. *Org. Lett.* **2017**, *19*, 1922–1925. (c) Adams, G. L.; Carroll, P. J.; Smith, A. B., III. *J. Am. Chem. Soc.* **2012**, *134*, 4037–4040. (d) Liang, X.; Jiang, S. Z.; Wei, K.; Yang, Y. R. *J. Am. Chem. Soc.* **2016**, *138*, 2560–2562. (e) Mason, J. D.; Weinreb, S. M. *J. Org. Chem.* **2018**, *83*, 5877–5896. (f) Mason, J. D.; Weinreb, S. M. *Angew. Chem., Int. Ed.* **2017**, *56*, 16674–16676. (g) Bihelovic, F.; Ferjancic, Z. *Angew. Chem., Int. Ed.* **2016**, *55*, 2569–2572.
- (8) (a) Yamauchi, T.; Abe, F.; Chen, R. F.; Nonaka, G. I.; Santisuk, T.; Padolina, W. G. *Phytochemistry* **1990**, *29*, 3547–3552. (b) Macabeo, A. P. G.; Krohn, K.; Gehle, D.; Read, R. W.; Brophy, J. J.; Cordell, G. A.; Franzblau, S. G.; Aguinaldo, A. M. *Phytochemistry* **2005**, *66*, 1158–1162.
- (9) HRDARTMS found  $m/z$  385.1760  $[M + H]^+$  (calcd for  $C_{21}H_{24}N_2O_5 + H$ , 385.1764).
- (10) Dugave, C.; Demange, L. *Chem. Rev.* **2003**, *103*, 2475–2532.
- (11) Zeches, M.; Ravao, T.; Richard, B.; Massiot, G.; Le Men-Olivier, L.; Verpoorte, R. *J. Nat. Prod.* **1987**, *50*, 714–720.
- (12) Akhmedov, N. G.; Myshakin, E. M.; Hall, C. D. *Magn. Reson. Chem.* **2004**, *42*, 39–48.
- (13) The coalescence temperature was shown to be between 40 and 50 °C.
- (14) Walser, A.; Djerassi, C. *Helv. Chim. Acta* **1964**, *47*, 2072–2086.
- (15) HRDARTMS found  $m/z$  343.1644  $[M + H]^+$  (calcd for  $C_{19}H_{22}N_2O_4 + H$ , 343.1658).
- (16) Lim, J. L.; Sim, K. S.; Yong, K. T.; Loong, B. J.; Ting, K. N.; Lim, S. H.; Low, Y. Y.; Kam, T. S. *Phytochemistry* **2015**, *117*, 317–324.
- (17) Szabo, L. F. *ARKIVOC* **2008**, *iii*, 167–181.
- (18) Lim, K. H.; Low, Y. Y.; Kam, T. S. *Tetrahedron Lett.* **2006**, *47*, 5037–5039.
- (19) Koyama, K.; Hirasawa, Y.; Zaima, K.; Hoe, T. C.; Chan, K. L.; Morita, H. *Bioorg. Med. Chem.* **2008**, *16*, 6483–6488.
- (20) Al-Khdhairawi, A. A. Q.; Krishnan, P.; Mai, C. W.; Chung, F. F. L.; Leong, C. O.; Yong, K. T.; Chong, K. W.; Low, Y. Y.; Kam, T. S.; Lim, K. H. *J. Nat. Prod.* **2017**, *80*, 2734–2740.
- (21) Yap, V. A.; Loong, B. J.; Ting, K. N.; Loh, S. H. S.; Yong, K. T.; Low, Y. Y.; Kam, T. S.; Lim, K. H. *Phytochemistry* **2015**, *109*, 96–102.



Contents lists available at ScienceDirect

## Tetrahedron Letters

journal homepage: [www.elsevier.com/locate/tetlet](http://www.elsevier.com/locate/tetlet)

# Alstobrogaline, an unusual pentacyclic monoterpene indole alkaloid with aldimine and aldimine-*N*-oxide moieties from *Alstonia scholaris*

Premanand Krishnan<sup>a</sup>, Chun-Wai Mai<sup>b,c</sup>, Kien-Thai Yong<sup>d</sup>, Yun-Yee Low<sup>e</sup>, Kuan-Hon Lim<sup>a,\*</sup><sup>a</sup> School of Pharmacy, University of Nottingham Malaysia, Jalan Broga, 43500 Semenyih, Selangor, Malaysia<sup>b</sup> School of Pharmacy, International Medical University, Bukit Jalil, 57000 Kuala Lumpur, Malaysia<sup>c</sup> Center for Cancer and Stem Cell Research, International Medical University, Bukit Jalil, 57000 Kuala Lumpur, Malaysia<sup>d</sup> Institute of Biological Sciences, Faculty of Science, University of Malaya, 50603 Kuala Lumpur, Malaysia<sup>e</sup> Department of Chemistry, Faculty of Science, University of Malaya, 50603 Kuala Lumpur, Malaysia

## ARTICLE INFO

## Article history:

Received 15 November 2018

Revised 19 December 2018

Accepted 8 February 2019

Available online 10 February 2019

## Keywords:

Monoterpene indole alkaloid

Aldimine

*Alstonia*

Apocynaceae

## ABSTRACT

Alstobrogaline (**1**), an unusual monoterpene indole alkaloid incorporating a third *N* atom and possessing two aldimine functions, with one being in the form of *N*-oxide, was isolated from the leaves of *Alstonia scholaris*. Its structure and relative configuration were determined by extensive NMR spectroscopic analysis, while its absolute configuration was established by X-ray diffraction analysis. A possible biogenetic pathway to **1** was proposed. Compound **1** displayed weak cytotoxic effects against MDA-MB-231 and MCF7 breast cancer cells.

© 2019 Elsevier Ltd. All rights reserved.

Plants of the genus *Alstonia* are known to be prolific producers of monoterpene indole alkaloids with intriguing polycyclic molecular skeletons and useful biological activities. *Alstonia scholaris*, which is widely distributed in tropical Asia, is used in traditional medicine in China, India, and Southeast Asia for the treatment of various diseases [1–3]. Although various samples of *A. scholaris* collected from different regions have previously been investigated [1,4,5], there was only one report on the Malaysian sample, which was collected from the east coast of Peninsular Malaysia. In the present study, the leaf sample of a cultivated *A. scholaris* collected from the west coast of Peninsular Malaysia was investigated, which resulted in the discovery of alstobrogaline (**1**), an unprecedented pentacyclic monoterpene indole alkaloid incorporating a third *N* atom as well as featuring an aldimine and an aldimine-*N*-oxide function (Fig. 1). Herein, we report the isolation, structure elucidation, and biogenetic pathway of compound **1**.

Alstobrogaline (**1**) was initially isolated as a light yellowish oil and subsequently crystallized from CHCl<sub>3</sub> as light orange block crystals, mp 187 °C (decomposed), [α]<sub>D</sub> = +93 (c 0.10, CHCl<sub>3</sub>). The IR spectrum showed NH and ester carbonyl absorption bands at 3249 and 1739 cm<sup>-1</sup>, respectively, while the UV spectrum showed characteristic dihydroindole absorption maxima at 235 and

290 nm. The HR-DART-MS measurements showed an [M + H]<sup>+</sup> peak at *m/z* 352.1674, which analyzed for C<sub>20</sub>H<sub>21</sub>N<sub>3</sub>O<sub>3</sub> + H. The molecular formula of **1** reveals the presence of 12 degrees of unsaturation, in addition to the presence of a third *N* atom, which is rare among monoterpene indole alkaloids.

The <sup>1</sup>H NMR data (Table 1) showed the presence of signals due to four aromatic hydrogens (δ<sub>H</sub> 6.73–7.10), an ester methyl at δ<sub>H</sub> 3.73 (s), an indolic NH at δ<sub>H</sub> 4.92 (br s), and an ethylidene side chain (δ<sub>H</sub> 1.75, d, 3H; δ<sub>H</sub> 5.84, q, 2H; *J* = 7.5 Hz). Additionally, two unusually deshielded signals at δ<sub>H</sub> 7.29 (br s) and 7.69 (s) were also observed. Consistent with the molecular formula established by HRMS measurements, the <sup>13</sup>C NMR spectrum (Table 1) indicated a total of 20 carbon resonances, while the HSQC spectrum revealed the presence of 11 downfield resonances (comprising seven *sp*<sup>2</sup> methine carbons, one *N*-bearing *sp*<sup>2</sup> tertiary carbon, two *sp*<sup>2</sup> quaternary carbons, and one ester carbonyl carbon) and nine upfield resonances (comprising two methyl carbons, two *sp*<sup>3</sup> methylene carbon, three *sp*<sup>3</sup> methine carbons, one *sp*<sup>3</sup> quaternary carbon, and one significantly deshielded non-H-bearing *sp*<sup>3</sup> carbon at δ<sub>C</sub> 98.8). The downfield resonances corresponding to the indolic benzene ring (δ<sub>C</sub> 111.3, 120.5, 123.0, 129.0, 136.3, and 145.7) and ethylidene side chain (δ<sub>C</sub> 130.0, 132.3, and 14.4) were readily assigned based on comparison with other indole alkaloids with a dihydroindole chromophore and an ethylidene unit [6], and these assignments were corroborated by HMBC and NOESY data (Figs. 2 and 3).

\* Corresponding author.

E-mail address: [Kuanhon.Lim@nottingham.edu.my](mailto:Kuanhon.Lim@nottingham.edu.my) (K.-H. Lim).<https://doi.org/10.1016/j.tetlet.2019.02.018>

0040-4039/© 2019 Elsevier Ltd. All rights reserved.

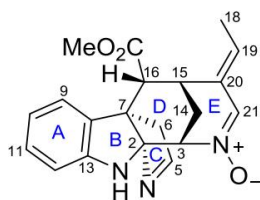


Fig. 1. Structure of alstobrogaline (**1**).

Table 1  
<sup>1</sup>H and <sup>13</sup>C NMR spectroscopic data of **1** in CDCl<sub>3</sub>.

Position	$\delta_c^a$	$\delta_H$ (J in Hz) <sup>a</sup>
2	98.8	
3	69.2	4.55 t (2.5) (eq)
5	167.9	7.69 br s
6	47.4	3.25 m
7	50.6	
8	136.3	
9	123.0	6.99 d (7.5)
10	120.5	6.75 t (7.5)
11	129.0	7.10 t (7.5)
12	111.3	6.73 d (7.5)
13	145.7	
14	28.8	2.24 dt (13.6, 3.8) (eq)
14'		2.46 dt (13.6, 2.1) (ax)
15	27.5	3.34 m (eq)
16	52.6	2.81 d (3.6) (ax)
18	14.4	1.75 d (7.5)
19	132.3	5.84 q (7.5)
20	130.0	
21	138.1	7.29 s
CO <sub>2</sub> Me	171.9	
CO <sub>2</sub> Me	51.9	3.73 s
NH		4.92 br s

<sup>a</sup> Recorded at 600 and 150 MHz.

The COSY spectrum revealed the presence of CHCHCHCH, NCHCH<sub>2</sub>CHCH, and =CHCH<sub>3</sub> partial structures corresponding to the C-9–C-10–C-11–C-12, N-C-3–C-14–C-15–C-16, and C-18–C-19 fragments in **2**, respectively (Fig. 2). The C-9–C-10–C-11–C-12 fragment was readily assigned to the four contiguous aromatic methines of the dihydroindole moiety, which was firmly established based on the HMBC three-bond correlations from H-9 to C-7 and C-13, from H-12 to C-8, and from NH to C-7 and C-8. The N-C-3–C-14–C-15–C-16 fragment was deduced to be attached to C-2 and C-7 based on the three-bond correlations observed from H-3 to C-7, from H-14 to C-2, and from H-16 to C-2, C-6, and C-8 (Fig. 2), thus completed the assembly of the six-membered ring D. The HMBC correlations from H-16 and OMe ( $\delta$  3.73) to the carbonyl carbon at  $\delta_c$  171.9 indicated the presence of the CO<sub>2</sub>Me group and its attachment to C-16.

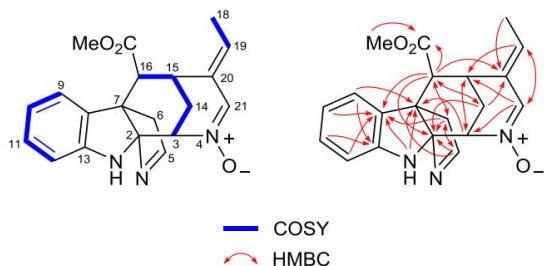


Fig. 2. COSY and selected HMBCs of **1**.

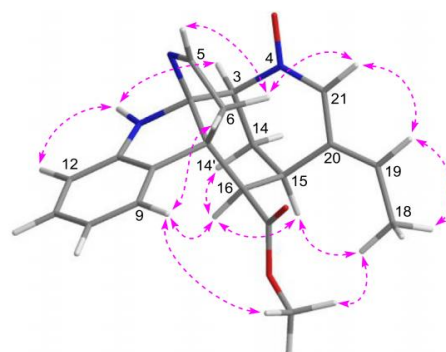


Fig. 3. Selected NOEs of **1**.

The C-18–C-19 fragment was deduced to be part of the ethylene side chain based on the HMBC three-bond correlation from H-18 to C-20. On the other hand, C-15 and C-21 ( $\delta_c$  138.1) were deduced to be attached to C-20 based on the correlations from H-19 to C-15 and C-21 and from H-21 ( $\delta_H$  7.29) to C-15, C-19, and C-20. Furthermore, the connection between C-21 and C-3 via N-4 was inferred by the HMBC correlation from H-21 to C-3, thus giving rise to the six-membered ring E. The unusually deshielded CH-21 ( $\delta_c$  138.1;  $\delta_H$  7.29) indicated the presence of a rare aldimine-N-oxide function at the N-4 – C-21 fragment [6]. Finally, ring C was constructed by linking C-6 to C-7, and C-5 to C-2 via an N atom as indicated by the HMBC correlations from H-6 to C-2, C-5, C-8, and C-16 and from H-5 to C-2, C-6, and C-7. The unusually deshielded CH-5 ( $\delta_c$  167.9;  $\delta_H$  7.69) supported it to be an aldimine carbon (CH-5 = N), whereas the chemical shift observed for C-2 ( $\delta_c$  98.8) is consistent with it being an aminal carbon. The resulting 2D structure, as shown in **1**, is in full agreement with the HMBC data (Fig. 2).

The relative configurations at the various stereocenters were deduced from the NOESY data (Fig. 3). The NOE observed for H-16/H-14' indicated a 1,3-diaxial relationship for H-16 and H-14', whereas the NOEs observed for H-3/NH and H-15/H-16 indicated that both H-3 and H-15 were equatorially oriented. These observations also inferred that ring D adopted a chair conformation, while the C-3–N-4 and C-15–C-20 bonds were axial. Furthermore, the NOE observed for H-6/H-21 required ring C and the N-4–C-21–C-20 fragment to be located on the same face of ring D. Taken together, the configurations at C-2, C-3, C-7, C-15, and C-16 were determined to be *rel*-(2*S*,3*S*,7*R*,15*R*,16*R*). Finally, the geometry of the C-19–C-20 double bond was deduced to be *E* based on the

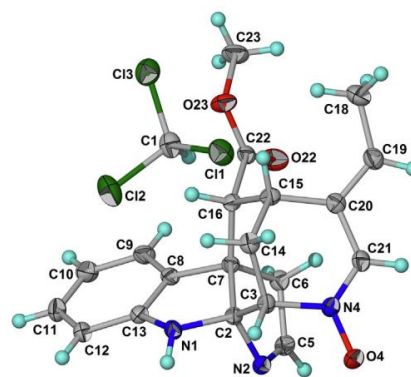
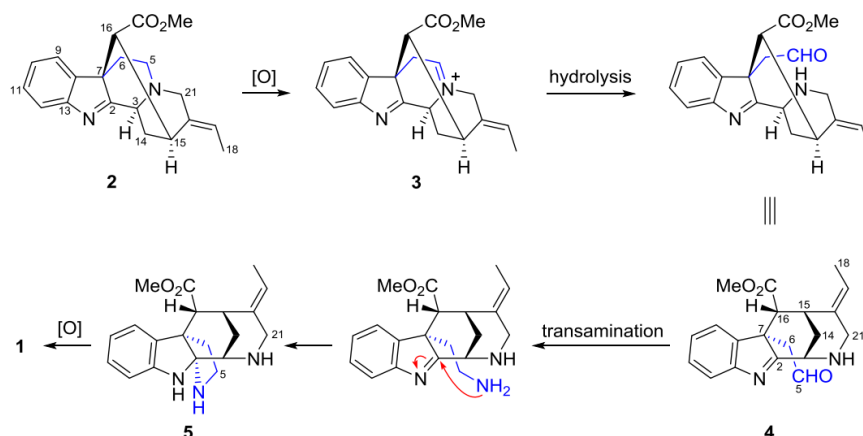


Fig. 4. X-ray crystal structure of **1** [Flack parameter,  $x = -0.02(2)$ ].

Scheme 1. Possible biogenetic pathway to **1**.

NOEs observed for H-19/H-21 and H-18/H-15. Since suitable crystals of **1** were obtained, X-ray diffraction analysis was carried out, which confirmed the absolute configurations at all stereocenters as 2*S*,3*S*,7*R*,15*R*,16*R* (Fig. 4) [7].

Alstobrogaline (**1**) represents a novel and unusual monoterpenoid indole alkaloid incorporating a third *N* atom, and possessing two aldimine functions, with one being in the form of *N*-oxide. To the best of knowledge, following the isolation of two 4,5-*seco*-picrinine-type alkaloids (i.e., alschomine and isoalschomine) [6], compound **1** represents the third instance in which a monoterpenoid indole alkaloid incorporates an aldimine-*N*-oxide function. A possible biogenetic pathway to **1** is shown in Scheme 1, starting from an akuammiline-type precursor such as strictamine (**2**). Firstly, **2** undergoes an oxidation to the C-5–*N*-4 iminium ion **3**, which following hydrolytic cleavage gives the amine-aldehyde **4**. Subsequently, transamination of the aldehyde in **4** gives a primary amine, which then performs a nucleophilic addition onto the imine C-2 to give the pentacyclic aminal **5**. Finally, oxidation of **5** gives the desired alkaloid, alstobrogaline (**1**), which incorporates an aldimine and an aldimine-*N*-oxide function at C-5 and C-21, respectively.

Alstobrogaline (**1**) was evaluated for its cytotoxicity against a panel of five breast cancer cell lines. Compound **1** was weakly cytotoxic against MDA-MB-231 and MCF7 cells (IC<sub>50</sub> 25.3 and 24.1 μM, respectively), but was not active against MDA-MB-468, SKBR3, and T47D cells (IC<sub>50</sub> > 30 μM) [8].

#### Acknowledgment

P.K. and K.H.L. thank University of Nottingham Malaysia for providing PhD scholarship and partial funding for research.

#### Appendix A. Supplementary data

Supplementary data (Experimental procedures, NMR and HRMS data of **1**, crystal data and structure refinement parameters of **1**) to this article can be found online at <https://doi.org/10.1016/j.tetlet.2019.02.018>. These data include MOL files and InChIKeys of the most important compounds described in this article.

#### References

- [1] M.S. Khyade, D.M. Kasote, N.P. Vaikos, J. Ethnopharmacol. 153 (2014) 1–18.
- [2] X.H. Cai, Z.Z. Du, X.D. Luo, Org. Lett. 9 (2007) 1817–1820.
- [3] T.S. Kam, K.T. Nyeoh, K.M. Sim, K. Yoganathan, Phytochemistry 45 (1997) 1303–1305.
- [4] T. Yamauchi, F. Abe, R.F. Chen, G.I. Nonaka, T. Santisuk, W.G. Padolina, Phytochemistry 29 (1990) 3547–3552.
- [5] A.P.G. Macabeo, K. Krohn, D. Gehle, R.W. Read, J.J. Brophy, G.A. Cordell, S.G. Franzblau, A.M. Aguinaldo, Phytochemistry 66 (2005) 1158–1162.
- [6] F. Abe, R.F. Chen, T. Yamauchi, N. Marubayashi, I. Ueda, Chem. Pharm. Bull. 37 (1989) 887–890.
- [7] Crystal data for alstobrogaline (**1**): Light orange block crystals, C<sub>20</sub>H<sub>21</sub>N<sub>3</sub>O<sub>3</sub>·CHCl<sub>3</sub>, Mr = 470.77, orthorhombic, space group P2<sub>1</sub>2<sub>1</sub>2<sub>1</sub>, a = 9.3566(3) Å, b = 12.8522(5) Å, c = 17.2351(5) Å, V = 2072.57(12) Å<sup>3</sup>, Z = 4, D<sub>calc</sub> = 1.509 g cm<sup>-3</sup>, crystal size 0.20 × 0.13 × 0.10 mm<sup>3</sup>, R(000) = 976, Mo Kα radiation (λ = 0.71073 Å), T = 169(2) K. A total of 17986 reflections were measured with 6305 independent reflections (R<sub>int</sub> = 0.0279, R<sub>sigma</sub> = 0.0369). The final R<sub>1</sub> value was 0.0435 [I ≥ 2σ(I)] and wR<sub>2</sub> value was 0.1068 (all data). The absolute configuration was determined on the basis of the Flack parameter [x = -0.02(2)], refined using 2637 Friedel pairs. Crystallographic data for the structure of **1** have been deposited with the Cambridge Crystallographic Data Centre (deposition no. CCDC 1878436). These data can be obtained free of charge via [www.ccdc.cam.ac.uk/data\\_request/cif](http://www.ccdc.cam.ac.uk/data_request/cif), or by emailing [data\\_request@ccdc.cam.ac.uk](mailto:data_request@ccdc.cam.ac.uk), or by contacting The Cambridge Crystallographic Data Centre, 12 Union Road, Cambridge CB2 1EZ, UK; fax: +44 1223 336033.
- [8] A.A.Q. Al-Khdhairawi, P. Krishnan, C.W. Mai, F.F.L. Chung, C.O. Leong, K.T. Yong, K.W. Chong, Y.Y. Low, T.S. Kam, K.H. Lim, J. Nat. Prod. 80 (2017) 2734–2740.